Secondary Minerals to Replace Cement in Stabilising an Alluvium

Paul Sargent

MSci (Hons) Dunelm MSc FGS

This thesis is submitted in partial fulfilment of the requirements for the degree of Doctor of Philosophy

School of Civil Engineering and Geosciences

Newcastle University

NE1 7RU

May 2015

Declaration

I hereby certify that this work is my own, except where otherwise acknowledged, and that it has not been submitted previously for a degree at this or any other university.

Signed:

.....

Paul Sargent MSci (Hons) Dunelm MSc FGS

Abstract

Ordinary Portland cement (CEM-I) is widely used across the construction industry. It is the most commonly used cementitious binder for ground improvement applications such as deep dry soil mixing (DDSM) in the UK, due to its high strength performances. However, CEM-I production is one of the world's most energy intensive and expensive industrial processes; contributing up to 7% of the world's total CO_2 emissions (McLellan et al., 2011). Hence, there is now significant pressure on the cement and construction industries to greatly reduce their CO_2 emissions by developing "greener" alternatives to CEM-I, which are both more environmentally and financially sustainable in the long-term.

Alkali activated industrial waste materials, known as geopolymers have been identified as potential alternatives to CEM-I. There are numerous advantages in recycling industrial waste materials such as ground granulated blast furnace slag (GGBS) and pulverised fly ash (PFA), including avoiding the need to transfer such materials to landfill, their abundant supply, negligible or zero production costs and for calcium-bearing wastes such as slags, their recently determined potential for carbon capture and storage (CCS).

This thesis presents recent laboratory research which focussed on the potential for utilising alkali activated industrial waste materials as sustainable binders in DDSM to enhance the geotechnical properties of soft soils. The laboratory testing programme deployed geotechnical and mineralogical tests to determine the performance of the binders when incorporated into a soft alluvial soil, typically found in abundance across the UK.

Comparisons with the strength and durability of untreated and stabilised soils have been made. The study indicates that from the by-products tested, soils stabilised with sodium hydroxide (NaOH) activated GGBS resulted in the greatest strength and durability improvements; with other materials tested showing smaller improvements. The addition of NaOH has been observed to allow pozzolanic reactions to occur, leading to improved mechanical properties; primarily strength, which increased with time.

The effectiveness of DDSM treatment in stabilising sections of high-speed railway lines with ground conditions dominated by soft and highly compressible soils, has previously been well demonstrated (Holm et al., 2002; Hughes and Glendinning, 2004). Traditionally, the monotonic strength properties of stabilised soils have been used to assess their suitability for stabilising railway embankments. However, the dynamic strength properties of such materials require investigation in order to provide better estimates of their field behaviour when subjected to complex loading conditions associated with high-speed railway embankments and high-frequency train traffic. Hence, this thesis combines monotonic and dynamic triaxial testing techniques to assess the suitability of the new GGBS-NaOH binder for stabilising high-speed railway embankments. After 28 days curing, the binder successfully demonstrated itself as an effective countermeasure against significant track displacements after the simulated passage of a typical InterCity 125 high-speed train.

This thesis advocates that there is great potential for using GGBS-NaOH as a more environmentally and financially sustainable binder over CEM-I for DDSM projects in the UK, such as the proposed HS2 and HS3 rail links. However, further research and collaboration with the construction industry is still required before the new binder may be used on a commercial scale.

Key terms: Stabilised soils, Sustainability, Alkali activation, Performance, High-speed rail.

This thesis is dedicated to my parents, Anne and John.

Acknowledgements

Firstly, I would like to thank my supervisors Dr. Paul Hughes and Dr. Mohamed Rouainia for all of their time, assistance, guidance and encouragement throughout this PhD. It is they who have truly inspired me to pursue a career in academia. I would also like to thank Mr. Stuart Patterson and Mr. Fred Beadle for all of the support, advice and training which they provided to make the laboratory testing programme of this research possible. I would also like to pay my gratitude to Dr. David Nash and Dr. Andrea Diambra from Bristol University, who kindly allowed me to use some of their advanced triaxial testing equipment and provided invaluable advice throughout my stay in Bristol.

I would like to thank St. James's Investments (New Bond Street, London) for providing a financial contribution towards funding this research. Thanks also go to all of my close friends and fellow PhD colleagues at Newcastle, who helped make my time as a PhD student in Newcastle such a fantastic experience. Finally, I would like to acknowledge all of the constant encouragement and financial support provided by my parents over the last four years; without whom I would not have been able to complete this project.

Table of Contents

List of Figures

List of Tables

List of Symbols and Acronyms

AA	Alkali activated sample
A	Sample cross sectional area
A_c	Triaxial sample's new cross sectional area post-consolidation
A_0	Original sample's cross sectional area
Aft	Hydrous calcium aluminate sulphate
Afm	Hydrous calcium aluminate ferrite
B	Triaxial sample saturation B-test
BCVG	Barry Clarke volume gauge
BET	Brunauer Emmett Teller nitrogen absorption specific surface area measurement method
C	Controlled (non-activated) sample
c'	Effective cohesion
C_c'	Compression index
C_s'	Swelling index
C_2S	Dicalcium silicate
C_3S	Tricalcium silicate
C_3A	Tricalcium aluminate
C_4AF	Tetracalcium aluminoferrite
C-A-H	Calcium alumina hydrate
CEC	Cation exchange capacity
CEM-I	Ordinary Portland cement (ASTM designation)
CH	Calcium hydrate
CID	Isotropically consolidated drained triaxial test
CIU	Isotropically consolidated undrained triaxial test
C-N-A-H	Calcium sodium alumina hydrate
C-N-S-H	Calcium sodium silica hydrate
C-N-A-S-H	Calcium sodium alumina silica hydrate

C-S-H	Calcium silica hydrate
CSL	Critical state line
CSR	Cyclic stress ratio
Cu	Undrained shear strength
C_v	Coefficient of consolidation
d_r	Strain rate
DDSM	Deep dry soil mixing
Dis	Disturbed/remoulded sample
D_0	Initial sample diameter
DSM	Deep soil mixing
DWSM	Deep wet soil mixing
e	Void ratio
e_n	Difference in void ratio between the NCL and ISL/ICL according to Gasparre and Coop's (2008) oedometer normalisation technique
e_0	Initial void ratio
e^*_{100}	Void ratio on the ICL at a vertical stress of 100 kPa
e^*_{1000}	Void ratio on the ICL at a vertical stress of 1000 kPa
E	Young's modulus
E'	Young's modulus derived from consolidated drained triaxial tests in terms of effective stresses
EDX/EDS	Energy dispersive X-ray analysis
ESEM	Environmental scanning electron microscopy
E_{sec}	Secant Young's modulus
E_{tan}	Tangent Young's modulus
E_u	Young's modulus derived from consolidated undrained triaxial tests in terms of effective stresses
F	Coefficient for calculating expected time to failure of triaxial samples - as defined in BS 1377 (BSI, 1990), depending on how many drains were used for consolidation
F'	Frequency of sine wave signal pulses for bender element measurements
f	Cyclic loading frequency

gL	Local LVDT gauge length
G	Shear modulus
G_{max}	Maximum/initial shear stiffness
G_s	Specific gravity
G_{sec}	Secant shear modulus
GGBS	Ground granulated blast-furnace slag
H	Height of oedometer testing sample
H_1	Oedometer sample height at the start of each loading increment
H_2	Oedometer sample height at the end of each loading increment
ΔH	Cumulative compression of oedometer samples from H_0
$\bar{H}$	Average sample height for each oedometer loading increment
H_0	Original height of oedometer testing sample
H_s	Equivalent height of soil particles
HST	High-speed train
HWC	High water content
IBP	Industrial by-product
ICL	Intrinsic compression line
ICVC	Imperial College volume cell
ISL	Intrinsic swelling line
Iv	Void index
K	Bulk modulus
K_{sec}	Secant bulk modulus
k_v	Coefficient of vertical permeability
$\Delta l/\delta l$	Change in sample length
L_c	Triaxial sample's new length post-consolidation
L_o	Original sample's length
LL	Liquid limit
LVDT	Linear variable differential transformer
LWC	Low water content
M	Slope of critical state line

M^*	Value of M in triaxial extension/slope of volumetric strain-shear strain for drained triaxial tests, used to calculate dilation angle
M_{ds}	Mass of water lost during drying of soil samples to calculate their moisture content
M_r	Resilient modulus
M_v	Coefficient of volume compressibility
M_w	Mass of dried soil samples to calculate their moisture content
NaOH	Sodium hydroxide
Na_2SiO_3	Sodium silicate
NCL	Normal compression line
p_1	Pressure at the top of triaxial sample during permeability test
p_2	Pressure at the bottom of triaxial sample during permeability test
P_1	Vertical stress applied to oedometer samples for the previous loading increment
P_2	Vertical stress applied to oedometer samples for the current loading increment
p'	Mean effective stress
p'_0	Initial mean effective stress
p_c	Pressure loss in triaxial system for rate of flow during permeability test
P_{max}	Maximum force experienced by samples during compression tests
PFA	Pulverised fly ash
PI	Plasticity index
PL	Plastic limit
PVC	Polyvinyl chloride
q	Deviatoric stress
q'	Flow rate during permeability test
r_0	Soil structure
RG	Red gypsum
R_t	Temperature correction factor for the viscosity of water during triaxial permeability test
R_u	Excess pore pressure ratio

S_σ	Stress sensitivity
SEM	Scanning electron microscopy
SS	Steel slag
SSA	Specific surface area
T	Period for one load-unload cycle during dynamic triaxial testing
t	Time
t_f	Expected time to failure during shearing for triaxial samples
t_m	Membrane thickness for triaxial tests
t_s	Shear wave arrival time
t_{90}	Time taken for 90% consolidation to be completed
t_{100}	Time taken for 100% consolidation to be completed
u	Pore water pressure
UCL	Undisturbed compression line
UCS	Unconfined compressive strength
Undis	Undisturbed sample
UUT	Quick undrained unconsolidated triaxial
U100	Undisturbed 100 mm diameter x 200 mm long soil sample
v*	Specific volume
v^*_0	Initial specific volume
V_c	Triaxial sample's new consolidated volume
ΔV_c	Change in triaxial sample's volume during consolidation
VCL	Virgin compression line
V_s	Shear wave velocity
V_0	Original sample volume
w	Moisture/water content
XRD	X-ray diffraction
y	Cumulative correction factor for deformation of oedometer apparatus during testing
YSR	Yield stress ratio
Z	Depth below ground level

ε_a	Axial strain
ε_{cq}	Cyclic shear strain
ε_r	Radial strain
$l\varepsilon_a$	Locally measured axial strain
$l\varepsilon_r$	Locally measured radial strain
ε_p	Volumetric strain
ε_q	Shear strain
ρ	Bulk density
ρ_d	Dry density
ρ_s	Particle density
ρ_w	Water density
σ'_1	Effective principle stress
σ'_3	Effective confining stress
σ_{mb}	Membrane correction factor for triaxial tests
σ_n	Normal stress
σ'_n	Effective normal stress
σ_v	Vertical stress
σ_y	Yield stress
τ	Shear stress
υ	Poisson's ratio
φ'	Effective angle of internal friction
ψ	Angle of dilation

Chapter 1:

Introduction

1.1 Introduction

This thesis investigates the potential of using industrial waste products and alkali activators as more sustainable alternative binders to ordinary Portland cement (CEM-I) and lime, for use in treating soft soils for engineering applications. Large areas of the ground surface in many countries such as the UK are characterised by soft soils including alluvium, peat and soft organic clays. These present challenging ground conditions for civil engineers; given their unfavourably high settlements, poor bearing capacity, shear strength and shrink/swell durability characteristics. Deep dry soil mixing (DDSM) is becoming an increasingly popular and effective ground improvement technique in the UK for treating such soils by creating cemented soil columns via auger mixing.

The driving force behind this research is the need for the cement and civil engineering industries to develop and use new "greener" cementitious binders which have smaller carbon footprints and lower financial costs than the traditionally used CEM-I and lime. The production of CEM-I accounts for 7% of the world's atmospheric CO_2 emissions (McLellan et al., 2011). There is also pressure for these industries to develop materials and processes to potentially sequester atmospheric carbon. Whilst meeting financial and environmental sustainability criteria, it is also crucial for new cementitious binders to achieve similar or better engineering performances compared with those obtained by the traditionally used binders.

Much research has been conducted over the last 20 years on the development of geopolymer cement mixtures using industrial by-products (IBP's) including ground granulated blastfurnace slag (GGBS) and pulverised fly ash (PFA), both in abundant supply in the UK. High calcium wastes such as GGBS have recently been shown to exhibit promising carbon capture and storage potential within urban soils. Geopolymers have been commercialised in Australia (Global Cement, 2011), thereby suggesting that they are serious contenders as alternative cementitious binders to CEM-I. However, the UK's cement and civil engineering industries are reluctant to use geopolymers over CEM-I and continue to opt for traditional binders given their well proven engineering performances.

Recently, the UK government has outlined firm plans to develop HS2 and HS3 lines to better connect major cities within the midlands and north of England to southern parts of the country and with the European high-speed railway networks by 2026 (HS2, 2014). Soft problematic ground conditions are likely to be experienced along the proposed routes, given their relative abundance in the UK. The treatment of such soils would be essential prior to the rail links coming into service to provide a means of counter measure against significant track and surface settlements, embankment slope instability and slower train speeds. These would inherently lead to high long-term maintenance costs and fines would be incurred to the rail link owner due to delayed trains. A potential treatment technique for treating such ground conditions would be DDSM, given its proven success in stabilising sections of Sweden's Vastkustbanan and the UK's Channel Tunnel Rail Link (a.k.a. CTRL or HS1) through the use of lime or lime/CEM-I binders to suit the structural requirements of the rail links.

For many years, the monotonic strength characteristics of stabilised soils have been used to assess their suitability for stabilising high-speed railway embankments. This is deemed insufficient in terms of accurately understanding the material's behaviour. The loading conditions associated with high-speed railway embankments are complex, due to the combination of the monotonic loads presented by the embankment and permanent railway structures; and the high-frequency dynamic loads presented by high-speed train traffic. Hence, another main driving factor behind this research is being able to use dynamic triaxial tests in addition to monotonic testing to more accurately simulate and understand the behaviour of untreated and geopolymerised soils when subjected to dynamic loads typically associated with high-speed railway traffic. To date, neither untreated nor stabilised soils have not been systematically characterised in this manner before. It is anticipated that such dynamic testing data will prove useful in providing civil and railway engineers with practical estimates for ground/track settlements during the geotechnical design of railway embankments for HS2 and HS3.

1.2 Aims and objectives

This research has two main aims. The first is to determine whether an optimised alkali-activated IBP binder mixture is suitable in terms of engineering performance and environmental/financial sustainability for stabilising a soft alluvial foundation soil typically found in the UK for a high-speed railway embankment under various atmospheric and loading conditions. The second aim is to discern the mineralogical and microstructural changes within the soil as a result of stabilisation associated with in the observed improvements in engineering performance.

To achieve these aims, the following objectives require fulfilment:

- To develop a new low carbon binder design and appropriate dosage, which when mixed into an alluvial soil meets stringent strength criteria according to EuroSoilStab (2002).
- To assess the effectiveness of alkali activation on the rates at which IBP-stabilised soils' engineering properties are enhanced.
- To determine the influence of a soil's physico-chemical properties and curing time on a stabilised soil's improved engineering performance.
- To apply oedometer and triaxial testing techniques to quantify the geotechnical properties of an optimum alkali activated IBP binder design for use in DDSM; whereby attention will be paid towards the. stabilised soil's behaviour under monotonic and dynamic loading to assess the its suitability for stabilising high-speed railway embankments.
- To assess the mineralogical and microstructural features of the stabilised soil through the use of X-ray diffraction and scanning electron microscopy, to identify the reaction mechanisms and cementitious mineral phases responsible for the enhanced engineering performances.
- To assess the commercialisation potential, environmental and financial sustainability of the new alkali activated IBP binder compared with that for CEM-I.

1.3 Thesis structure

This thesis comprises ten chapters. Following this introduction, chapter 2 presents a literature review of the principles involved in chemical soil stabilisation and the processes involved in shallow and deep soil mixing. The chapter also reviews the binder materials which have been traditionally used in soil mixing since the technique was developed in the 1960's, along with the development of alkali activated waste products (a.k.a. geopolymers) as potentially more environmentally and financially sustainable alternatives to cement and lime. The final sections of the literature review present laboratory studies on the geotechnical and mineralogical characterisation of geopolymerised soil mixtures, plus recent efforts in developing constitutive soil models to numerically model the behaviour of cemented soils.

Chapter 3 presents the laboratory testing and analytical methodologies adopted by the author for the components of this research programme. Also, details of all the pieces of apparatus, data analyses, correction factors and interpretation techniques used are provided.

Chapter 4 presents the findings obtained from a suite of standard geotechnical and physico-chemical tests performed on an artificial silty sand, which was stabilised with various controlled and alkali activated IBP binder mixtures. Immediately following this dosage trial, a natural soft alluvial soil was sourced from Lanton in Northumberland (UK). The soil's geotechnical and physico-chemical index properties are characterised at the start of chapter 5. The results from chapter 4 formed the basis for a similar stabilisation study conducted on the Lanton alluvium, involving the use of similar controlled and alkali activated IBP binders to those described in chapter 4. The results from the Lanton alluvium's stabilisation study are also presented in chapter 5.

Based on the engineering performance results presented in chapter 5, environmental and financial sustainability issues, an optimum binder of GGBS-NaOH and corresponding dosage of 107 kg m^{-3} was selected for further study in this research. Results from a mineralogy and microstructure study conducted on the Lanton alluvium (untreated and stabilised with the GGBS-NaOH binder) are presented in chapter 6.

Based on oedometer testing results in chapter 5, the Lanton alluvium was deemed a highly sensitive soil, possessing a relatively high degree of post-sedimentation

bonding-based structure in its undisturbed state. Given the complexity of loads associated with high-speed railway embankments, chapter 7 presents a detailed monotonic and dynamic triaxial characterisation of the Lanton alluvium in its reconstituted and undisturbed states.

The final results chapter (chapter 8), presents findings from a comprehensive monotonic and dynamic triaxial study conducted on the GGBS-NaOH stabilised Lanton alluvium, following 28 days curing.

A discussion of the results in chapters 4–8 is provided at the end of each of these chapters. Chapter 9 presents a final discussion for the whole research study, drawing upon the results and discussions in chapters 4–8. The main themes are based on the engineering performance, sustainability and potential application to high-speed rail for the optimum binder. Finally, chapter 10 summarises the main conclusions from this research, along with a number of recommendations for future study.

It has become widely recognised within the geotechnical community that in terms of soil testing, local small strain measurements need to be conducted as these provide more reliable estimates of soil stiffness compared with global (external) strain measurements. These in turn may be used in numerical simulations, which should assist in avoiding higher project costs arising from overdesigning geotechnical structures such as railway embankments. Hence, two undrained small strain triaxial tests were conducted on samples of untreated undisturbed and 28day cured GGBS-NaOH treated Lanton alluvium at Bristol University. The results are presented in Appendix 5.

Chapter 2:

Literature Review

2.1 Introduction

In many countries, large areas of the ground surface are covered by soft soils (e.g. alluvium and peats). These can be problematic, due to their unfavourable bearing capacity, strength, shrink/swell, settlement and durability characteristics. Alluvial soils contain large quantities of silt, which present difficult ground conditions for construction purposes. In both wet and dry conditions they have low levels of cohesion, which can cause wall collapses within excavations and slope instability. The low strengths and stiffnesses of such soils can also lead to bearing capacity problems. Alluvial soils are found abundantly across the UK, especially on floodplains within river valleys where housing and industrial developments are often concentrated. Hence, the treatment of such alluvial soils forms the main basis of this research.

To improve such conditions, several stabilisation techniques are available, including compaction/consolidation, mechanical stabilisation and chemical (admixture) soil mixing with cementitious binders (Sherwood, 1993). This research focusses on chemical soil mixing, specifically deep dry soil mixing, which introduces cementitious materials to soft problematic soils; with a view to improving their engineering properties including strength and durability. Portland cement (CEM-I; BS EN: 197-1) and lime have long been utilised as binders. The former is considered more favourable in providing rapid strength enhancements (Rogers et al., 2000, Hossain, 2010 and Jegandan et al., 2010). The presence of soil water and calcium silicates/aluminates within the binders react to form hydration products including calcium silica hydrate (C-S-H) and calcium aluminate hydrate (C-A-H) gels.

Negative environmental and financial issues are associated with utilising CEM-I and lime as binders; specifically high energy consumption, financial cost, greenhouse gas and carbon emissions. The continued use of these binders is unsustainable - hence, there is a need to identify more environmentally and financially sustainable replacement binders. These binders should provide engineering performances that compare with or surpass those of CEM-I and lime within similar curing times.

A popular route for selecting new binders has been to recycle industrial by-products (IBP's); preferably those which are alumino-silicate based (i.e. pozzolanic). The introduction of alternative alkali activators such as sodium hydroxide to these IBP's,

can increase the rate at which the mechanical properties of stabilised soils are improved by increasing soil pH; thereby allowing pozzolanic reactions and cementitious bonding to occur (Palomo et al., 1999).

This chapter aims to present an up-to-date literature on the development and use of alkali activated cements as binders for chemical soil stabilisation. The first few sections address the basic mechanisms of chemical soil stabilisation, traditionally used binders and this technique's applicability in geotechnics. Recent environmental and financial costs findings are then presented, demonstrating the need for new sustainable binders. The final sections present findings from recent laboratory-based research on the development of new alkali activated cement mixtures and possible future trends in this research area.

2.2 Basic mechanisms of chemical soil stabilisation

There are five main reactions which occur between the binder and the soil to be stabilised: flocculation/agglomeration, cation exchange, hydration, pozzolanic reactions and potentially carbonation. Cation exchange and flocculation/agglomeration occur immediately upon mixing and can last up to a few hours afterwards. Hydration takes place up to one month post-mixing, whereas pozzolanic reactions occur over a longer time-scale – i.e. months and years.

2.2.1 Cation exchange

Immediately upon mixing, the introduction of a binder to the soil releases calcium ions, which can exchange with metal ions (e.g. Na^{+} and Al^{3+}) incorporated within the soil's clay lattice (Rogers and Glendinning, 1996). This process is referred to as cation exchange, resulting in numerous physical changes to the soil. One of the first changes is a reduction in the electric double (adsorbed water) layer surrounding clay particles (Rogers and Glendinning, 1996). The physical arrangement of clay particles dictates the size of the electric double layer. Parallel arrangements allow larger envelopes to form compared with "edge-to-face" arrangements. A reduced electric double layer

thickness means clay particles are less prone to the addition of water. The second change experienced is flocculation. Van der Waals forces overcome the repulsion of the negatively charged clay particles, bringing them into close proximity with each other and further reducing the thickness of the adsorbed water layer (Figure 2.1).

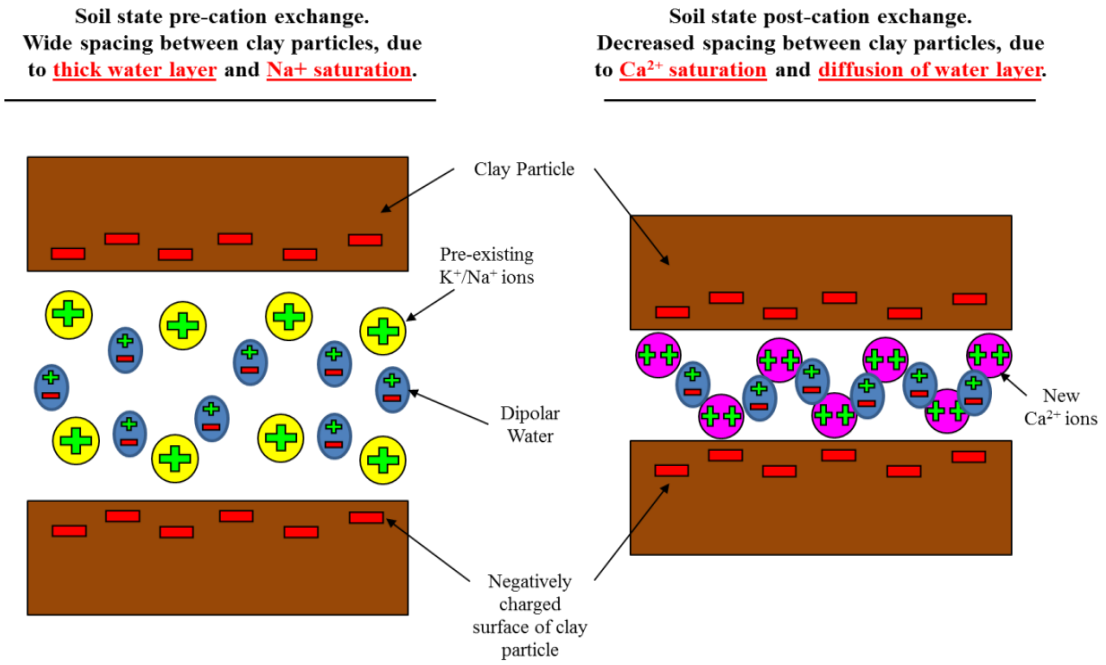

Figure 2.1: Diagram demonstrating cation exchange within soils, occurring immediately upon introducing a binder such as lime or cement.

These changes result in numerous textural and strength changes within the soil; namely a transition from a medium-high plastic clay to a more granular and friable soil characterised by a lower Plasticity Index. This causes an increase in the friction angle between agglomerate matter; and consequently an increase in shear strength (Rogers and Glendinning, 1996). Common cations involved in cation exchange include aluminium (Al^{3+}), calcium (Ca^{2+}), magnesium (Mg^{2+}), potassium (K^{+}), ammonium (NH_4^{+}), sodium (Na^{+}) and hydrogen (H^{+}). A cation's adsorption potential is influenced by valence and atomic weight. The higher these values, the higher the cation's adsorption level.

2.2.2 Flocculation

Flocculation/agglomeration occurs immediately post-mixing, involving the restructuring of negatively charged clay particles surrounded by a positively charged cation shell. The thickness of the shell depends on the level of charge; the higher the charge the thicker the shell. Initially, the clay particles are dispersed and occur in a parallel arrangement, due to their negative surface charge and positively charged cation shells repelling each other. This repulsion may be overcome by Van der Waals forces, causing particles to flocculate and give a new edge-to-face orientation (Figure 2.2).

There are two divisions of flocculators; good flocculators are ions with larger hydrated radii and higher valences (≥2+) (Sumner and Naidu, 1998), including Ca^{2+} and Mg^{2+}. Poor flocculators include ions with smaller hydrated radii and lower valences; including Na^{+} and K^{+}. Because of flocculation, soils gain improved engineering performances; specifically by increasing the plastic limit, increasing shear strength and the development of a granular texture.

2.2.3 Hydration

Hydration occurs when combining water with lime or cement (Equation 2.1). The hydration of quicklime is exothermic (Figure 2.3). Occasionally the amount of heat produced causes a soil's pore water to boil (Bergado et al., 1996). Upon mixing, the soil's water content instantly decreases as the water is consumed during hydration. This drying process is key in improving soft soils with high moisture contents. Per Bergado et al. (1996), the soil's moisture content must be sufficiently high for the quicklime to be completely slaked. There must also be sufficient amounts of water post-evaporation due to the heat produced during slaking, to ensure that ion exchange occurs between calcium ions of hydrated lime and alkali ions of clay minerals.

$$CaO + H_2O \rightarrow Ca(OH)_2 + Heat \qquad \textbf{(Equation 2.1)}$$

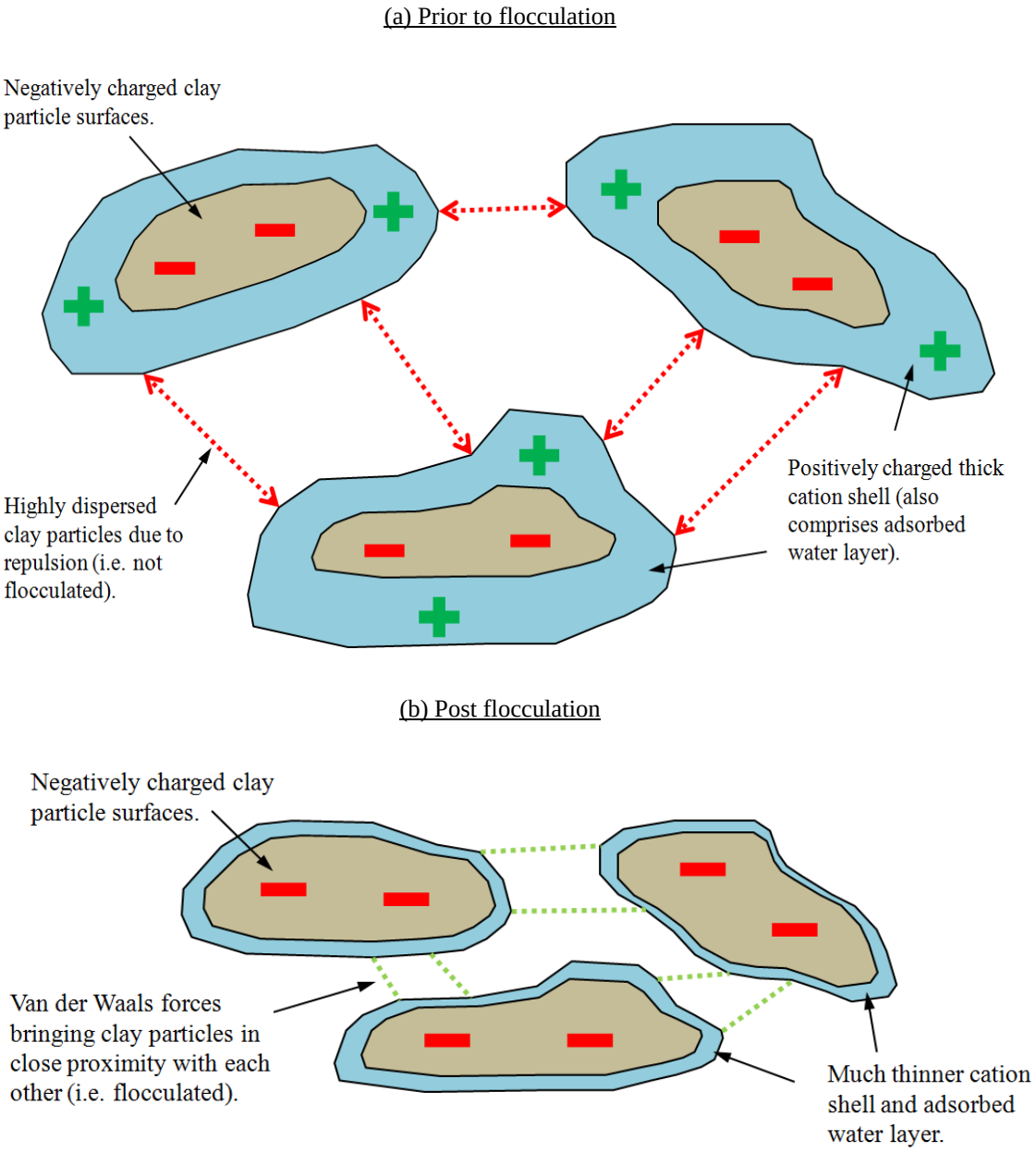

Figure 2.2: Illustration of the state of a soil both: (a) before and (b) post flocculation.

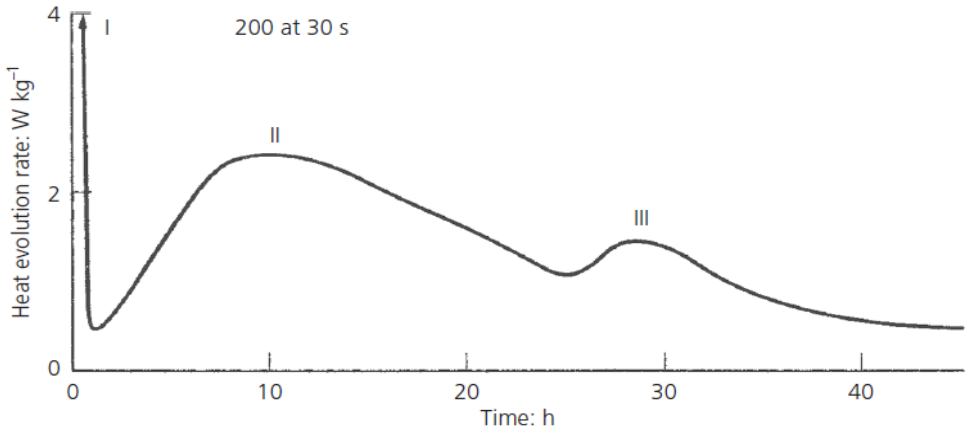

Figure 2.3: Heat evolution during hydration of ordinary Portland cement at 20°C and a water-cement ratio of 0.4. Note the three maxima (I, II and III) in hydration reaction rates. Courtesy of Bye (2011). Reproduced with permission from the Institution of Civil Engineers.

The calcium oxide reaction product from Equation 2.1 dissociates in the pore water, which increases its electrolytic concentration and pH (Equation 2.2); thereby dissolving SiO_2 and Al_2O_3 from the soil's clay particles (Bergado et al., 1996). These will collectively allow ion exchange, flocculation and pozzolanic reactions to occur (Bergado et al., 1996).

$$Ca(OH)_2 \rightarrow Ca^{++} + 2(OH)^- \qquad \textbf{(Equation 2.2)}$$

Two mechanisms occur during hydration, "Through solution" and "Topochemical" (Kurtis, 2007). Through solution involves the dissolution of anhydrous compounds towards their ionic constituents, hydrate formation within the solution and ultimately their precipitation, given their low solubility (Kurtis, 2007). The topochemical mechanism (solid state hydration) involves reactions occurring on anhydrous cement compound surfaces without going into solution (Kurtis, 2007). Five key phases occur upon mixing cement with soil water. Firstly the cement particles undergo dissolution followed by increases in ionic concentration levels within the water. Once ionic concentrations have become sufficiently high, compounds develop within solution. Once ionic concentration has become saturated these compounds precipitate as solid hydration products, which form close to or on the surfaces of anhydrous cement particles (Kurtis, 2007).

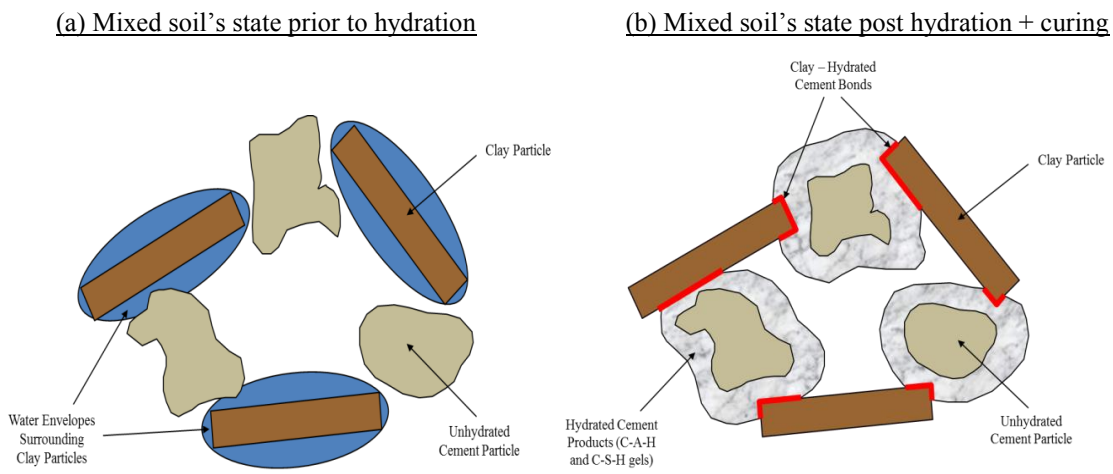

Figure 2.4: The typical state of a soil mixed with cement both: (a) prior to hydration and (b) after a few weeks curing, whereby the cement has reacted with the soil water and produced hydrated cementitious gels.

Four main strength-producing compounds exist within CEM-I, two are silicate-based, two are aluminate-based. Tricalcium silicate (C_3S) hydrates and hardens quickly and accounts for any early setting and strength gains (3 hours – 14 days post-mixing).

The second main hydrated cement compound is dicalcium silicate (C_2S) which hydrates and hardens relatively slowly. Rather than contributing towards initial strength gains, the strengthening effects of C_2S are observed later; normally between 7 and 14 days (Kurtis, 2007). Higher levels of heat are associated with C_3S hydration than with C_2S. The two aluminate-based hydrated cement compounds are tricalcium aluminate (C_3A) and tetracalcium aluminoferrite (C_4AF). The former releases a lot of heat during the first couple of days of curing and is most useful for initial strength development. C_4AF hydrates quickly and decreases the clinkering temperature; contributing very little towards strength development (Kurtis, 2007).

All four compounds are important for providing strength gains. Immediately upon mixing, the cement hydrates rapidly and produces primary cementitious products (a.k.a. major hydration products) – these being hydrated calcium silicates (C_2SH_x and $C_3S_2H_x$) and aluminates (C_3AH_x and C_4AH_x) and hydrated lime (Bergado et al., 1996). The cement particles then create bonds between adjacent cement grains and undisturbed soil particles during the hardening phase, ultimately creating a stronger soil-cement skeleton.

By hydrating both C_3S and C_2S, C-S-H and calcium hydrates (CH) are produced (Figure 2.4). However C_2S produces significantly less CH, which is vital for durability purposes within sulphate-bearing soils (Kurtis, 2007). As with most chemical reactions, temperature influences the rate of hydration.

C-S-H gels' mineralogical structures are generally poorly understood, due to the wide variation from amorphous to poorly crystalline (Kurtis, 2007). C-S-H is the primary strengthening mineral within CEM-I via ionic and Van der Waals bonds. It takes up to 60% of the hydrated cement paste and takes up large surface areas of up to 700 m^2/g (Kurtis, 2007).

Per Kurtis (2007), as the hydration rates of the five phases can significantly differ. Factors such as the rate of cement hardening, the time required for cement to stiffen and the setting time will ultimately depend on cement composition. Cement hydration also leads to an increase in the soil pore water's pH as a direct consequence of the dissociation of the hydrated lime (Bergado et al. (1996).

2.2.4 Pozzolanic reactions

Pozzolanic reactions occur over long timescales (months – years). The main mechanism involves the transportation of calcium hydroxide [$Ca(OH)_2$] via water within the soil to combine with the aluminate and/or silicate clay minerals (Duxson et al., 2007). The high surface area aluminate and silicate minerals are pozzolan phases, which in the presence of water and an alkali (e.g. calcium) produce cementitious materials; comprising calcium silicates and aluminate hydrates (Bergado et al., 1996). Any dissolved Ca^{2+} ions within the soil then react with any dissolved SiO_2 and Al_2O_3 located on clay particles to produce hydrated gels of C-S-H and C-A-H, which cement soil particles together as seen in Figure 2.5.

$$Ca^{2+} + 2(OH)^- + SiO_2 \quad \rightarrow \quad C-S-H \qquad \textbf{(Equation 2.3)}$$

$$Ca^{2+} + 2(OH)^- + Al_2O_3 \quad \rightarrow \quad C-A-H \qquad \textbf{(Equation 2.4)}$$

Pozzolanic reactions consume part of the soil's water, which enhances the engineering performance of stabilised soil. The material becomes stiffer and less susceptible to volume shrinkage/swelling. The soil-binder mixtures cure and produce stronger, cementitious soil matrices known as "Geopolymers" (Sherwood, 1993), which resist dissolution and soil erosion.

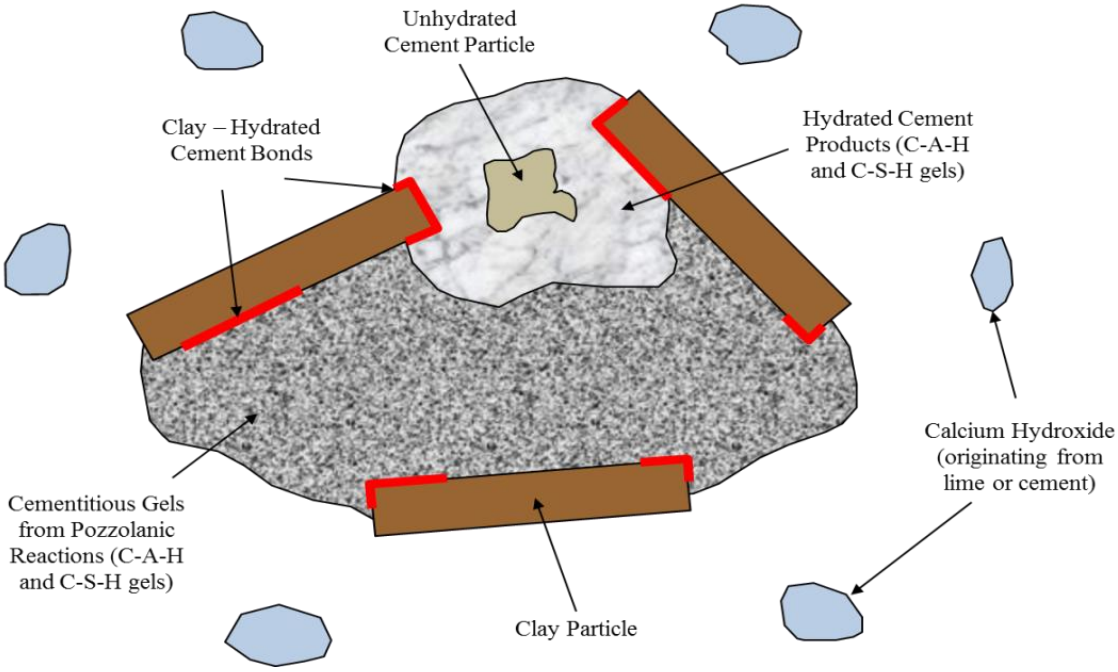

Figure 2.5: Cementitious bonding products formed during hydration and long-term pozzolanic reactions.

Per Bergado et al. (1996) and Diamond and Kinter (1965), pozzolanic reactions are incomplete until five years post-mixing. The solubility potential of silicates and aluminates within the soil, their likelihood of reacting with lime/cement and cementitious bond formation heavily rely on soil pH. Per Davidson et al. (1965), pozzolanic reactions only occur when soil pH is $\geq$10.5, i.e. when SiO_2 and Al_2O_3 become soluble. Broms, (1984) and Palomo et al. (1999) suggest that if samples cure at higher temperatures during the first 5 hours post-mixing; reaction rates are increased, producing further improved strengths.

2.3 Chemical stabilisation techniques

Chemical treatment is a versatile ground improvement technique, suitable for stabilising various soils up to 25 metres depth. A key advantage of this technique is that many binders are available; each possessing unique physicochemical properties that are advantageous in soil stabilisation. Both the soil's and binder's material properties must be carefully studied prior to stabilisation, as a binder may show impressive strength gains within one soil and damaging effects in another.

2.3.1 Surface and shallow soil mixing

Surface and shallow mixing are low cost techniques for enhancing the mechanical properties of soft soils, which cover large areas (Topolnicki, 2004). Surface mixing involves incorporating a lime or cement-based binder (dry or wet) within the top 250 mm of soil at air temperatures >7^{o}C (Figure 2.6). This technique has long been used in the USA and Australia for treating soft subgrades.

Figure 2.6: Photograph of surface mixing in India (courtesy of Wirtgen Group, 2014).

Prior to mixing, the binder may be applied by spreading either a dry powder or slurry. Soils which are most suitable for surface mixing are characterised by clay contents >10%, plasticity index (PI) >20, an activity PI – clay content ratio >0.75 and a sulphate content <1%.

For stabilising the subgrade, the typical binder dosage should be >2.5%. Once the binder has been mixed into the soil, an uneven surface is produced. Thus, a roller follows behind the mixer to compact the stabilised soil. The main advantage for using surface mixing is that it avoids removing poor soil from site. Onsite stabilisation reduces the amount of binder/aggregate required if significant quantities of poor soil require replacing. Depending on the soil and binder type, additional binder may be introduced to increase strength gain rates. Numerous disadvantages are associated with surface mixing; the most serious being dust and atmospheric pollution caused by plant equipment.

Shallow mixing involves treatment up to 3m depth. Large diameter augers and mass mixers stabilise a specific volume of soil (Topolnicki, 2004); commonly called "mass stabilisation". The uppermost soil layers may be insufficiently strong to support heavy mixing equipment. Therefore mass mixers/augers should either be suspended from a crane or mounted to a cantilever. It is normal practice to initially stabilise a 2m wide x 5m long x 3m deep block of soil positioned onsite within the crane's operational range (Topolnicki, 2004). One major disadvantage with shallow mixing is high emissions. To reduce such emissions, mixing tools may be fitted with a hood/bottom-opened cylinder, temporary low-pressure blowers, vacuum pumps, dust collectors, fume incinerators and activated carbon scrubbers (Topolnicki, 2004).

2.3.2 Deep soil mixing

Deep soil mixing (DSM) is used for various geotechnical applications on and off shore, ranging from environmental remediation to ground improvement for construction purposes including foundations, excavation wall support, liquefaction mitigation, slope stabilisation and embankment hydraulic cut-off walls. DSM involves the mechanical disturbance of a soil via auger mixing to depths of 25m (Quasthoff, 2012). Once the auger has been drilled to the required depth, its rotation direction is reversed and retrieved whilst a binder is pumped through the auger drill bit. The auger's rate of rotation and binder flow must remain constant during mixing to ensure homogeneous stabilised soil columns are produced. Various auger drill bits are available, whereby the drill bit used depends upon the DSM column diameter required and the soil being

stabilised. All drill bit's fins are orientated to ensure compaction occurs along the column's length upon auger retraction.

DSM has numerous advantages over other deep ground improvement techniques; including its applicability within a wide variety of soils and its minimal environmental impact due to low levels of vibration, noise and spoil. DSM has high levels of productivity, making it economical for larger projects (Topolnicki, 2004). The desired engineering properties of DSM soils are easily adjustable, as are the column spacings and their installation pattern (Figure 2.7).

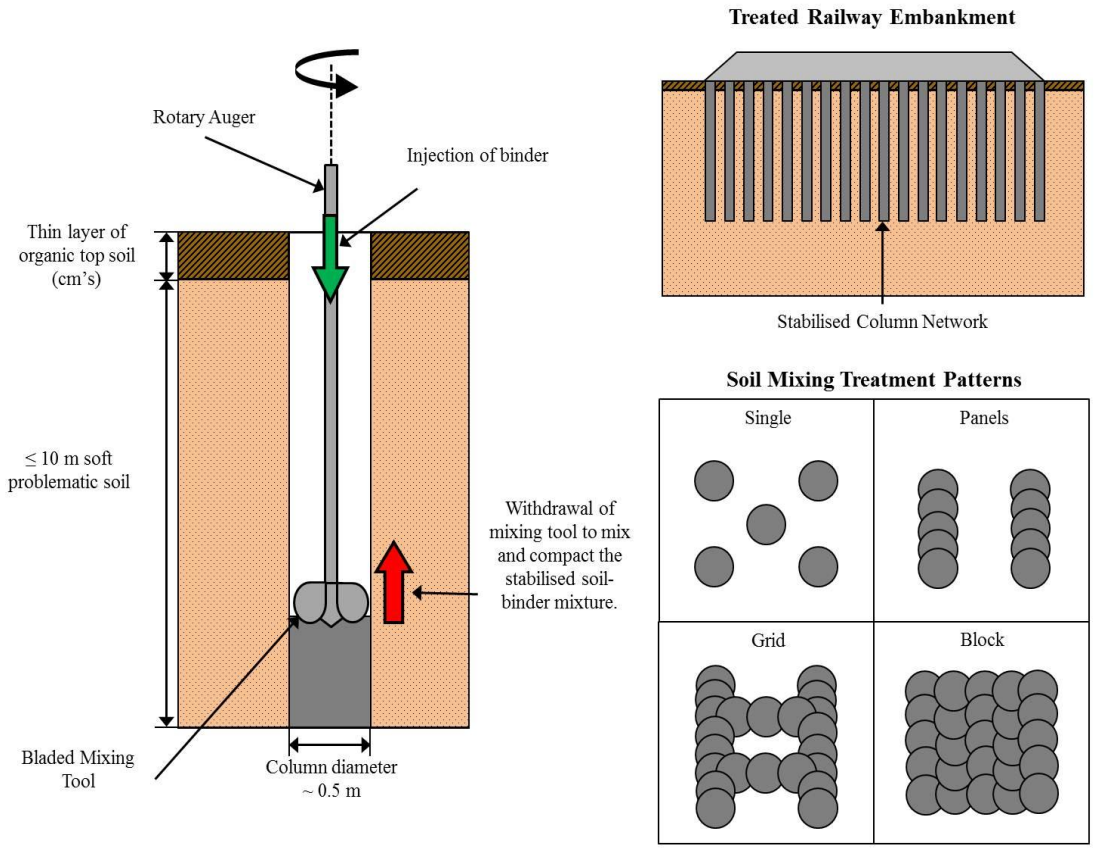

Figure 2.7: Illustration of the DSM technique and its application in ground improvement.

For chemical treatment, there are dry and wet mixing methods. Deep dry soil mixing (DDSM) involves injecting a dry binder under compressed air into the surrounding soil via nozzles at the tips of the auger mixing tool's blades (Figure 2.7). A similar process is involved for deep wet soil mixing (DWSM). The binder slurry is supplied from a delivery pump; but more expensive plant equipment is required; namely a

water tank, a temporary storage tank and large silos (Topolnicki, 2004). When selecting DDSM or DWSM, the soil's moisture content must be considered. Cohesive soils with moisture contents of 60–200% are most suited for dry mixing (Topolnicki, 2004).

For soils with moisture contents <20% and/or lower than the soil's plastic limit, the volume of water within the soil is insufficient for hydration. For DSM projects where high strength columns are essential, DWSM should be used as it provides higher levels of homogeneity due to longer mixing times. DDSM tends to be used when using either a combination of cement and lime or IBP's as binders.

DDSM is preferred over DWSM in regions where long periods of cold temperatures, freeze and thaw cycles are experienced (e.g. Scandinavia) as water based delivery systems are prone to freezing (Topolnicki, 2004; Quasthoff, 2012). Additionally, DWSM is generally more expensive as it requires more expensive pieces of plant equipment and storage for producing, storing and delivering the binder slurry into the soil (Topolnicki, 2004). When installing DSM columns through harder stratified soils, DWSM should be used as the slurry acts as a lubricant which aids/ensures higher torque capacity and consistent strengths along the length of the columns (Topolnicki, 2004).

Since pioneered in Scandinavia and Japan during the 1960's, the DSM technique has become increasingly popular. Countries including Belgium, Germany, China and USA commonly use it (Topolnicki, 2004); whereas the UK only began using it in the 1990's (Al-Tabbaa, 2003). For DDSM and DWSM, lime and cement have predominantly been used as binders since the 1970's, based on their high strength performances. Where DSM is used for environmental remediation, cementitious binders are substituted with chemical oxidation agents and reactive materials (Topolnicki, 2004).

Figure 2.8: Dense network of solidified DSM columns (courtesy of Treviicos, 2013).

DSM soil strength depends on numerous factors, including the blade rotation number, the mixing energy used, the binder dosage and soil type (Topolnicki and Pandrea, 2012). Table 2.1 summarises the expected engineering properties of DSM soils after 28 days.

Table 2.1: Summary of typical UCS and permeability values expected after 28 days curing for various soil types and binder dosages. Data courtesy of Geo-Con, Inc. (1998) and FHWA (2001).

Soil Type	**Binder Dosage (kg/m^3)**	**Expected Permeability, k (ms^{-1})**	**Expected UCS (MPa)**
Sludge	250–400	$1x10^{-8}$	0.1–0.4
Peat/Organic silts and clays	150–350	$5x10^{-9}$	0.2–1.2
Soft clays	150–300	$5x10^{-9}$	0.5–1.7
Medium – hard clays	120–300	$5x10^{-9}$	0.7–2.5
Silts and silty sands	120–300	$1x10^{-8}$	1.0–3.0
Fine – medium sands	120–300	$5x10^{-8}$	1.5–5.0
Coarse sands and gravels	120–250	$1x10^{-7}$	3.0–7.0

2.4 Soil suitability for chemical treatment

The characteristics of both the stabilisation reactions and the end-products are controlled by factors associated with the soil's nature; namely mineralogy, soil grading, CEC, surface area and moisture content. As these properties vary greatly between soils, chemical stabilisation may not be suitable for treating all soils.

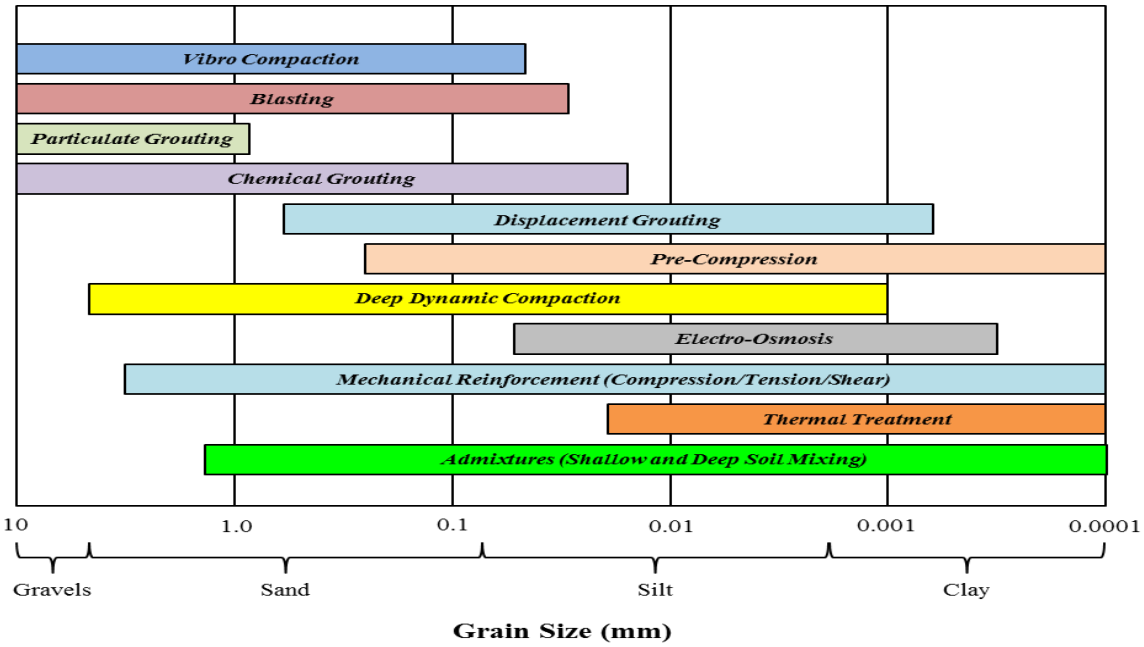

Figure 2.9: Graph showing the influence of a soil's particle size distribution on the applicability of various ground improvement techniques. After Mitchell (1972).

From Figure 2.9, chemical treatment may be used for soils comprising fine clays to medium/coarse sands. Soils deemed suitable for soil mixing include most silts, clays, peats and some non-cohesive granular soils; but require a moisture content of ≥20% for DSM to be effective (Quasthoff, 2012). Generally, cohesive fine grained soils achieve better engineering performances after chemical treatment compared with non-cohesive coarse grained soils

To understand a soil's capacity to react with binders and ultimately produce cementitious gels, researchers have determined it is necessary to conduct specific surface area and CEC analyses. Other factors including the organic and sulphate

contents of soils also have a role in assessing whether a soil is suitable for chemical treatment.

2.4.1 Surface area and cation exchange capacity

Quantifying a soil's specific surface area provides insights into its CEC and particle size distribution. Clay particles have high surface areas. Therefore soils with high surface area values indicate high clay contents. This implies the soil's CEC is likely to be high; suggesting it would be well suited to chemical stabilisation. A common technique for determining the specific surface area of soils is the Brunauer Emmet Teller (BET) method, involving nitrogen gas adsorption on particle surfaces (Brunauer et al., 1938).

CEC provides an estimate of the net negative charge on soil particulate matter through isomorphous substitution and broken bonds at boundaries (Terzaghi et al., 1996); i.e. the number of sites within a soil which can attract, retain and exchange cations. Large proportions of most soils comprise clay minerals and organic matter; both are characterised by negative surface charges, implying they must attract cation elements of the opposite charge. Cations which neutralise negative surface charges within water can be exchanged with other cations; depending upon the cation concentrations within the soil water and their electrovalences (Terzaghi et al., 1996).

Out of kaolinite, illite and montmorillonite, montmorillonite has the highest CEC (Table 2.2), as its structure comprises multiple single unit sheets (Terzaghi et al., 1996).

Table 2.2: Summary of CEC values of the three principal clay minerals (values courtesy of Terzaghi et al., 1996). Reproduced with permission from John Wiley & Sons, Inc.

Clay Mineral	**CEC (meq/g)**
Kaolinite	0.03–0.1
Illite	0.2–0.3
Montmorillonite	0.8–1.2

Soils containing clay minerals with high CEC values experience more significant mechanical changes upon mixing compared with those containing clay minerals with low CEC values (Rogers and Glendinning, 1996). Low CEC values are representative of soils characterised by low organic matter contents and low clay/high sand contents (Figure 2.10); as expected from river alluvium deposits (Cooper, 2009). A soil's surface area can influence its physical and chemical characteristics. Larger surface areas provide more cation exchange surfaces.

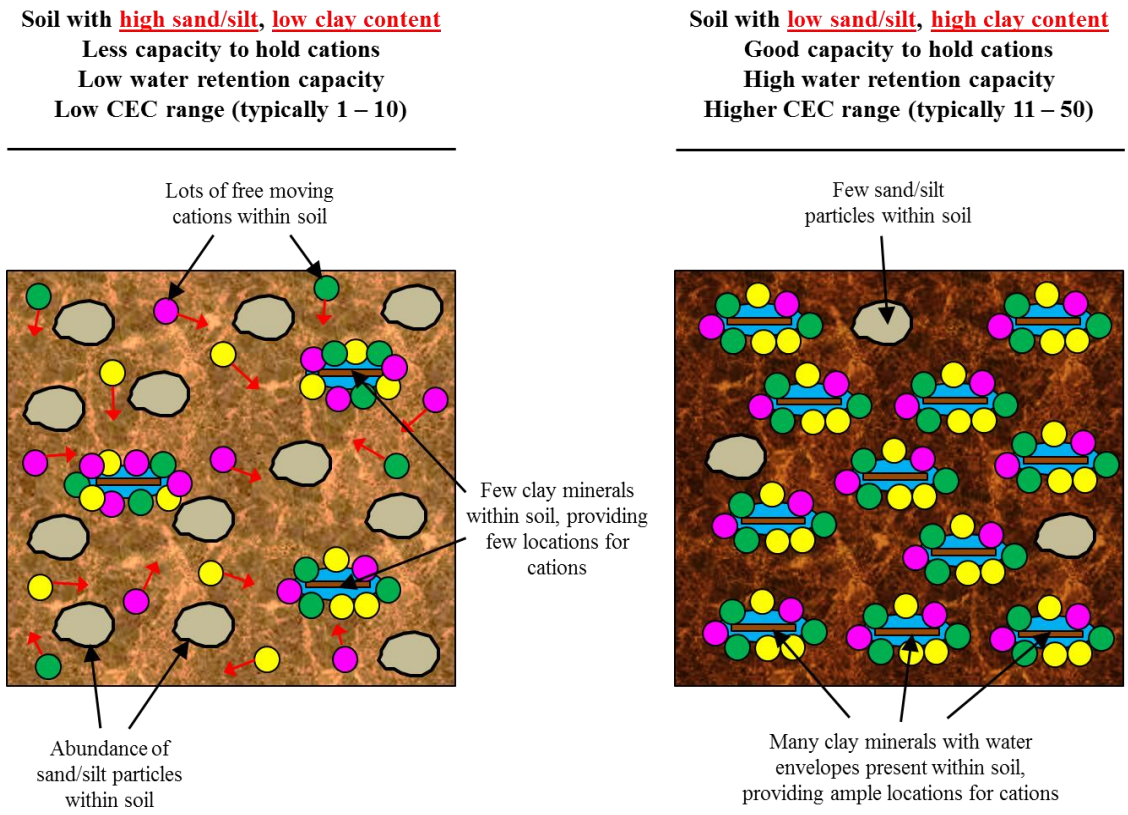

Figure 2.10: Schematic showing cation exchange capacity variability between soils that are predominantly composed of sand/silt and those of mainly clay particles.

Knowledge about a soil's CEC and surface area properties provides insights into its potential cementitious gel formation. By using CEC values obtained from laboratory testing and Equation 2.5 (Meunier, 2005), the CEC-related charge density (σ_{CEC}) may be calculated:

$$\sigma_{CEC} = \frac{e\ (CEC\ x\ 10^{-2})}{2\ ab} \qquad \textbf{(Equation 2.5)}$$

(e = the elementary charge, which has a constant value of 1.6022 x 10^{-2} C. a and b are unit cell parameters for the clay mineral in the x-y plane. For kaolinite a = 0.531 nm and b = 0.92 nm. Values taken from Meunier, 2005.)

Per Table 2.3, low surface area, organic matter and CEC values can be expected of sandy and silty soils such as loam and alluvium (Ersahin et al., 2006).

Table 2.3: Summary of surface area, organic matter and CEC characteristics typically expected for various soils. (Adapted from Ersahin et al., 2006). Reproduced with permission from Elsevier.

Soil No.	**Particle Size Distribution (%)**			**Texture Class**	**Specific Surface Area (m^2/g)**	**Organic Matter (%)**	**CEC (cmol/kg)**
	Clay	**Silt**	**Sand**				
1	61.2	11.4	27.3	C	234.1	2.0	37.4
2	35.7	11.3	53.0	SiCL	122.6	1.8	22.8
3	14.0	27.5	58.5	SiL	68.4	1.3	14.6
4	35.0	26.0	39.0	CL	133.7	2.4	26.1
5	7.7	58.3	34.0	SL	43.0	0.65	11.0
6	49.0	25.0	26.0	SCL	146.0	2.4	19.3
7	18.0	33.0	49.0	L	53.4	1.2	14.8

(C = Clay, SiCL = Silty Clay Loam, SiL = Silty Loam, CL = Clay Loam, SL = Sandy Loam, SCL = Sandy Clay Loam and L = Loam. The texture classification scheme used by Ersahin et al. (2006) was that of the USDA.)

2.4.2 Other factors

Although CEC and surface area have a considerable role in dictating a soil's suitability for chemical treatment, other relevant parameters include particle size distribution, organic and sulphate contents.

Chemically treated soils containing high fines contents produce the most impressive strengths (Puppala et al., 2008). This is related to surface area characteristics. Soils with higher surface areas are characterised by relatively high CEC values, which are ideal for cementitious bonding and strength developments.

Chemical treatment has long been applicable for soft clayey soils with high degrees of total organic matter (TOM). However, the level of improvement gained for soils with high TOM values will be lower compared with that achieved by soils with low TOM values. Delle Site (2000) provides a conversion factor of 1.724 to convert total organic carbon (TOC) values to TOM.

Organics interfere with the chemical reactions occurring between the soil and binder. Soils with higher organic matter decomposition (OMD) produce higher strengths upon stabilisation. Prior to stabilisation, a soil's TOM value affects its Atterberg limits and pH (Puppala et al., 2008). Oven and air drying such soils increases acidity and reduces plasticity. Once treated with lime-cement, Puppala et al. (2008) documented poor strength developments, which were attributed to the soil becoming more plastic rather than more acidic. A large fraction of a soil's organic content comprises humified material, which has adverse effects on strength development (Puppala et al., 2008). The presence of lime in organic soils inhibits strength development, as it increases organic solubility; resulting in higher degrees of homogenisation in terms of organic distribution within the soil (Puppala et al., 2008). Hence for organic soils, CEM-I is preferred over lime or lime-cement.

The final aspect of a soil's chemistry to consider is sulphate content. Soils with sulphate contents >3000 ppm are problematic and ettringite formation is likely. For such soils, Nair and Little (2009) recommend that whilst it is impossible to fully solubilise all sulphates, water should be used to thoroughly mix the soil to ensure sulphates and all possible ettringite formation sites are homogeneously distributed.

Sulphates occur as gypsum but are distributed unevenly through the soil column, most commonly occurring within seams or as lenses. Climate impacts on ion movement within soils. In dry arid climates where evaporation is common, sulphates are located within the shallow surface. For wet humid climates, sulphates are found at greater depths due to water infiltration. However, capillary action can cause water and sulphate sources to rise towards the surface (Nair and Little, 2009). Local terrain,

geological and hydrological conditions also influence sulphate distribution. In regions characterised by hilly topography, (gravitational) surface and sub-surface water flow are common, resulting in soils with high moisture and sulphate contents, plus high potential for ettringite formation and surface heave on valley floors.

Clay-rich soils have higher moisture-retention capabilities, higher sulphate and salinity contents compared with most other soils (Nair and Little, 2009). These characteristics are key for ettringite and thaumasite production, which are hydrous calcium aluminate sulphate (Aft) minerals per Figure 2.11 (Wilkinson et al., 2010). These cause volumetric expansion within soils stabilised with calcium-based binders (Nair and Little, 2009). In contrast to soils containing high organic contents, the presence of lime does not inhibit strength development as it decreases organic solubility and does not interfere with chemical reactions between the soil and lime (Puppala et al., 2008).

The high surface areas of ettringite and thaumasite provide high reactivity rates, allowing reactants to become available as soluble ions (Nair and Little, 2009). Hence, ettringite formation in CEM-I concrete is rapid and relies on the matrix sulphate content, whereas for stabilised soils, ion availability in solution depends on the soil's mineralogy, degree of initial flocculation and dissolution properties (Nair and Little, 2009).

In chemical stabilisation, there are two phases of ettringite formation (Nair and Little, 2009); the first occurs during initial hydration and does not present any damaging effects. The second occurs later in the curing process when the soil's cemented matrix has been established, possibly leading to deterioration. The environmental and weathering conditions soil particles are subjected to create higher levels of heterogeneity compared with CEM-I, meaning that fewer ions are available in solution to produce ettringite in stabilised soils compared with cement pastes (Nair and Little, 2009). Thus, ettringite forms less rapidly in stabilised soils compared with in cement.

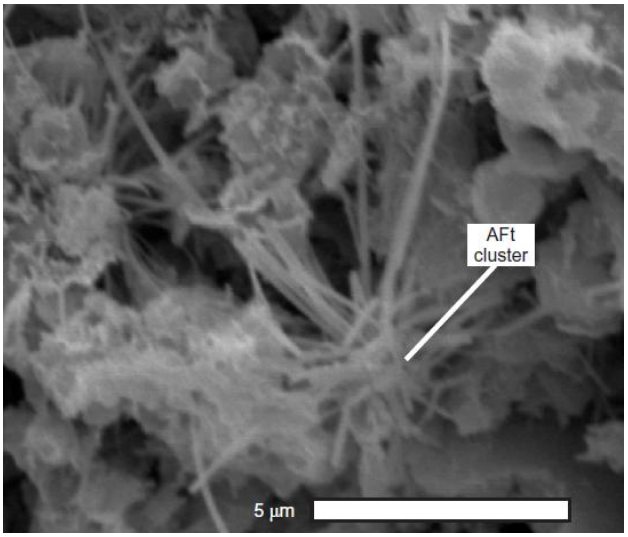

Figure 2.11: Ettringite (AFt) formation within PFA-stabilised Ginifer soil after 28 days. Courtesy of Wilkinson et al. (2010a). Reproduced with permission from the Institution of Civil Engineers.

No single binder is suited for stabilising all problematic soil types, given the natural complexity of soils. Binders commonly comprise 2 – 3 materials, as the chemistry of a single material may not be as efficient in creating the ideal conditions for cementitious bond formation as 2 – 3 materials. A soil's chemistry and basic geotechnical classification dictate the optimum binder design for its stabilisation. Studying EuroSoilStab (2002) is strongly advised prior to treatment to assist in selecting the most appropriate binder mix for stabilising problematic soils.

2.5 Traditional binder materials

Since the 1960's, various binders have been widely used; depending on the soil type to be stabilised. The ideal binder should bond soil particles together and waterproof the material. However, not all binders are able to do both within all soils. The performance of binders whose primary aim is to bond soil particles depends upon the strength of the stabilised soil's matrix, whether bonds form between soil particles and the matrix and whether individual or agglomerations of soil particles are bonded with each other (Sherwood, 1993). Binders will not completely waterproof a soil, however they will ensure less water absorption. Their purpose is to ensure the soil's moisture

content is kept to a minimum. The performance of such binders is measured by the reduction in the soil's permeability (Sherwood, 1993).

The presence of soil water and calcium silicates/aluminates within binders reacts to form C-S-H and C-A-H gels via long-term pozzolanic reactions when soil pH levels are ≥10.5 (Davidson et al., 1965). The mixtures then cure and produce stronger, cementitious soil matrices known as "Geopolymers" (Sherwood, 1993). Cement and lime have long been utilised as binders. The former is more favourable in providing rapid strength enhancements (Rogers et al., 2000; Hossain, 2010; Jegandan et al., 2010). Portland cement primarily comprises tri- and di-calcium silicates. Other constituents can be added to produce advanced cement blends that are more suitable than type-I cement (CEM-I) for specific engineering purposes. CEM-I is most commonly used in soil stabilisation, due to its availability and low cost over other cements (Bergado et al., 1996).

Table 2.4: Summary of the type I and related Portland cements used in the UK. Taken from Bye (2011).

Portland cement type	**Characteristics**	**Corresponding British Standard & Eurocode**	**Corresponding ASTM classification**
Ordinary	Specific surface: 330-380 m^2/kg strength (class 42.5 N SO_3; ≤ 3.5%	BS 12: 1996 (SS) BS EN 197-1:2000 (C)	I
Rapid Hardening	Specific surface: 400-450 m^2/kg strength (class 42.5 R or 52.5 N)	BS 12: 1996 (SS) BS EN 197-1:2000 (C)	III
White	Fe_2O_3 < 0.3%	BS 12: 1996 (SS) BS EN 197-1:2000 (C)	-
Controlled Fineness	Specific surface requested by customer	BS 12: 1996 (SS) BS EN 197-1:2000 (C)	-
Low Heat	Heat hydration < 250 Joules/g at 7 days, < 290 Joules/g at 28 days	BS 1370: 1979 (C)	IV
Low Alkali	Na_2O% + 0.658 K_2O% 62/94 < 0.6%	BS 4027: 1996 (SS) BS EN 197-1:2011 (C)	-
Sulphate-resisting	C_3A ≤ 3.5%, SO_3 ≤ 2.5%	BS 4027: 1996 (SS) BS EN 197-1:2011 (C)	V
Modified	C_3A ≥ 8%	-	II

[Note: SS = superseded, C = current.]

Some problematic soils have contaminated mineralogical compositions or are rich in natural sulphates, such as salts of sodium, potassium, calcium and magnesium (Bye, 2011). In alkaline soils, Bye (2011) states that the aggressiveness of sulphate solutions flowing through the soils decreases as soil pH increases towards 12.5. When deep mixing is conducted within such soils, it is likely that the soil-cement columns will become susceptible to sulphate attack and subsequent ettringite and/or thaumasite formation. This can cause severe soil swelling and ultimately lead to the structural degradation of the stabilised soil's matrix. Per Bye (2011), it has been known that damage to concrete and cement by sulphate-rich solutions results in ettringite formation since the 19th century. Ettringite precipitates in conditions characterised by high pH and high levels of Ca^{2+}, $Al_{(aq)}$ and SO_4^{2-} activity (Nair and Little, 2009).

According to Bye (2011), it is the delayed expansive formation of ettringite and thaumasite within a pre-existing hard material (i.e. deep mixed columns) that has a limit of elasticity, which is the primary cause of these minerals' damaging effects. Although ettringite forms as tubular needle-like micron-sized crystals, the precise mechanism associated with ettringite precipitation and expansion, along with the relationship between the amount of ettringite produced and the amount of volume change within the stabilised soil-cement matrix are all still under debate (Nair and Little, 2009). A study by Nair and Little (2009) documented the presence of water as a necessity in ettringite formation and that the timing of additional water being introduced to a soil dictates the extent of soil matrix expansion. Additionally, Nair and Little (2009) found that almost all ettringite within cement stabilised soil mixtures forms within the first 72 hours of curing, and that when subject to an external influx of water (sulphate or non-sulphate rich), the soil's volume increases considerably due to ettringite formation.

To address the problems presented to concretes and cements by sulphate attack, sulphate-resistant Portland cement has been developed by the cement industry. Such sulphate-resistant cements are characterised by a low C_3A content and a lower alumina/iron oxide ratio of 0.7 for the cement's raw material. This is achieved by replacing some of the clay/shale within the kiln feed with a by-product iron oxide and a silica-rich material to ensure the calcium silicate content is sufficiently high (Bye, 2011).

Lime originates from the calcination products of chalk or limestone (see Equation 2.6 below). Calcitic lime may be utilised as either quicklime [calcium oxide, CaO] or slaked lime [$Ca(OH)_2$]. When combined with water, quicklime reacts to form slaked lime; during which large amounts of heat (17×10^9 Joules/kg of quicklime; Sherwood, 1993) are produced (see Equation 2.7 below). When combining slaked lime with water, such an exothermic reaction is not observed given the lower calcium to weight ratio of the slaked lime compared with quicklime, and the hydrated lime converts to calcium carbonate upon exposure to air (see Equation 2.8) (Sherwood, 1993).

$$CaCO_3 + Heat \rightarrow CaO + CO_2 \qquad \textbf{(Equation 2.6)}$$

$$CaO + H_2O \rightarrow Ca(OH)_2 + Heat \qquad \textbf{(Equation 2.7)}$$

$$Ca(OH)_2 + CO_2 \rightarrow CaCO_3 + H_2O \qquad \textbf{(Equation 2.8)}$$

Of the products from these three reactions, Sherwood (1993) states that only CaO and $Ca(OH)_2$ will react with a soil. Calcium carbonate may be used in agriculture but not for civil engineering purposes. Magnesium rich dolomitic limes may also be used as a binder due to their reactive silicate and aluminate contents as similarly found in CEM-I. Albeit their immediate strength-gains may be less than calcium-rich limes, dolomitic limes may potentially produce higher strengths in the long term (Sherwood, 1993). For use in soil mixing, hydrated lime is generally available as a fine grained dry powder; whereas quicklime is available either as a fine grained powder or alternatively as coarse grained granules.

Per Christopher et al. (2006), lime treatment involves adding up to 3% lime to dry it and allow compaction to take place. Lime may also be used to modify expansive soils characterised by high swelling potential due to the high water content absorbed by the clay minerals. Additionally, lime treatment may also be used to prepare problematic soils for subsequent cement stabilisation (Christopher et al., 2006).

Quicklime has several advantages over hydrated lime, whereby it is more economical as it contains up to 25% more available lime, has a faster drying rate within highly

saturated soils and has faster rates of reaction (Sherwood, 1993). However, quicklime requires higher quantities of water than hydrated lime for stabilising soils, which Sherwood (1993) points out as being problematic on dry sites. There are also environmental and health risks associated with quicklime, including the amount of dust produced, which makes it unsuitable for use in highly populated areas (Sherwood, 1993). Whereas the dust emissions associated with using hydrated lime are comparable with those of cement. There is also the risk of skin and/or eye burns to site workers as lime is an irritant; so site workers should wear the necessary safety equipment.

Both lime and cement are available as fine grained powders, making them ideal for dry soil mixing. However, they may also be combined with water to produce slurries (Sherwood, 1993). This eliminates dust emissions and produces more homogeneous soil-binder mixtures, although using slurries is less applicable in highly saturated soils compared with dry powders.

2.6 Applications of chemical (admixture) soil stabilisation

Chemical admixture soil stabilisation has several applications in geotechnical ground improvement, given its versatility. A primary aim of chemical (admixture) soil stabilisation is to produce stiffer, more stable ground conditions. Stiffer soils produce higher bearing capacities, increased stability of natural slopes, railway embankments (e.g. the Channel Tunnel Rail Link), levees (e.g. stabilisation of levees in Louisiana after Hurricane Katrina, 2005); and reduce the active loads acting on retaining walls. Chemical treatment also acts to enhance a soft soil's deformational properties when subjected to static loads; specifically in terms of reducing surface settlements, horizontal displacements and the time taken for such ground deformations to occur (EuroSoilStab, 2002).

Besides improving the mechanical properties of soft soils subject to static loading, chemical treatment may also improve their dynamic stiffness's. Common examples of dynamic loads experienced by soils on a day-to-day basis include passing railway traffic on railway embankments and specifically in tectonically active regions,

earthquake phenomena. Regarding chemical soil stabilisation around railway embankments, the treatment also acts to decrease the magnitude of train-induced vibrations felt in the immediate surroundings (EuroSoilStab, 2002; Liu et al., 2010).

In tectonically active regions, earthquakes can cause liquefaction phenomena within soft soils characterised by low levels of cohesion such as sandy fluvial/alluvial soils. Such soils have usually been deposited in a loose state through monotonic, transient or repeated disturbance (Kramer, 1996). Liquefaction only tends to occur within poorly graded saturated soils containing a large proportion of rounded grains, which are more likely to densify over angular grains (Kramer, 1996). During loading, excess pore water pressures develop via the densification of the soil; thereby severely degrading the soil's effective strength and causing it to behave as a fluid. Work on using DSM to remediate liquefaction-prone soils has been active in numerous seismically active regions such as Japan (Figure 2.12 below), USA and more recently the Caribbean.

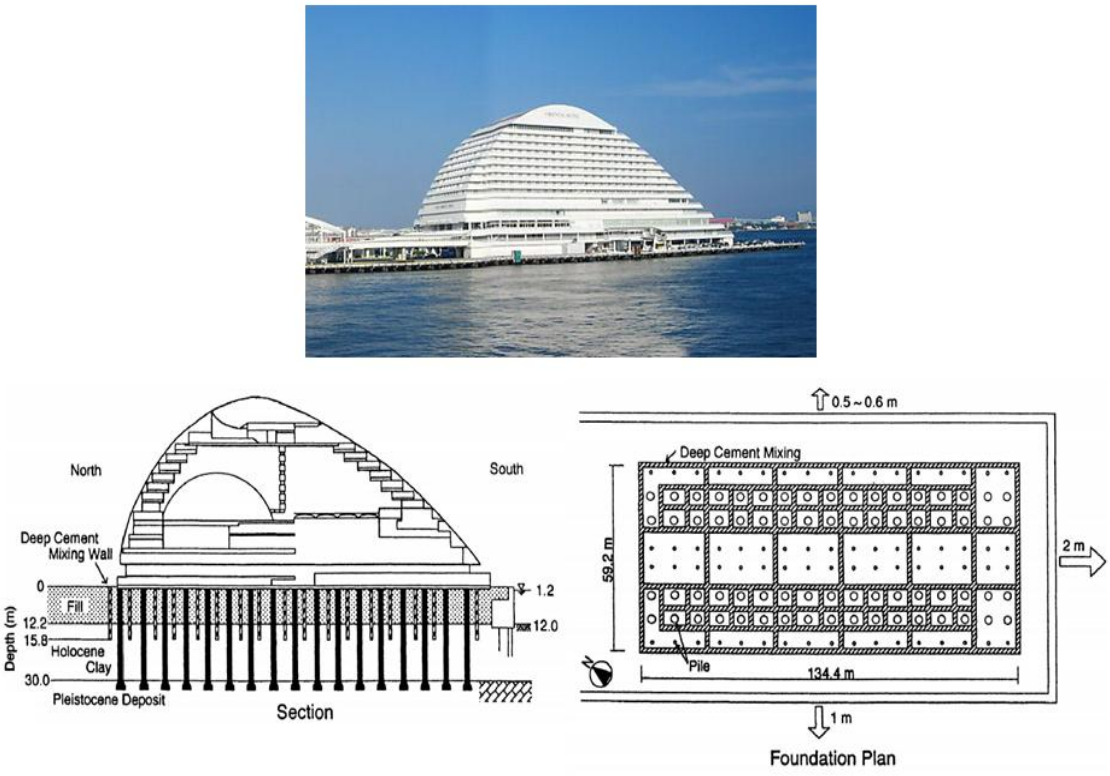

Figure 2.12: Photographs and schematics of the Kobe Oriental Hotel's effective pile and deep mixed caisson foundation design in preventing liquefaction during the 1995 earthquake. Adapted from Porbaha et al. (1999).

The final main application of chemical (admixture) stabilisation is in environmental remediation; particularly in treating contaminated land. On sites formerly or currently occupied by the likes of chemical plants, oil refineries, fuel and power stations; it is likely that there have been spillages of contaminants, including heavy metals, inorganics and petroleum hydrocarbons. If such contaminants infiltrate shallow sub-surface soils, they will pollute local ground water and consequently have long-term adverse effects on local ecosystems. In such instances chemical soil stabilisation aims to create a relatively high strength, impervious geohydrological barrier/cut-off wall surrounding the contaminated site (Figure 2.13), ensuring that any contaminants are contained and do not pollute the immediate surroundings via local ground water flow regimes.

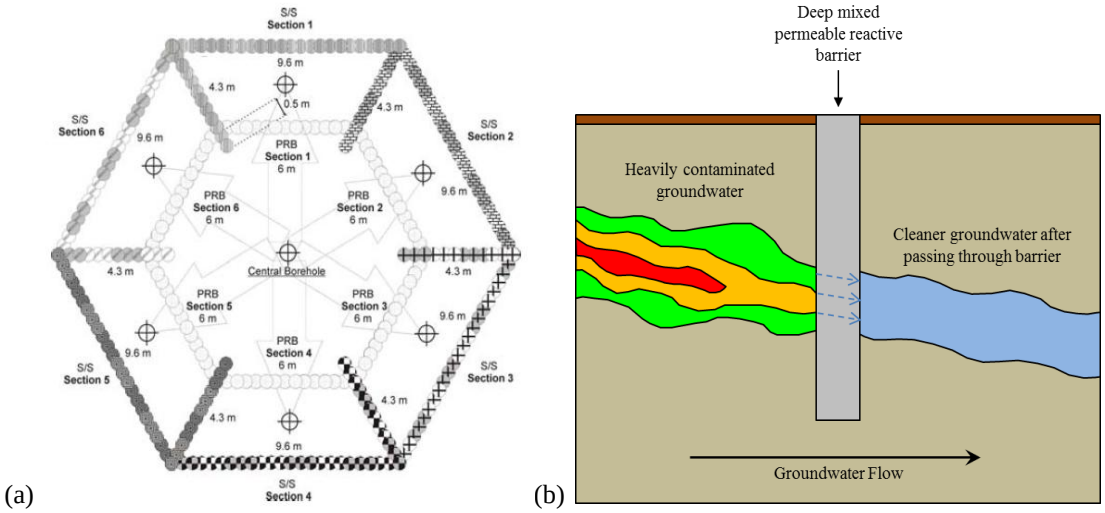

Figure 2.13: (a) Hexagonal permeable reactive barrier system installed by Al-Tabbaa et al. (2012) (courtesy of Al-Tabbaa et al., 2012). (b) Diagram illustrating the concept of the permeable reactive barrier in treating local contaminated groundwater.

Much research has been conducted in the UK since the 1990's in the development of chemical soil stabilisation as a remediation technique for treating contaminated sites. Most studies have been collaborative between academic institutions, namely Al-Tabbaa from Cambridge University, UK; and numerous industrial partners including May Gurney and Bachy Soletanche (Al-Tabbaa, 2003).

2.7 Alkali activated waste products as environmentally sustainable alternatives

Negative environmental issues are associated with CEM-I and lime in soil stabilisation. Their production requires large amounts of energy. Dust and sulphur dioxide (SO_2) aerosol emissions from manufacturing plants can pose serious health risks including long-term respiratory diseases. SO_2 is also a primary contributor to trans-boundary pollution via acid rain. CEM-I, lime and steel manufacture also produces high CO_2 emissions; whereby cement alone accounts for 5–7% of global CO_2 emissions (Bye, 2011; McLellan et al., 2011). Heavy elements including lead are present within the raw materials and fuels involved in cement manufacture (Bye, 2011), which can be toxic at high concentrations. Environmental pollution has been regulated in the UK since 1805 by the UK Alkali Act and by the Integrated Pollution Prevention and Control directive (IPCC) in the EU (Bye, 2011).

It has become a priority for the cement/lime manufacture and construction industries to develop new cementitious binders that are more environmentally sustainable in terms of energy consumption and greenhouse gas emissions associated with their production. Given the high greenhouse gas concentrations currently within the atmosphere, there is now real pressure on the civil engineering/geoscience academic and industrial communities to develop new techniques and processes in sequestering significant quantities of atmospheric carbon and storing it safely over geological timescales.

Soils are considered vital tools for controlling rising atmospheric CO_2 concentrations. The 1997 Kyoto Protocol identified soils as a major carbon storage facility (Washbourne et al., 2012). Hence, cement industries involved in designing and manufacturing new cementitious binders for soil stabilisation should also consider a binder's carbon sequestration potential. New binders should also provide engineering performances that compare with or surpass those of CEM-I and lime within similar curing times. A popular route for selecting new materials has been the development of geopolymers, which are synthetic alkali alumino-silicates produced when combining a solid alumina-silicate with a highly concentrated aqueous alkali hydroxide or silicate solution (Duxson et al., 2007). Geopolymers commonly use alumino-silicate based (i.e.

pozzolanic) industrial by-products (IBP's) (Bye, 2011), which are able to produce high compressive strengths, low shrinkage levels, acid and fire resistance and low thermal conductivity (Duxson et al., 2007; Weil et al., 2009). Also, IBP geopolymers production costs are up to 30% lower than that for CEM-I (Duxson et al., 2009). McLellan et al. (2011) conducted a sustainability comparison study between CEM-I and Australian geopolymers, revealing that geopolymers are capable of reducing greenhouse gas emissions by 44–64%.

Tanaka and Stigson (2009) plus Duxson et al. (2007) point out that the performance of geopolymers is directly influenced by the incorporation of alumina, the composition of source materials, the concentration of the soluble silicates and the sodium hydroxide and potassium hydroxide activators. Regarding source material, GGBS and PFA may contain impurities including calcium and iron, thereby adding further reaction pathways during geopolymerisation and inherently changing the material's final properties through alterations in setting time, strength and shrinkage (Duxson et al., 2007). However, the literature now indicates that even with the presence of such impurities, the network forming cations are still silicon and aluminium; thereby suggesting impurity cations' importance in changing geopolymerisation products. According to Duxson et al. (2007), although calcium is considered an impurity within materials such as PFA, it is known to react with silicon and aluminium when combined with water to produce C-S-H and C-A-H phases. Ultimately, the quantity and form of calcium present within the raw materials have major roles in determining reaction pathways and the physical properties of the geopolymer (Duxson et al., 2007). When using the most ideal formulations of raw materials and processing conditions, geopolymers can produce high compressive strengths, low levels of shrinkage, acid and fire resistance, plus low thermal conductivity (Duxson et al., 2007).

Adding any calcium-based binders to sulphate-bearing soils may result in the formation of ettringite and/or thaumasite minerals, plus subsequent volumetric changes within the soil. This forms another basis for finding alternative binder materials, which are still able to achieve high strengths but less likely to cause problems such as heave. One favourable option is using binders containing an abundance of readily soluble silica; such as pulverised fly ash and ground granulated blast furnace slag. Nair and Little (2009) stated the presence of such high quantities of readily soluble silica tends to result in the formation of C-S-H minerals rather than

ettringite. However, for such binders to be effective in producing strength gains through pozzolanic reactions, alkali activation is required. Although it is necessary for soil pH to be ≥10.5 for pozzolanic reactions to occur, Nair and Little (2009) state that ettringite starts precipitating in soils with pH values of ≥10.7. Hence, increasing soil pH through alkali activation leads to favourable conditions for ettringite and thaumasite formation and thus creates the chance of deterioration within the stabilised soil's matrix.

Popularly used IBP's for geopolymers include ground granulated blast furnace slag (GGBS), steel slag (SS) and pulverised fly ash (PFA). PFA is a synthetic pozzolanic material produced from combustion processes within coal-fired power stations. Type C PFA is preferred over type F PFA (ASTM C618-12a, 2012) due to its higher lime content and therefore better reactivity and cementitious properties (McCarthy et al., 1984). SS is a by-product of steel manufacture comprising a mixture of silicates and oxides that forms upon the separation of molten steel from impurities within the furnace, which ultimately cools and solidifies (FHWA, 2012). GGBS is a latent hydraulic cement produced during pig iron manufacture, whose chemical composition partly resembles that of CEM-I cement. The slag is required to be in a granulated form in order for it to be reactive (EuroSoilStab, 2002). Red gypsum (RG) is a by-product of Titanium Dioxide manufacture (an extensively used white pigment), which occurs in a filter cake form during sulphuric acid neutralisation. This is produced in the UK by Huntsman Tioxide Europe Ltd. and has recently been developed as a binder (Hughes et al., 2011; Gazquez et al., 2013).

From these materials, GGBS and type C PFA tend to be the preferred binders due to the high strengths which they typically achieve. Regarding SS, type F PFA and RG, these tend to be used in combination with other cementitious wastes (GGBS) to produce higher strengths, due to factors including low Tricalcium silicate content (Shi et al., 2006). Ashes produced from burning certain organic materials including rice husk and wood may also be used as binders, due to their high levels of pozzolanicity and reactivity; and their high CaO and silica contents (Abu Bakar et al., 2011; Zain et al., 2011; Supancic and Obernberger, 2012).

Certain IBP's require alkali activation to initiate pozzolanic reactions, cementitious bond formation and to increase the rate at which mechanical properties are improved by increasing soil pH (Palomo et al., 1999). Such materials may be sourced naturally

or synthetically; although the latter incurs high costs and negative environmental impacts. Alkali silicates (sodium silicate) are the most useful activators. Lime and metakaolin are less popular due to environmental impacts, poor early strength development, long setting times (Moranville-Regourd, 1998; Shi et al., 2006) plus metakaolin requires large volumes of water, which increases a soil's porosity and decreases its stiffness (Duxson et al., 2007).

Research by Renforth et al. (2009), Washbourne et al. (2012) and Sanna et al. (2012) have focussed on the potential in using inorganic industrial mineral waste materials within soils for atmospheric carbon sequestration and storage by mineralisation. Calcium and magnesium bearing waste silica materials including SS and GGBS, along with calcium and magnesium bearing minerals within basaltic igneous rocks (dolerite) have already demonstrated impressive potential when incorporated within urban soils in sequestering atmospheric carbon. These have theoretical CO_2 uptakes of 29–52 and 20–44 wt.%, respectively (Sanna et al., 2012). A study recently conducted by Washbourne et al. (2012) on the "Science Central" site in Newcastle upon Tyne demonstrated that the top metre of soil for the 10 hectare site has the potential to capture and store 64,000 Mg of atmospheric CO_2 in the form of carbonate minerals, half of which was captured within 3 years at an annual rate of 325 Mg C ha^{-1}. These CCS potential figures for demolition rubble-bearing urban soils appear to be very high, to the extent that they seem unbelievable. However, similar figures were also calculated for similarly mixed quarry soils (Barrasford, UK); namely 300 Mg C ha^{-1}, whereby this was observed down to depths of three metres over a period of ten years (Manning et al., 2013). Such differences in sequestration rates were attributed to differing soil mineralogies; whereby urban soils at Science Central contained cementitious rubble material (calcium silicates and calcium hydroxide) which produce greater rates of carbonation compared with Barrasford quarry soil (Manning et al., 2013). Globally, construction and development site soils are considered able to capture and store 290 million tonnes of atmospheric carbon within soil matrices per year (Renforth et al., 2009).

It should be considered that CEM-I, lime and steel production entail such high CO_2 emissions that they overcome the current sequestration potential of their resulting waste products. Per Manning et al. (2013), artificial minerals derived from CEM-I such as calcium silicates and calcium hydroxide possess a high embedded carbon

value corresponding to the loss of CO_2 caused during calcining and fuel combustion during CEM-I manufacture. Therefore, it is the author's opinion that whilst the use of high Ca-bearing IBP's as binders within geopolymers and carbon capture gardens certainly make a valuable contribution towards sequestering atmospheric CO_2, they cannot be solely relied upon as solutions to fully sequester the large quantities of CO_2 originally emitted from CEM-I, lime and steel production. CCS by reaction of such artificial minerals are deemed to be only capable of compensating for CO_2 lost during calcining (Manning et al., 2013). This implies that further more effective, larger scale sequestration technologies require development to solve the current high atmospheric CO_2 levels problem.

2.8 Traditional versus alkali activated waste binders

Cement manufacture is documented as having several associated environmental and financial issues. Processes involved in cement manufacture consume much energy through electricity and fuel to produce clinker, crush raw materials and clinker, vent gases through the main kiln and delivering materials from quarries to dispatch (Bye, 2011). Hence, cement manufacture also incurs considerable financial expense. Based on the nature of the raw materials, the processes and amount of energy involved in the manufacturing process; environmental pollution of local air quality, groundwater and land is a problem and has been strictly regulated since 1805 by the UK Alkali Act (Bye, 2011). Current environmental regulation in the EU has been governed by the Integrated Pollution Prevention and Control directive (IPCC), which was updated as the Industrial Emissions Directive in 2010 (Bye, 2011). Within the IPCC is a principle that European cement manufacture plants employ the best available techniques (BAT) with a view to reducing their environmental and health impacts (Bye, 2011).

2.8.1 Environmental and health impacts

2.8.1.1 Dust emissions

Dust emissions have long been considered to be a major aerosol emission from cement manufacturing production; which is a major health risk concern. Similar to volcanic ash, particulate matter is released into the air from the quarrying of limestone, which is subsequently fed into kilns within cement manufacturing plants. Any particulates with dimensions of 10µm or smaller can be inhaled, penetrate the respiratory tract, enter the lungs and potentially cause asthma or other long-term respiratory diseases (Sargent, 2009). However, dust emissions produced from the burning of limestone within cement manufacturing plants are kept to a minimum, whereby the alkaline kiln dust is trapped within chimney filters.

2.8.1.2 CO_2 emissions and global warming

As calcium carbonate-bearing raw materials such as limestone are used to produce CEM-I, the calcination of these materials and the combustion of carbon within fossil fuels to power the cement manufacturing process inherently results in high CO_2 emissions. Cement production alone contributes 5–7% of global CO_2 emissions (McLellan et al., 2011). Per figures by Bye (2011), the cement manufacturing industry is responsible for producing about 5% of global CO_2 emissions. Increases in atmospheric greenhouse gases such as CO_2 have been known to have adverse effects on the global climate for over 50 years. Consequences of such increases in atmospheric CO_2 may be severe in the long term. It is anticipated that global warming will adversely affect global climates, resulting in changing weather patterns, melting of the Earth's ice caps, subsequent rising sea levels and ocean acidification. These effects will have potentially major impacts on marine and land based life. Therefore, it has become extremely important for industries such as the cement and construction industries to become more sustainable and more environmentally friendly by using

less fossil fuels and move towards using cleaner waste products or renewable energy sources.

According to Bye (2011), in 2008 the British Cement Association reported that CO_2 emissions steadily declined between 1990 and 2007 by 11.4% to 819 kg CO_2 per tonne of clinker produced. Bye (2011) stated this was mainly achieved through using alternative waste products as fuels and the addition of secondary components within cements such as GGBS and fly ash. Based on these figures, the cement industry has been taking steps to reduce its carbon footprint. However many parties feel further steps need to be taken to avoid severe climate change.

McLellan et al. (2011) recently conducted a detailed sustainability comparison study between CEM-I and geopolymer cements in terms of their costs and carbon emissions. The three main factors considered were energy (direct fuel and electricity consumption), greenhouse gas emissions and financial cost. Other factors considered included technical performance, leaching, water usage, hazardous materials content and the volume of waste produced. Several previous works were considered in this sustainability study; notably that of Weil et al. (2009) who assessed the financial cost and CO_2 emissions (kg CO_2-eq/m^3) produced for feedstock and transport. McLellan et al. (2011) conducted a detailed comparison analysis between four typical Australian geopolymers mixtures and CEM-I. The composition of the four geopolymers studied is provided in Table 2.5.

Table 2.5: Compositional summary of the four geopolymer mixtures analysed by McLellan et al. (2011). (Quantities provided as weight % with no added water).

Geopolymer component	Mix 1	Mix 2	Mix 3	Mix 4
PFA	84	91	85.2	78
NaOH	11	7.2	7.6	11
Sodium silicate	0	1.8	7.2	0
Silica fume	5	0	0	9
Gibbsite	0	0	0	2

A comparison between the four geopolymers mixtures and CEM-I for greenhouse emissions (specifically CO_2) produced during their manufacture and transport is given in Figure 2.14. The data in Figure 2.14 shows that geopolymers mixes 1-3 produce considerably lower greenhouse gas emissions overall as a material and for their transport compared with CEM-I. This is a major contributing factor in promoting geopolymers as sustainable alternatives to CEM-I.

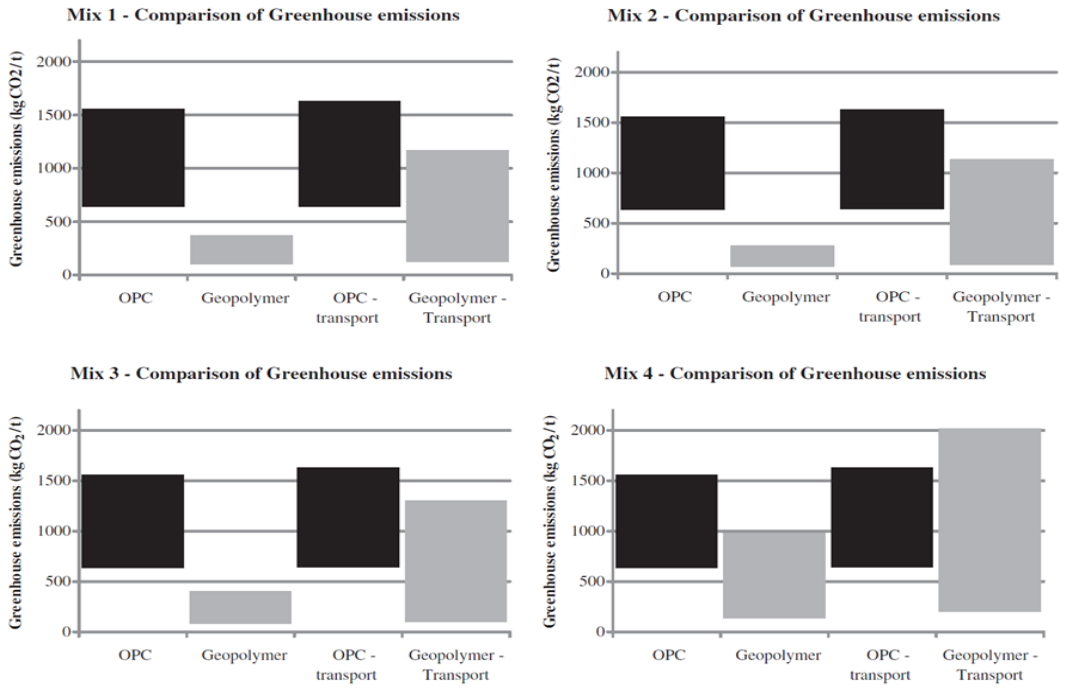

Figure 2.14: Summary of the greenhouse emissions produced during the production and transport of the four geopolymers compared with CEM-I. Taken from McLellan et al. (2011).

Per Weil et al. (2009), for a geopolymer comprising 78% gravelly soil and 22% binder (9.6% GGBS, 2.4% PFA, 3.5% reactive waste, 1.4% Na_2SiO_3, 1% NaOH and 4% deionised water), a reduction of 131 kg CO_2-eq/m^3 was observed for the combined manufacture and transport of the binder compared with that for CEM-I. Thus, McLellan et al. (2011) concluded that geopolymers have high potential for reducing the environmental impacts of cement production. Based on a proposed Australian geopolymer mix (mix 2), McLellan et al. (2011) estimated a significant greenhouse gas emission reduction of 44–64% compared with CEM-I.

2.8.1.3 Toxicity

Other environmental concerns include the presence of trace amounts of heavy metals. Bye (2011) states that heavy elements such as mercury and lead naturally occur within the raw materials and fuels (i.e. coal) fed into the kiln during cement manufacture. This inherently implies that such heavy metals are likely to be present within PFA. If such heavy metals are present at high concentrations, they are likely to be toxic and potentially have negative effects on the reactivity of the cement. This has further encouraged the drive to develop alternative materials/fuels in cement manufacture and to introduce stricter emission limits (Bye, 2011). More heavy and potentially toxic metals tend to be vaporised at higher temperatures. To reduce such emissions, kiln exhaust temperatures can be lowered or alternative fuels containing less heavy metals can be sought.

2.8.1.4 SO_2 and other gas emisions

Emissions of sulphur dioxide from the burning of raw fuel materials such as coal are also problematic. Such emissions are documented by Bye (2011) as linked with respiratory problems of workers and populations surrounding cement plants, and are also considered to be a primary contributor to trans-boundary pollution via acid rain. Consequently, acid rain can acidify water within lakes, rivers and local soils; thereby imposing an environmental hazard on local public water supplies. Other gases

documented by Bye (2011) which are created by burning raw fuels and cause acid rain along with consequent respiratory problems, are nitrogen oxides including nitric oxide and nitrogen dioxide.

2.8.2 Financial costs

The financial cost of energy consumption, transportation and market price is a significant factor in determining whether alkali activated geopolymers can become sustainable replacements for CEM-I/lime. If geopolymers are to become serious competitors, their financial cost must be similar or lower than that for CEM-I and lime. The inclusion of alkali activators within geopolymers significantly increases their overall cost due to the amount of fuel and electricity required in their production (Figure 2.15) (McLellan et al., 2011).

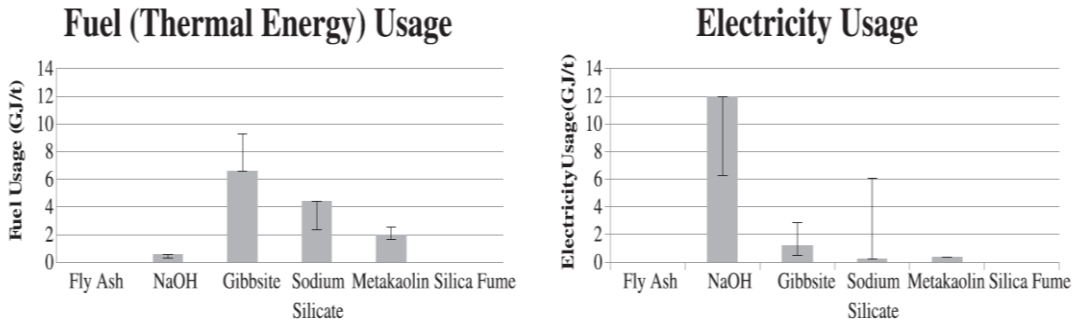

Figure 2.15: Energy usage for geopolymers feedstock production in Australia. Taken from McLellan et al. (2011). Reproduced with permission from Elsevier.

However, as IBP's have no production costs and constitute >80% by dry weight of geopolymers, their inclusion compensates for the high cost of alkali materials. For the Australian geopolymers studied by McLellan et al. (2011), the overall cost of most mixtures was slightly greater than for CEM-I; although transportation costs were considerably higher (Figure 2.16). This therefore questions the merits of using geopolymers.

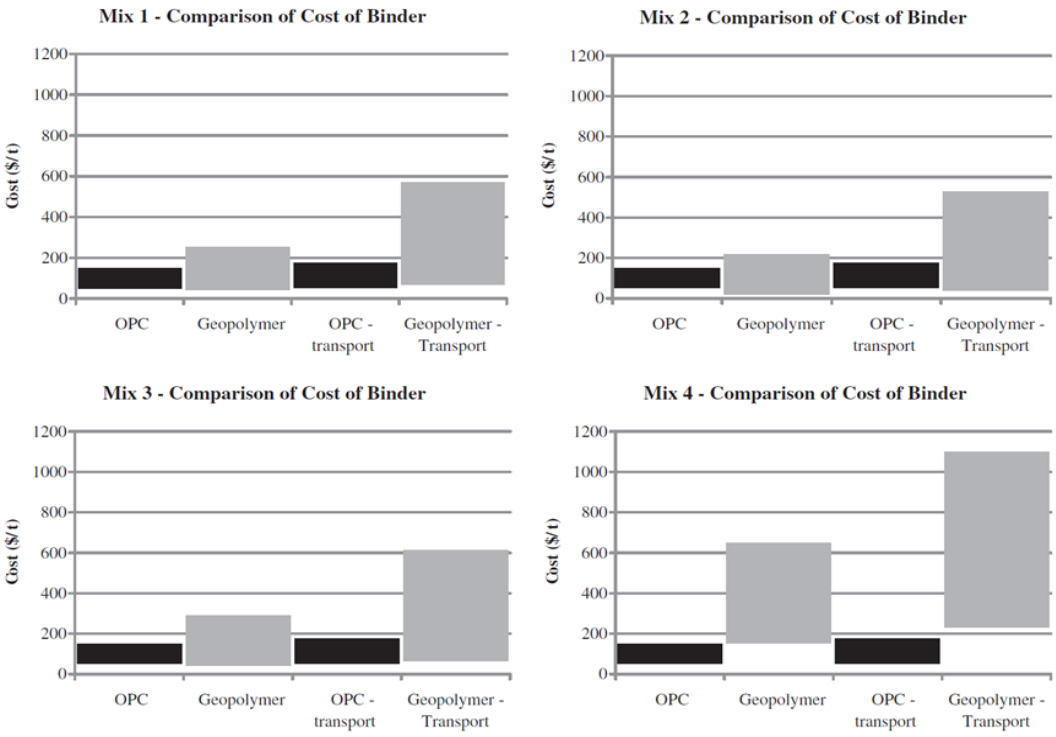

Figure 2.16: Summary of the overall costings for the four Australian geopolymers compared with CEM-I. Taken from McLellan et al. (2011). Reproduced with permission from Elsevier.

However, McLellan et al.'s (2011) findings were restricted to production and transportation within Australia, where transportation distances can greatly vary. Hence, McLellan et al.'s (2011) findings may not be truly representative of transportation costs incurred elsewhere in the world where geopolymers are manufactured.

Wherever geopolymers are intended for use, careful assessments should be conducted to ensure that the distances between the binder source and treatment site are minimised, as this influences their overall sustainability, market price and competitiveness against CEM-I/lime. The market price of NaOH and sodium silicate are considerably higher than other alkalis and IBP's. However, alkalis are only required in small quantities to activate pozzolanic reactions.

To summarise, although the inclusion of alkalis within geopolymers can incur high costs due to their production and transport; and appear to make geopolymers less competitive against CEM-I/lime, geopolymers are capable of achieving strengths surpassing those for CEM-I/lime. Hence, the scope of this thesis is to take advantage of the convenient large stockpiles of IBP's in the UK, which are pozzolanic, capable

of producing strength gains either at comparable rates or more rapidly than CEM-I; whilst entailing significantly lower CO_2 emissions and being economically more feasible than using CEM-I or lime.

2.9 Recent research into the engineering behaviour of stabilised soils

There is extensive literature on the laboratory investigation of chemically stabilised soils. There are two main types of laboratory investigations which are conducted on chemically treated soils; those examining the mechanical (engineering) performance and those examining how the mineralogy of stabilised soils change with curing, in order to account for engineering performance enhancements. Several studies from both types of investigation are hereby presented.

2.9.1 Al-Tabbaa et al. – Cambridge University, UK

Some of the first studies on the laboratory characterisation of stabilised soils in the UK using IBP-based binders were those by Al-Tabbaa and Evans (1998 and 1999). Their studies aimed to develop soil-grout mixtures that were suitable for stabilising soils (made ground, sands and gravels) in terms of strength and environmental remediation, which had been contaminated with organic compounds and heavy metals on a former chemical works site in West Drayton, Middlesex. There was also an emphasis on using as little cement/grout as possible to meet economic and environmental criteria. The binders used included CEM-I, PFA, bentonite and lime to increase soil pH. A soil-grout ratio of 5:1, a water-dry grout ratio of 0.42:1 and a soil-dry grout ratio of 5:1/7:1 were always maintained. After 28 days curing, the mixtures tested reached UCS values of 350–1100 kPa, leachate pH values of 6.5–10.5, reasonable wet-dry but poor freeze-thaw durability performances, low permeabilities of 0.2–2.0 x 10^{-9} ms^{-1} and low Mv values of $2x10^{-6}$ m^2/kN. These results suggested that Al-Tabbaa and Evans' (1998) treatment methodology was appropriate for the West Drayton site. This led to their 1999 paper, which simplified (in terms of the contaminants present) and

homogenised the West Drayton's site conditions; thereby allowing correlations to be made between the 1998 treatability study and the properties of the lab-scale in-situ treated soil, and secondly between the lab and field scale modelling of the soil stabilisation conducted.

2.9.2 Hughes et al. – Newcastle University, UK

Hughes and Glendinning (2004) stabilised a site near Sandling in Kent (UK) characterised by 5 metres of problematic peaty soils, underlying a section of the Channel Tunnel Rail Link (CTRL). Given the poor ground conditions and the CTRL's importance, stabilised soils were required to achieve minimum undrained shear strengths of 100kPa and a Young's modulus of 10MPa after 28 days (Hughes and Glendinning, 2004). The study's main aim was to assess RG's suitability when combined with GGBS as an alternative to lime/CEM-I, in terms of cost and engineering performance. The researchers conducted both field and laboratory testing using a range of GGBS/RG ratios at a dosage of 200kg m^{-3}. Once 27 DSM columns had been installed, they conducted in-situ standard column penetration (SCPT) and cone penetration tests after 7 and 56 days curing. Cores were recovered from the columns for laboratory testing; namely quick undrained unconsolidated triaxial, durability (wet-dry and freeze-thaw) pH and mineralogical analyses (XRD, SEM).

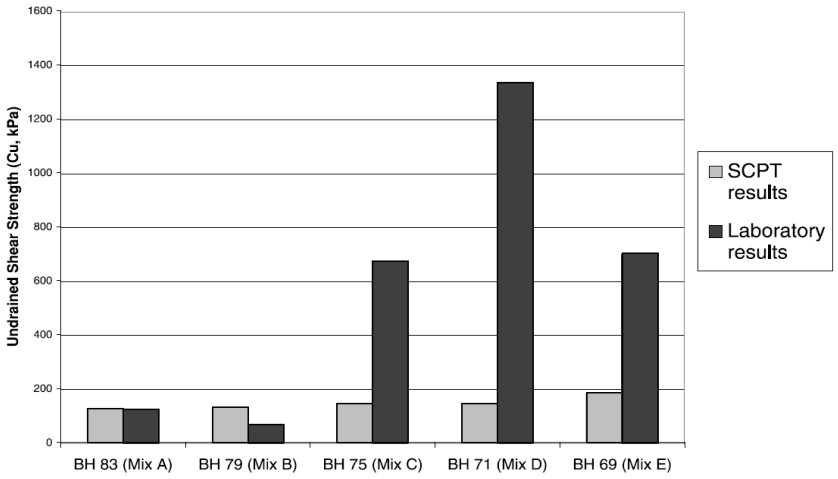

Figure 2.17: Variations in undrained shear strengths obtained for five GGBS-RG columns from in-situ SCPT and laboratory testing. Taken from Hughes and Glendinning (2004). Reproduced with permission from the Geological Society of London.

These researchers documented a good correlation between the in-situ SCPT and laboratory undrained shear strengths. However, there were a few exceptions (Figure 2.17). Higher laboratory strengths may be attributed to continued strength development of laboratory samples between sample recovery and testing. Unusually low laboratory strengths may be due to sample disturbance and weakening during transport.

Using a GGBS-RG ratio of 75:25 produced the most impressive strengths, met the required design criteria and exceeded those achieved by using CEM-I. Durability results were also encouraging, whereby little damage was incurred to the columns and the GGBS-RG's overall performance was comparable to CEM-I.

Although pH may have an impact on DSM column strength development, pH values >10.5 did not guarantee higher shear strengths. Humic acids within the peaty soils interfered with the soil-cement reactions, which may explain the low pH and strength values of certain mixtures. Using an alkali activator is recommended to raise the pH of such samples and thus promote pozzolanic reactions.

Further to their 2004 study, Hughes et al. (2011) investigated RG's effectiveness in terms of strength/stiffness development over 28 days at 55% relative humidity when combined with GGBS, PFA and basic oxygen steel slag (BOSS). The RG-IBP ratios varied between 9:1 and 5:5. 1 $Ca(OH)_2$ was also added to ensure pH was >10.5. UCS results revealed the most effective mixture was RG-GGBS at a ratio of 10:90 and moisture content of 35%, producing strengths of 39.7MPa. For the lower moisture contents tested by Hughes et al. (2011), RG-BOSS mixtures produced the highest UCS values; but also highly brittle failures that could prove problematic when dynamically loaded. Although the highest strengths were achieved by RG-GGBS using a ratio of 10:90; the RG-GGBS ratio of 50:50 was deemed most favourable as it used as much IBP material as possible; whilst achieving high strengths.

Further to the above, Hughes et al. (2011) assessed RG-GGBS's performance in stabilising numerous UK soils; including an artificial alluvium, London Clay, Northumberland Glacial Till and Irish Moss Peat. For triaxial testing, confining pressures of 100kPa and a strain rate of 1.23 mm/min were used. Samples were wet and dry cured for up to 112 days. For the former an 18kPa surcharge was exerted on top of samples to simulate realistic confining pressures beneath the water table.

For stabilised artificial alluvium samples, soak- and dry-cured samples achieved strengths of ~ 2.7MPa and 5MPa respectively (Figure 2.18). Their rate of stiffness development was slower than for CEM-I stabilised samples. Stabilised till samples developed lower undrained shear strengths (0.5MPa) than those for CEM-I-stabilised samples (3MPa). Any considerable strength developments were only observed after 28 days.

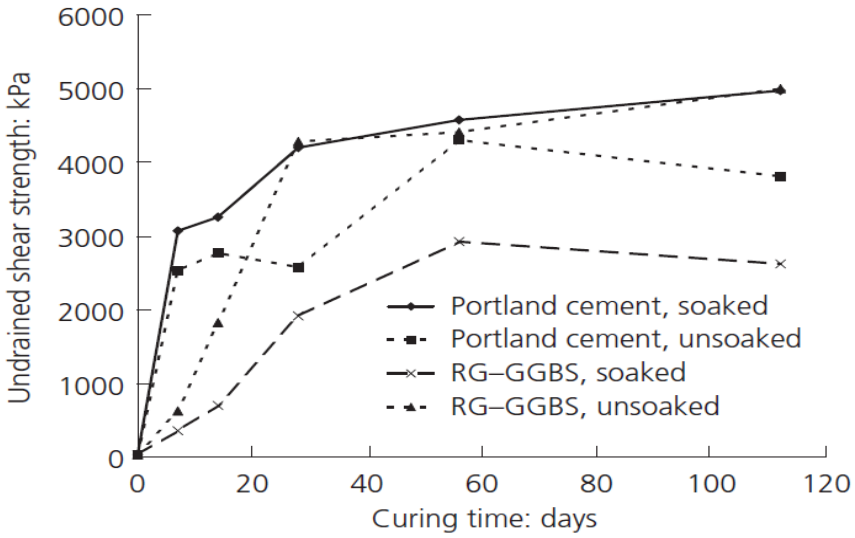

Figure 2.18: Undrained shear strength development of stabilised silty sand samples tested by Hughes et al. (2011). Taken from Hughes et al. (2011). Reproduced with permission from the Institution of Civil Engineers.

Significantly lower shear strength values were obtained for stabilised peat samples; even when additional lime was incorporated. However, such results were expected given the high water and organic contents and low pH levels, which inhibit pozzolanic reactions. The highest undrained shear strength recorded after 14 days was 10kPa for samples containing 30% lime. Similar to stabilised peat, negligible strength developments were observed for stabilised London Clay, reaching ≤150kPa which was 10 times lower than that for CEM-I samples. These results indicate that further work on binder chemistry and dosage is required for stabilising London Clay and soft organic peat soils.

2.9.3 Horpibulsuk et al. – Suranaree University of Technology, Thailand

Horpibulsuk et al. (2010) suggested that strength development within stabilised soils may be split into three zones (Figure 2.19a): 1) an active zone within which the volumes of pores <0.1 μm decreased through incorporating a binder and the development of cementitious minerals; 2) an inert zone within which pore size distribution and volume of cementitious minerals undergo negligible change with increasing cement dosage and hence minimal strength enhancements; and 3) a deterioration zone where the amount of pore water present is insufficient for hydration given the relative excess of binder.

The cluster theory states there are two pore types within stabilised soils: inter- (>0.01 μm) and intra-aggregate (<0.01 μm) (Horpibulsuk et al., 2010). Immediately post-mixing, the volume occupied by inter-aggregate pores decreases due to clay-cement agglomeration formation whilst the volume of larger inter-aggregate pores increases. With cementitious mineral growth, inter-aggregate pores become occupied and the soil's total pore volume decreases. The researchers confirmed this after 7 days curing, where large pore volumes and total pore volumes within samples decreased as the volume of small pores (<0.01 μm) increased due to cementitious mineral growths (Figure 2.19b).

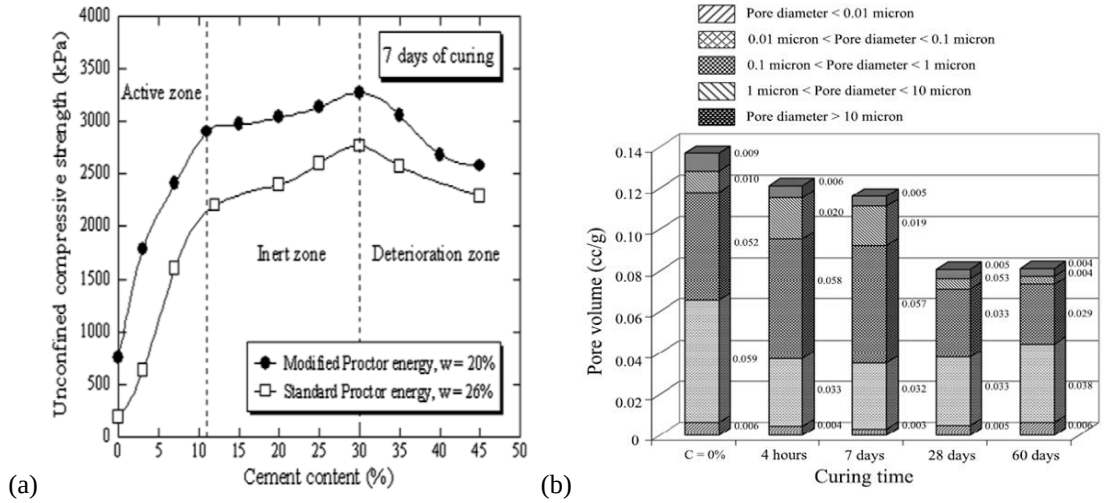

(a) (b)

Figure 2.19: (a) Three zones of strength development within cemented soils; (b) Chart showing pore size distribution for samples stabilised with 10% CEM-I. Taken from Horpibulsuk et al. (2010). Reproduced with permission from Elsevier.

The researchers investigated UCS development of PFA-biomass ash stabilised Bangkok clay. The effects of various water contents (89, 119 and 149%), cement (0–30%) and PFA/biomass ash (0–60%) dosages were investigated for curing periods up to 120 days at 20^{o}C. An optimum PFA content of 25% produced the highest strengths (1900 kPa for 89% moisture content) after 28 days. This PFA dosage was also the most economic mixture. It reduced the amount of binder required to stabilise the soil by 16% compared with using CEM-I. Horpibulsuk et al. (2011) observed that the relationship between sample strength, clay-water/cement ratio and curing times was useful in estimating laboratory strengths and the required cement dosages within soils of different in-situ and field moisture contents (Figure 2.20).

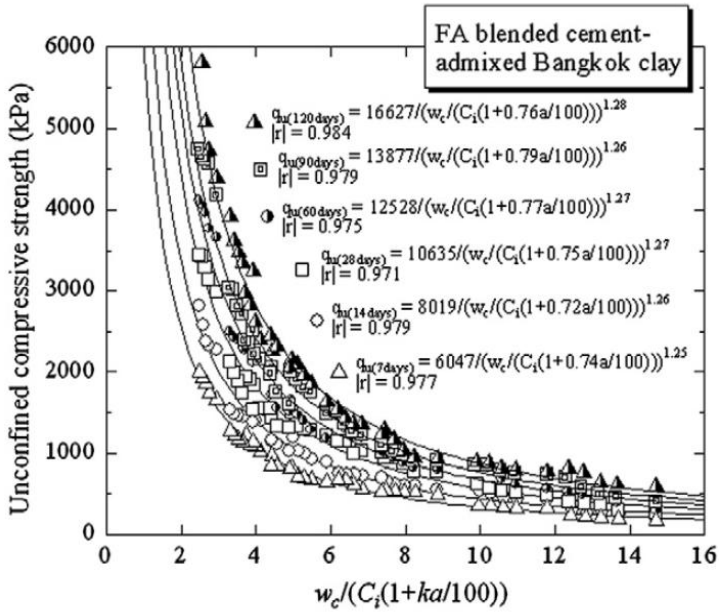

Figure 2.20: Relationship between UCS and clay-water/cement ratio for PFA-cement stabilised Bangkok clay. Taken from Horpibulsuk et al. (2011). Reproduced with permission from Elsevier.

PFA stabilised soil mixes are expected to achieve strengths of 0.6–3.0 MPa after 28 days (Horpibulsuk et al., 2011). In relation to CEC, ash, silt and sand particles within such mixtures are non-interacting particles given their low specific surface areas and non-electrical nature; whereas cement and clay particles can undergo physicochemical interactions with soil water. As a result of the clay's interactions, a micro-fabric develops which strengthens when cement is mixed into the soil; thereby creating large clay-cement agglomerations.

Although PFA is silica and alumina rich, its pozzolanicity is very low. This contrasts with how previous authors and industrial standards have characterised PFA as having good pozzolanicity levels (e.g. ASTM D5239–04). Rather than the conventional pozzolanic strength gain mechanism of $Ca(OH)_2$ produced via hydration by cements; PFA is only able to disperse large clay-cement agglomerations. This leads to increases in the reactive surface area of cement particles and subsequent strength enhancements. The researchers confirmed this through using SEM, mercury intrusion porosimetry and thermal gravitimetry analyses. Thus, Horpibulsuk et al. (2011) proposed a new hypothesis on how strength develops within blended cement-clay admixtures, postulating strengths achieved solely depend on the clay-water/cement ratio. Given PFA's poor pozzolanicity, the equivalent cement content within a stabilised soil thus depends on the dispersing potential of the material, which is controlled by the PFA content.

2.9.4 Ahnberg – Swedish Geotechnical Institute

Many previous laboratory studies examining the strength of stabilised soft soils have used UCS, due to its simplicity, low cost and usefulness in comparing the effects of different binders/other factors in influencing their strengths. However, Ahnberg (2007) amongst others believe that to develop a more detailed understanding of stabilised soil's mechanical behaviour, triaxial testing is more appropriate as they fail in shear.

Little literature exists on yield stresses within stabilised soils and their effects on strength behaviour. Yield stresses are largely influenced by cementation (Ahnberg, 2007). However, stresses acting on stabilised soils during curing also play a role. To examine the impact of these factors, effective stress path and shear strength behaviour of stabilised soils, Ahnberg (2007) carried out consolidated drained and undrained triaxial testing on two stabilised Swedish post-glacial clays; characterised by moisture contents 80–90%, plastic and liquid limits of 24% and 68% respectively, high clay contents (>60%), low organic contents (1%), sensitivities of 20–25 and low undrained shear strengths (8–15kPa).

The dry binder mixtures used included CEM-II, quick lime, CEM-II+quick lime, CEM-II+GGBS, CEM-II+PFA and GGBS+quick lime. Composite binders comprised

a 50:50 ratio of each material. The binder dosage used for both soils was 100kg/m^3. Ahnberg (2007) used two curing methods; most samples were stored within sealed plastic tubes and cured for 1, 28 and 360 days at 8^{o}C per Swedish testing standards. However, some CEM-II & quick lime stabilised samples were cured within triaxial cells under numerous vertical stresses. Prior to shearing, Ahnberg (2007) mounted samples within the triaxial cells and subjected them to K_0 consolidation and curing under the same stresses for 28 days. Effective confining pressures of 20–60kPa and vertical effective stresses of 40–120kPa were applied. For comparison, Ahnberg (2007) also stored non-stressed stabilised samples for 28 days which were saturated from both ends. Given stabilised soil's high stiffnesses and low permeabilities, Ahnberg (2007) saturated samples by using back pressures of ≥400 kPa. Subsequently, samples were consolidated for 7.5 hours to achieve a K_0 of 0.5. For shearing, a constant strain rate of 0.02%/min was used for all tests. A variation in shear strength was recorded for the different stabilised mixtures of 50–1500kPa (Figure 2.21).

Samples consolidated at stresses lower than their yield stresses behaved in an overconsolidated manner; whereas those consolidated at stresses higher than their yield stresses behaved as normally consolidated soils. The majority of yield stress values were evaluated from oedometer tests, depicting a stress dependency of stabilised soils' undrained shear strength behaviour.

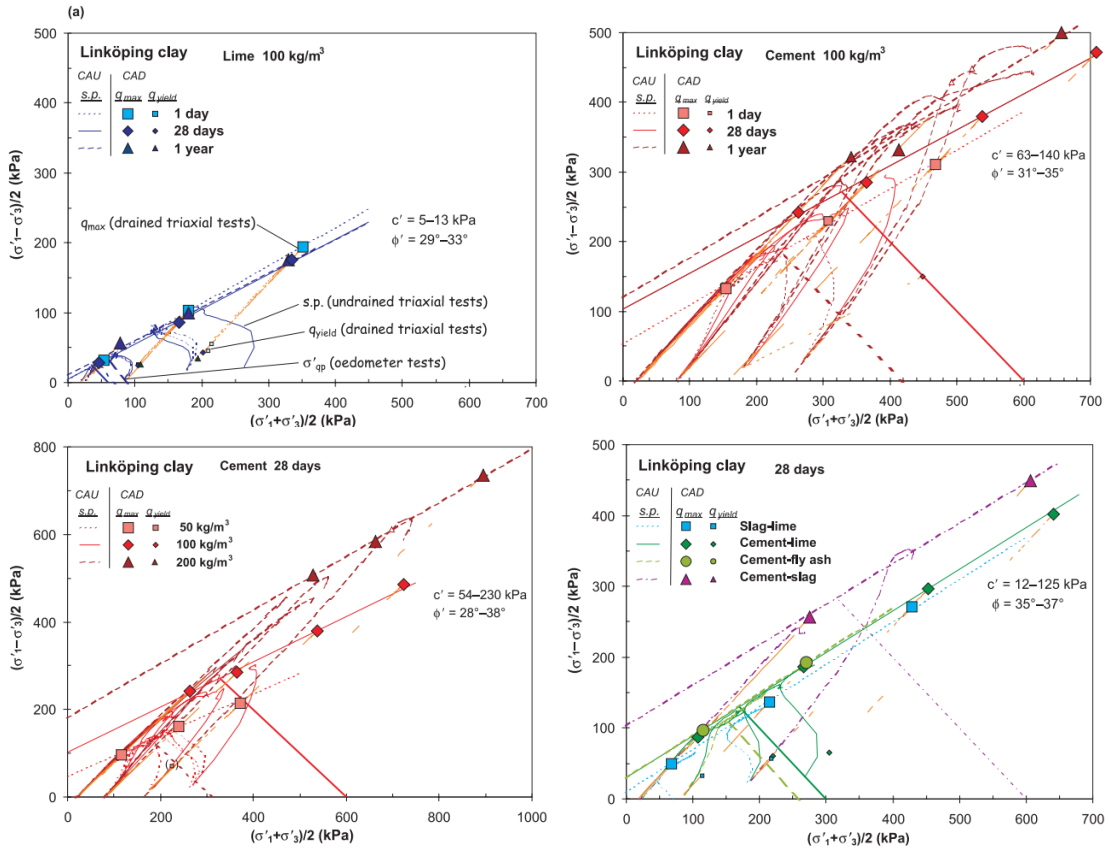

Figure 2.21: Measured effective stress paths in the s–t plane for stabilised Linköping clay mixtures. Taken from Ahnberg (2007). © 2008 Canadian Science Publishing or its licensors. Reproduced with permission.

Ahnberg (2007) recorded high effective friction angles (30–36^{o}) and effective cohesion values (up to 175kPa). Such increases in effective cohesion were attributed to simultaneous increases in undrained shear strength. However, Ahnberg (2007) noted this did not always apply; namely for lime-stabilised mixtures where using lime had negligible strengthening effects. Such poor performances are common when using high lime dosages within soils containing high moisture contents. Locat et al. (1990) confirmed that high lime dosages results only in long-term strength increases for soils with high moisture contents (Figure 2.22).

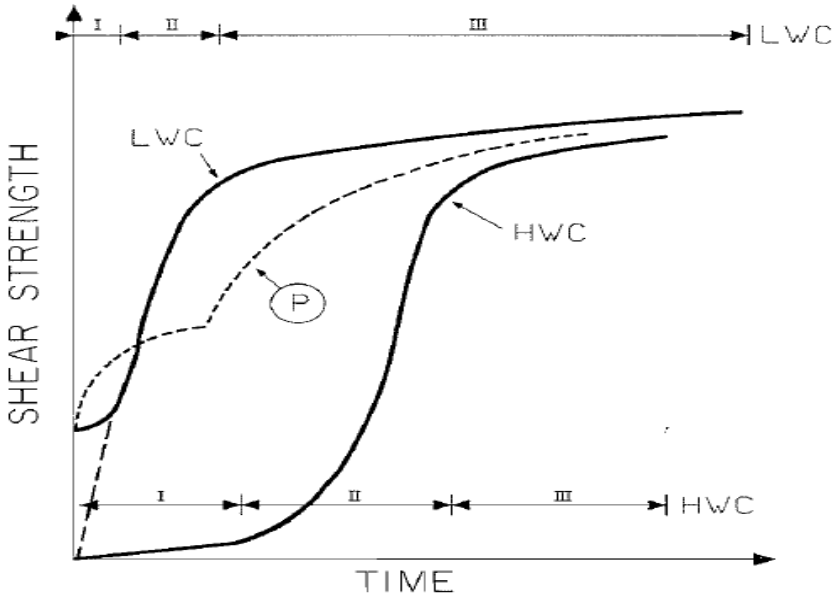

Figure 2.22: A mechanical conceptual model of shear strength development within lime stabilised sensitive clays at both low and high moisture contents. (LWC – Low water content; HWC – High water content, P – Perret model for silty soils.) Taken from Locat et al. (1990). © 2008 Canadian Science Publishing or its licensors. Reproduced with permission.

Drained triaxial tests revealed that yield points for lower strength samples were recorded at low strains; whereas failure occurred at much greater strains. However, Ahnberg (2007) noticed that yielding became less distinguishable within higher strength samples, which occurred at stresses and strains close to failure.

Although significant variations in strength were seen by Ahnberg (2007) due to factors including soil type, binder type and curing period; relatively similar stress-strain behaviour was recorded for the different stabilised mixtures. This was linked to samples' degree of overconsolidation. For samples under drained conditions failing at smaller strains, large reductions in shear strength with increasing strain post-failure were seen. Ahnberg (2007) noted this behaviour for samples that had been consolidated at lower stresses than their yield stresses.

Under undrained conditions, Ahnberg generally recorded little changes in deviator stress post-failure. The strains experienced at failure for normally consolidated untreated and stabilised samples were similar. Both experienced near-perfect plastic behaviour with no considerable strength degradations post-failure. For highly

overconsolidated samples, brittle behaviour was experienced at small strains, followed by significant strength degradation post-failure.

Ahnberg (2007) identified a "phase-transformation" point during undrained tests where changes in pore pressure were zero and the stress paths of overconsolidated samples changed direction to follow the critical state line. Ahnberg interpreted this as depicting a yield surface and that Larsson's (1977) yielding model closely described this behaviour.

Ahnberg (2007) assumed that the effects of increased external stresses are related to the compression of the stabilised soil; inferring that increased stresses due to external loads ought to be applied shortly after stabilisation. This ensures that the material becomes compressed, allowing for cementation and increases in yield and overall shear strength to occur.

2.9.5 Wilkinson et al. – Department of Transport/Monash University, Australia

Wilkinson et al. (2010b) studied pH, plasticity and undrained shear strength development of various soil-binder mixtures with curing. Four soil types were stabilised; two high plasticity (Ginifer and Leeville), one low plasticity (Boambee) and one engineered clay soil (Table 2.6). The binders used included lime, lime activated GGBS and lime activated PFA, which were added at a dosage of 10% by dry weight.

Table 2.6: Summary of the soil's geotechnical, chemical, CEC and mineralogical characteristics stabilised by Wilkinson et al. (2010a,b). Reproduced with permission from the Institution of Civil Engineers.

Soil	Plasticity Index (%)	Clay mineralogy	CEC (meq/100g)	pH at 1:3 soil/water ratio	Organic carbon content (%)
Ginifer	68.8(high)	Smectite dominant	33.1	8.25	0.08(low)
Leeville	47.9(high)	Smectite dominant	18.1	5.38	1.22(high)
Boambee	31.(low)	Kaolinite dominant	6.0	4.45	0.35(high)
Engineered Soil	59.0(high)	Kaolinite dominant	18.2	8.2	0

Davidson et al. (1965) determined that for pozzolanic reactions to occur within stabilised soils, a minimum pH of 10.5 was required. Based on the four soils' pH values in Table 2.6, each required alkali activation. Initial pH values post-stabilisation all exceeded 12 but degraded towards 11.5 over one year. Hence, pozzolanic reactions could occur within all samples and a relationship existed between decreasing soil pH with increasing strength as curing progressed. The mechanism causing this involves $Ca(OH)_2$ acting as an electrolyte to fuel modification reactions and as a caustic agent, allowing stabilisation to occur through increasing pH for pozzolanic reactions to occur (Rogers and Glendinning, 2000; Wilkinson et al., 2010b). Pozzolanic reactions then consume hydroxyl ions from soil and binder particle surfaces, combining with pore water to precipitate cementitious minerals.

The researchers' results show that the most successful binder in the short and long term was lime activated GGBS (Figure 2.23). Ginifer soil stabilised with this binder produced the highest undrained shear strengths (388kPa) out of all twelve mixtures tested after 28 days.

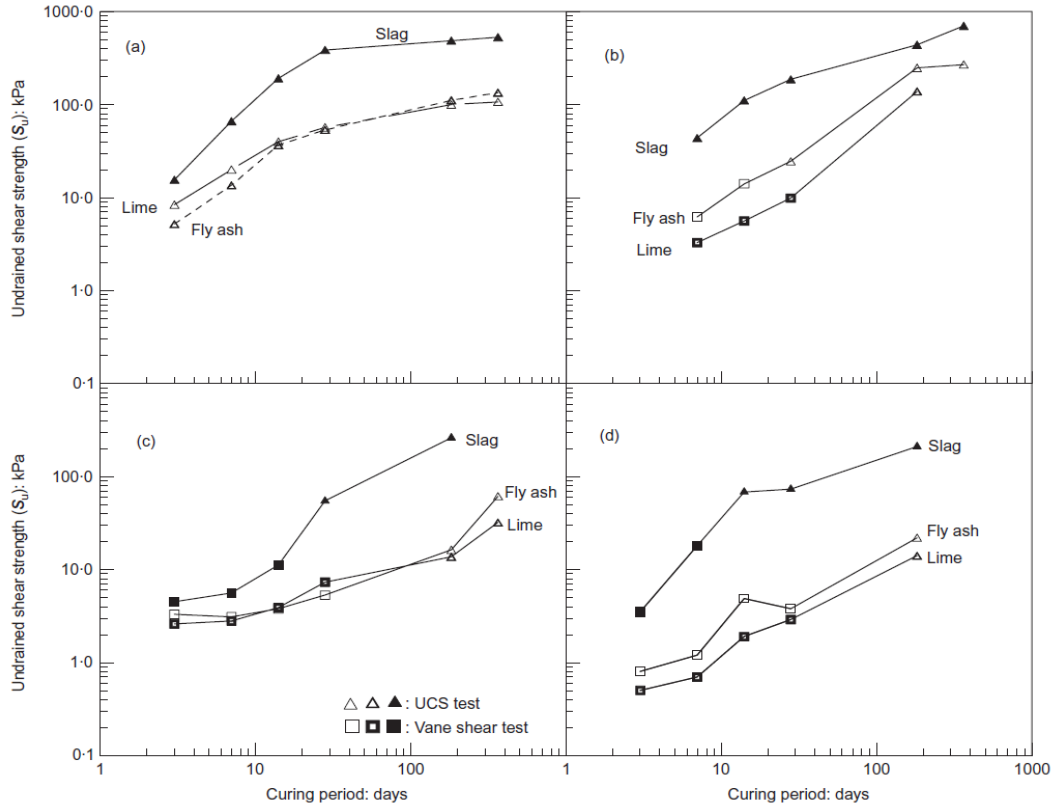

Figure 2.23: Undrained shear strength development of all stabilised soil mixtures tested by Wilkinon et al. (2010b): (a) Ginifer (b) Engineered clay (c) Leeville (d) Boambee. Taken from Wilkinson et al. (2010b). Reproduced with permission from the Institution of Civil Engineers.

Activated PFA and lime binders exhibited similar performances within smectite-based clays; whereas activated PFA produced preferable performances over lime for the kaolinite-dominated soils. Work by Bell (1996) on the lime stabilisation of clay soils determined that smectite has higher short term pozzolanicity compared with kaolinite, attributable to smectite's higher surface area and CEC. These characteristics along with the higher organic content of the Ginifer soil may explain the GGBS activated engineered soil producing higher strengths than the GGBS activated Ginifer soil after one year curing.

Plasticity testing revealed that clay particles had been altered during cementation (as confirmed by SEM imagery). The smectite-bearing soils demonstrated reductions in PI values through smectite consumption. Contrastingly, kaolinite-bearing soils exhibited increases in PI values as cementation occurred.

2.9.6 Verástegui Flores et al. – Ghent University, Belgium

A triaxial study was conducted by Verástegui Flores and Van Impe (2009) on artificially cemented kaolin clay samples to distinguish between the material behaviour of stabilised and untreated kaolin. Untreated samples had a moisture content of 57.7%, to simulate a very soft soil. This study used a more advanced triaxial set-up than Ahnberg (2007), involving bender elements to gain insights into the small strain stiffness behaviour of cemented soils. The binder used was CEM-I at dosages of 5 – 20 % by dry mass.

Once saturated, untreated samples were isotropically consolidated to an effective stress of 50kPa prior to shearing. Treated samples containing binder dosages of 10 and 20% were isotropically consolidated under effective stresses of 100kPa and 300kPa, respectively. During consolidation, values of initial shear stiffness (G_0) were recorded by using bender elements. Shear waves were generated by 1 cycle of a sinusoidal electrical pulse at a frequency of 10kHz. Initially high G_0 values were observed to decrease with increasing isotropic consolidation stresses to a minimum value, straight after which they increased. Verástegui Flores and Van Impe (2009) stated that this behaviour is typical of non-cemented frictional soils, and that the transition from G_0 decreasing to increasing again denotes the point at which the material's structure degrades from cemented to non-cemented behaviour; defining the yield stress (p'_y) (Figure 2.24a).

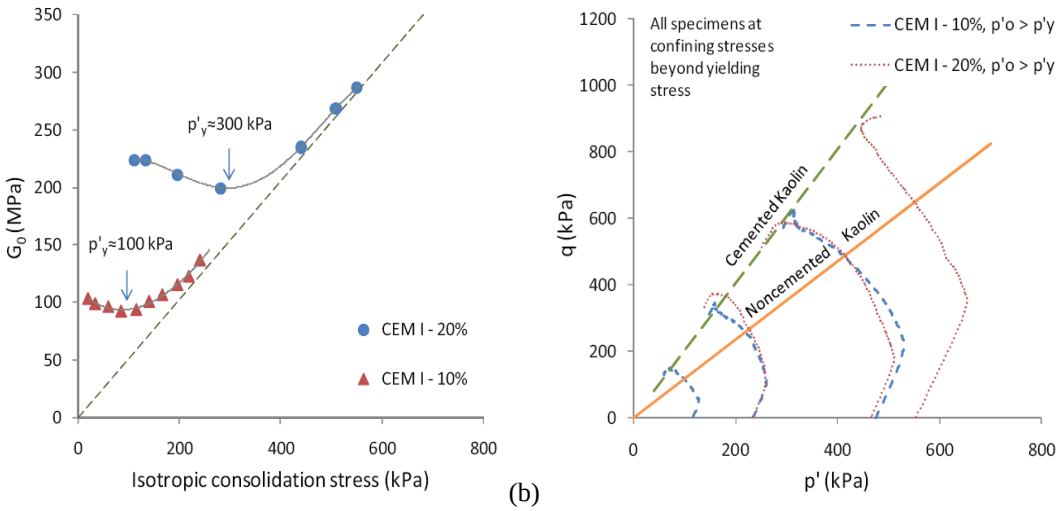

Figure 2.24: (a) Bender element measurement of G_0 for CEM-I stabilised kaolin mixtures; (b) Effective Cambridge stress path plot of treated and untreated kaolin samples. Reprinted from Verástegui Flores, R. D. and Van Impe, W. F. (2009). Copyright 2009, with permission from IOS Press.

At low confining pressures, shear strength behaviour was influenced by the level of cementation; whereas at higher confining pressures the behaviour was influenced by isotropic consolidation stresses. All treated samples produced a linear peak failure envelope, located above that defined for untreated samples (Figure 2.24b). Based on this observation, the researchers interpreted that an unbound granular macro structure existed within cemented samples. These findings should therefore encourage using bender elements on soils stabilised with alkali activated IBP's in the future, to gain further insights into their mechanical behaviour at small strains.

2.10 Recent research into the mineralogical and microstructural characteristics of alkali activated binders for soil stabilisation

2.10.1 Al-Tabbaa et al. – Cambridge University, UK

Following their 1998 study, Al-Tabbaa and Evans (1999) used XRD and SEM techniques to examine the microstructural and physico-chemical characteristics of the same stabilised mixtures after 7 and 28 days curing. XRD and SEM results (Figure 2.25) confirmed the presence of hydrating cementitious compounds, and that the presence of most contaminants within the soil-grout mixtures did not inhibit the development of cementitious minerals. However, the presence of lead nitrate appeared to inhibit cementitious mineral growth as much as mineral oil and lead nitrate combined.

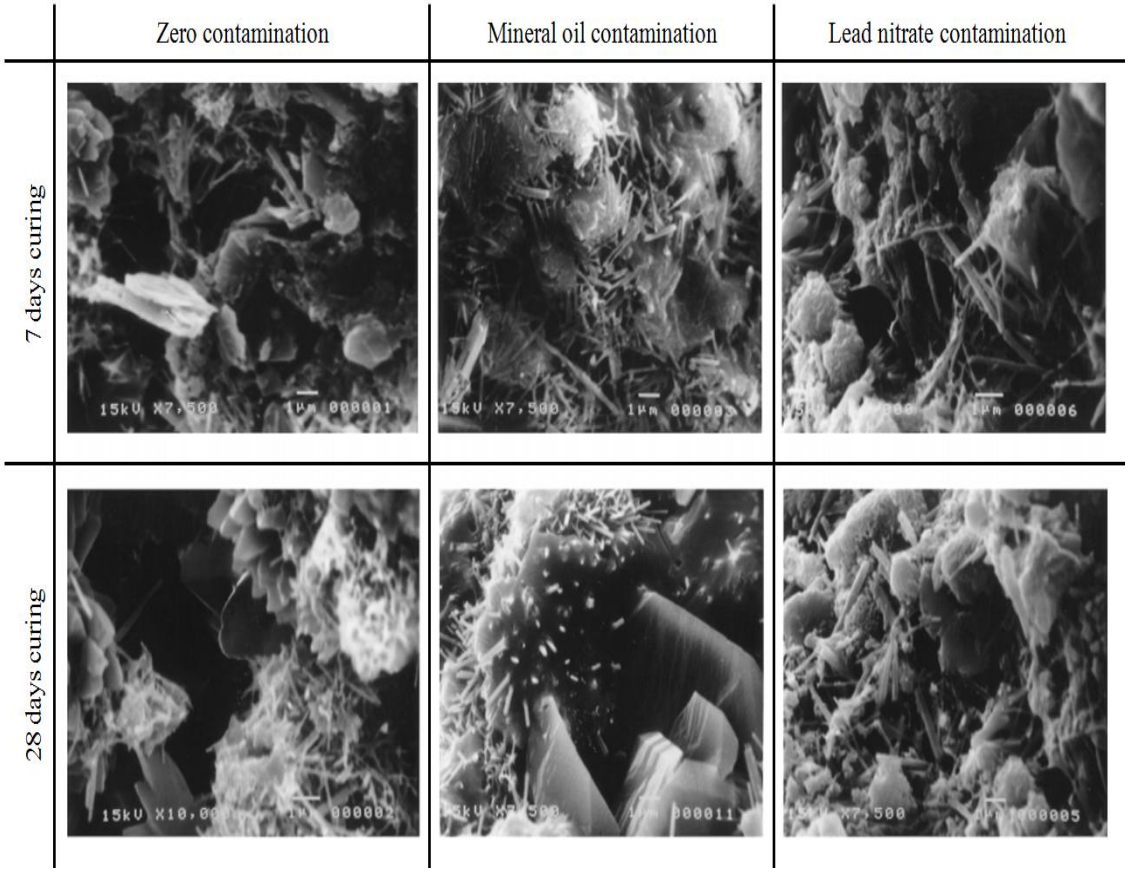

Figure 2.25: SEM micrographs of West Drayton soil in both uncontaminated and contaminated states after 7 and 28 days curing. Adapted from Al-Tabbaa and Evans (1999). Reproduced with permission from the Institution of Civil Engineers.

2.10.2 Hughes et al. – Newcastle University, UK

Besides their geotechnical testing, Hughes and Glendinning (2004) conducted SEM and XRD analyses on samples recovered from the 27 DSM columns installed. XRD analyses revealed no evidence of ettringite or thaumasite within any of the samples, indicating that the GGBS-RG columns were not susceptible to sulphate attack for up to 56 days post-treatment. However, the detection of hydrated cementitious minerals within samples was not possible by using XRD, due to their amorphous nature. SEM techniques (including the EDS point elemental analysis tool) identified hydrated cementitious minerals infilling void spaces due to pozzolanic reactions. Some of the SEM micrographs taken showed the presence of a few needle-shaped minerals (Figure 2.26), suggesting the presence of ettringite/thaumasite. However, the SEM-EDS

system determined these minerals as RG and posed no threat towards the soil's mechanical structure.

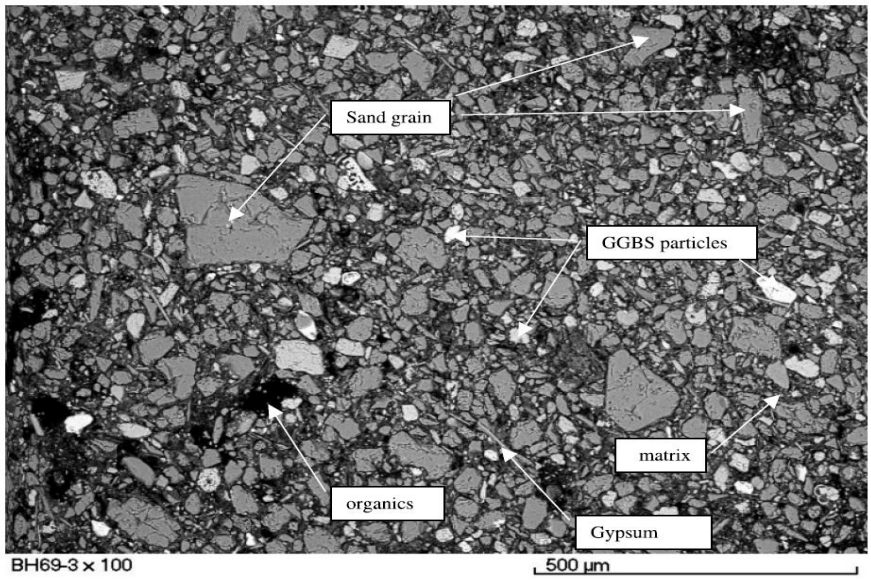

Figure 2.26: SEM micrograph of a polished sample section, which has been EDS analysed. Taken from Hughes and Glendinning, 2004). Reproduced with permission from the Geological Society of London.

The researchers also conducted XRD and SEM analyses on treated and untreated samples of artificial silty sand, Northumberland till, London Clay and Irish peat (Table 2.7).

Table 2.7: Summary of mineral phases observed in each sample analysed by Hughes et al. (2011) using XRD. Reproduced with permission from the Institution of Civil Engineers.

	RG-GGBS stabilised		**CEM-I stabilised**	
	Dry-Cured	***Soak-Cured***	***Dry-Cured***	***Soak-Cured***
Artificial Alluvium	Kaolinite, Gypsum, Ettringite, Quartz & C-S-H.	Kaolinite, Gypsum, Ettringite, Quartz & C-A-O-H.	Kaolinite, Portlandite, Calcite, Quartz, C-S-H & C-A-O-H.	Kaolinite, Portlandite, Calcite, Quartz, Calcium Silicate & C-A-O-H.
London Clay	Gypsum, Ettringite, Quartz & Muscovite.	-	Kaolinite, Calcite, Ettringite, Quartz, Muscovite & C-S-H.	Ettringite, Quartz, Muscovite & Calcite.
Northumberland Glacial Till	Kaolinite, Gypsum & Quartz.	Kaolinite, Gypsum, Ettringite, Quartz & C-S-H.	Kaolinite, Portlandite, Calcite, Quartz & C-S-H.	Kaolinite, Portlandite, Calcite, Quartz & C-S-H.

[The symbol (-) denotes no sample was analysed.]

From the SEM-EDS analyses on polished sections of the mixtures in Table 2.7, little mineralogical differences existed between samples containing RG-GGBS or CEM-I. The researchers did not recommend using the EDS tool, as it can only identify elements with atomic numbers >5; thus being unable to detect hydrogen.

The effectiveness of RG-GGBS in producing improved engineering performances was influenced by soil mineralogy and pH. For the artificial alluvium tested, the addition of lime was needed to raise pH to >10.5. In contrast, the mineralogy (specifically sulphate content) of the Northumberland glacial till, peat and London Clay caused pH levels to decrease with curing. The lime added was insufficient to raise pH levels, resulting in the unsuccessful activation of the RG-GGBS. Although the strengths achieved were lower compared with CEM-I, the researchers believed that RG-GGBS should still be considered as a sustainable alternative to CEM-I which meets construction specifications.

Wax-sealing samples for curing was more effective in preventing sample evaporation compared with cling film wrapping samples, as adopted by Rahman et al. (2008). Hughes et al.'s (2011) RG preparation method was more effective than that adopted by Rahman et al. (2008) in producing higher strengths, which involved oven drying the moist RG filter cake at 40^{o}C and then manually grinding it into a powder. The strengths of activated GGBS mixtures exceeded those achieved by CEM-I. Hence, the performance of the activated GGBS may conceal any effects due to the presence of RG.

2.10.3 Wilkinson et al. – Department of Transport/Monash University, Australia

Similar to Hughes et al. (2004, 2011), Wilkinson et al. (2010 a,b) investigated using lime activated PFA and GGBS to stabilise numerous Australian clayey soils. SEM and XRD were used to examine mineralogical changes within stabilised mixtures at various curing periods up to one year. SEM images revealed the occurrence of flocculation and agglomeration once the soils had been stabilised. These researchers also observed the development of neoform products including AFt (aluminate ferro tri-) phases (ettringite and thaumasite; Figure 2.27a), $Ca(OH)_2$ (Figure 2.27b), AFm (aluminate ferrite mono-) phases (i.e. strätlingite and calcium monosulphate hydrate;

Figure 2.28a) and C-S-H (Figure 2.28b). These products grew within pore spaces binding the soil structure together.

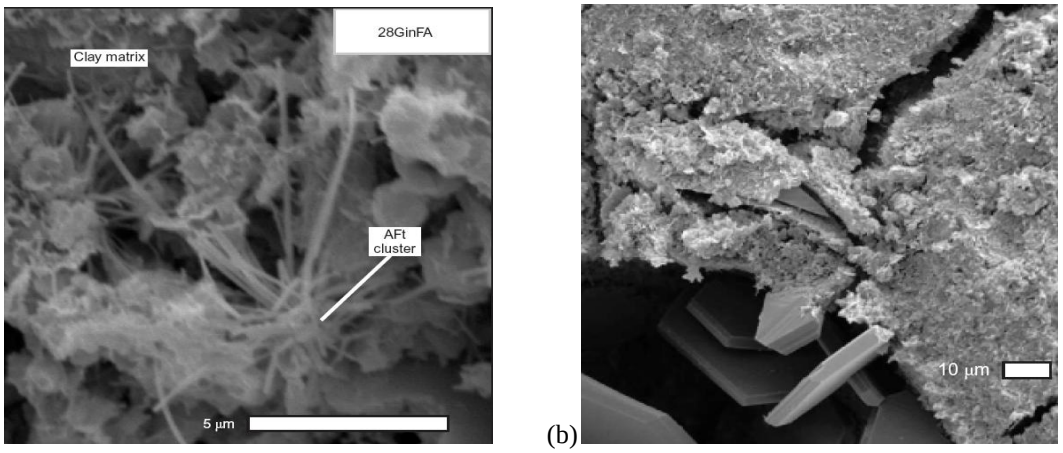

(a) (b)

Figure 2.27: SEM images of a) AFt phase ettringite and b) CH minerals. Taken from Wilkinson et al. (2010a). Reproduced with permission from the Institution of Civil Engineers.

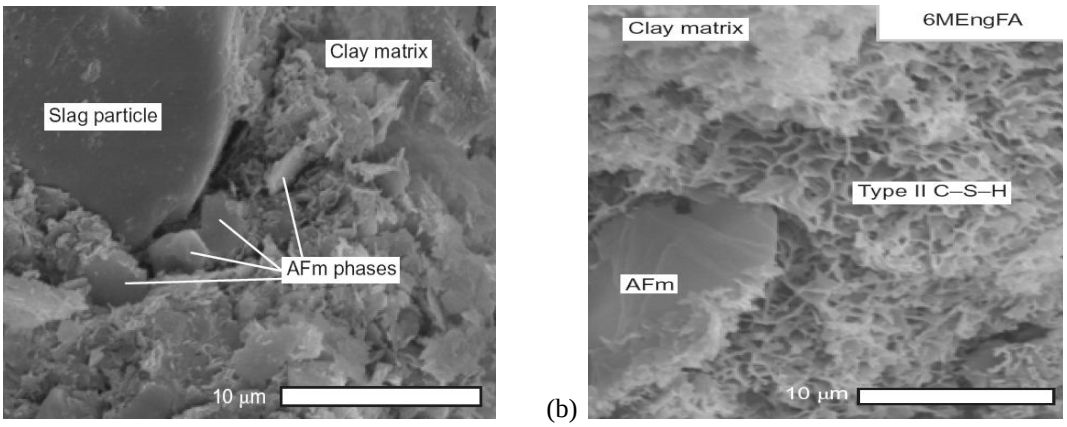

(a) (b)

Figure 2.28: SEM images of a) AFm phase and b) type II C-S-H minerals. Taken from Wilkinson et al. (2010a). Reproduced with permission from the Institution of Civil Engineers.

The abundance of AFt, AFm and C-S-H mineral phases increased with curing. C-S-H minerals were most abundant after 182 days (Wilkinson et al., 2010a). XRD analyses also confirmed the changing mineralogy of samples over time (Figure 2.29).

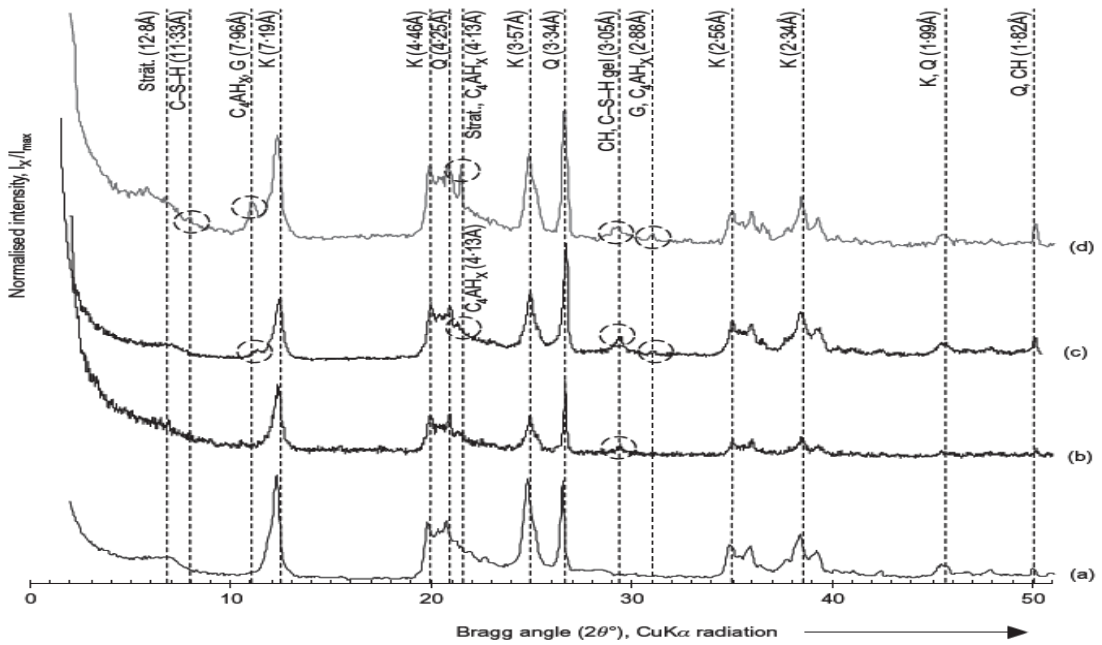

Figure 2.29: XRD traces of samples analysed by Wilkinson et al. after various curing periods: a) untreated clay at 0 days, b) with hydrated lime at 6 months, c) activated PFA at 1 year and d) activated GGBS at 6 months. [*K = kaolinite, Q = quartz, G = gypsum, C_4AH_x = calcium aluminate oxide (carbonate) hydroxide.*] Courtesy of Wilkinson et al. (2010a). Reproduced with permission from the Institution of Civil Engineers.

Overall, the activated PFA and GGBS were seen to influence the type and form of growing mineral phases. Finally, soil organic content was observed to hinder cementitious mineral growths and thus subsequent strength developments.

2.10.4 Zhang et al. – Worcester Polytechnic Institute, USA/ Northwest A&F University, China

Zhang et al. (2013) stabilised a low-plasticity synthetic clay soil in the laboratory and subjected it to UCS, volumetric strain, and mineralogical/microstructural testing; specifically XRD and SEM-EDX (energy dispersive X-ray spectroscopy). The stabiliser used was metakaolin at dosages of 3-15%. Samples were cured for up to 28 days in cling film. For samples containing a Si/Al ratio of 1.7 and a 15% binder dosage, impressive 28 day UCS values of 31MPa were achieved, even though cling-filming samples for curing is less desirable than wax-sealing and that Duxson et al.

(2007) believe metakaolin should not be used in geopolymers due to the large volumes of water required and the consequent increase in the material's porosity.

Using SEM-EDX was successful in qualitatively identifying the presence of cementitious gels within samples and that sample homogeneity (and thus strength) enhanced through increasing binder dosage. Per Figure 2.30, sodium was detected in all EDX analyses of metakaolin-stabilised samples, probably associated with the geopolymers gels (Zhang et al., 2013). Upon blending the metakaolin with the soil, the reaction was observed to be rapid due to the metakaolin's fineness and high amorphous content. Regarding XRD analyses, a negligible difference between stabilised and untreated samples was recorded; indicating that there was no reaction between the metakaolin and the soil minerals and that the strength enhancements were attributed solely to geopolymer gels.

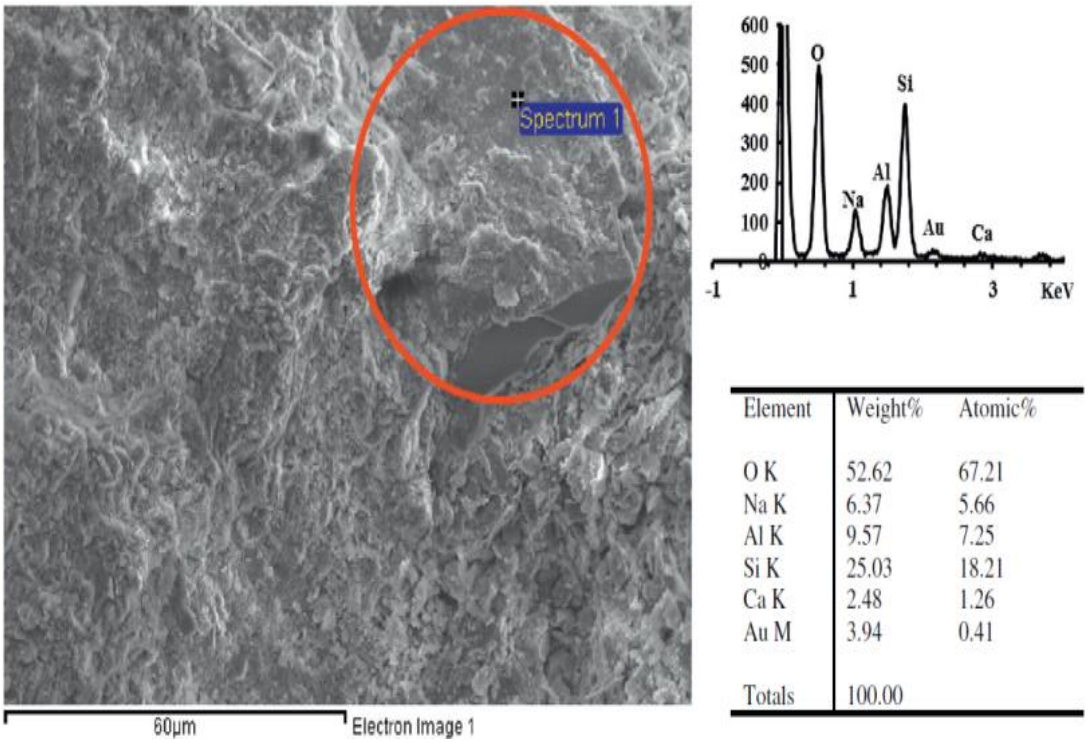

Element	Weight%	Atomic%
O K	52.62	67.21
Na K	6.37	5.66
Al K	9.57	7.25
Si K	25.03	18.21
Ca K	2.48	1.26
Au M	3.94	0.41
Totals	100.00	

Figure 2.30: EDX spectra of metakaolin geopolymers after 28 days curing. Taken from Zhang et al. (2013). Reproduced with permission from Elsevier.

However, metakaolin is costly and has been documented as unsuitable for chemical stabilisation (Duxson et al., 2007) and must be used at high dosages (>11%) to

produce comparable performances to 5% CEM-I (Zhang et al., 2013). Hence, other alkalis ought to be used for activating IBP-based geopolymers.

2.11 Modelling the behaviour of stabilised soils

Natural soils have widely been documented to possess an intitial degree of structure (Rouainia and Muir Wood, 2000), which has been attributed to the natural arrangement of particles within the soil matrix, inter-particle forces and the presence of weak cementitious bonding between particles (Gasparre and Coop, 2008). Vatsala et al. (2001) state that such cementation has a major influence on a soil's mechanical behaviour. Soft soils such as alluvium and peat tend to exhibit little structure or natural cementation and therefore often require treatment, such as DSM. Artificially cemented soils were considered by Vatsala et al. (2001) to fall into a similar "grey" area as soft rocks. Their behaviour is considered to be intermediate between soils and rocks and has yet to be fully defined and understood (Figure 2.31).

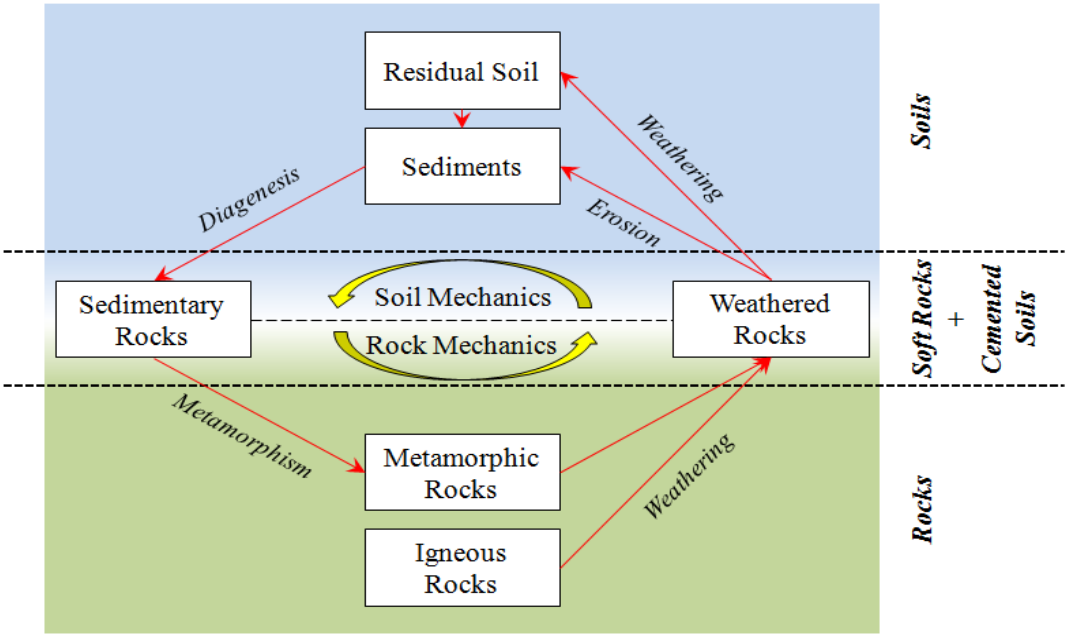

Figure 2.31: Diagram showing the concept of cemented soils in relation to rocks and soils in terms of their behaviour. Adapted from Dobereiner and De Freitas (1986).

Through personal communication with Hayward Baker (2012), geotechnical consultancies specialising in DSM treatment of soils tend to model the behaviour of cemented soils using the linear elastic-perfectly plastic Mohr-Coulomb model. The reasoning behind using such a simplistic constitutive soil model is the high levels of strength and stiffness achieved by stabilised soils over a relatively short period of time; exhibiting behaviour that is typical of concrete. Albeit the limit of elasticity and stiffness of stabilised soils far exceed those of natural untreated soils, stabilised soils are still complex materials demonstrating non-linear elasticity prior to yielding and plasticity post-yielding.

Based on these factors, research efforts have started to focus on developing constitutive models that are more capable of accurately capturing the behaviour of cemented soils. Vatsala et al. (2001) modelled the behaviour of a cemented soil by combining the behaviour of the untreated soil through using modified Cam clay and a new strain softening elastoplastic model for the cementation bond strength. Once cementitious bonds have developed within a stabilised soil and are able to withstand high stresses before failure, they would be assumed to be rigid and exhibit highly brittle deformation upon failure. However, testing by Vatsala et al. (2001) indicated that the cement bonds behaved inelastically in compression and shear; and were therefore modelled as an Elasto-plastic material. Hence, linear elasticity was used to describe the cement bonds' behaviour up to the cemented soil's yield stress, beyond which Elasto-plasticity was utilised.

Vatsala et al. (2001) verified their model by using their new elastoplastic model to predict the soil behaviour of various soft to very stiff clayey to non-clayey soils. The model's predictions compared reasonably well with literature data, given its relative simplicity. The researchers combined modified Cam clay-elastoplastic model captured the essential behavioural properties of cemented soils, including: 1) the sudden structural collapse of the cemented matrix upon compression, 2) the unusual shape of the K_0 path, 3) the progression from brittle to ductile behaviour upon yielding, 4) the material's stress-strain behaviour particularly in depicting strain softening, 5) the generation of positive and negative pore pressures and 6) positive and negative volume changes, depending on the soil's state and confining stress.

The most notable work building on that by Vatsala et al. (2001) was the development of a structured Cam clay model by Horpibulsuk et al. (2010), which was based on

works by Liu and Carter (2002, 2005). In terms of the compressional behaviour of cemented soils, Horpibulsuk et al. (2010) noted that they bore close resemblances with naturally structured clays. However, several differences were noted, including:

1) The cemented structure of stabilised clays results in a higher void ratio than natural clays.
2) When cemented clays yield, their level of cementation degrades and causes a reduction of the void ratio sustained by the cemented structure.
3) For highly saturated clays, the added voids ratio sustained by cemented structure is higher than that for the natural clay's structure.
4) The degradation rate of cementation within stabilised clays is higher than that for naturally structured clays; per the sudden high levels of compression post-yielding.
5) The isotropic compression curve of cemented clays is not asymptotic as observed for reconstituted natural clays.
6) The size of a cemented clay's initial yield surface increases along with tensile strength as cementation bond strength increases.
7) Cemented clays are characterised by elastic behaviour when stress states are located within the yield surface.
8) The higher the level of cementation, the higher the virgin yielding compression index. Hence, with increasing yield strength, the more resistance the material exhibits towards plasticity.
9) Strain softening occurs when cemented clays are loaded either at several locations within or on the material's yield surface. This softening is considered different from that expected for reconstituted clays, occurring when it is loaded within the yield surface and caused by the break-up of clay agglomerations.
10) The shear strength and shear stress ratio characteristics of cemented clays are higher than those for naturally structured or reconstituted clays.
11) Variations in the mechanical properties of cemented clays are isotropic.

For Horpibulsuk et al.'s (2010) model, the cemented soil material was assumed to be isotropic and characterised by elastic and virgin yielding behaviour. Its yield surface changed isotropically with increasing plastic volumetric deformation. Several modelling assumptions/conditions were made. Firstly, stress states within the structural yield surface were assumed elastic with elastic deformation being described according to Hooke's law. Virgin yielding was assumed to occur for stress states along the yield surface or those originating on the structural surface. In line with the Modified Cam clay model, the cemented soil's yield surface was assumed elliptical (Figure 2.32b). The reconstituted compression line was used as a reference for describing the cemented soil's compression curves. The cemented soil was assumed to use the same flow rule conditions as if the material's cemented structure had been removed. The researchers associated the destructuration of the cemented soil with progressive shearing, with failure only being achieved once all cementation had been removed. Softening was considered to occur once the material reached its peak strength state, due to localisation of deformation and degradation of the soil-cementation structure. Finally, the cemented soil was defined as reaching critical state once the stress ratio equalled the slope of its failure envelope and when the cementation structure equalled the additional voids ratio.

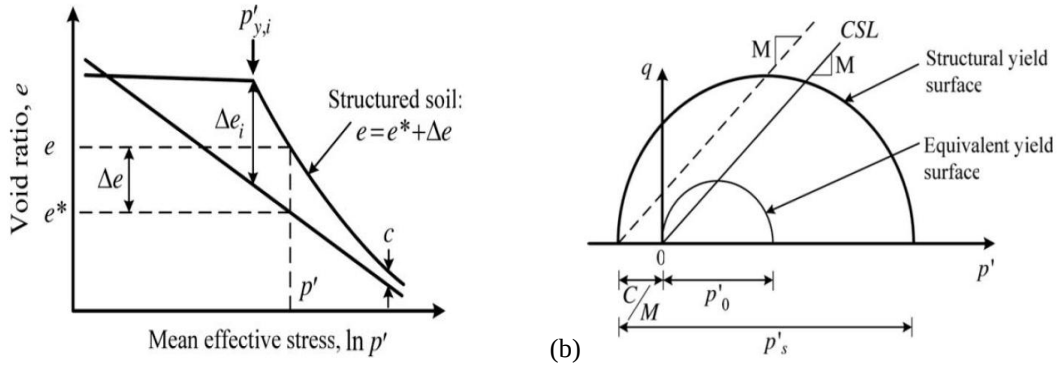

Figure 2.32: Material idealisation of structured cam clay for cemented clays in terms of: (a) compressional behaviour and (b) structural and equivalent yield surfaces. Taken from Horpibulsuk et al. (2010).

The researchers validated their model by conducting a suite of compression tests and isotropic drained and undrained triaxial tests on remoulded and cemented Ariake, kaolin, Hong Kong and Aberdeen clays containing a 9% cement dosage (Figure 2.33a).

Numerical simulation and experimental results (Figure 2.33b) were observed to compare favourably, capturing the following behavioural features:

1) Increasing size of the initial yield structural surface and strength with increasing cement content.

2) For cemented clays with high over-consolidation ratios, undrained stress paths initially rise vertically up to a peak, followed by softening and negative excess pore pressure generation as the stress path moves towards the CSL. The stress path then moves down and approaches the CSL causing positive excess pore pressures and ultimately sample failure.

3) For cemented clays with normal or lightly over-consolidated states, undrained stress paths initially rise and curve towards the CSL (indicating plastic deformation/virgin yielding). Subsequently, the stress path passes through the CSL through the effects of cementation, reaching its peak strength state and producing positive pore pressures and degradations in strength and cementation structure.

4) Cemented clays sustain higher void ratios than reconstituted samples; hence values for the critical state strength of reconstituted samples are zero compared with much higher values for cemented samples.

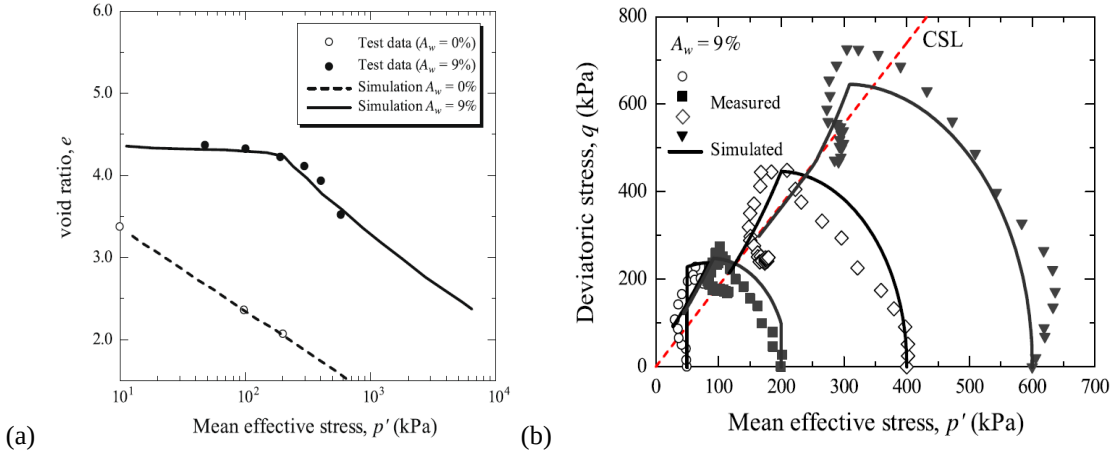

Figure 2.33: (a) Compression results for cemented Ariake clay; (b) Undrained effective stress paths for cemented Ariake clay in p'-q stress space. Taken from Horpibulsuk et al. (2010).

2.12 Conclusions and future trends

This chapter presents a detailed review of the processes and materials typically involved in chemical soil stabilisation, alongside the development of new more sustainable alkali activated mixtures as alternatives to lime and CEM-I. The key points are summarised below:

- Factors including high levels of versatility, low dust and noise emissions make DSM techniques ideal for improving ground conditions characterised by soft clayey and/or organic soils. This technique has successfully been used in stabilising local ground conditions for numerous major engineering projects; including the construction of the CTRL and the repair of levees in New Orleans after Hurricane Katrina in 2005.
- To ensure the soil and binder react and that maximum engineering improvements are achieved, a detailed understanding of the various binder materials available for chemical treatment is essential. Additionally, thorough soil assessments must be made including particle size distribution, surface area/reactivity, mineralogical and chemical characteristics. Soils ideally suited to chemical treatment contain fines (>10% clays of smectite or montmorillonite composition), low organic and sulphate contents; as organics can interfere with cementation reactions and sulphates can produce unfavourable minerals including ettringite and thaumasite.
- Although lime and CEM-I have been used in previous projects and produced high strengths and durabilities, there are numerous environmental and financial problems associated with their production and usage. The production of these materials incurs high costs due to their high levels of energy consumption and high greenhouse gas and carbon emissions. Their continued use as binders is unsustainable and hence the need for designing new sustainable binders; specifically in terms of energy consumption, greenhouse gas emissions, production and transport costs. To ensure such materials are competitive, they should provide engineering performances which compare with or surpass those of CEM-I and lime within similar curing times and also demonstrate credible carbon sequestration potential.

- Research into developing new alternative materials has continued since the mid-1990's. A preferred criterion for selecting new binders has been recycling IBP's to form geopolymers. Such binders could be substituted for CEM-1 and lime with only minimal modification to existing plant and equipment or reduction in the efficiency of the installation process.
- Recent laboratory and field-based research has demonstrated that IBP's have great potential as sustainable lime/CEM-I replacements. However, the inclusion of alkali activators is necessary to enhance the rates at which their mechanical properties are improved by increasing pH. This thereby promotes the conditions required for pozzolanic reactions and cementitious bonding to occur. Alkali activated GGBS is known to produce excellent short and long term engineering performances, comfortably surpassing those exhibited by lime and CEM-I.
- The cost of any chemical soil stabilisation project involving alkali activated mixtures is quite high. It is common for geopolymers components to come from various locations. The distances between some sourcing plants and stabilisation sites can be considerable. As modern transportation costs are high, careful planning must be conducted to keep delivery distances to a minimum. This will help geopolymers become more sustainable and competitive than lime or CEM-I.
- Until recently, much geotechnical experimental research into the mechanical behaviour of cement stabilised soils involved relatively simplistic testing techniques such as UCS. As such materials are now recognised to exhibit more complex non-linear elasto-plastic behaviour than the Mohr-Coulomb model, it is essential to characterise these materials through advanced triaxial testing techniques. Given the necessity to examine the small strain behaviour for natural uncemented soils, a similar approach should be adopted for the triaxial testing of cemented soils when subject to monotonic and dynamic loading conditions. Such data will prove very valuable in the further development of cemented soil constitutive models and ultimately in modelling current and future geotechnical problems involving the installation of DSM columns.

Chapter 3:

Testing and Analysis Methods

3.1 Introduction

The laboratory testing and analysis methods presented in this chapter were carefully developed to meet the aims and objectives of this research. Wherever possible, testing methodologies were conducted per British or ASTM standard procedures and with the latest methodologies in the academic literature.

The primary aims of the laboratory testing programme included:

1) Based on the industrial by-products (IBP) and alkali activator (AA) materials identified within the literature review, determining which IBP-AA binder mixtures produce the most desirable engineering performances after 28 days when mixed within an artificial alluvial soil, and thus have potential for use as alternative binders to lime and CEM-I in DDSM.
2) Determining the optimum IBP-AA binder mixture and dosage which achieves engineering performances meeting/surpassing those of lime and CEM-I, whilst also meeting 28 day strength criteria per EuroSoilStab (2002).
3) Identifying the most financially and environmentally sustainable IBP-AA binder mixture relative to lime, CEM-I and other IBP-AA binders, based on criteria in the literature review (see sections 2.7 and 2.8).
4) Assessing the potential for using the new binder in civil engineering applications; particularly focussing on stabilising high speed railway embankments, which experience monotonic and dynamic/cyclic loading conditions on a daily basis.

Hence, the objectives of the laboratory testing programme were to:

1) Design an optimum binder mixture by mixing various IBP and AA materials at different ratios within an artificial alluvial soil at various dosages (by dry weight) and testing their engineering performances in terms of compressive/shear strength, stiffness, compressibility and durability over various curing periods; with CEM-I and lime used as controls.
2) Based on the performances from the stabilised artificial alluvium mixtures, design an optimum binder mixture for mixing within a natural soft alluvial soil

from Northumberland; using the same IBP's, AA's, CEM-I/lime controls, sample mixing and testing techniques as employed for the first objective.

3) Conduct mineralogical and microstructural analyses on stabilised Northumberland alluvium samples displaying the most desirable engineering performances to determine how the microstructure of the stabilised material changes with increasing curing time and to identify the formation of new cementitious minerals.

4) Characterise the geotechnical behaviour of the Northumberland alluvium in its natural untreated state by using oedometer, monotonic and dynamic triaxial testing. These results will provide insights into the soil's initial degree of structure, which would be lost when subjected to dynamic loads associated with DSM and passing high speed trains.

5) Incorporate the selected optimum IBP-AA binder and dosage within the Northumberland soil, cure for 28 days and assess its performance when subjected to the same oedometer and monotonic/dynamic triaxial testing conditions per the previous objective.

3.2 Experimental plan

The laboratory testing programme presented for this research is divided into three phases:

Phase 1: Initial binder development and preliminary performance testing for stabilising an artificial alluvium (aims 1–3; objectives 1–2)

Phase 2: Binder development, optimisation and performance testing for stabilising Lanton alluvium (aims 1–3; objective 2)

Phase 3: Detailed performance, mineralogical and microstructural studies on an optimised binder for stabilising Lanton alluvium (aims 1–4; objectives 3–5)

Figure 3.1 presents a flow chart, which defines the test types, binder materials, dosages and curing times used during each phase of this research experimental programme, along with the order in which they were conducted.

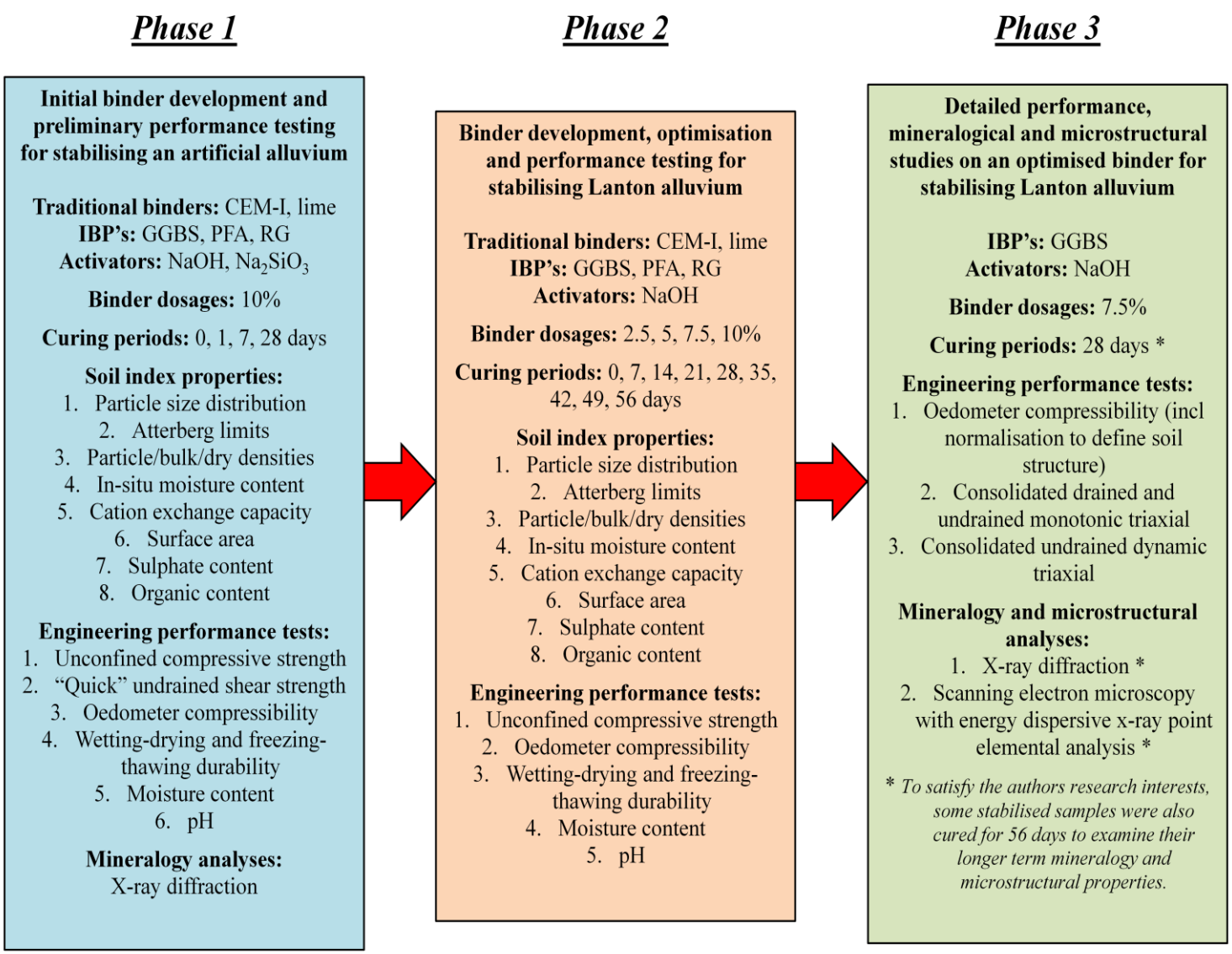

Figure 3.1: Flow chart defining the details and planned progression of this research programme's three experimental phases.

3.2.1 Phase 1

Phase 1 comprised a suite of geotechnical laboratory tests to investigate the mechanical strength and durability of a synthetic alluvial soil in its untreated state and when stabilised with traditional and various new alkali activated IBP binder mixtures. The laboratory prepared synthetic soil was chosen for study to ensure sample consistency and that findings were directly comparable with those published by Hughes et al. (2011). A suite of geotechnical and physico-chemical index property tests were also conducted to characterise the nature of the synthetic alluvium. The rationale behind conducting these tests is presented in section 3.3.1. The performances of alkali activated and non-activated GGBS (supplied by Frodingham Cement Ltd), PFA (supplied by ScotAsh Ltd) and RG (by Huntsman Tioxide Europe Ltd) as binders were examined. The NaOH and Na_2SiO_3 activators were supplied by Fisher Scientific UK Ltd. These materials were mixed within the soil both individually and in combination with each other to determine the most effective mixture for general engineering performance. For comparison, the soil was stabilised with the more traditional binders of CEM-I (supplied by Lafarge) and lime (supplied by Fisher Scientific UK Ltd). The binder mixtures tested in phase 1 are summarised in Table 3.1.

Table 3.1: Summary of the binder compositions used for phase 1 testing. (Note: C denotes non-alkali activated samples, AA denotes alkali activated samples.)

Mix	Composition (by dry weight of soil)
PFA-C	Artificial alluvium (15% grav. water) + 10% PFA
PFA-AA	Artificial alluvium (15% grav. water) + 7.2% PFA + 2.8% AA
RG-C	Artificial alluvium (15% grav. water) + 10% RG
RG-AA	Artificial alluvium (15% grav. water) + 7.2% RG + 2.8% AA
GGBS-C	Artificial alluvium (15% grav. water) + 10% GGBS
GGBS-AA	Artificial alluvium (15% grav. water) + 7.2% GGBS + 2.8% AA
PFA-RG-C	Artificial alluvium (15% grav. water) + 5% PFA + 5% RG
PFA-RG-AA	Artificial alluvium (15% grav. water) + 3.6% PFA + 3.6% RG + 2.8% AA
PFA-GGBS-C	Artificial alluvium (15% grav. water) + 5% PFA + 5% GGBS
PFA-GGBS-AA	Artificial alluvium (15% grav. water) + 3.6% PFA + 3.6% GGBS + 2.8% AA
GGBS-RG-C	Artificial alluvium (15% grav. water) + 5% GGBS + 5% RG
GGBS-RG-AA	Artificial alluvium (15% grav. water) + 3.6% GGBS + 3.6% RG + 2.8% AA
Lime	Artificial alluvium (15% grav. water) + 10% Lime
CEM-1	Artificial alluvium (15% grav. water) + 10% CEM-1

Several common laboratory tests were conducted to assess the performance of the various binders. These were unconfined compressive strength (UCS), "quick" undrained unconsolidated triaxial shear strength (UUT), oedometer compressibility, durability (freezing-thawing and wetting-drying), moisture content and pH. The reasoning behind using this suite of tests include their high levels of robustness in terms of geotechnical testing, ease of repeatability, capable of providing material parameters typically required by practitioners in geotechnical design and the EuroSoilStab (2002) standard. These in turn enable comparisons with engineering performance data previously published in the literature by workers including Al-Tabbaa et al., Hughes et al., Horpibulsuk et al. and Ahnberg et al. (please refer to chapter 2). Table 3.2 summarises the number of samples tested for each laboratory test. Triplicate samples of each mixture for all of the required curing periods and tests were produced to eliminate bias, enable the identification of any anomalous results and ultimately make the data sets more reliable.

Table 3.2: Summary of the number of samples tested for each mixture, curing period and geotechnical test for phase 1 of the experimental programme (continues overleaf).

Mix	Curing period (days)	Number of testing samples						
		UCS	UUT	Oedometer	Durability (w-d)	Durability (f-t)	Water content	pH
Synthetic alluvium	0	3	3	-	-	-	3	3
	1	3	3	-	-	-	3	3
	7	3	3	-	-	-	3	3
	28	3	3	3	3	3	3	3
PFA-C	0	3	3	-	-	-	3	3
	1	3	3	-	-	-	3	3
	7	3	3	-	-	-	3	3
	28	3	3	3	3	3	3	3
PFA-AA	0	3	3	-	-	-	3	3
	1	3	3	-	-	-	3	3
	7	3	3	-	-	-	3	3
	28	3	3	3	3	3	3	3
RG-C	0	3	3	-	-	-	3	3
	1	3	3	-	-	-	3	3
	7	3	3	-	-	-	3	3
	28	3	3	3	3	3	3	3
RG-AA	0	3	3	-	-	-	3	3
	1	3	3	-	-	-	3	3
	7	3	3	-	-	-	3	3
	28	3	3	3	3	3	3	3
GGBS-C	0	3	3	-	-	-	3	3
	1	3	3	-	-	-	3	3
	7	3	3	-	-	-	3	3
	28	3	3	3	3	3	3	3
GGBS-AA	0	3	3	-	-	-	3	3
	1	3	3	-	-	-	3	3
	7	3	3	-	-	-	3	3
	28	3	3	3	3	3	3	3
PFA-RG-C	0	3	3	-	-	-	3	3
	1	3	3	-	-	-	3	3
	7	3	3	-	-	-	3	3
	28	3	3	3	3	3	3	3

Mix	Curing period (days)	Number of testing samples						
		UCS	**UUT**	**Oedometer**	**Durability (w-d)**	**Durability (f-t)**	**Water content**	**pH**
PFA-RG-AA	0	3	3	-	-	-	3	3
	1	3	3	-	-	-	3	3
	7	3	3	-	-	-	3	3
	28	3	3	3	3	3	3	3
PFA-GGBS-C	0	3	3	-	-	-	3	3
	1	3	3	-	-	-	3	3
	7	3	3	-	-	-	3	3
	28	3	3	3	3	3	3	3
PFA-GGBS-AA	0	3	3	-	-	-	3	3
	1	3	3	-	-	-	3	3
	7	3	3	-	-	-	3	3
	28	3	3	3	3	3	3	3
GGBS-RG-C	0	3	3	-	-	-	3	3
	1	3	3	-	-	-	3	3
	7	3	3	-	-	-	3	3
	28	3	3	3	3	3	3	3
GGBS-RG-AA	0	3	3	-	-	-	3	3
	1	3	3	-	-	-	3	3
	7	3	3	-	-	-	3	3
	28	3	3	3	3	3	3	3
Lime	0	3	3	-	-	-	3	3
	1	3	3	-	-	-	3	3
	7	3	3	-	-	-	3	3
	28	3	3	3	3	3	3	3
CEM-1	0	3	3	-	-	-	3	3
	1	3	3	-	-	-	3	3
	7	3	3	-	-	-	3	3
	28	3	3	3	3	3	3	3

3.2.2 Phase 2

Findings from phase 1 were then used as the basis for phase 2 of testing. This examined the stabilising potential of the more successful alkali activated IBP binders from phase 1 when mixed at various dosages within a natural soft alluvium sourced from Lanton, near Wooler in Northumberland. A similar laboratory testing suite to that used for phase 1 was also used for phase 2, which aimed to determine the most effective "optimum" binder mixture for general engineering performance. As part of the design optimisation process, binders and activators which either produced poor engineering performances in phase 1 or were considered impractical for use in DDSM were not selected for further study in phases 2 or 3. The author recognises that artificial neural networks and Taguchi techniques would have been useful in the binder design optimisation process through the use of statistics. Therefore, these would be encouraged for use in future research. Table 3.3 summarises the binder mixtures tested in phase 2. Summarised in Table 3.4 is the number of samples which were tested for UCS, UUT, oedometer, durability, moisture content and pH testing. As for phase 1, triplicate samples of each mixture were produced for each curing period to maximise the reliability of the resulting data sets.

Table 3.3: Summary of the binder compositions used for phase 2 of the experimental programme.

Soil – Binder Mixture	Composition
Lanton	Lanton (25% grav. water)
Lanton + 5% Lime	Lanton (25% grav. water) + 5% lime
Lanton + 10% Lime	Lanton (25% grav. water) + 10% lime
Lanton + 5% CEM-1	Lanton (25% grav. water) + 5% CEM-I
Lanton + 10% CEM-1	Lanton (25% grav. water) + 10% CEM-I
Lanton + 10% PFA	Lanton (25 % grav. water) + 10 % PFA
Lanton + 10% PFA-NaOH	Lanton (25% grav. water) + 6.67% PFA + 3.33% NaOH
Lanton + 5% GGBS	Lanton (25% grav. water) + 5% GGBS
Lanton + 10% GGBS	Lanton (25% grav. water) + 10% GGBS
Lanton + 2.5% GGBS-NaOH	Lanton (25% grav. water) + 1.67% GGBS + 0.83% NaOH
Lanton + 5% GGBS-NaOH	Lanton (25% grav. water) + 3.33% GGBS+ 1.67% NaOH
Lanton + OLD 7.5% GGBS-NaOH	Lanton (25% grav. water) + 5% GGBS + 2.5% NaOH
Lanton + NEW 7.5% GGBS-NaOH	Lanton (25% grav. water) + 5% GGBS + 2.5% NaOH
Lanton + 10% GGBS-NaOH	Lanton (25% grav. water) + 6.67% GGBS + 3.33% NaOH

Table 3.4: Summary of the number of samples tested for each mixture, curing period and geotechnical test for phase 2 of the experimental programme (continues overleaf).

Mix	Curing period (days)	Number of testing samples					
		UCS	Oedometer	Durability (w-d)	Durability (f-t)	Water content	pH
Lanton alluvium	0	3	3	-	-	3	3
	7	3	-	-	-	3	3
	14	3	-	-	-	3	3
	21	3	-	-	-	3	3
	28	3	-	3	3	3	3
	35	3	-	-	-	3	3
	42	3	-	-	-	3	3
	49	3	-	-	-	3	3
	56	3	-	-	-	3	3
Lanton + 5% Lime	0	3	-	-	-	3	3
	7	3	-	-	-	3	3
	14	3	-	-	-	3	3
	21	3	-	-	-	3	3
	28	3	-	3	3	3	3
	35	3	-	-	-	3	3
	42	3	-	-	-	3	3
	49	3	-	-	-	3	3
	56	3	-	-	-	3	3
Lanton + 10% Lime	0	3	-	-	-	3	3
	7	3	-	-	-	3	3
	14	3	-	-	-	3	3
	21	3	-	-	-	3	3
	28	3	-	3	3	3	3
	35	3	-	-	-	3	3
	42	3	-	-	-	3	3
	49	3	-	-	-	3	3
	56	3	-	-	-	3	3
Lanton + 5% CEM-1	0	3	-	-	-	3	3
	7	3	-	-	-	3	3
	14	3	-	-	-	3	3
	21	3	-	-	-	3	3
	28	3	-	3	3	3	3

Mix	Curing period (days)	Number of testing samples					
		UCS	**Oedometer**	**Durability (w-d)**	**Durability (f-t)**	**Water content**	**pH**
	35	3	-	-	-	3	3
	42	3	-	-	-	3	3
	49	3	-	-	-	3	3
	56	3	-	-	-	3	3
Lanton + 10% CEM-1	0	3	-	-	-	3	3
	7	3	-	-	-	3	3
	14	3	-	-	-	3	3
	21	3	-	-	-	3	3
	28	3	-	3	3	3	3
	35	3	-	-	-	3	3
	42	3	-	-	-	3	3
	49	3	-	-	-	3	3
	56	3	-	-	-	3	3
Lanton + 10% PFA	0	3	-	-	-	3	3
	7	3	-	-	-	3	3
	14	3	-	-	-	3	3
	21	3	-	-	-	3	3
	28	3	-	3	3	3	3
	35	3	-	-	-	3	3
	42	3	-	-	-	3	3
	49	3	-	-	-	3	3
	56	3	-	-	-	3	3
Lanton + 10% PFA-NaOH	0	3	-	-	-	3	3
	7	3	-	-	-	3	3
	14	3	-	-	-	3	3
	21	3	-	-	-	3	3
	28	3	-	3	3	3	3
	35	3	-	-	-	3	3
	42	3	-	-	-	3	3
	49	3	-	-	-	3	3
	56	3	-	-	-	3	3
Lanton + 5% GGBS	0	3	-	-	-	3	3
	7	3	-	-	-	3	3
	14	3	-	-	-	3	3
	21	3	-	-	-	3	3
	28	3	-	3	3	3	3

Mix	Curing period (days)	Number of testing samples					
		UCS	**Oedometer**	**Durability (w-d)**	**Durability (f-t)**	**Water content**	**pH**
	35	3	-	-	-	3	3
	42	3	-	-	-	3	3
	49	3	-	-	-	3	3
	56	3	-	-	-	3	3
Lanton + 10% GGBS	0	3	-	-	-	3	3
	7	3	-	-	-	3	3
	14	3	-	-	-	3	3
	21	3	-	-	-	3	3
	28	3	-	3	3	3	3
	35	3	-	-	-	3	3
	42	3	-	-	-	3	3
	49	3	-	-	-	3	3
	56	3	-	-	-	3	3
Lanton + 2.5% GGBS-NaOH	0	3	-	-	-	3	3
	7	3	-	-	-	3	3
	14	3	-	-	-	3	3
	21	3	-	-	-	3	3
	28	3	3	3	3	3	3
	35	3	-	-	-	3	3
	42	3	-	-	-	3	3
	49	3	-	-	-	3	3
	56	3	-	-	-	3	3
Lanton + 5% GGBS-NaOH	0	3	-	-	-	3	3
	7	3	-	-	-	3	3
	14	3	-	-	-	3	3
	21	3	-	-	-	3	3
	28	3	3	3	3	3	3
	35	3	-	-	-	3	3
	42	3	-	-	-	3	3
	49	3	-	-	-	3	3
	56	3	-	-	-	3	3
Lanton + OLD 7.5% GGBS-NaOH	0	3	-	-	-	3	3
	7	3	-	-	-	3	3
	14	3	-	-	-	3	3
	21	3	-	-	-	3	3
	28	3	3	3	3	3	3

Mix	Curing period (days)	Number of testing samples					
		UCS	**Oedometer**	**Durability (w-d)**	**Durability (f-t)**	**Water content**	**pH**
	35	3	-	-	-	3	3
	42	3	-	-	-	3	3
	49	3	-	-	-	3	3
	56	3	-	-	-	3	3
Lanton + NEW 7.5% GGBS-NaOH	0	3	-	-	-	3	3
	7	3	-	-	-	3	3
	14	3	-	-	-	3	3
	21	3	-	-	-	3	3
	28	3	3	3	3	3	3
	35	3	-	-	-	3	3
	42	3	-	-	-	3	3
	49	3	-	-	-	3	3
	56	3	-	-	-	3	3
Lanton + 10% GGBS-NaOH	0	3	-	-	-	3	3
	7	3	-	-	-	3	3
	14	3	-	-	-	3	3
	21	3	-	-	-	3	3
	28	3	3	3	3	3	3
	35	3	-	-	-	3	3
	42	3	-	-	-	3	3
	49	3	-	-	-	3	3
	56	3	-	-	-	3	3

3.2.3 Phase 3

The alkali activated IBP binder which produced the most impressive performances from phase 2, was selected for stabilising the Lanton alluvium during phase 3 of the testing programme. However, in terms of selecting the optimum binder dosage for phase 3, this was not solely based on the engineering performances, but also on environmental and financial sustainability grounds.

3.2.3.1 Part 1: Mineralogical and microstructural characterisation

As identified by Van Impe and Verastegui-Flores (2006) and Wilkinson et al. (2010), interactions between soil and cementitious particles are still poorly understood and require further research. To quantify the engineering performances observed for the stabilised Lanton alluvium by using the optimum alkali activated IBP binder and dosage, it was important to gain insights into the mineralogical and microstructural changes occurring within the material during the curing process, via XRD and SEM-EDX techniques. To enable mineralogical and microstructural comparisons, samples of the untreated Lanton alluvium and binder were also analysed.

3.2.3.2 Part 2: Definition of soil structure

Oedometer testing was conducted during phase 2 on Lanton alluvium in its remoulded, undisturbed and stabilised states. The rationale behind conducting this testing stems from studies by Rouainia and Muir Wood (2000) and Gasparre and Coop (2008); whereby most natural soils are defined as having a degree of structure, which provides a degree of additional strength to the soil. Such soil structure is owed to its fabric (i.e. arrangement of particles and fissures, layering and any other inhomogeneities) and inter-particle bonding/cementation. The nature of a soil's structure is a direct result of its geological history; namely the depositional and post-depositional processes (Gasparre and Coop, 2008). Introducing an auger mixer to Lanton alluvium for DDSM

treatment will inevitably result in the removal of the soil's structure, given the unfavourable strength properties associated with alluvial soils (as defined in chapter 2). Therefore, results from oedometer tests were normalised according to the method defined by Gasparre and Coop (2008), to define the degree of initial structure within the Lanton alluvium and the level of DDSM treatment required to compensate for destructuration and provide the necessary strength gains required by EuroSoilStab (2002).

3.2.3.3 Part 3: Monotonic and dynamic triaxial characterisation

The final component of phase 3 of the experimental programme involved the monotonic and dynamic triaxial characterisation of remoulded, undisturbed and stabilised Lanton alluvium. Triaxial testing is viewed as one of the most versatile (Gasparre, 2005) and widely used geotechnical laboratory tests for investigating the shearing behaviour of geomaterials under a wide range of stress and strain conditions. All stress and strain conditions can be accurately monitored and controlled during tests. Through advancements in testing methodologies and testing equipment, the data obtained is generally of high quality.

In order to gain a comprehensive understanding of the short and long term behaviour of three materials, particularly in defining their respective critical state lines, yield surfaces and effective shear strength properties; consolidated drained and undrained monotonic tests were conducted under a minimum of four effective confining stress conditions. The same experimental plan was followed for dynamic tests, with the exception that only required consolidated undrained tests as a dynamic loading event due to a passing HST is a short-term event where generated pore pressures have not had sufficient time to dissipate. Triplicate samples of each material were tested for each effective confining stress used for undrained and drained tests to remove bias, identify anomalies and increase the overall reliability of the data recorded for subsequent analysis and interpretation. Tables 3.5-3.10 summarises details of all the samples tested and effective confining stresses used for the triaxial testing programme.

Table 3.5: Summary of the testing schedule followed for all static consolidated undrained triaxial tests on Lanton alluvium.

Sample ID	Sample type	Test type	Drainage conditions	Sample length (mm)	Sample diameter (mm)	Effective confining stress, p'_0 (kPa)
DisCIU1 (p'0 50)	Reconstituted	Monotonic, l	Undrained	202.96	100.64	50
DisCIU1 (p'0 100)	Reconstituted	Monotonic, l	Undrained	201.85	100.05	100
DisCIU1 (p'0 250)	Reconstituted	Monotonic, l	Undrained	201.55	99.33	250
DisCIU2 (p'0 50)	Reconstituted	Monotonic, l	Undrained	186.84	105.25	50
DisCIU2 (p'0 100)	Reconstituted	Monotonic, l	Undrained	185.09	104.25	100
DisCIU2 (p'0 150)	Reconstituted	Monotonic, l	Undrained	183.94	103.60	150
DisCIU3 (p'0 100)	Reconstituted	Monotonic, l	Undrained	177.72	101.52	100
DisCIU3 (p'0 150)	Reconstituted	Monotonic, l	Undrained	176.41	100.77	150
DisCIU4 (p'0 50)	Reconstituted	Monotonic, l-u-r	Undrained	175.63	110.93	50
DisCIU4 (p'0 150)	Reconstituted	Monotonic, l-u-r	Undrained	174.01	109.87	150
DisCIU4 (p'0 250)	Reconstituted	Monotonic, l-u-r	Undrained	173.14	109.32	250
DisCIU5 (p'0 50)	Reconstituted	Monotonic, l-u-r	Undrained	188.91	103.22	50
DisCIU5 (p'0 150)	Reconstituted	Monotonic, l-u-r	Undrained	187.10	102.23	150
DisCIU5 (p'0 250)	Reconstituted	Monotonic, l-u-r	Undrained	185.92	101.57	250
DisCIU6 (p'0 50)	Reconstituted	Monotonic, l-u-r	Undrained	187.96	103.06	50
DisCIU6 (p'0 150)	Reconstituted	Monotonic, l-u-r	Undrained	186.21	102.08	150
DisCIU6 (p'0 250)	Reconstituted	Monotonic, l-u-r	Undrained	185.09	101.41	250
UndisCIU1 (p'0 50)	Undisturbed	Monotonic, l	Undrained	198.17	103.42	50
UndisCIU1 (p'0 150)	Undisturbed	Monotonic, l	Undrained	189.65	98.87	150
UndisCIU1 (p'0 250)	Undisturbed	Monotonic, l	Undrained	187.37	97.73	250
UndisCIU1 – Bristol	Undisturbed	Monotonic, l	Undrained	177.03	102.57	50

Table 3.6: Summary of the testing schedule followed for all static consolidated drained triaxial tests on Lanton alluvium.

Sample ID	Sample type	Test type	Drainage conditions	Sample length (mm)	Sample diameter (mm)	Effective confining stress, p'_0 (kPa)
DisCID1 (p'0 50)	Reconstituted	Monotonic, l	Drained	188.65	103.40	50
DisCID3 (p'0 50)	Reconstituted	Monotonic, l	Drained	178.81	106.94	50
DisCID4 (p'0 50)	Reconstituted	Monotonic, l	Drained	189.65	101.48	50
DisCID5 (p'0 50)	Reconstituted	Monotonic, l	Drained	191.40	101.11	50
DisCID6 (p'0 50)	Reconstituted	Monotonic, l	Drained	186.91	102.63	50
DisCID7 (p'0 150)	Reconstituted	Monotonic, l	Drained	186.87	102.21	150
DisCID8 (p'0 150)	Reconstituted	Monotonic, l	Drained	184.19	101.13	150
DisCID9 (p'0 150)	Reconstituted	Monotonic, l	Drained	186.90	100.07	150
DisCID11 (p'0 200)	Reconstituted	Monotonic, l	Drained	189.12	101.07	200
DisCID12 (p'0 200)	Reconstituted	Monotonic, l	Drained	188.26	99.84	200
DisCID13 (p'0 200)	Reconstituted	Monotonic, l	Drained	185.23	102.24	200
DisCID14 (p'0 50)	Reconstituted	Monotonic, l-u-r	Drained	189.06	101.40	50
DisCID15 (p'0 50)	Reconstituted	Monotonic, l-u-r	Drained	192.41	101.37	50
DisCID16 (p'0 50)	Reconstituted	Monotonic, l-u-r	Drained	191.28	101.31	50
DisCID17 (p'0 150)	Reconstituted	Monotonic, l-u-r	Drained	187.59	100.75	150
DisCID18 (p'0 150)	Reconstituted	Monotonic, l-u-r	Drained	186.28	99.97	150
DisCID19 (p'0 150)	Reconstituted	Monotonic, l-u-r	Drained	183.83	99.76	150
DisCID20 (p'0 200)	Reconstituted	Monotonic, l-u-r	Drained	185.17	100.32	200
DisCID21 (p'0 200)	Reconstituted	Monotonic, l-u-r	Drained	182.42	101.83	200
DisCID22 (p'0 200)	Reconstituted	Monotonic, l-u-r	Drained	186.61	99.63	200
UndisCID1 (p'0 50)	Undisturbed	Monotonic, l	Drained	125.57	49.76	50
UndisCID2 (p'0 150)	Undisturbed	Monotonic, l	Drained	123.48	49.64	150
UndisCID3 (p'0 200)	Undisturbed	Monotonic, l	Drained	103.22	47.89	200

Table 3.7: Summary of the testing schedule followed for all dynamic consolidated undrained triaxial tests on Lanton alluvium.

Sample ID	Sample type	Test type	Drainage conditions	Sample length (mm)	Sample diameter (mm)	Effective confining stress, p'_0 (kPa)
Dis-3m_1	Reconstituted	Dynamic	Undrained	186.13	99.83	60
Dis-3m_2	Reconstituted	Dynamic	Undrained	185.15	99.72	60
Dis-3m_3	Reconstituted	Dynamic	Undrained	185.62	98.98	60
Dis-7.5m_1	Reconstituted	Dynamic	Undrained	188.44	99.66	108.65
Dis-7.5m_2	Reconstituted	Dynamic	Undrained	188.80	100.34	108.65
Dis-7.5m_3	Reconstituted	Dynamic	Undrained	189.21	99.54	108.65
Dis-12m_1	Reconstituted	Dynamic	Undrained	186.55	99.74	147.48
Dis-12m_2	Reconstituted	Dynamic	Undrained	188.03	99.68	147.48
Dis-12m_3	Reconstituted	Dynamic	Undrained	187.62	97.91	147.48
Undis-3m_1	Undisturbed	Dynamic	Undrained	117.70	48.65	60
Undis-3m_2	Undisturbed	Dynamic	Undrained	106.59	50.21	60
Undis-7.5m_1	Undisturbed	Dynamic	Undrained	111.69	49.26	108.65
Undis-7.5m_2	Undisturbed	Dynamic	Undrained	109.28	49.41	108.65
Undis-12m_1	Undisturbed	Dynamic	Undrained	110.03	49.48	147.48
Undis-12m_2	Undisturbed	Dynamic	Undrained	108.73	50.07	147.48

Table 3.8: Summary of the testing schedule followed for all monotonic consolidated undrained triaxial tests on GGBS-NaOH stabilised Lanton alluvium.

Sample ID	Sample type	Test type	Drainage conditions	Sample length (mm)	Sample diameter (mm)	Effective confining stress, p'_0(kPa)
28d CIU 1 (p'0 50)	28 day cemented	Monotonic, l	Undrained	75.51	39.07	50
28d CIU 2 (p'0 50)	28 day cemented	Monotonic, l	Undrained	76.64	38.82	50
28d CIU 3 (p'0 100)	28 day cemented	Monotonic, l	Undrained	76.20	39.23	100
28d CIU 4 (p'0 100)	28 day cemented	Monotonic, l	Undrained	75.47	38.71	100
28d CIU 5 (p'0 100)	28 day cemented	Monotonic, l	Undrained	87.50	38.99	100
28d CIU 6 (p'0 200)	28 day cemented	Monotonic, l	Undrained	83.11	38.99	200
28d CIU 7 (p'0 200)	28 day cemented	Monotonic, l	Undrained	77.08	38.88	200
28d CIU 8 (p'0 200)	28 day cemented	Monotonic, l	Undrained	90.07	38.84	200
28d CIU 9 (p'0 400)	28 day cemented	Monotonic, l	Undrained	85.37	38.92	400
28d CIU 10 (p'0 600)	28 day cemented	Monotonic, l	Undrained	89.13	39.12	600
28d CIU 11 (p'0 600)	28 day cemented	Monotonic, l	Undrained	89.38	38.90	600
28d CIU 12 (p'0 50)	28 day cemented	Monotonic, l	Undrained	75.94	38.84	50
28d CIU 13 (p'0 400)	28 day cemented	Monotonic, l	Undrained	87.56	38.93	400
28d CIU 14 (p'0 400)	28 day cemented	Monotonic, l	Undrained	86.78	38.88	600
28d CIU 15 (p'0 600)	28 day cemented	Monotonic, l	Undrained	87.68	38.88	600
28d CIU 1 (CP' 50) – Bristol	28 day cemented	Monotonic, l	Undrained	179.0	104.03	50

Table 3.9: Summary of the testing schedule followed for all monotonic consolidated drained triaxial tests on GGBS-NaOH stabilised Lanton alluvium.

Sample ID	Sample type	Test type	Drainage conditions	Sample length (mm)	Sample diameter (mm)	Effective confining stress, p'_0(kPa)
28d CID 1 (p'0 200)	28 day cemented	Monotonic, l	Drained	89.93	38.89	200
28d CID 2 (p'0 200)	28 day cemented	Monotonic, l	Drained	89.88	38.89	200
28d CID 3 (p'0 400)	28 day cemented	Monotonic, l	Drained	89.83	39.02	400
28d CID 4 (p'0 400)	28 day cemented	Monotonic, l	Drained	90.09	38.88	400
28d CID 5 (p'0 600)	28 day cemented	Monotonic, l	Drained	89.02	39.19	600
28d CID 6 (p'0 600)	28 day cemented	Monotonic, l	Drained	89.98	38.84	600
28d CID 7 (p'0 200)	28 day cemented	Monotonic, l	Drained	89.14	38.81	200
28d CID 8 (p'0 400)	28 day cemented	Monotonic, l	Drained	87.63	38.45	400
28d CID 9 (p'0 600)	28 day cemented	Monotonic, l	Drained	89.17	38.91	600

Table 3.10: Summary of the testing schedule followed for all dynamic consolidated undrained triaxial tests on GGBS-NaOH stabilised Lanton alluvium.

Sample ID	Sample type	Test type	Drainage conditions	Sample length (mm)	Sample diameter (mm)	Effective confining stress, p'_0 (kPa)
-3m_1	28 day cemented	Dynamic	Undrained	88.83	39.16	60
-3m_2	28 day cemented	Dynamic	Undrained	89.08	38.98	60
-3m_3	28 day cemented	Dynamic	Undrained	89.07	38.98	60
-7.5m_1	28 day cemented	Dynamic	Undrained	89.18	38.91	108.65
-7.5m_2	28 day cemented	Dynamic	Undrained	88.91	38.73	108.65
-7.5m_3	28 day cemented	Dynamic	Undrained	88.90	38.73	108.65
-12m_1	28 day cemented	Dynamic	Undrained	90.02	38.86	147.48
-12m_2	28 day cemented	Dynamic	Undrained	89.84	38.75	147.48
-12m_3	28 day cemented	Dynamic	Undrained	89.83	38.74	147.48

Two advanced monotonic consolidated undrained triaxial tests were conducted on the undisturbed and stabilised Lanton alluvium at Bristol University, which involved small strain measurements. The rationale behind conducting these tests was to gain insights into the behaviour of these two materials at small strain levels, which typically occur around geotechnical structures (Clayton, 2011) and therefore are of importance in geotechnical design. The reader is forwarded to Appendix 5 for the results obtained from these tests.

3.3 Testing methods

3.3.1 Index properties testing

As defined by Terzaghi et al. (1996), the design of all geotechnical structures is based upon simple empirical rules, which may only be adopted by experienced engineers. Geotechnical engineers rely upon adequate soil descriptions made by themselves and others as a key part of the design process. To reduce the number of ambiguities when working with soils, given their high levels of variability, it has become important to define simple methods for distinguishing between soil types (Terzaghi et al., 1996). The properties upon which distinctions are based are labelled "index properties".

To characterise both the artificial and natural Lanton alluvial soils in terms of their geotechnical index properties, a series of classification tests were conducted in accordance with procedures presented within BS 1377 parts 2 and 4 (BSI, 1990). The tests conducted were particle size distribution (PSD) through wet sieving and sedimentation, Atterberg limits (to determine the soil's liquid and plastic limits and plasticity indices), particle density, natural in-situ moisture contents and compaction testing to determine the soil's optimum moisture contents, bulk and dry densities. Based on the results obtained from these classification tests and field descriptions of the soils, an engineering soil description and final classification per BS 5930 (BSI, 1999) criteria was then assigned to the synthetic and natural alluvial soils.

Further to these classification tests, both the synthetic and Lanton soils were subjected to a series of physico-chemical tests to gain an understanding of their capacities to react with binders and ultimately produce cementitious gels. The pH of the synthetic and Lanton soils in their untreated and stabilised states after various curing periods were measured per the procedure outlined within BS 1377 part 3 (BSI, 1990). The equipment used to determine soil pH was a Camlab ultrameter 6P.

Cation exchange capacity (CEC) and specific surface area testing was then conducted. The former provides an estimate of the number of sites on clay minerals within a soil where cation exchange may occur. Inherently, soils with high surface area values (i.e. those characterised by higher clay contents) result in higher CEC values. Hence, knowledge about a soil's CEC and surface area properties provides a crucial insight into its potential for undergoing future reactions between soil particles and the cementitious binder, and therefore the formation of cementitious gels. The method used for CEC analysis was BS: 7755, Section 3.12:1996, ISO 13536:1995, using barium chloride solution buffered at a pH of 8.1. For CEC analyses, the equipment used was a Varian Spectraa 400 Atomic Absorption Spectrometer (AAS); whereby 15 g samples were required to be oven dried and passing a 2 mm sieve. By using the CEC values obtained, the CEC-related charge density (σ_{CEC}) for the soils was obtained from Equation 3.1 as stated by Meunier (2005):

$$\sigma_{CEC} = \frac{e\ (CEC\ x\ 10^{-2})}{2\ ab} \qquad \textbf{(Equation 3.1)}$$

where e = the elementary charge, which has a constant value of 1.6022 x 10^{-2} C. a and b are unit cell parameters for the clay mineral in the x-y plane. (For kaolinite a = 0.531 nm and b = 0.92 nm; Meunier, 2005.)

The surface area of a soil can influence its physical and chemical characteristics. For CEC, larger surface area provides more exchangeable surfaces. For determining the surface areas of the soils, the Brunauer Emmett Teller (BET) nitrogen absorption method was adopted (Brunauer et al., 1938) by using a Micromeritics Tristar 300 machine. Besides the CEC and BET surface area testing, given the natural

Northumberland alluvium was chemically and mineralogically more complex than the synthetic alluvium, it was also subjected to total organic carbon and total organic matter testing. Per Nair and Little (2009), the presence of sulphates within soils can have detrimental effects on their long-term engineering performances when stabilised with cementitious binders. This arises from the likely formation of ettringite and/or thaumasite minerals, which swell upon contact with water. Hence, the Northumberland soil was also tested for its sulphate content. The equipment used was a Dionex Ion-Chromatography ICS-1000 and samples were 0.2 micron filtered.

3.3.2 General engineering performance testing

3.3.2.1 Laboratory tests

Several laboratory tests were conducted to assess the performance of the various binders. Strength and stiffness was primarily assessed via unconfined compressive strength (UCS) through using an Instron 5585H testing frame, according to BS 1377: Part 7: Clause 7 (BSI 1990). The strain rate used for all compression tests was 1.5 mm/min and samples were tested either to failure or to a maximum axial strain of 15%. Strength and stiffness was also assessed through UUT testing in accordance with BS 1377: Part 7: Clause 8 (BSI 1990). Samples were tested at a constant strain rate of 1.27 mm/min either to failure or a maximum of 15% axial strain. Three confining stresses were used to more accurately define an average undrained shear strength of the materials; namely 50, 100 and 200 kPa. Compressibility was assessed by oedometer testing (BS 1377: Part 5, BSI 1990), whereby tests involved conducting a series of unload-reload loops up to a maximum vertical stress of 1600 kPa.

Durability was assessed by wetting-drying and freeze-thaw durability tests (ASTM D559 and ASTM D560 respectively, ASTM 1996a and 1996b). In the UK, wetting-drying cycles actively occur within soils up to depths of 3.5 metres, whereas freeze-thaw processes can occur up to 2 metres; subject to some variation between locations due to in-situ soil and vegetation conditions (Clarke and Smethurst, 2010). For temperate maritime climates similar to that experienced in the UK, rainfall occurs

throughout the year and therefore any related surface water is likely to percolate through the sub-surface. Thus, in locations where DDSM columns are installed, there is potential for water to percolate through or around the columns, causing swelling during wetting or thawing periods and shrinkage during drier or freezing periods. Therefore, should IBP binders be mixed into problematic soils via DDSM, they must be able to endure such wetting-drying and freezing-thawing cycles and provide resistance against soil-cement losses, volume and water content changes to prevent the failure of DDSM columns and any consequential adversities for overlying loads or structures. Considering the UK's temperate maritime climate, the ASTM 559 and 560 standards for conducting wetting-drying and freezing-thawing durability testing on stabilised alluvium may be considered fairly extreme, given the climatic conditions typical in the UK. Hence, the standard followed in this study is probably more representative of climatic conditions in other countries.

As sufficient volumes of water within soils and a minimum pH value of 10.5 are required to promote pozzolanic conditions for long-term strength development (Davidson et al., 1965), the moisture content and pH of all stabilised soil mixtures were tested before and after each curing period. Sample moisture contents were measured according to BS 1377: Part 2 (BSI, 1990) and pH was measured by using a Camlab ultrameter 6P (BS 1377: Part 3; BSI, 1990).

3.3.2.2 Sample preparation

To create test samples, various alkali activated and non-activated binder combinations were added to the synthetic and Lanton alluvial soils at numerous dosages between 2.5 and 10% by dry weight to identify the most effective binder and corresponding dosage. For phase 1 of testing, the artificial soil was produced by mixing fine silica sand (produced by WBB Minerals Ltd) with grade E kaolin (produced by English China Clay International Europe Ltd) at a ratio of 70:30 and water was added to achieve a gravimetric moisture content of 15% (Hughes et al., 2011). The new activator used in this study was created by mixing NaOH and Na_2SiO_3 at a ratio of 1:2, which was added to the IBP binders at a concentration of 20% by dry weight.

For phase 2 of testing, samples of the Northumberland alluvium were obtained from the field and oven dried at 110^{o}C for 24 hours. Once the soil had been dried, crushing was required to break down large soil agglomerations (up to 70 mm diameter) into a fine powder (particle size ≤1 mm); thereby increasing practicality when mixing binders within the soils in the laboratory. Stabilised samples were then mixed by using a rotary mixing machine for 10 minutes (Figure 3.2). Water was added to the stabilised mixtures to achieve the required pre-treatment (in-situ) soil moisture content of 25%.

Figure 3.2: Hobart rotary mixing machine used for mixing stabilised soil samples.

All the industrial by-product (IBP) materials examined in this research came as fine powders prior to soil mixing, with the exception of RG, which required additional preparation before use. RG, in its raw form contains water and thus was inappropriate for mixing, given that DDSM involves the use of dry cementitious powders. Thus, the RG required oven drying and milling down to a fine powder before use as a binder.

Samples were created by tamping and compressing the stabilised soils into split-sample moulds (Figure 3.3), which were then placed in a hydraulic press to compact the material to the correct dimensions. This allowed the production of samples with consistent dimensions, water contents and density at relatively rapid rates. For UCS and UUT tests, 38 mm diameter, 76 mm long samples were created. For oedometer

compressibility testing, 76 mm diameter x 18 mm thick samples were prepared and cured within oedometer rings and sealed using three layers of cling film. Finally, 105 mm diameter 115 mm long samples were prepared and cured for durability testing. All samples were prepared based on optimum compaction criteria.

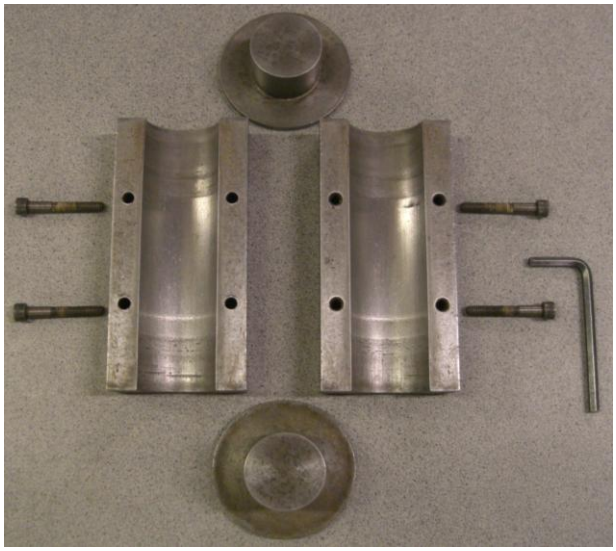

Figure 3.3: Split sample mould used to prepare stabilised soil specimens for compressive and shear strength testing.

For strength testing, samples were cured within wax-sealed PVC sample moulds for periods of 0 (day of mixing), 1, 7, 14, 21, 28, 35, 42, 49 and 56 days, and were stored within a temperature controlled room (55% relative humidity, 20^{o}C ambient air temperature). For compressibility and durability (wetting-drying and freezing-thawing) testing, samples were cured for 28 days before testing, based on construction specifications defined by Hansson et al. (2001). Once cured, the samples were extruded, trimmed (or carefully ground down for stiffer samples according to ASTM D4543-08 to tolerances not exceeding 25µm; ensuring they were smooth, flat, parallel to each other and perpendicular to the samples' longitudinal axes) to the appropriate dimensions and then tested. The author acknowledges that leaching testing of the stabilised soil mixtures is also required, and is therefore mentioned in Chapter 10 as a recommendation for future works.

3.3.3 Mineralogical and microstructural investigations

Upon completing the geotechnical testing components of phases 1 and 2 of the experimental programme on the stabilised synthetic and Lanton alluvium soil mixtures, their mineralogical properties when untreated and stabilised with the range of IBP binders used were analysed using X-ray diffraction analysis (XRD). The XRD technique involves a focussed X-ray beam being directed onto a powdered sample. The diffracted X-rays are then recorded. The pattern produced determines the mineralogy of grains within the material. Although XRD is very useful in determining the mineralogy of the untreated soil and the raw binder, it has difficulty in identifying new cementitious minerals. As recognised by Hughes and Glendinning (2004), this arises from their amorphous nature and cement minerals are hydrates. XRD cannot detect minerals whose elemental composition are characterised by low atomic numbers (i.e. hydrogen = 1).

3.3.3.1 XRD apparatus

XRD analyses were conducted by research staff (Ms Maggie White) within Newcastle University's Advanced Chemical and Materials Analysis unit. The equipment used was a PANalytical X'Pert Pro MPD, powered by a Philips PW3040/60 X-ray generator and fitted with an X'Celerator detector (Figure 3.4). Diffraction data was obtained by exposing dried powder samples of Lanton alluvium to Cu-Kα X-ray radiation, with a wavelength of 1.5418 Å. X-rays were generated from a Cu anode supplied with 40 kV and a current of 40 mA. Post analysis, mineral phases were identified by using the X'Pert accompanying software program PANalytical High Score Plus, in conjunction with the ICDD Powder Diffraction File 2 Database, sets 1-49 (ICDD, 1999), ICDD Powder Diffraction File 4 - Minerals (2012), the American Mineralogist Crystal Structure Database (March 2010) and the Crystallography Open Database (February 2012; www.crystallography.net).

(a)  (b) 

Figure 3.4: PANalytical X'Pert Pro MPD diffractometer: (a) 15 berth sample magazine autochanger and (b) a sample loaded onto the spinning stage. Photographs courtesy of ACMA (2014).

3.3.3.2 XRD sample preparation

For XRD analyses, all the stabilised sample mixtures tested were required to be in a fine and dried powder form (i.e. grain size of <1-2 mm). The stabilised samples required air drying and were carefully ground down to a fine powder by using a mortar and pestle. Per Hughes (2005), the raw GGBS binder was not analysed using XRD due to its amorphous glassy nature.

3.3.3.3 SEM apparatus

In addition to having their mineralogy examined through XRD, the microstructure and chemical composition of the most impressive binder mixture in stabilising Lanton alluvium soil was examined by using scanning electron microscopy (SEM). SEM is able to provide a direct means of observing cementation processes within stabilised samples and identifying newly formed cementitious gels. The chemical composition of individual grains and cementitious gels was quantified by using energy dispersive X-ray (EDX) point element analysis, undertaken whilst performing SEM analysis.

However, intelligent interpretation was required to determine which minerals were present within the samples by using the EDX and XRD data sets. The equipment used for SEM-EDX analyses was a Philips XL30 ESEM-FEG (Figure 3.5). Assistance in using the equipment was provided by research staff within Newcastle University's Advanced Chemical and Materials Analysis unit.

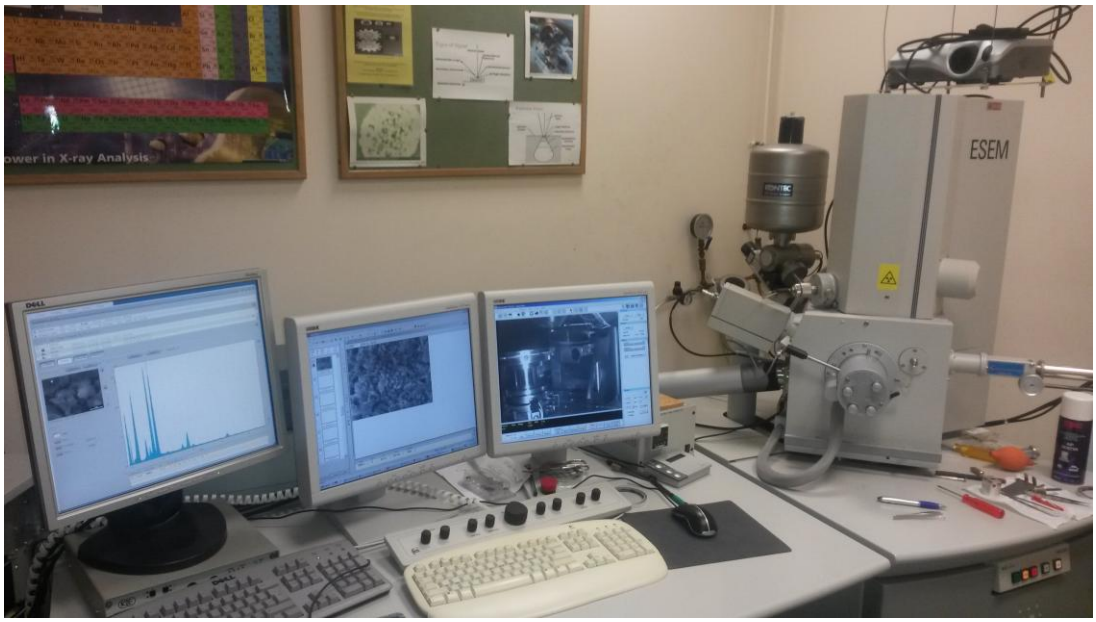

Figure 3.5: Photograph of Philips XL30 ESEM-FEG at Newcastle University (ACMA).

Due to financial and time constraints, not all of the stabilised soil mixtures tested from phases 1 and 2 could be analysed. Samples which produced the most impressive engineering performances after curing periods of 28 and 56 days and demonstrated encouraging sustainability potential were prioritised for mineralogical and microstructural analysis.

3.3.3.4 SEM sample preparation

For SEM-EDX analyses, 5-10 g sprinklings of dried Lanton alluvium and GGBS powders were placed onto sticky tabs and then mounted onto aluminium stubs. The GGBS used to stabilise Lanton alluvium was provided by Hansen Cements UK in a

dried powder form, whose grain size passes the 63 μm sieve with a surface area of 4000 – 6000 cm^2/g (BS EN 15167-1; Leung and Wong, 2010) and therefore required no further sample preparation for SEM-EDX analysis. It was important that any excess powder was removed from the tabs, as these would be likely to move when analysed in the SEM. For analysing GGBS-NaOH stabilised Lanton alluvium samples, small 10 mm diameter sub-samples were simply broken off from their original 76 mm long 38 mm diameter cured samples. These samples were then mounted and secured to the aluminium stubs by using a silver electrodag glue. Coating SEM samples with gold makes them electrically conductive (Wilkinson et al., 2010a), which is preferable for taking high quality SEM micrographs. However, samples in this study were not gold coated as it would prevent EDX analyses from accurately determining the elemental composition of cemented soil samples. This is imperative in identifying which cementitious mineral phases formed during the curing process. SEM micrographs were taken at magnifications of x800 and x2000 to visualise both the overall microstructure of treated and untreated samples, besides any cementitious bonding between soil and binder particles.

3.3.4 Monotonic and dynamic triaxial testing

3.3.4.1 Triaxial apparatus

At Newcastle, a conventional effective stress path triaxial apparatus was used to conduct both monotonic consolidated drained/undrained and dynamic consolidated undrained triaxial tests on cylindrical samples up to 100 mm diameter, which had height-diameter ratios of 2 and were enclosed within sealed latex rubber membranes. The specific equipment used was an electro-mechanical GDS Enterprise Level Dynamic Triaxial Testing system (ELDYN), whose maximum operating frequency for dynamic tests was 5 Hz. Detailed sketches of the ELDYN apparatus are presented in Figures 3.6 – 3.8. Samples were mounted on the base pedestal and fully submerged in pressurised water within the triaxial cell. Base pedestal adaptors for 38, 50 and 100 mm diameter samples were designed and manufactured in-house at Newcastle

University. Sample drainage, measurement of pore pressures and the application of back pressures to samples were enabled by connecting a thin nylon tube between the back pressure lines and the top cap. This also allowed water to pass from sample bases to the back pressure lines via the base pedestal. The maximum load capacity of the ELDYN's electro-mechanical actuator and therefore for all tests was 5 kN; albeit the capacity of the submersible load cell was 8 kN.

The cell and back pressures were supplied by a compressor (maximum capacity 10–16 bar). The air pressures provided were applied to testing samples in the form of hydraulic pressures via air-water interfaces. Given the relatively low pressures required for testing Lanton alluvium, cell and back pressures were regulated manually by using Norgren pressure regulators, which had maximum capacities of 10 bar. To accurately measure the cell, back and pore pressures during triaxial tests, Druck pressure transducers (maximum capacity 15 bar) were fitted, all having been calibrated using a 4 MPa capacity GDS standard pressure volume controller.

Two separate volume change units were attached to the triaxial apparatus. The unit primarily used due to higher levels of accuracy was the Imperial College volume cell (ICVC), which had a maximum capacity of 50 ml. The ICVC unit contains a belloframe and sealed piston, which moves up when there is an increase in air pressure and decrease in water pressure – causing water to flow into the sample, and vice versa. When a sample is fully saturated and assuming water is incompressible, a change in the volume of water within the ICVC corresponds to a change in sample volume. To accurately monitor changing volumes within the ICVC and therefore volumetric strains within the sample, a linearly variable differential transformer (LVDT) was attached to the ICVC.

The second volume change unit used was the Barry Clarke volume gauge (BCVG), which had a maximum capacity of approximately 150 ml. The BCVG is based on a simple air-water interface. An increase in air pressure and decrease in water pressure would result in water flowing out from the bottom of the BCVG and into the sample. The BCVG comprises 15 mm and 5 mm diameter transparent plastic tubes, whereby the former is more suited to measuring larger volumetric strains and the latter for smaller volumetric strains. To measure the volume of water present within the BCVG during testing, a transducer and digital volt meter were fitted to the base of the unit and calibrated such that a certain volume of water corresponded to a specific voltage

output. The BCVG unit was used as a secondary volume change unit and predominantly served to conduct permeability tests besides acting as a means of filling and emptying the Imperial College volume cell between triaxial tests.

The triaxial cell's submersible load cell worked in conjunction with the electro-mechanical actuator to record changes in load and axial displacement experienced by samples. This provided an external means of axial strain measurement. Although all these transducers had been calibrated and fitted to the triaxial apparatus, only four transducer ports were available on the GDS ELDYN's data logger. Hence, for all tests, the GDS Lab data acquisition software recorded all raw data for cell pressure, back pressure/pore pressure at the sample base, volume change using the ICVC and load/displacement via the triaxial cell's submersible load cell. Besides the digital recording of cell, back and pore pressures during testing via the Druck pressure transducers, a secondary pressure indicating panel was utilised for pressure monitoring purposes.

The method used to pressurise the triaxial cell depended on whether samples were to be tested monotonically or dynamically. For monotonic tests, the triaxial cell was completely filled with de-aired water; thereby completely submerging samples and pressurised using an air/water bladder interface. The bladder served as both a reservoir and interface between the de-aired water and compressed air, which could provide cell pressures to approximately 800kPa.

For dynamic tests, per ASTM D5311-11 (ASTM, 2012) samples were completely submerged in de-aired water whilst ensuring that an air pocket remained at the top of the triaxial cell to ensure ease of movement of the piston/submersible load cell in and out of the triaxial cell. This also prevented any cell pressure fluctuations during dynamic tests. Once this had been achieved, the water within the triaxial cell was pressurised using compressed air directly from an air line leading directly into the top of the triaxial cell.

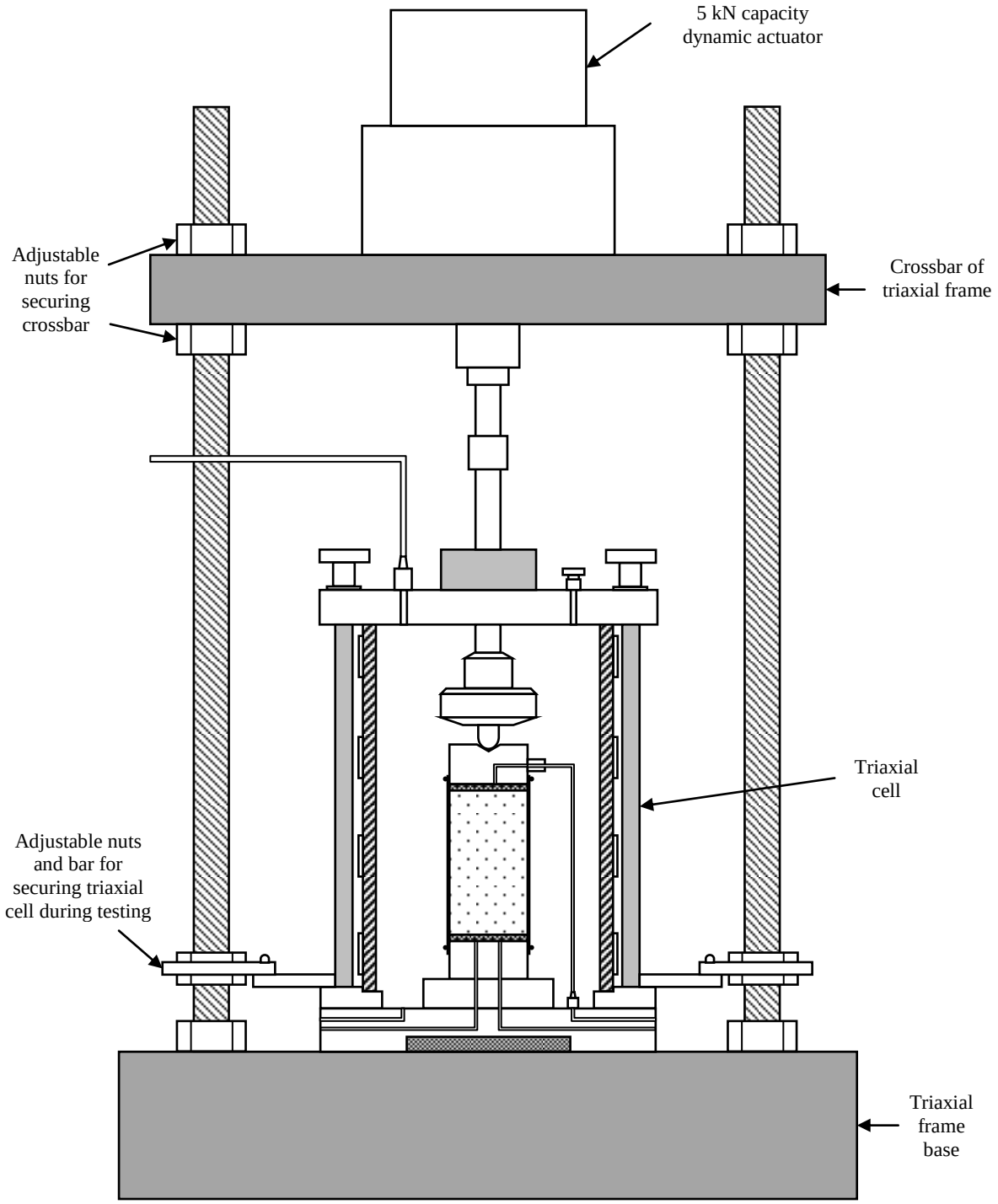

Figure 3.6: Schematic of the ELDYN triaxial frame at Newcastle University.

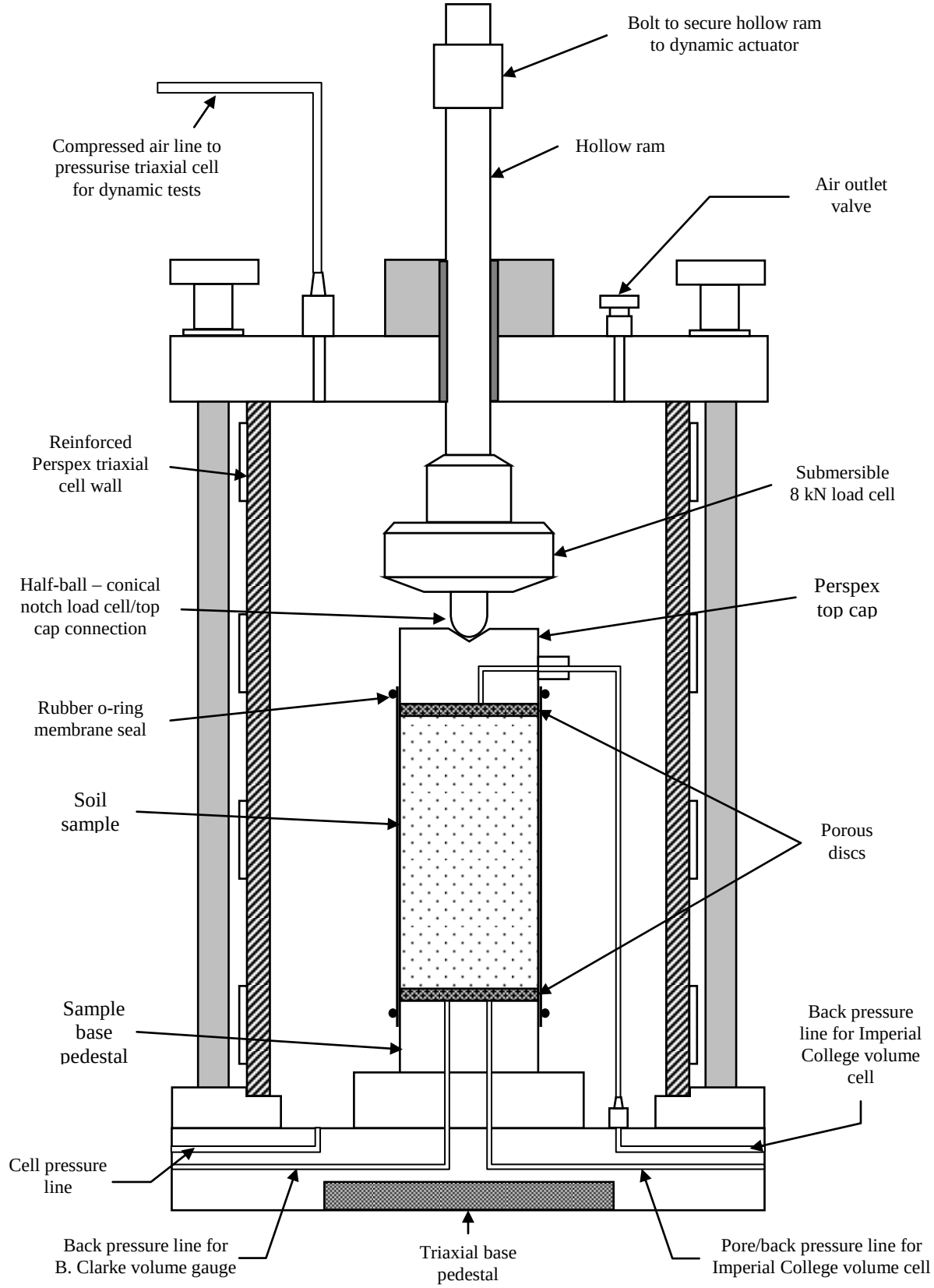

Figure 3.7: Detailed schematic of the ELDYN triaxial cell.

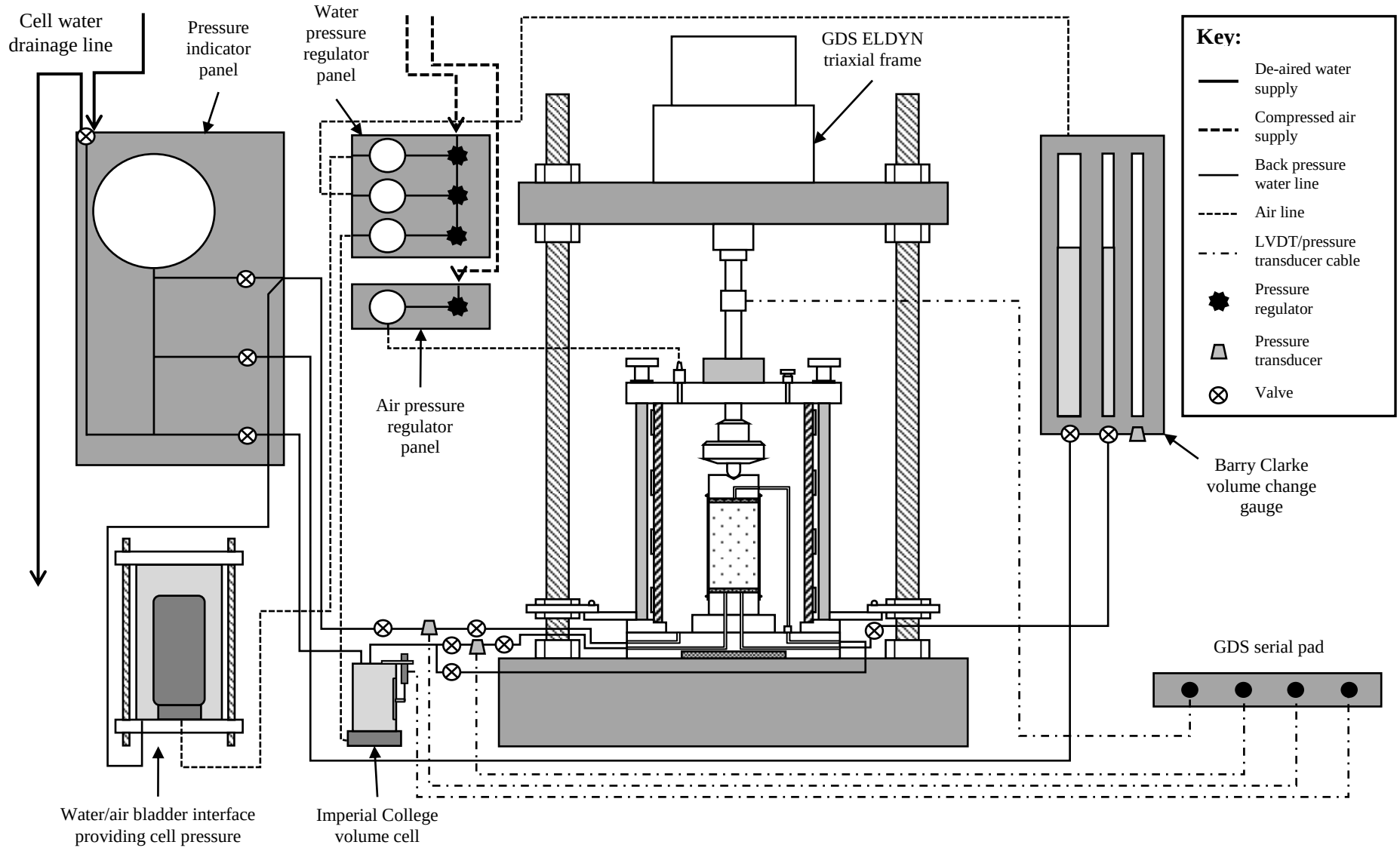

Figure 3.8: Schematic of complete ELDYN triaxial apparatus; including pressure regulators/indicators, back pressure lines, volume change and serial pad devices.

During the early phases of testing, sample top caps were docked with the submersible load cell by using the half-ball connection, where the half ball conical fitting on the end of the load cell was seated within a concave depression on the surface of the top cap (Figure 3.9a). To ensure a constant contact was maintained between the load cell and the top surfaces of samples during saturation, consolidation and at the start of shearing; the constant deviator stress function within the GDS Lab software was utilised. However, similar to observations by Gasparre (2005), using this half-ball connection caused sample bedding errors through sample tilting and consequent sample disturbances. To reduce such bedding and alignment errors, besides ensuring load cell-sample contacts were maintained during dynamic tests, a rigid connection was used (Figure 3.9b). As with the half-ball connection, the constant deviator stress function within GDS Lab was also used for tests using the rigid connection.

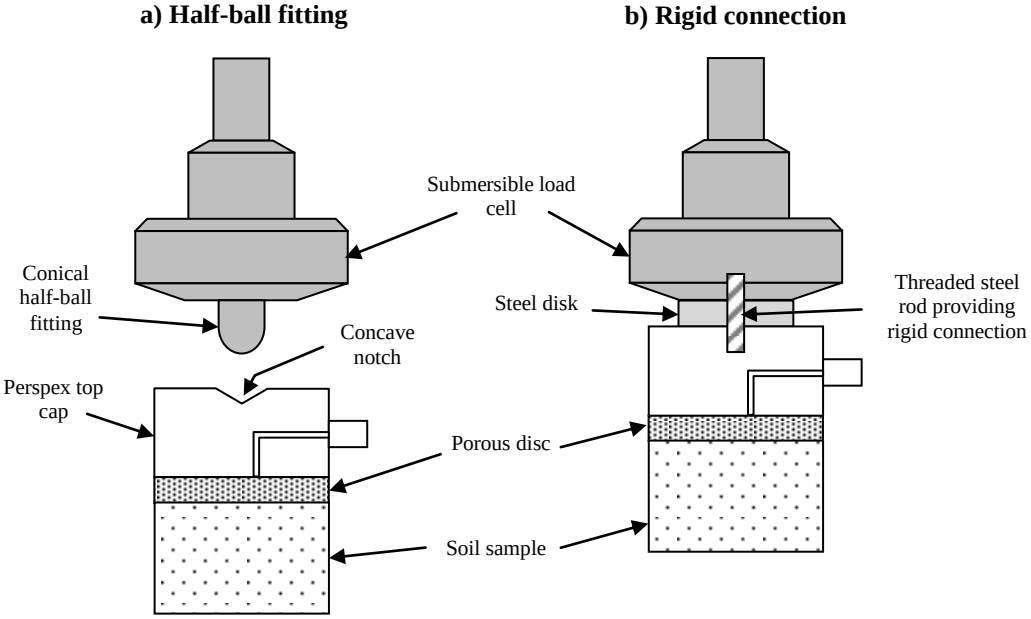

Figure 3.9: Schematics of: (a) half-ball fitting and (b) rigid load cell – top cap connections used during triaxial tests.

3.3.4.2 Testing procedures

Careful sampling techniques were adopted to retrieve undisturbed U100 sized samples from Lanton, Northumberland. As no excavation or rotary core equipment was available to obtain undisturbed samples, a shallow excavation was created manually and U100 sample tubes were manually driven into the base of the excavation at a depth of 1.5–2.0 metres. Disturbed samples were also taken from the same and sealed within plastic bags. To ensure the in-situ moisture contents of U100 undisturbed samples were retained up to testing, samples were wax sealed on site. During transport from site to the laboratory, the samples were carefully wrapped in several layers of bubble wrap, placed within a foam lined suitcase and subsequently laid down and wedged within the foot well of the transport vehicle. Isotropically consolidated drained/undrained monotonic and undrained dynamic triaxial tests were conducted on both natural undisturbed and reconstituted samples with sizes of 50 and 100 mm diameter.

3.3.4.2.1 Sample preparation

To ensure the highest quality of triaxial test results, care was taken in preparing samples of both natural (remoulded/undisturbed) and stabilised alluvium samples. However, undisturbed samples were generally prepared with higher degrees of precision and delicacy to preserve their initial degrees of internal structure. The techniques utilised to prepare such samples for monotonic and dynamic triaxial tests are described forthwith.

3.3.4.2.1.1 Reconstituted untreated samples

Once all the disturbed soil samples were brought back to the laboratory, they were stored within a temperature controlled room. The relative humidity and temperature conditions were set to 55% and 20^{o}C, respectively. To prepare remoulded (and

stabilised) soil samples, two sealed sample bags were taken at a time and oven dried at 100^{o}C for 48 hours. Once dried, the soil was crushed to a fine powder to ensure that soil particles/agglomerations were <3 mm diameter for ease during sample mixing and therefore more practical. For triaxial testing, 100 mm diameter, 200 mm long cylindrical samples were prepared by initially mixing the dried crushed soil with a moisture content of 25% by dry weight (per the soil's in-situ moisture content) within a Hobart rotary mixer for 5 minutes. Once the soil had been thoroughly mixed, samples were made by compacting the soil into three layers within a standard 100 mm diameter compaction mould in accordance with BS 1377 (BSI, 1990). The mass of the sample was then noted by subtracting the mass of the mould from the overall mass of the mould containing the sample. Once the sample had been compacted and any excess material trimmed off, the sample was then carefully extruded (Figure 3.10a). Due to the soil's high silt content, low levels of cohesion and relatively high moisture content, remoulded samples tended to display some slumping upon extrusion per Figure 3.10b.

To reduce the time required to saturate and consolidate samples, circumferential filter paper was applied to all samples to facilitate radial drainage. Porous discs were placed at both ends of the samples, which had previously been cleaned and de-aired by placing them into a tray of boiling water for two hours and then into a vacuum pump for a further two hours. Samples were then carefully transferred onto the base pedestal of the triaxial cell and had their dimensions accurately measured using a set of digital calipers accurate to two decimal places. A latex rubber membrane was then carefully placed over the samples by using a suction sleeve stretcher.

Once samples were encased within their rubber membranes, they were sealed by firstly placing three rubber o-rings over the membrane around the base pedestal. A perspex top cap was subsequently placed on top of the samples, followed by three further rubber o-rings over the membrane around the top cap. The triaxial cell was then placed over the top of the sample, taking care not to disturb the sample and sealed by manually tightening. The ram and submersible were then gently lowered to establish contact with the sample either by using the half-ball or rigid load cell connection types. Once all of the equipment was assembled, an "Advanced loading" stage in the GDS Lab software was set up to linearly record raw data measurements from all transducers and perform calculations for values including mean effective stress (p'),

deviator stress (q) and effective stress ratio every 30 seconds; whilst maintaining a constant q value of 0 kPa throughout saturation and consolidation. The constant measurement of changing sample height throughout the test was therefore enabled, and was more accurate than simply conducting post-consolidation sample height calculations per BS 1377. Finally, de-aired water was introduced to the triaxial cell in preparation for saturation.

(a)  (b) 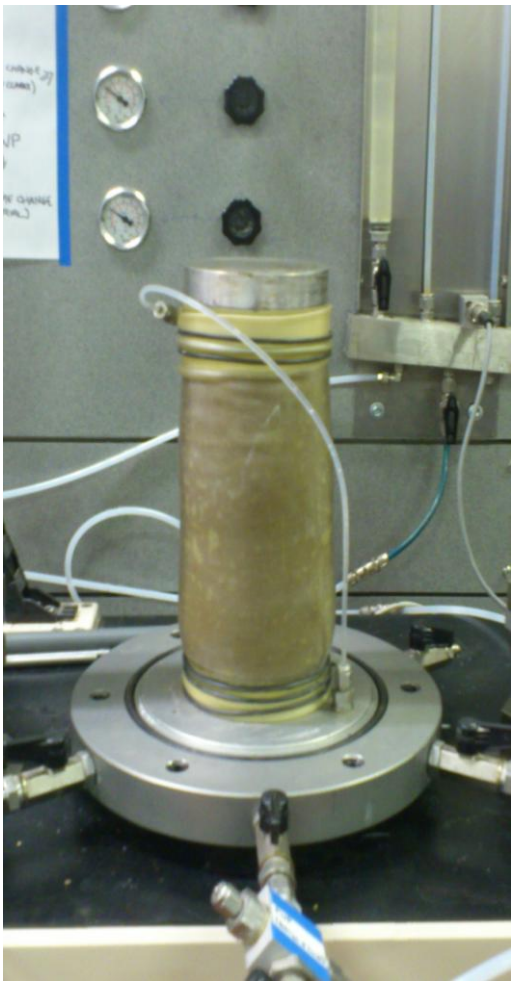

Figure 3.10: (a) Extrusion of remoulded 100 mm diameter samples from a compaction mould; (b) remoulded samples mounted on the triaxial base pedestal, showing signs of slumping towards the sample base.

3.3.4.2.1.2 Undisturbed untreated samples

As only four U100 sized undisturbed soil samples were obtained from the sampling site in Lanton, both 50 and 100 mm diameter samples were used for triaxial testing. 100 mm diameter samples were extruded directly from their U100 sample tubes and carefully trimmed to the appropriate length using a sharp stanley knife. As with reconstituted samples, undisturbed samples were then weighed, very carefully transferred to the triaxial base pedestal with porous discs placed at both ends and their dimensions recorded. Once completed, circumferential filter paper was placed onto the samples, followed by the placement of the perspex top cap and lastly encapsulation within an o-ring sealed latex rubber membrane. One of the most significant observations made from undisturbed samples upon their extrusion and after being fully prepared for triaxial testing was their significantly lower degrees of slumping (Figure 3.11a). By comparing this observation with the slumping feature noted for reconstituted samples, an indication of the undistrubed sample's initial degrees of sedimentation structure was provided.

(a) 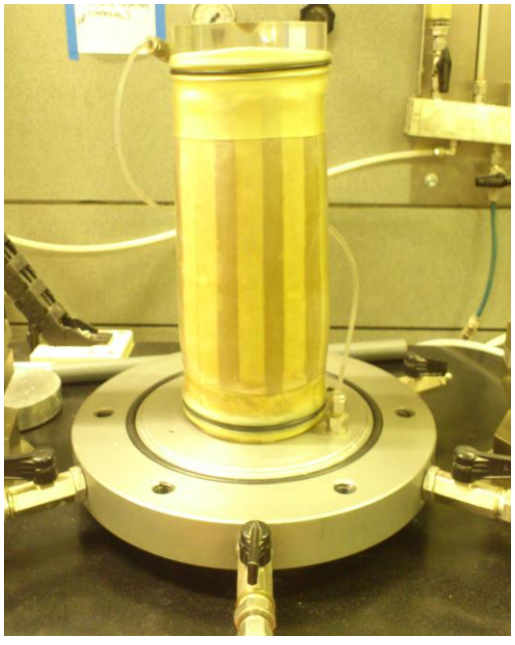 (b) 

Figure 3.11: (a) Undisturbed 100 mm diameter Lanton alluvium sample mounted for triaxial testing; (b) preparation of multiple 50 mm diameter undisturbed samples from a 100 mm diameter sample.

3.3.4.2.1.3 Stabilised samples

Based on previous works by Hughes et al. (2011) and testing results from phases 1 and 2 of the experimental programme, the author anticipated that the failure loads likely to be experienced in testing 100 mm and potentially 50 mm diameter stabilised samples would exceed the 5 kN capacity of the GDS ELDYN triaxial apparatus. Hence, as followed for phases 1 and 2, 38 mm diameter x 76 mm long stabilised samples were tested. The procedure followed for preparing cured stabilised samples is outlined above in section 3.3.2.2.

Once stabilised samples had been extruded from their wax sealed PVC curing tubes, their top and base surfaces required further preparation to reduce any bedding errors during triaxial testing. Per ASTM D4543-08, the ends of the samples were carefully ground down using a surface grinder to tolerances not exceeding 25µm, to ensure they were smooth, flat, parallel to each other and perpendicular to the samples' longitudinal axes. Once complete, the samples were then weighed, carefully transferred to the triaxial base pedestal with porous discs placed at both ends and their dimensions recorded. Finally, the perspex top cap was placed on top of the samples and then encapsulated within an o-ring sealed latex rubber membrane.

3.3.4.2.2 Saturation

Once samples had been fully submerged in de-aired water within the triaxial cell, samples were saturated by applying increments of cell pressure and back pressure. To ensure that any air bubbles within the sample and back pressure system had dissolved into solution prior to assessing the saturation state of samples, the cell and back pressures were increased simultaneously whilst maintaining a 20 kPa differential, up to reaching a minimum back pressure value of 320 kPa. This was conducted per BS 1377 (BSI, 1990) to ensure no leaks occurred during testing. Once these pressure conditions were achieved, the pore pressures within samples were then left to stabilise for 12–24 hours. Once the pore pressures had become stable, the level of saturation within samples was determined by conducting a B-test. This involved increasing the

cell pressure by 50 kPa and monitoring the pore pressure response at both the top and bottom of the samples, whilst maintaining the same back pressure and closing all back pressure valves leading into the sample. The B-test calculation involved using the following formula:

$$B = \frac{\Delta u}{\Delta \sigma_r} \qquad \textbf{(Equation 3.2)}$$

where Δu is the change in pore pressure within the sample in response to a change in cell pressure/radial stress ($\Delta\sigma_r$).

To ensure samples were saturated, a minimum B-value of 0.95 was sought. If samples did not reach this value after 24 hours, further stages of saturation were required. This involved increasing the cell and back pressures to reduce the sample's p' value to 10 kPa and thereby introduce more water to the samples. For untreated Lanton alluvium samples, saturation was generally achieved within 24-48 hours by using back pressures of 320 kPa. However, much higher back pressures of 650–750 kPa were required to achieve saturation within stabilised Lanton alluvium samples. Given the material's much lower permeability, the considerable volume of the material's water content which had been consumed in producing cementitious bonds and the relatively simplistic nature of the back pressure system at Newcastle compared with computer controlled pressure controllers; saturation generally required up to four days to complete.

Occasionally, air bubbles were observed within the back pressure lines at pressures above 320 kPa. These bubbles were manually flushed out the system very slowly, to ensure that only small volumes of water within the back pressure lines were lost. In general, all samples reached B-values between 0.95 and 0.97. To reduce the likelihood of air bubbles becoming trapped during triaxial tests, the back pressure system was pressurised between tests.

3.3.4.2.3 Isotropic consolidation

Once samples were saturated, a minimum back pressure of 320 kPa was maintained for subsequent consolidation and shearing stages, whilst the cell pressure was increased to produce the required effective confining stress (σ_r'). The effective stress conditions used for consolidating and shearing samples were selected based on the unit weight of Lanton alluvium in both saturated (18.44 kN/m^3) and unsaturated (14.5 kN/m^3) conditions, the typical depth range which DSM may be applied (15–20 metres) and finally the zone of influence (where the increase in vertical load was 20% of the original overburden) due to a passing high speed train, based on Newmark calculations (Tomlinson, 2001).

On the UK's East Coast mainline, most high speed trains (HST) travel at 125 mph and have a configuration comprising two Class 43 diesel locomotives and nine Mark 3 coaches. Table 3.11 presents the dimensions and loads for the train when heavily loaded with passengers and luggage.

Table 3.11: Summary of the weight and dimensions for each component of an Intercity 125 train set. Data obtained from Wikipedia (2012).

Intercity 125 HST	**Weight**	**Length**	**Width**
	Tonnes	***m***	***m***
Class 43 Locomotive	70.25	17.79	2.74
Mark 3 Coach	33.0	23.0	2.74

Per Powrie et al. (2007), railway embankment fill tends to comprise three layers of different materials; ballast (16.66 kN/m^3), sub-ballast (22.54 kN/m^3) and prepared subgrade (19.6 kN/m^3). For simplicity, an average unit weight of 20 kN/m^3 was assumed for the entire embankment, which corresponds with the value used by Han et al. (2007). According to Newmark calculations, if a 3 metre high high-speed railway embankment is founded upon Lanton alluvium soil, which is fully saturated at a depth of 1 metre below initial ground level; the zones of influence due to the Class 43 locomotive and Mark 3 coaches are 11.89 metres and 9.10 metres, respectively. Hence, given the difference in these values, the maximum zone of influence for the

entire train is assumed to be 11.89 metres; whereby the corresponding σ_r' is 147.48 kPa.

To capture the behaviour of Lanton alluvium at various σ_r' conditions both within the zone of influence for these trains and within the depth range of DSM, the σ_r' conditions used for consolidation and shearing Lanton alluvium ranged between 50 and 250 kPa. However, the behaviour of Lanton alluvium at σ_r' values of 50, 100 and 150 kPa were of key interest, given the overlap of the train's zone of influence and the depth range of DSM. Figure 3.12 presents a schematic of the conceptual high speed railway embankment situation considered in this triaxial testing programme and also identifies the depths/σ_r' conditions of key interest.

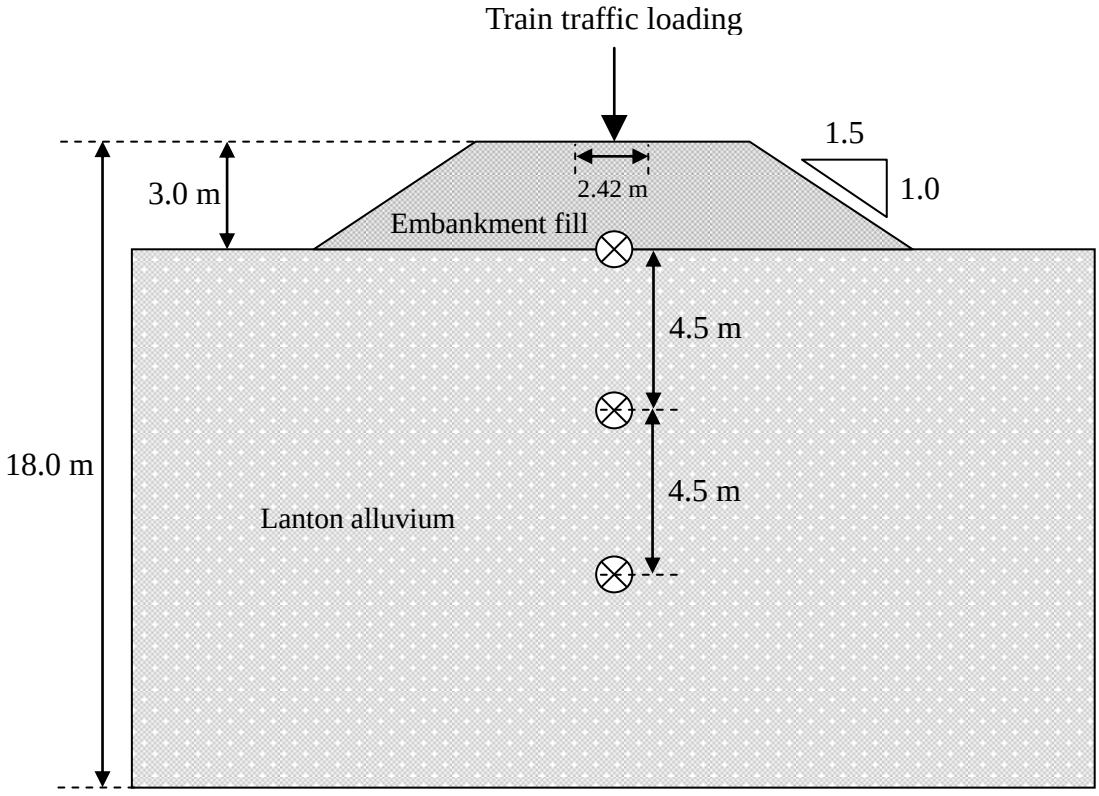

Figure 3.12: Stress points of interest for Newmark calculations and effective confining stresses for use in the triaxial testing of Lanton alluvium, which underlies a theoretical high-speed railway embankment.

All samples were isotropically consolidated via the radial drains provided by the filter paper and also drained from the top end of the sample. This allowed pore water pressure dissipation to be recorded using the pressure transducer located at the base of

the sample. Samples were considered consolidated once the required effective stress condition was achieved and when volumetric strain had fully stabilised. There were several occasions when very lengthy consolidation times were observed for reconstituted samples and it was necessary to consolidate the sample using the radial, top and bottom drains. Pore water pressure dissipation could not be recorded, given the absence of a mid-height pore pressure probe but was periodically measured manually by quickly pausing the test, closing the top and base drain valves, recording pore pressure readings and then reopening drainage valves. Generally, samples were left to consolidate for a minimum of 24–36 hours.

Once samples were consolidated, the top and bottom drainage valves were closed and the test within the GDS Lab/Triax software was paused. Calculations were then carried out per BS 1377 (BSI, 1990) to determine the post-consolidation dimensions of samples. The following equations were used:

Volume change during consolidation: $$V_c = V_o - \Delta V_c$$ (**Equation 3.3**)

where V_c is the sample's new consolidated volume, V_o is the original volume, ΔV_c is the change in volume during consolidation; all measured in cm^3.

Area change during consolidation: $$A_c = A_o \left[1 - \frac{2}{3}\frac{\Delta V_c}{V_o}\right]$$ (**Equation 3.4**)

where A_c is the sample's new cross sectional area post-consolidation and A_o is the original cross sectional area; all measured in cm^2.

Length change during consolidation: $$L_c = L_o \left[1 - \frac{1}{3}\frac{\Delta V_c}{V_o}\right]$$ (**Equation 3.5**)

where L_c is the sample's new length post-consolidation, L_o is the original length; all measured in mm.

Subsequent to calculating the sample's new dimensions, by plotting a root-time vs. back volume graph, a value for t_{100} could be determined using the method shown in Figure 3.13.

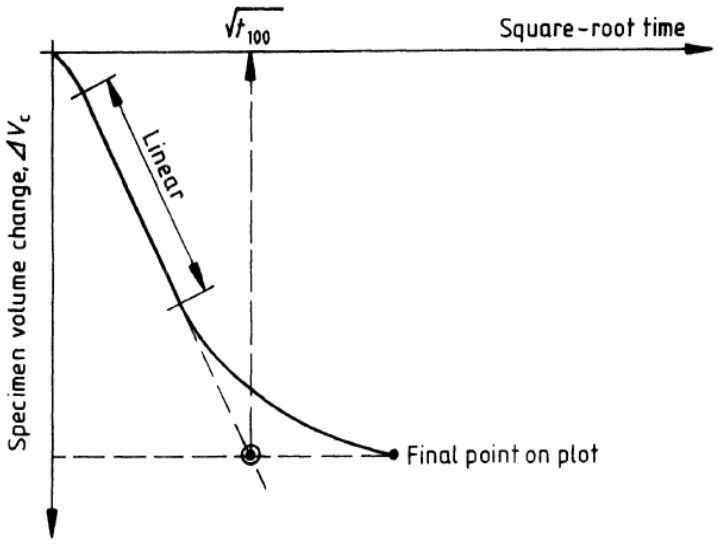

Figure 3.13: Ideal consolidation curve for triaxial samples. Courtesy of BS 1377 (BSI, 1990).

The next stage of calculations was to determine the rate of strain required for shearing samples. A value obtained for t_{100} was then used to calculate the expected time to failure during shearing (t_f), using the following formula:

Expected time to failure: $t_f = F \,.\, t_{100}$ (**Equation 3.6**)

where t_f is measured in minutes, F is a coefficient that is dependent on the whether the test is undrained or drained and how many drains were used during consolidation (i.e. top, end, radial). Values for F can be determined using BS 1377 (BSI, 1990).

Using this value for t_f, the strain rate (d_r) required for shearing the sample could then be determined via the following formula:

Strain rate: $$d_r = \frac{\varepsilon_f \,.L_c}{t_f}$$ (**Equation 3.7**)

where εf is the significant strain interval for the shearing test and d_r is measured in mm/min.

Based on values obtained from calculations using these equations, the strain rates used for undrained and drained tests were 0.05 and 0.01 mm/min, respectively. For all undrained samples, multi-stage shearing was conducted. Three shearing tests were conducted at three different effective confining stresses, separated by a consolidation stage to repair the sample from its previous shearing test.

3.3.4.2.4 Permeability

For several reconstituted and undisturbed samples, permeability tests were conducted immediately post-consolidation in accordance with BS 1377 (BSI, 1990). This required using both the ICVC and BCVG units and a "Just-log" test was set-up in the GDS Lab software. To present a hydraulic gradient across samples whilst ensuring any air bubbles within the soil and/or back pressure lines remained dissolved in solution, a pressure differential of 30 kPa was created between the back pressure at the top ($p_1 \geq$ 320 kPa) and that at the bottom ($p_2 \geq 350$ kPa) of the sample. The apparatus was set up to enable water to flow from the ICVC, upwards through the sample and into the BCVG. DVM readings for monitoring the volume of water entering the BCVG unit during testing were recorded manually every 5–10 minutes for 6 hours.

Once permeability testing had been conducted, the back pressure valves for the top and base of the sample were closed. Once the volume of water which had passed through the sample over the 6 hour testing period had been determined, a flow rate (q′) was calculated. Hence, to determine the coefficient of permeability for samples, the following equation was utilised:

Coefficient of permeability: $$k_v = \frac{1.63 \,.q\prime \,.L_c}{A_c[(p_1 - p_2) - p_c]} \,.R_t \,.10^{-4}$$ (**Equation 3.8**)

where k_v is measured in m/s, L_c is the sample's length post-consolidation, A_c is the sample's area post-consolidation, p_1 is the pressure at the top of the sample (kPa), p_2 is the pressure at the bottom of the sample (kPa), R_t is the temperature correction factor for the viscosity of water (which at a laboratory temperature of 22^{o}C is 0.95) and finally p_c is the pressure loss in the system for rate of flow, which was assumed to be zero. Darcy's law traditionally defines the movement of water through fully saturated soils. However, in triaxial samples 100 % saturation is not always guaranteed. Small amounts of air are likely to be present within soils post-consolidation – especially under confining stress conditions <300 kPa, which is generally considered as the minimum pressure under which air has mostly dissolved into solution. Hence, the 1.63 x 10^{-4} m/s coefficient in Equation 3.8 accounts for the viscosity of air within the soil.

3.3.4.2.5 Shearing

3.3.4.2.5.1 Monotonic tests

For the monotonic shearing of samples, another "Advanced loading" test was created in the GDS Lab software for the Newcastle triaxial apparatus, or a "Shear" stage within Triax for the Bristol apparatus. Samples' post-consolidation dimensions were used to determine the maximum amount of axial strain to be experienced by samples during shearing. Given that samples had reduced in volume and therefore in height during saturation and consolidation, a positive value for axial displacement was recorded. This value was zeroed before shearing was initiated.

Several failure criteria may be used for monotonic triaxial tests. Some of the most commonly used include maximum deviatoric stress and maximum effective stress ratio with axial strain. It should be noted that the points at which maximum deviatoric stress and maximum effective stress ratio are reached may differ between samples. Therefore, the failure criterion selected for this research was maximum effective stress ratio, as this is a function of pore water pressure. Besides conventional monotonic triaxial tests where samples are simply loaded to failure, several samples were

subjected to a series of unload-reload loops prior to sample failure under both undrained and drained conditions. This was conducted to gain insights into Lanton alluvium's initial stiffness. The following load-unload-reload sequences were followed for their respective effective confining stress conditions, as defined in section 3.4.3.3:

σ_r' = 50 kPa:

- Initial loading: sample sheared to 2.5% axial strain.
- Unloading: sample unloaded back to 2.3% axial strain.
- Reloading: sample sheared to failure (approx. 5% axial strain).

σ_r' = 100 kPa:

- Initial loading: sample sheared to 5% axial strain.
- Unloading: sample unloaded back to 4.8% axial strain.
- Reloading: sample sheared to failure (approx. 7.5% axial strain).

σ_r' = 150 kPa:

- Initial loading: sample sheared to 7.5% axial strain.
- Unloading: sample unloaded back to 7.3% axial strain.
- Reloading: sample sheared to failure (approx. 10–15% axial strain).

3.3.4.2.5.2 Dynamic tests

Per GDS (2014), soils in many geotechnical projects experience dynamic/cyclic loading, possibly due to anthropogenic activity such as vibrating machinery and passing rail/road traffic or natural environmental factors including earthquakes and storms. Dynamic loading caused by passing railway traffic can potentially cause the subgrade within railway embankments to undergo progressive rotational slip (shear) failures. Hence, the primary aim of the dynamic triaxial testing conducted for this research was to examine the behaviour of Lanton alluvium in both its untreated and

treated states, when subject to dynamic loads that are typically presented by high-speed trains in the UK.

It is generally considered that the behaviour displayed by soils when dynamically loaded is more complex than that exhibited during monotonic loading conditions. Per GDS Ltd. (2014), there are two key differences in terms of a soil's response to dynamic/cycling loading and monotonic loading; 1) the oscillation between increasing and decreasing deviatoric stresses exerted on a soil sample and 2) the rate-dependency of a soil's response.

For cyclic and dynamic triaxial tests intended to simulate railway traffic loading, it is necessary to initially place samples under a "seat load" to ensure contact is maintained between the sample and the load cell during tests, given the oscillation of deviatoric stress exerted on samples (Aursudkij et al., 2009). This method is referred to as "one-way loading", which ensures that the applied deviatoric stresses remain positive throughout tests. The second method is "two-way loading", where the deviatoric stresses exerted on samples alternates between positive and negative values. Figure 3.14 presents a visualisation of the two cyclic/dynamic loading patterns for the deviator stresses applied to samples during tests. However, for such two-way tests an extension top cap with a vylastic sleeve is usually required, per Figure 3.15.

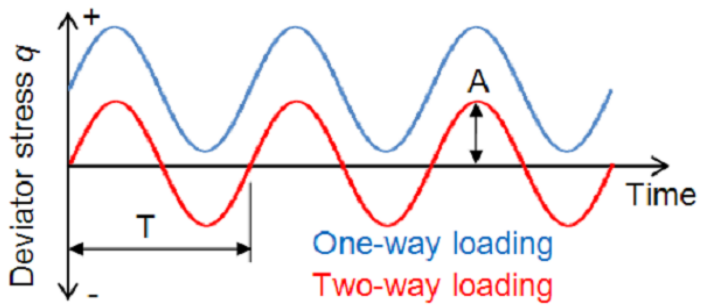

Figure 3.14: Visualisation of one- and two-way loading patterns in dynamic/cyclic triaxial tests (A = loading amplitude, T = loading period/wavelength). Taken from GDS Ltd. (2014).

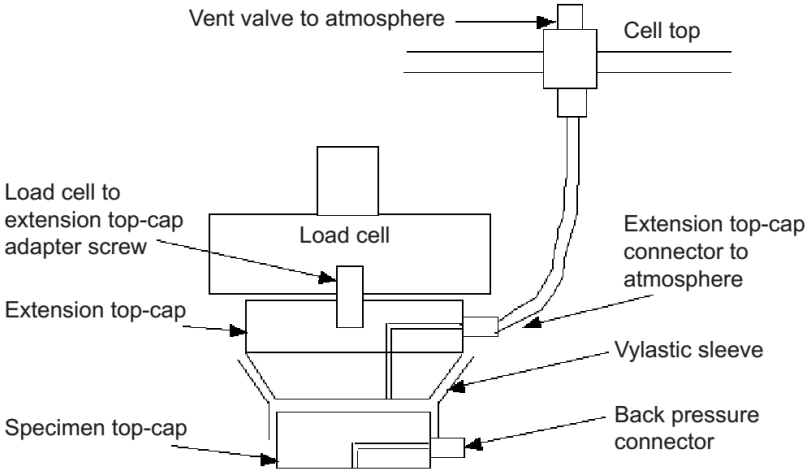

Figure 3.15: Extension top cap with vylastic sleeve configuration provided by GDS Ltd. for two-way dynamic/cycle loading triaxial tests. Taken from GDS Ltd. (2014).

To determine the magnitude and frequency of the dynamic loading to be applied to Lanton alluvium samples during testing when simulating a high speed train travelling at 125 mph, several calculations based on the data in Table 3.11 and assumptions have been made. Firstly, it was assumed that the loads exerted by the Class 43 locomotives and the Mark 3 coaches was distributed across four railway sleepers at any one time via four axles (i.e. two bogeys). Per Powrie et al. (2007) the typical dimensions of railway sleepers are 2.42 m long, 0.242 m wide and 0.2 m high; giving an area of 0.59 m^2. These sleeper types are incorporated into the typical track design recommended by the International Union of Railways Code 719R, and have been used to construct the UK Channel Tunnel high speed rail link (Powrie et al., 2009). Table 3.12 summarises the stresses exerted by the Class 43 locomotive and Mark 3 coach across the area of four sleepers.

Table 3.12: Summary of stresses exerted by each component of an Intercity 125 train set across four sleepers.

Intercity 125 HST	**Weight**	**Stress across four 0.59 m^2 sleepers (2.34 m^2)**
	kN	***kPa***
Class 43 Locomotive	688.45	293.89
Mark 3 Coach	323.40	138.05

Regarding the rate dependency of a soil's response to dynamic/cyclic loads, the effects of loading rate are generally observed once a soil has started to experience elasto-plastic behaviour, and may be attributed to the soil's inter-particle viscosity (for non-granular sand/gravel based soils only) and the ability of the soil to dissipate excess pore water pressure (GDS Ltd., 2014). Hence, by assuming constant undrained conditions during the application of high-frequency dynamic/cyclic loads, GDS Ltd. (2014) state that the response of granular soils is considered to be relatively independent of loading rate. Generally, faster (higher frequency) loading rates cause stiffer responses within cohesive soils. If granular soils characterised by high permeability values are dynamically loaded at a slow rate, there is sufficient time for pore water pressure to dissipate and drain away. Conversely, soils with low permeabilities which are dynamically loaded at a fast rate cause excess pore pressure build up, a reduction in the soil's effective stress towards zero and consequently results in soil failure – e.g. liquefaction of dense sands.

The typical loading frequencies exerted by passing railway traffic are generally much higher than those typically presented by seismic activity (1 Hz), wave or wind action (0.1–1.0 Hz). When assuming an axle wheel spacing of 2.6 m and high-speed train velocities of 70–125 mph, Aursudkij et al. (2009) state that loading frequencies can be around 30 Hz. Figure 3.17 shows a schematic of an HST Intercity 125's geometry and loads, which were simulated during the dynamic triaxial testing programme. To calculate the frequency of loading to be applied during testing, the period for one complete load-unload was determined as 0.036 seconds when the train travels at 125 mph. From this, the frequency can be calculated using Equation 3.9:

Loading frequency: $$f = \frac{1}{T}$$ (**Equation 3.9**)

where f is measured in Hz, T is the period for one load-unload cycle measured in seconds.

When travelling at 125 mph, the loading frequency of the Intercity 125 HST was calculated to be 27.94 Hz. This frequency far exceeded the 5 Hz frequency capability

of the ELDYN triaxial apparatus. Therefore for dynamic tests the loading frequency had to be scaled down by a factor of 10 to 2.794 Hz. There are a number of implications which arise from using this lower frequency, the first of which includes subjecting samples to dynamic loads that are still not a true representation of HST loading. This ultimately suggests that there will be an underestimation of the induced strains and pore pressure increases experienced by samples during loading and thus their liquefaction potential.

Following the above sets of assumptions and train load/stress calculations, a series of Newmark calculations were performed per Tomlinson (2001) to determine how the stresses exerted by the passing high-speed train (q) vary with depth (Z) beneath the railway embankment (Figure 3.16).

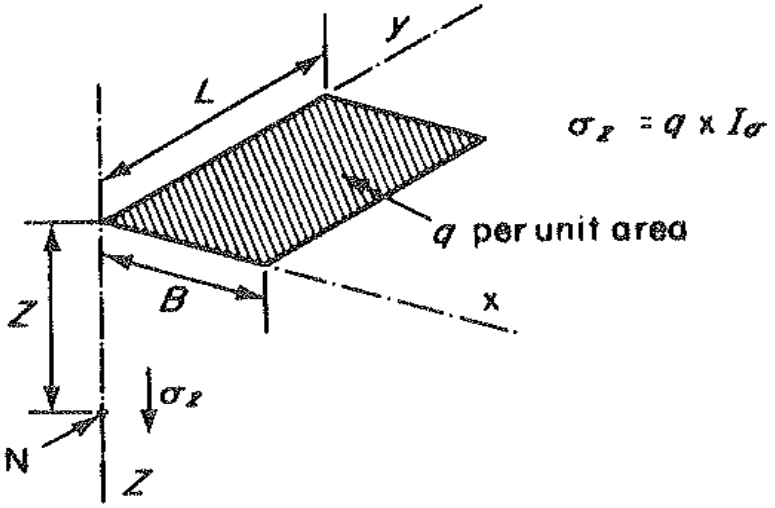

Figure 3.16: Schematic of the Newmark (Bousinesque) principle used to calculate influence values for vertical normal stresses at specified depths (point N) beneath a corner of the Class 43 locomotive and Mark 3 coaches. Taken from Tomlinson (2001).

The dynamic behaviour of Lanton alluvium was examined under the same effective stress conditions as those defined in section 3.3.4.2.3. The dynamic loads to be applied to triaxial specimens at these effective confining stresses, which are intended to simulate an HST passing at 125 mph were calculated via Newmark's method and are per Table 3.13.

Table 3.13: Summary of the dynamic loads and stresses to be applied to 100 mm samples during testing.

Effective confining stress (kPa)	**Class 43 Locomotive**		**Mark 3 Coach**	
	Dynamic load for 100 mm samples (kN)	***Corresponding dynamic stress (kPa)***	***Dynamic load for 100 mm samples (kN)***	***Corresponding dynamic stress (kPa)***
60.0	1.26	160.86	0.59	75.57
108.65	0.53	67.39	0.25	31.66
147.48	0.22	28.45	0.10	13.36

To set up a dynamic test in the GDS Lab software, the dynamic loading function was selected. To simulate a passing HST, three dynamic shear stages were required:

Stage 1: passage of the first Class 43 locomotive (2 bogeys).

Stage 2: passage of nine Mark 3 coaches (18 bogeys).

Stage 3: passage of the final Class 43 locomotive (2 bogeys).

Details of the loading conditions used for the three dynamic shear stages at each effective confining stress are per Table 3.14 below. As an extension top cap and vylastic sleeve configuration was not available for this dynamic testing programme, two-way loading was not possible. Therefore, one-way loading was utilised for dynamic tests by using the rigid load cell connection (per Figure 3.17 and work by Aursudkij et al. (2009)).

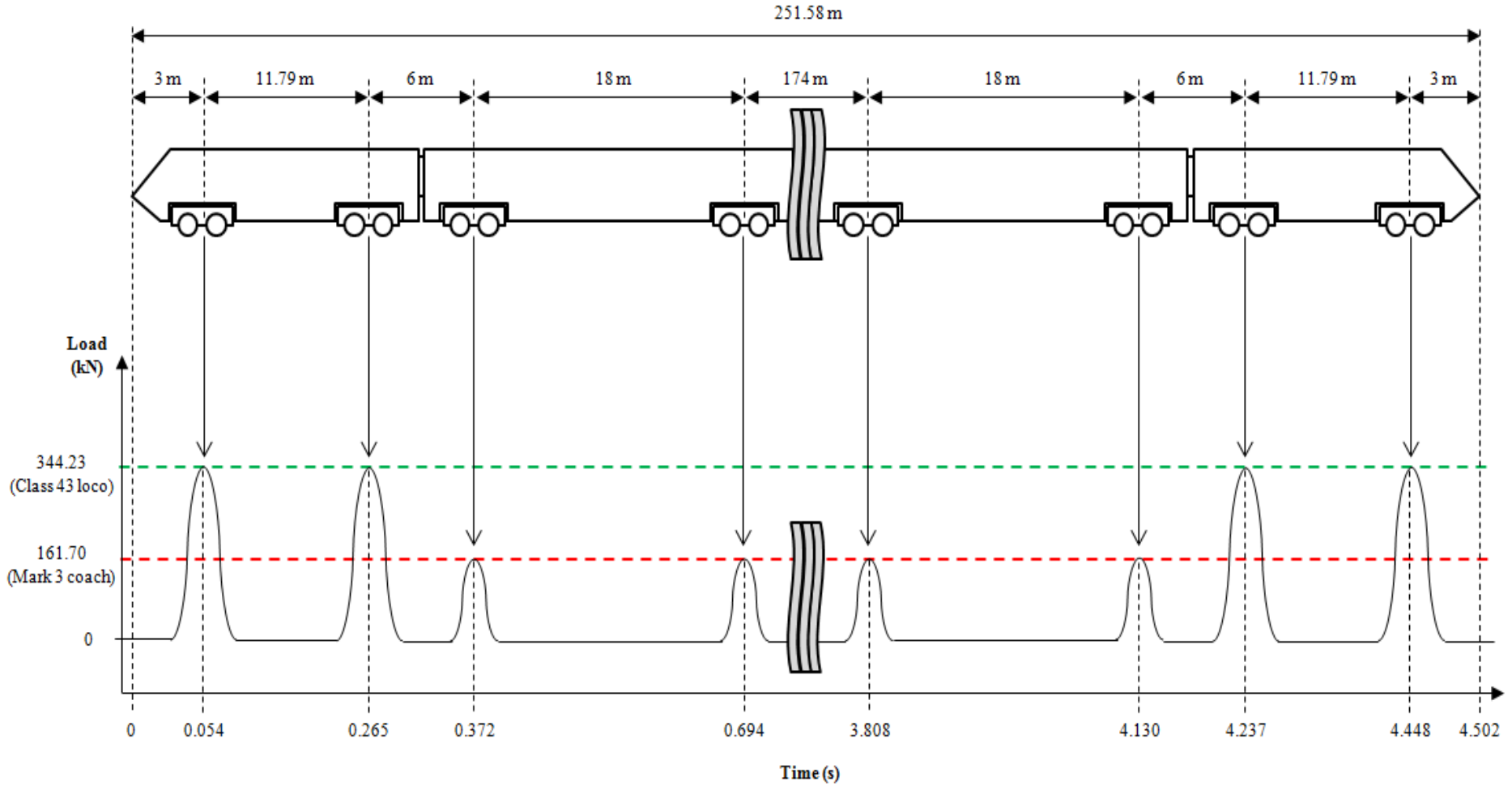

Figure 3.17: Geometry and loading of an Intercity 125 high speed train travelling at 125 mph, to be simulated for dynamic testing.

Table 3.14: Summary of testing parameters used for dynamic shear strength tests on 100 mm diameter samples.

Effective confining stress (kPa)	**Class 43 Locomotive**			**Mark 3 Coach**		
	Number of load-unload cycles	***Load amplitude (kN)***	***Load datum (kN)***	***Number of load-unload cycles***	***Load amplitude (kN)***	***Load datum (kN)***
60.0	2	0.630	0.830	18	0.296	0.496
108.65		0.264	0.464		0.124	0.324
147.48		0.112	0.312		0.053	0.253

To obtain sufficient data to define the dynamic behaviour of Lanton alluvium, whilst taking care not to create over-large data files; 200 data points were recorded per loading cycle. An additional parameter required within the GDS Lab software during load-controlled dynamic tests was the provision of a stiffness estimate for the soil. A maximum value of 10 kN/mm could be used (the stiffer the soil being tested, the higher the stiffness estimate). Defining a stiffness estimate sets the servo loop gain for load control; ultimately ensuring that the load-unload curves were as smooth as possible during testing. As outlined in the GDS handbook for the ELDYN triaxial system, a soil's stiffness can only be determined through experience gained from static loading triaxial testing of the soil. If the stiffness estimate chosen was too low, it would cause the ELDYN's actuator/servo to start oscillating. Therefore, the stiffness estimate values chosen for Lanton alluvium ranged between 1–2 kN/mm.

3.4 Data analysis techniques

3.4.1 General engineering performance

3.4.1.1 Unconfined compressive strength

The maximum UCS value achieved by samples may be calculated using the following equation:

$$UCS = \frac{P_{max}}{A} \qquad \textbf{(Equation 3.10)}$$

where P_{max} is the maximum force (i.e. load) experienced by the sample during compression and A is the sample's cross sectional area at failure.

3.4.1.2 "Quick" undrained unconsolidated shear strength

Figure 3.18 below illustrates the Mohr circles produced from UUT tests and the derivation of undrained shear strength (Cu) and maximum deviator stress (q); whereby σ_3 is the confining stress used and σ_1 is the maximum normal stress applied to samples during tests. (Note: the UUT test does not involve pore pressure measurements, therefore measures total stresses rather than effective stresses.)

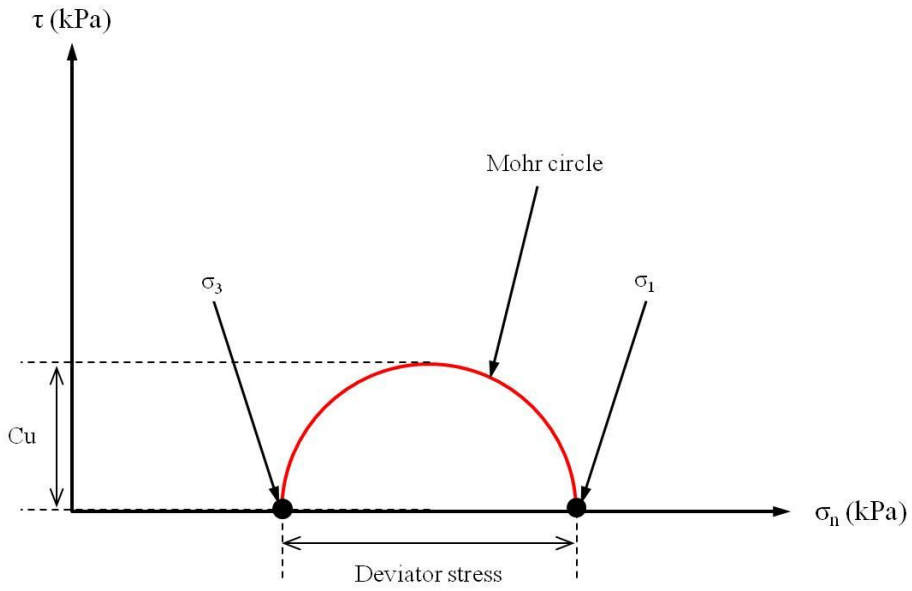

Figure 3.18: Definition of Mohr circles and undrained shear strength from UUT tests.

Equations 3.11 - 3.13 below were used to calculate values for q, σ_1 and Cu (also see Equation 3.35 for calculating q in terms of effective stresses):

Maximum deviatoric stress: $q = \frac{P_{max}}{A}$ (**Equation 3.11**)

where P_{max} is the maximum axial force measured during sample compression.

Maximum normal stress: $\sigma_1 = q + \sigma_3$ (**Equation 3.12**)

Undrained shear strength: $Cu = \frac{q}{2}$ (**Equation 3.13**)

For convenience, an empirical relationship exists between the UCS and Cu values for a cohesive soil, as defined in Equation 3.14 below:

$$Cu = \frac{UCS}{2} \quad \text{(Equation 3.14)}$$

3.4.1.3 Oedometer compressibility

According to BS 1377: Part 5 (BSI, 1990), the following Equations 3.15 - 3.20 were used to calculate the changing height (H) and void ratio (e) of samples during one-dimensional compression, and therefore their coefficients of consolidation (Cv) and compressibility (Mv):

Equivalent height of solid particles: $H_s = \frac{H_0}{1+e_0}$ (**Equation 3.15**)

where H_0 and e_0 are the initial height and void ratio of testing samples.

Initial void ratio: $e_0 = \left(\frac{\rho_d}{\rho_s}\right) - 1$ (**Equation 3.16**)

where ρ_d and ρ_s are the sample's dry density and particle density respectively.

Changing sample height: $$H = H_0 - (\Delta H - y)$$ (**Equation 3.17**)

where ΔH is the cumulative compression of samples from H_0 and y denotes the cumulative correction for deformation of the oedometer apparatus under the pressures used during testing.

Changing void ratio: $$e = \frac{H - H_s}{H_s}$$ (**Equation 3.18**)

Coefficient of consolidation: $$C_v = \frac{0.111\,\bar{H}^2}{t_{90}}$$ (**Equation 3.19**)

where $\bar{H}$ is the average sample height for each load increment and t_{90} is the time taken for 90% sample consolidation to have occurred.

Coefficient of volume compressibility: $$M_v = \left(\frac{H_1 - H_2}{H_1}\right)\left(\frac{1000}{P_2 - P_1}\right)$$ (**Equation 3.20**)

where H_1 and H_2 are the sample heights at the start and end of loading increments respectively, P_1 and P_2 are the stresses applied to samples for the previous and current loading increments respectively.

3.4.1.4 Durability

For both wetting-drying and freezing-thawing testing, samples were measured in terms of their volume (V) and moisture contents (w) post submersion, oven drying and

sample scratching (ASTM D559 and D560). Equation 3.21 was used to calculate sample's volumetric changes:

Sample volume: $$V = V_0 - \Delta V$$ (**Equation 3.21**)

where V_0 denotes sample's initial volume before testing and ΔV is the change in volume experienced by samples after each cycle of submersion, oven drying and scratching. Sample moisture contents were calculated using Equation 3.22 below.

3.4.1.5 Moisture content

The moisture content of all UCS, triaxial, oedometer and durability samples were recorded in general accordance with the procedure outlined in BS 1377: Part 2 (BSI, 1990). Samples were left to dry within a 100^{o}C oven for 24-36 hours. The following equation was used to determine sample moisture contents:

Moisture content: $$w = \left(\frac{M_w}{M_{ds}}\right)$$ (**Equation 3.22**)

whereby M_w and M_{ds} correspond to the mass of water lost during drying and the mass of the dried soil, respectively.

3.4.2 Oedometer testing - defining soil structure

Oedometer testing was initially conducted on Lanton alluvium in its remoulded and undisturbed natural states. The rationale behind conducting this testing on the alluvium in these two states stems from studies by Rouainia and Muir Wood (2000) and Gasparre and Coop (2008); whereby most soils are defined as having a degree of structure which is owed to its fabric (i.e. arrangement of particles and fissures,

layering and any other inhomogeneities) and inter-particle bonding/cementation. The nature of a soil's structure is a direct result of its geological history; namely the depositional and post-depositional processes (Gasparre and Coop, 2008).

Introducing an auger mixer to Lanton alluvium for DDSM treatment will inevitably result in its complete destructuration. Therefore, results from this oedometer testing are intended to define the degree of initial structure within the soil and ultimately assist in defining the level of DDSM treatment which is required to compensate for this structure loss and to provide the necessary strength gains required per EuroSoilStab (2002) criteria. To define the degree of initial structure within the undisturbed Lanton alluvium, a similar approach to that taken by Gasparre and Coop (2008) will be adopted, as seen in Figure 3.19. Gasparre and Coop (2008) state that normally consolidated soils possess a sedimentation structure, whereas overconsolidated soils possess a post-sedimentation structure. The typical behaviour for normally and over-consolidated soils can be seen in Figure 3.19a and b, respectively.

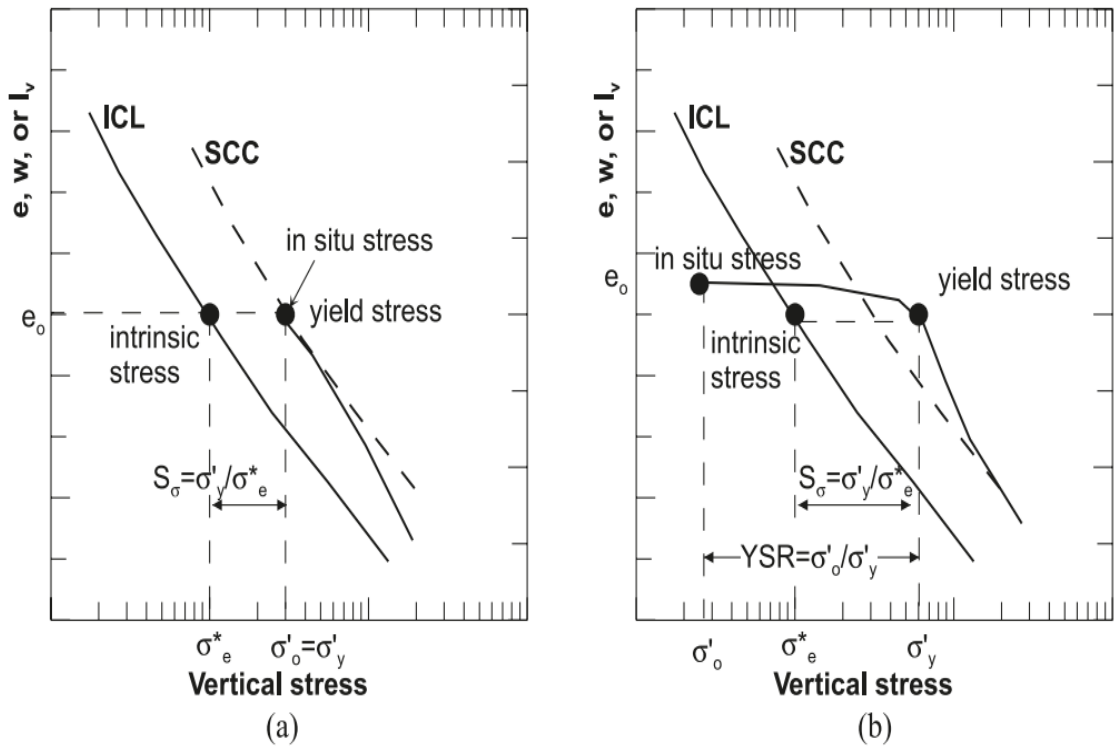

Figure 3.19: Definition of initial degree of structure within soils characterised by a: (a) sedimentation structure and (b) post-sedimentation structure. Taken from Gasparre and Coop (2008).

For normally consolidated soils, their gross yield and preconsolidation stresses coincide and the material yields along its sedimentation compression curve (SCC), which is defined by the locus of in-situ stress states with increasing depth as the soil experiences virgin compression (Gasparre and Coop, 2008). Whereas for overconsolidated soils, the yield stress is higher than values depicting the SCC before undergoing virgin compression. According to Gasparre and Coop (2008), considerable volumetric changes occur within a soil once the yield stress (σ'_y) has been exceeded, which in turn may be unrelated to the soil's stress history. To quantify the degree of structure within Lanton alluvium soil, a number of parameters require derivation by using the raw oedometer data. The yield stress ratio (YSR) must firstly be calculated to accurately define the in-situ state for a soil and may be calculated via the following equation:

$$YSR = \sigma'_y / \sigma'_0 \qquad \textbf{(Equation 3.23)}$$

Stress sensitivity (S_σ) must then be defined, which is the ratio between the undisturbed soil's σ'_y value to the vertical stress on the intrinsic compression line (ICL) at the same void ratio (σ^*_e). This parameter may be considered as one that incorporates variations in microstructure of soils in both their undisturbed and remoulded states (Gasparre and Coop, 2008) and may be defined via the following equation:

$$S_\sigma = \sigma'_y / \sigma^*_e \qquad \textbf{(Equation 3.24)}$$

The S_σ value for a soil quantifies the amount of spacing between the undisturbed soil's compression curve and the ICL, which may increase with increasing vertical stress – depending upon the compression curve shape and σ'_y value (Gasparre and Coop, 2008).

For direct comparisons to be made between Lanton alluvium and various different soils in terms of their structure, normalising the compressional behaviour for the grading and mineralogy of the soil must be conducted. Gasparre and Coop (2008)

utilised Burland's (1990) void index (Iv) instead of the void ratio (e), which may be calculated via the following equation:

$$I_v = \frac{e - e^*_{100}}{e^*_{100} - e^*_{1000}} \quad \textbf{(Equation 3.25)}$$

whereby e^*_{100} and e^*_{1000} are void ratios on the ICL at vertical stresses of 100 and 1000 kPa, respectively. Gasparre and Coop (2008) suggested that any normalisation must account for the comparison between the compression path of the undisturbed soil with the ICL as well as the effects of structure at lower vertical stresses before the compression path first crosses the ICL. Thus, Gasparre and Coop (2008) presented a new normalisation method, which considers the location of the undisturbed soil's compression curve with reference to the intrinsic swelling and compression lines. Ultimately, they defined the effect of structure on a soil's compressive behaviour as the difference in void ratio (e_n) between the undisturbed soil's compression curve and 1) the intrinsic swelling line (ISL) when the vertical stress (σ_v) is less than σ_n (the stress denoted by the intersection between the intrinsic swelling and compression lines); and 2) the ICL when σ_v is greater than σ_n. Figure 3.20 provides a visualisation for conducting Gasparre and Coop's (2008) normalisation technique.

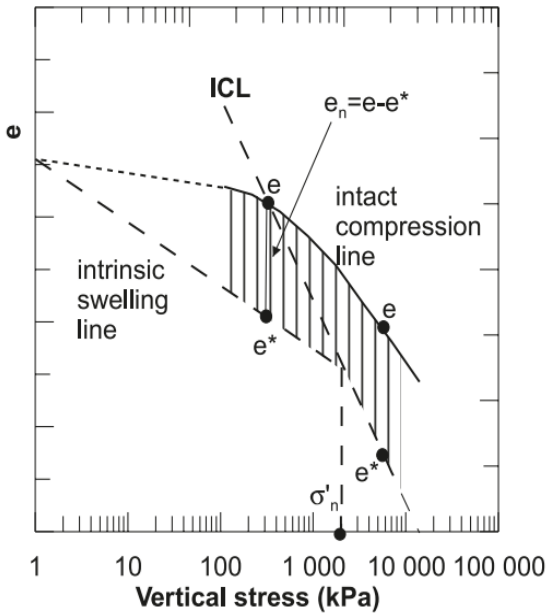

Figure 3.20: Visualisation of Gasparre and Coop's (2008) technique for normalising the effects of soil structure. Taken from Gasparre and Coop (2008).

3.4.3 Triaxial testing

Although the GDS Lab and Triax software packages could provide values for several engineering parameters in real time as triaxial tests progressed, all parameters were calculated manually as some of the GDS/Triax calculated values were insufficiently accurate, particularly with strain measurements. All of the calculations made for both reconstituted and undisturbed Lanton alluvium samples are hereby presented.

3.4.3.1 Strains

For determining the degree of axial strain (ε_a) experienced by samples using external LVDT (global) measurements, the following formula may be used:

Global axial strain: $$\varepsilon_a = \left(\frac{\delta L}{L}\right)$$ (**Equation 3.26**)

where δL is the change in length experienced by the sample during testing and L is the original length of the sample prior to straining. All strain values are expressed as a percentage. Understanding the small strain behaviour of soils is crucial in designing geotechnical structures (Clayton, 2011). Based on the bedding errors, end restraint effects and machine compliance issues, it has become increasingly important to measure strains within samples using local LVDT's compared with external LVDT's. Figure 3.21 demonstrates the significant difference in Young's modulus values obtained between using external and local LVDT measurements. Results obtained from local LVDT's can accurately capture higher stiffnesses at small – very small strain levels and therefore considered to be a much better representative of a soil's behaviour compared with using external LVDT's.

For measuring local strains experienced by samples ($l\varepsilon_a$), changes in sample length are assessed relative to the LVDT's gauge length (gL) rather than the total length of the sample. The following equation may be used for calculating local axial strains:

Local axial strain: $l\varepsilon_a = \left(\frac{\delta gL}{gL}\right)$ (**Equation 3.27**)

For measuring local radial strains ($l\varepsilon_r$), the displacement values recorded by the radial LVDT are approximately double the actual diametrical displacement experienced. Therefore, these values required correction by simply dividing them by two. This arises from the caliper's geometry. The pivot of the radial caliper was diametrically opposite the local radial LVDT, which was aligned normal to the sample's diameters and was fixed at the centre of the samples. Therefore, the formula used to calculate local radial strain is given as follows:

Local radial strain: $l\varepsilon_r = \left(\frac{\delta gL/2}{gL}\right)$ (**Equation 3.28**)

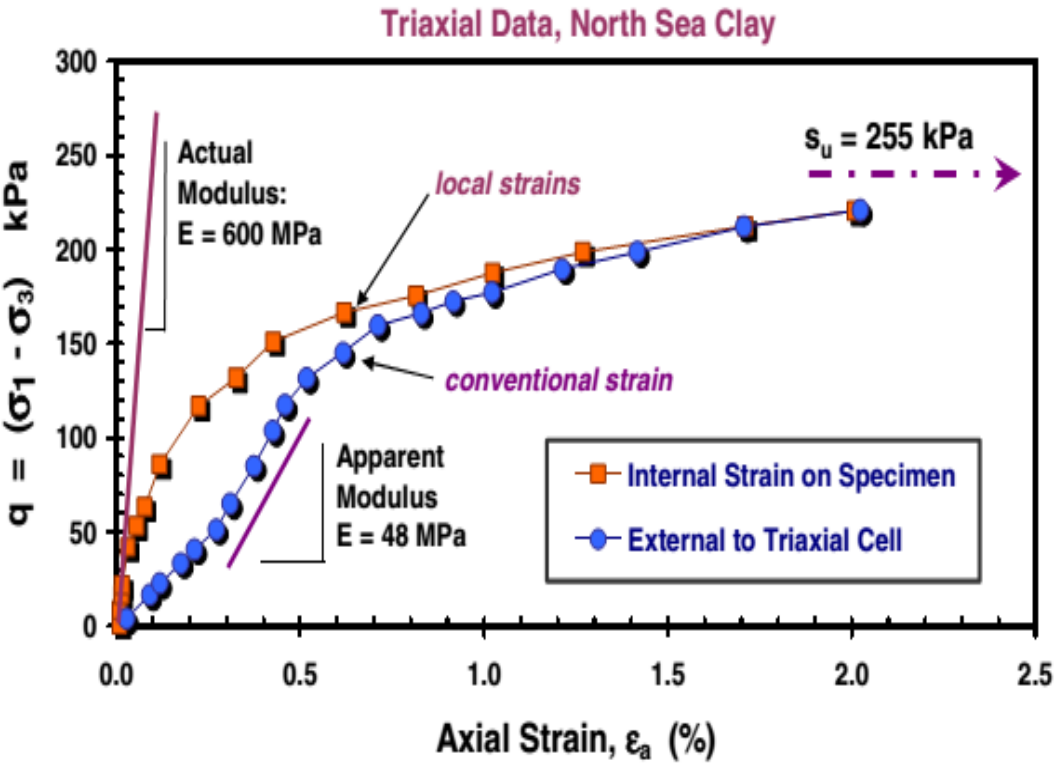

Figure 3.21: Comparison in stress-strain plots produced for North Sea Clay when using local and external LVDT's. After Mayne et al. (2009).

From raw drained triaxial data, the following formula from Muir Wood (1990) determines the volumetric strain (ε_p) experienced by a sample:

Volumetric strain: $$\varepsilon_p = \frac{-\delta V/V}{V}$$ (**Equation 3.29**)

where –δV is the change in volume experienced by the sample, relative to its initial volume (V). Without the presence of local strain equipment at Newcastle University, the following formulae from Muir Wood (1990) enable radial and shear strains encountered by samples to be calculated, which are based on samples' volumetric changes:

Radial strain: $$\varepsilon_r = \frac{-\delta V/V + \delta l/l}{2}$$ (**Equation 3.30**)

Shear strain: $$\varepsilon_q = \frac{-\delta l}{l} + \frac{\delta V/V}{3}$$ (**Equation 3.31**)

Intuitively, the amount of ε_p experienced by samples may be split into ε_a and ε_r components. Hence, ε_p may also be calculated by using the following equation when local strain measurements are available:

Volumetric strain: $$\varepsilon_p = \varepsilon_a + (2\varepsilon_r)$$ (**Equation 3.32**)

When local strain measurements can be taken during triaxial tests, the following equations may also be used to determine values for ε_q, K_{sec} and G_{sec}, respectively for comparison purposes:

Shear strain: $$\varepsilon_q = \frac{2}{3}(\varepsilon_a - \varepsilon_r)$$ (**Equation 3.33**)

Although the degree of ε_a experienced by soils during dynamic/cyclic triaxial testing is very useful in calculating M_r and surface settlements, another strain parameter which is directly related to ε_a and well suited for analysing the dynamic/cyclic behaviour of soils is cyclic shear strain (ε_{cq}), which may be defined through the following equation:

Cyclic shear strain: $$\varepsilon_{cq} = 1.5 \,.\, \delta\varepsilon_a$$ (**Equation 3.34**)

3.4.3.2 Stresses and stiffnesses

3.4.3.2.1 Monotonic tests

In conventional triaxial testing, several testing parameters can considerably influence the final results obtained from tested soil samples; including the effective confining stress, strain/loading rate and the orientation of applied stresses on samples. Effective Cambridge stress paths are the most common means of visualising the effects of these two testing parameters along with natural material properties on soil behaviour. The parameters used to produce effective Cambridge stress paths are deviatoric stress (q) and mean effective stress (p'), which are calculated directly from raw triaxial data from the following formulae:

Deviatoric stress: $$q = \sigma'_1 - \sigma'_3$$ (**Equation 3.35**)

Mean effective stress: $$p' = \frac{(\sigma'_1 + [2\sigma'_3])}{3}$$ (**Equation 3.36**)

where σ'_3 is the effective confining stress (i.e. cell pressure minus pore water pressure) used within the triaxial cell for shearing and σ'_1 is the sum of σ'_3 and the effective axial stress caused by the compression of the samples.

As conducted by Gasparre (2005), stress paths are also very effective in defining the locations of various yield surfaces for soils, which attempt to separate zones of: 1) linear elasticity with fully recoverable strains; 2) non-linear elasticity/plasticity where non-recoverable plastic strains start developing and finally 3) plasticity where non-recoverable plastic strains dominate (Figure 3.22). The boundary between zones 1 and 2 is termed as Y1 (a kinematic surface), the maximum extent of zone 2 is called Y2 (a kinematic surface) and finally the outer limit of zone 3 is Y3, which is a bounding surface.

Prior to yielding, soils exhibit hardening behaviour. Simple elasto-plastic models such as Mohr-Coulomb assumed perfect plasticity post-yielding, which is incorrect. Per Potts and Zdravkovic (1999), once yielded, soils tend to either undergo strain softening (usually observed for overconsolidated soils) or further strain hardening (typically observed for normally consolidated soils).

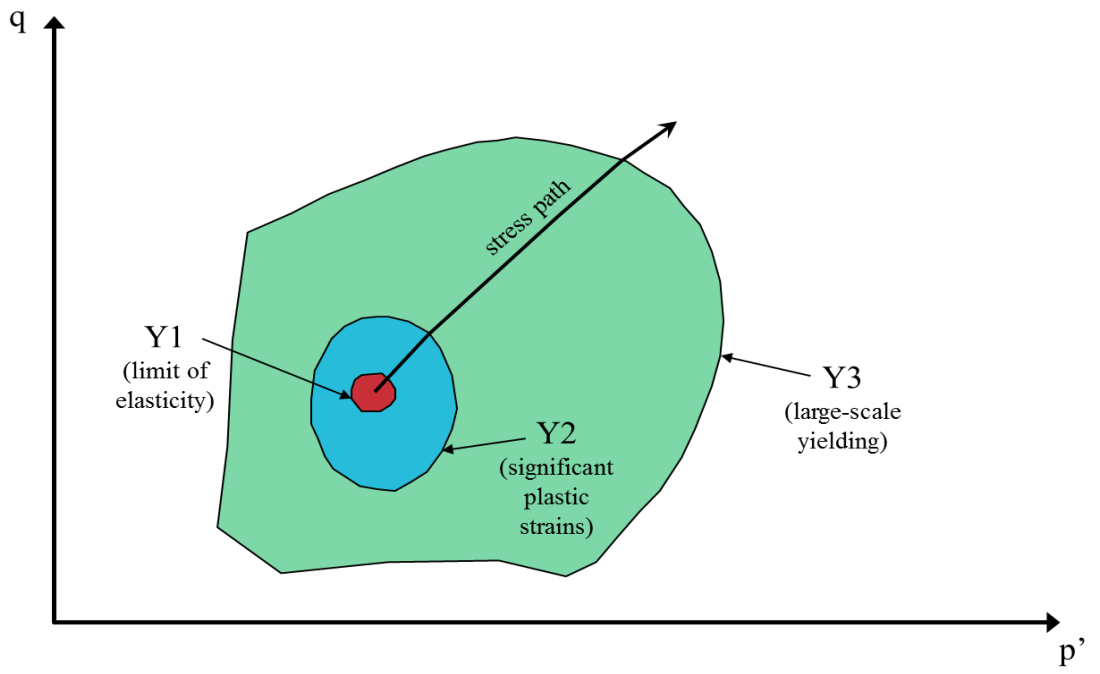

Figure 3.22: Yield surfaces for London Clay, produced by effective Cambridge stress paths. Adapted from Gasparre et al. (2007).

It is important for constitutive soil models to capture both hardening and softening behaviour, which is exhibited by most soils (Figure 3.23).

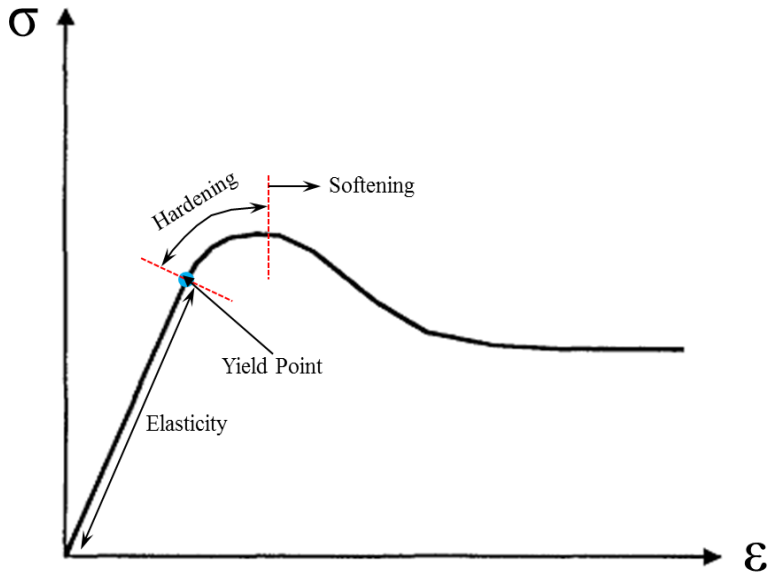

Figure 3.23: Softening and hardening behaviour of soils. Adapted from Potts and Zdravkovic (1999).

There are two types of hardening which can occur as plastic straining occurs within a soil (Figure 3.24); the first is isotropic hardening, where the yield surface remains centred about the same location in p'-q stress space and increases in size. The second type of hardening is kinematic, which involves a yield surface moving within the p'-q stress space, whilst maintaining its initial shape and dimensions (Potts and Zdravkovic, 1999).

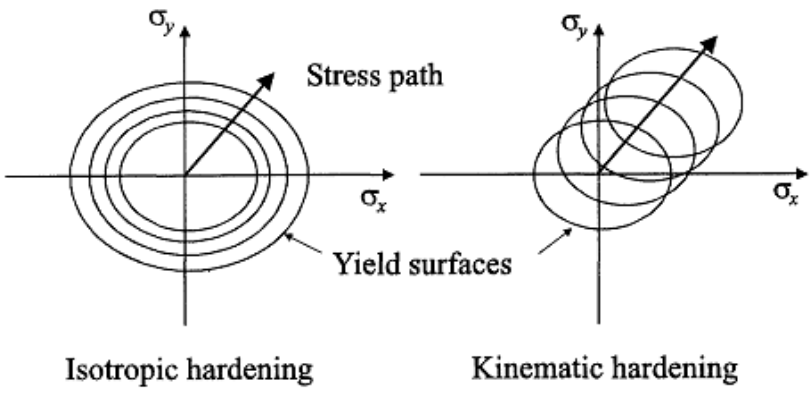

Figure 3.24: Illustration of isotropic and kinematic hardening. Taken from Potts and Zdravkovic (1999).

The stiffness of a soil is simply the relationship between the stress applied to a soil body [σ (kPa) = force (kN) / area (m^2)] and the resulting axial strain (ε_a). Assuming soils exhibit perfectly linear elasticity or plasticity is too simplistic. Instead, soils are generally characterised by complex non-linear behaviour, both for elasticity and plasticity. However, at very small strain levels, soils are likely to display stress-strain behaviour that closely resembles linear elasticity (Figure 3.21). To determine the initial stiffness of a soil at such strain levels, Young's modulus may be calculated via the following formula:

Young's modulus: $$E = \frac{\delta\sigma}{\delta\varepsilon_a}$$ **(Equation 3.37)**

The changing stiffness of a soil with progressive straining may also be monitored via this formula. However, there are two methods which may be adopted to determine Young's modulus; namely the tangential and secant methods. Figure 3.25 below illustrates how tangential (E_{tan}) and secant (E_{sec}/E_{50}) stiffness values may be obtained.

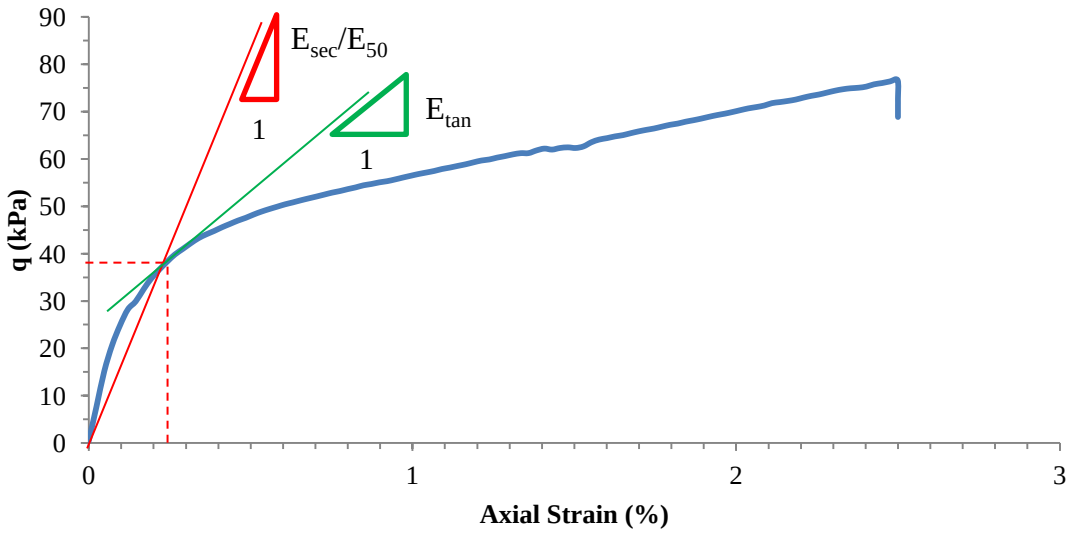

Figure 3.25: Determination of secant and tangential stiffnesses for any given point on a non-linear stress-strain curve. Green = tangential method, red = secant method.

Although Jardine et al. (1986) documented that a large proportion of numerical modelling analyses used secant or tangential Young's modulus values to quantify the changing stiffnesses of materials such as soils with strain, its sole use for examining stiffness degradation within soils was inappropriate. This is primarily due to soils being both compressible and anisotropic materials. When soils are subjected to compressional/shear stresses, individual particles within the material can rearrange themselves into different configurations and therefore displace air and/or water from pore spaces through drainage. Hence, these deformation processes imply that a soil is able to change volume as well as shape during compression/shearing, as demonstrated in Figure 3.26.

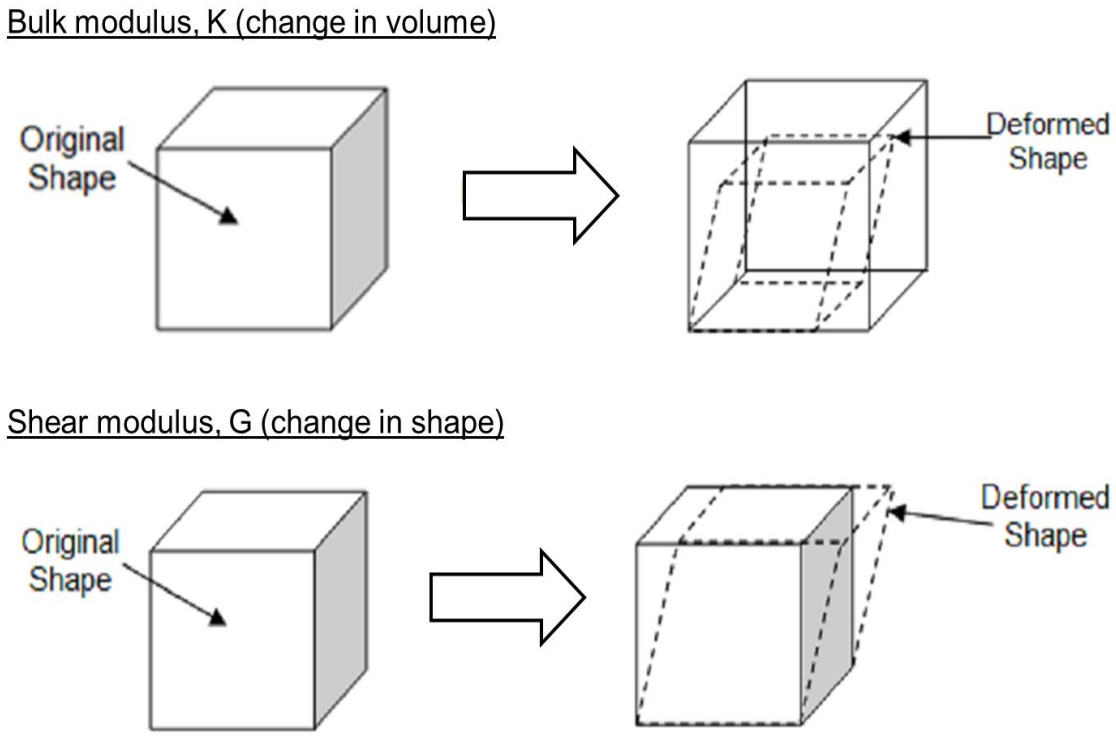

Figure 3.26: Illustrations of shear and bulk moduli, used to define a soil's elastic behaviour.

Therefore, the elasticity of a soil may be defined for its bulk (K) modulus (volumetric changes) and shear (G) modulus (distortional changes). Both parameters can be calculated by using values for Young's modulus (E) and Poisson's ratio (υ), with the latter being calculated through the following equation from Muir Wood (1990):

Poisson's ratio: $$\upsilon = \frac{-\delta d/d}{\delta l/l}$$ (**Equation 3.38**)

Poisson's ratio is a dimensionless parameter, which is simply the ratio between diametric and axial strains occurring during sample compression/shearing. The change in diameter is denoted by δd, with respect to its original diameter (d). The formulae required to calculate values for G and K based on known values for E and υ are provided below (obtained from Muir Wood, 1990):

Bulk modulus: $$K = \frac{E}{3(1-2\upsilon)}$$ (**Equation 3.39**)

Shear modulus: $$G = \frac{E}{2(1+\upsilon)}$$ (**Equation 3.40**)

To derive shear modulus values, either conventional undrained or drained triaxial tests may be conducted. However, values for bulk modulus can only be obtained from drained triaxial tests. Secant bulk and shear moduli may also be derived from ε_p & p' and ε_q & q measurements, respectively by using the following formulae:

Secant bulk modulus: $$K_{sec} = \frac{\delta p'}{\delta \varepsilon_p}$$ (**Equation 3.41**)

Secant shear modulus: $$G_{sec} = \frac{\delta q}{(3\,.\,(\delta \varepsilon_q))}$$ (**Equation 3.42**)

Figures 3.27 and 3.29 below provide a summary of all the combinations of graphs using data from drained and undrained triaxial tests, which are used to derive values for E, G and K.

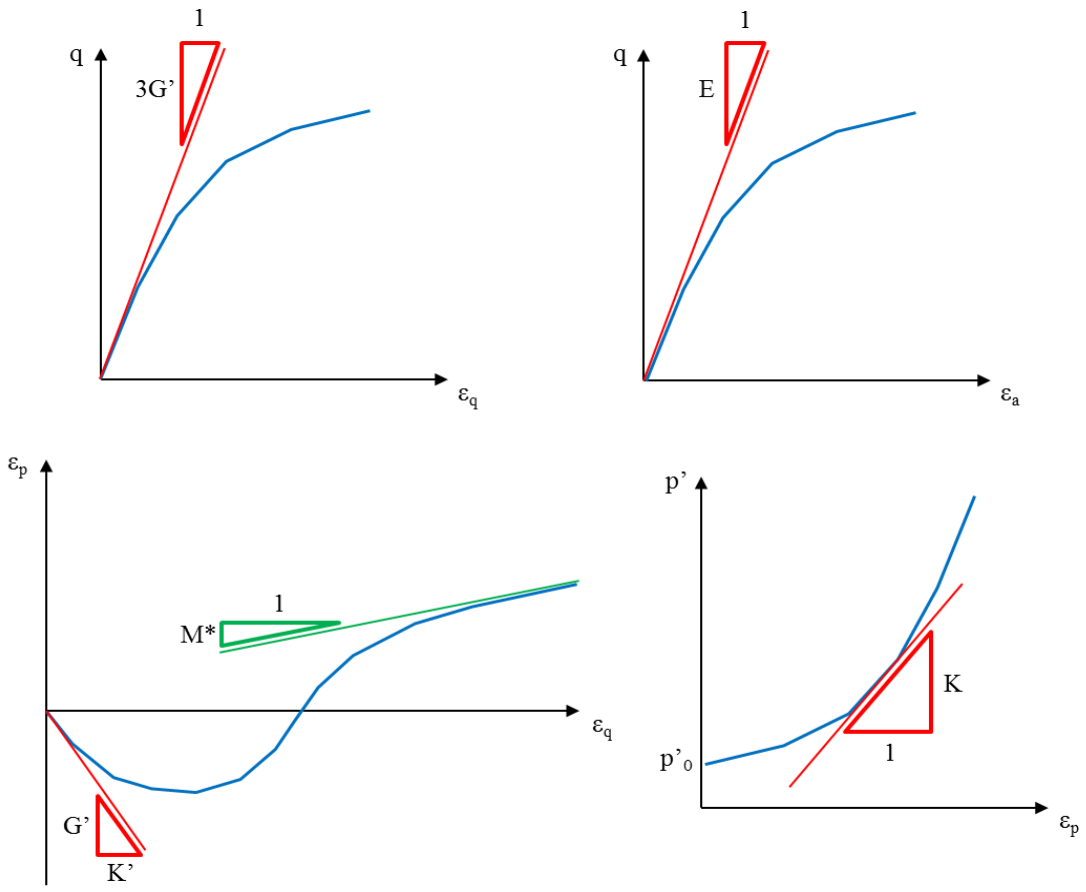

Figure 3.27: Elastic parameters derived from consolidated drained triaxial tests. Adapted from Muir Wood (1990).

Hence, a series of stress v strain plots were produced from the data obtained from all the triaxial tests conducted (including q v p', q v ε_a, q v ε_q, ε_p v ε_q, p' v ε_p and u v ε_q) to derive values for K and G using both tangential and secant methods at numerous strain levels. Curves for both shear and bulk stiffness degradation with increasing shear strain were then subsequently produced. The ε_p v ε_q plot was also used to determine a value for M*, which is used to determine the soil's dilatancy angle:

Dilatancy angle (degrees): $$M^* = \frac{(1-sin\psi)}{(2sin\psi)}$$ **(Equation 3.43)**

The derivation of values for (1-sinψ) and (2sinψ) from drained triaxial testing data can be seen in Figure 3.28 below, according to Schanz et al.(1999):

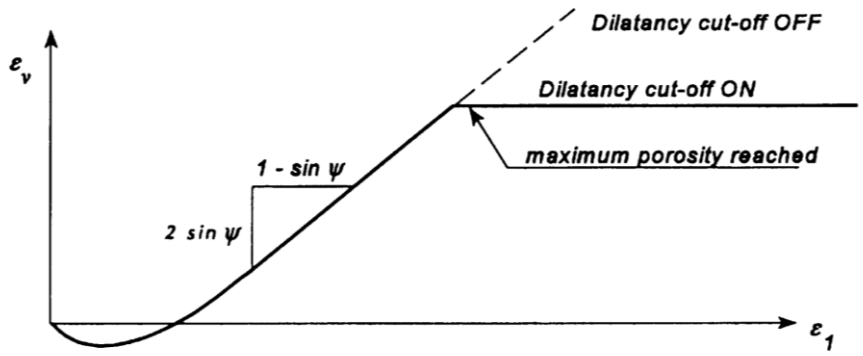

Figure 3.28: Derivation of dilation angle from a standard drained triaxial test. Taken from Schanz et al. (1999).

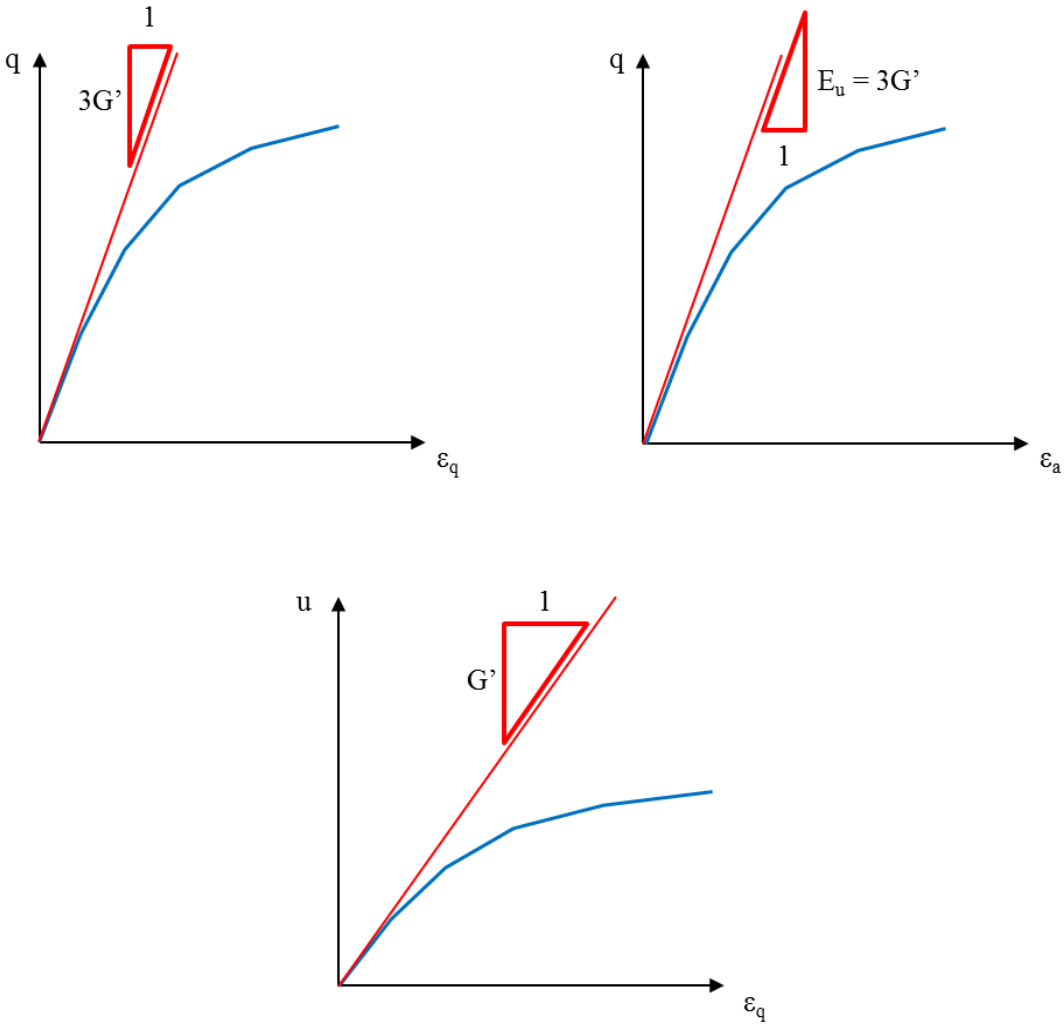

Figure 3.29: Elastic parameters derived from consolidated undrained triaxial tests. Adapted from Muir Wood (1990).

In addition to the effects strain on dilatancy behaviour, stress dilatancy may also be examined, further to triaxial data analysis methods used by Rios et al. (2014) on natural (Figure 3.30) and cemented sands. The parameters to be considered for examining stress dilatancy include the stress ratio, M and the volumetric-shear strain ratio, which are defined below in Equations 3.44 and 3.45 respectively:

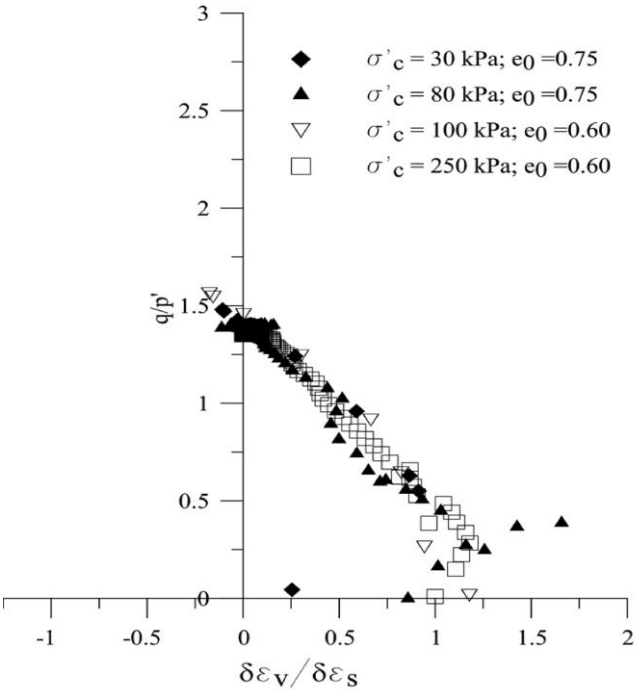

Figure 3.30: Assessment of stress dilatancy behaviour for natural sands. Taken from Rios et al. (2014).

Stress ratio M: $M = \frac{q}{p\prime}$ (**Equation 3.44**)

Volumetric - shear strain ratio: $\frac{\varepsilon_v}{\varepsilon_p}$ (**Equation 3.45**)

As the influence of initial mean effective stress conditions (p'_0) on the behaviour of Lanton alluvium was investigated in this research, it was anticipated that higher initial shear and bulk stiffness values would be calculated for tests conducted at higher p'_0 values. To make the bulk and shear stiffness data sets obtained from all samples directly comparable, the bulk and shear stiffness values were normalised against p' to

negate any effects associated with p'_0 conditions (Simpson and Rouainia, 2012). Hence, the following formulae were used to normalise K_{sec} and G_{sec} data:

Normalised K_{sec}: $$K_{sec} = \frac{K}{p'}$$ (**Equation 3.46**)

Normalised G_{sec}: $$G_{sec} = \frac{3G_{sec}}{p'}$$ (**Equation 3.47**)

3.4.3.2.2 Dynamic tests

As the passing of an HST over a mass of soil is a very quick dynamic event, any pore pressures generated within the soil will have insufficient time to dissipate. Hence, all dynamic tests simulating a passing HST were undrained. As previously mentioned, the behaviour displayed by soils during cyclic and dynamic triaxial tests is generally more complex than that displayed during monotonic tests. According to ASTM D5311-11 (2012), other material parameters concerning the loading-unloading stiffness and pore pressure response of a soil due to dynamic loading must be derived besides those derived from monotonic tests. Other such material properties include the cyclic stress ratio (CSR), defined by the following equation:

Cyclic stress ratio: $$CSR = \frac{q}{2p'_0}$$ (**Equation 3.48**)

q is the deviatoric stress being exerted on the soil sample, which had been consolidated to a specified mean effective stress (p'_0). The excess pore pressure ratio (R_u) may be defined to quantify how a soil's changing pore pressure (δu) changes during cyclic/dynamic loading with respect to the sample's p'_0 value. The following equation may be used:

Excess pore pressure ratio: $$R_u = \frac{\delta u}{p'_0}$$ (**Equation 3.49**)

Dynamic/cyclic triaxial testing is often conducted to determine whether a soil will undergo liquefaction. When using pore pressure criteria, a soil is considered to liquefy when an R_u value of 1 is achieved. This implies that the pore pressure increase due to dynamic/cyclic loading equals to the soil's p'_0 value. Although remarkably similar to using Young's modulus, Resilient modulus (M_r) is a much more effective means of calculating and monitoring how a soil's stiffness changes during cyclic or dynamic triaxial tests. The M_r value of a soil for any load-unload cycle during dynamic triaxial tests is per Figure 3.31; and may be calculated via the following equation:

Resilient modulus (MPa): $$M_r = \left(\frac{q_{max} - q_{min}}{\epsilon_{a\,max} - \varepsilon_{a\,min}}\right)$$ (**Equation 3.50**)

where q_{max} is the maximum deviatoric stress experienced during the loading segment of a cycle and q_{min} is the minimum deviatoric stress recorded for the unloading segment. The axial strains corresponding to q_{max} and q_{min} are $\varepsilon_{a\ max}$ and $\varepsilon_{a\ min}$ respectively.

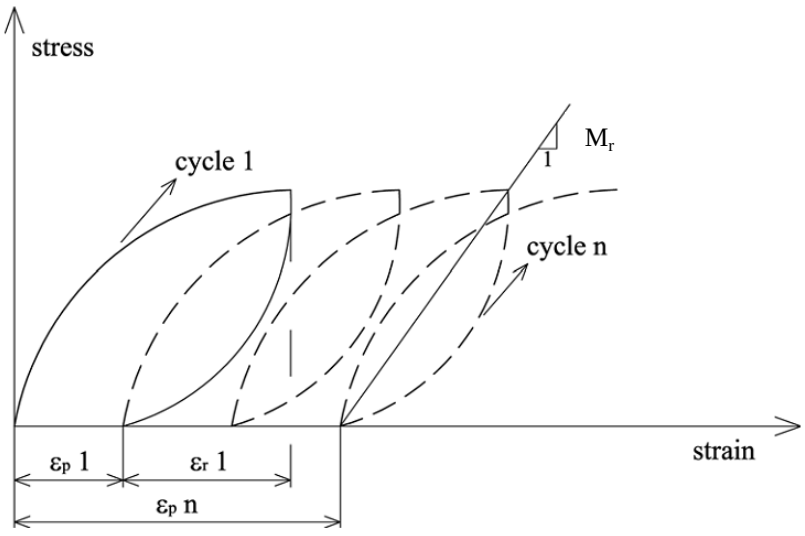

Figure 3.31: Definition and derivation of resilient modulus (M_r) and permanent plastic strains from dynamic/cyclic triaxial tests. Taken from Viana da Fonseca et al. (2013).

Per Viana da Fonseca et al. (2013), the degradation of stiffness and structure within granular soils due to dynamic/cyclic loading is defined by the "shakedown" theory, which assumes that below a certain magnitude of dynamic/cyclic load (i.e. the "shakedown load"), the soil will be completely elastic with no accumulations of plastic strains. Beyond the shakedown load, uncontrolled plastic deformations will result. Three modes of behaviour have been defined by the European Standard Committee for unbound granular materials under cyclic loads (CEN, 2004), based on works by Werkmeister et al. (2005):

1) Plastic shakedown – stable deformation behaviour (Range A)
2) Plastic creep – failure at a high number of loading cycles (Range B)
3) Incremental collapse – failure at low number of loading cycles (Range C)

Illustrations of these three modes are presented in Figure 3.32 for accumulated permanent strain versus number of loading cycles.

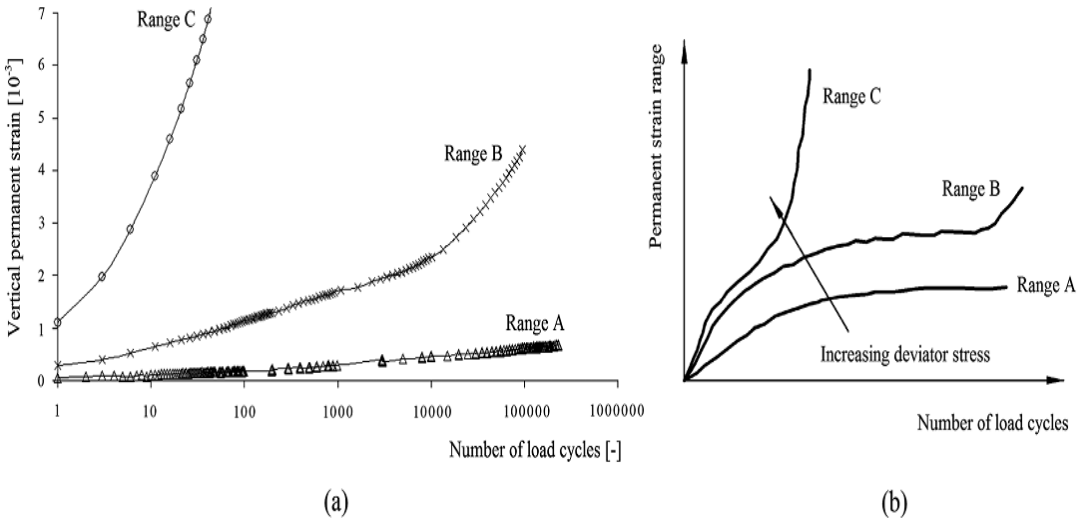

Figure 3.32: Modes of behaviour for permanent strain behaviour with increasing number of loading cycles, per: (a) Werkmeister et al. (2005) and (b) CEM (2004). Taken from Viana da Fonseca et al. (2013).

3.4.3.3 Specific volume

Besides producing effective Cambridge plots for the consolidated drained monotonic triaxial tests conducted, a series of volumetric stress paths (i.e. isotropic normal compression lines [NCL's]) within the specific volume (υ*) – p' compression plane were also produced to define a possible location for Lanton alluvium's critical state line (CSL). To calculate the initial volume for saturated soils (υ^*_0), the following equation may be used:

Initial specific volume: $$\nu^*_0 = 1 + G_s\, w$$ (**Equation 3.51**)

where w is the soil's moisture content and G_s denotes the soil's specific gravity, which may be calculated by using the following equation:

Specific gravity: $$G_s = \frac{\rho_s}{\rho_w}$$ (**Equation 3.52**)

where ρ_s is the soil's particle density (untreated Lanton = 2.606 Mg/m^3, GGBS-NaOH stabilised Lanton = 2.660 Mg/m^3) and ρ_w is the density of water (1.0 Mg/m^3). Hence, Gs for untreated and GGBS-NaOH stabilised Lanton alluvium is 2.606 and 2.660, respectively and is a dimensionless parameter. As the shearing samples progressed during shearing, the changing υ* of samples was monitored via the following equation:

Current specific volume: $$\nu^* = \nu^*_0\left[1 - \varepsilon_p\right]$$ (**Equation 3.53**)

whereby ε_p refers to the volumetric strain experienced by the samples during their compression, which was measured by the ICVC unit. Higher resolution data regarding volumetric strains experienced by samples could also be obtained directly from local

strain tests. However, no small strain consolidated drained triaxial tests could be conducted during this testing programme.

3.4.3.4 Correction factors

During shearing, the majority of reconstituted and natural undisturbed samples exhibited evidence of barrelling. This implies that the current area of samples (A) changed throughout the shearing process. Therefore, assuming that samples deformed as a right cylinder, the following area correction factor was applied to obtain more accurate values for q and p':

Corrected sample area: $$A = \frac{A_c}{1 - \varepsilon_a}$$ (**Equation 3.54**)

whereby A_c is the post-consolidation/pre-shearing area of the sample and ε_a is the amount of axial strain experienced by the sample during shearing.

Per BS 1377: Part 8 (BSI, 1990), the restraining effects of 0.2 mm thick latex rubber membranes on the q values calculated for 38 mm diameter samples during shearing can be considerable. Hence, for any 38 mm diameter samples tested, the following membrane correction factor (σ_{mb}) was applied to q values:

Membrane correction factor: $$\sigma_{mb} = \frac{38}{D_0} . \frac{t_m}{0.2}$$ (**Equation 3.55**)

where D_0 is the initial sample diameter, tm is the thickness of the latex rubber membrane enclosing the sample. The final correction factor to be added was solely for samples which had vertical side drains fitted around their circumferential surface, once axial strains >2% were experienced. The vertical side drain correction factor (σ_{dr}) to be applied depends on the diameter of the sample being tested. The appropriate factor from Table 3.15 may be applied to samples accordingly.

Table 3.15: Vertical side drain correction factors. Values taken from BS 1377 (part 8) (BSI, 1990).

Sample diameter (mm)	Drain correction (kPa)
38	10
50	7
70	5
100	3.5

Chapter 4:

Phase 1: Initial Binder Dosage Trials

4.1 Introduction

This chapter presents results from a suite of laboratory tests investigating the mechanical strength and durability of natural and alkali activated IBP-stabilised alluvial soils. The performances of various IBP binder combinations within an artificial soil are examined to help identify the most effective binder in general engineering performance and environmental sustainability terms. The findings will prove useful in selecting the most suitable binder for stabilising a soft natural alluvial soil, which is addressed in the next chapter.

4.2 Laboratory testing

4.2.1 Materials

For consistency an artificial silty sand was produced in the laboratory in order to represent a soft alluvial soil typically found in the UK. The IBP binders used were PFA, GGBS and RG. The chemical composition of RG is presented in Table 4.1.

Table 4.1: Summary of the chemical composition of red gypsum. After Hughes et al. (2011).

Component	Content (% dry weight)	Component	Content (mg/kg)
Gypsum ($CaSO_4.2H_2O$)	58.5 – 59.3	Chromium (Cr)	500 – 800
Iron Oxide (Fe_2O_3)	32.9 – 36.6	Zinc (Zn)	200 – 400
Titanium (Ti)	1.0 – 1.3	Strontium (Sr)	100 – 300
Aluminium (Al)	0.1 – 0.8	Nickel (Ni)	50 – 60
Magnesium (Mg)	0.5 – 0.6	Cobalt (Co)	20 – 30
Manganese (Mn)	0.2 – 0.5	Barium (Ba)	1 – 3
Silicon (Si)	0 – 0.5	Lead (Pb)	1 – 2
Chlorine (Cl)	0.002 – 0.2		

Previous studies (Hughes et al., 2010, 2011) have investigated the use of lime as an alkali activator in a range of similar soils/IBP binders. In these studies, whilst some soil/binder combinations exhibited significant mechanical improvement, not all IBP's investigated were seen to improve the strength of all the soils investigated. The low strength development could at least be partially attributed to insufficiently high pH being generated by the lime activator. Durability was also identified as a potential concern when using these binders. Therefore in this study a new alternative alkali activator was added to the IBP's by mixing sodium hydroxide (NaOH) flakes and sodium silicate (Na_2SiO_3) solution, both being sourced from Fisher Scientific UK Ltd. For comparison purposes, non-activated binders, lime (supplied by Fisher Scientific UK Ltd) and CEM-I (supplied by Lafarge Cement UK Plc) were tested in addition to activated samples.

4.2.2 Soil characterisation

Based on the particle size distribution of the artificial soil (see Figure 4.1), it may be classified as a silty sand per BS 5930 (1999) criteria. Regarding the soil's Atterberg limits, it had a liquid limit of 23.48 and a plasticity index of 12.02, thereby indicating a low plasticity (Figure 4.2). Based on optimum compaction criteria for the artificial silty sand, all samples had a bulk density of 2.2 Mg/m^3, a dry density of 1.9 Mg/m^3 and an initial gravimetric moisture content of 15%. Per Tomlinson (2001), the dry density of the artificial silty sand falls within the category of fine and silty sands (1.75 – 2.15 Mg/m^3).

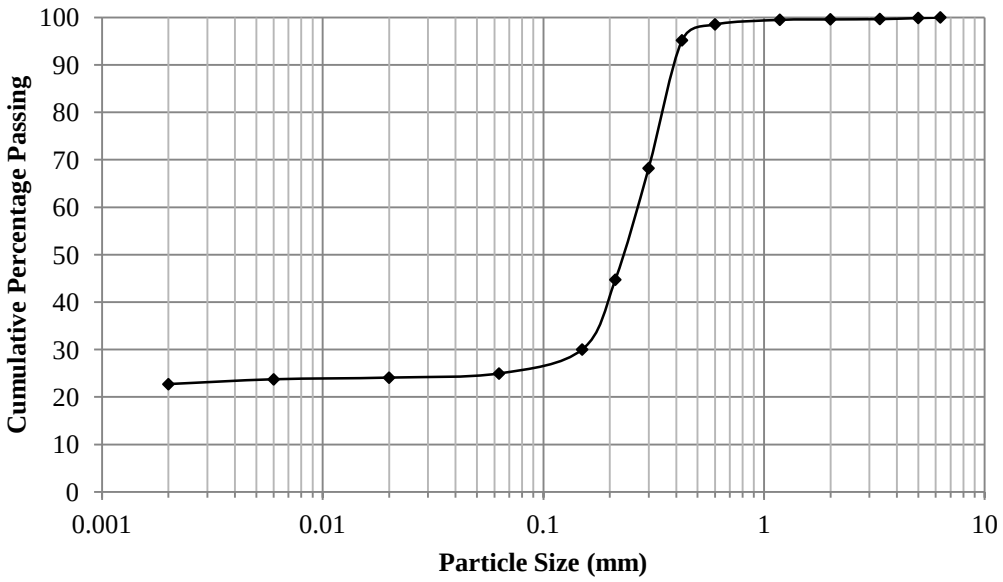

Figure 4.1: Soil grading curve of the artificial silty sandy clay.

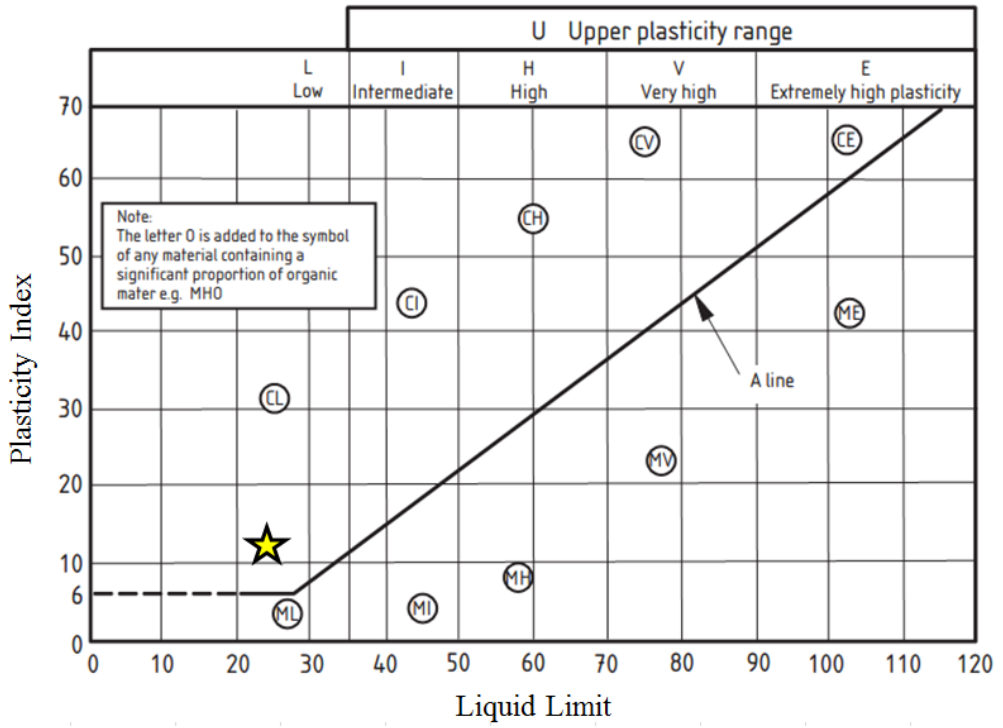

Figure 4.2: Atterberg limits of the artificial silty sandy clay per BS 5930 (1999).

According to results obtained from CEC analysis (BS: 7755, Section 3.12:1996, ISO 13536:1995), a CEC value of 1.96 cmol/kg (or 1.96 meq/100g) and CEC-related charge density (σ_{CEC}) of 0.00032 C m^{-2}were determined for the artificial silty sand. Such a low CEC value is representative of soils characterised by low organic matter

contents and relatively low clay/high sand contents; typically from river alluvium deposits (Cooper, 2009). The surface area of a soil can influence its physical and chemical characteristics. In terms of CEC, larger surface areas provide more exchangeable surfaces. Generally, the higher the soil's clay content, the greater the surface area; and hence a major impact on the soil's CEC. Through BET analysis, the artificial silty sand's surface area had a very low value of 2.275 m^2/g. According to a study by Ersahin et al. (2006), low surface area and CEC values can be expected of alluvial soils; particularly those classed as sandy loams (comprising approximately 10% clay, 30% silt and 60% sand). However, the surface area and CEC values obtained for the artificial silty sand from this study are even lower than those documented by Ersahin et al. (2006). This can be explained by the large proportion of sand sized particles and the relatively little silt and clay content.

4.2.3 Results

4.2.3.1 Compressive strength and stiffness

Figure 4.3 shows stress strain plots from the UCS testing of the individual IBP binder soil mixes. Figure 4.4 shows the average maximum strengths attained compared with soils mixed with CEM-1 and untreated soil. When the IBP's were used individually as binders, alkali activation had little effect on the strength of RG samples. The strength of the alkali activated PFA samples increased with time whereas the non-activated PFA samples did not. Compared with the natural performance of the artificial silty sand, the benefits in using activated PFA or RG binders appear negligible. The alkali activated GGBS samples showed the largest and most rapid strength and stiffness improvements with curing time. After 28 days curing, the activated GGBS binder exhibited twice the strength of standard CEM-1 cement, averaging 6 MPa after 28 days. However, as similarly observed for the non-activated PFA and RG, non-activated GGBS showed very little strength gain over the testing period. Generally, the behaviour of the activated GGBS samples after each curing period upon failure was brittle, compared with more ductile behaviour observed for other stabilised mixtures.

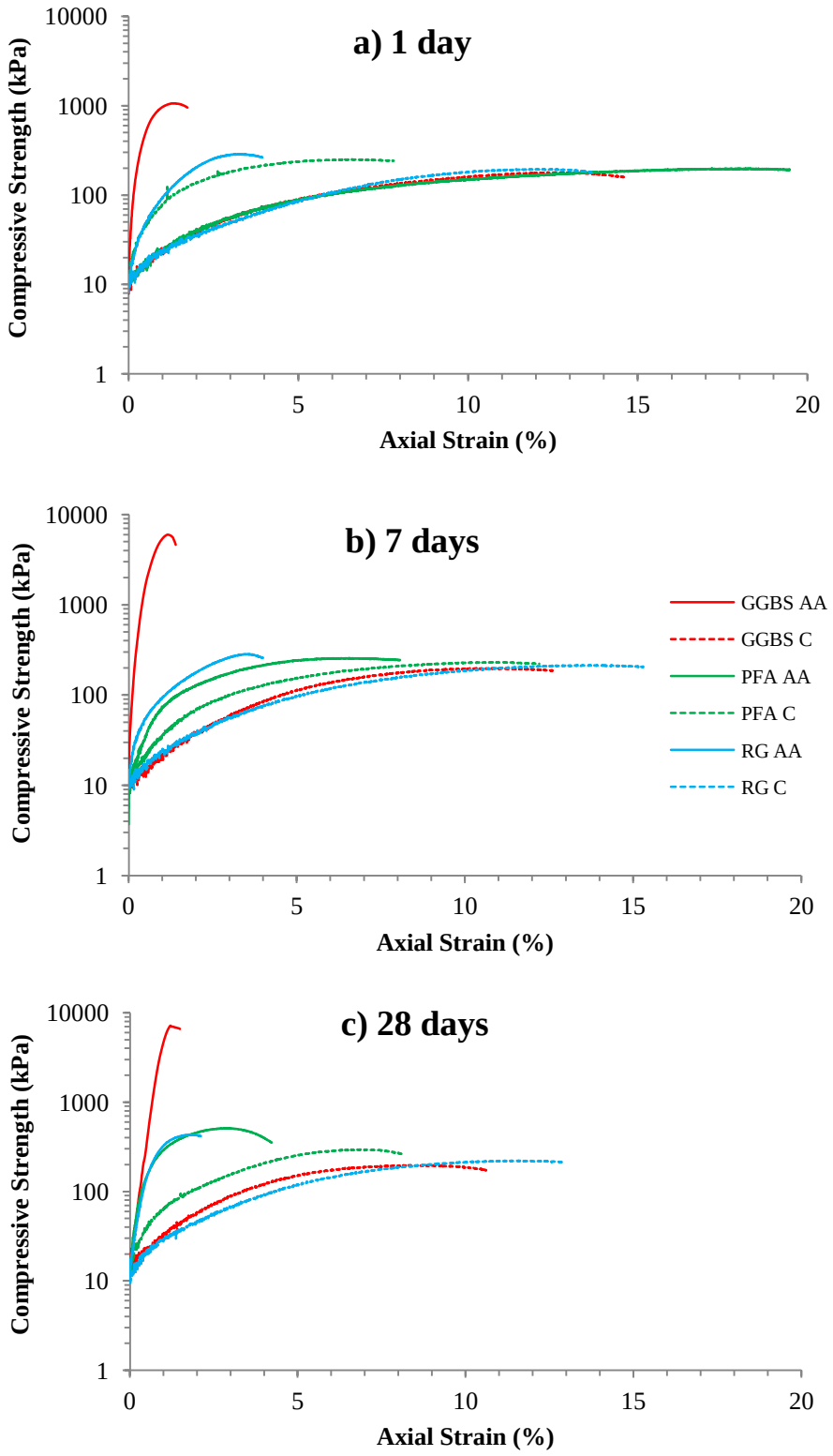

Figure 4.3: Stress strain plots from UCS testing for single IBP binder mixes after curing periods of: a) 1 day, b) 7 days and c) 28 days. Note: legend is the same for all graphs.

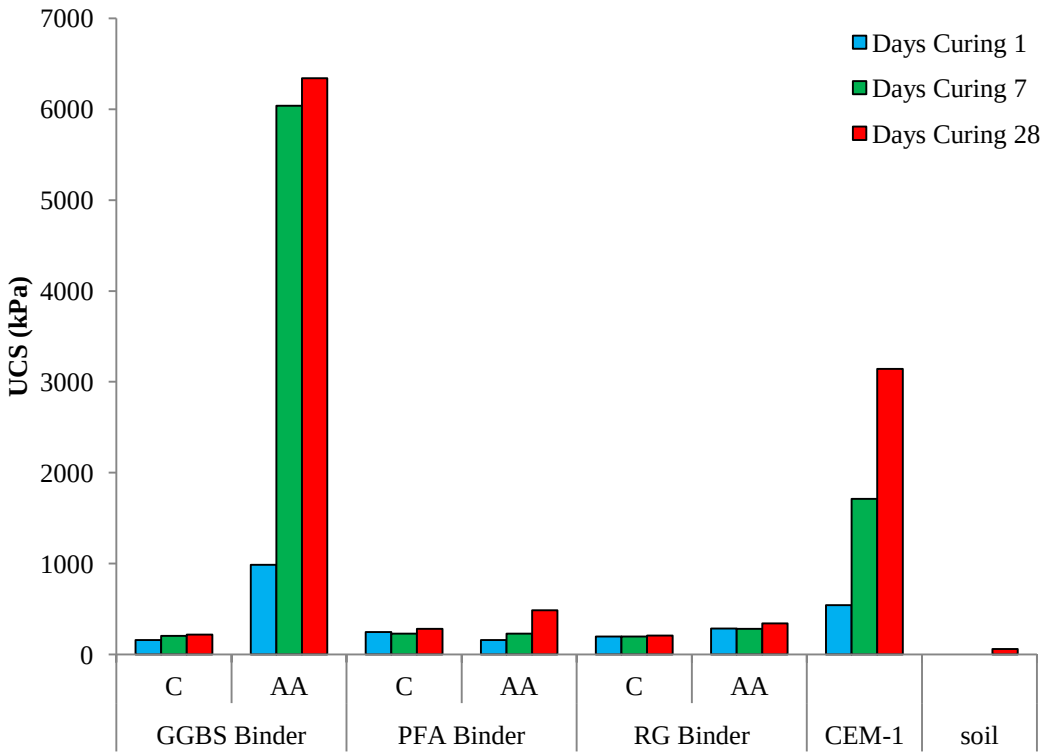

Figure 4.4: Average maximum unconfined compressive strengths for single IBP binders (average of three tests per curing period).

Figure 4.5 presents a selection of stress strain plots from the UCS testing of combined IBP binder soil mixes, and in Figure 4.6 a summary of average maximum strengths with curing time compared with soils mixed with CEM-1 and untreated soil. Alkali activation clearly increased the strengths developed in all of the combined IBP binders. The combination of GGBS–RG exhibited the highest strength (5 MPa after 28 days) and GGBS–PFA also showed significant strength gain (3.5 MPa after 28 days). Both these IBP combinations exhibited higher strengths than the CEM-1 binder. Contrastingly, the combination of PFA and RG exhibited the lowest strength gains. Figure 4.6 also shows these samples having the lowest levels of stiffness.

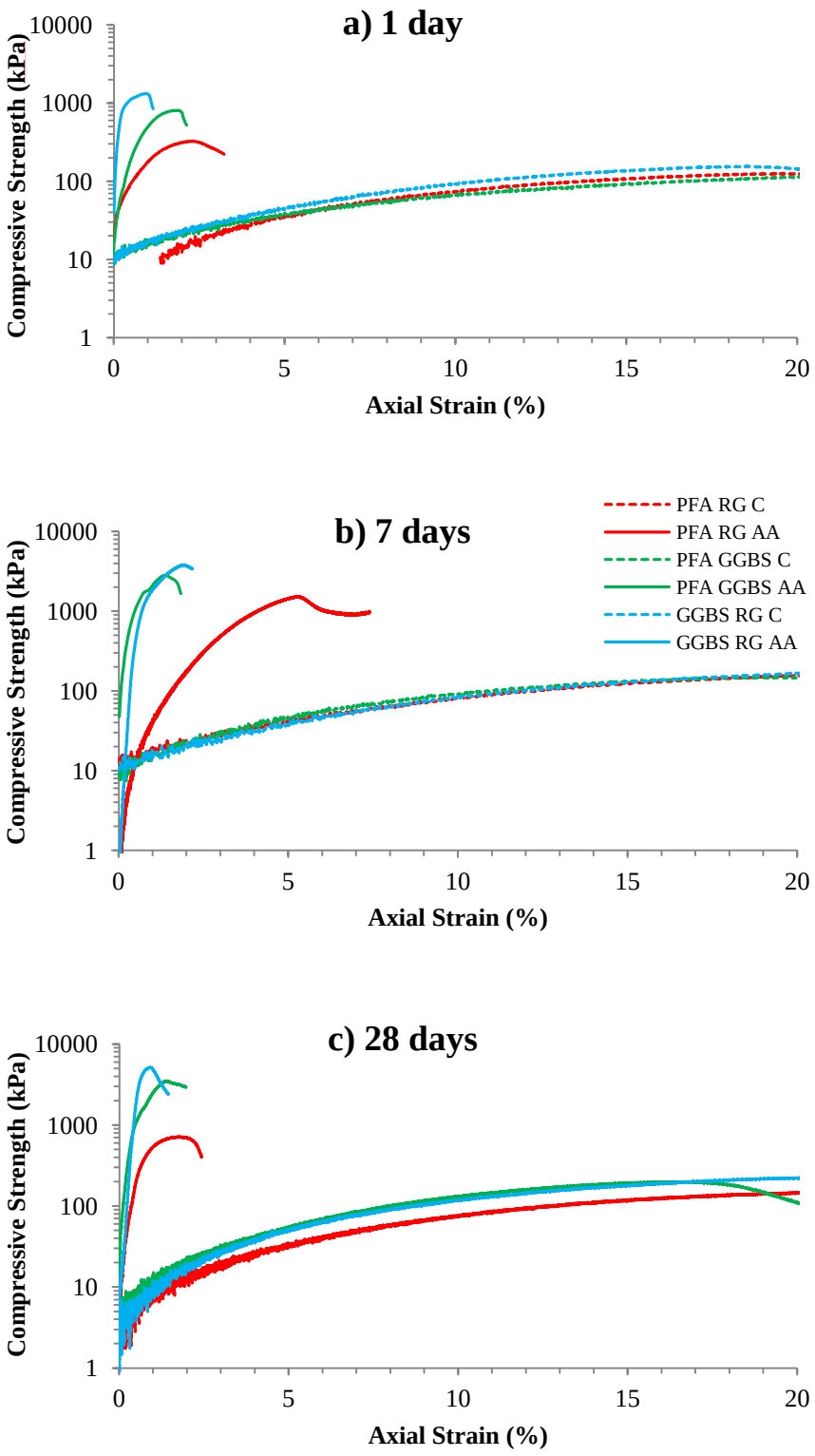

Figure 4.5: Stress strain plots from UCS testing for combined IBP binder mixes after curing periods of: a) 1 day, b) 7 days and c) 28 days. Compared with Figure 4.3, although maximum compressive stresses for combined binders were achieved at similar strains as individual binders, activated combined binders achieved lower strengths after each curing period. Note: legend is the same for all graphs.

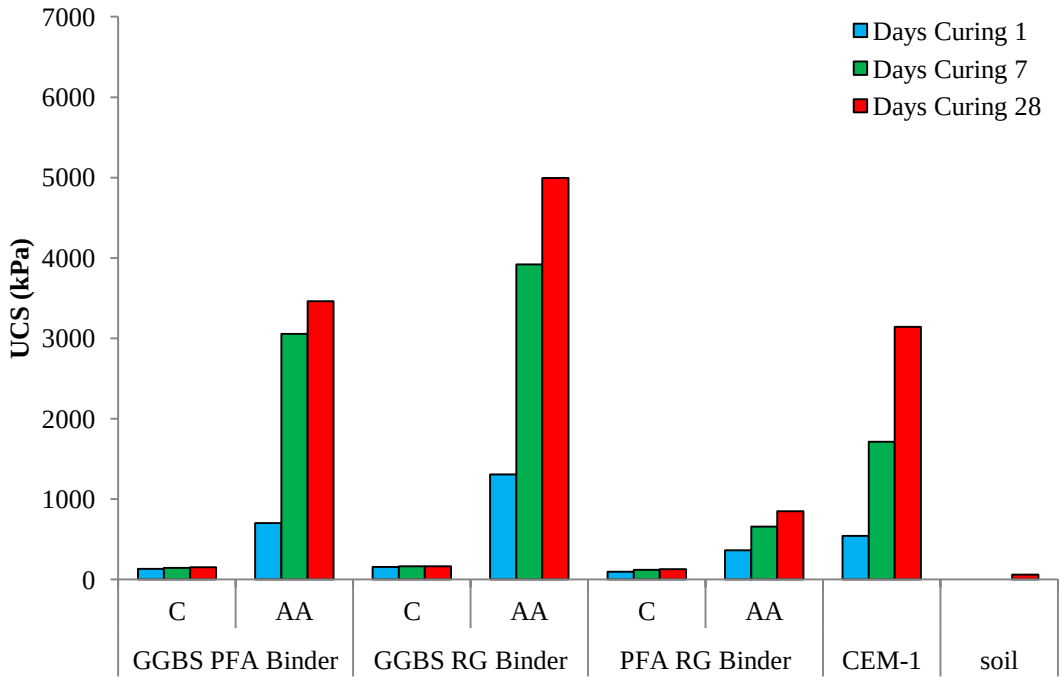

Figure4.6: Average maximum unconfined compressive strengths for combined IBP binders.

As for the UCS testing of the individual binders, the behaviour of samples containing a GGBS-based binder and had been alkali activated exhibited brittle behaviour upon failure. Contrastingly, the activated PFA-RG samples were characterised by more ductile behaviour at failure. Based on the compressive strength results obtained for the GGBS-based binders above, there seemed little logic in pursuing other alternative IBP binder combinations. However, through personal communication with D. Adams from Keller Geotechnique (2011), construction companies specialising in carrying out deep soil mixing have a keen interest in using PFA as an alternative binder to lime and CEM-I, given it is as abundant as GGBS and also is of lower cost.

4.2.3.2 Quick undrained shear strength

Results from the "quick" undrained triaxial tests are presented in Figure 4.7. Relatively similar results to those in Figure 4.5 for compressive strength are evident. The alkali activated GGBS-RG and GGBS-PFA binder combinations produced the highest shear strengths after 28 days. Interestingly between 28 and 56 days, the

strength of the activated GGBS-RG specimen decreased from 2.1 to 1.7 MPa. However, even after this strength reduction, the GGBS-RG binder's strength exceeded that of most other binders tested. The non-activated binder combinations showed low strengths of 100–200 kPa.

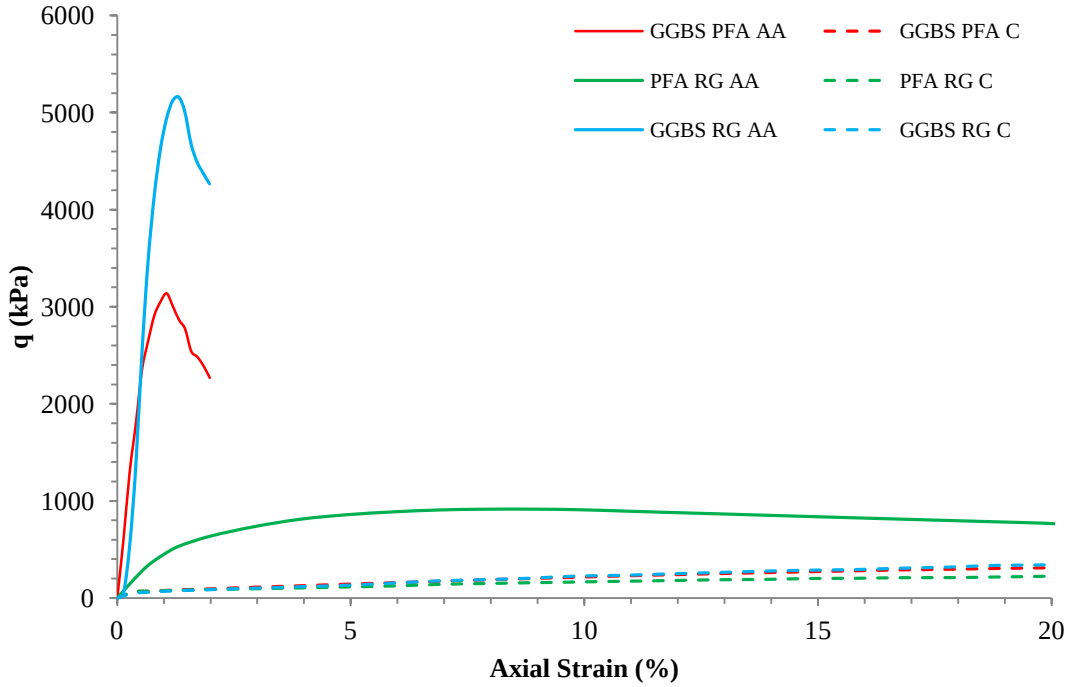

Figure 4.7a: Deviatoric stress ($q = \sigma_1 - \sigma_3$) –axial strain behaviour of samples after 28 days curing.

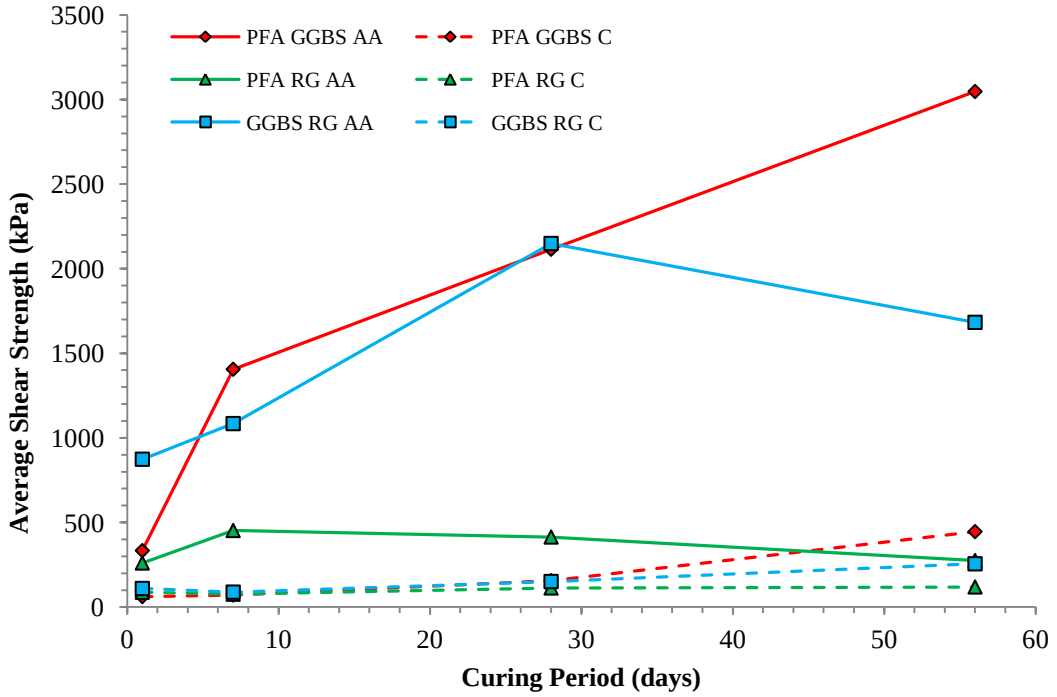

Figure 4.7b: Development of average shear strength (i.e. 0.5 x q) over 28 days for all samples tested.

However, after 28 days Figure 4.7 shows evidence to suggest that the non-activated GGBS-PFA and GGBS-RG binders started to slowly develop higher strengths, increasing up to 300–400 kPa at 56 days.

4.2.3.3 Compressibility

Oedometer studies were conducted according to BS 1377: Part 5 (BSI, 1990). Both non-activated and activated soil-binder mixtures of GGBS-RG, GGBS-PFA and PFA-RG were tested. The coefficients of volume compressibility (M_v) – defined as the volume change per unit volume per unit increase in effective stress (Craig, 2004), was calculated to gain an understanding of the compressible nature of IBP-stabilised silty sand. Samples were allowed to cure for 28 days and then subjected to 50, 100, 200, 400 and 800 kPa loading stages. Compression curves from oedometer testing and a summary of the calculated M_v values are shown in Figures 4.8 and 4.9 respectively.

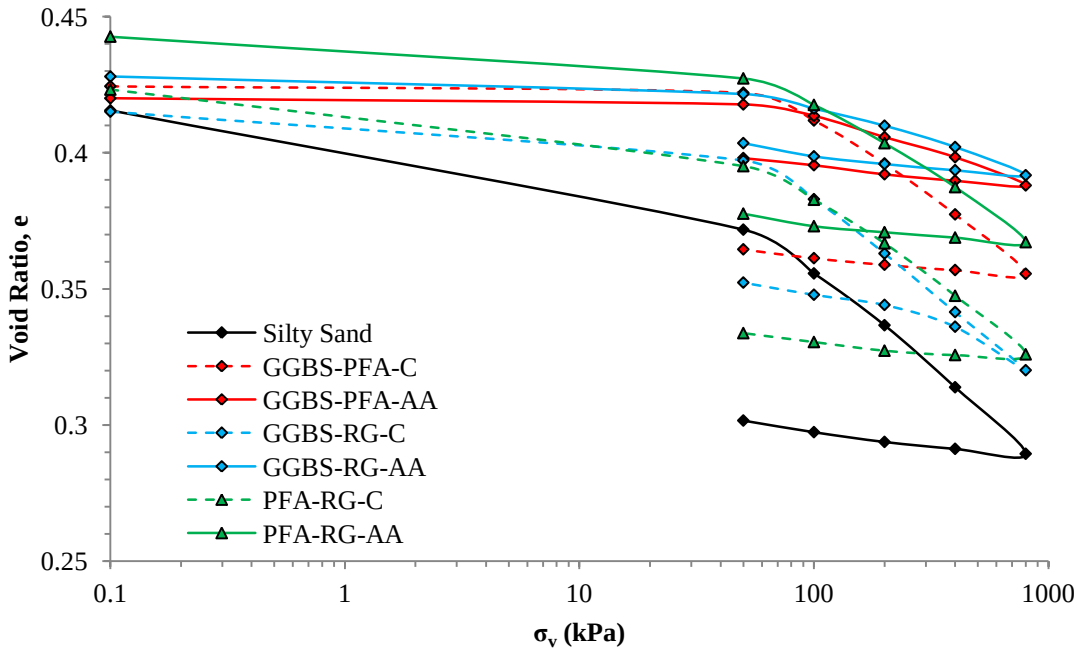

Figure 4.8: Oedometer compression curves of the natural and stabilised silty sand samples.

Per Figure 4.8, the compression curve for the untreated silty sand is located below the compression curves for all the stabilised soil mixtures tested as a result of the silty

sand experiencing more compression compared with the other stiffer stabilised samples.

Table 4.2: Summary of the compression and swelling indices recorded for treated and untreated silty sand after 28 days curing.

Soil – Binder Mixture	Compression index (Cc')		Swelling index (Cs')	
	Non-AA (C)	AA	Non-AA (C)	AA
Silty sand	0.078		0.012	
GGBS-PFA	0.067	0.029	0.008	0.009
GGBS-RG	0.071	0.030	0.014	0.008
PFA-RG	0.068	0.060	0.009	0.010

Regarding the compression indices (C_c) exhibited by samples (see Table 4.2), the stabilised samples had lower values compared with that recorded for the untreated silty sand (0.078). When comparing the C_c values obtained for the stabilised samples, the alkali activated GGBS-RG and GGBS-PFA samples have the lowest values of 0.030 and 0.029 respectively; whereas their respective non-activated samples along with the non-activated and activated PFA-RG samples had C_c values between 0.067 and 0.071. This indicates that the activated GGBS-RG and GGBS-PFA binders were much less compressible compared with the untreated silty sand and other binder combinations. Additionally, the C_c values obtained for the non-activated GGBS-RG, GGBS-PFA and PFA-RG were more comparable with that obtained for the untreated silty sand. This therefore suggests that alkali activation is certainly required in order to observe any marked reduction in compression and therefore C_c value.

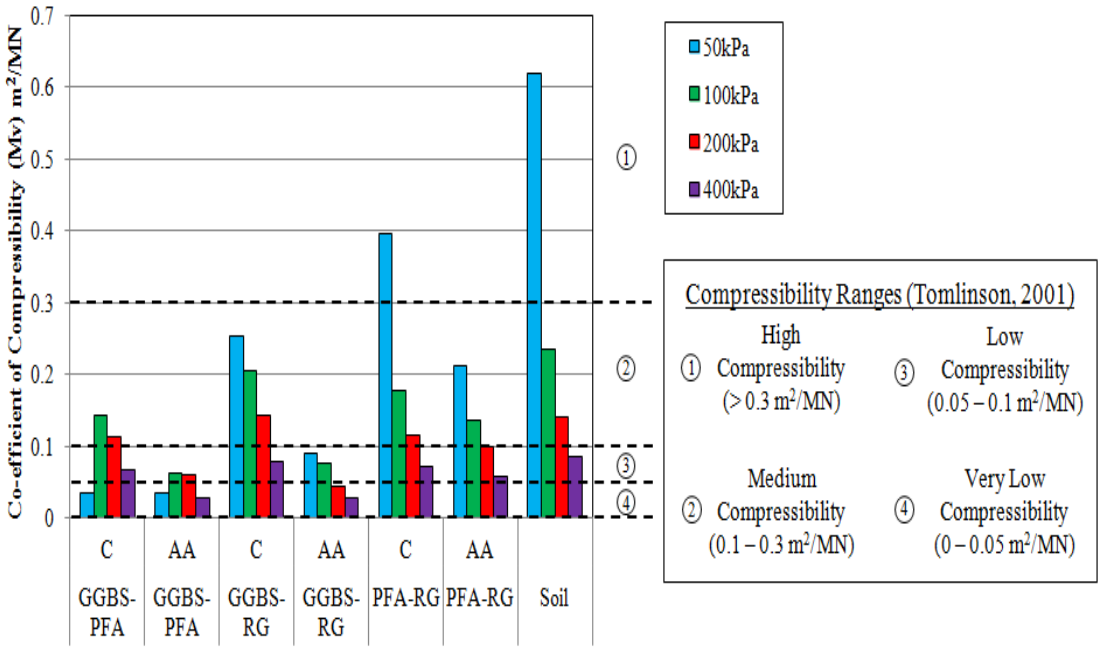

Figure 4.9: Summary of the M_v values (m^2/MN) calculated from oedometer tests after 28 days.

Figure 4.9 shows that all the binders tested reduced the compressibility of the silty sand soil and that the alkali activated binders reduced its compressibility by a greater extent than the non-activated binders. The initial M_v of the untreated soil was calculated as 0.6 m^2/MN, which is typical of normally consolidated alluvial clays and is considered highly compressible (Tomlinson, 2001). In the samples mixed with alkali activated IBP binders, the compressibility was reduced to an M_v of 0.06-0.21 m^2/MN and therefore considered to be a soil of low to medium compressibility (Tomlinson, 2001).

Of the alkali activated binders, the GGBS-PFA binder is the most effective in reducing compressibility with GGBS-RG slightly less effective and PFA-RG significantly less effective.

4.2.3.4 Durability

4.2.3.4.1 Wetting-Drying

Wetting-drying durability testing was conducted to determine soil cement losses, changes in volume and water contents due to wetting and drying cycles. The wetting and drying test results are shown in Figures 4.10 and 4.11 and Table 4.3.

Table 4.3: Average number of testing cycles survived by soil-binder mixtures during wetting-drying testing.

Binder Mixture	No. cycles survived
GGBS-AA	12
GGBS-C	0
PFA-AA	12
PFA-C	0
RG-AA	0
RG-C	0
GGBS-RG-AA	12
GGBS-RG-C	12
GGBS-PFA-AA	12
GGBS-PFA-C	0
PFA-RG-AA	5
PFA-RG-C	0
CEM-I	4.5

Of the individual IBP binders; non activated GGBS, PFA and RG all disintegrated upon their first immersion in water, as did alkali activated RG. Alkali activated GGBS and PFA survived the full 12 cycles with their water content and volume remaining reasonably constant. Of the combined IBP binders, all the non-activated samples disintegrated during the first cycle of testing. Alkali activated PFA-RG survived for 6 cycles but displayed a rapid reduction in volume during preceding cycles. Alkali activated GGBS-RG and GGBS-PFA survived the full 12 cycles. Specimens mixed with CEM-I initially showed reasonably constant water content and volume; but disintegrated at 4 and 5 cycles.

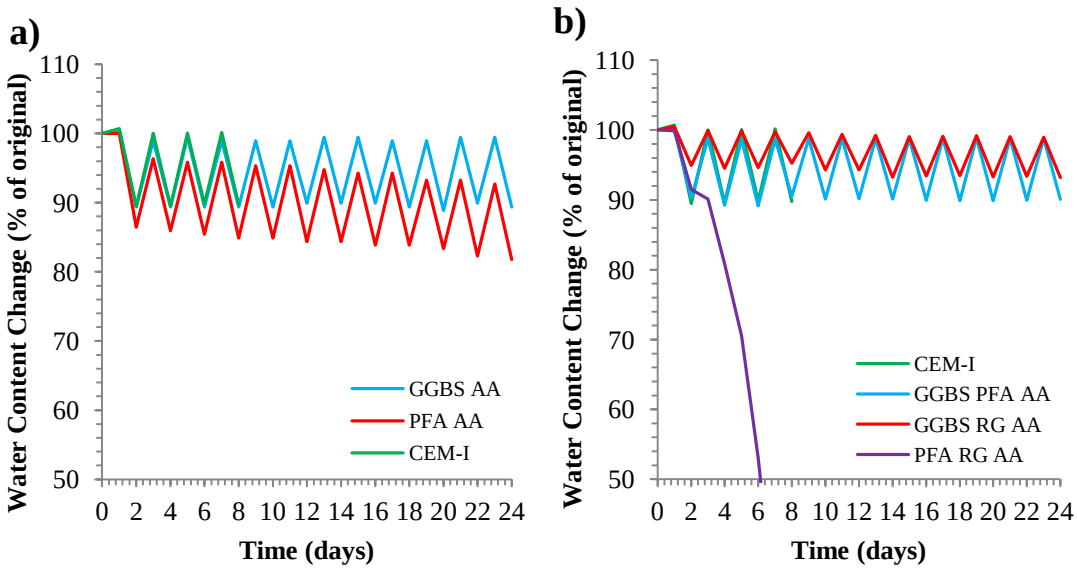

Figure 4.10: Water content changes experienced during wetting-drying testing by: a) single binders and b) multi binders.

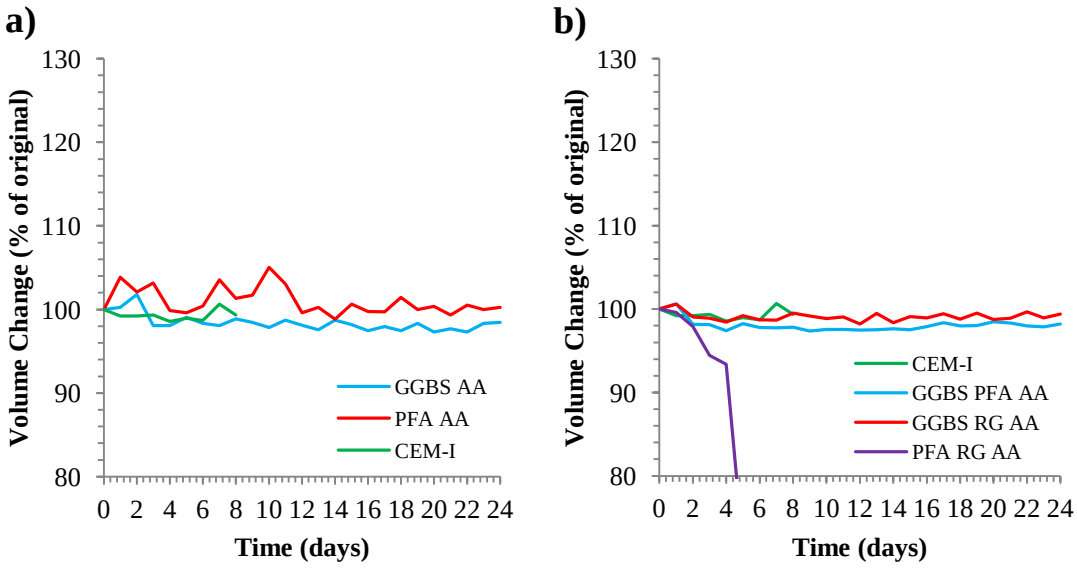

Figure 4.11: Volume changes experienced during wetting-drying testing by: a) single binders and b) multi binders.

4.2.3.4.2 Freezing-Thawing

The volumetric and moisture content results from the freeze-thaw tests are presented in Figures 4.12 and 4.13 and Table 4.4.

As for the individual IBP binders during wetting-drying testing, all non-activated samples disintegrated upon their first immersion in water. The alkali activated RG binder survived 3 cycles. The alkali activated PFA exhibited a significant reduction in water content and variation in volume after the 7^{th} cycle. The alkali activated GGBS binder sample survived for the full 12 cycles and showed only slight fluctuations in water content and volume.

With the exception of GGBS-PFA, the non-activated combined IBP binders exhibited low durability. Non-activated PFA-RG survived for 4 cycles and non-activated GGBS-RG survived for 8 cycles. The alkali activated combined binders survived the full 12 cycles with the exception of GGBS-RG, which disintegrated after 9 cycles. Despite surviving 12 cycles, the PFA-RG-AA and GGBS-PFA-C specimens showed significant variation in water content and volume throughout testing. Only the GGBS-PFA-AA specimen showed consistent water content and volume over 12 cycles.

Samples stabilised with CEM-I survived 4 cycles, exhibited small variations in volume and showed a slight decrease in water content.

Table 4.4: Average number of testing cycles survived by soil-binder mixtures during freezing-thawing testing.

Binder Mixture	No. Cycles survived
GGBS-AA	12
GGBS-C	0
PFA-AA	12
PFA-C	0
RG-AA	3
RG-C	0
GGBS-RG-AA	8.75
GGBS-RG-C	7.5
GGBS-PFA-AA	12
GGBS-PFA-C	12
PFA-RG-AA	12
PFA-RG-C	3.75
CEM-I	4.5

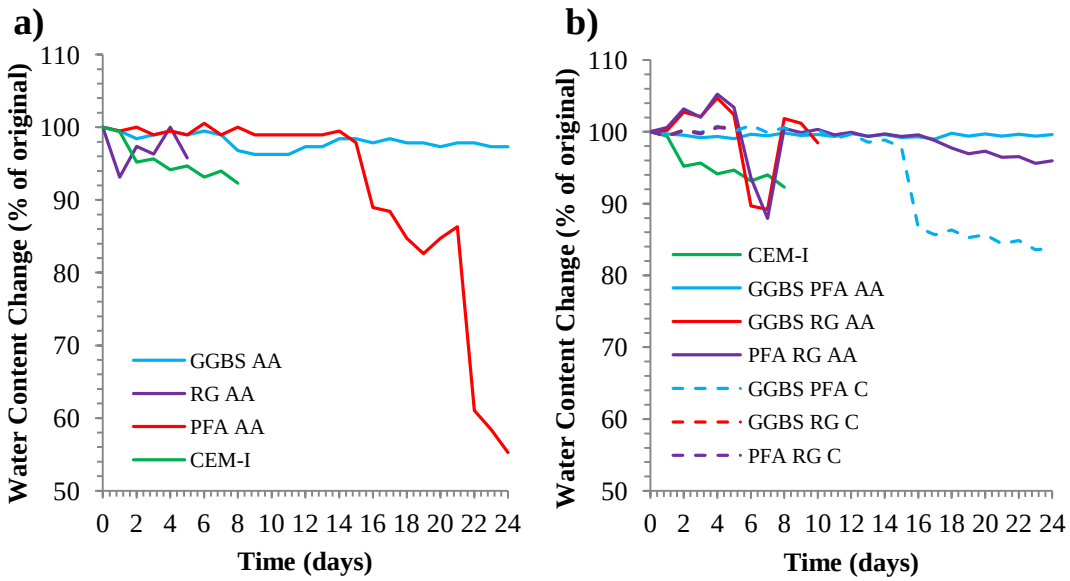

Figure 4.12: Water content changes experienced during freezing-thawing testing by: a) single binders and b) multi binders.

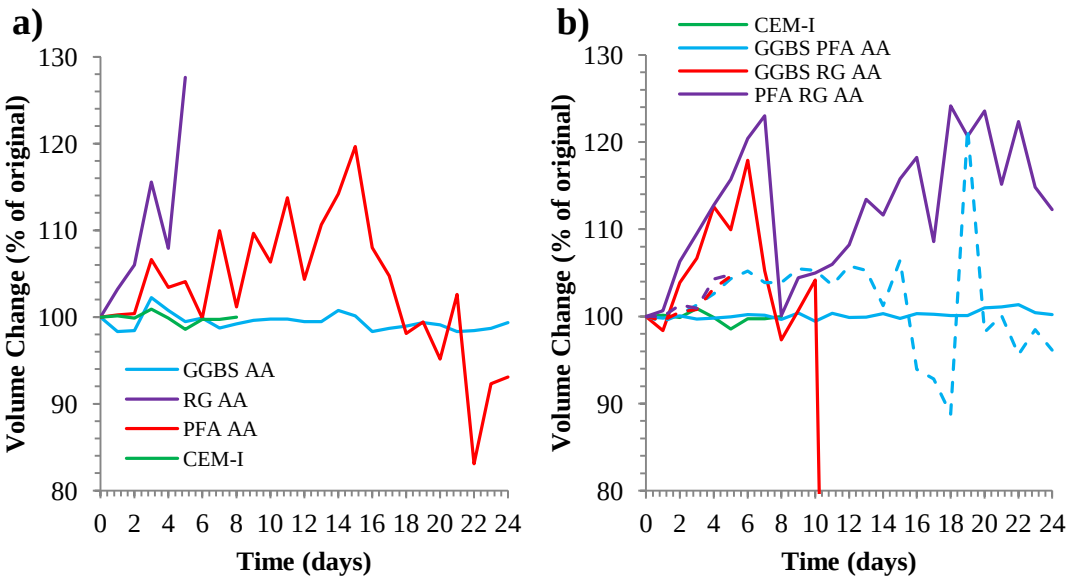

Figure 4.13: Volume changes experienced during freezing-thawing testing by: a) single binders and b) multi binders.

4.2.3.5 Water content testing

To determine whether there was sufficient water within the samples for continuing hydration and formation of cementitious gels, sub-samples were retained for water content testing immediately after strength testing. Testing was carried out per BS 1377: Part 2 (BSI, 1990) with an adjustment to the testing procedure for samples containing gypsum. As the conventional test requires samples to be dried at 110 ^{o}C, exposure to such high temperatures will cause gypsum to convert to anhydrite; and induce an incorrect water content reading. Therefore gypsum samples were dried at 45 ^{o}C for twice the standard drying time.

Table 4.5: Average changes in water content observed with increasing curing time for non-activated and alkali activated soil-binder mixtures.

Binder	Water content (%) with increasing curing time			Reduction in water content (%)
	1 day	7 days	28 days	
GGBS-AA	12.90	12.30	12.20	0.70
GGBS-C	12.80	12.90	12.70	0.10
PFA-AA	12.70	12.60	11.20	1.50
PFA-C	12.30	12.10	11.70	0.60
RG-AA	14.50	14.10	14.10	0.40
RG-C	13.30	12.90	12.50	0.80
GGBS-PFA-AA	13.0	12.12	11.85	1.15
GGBS-PFA-C	13.68	12.68	11.12	2.56
GGBS-RG-AA	12.11	11.41	11.08	1.03
GGBS-RG-C	13.95	13.65	11.45	2.50
PFA-RG-AA	13.10	12.51	12.04	1.06
PFA-RG-C	13.46	13.46	12.64	0.82
CEM-I	15.29	13.25	11.92	3.37

From Table 4.5, most samples had water contents between 12 and 14% over the 28 day curing period. However, a few samples had water contents of ~11% after 28 days such as the GGBS-RG-AA samples. This indicates that there was sufficient water volume within the samples for hydration to occur throughout the 28 day testing periods.

4.2.3.6 pH Testing

Previous studies (Hughes et al., 2011) have identified that insufficient pH (< 10.5) within soils stabilised with pozzolanic material can result in low strength development. Therefore in this study, sub-samples were retained after strength testing at 28 days and their pH checked according to BS 1377: Part 3 (BSI, 1990). pH results are presented in Figure 4.14.

Average pH values of 9.0, 6.23 and 9.7 were recorded for non-activated GGBS, RG and PFA-stabilised soils, respectively; whereas values of 11.47, 11.1 and 11.7 were achieved for their respective activated mixtures. pH values obtained for activated samples comprising two IBP's were greater than those above; whereby GGBS-PFA, GGBS-RG and PFA-RG samples ranged between 12.4 – 12.7, 11.9 – 12.4 and 12.1 – 12.5, respectively.

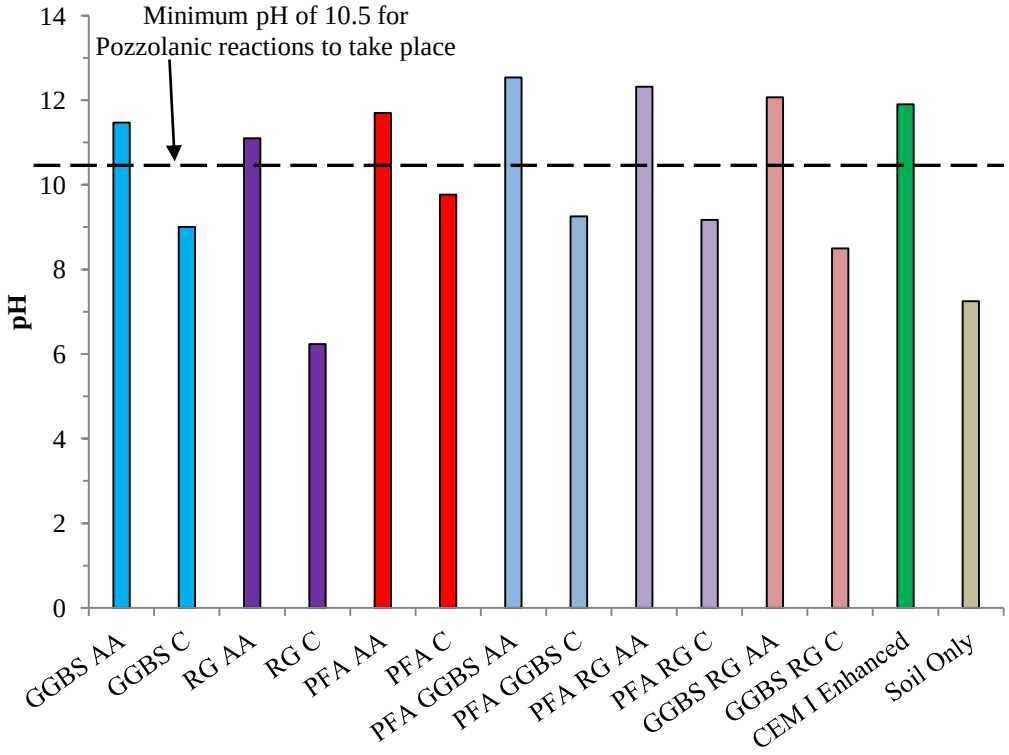

Figure 4.14: Bar chart showing the average pH values obtained by all non-activated and alkali activated samples over a curing period of 28 days.

4.2.3.7 Mineralogy

The 28 day cured UCS samples were retained after strength testing for a qualitative XRD analysis to examine the mineralogy of the combined IBP-stabilised samples. The focus was to determine whether cementitious minerals (such as C-S-H and C-A-H) were present within samples. Such minerals have been documented to cause strength development within stabilised soils. Additionally, problematic minerals such as Ettringite were searched for as they are known for their potential to cause soils to swell and ultimately lead to the structural degradation of their matrices through sulphate attack. The results of the analysis (Table 4.6) demonstrate that alkali activated binders which exhibited the highest strength gains during UCS testing also contained common hydrated cement minerals. Conversely, samples exhibiting lower strengths during UCS testing did not present any evidence of cementitious bond formation. Analyses showed that kaolinite and quartz mineral phases were present within all samples, which was expected as they were the artificial silty sand's two key constituents. Cementitious C-S-H minerals were observed within GGBS-PFA-AA (aluminium oxide) and PFA-RG-C (calcium aluminium oxide hydrate) samples. Thenardite was observed within PFA-RG-AA samples, which is an anhydrous sodium sulphate mineral causing unfavourable sulphate attack within concrete and masonry and consequently reducing strength through expansion and leading to degradation (Rodriguez-Navarro et al., 2000).

Table 4.6: Summary of the cementitious and problematic mineral phases found during XRD analyses of samples.

Binder Mixture	Cementitious Mineral Phases Recorded
GGBS-RG-AA	Calcium sulphate hydrate, calcium aluminium oxide hydrate
GGBS-RG-C	Ettringite
GGBS-PFA-AA	Calcium Silicate Hydrate
GGBS-PFA-C	Gypsum
PFA-RG-AA	Aluminium Oxide and Thenardite
PFA-RG-C	Calcium Silicate
CEM-I	Portlandite and Calcium Silicate Hydrate

4.2.4 Discussion

4.2.4.1 Strength

Testing results indicate that more cementitious bonds formed over 28 days within all alkali activated samples. Samples solely using the RG binder showed disappointing strength developments and plastic behaviour. This suggests that their use along with alkali activation as single binders within artificial alluvium is not recommended. RG's poor performance was at least partly attributed to the method its filter cake was prepared for testing, whereby it was dried and then ground down to a powder using a mortar and pestle. This may have produced a powder that was coarser and less uniform than the GGBS or PFA powders used. Drying the filter cake would have altered RG's micro-chemical structural properties, which includes water; a large proportion of which would have evaporated and consequently weakened its mineralogical structure. Per Beretka et al. (1996), RG is not pozzolanic and has not been greatly researched for use as a binder. Thus, this dosage trial study examined RG's use in combination with GGBS and PFA to form binders. Strengths significantly improved when RG was combined with GGBS and had been activated; whereas those achieved by PFA-RG samples were much lower. Although Hughes (2005) found GGBS-RG to be more favourable than CEM-I, GGBS-AA specimens from this study showed compressive strength enhancements exceeding those of both GGBS-RG and CEM-I, reaching values over 6 MPa after 28 days.

Per Fraay et al. (1989), PFA retards cementitious bond development; whereby pozzolanic reactions can take over a week to initiate, resulting in intial slow strength developments. However, this was not observed during this study. Given that Fraay et al.'s (1989) experiments were not activated to raise water pH and initiate pozzolanic reactions; the use of the $NaOH–Na_2SiO_3$ activator for PFA in this study resulted in strength gains within the first week of testing. However, the same cannot be said with the use of lime or SS as an activator. For such samples, any notable strength developments were only observed after 28 days curing; and even at that point, the strengths achieved were considerably lower when compared with other activated samples.

With reference to the values obtained for the artificial silty sand's low CEC, charge density and surface area, it appears that they resemble a sandy loam alluvial soil per Ersahin et al. (2006). Such a low clay and high sand content within the artificial soil provides a limited number of sites within the soil for cation exchange and subsequent hydration and pozzolanic reactions to occur. Thus, it is possible that adding the alkali activator within certain IBP-soil mixtures has over-compensated for the lack of cation exchange surfaces available by increasing the soil's pH. This has ultimately led to the dissolution of silica from the clay particles and subsequent formation of cementitious gels. There are several previous studies which have used (low-alkaline) PFA as a binding agent and have shown much more encouraging strength performances than those recorded in this chapter; notably that by Horpibulsuk and Raksachon (2010). Although their study used cement in combination with the PFA, they stabilised a silty clay comprising 2% sand, 45% silt and 53% clay. Therefore, based on basic CEC theory in terms of soil stabilisation, their soil would have provided a significantly higher number of cation exchange sites than that provided by this study's artificial silty sand. Should a future artificial soil be manufactured with a different clay of higher CEC, it is postulated that the performances of the various alkali activated PFA binders would surpass those observed in this study.

In addition to strength enhancements, alkali activation caused considerable increases in stiffness; as observed for GGBS-AA samples. Such soils were liable to experience brittle failure, which is geotechnically unfavourable, e.g. when dynamically loaded. Per Rowles and O'Connor (2003), higher silica to alumina ratios result in higher compressive strengths being achieved by alkali activated samples. This explains the low strengths achieved by PFA (comprising a low silica to alumina ratio) during this study. Additionally, higher silica ratios within a material have been documented to enhance elasticity (Rowles and O'Connor, 2003).

Results from both shear and compressive strength testing demonstrate that the length of curing imposed on samples has a considerable influence on the final strengths achieved; and ultimately on the performance of the alkali activation (Hughes et al., 2011). Even though alkali activation during this study increased strength gain rates for numerous samples that had been cured at 20^{o}C, work by Palomo et al. (1999) suggests that if samples are cured at higher temperatures, specifically during the first 5 hours of curing; reaction rates are increased even further and therefore result in further

improved strength properties. However, the practicality of applying such heating conditions on site may be limited and could also potentially undermine the objective of financial and environmental sustainability.

4.2.4.2 Compressibility

Per criteria stated by Tomlinson (2001), the study's oedometer results demonstrated that each binder improved the artificial soil's initially high level of compressibility to at least a medium to low level. Alkali activated specimens also resulted in much greater improvements than those which had not, particularly those which contained the GGBS-PFA binder. Thus, as similarly observed for compressive strength testing after 28 days curing, alkali activated GGBS-PFA oedometer samples exhibited the least amount of compression due to its high level of stiffness; closely followed by activated GGBS-RG samples. Although the activated and non-activated PFA-RG samples produced lower Mv values than those achieved by the untreated silty sand after each loading stage, the compression indices for the PFA-RG samples were still comparable with that of the silty sand. Therefore, rather than creating cementitious bonds to reduce compressibility, the PFA-RG binder has acted as a bulking agent. Further to the discussion of the strength results, it is anticipated that improved compressibility performances of the GGBS and PFA binders may be observed within a soil that has a higher surface area and cation exchange capacity. However, stabilised soils with high strengths and stiffness after 28 days curing may experience unfavourable brittle failure, should any large static or dynamic stresses be exerted. Should further oedometer testing be conducted on these IBP binders, it would be the intention to conduct a testing procedure comprising several unloading and reloading stages to more accurately define each binder's compressibility and swelling behaviour.

4.2.4.3 Durability

Overall, the addition of alkali activated GGBS or GGBS-PFA binders to the artificial silty sand produced the most enhanced durability performances. Albeit a GGBS-based

binder, a brittle failure was observed for a GGBS-RG-AA sample whilst thawing, due to crack formation during freezing. Samples containing RG or PFA-RG binders were considered the least durable, due to their premature disintegration during wetting-drying testing and disintegration for an activated specimen after the third cycle during freeze-thaw testing. As previously discussed, the technique used to prepare RG produced non-uniform coarse-grained samples that were potentially less dense and more permeable than GGBS or PFA. This would have enabled water to permeate through RG-stabilised samples and consequently result in swelling; thereby making the material prone to disintegration. The presence of Thenardite within activated PFA-RG samples may have also promoted sample swelling and degradation during durability testing.

As generally demonstrated by samples mixed with GGBS, GGBS-PFA and GGBS-RG; alkali activation proved successful in producing denser and less porous/permeable materials, which reduced the likelihood of water absorption and consequent sample degradation through shrinkage and swelling due to wetting-drying and freezing-thawing cycles. However, based on the soil and binder dosages examined, the future potential of RG and PFA as binders in enhancing the durability performance of sandy soils appears to be limited and therefore requires further research.

4.2.4.4 Water Content

For binders to hydrate and cementitious bonds to form within stabilised samples, sufficient quantities of natural soil water are required within samples. When the stabilised samples were produced, their initial water contents were recorded to be approximately 15%. After each curing period, sample's water contents were measured after compressive strength testing. Generally, water contents decreased over 28 days by a maximum of 3%; thereby suggesting all samples contained sufficient quantities of water for hydration reactions to occur and therefore the formation of cementitious bonds.

Part of activated sample's water contents gets consumed by pozzolanic reactions (Duxson et al., 2007). CaOH is transported via water to combine with siliceous and aluminate minerals, which dissolve to form strengthening C-S-H/C-A-H gels. During

this study, samples' compressive strengths increased with decreasing water content, which corresponds with Duxson et al.'s (2007) findings, who also determined that water gets consumed during dissolution of geopolymeric reactions; whereby solid aluminosilicates break down through alkaline hydrolysis, resulting in silicate and aluminate species. This also suggests that activated samples have lower water contents than non-activated samples. However, this may not always apply and non-activated samples may lose similar volumes of water via evaporation before testing.

Albeit there is clearly evidence for slight decreases in samples' water contents, possibly attributable to hydration and pozzolanic reactions; based on the low surface area and CEC of the artificial silty sand, it is possible that the binders demonstrating relatively poor performances in this study may be more successful within other soils comprising higher clay contents. Such soils contain more cation exchange sites and therefore have a greater potential for cementitious bonds to form through hydration and pozzolanic reactions; thereby resulting in greater reductions in water content compared with those observed in this study over similar curing periods.

As all samples were produced through compaction within a mould, it is possible that negative pore water pressures may have developed during this process, as observed by Hughes et al. (2011). This in turn may have slightly increased the strength values recorded. Soils with higher clay contents than the samples tested during this study would be characterised by low levels of permeability; and would significantly limit the amount of water accessible for hydration reactions to occur in the field (Hughes et al., 2011).

4.2.4.5 Mineralogy and pH

Previous studies have demonstrated that a soil's pH may strongly influence its strength development; whereby higher UCS values (i.e. > 1 MPa) are achieved by alkali activated samples whose pH values are > 10.5. This allows long-term pozzolanic reactions to occur. However, several samples with high pH levels did not achieve high compressive strengths; e.g. activated/non-activated RG, PFA-RG-AA and SS/lime activated PFA specimens. If oxidising reactions and subsequent pH reduction occur within IBP-stabilised samples, pozzolanic reactions and strength gains can become

inhibited. It is therefore essential to make an assessment of the quantity of alkali activator to be added to soils prior to treatment to ensure that pH remains above 10.5 for a sufficient period for curing to occur.

Mineralogically, XRD analyses from this study provided evidence for the existence of cementitious calcium silicate hydrate and calcium aluminium oxide hydrate minerals within certain alkali activated samples. Thenardite was observed within a PFA-RG-AA sample, which can cause sulphate attack and strength degradations within concrete (Rodriguez-Navarro et al., 2000) and therefore potentially cemented soils. No Thaumasite was observed within any samples, however Ettringite was observed within one GGBS-RG-AA sample. The presence of Ettringite and/or Thaumasite within calcium-based stabilised sulphate-bearing clay soils can cause structural distress (Little et al., 2005). However, in the case of this study and that by Wild et al. (1998) for clay-lime-GGBS-gypsum systems with high lime – low GGBS compositions; Ettringite may not have weakened the soils by swelling, but instead strengthened them.

4.2.4.6 Alkali activators

The new alkali activator primarily used in this dosage trial study comprised two parts Na_2SiO_3 solution to one part NaOH. It effectively raised pH and produced strength improvements, particularly for GGBS-based binders. The addition of these constituents to any commercial binder would have an associated cost and add to the complexity and risk of the mixing process. Particularly for the Na_2SiO_3 solution component, this alkali can be expensive to produce and the environmental impact resulting from its manufacture is fairly significant (Habert et al., 2011). Additionally, liquid-form Na_2SiO_3 was used, which would not be applicable to deep dry mixing. Hence, substituting these with a high alkalinity waste-based powder would be desirable to make these binders more commercially viable and easier to use on site. Habert et al. (2011) document that the financial cost and environmental impact associated with NaOH production is significantly lower compared with Na_2SiO_3 solution. Therefore, a potential recommendation for further study is to primarily use NaOH as an alkali activator. Finally, Habert et al. (2011) also state that using sodic slags as a replacement for Na_2SiO_3 may be a viable option.

4.3 Chapter summary and conclusions

Detailed binder dosage trials were first conducted on a replica alluvium soil to determine the most appropriate IBP materials for use as a binder in deep dry soil mixing. Results from a series of mechanical strength, durability, chemical and mineralogical tests revealed that alkali activated IBP stabilised samples, specifically those comprising GGBS; have much potential as replacements for lime and CEM-I in soil stabilisation. Binder dosages of 10% by dry weight were added to the soil. Based on the engineering performances of the GGBS-AA binder, such a high dosage may not be required to meet engineering specifications for most deep dry mixing applications. With strengths reaching around 6 MPa when using the GGBS-AA, such stabilised soil mixtures would become prone to brittle failures when subjected to dynamic loads; such as those from passing train traffic. In such instances the binder mixture to be used should be designed so that it has a lower level of stiffness.

As predicted from the findings in the literature, the combination of NaOH flakes and Na_2SiO_3 solution proved very effective as an alkali activator in raising soil pH to allow for pozzolanic reactions and subsequent strength enhancements. However, the practicality in using Na_2SiO_3 solution for deep dry soil mixing becomes problematic. Additionally, the environmental and economic costs associated with Na_2SiO_3 solution production and usage is fairly high. Hence, substituting Na_2SiO_3 with an alternative alkali activator for future binder mixtures would be preferable. However, NaOH alone as an alkali activator may be sufficient to raise soil pH to at least 10.5 and allow for pozzolanic reactions.

Based on the results and conclusions within this chapter, the IBP which should form the main basis of the binder for stabilising the Lanton alluvium would be GGBS. To reduce environmental and financial costs, simplify binder design and optimise engineering practicality for DDSM, a single alkali activator material should be used within a cementitious binder mixture rather than multiple activators. Given the nature of DDSM as a process, Na_2SiO_3 solution will no longer be used as an alkali activator in this research. It is anticipated that the sole use of NaOH will be sufficient in raising soil pH and ultimately activating long-term cementation reactions.

Chapter 5:

Phase 2: Stabilisation of Lanton Alluvium

5.1 Introduction

This chapter builds upon the findings in previous chapters and investigates the suitability of various IBP materials in both their activated and non-activated states as cementitious binders when added to a natural alluvial soil. This involves a suite of geotechnical laboratory testing techniques, focussing on each of the binders abilities to produce strength enhancements within a natural alluvial soil from Northumberland, which are typically expected of cemented soils in industrial practices according to EuroSoilStab (2002).

Once the most appropriate binder and optimum dosage was identified by compressive strength, pH, moisture content, durability, financial and environmental cost criteria, the binder was then assessed for its effectiveness in reducing the natural alluvium's compressibility through oedometer testing. Additionally, the compressional behaviour of the alluvium in both its undisturbed and remoulded states is characterised. All the results from this chapter ultimately form the basis for subsequent chapters, focussing on the triaxial characterisation of the alluvium in both its natural and stabilised states.

5.2 Laboratory testing

Findings from the previous chapter demonstrated that alkali activated GGBS-based binders produce high strength and durability performances within an artificial alluvial soil. Whilst it is clear from the academic literature that GGBS-based binders are known to produce such preferable performances, other IBP's such as PFA which are in abundant supply have also been known to produce excellent engineering performances within certain soils (Horpibulsuk et al., 2011). From the literature review chapter, numerous factors associated with a soil's natural state have an influence on the likelihood of cementitious reactions taking place; namely moisture content, clay mineralogy, CEC, surface area, organic and sulphate contents. Given that no two soils are identical regarding these material properties, the effectiveness of numerous IBP binders is assessed in this chapter for stabilising a natural alluvial soil as IBP binders

which proved effective in producing strength gains within an artificial silty sand may not prove as successful within a natural alluvium, or vice versa.

5.2.1 Materials

5.2.1.1 Lanton Alluvium

The natural alluvial soil chosen for stabilisation was sourced from the flood plain of the River Glen in Lanton (grid ref: NT 95893030), 4 km North West of Wooler in Northumberland (see Figure 5.1). Disturbed and undisturbed U100 samples from a depth of 1.5–2.4 metres were obtained from the site with the permission of the site owner, Tarmac Ltd.

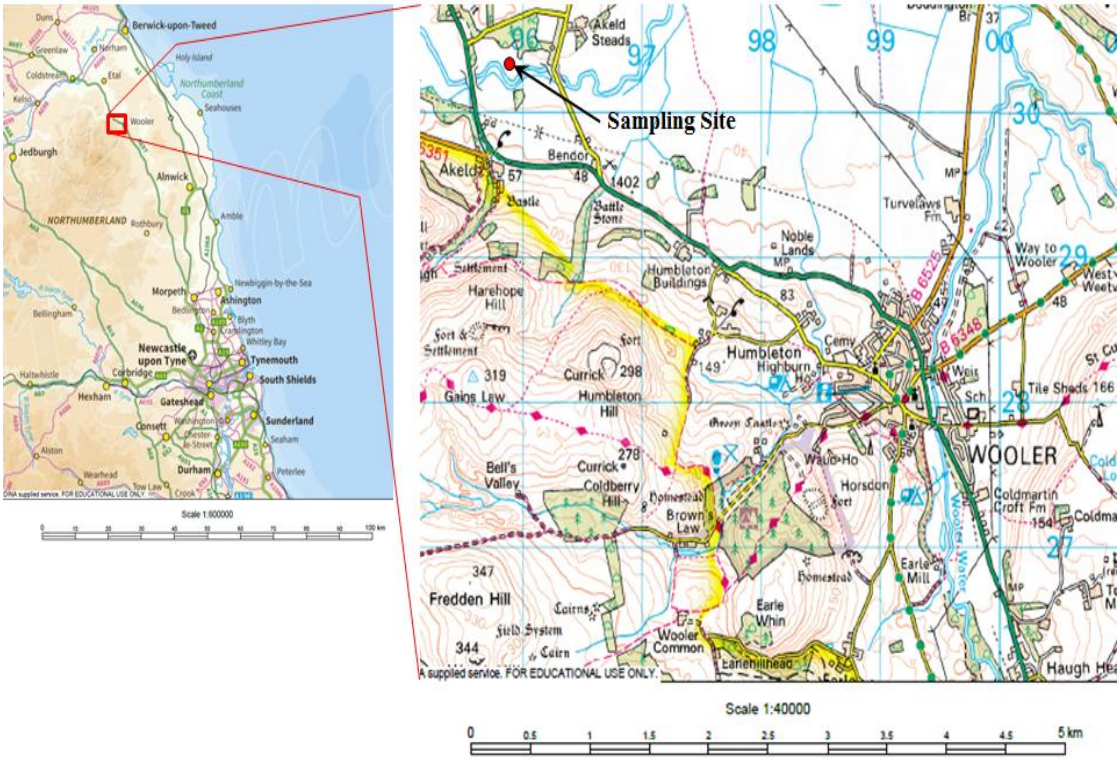

Figure 5.1: Location of soil sampling site at Lanton, Northumberland. Maps courtesy of Edina Digimap (2013).

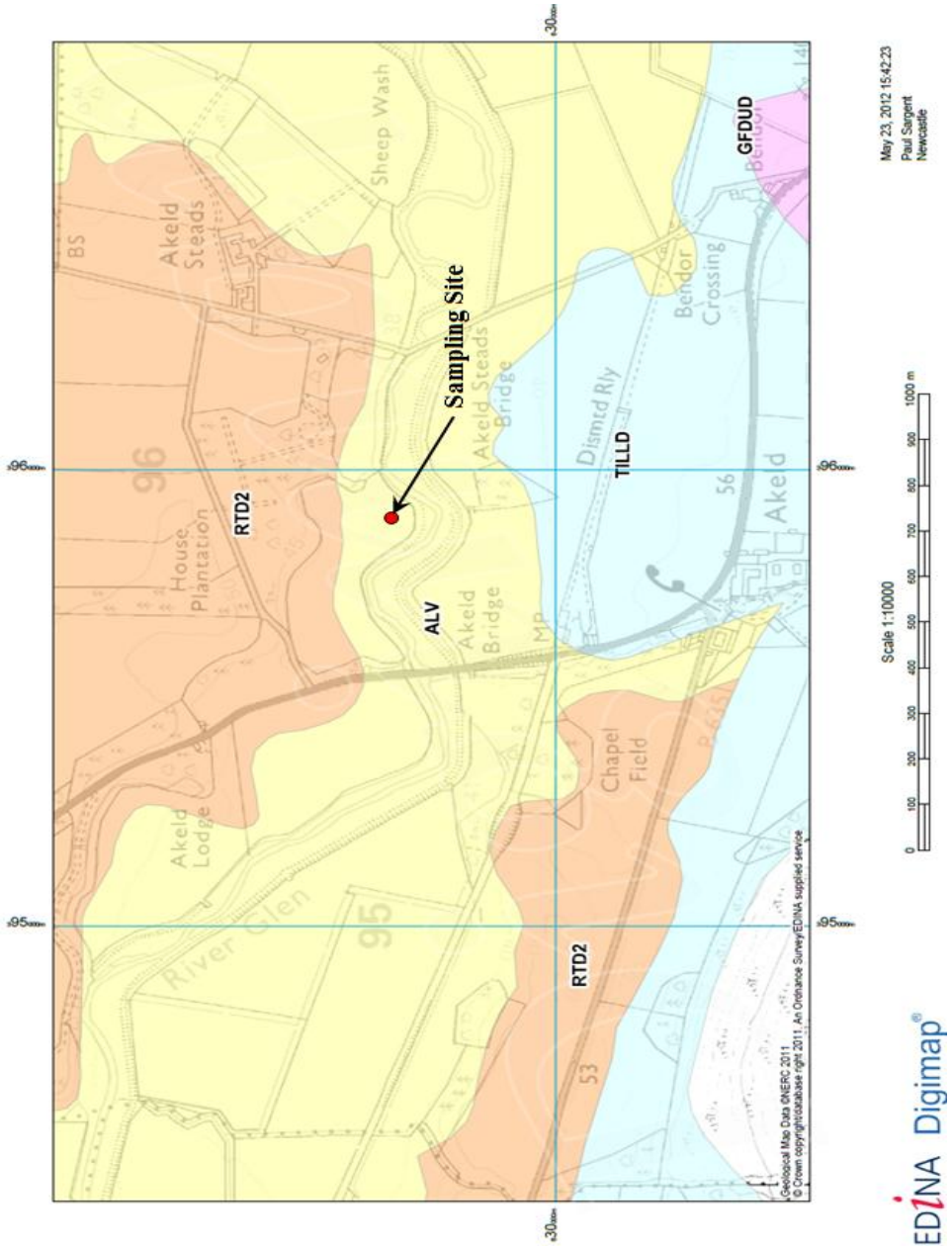

Figure 5.2: Superficial geological map of the sampling site at Lanton. (Abbreviations: ALV = alluvium, RTD = river terrace deposits, TILLD = Devensian glacial till and GFDUD = Devensian glaciofluvial deposits). Map courtesy of Edina Geology Digimap (2012).

According to the superficial geological map of the sampling site (Figure 5.2 above), the site's superficial geology was characterised by fairly widespread Holocene alluvium deposits along the course of the River Glen, which were bounded to the north and south by a series of river terrace sand and gravel deposits, along with Devensian glacial till and fluvioglacial deposits. Soil cores have previously been obtained from this site by Allen (2007) for pollen analyses; whereby cores were retrieved from 0.5–2 metres depth and stratigraphically logged in detail (Figure 5.3).

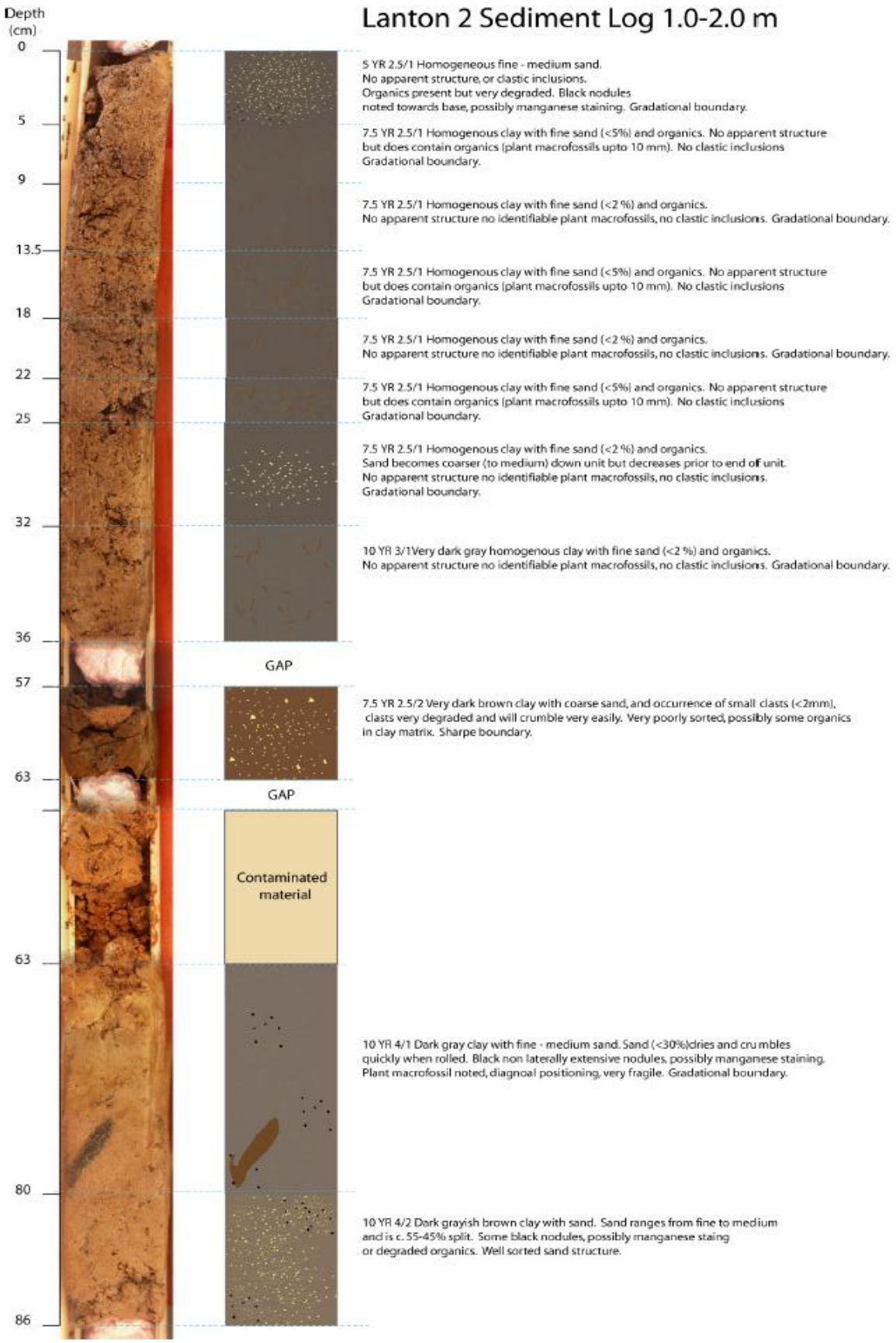

Figure 5.3: Detailed stratigraphic soil log of Lanton alluvium soil. Courtesy of Allen (2007).

5.2.1.2 Binders

Similar to the previous chapter, the IBP binders used were PFA and GGBS. RG was not selected for further use as a binder in this research, due to its negligible effects in enhancing the strength of the artificial silty sand (see chapter 4), along with the difficulties involved in preparing an RG filter cake so that it is suitable for dry soil mixing. For comparison purposes, non-activated IBP binders and traditional binders including CEM-I and lime were also used to stabilise the Lanton alluvium.

Upon reviewing an evaluation study by Habert et al. (2011) on geopolymer production, it was shown that the use of Na_2SiO_3 solution within binders was environmentally unsustainable. Habert et al. (2011) quoted a high global warming potential of 117.8 kg CO_2eq, a high human toxicity level of 82.75 kg 1,4-DB eq and a high freshwater ecotoxicity of 21.84 kg 1,4-DB eq. Therefore, to ensure that the binder ultimately incorporated within Lanton alluvium was environmentally and financially sustainable, the Na_2SiO_3 solution activator was discarded from the remainder of this study. However, per Habert et al. (2011) lower financial and environmental costs are associated with the production of NaOH flakes; (3.71×10^{-1} kg CO_2eq, human toxicity level of 15.84 kg 1,4-DB eq and a freshwater ecotoxicity of 3.98 kg 1,4-DB eq). Thus, the use of NaOH as an alkali activator continued for this phase of study.

As the GGBS used in the previous chapter had been exposed to the ambient temperature (20–25^{o}C) and relative humidity (>55%) conditions of the laboratory where it was stored for two years, it is likely that the material may not be as reactive when mixed into a soil. Numerous cement industry sources (e.g. Ability Products, Australia) document that GGBS may have a limited shelf-life when it has been: 1) stored in a non-sealed bag/container, 2) exposed to sun light, 3) exposed to high humidity (i.e. >50%) and temperatures (>25^{o}C). To assess whether these factors influence the engineering performance of the GGBS as a binder, this study compares performances achieved when using the older GGBS (provided by Frodingham Cement Ltd.) against using a fresh batch of GGBS (provided by Hansen Cements Ltd). The new GGBS was stored within sealed containers in a temperature controlled laboratory (20^{o}C, <50% relative humidity), away from any direct sunlight.

5.2.2 Soil characterisation

The geotechnical characterisation of Lanton alluvium soil was conducted in strict accordance with BS 1377 (BSI, 1990). The tests included particle size distribution (PSD) through wet sieving and sedimentation (Figure 5.4), Atterberg limits (LL = 35.66, PL = 20.71, PI = 14.95; see Figure 5.5), particle density (2.606 Mg/m^3), compaction (to determine optimum moisture content of 14.7%, a bulk density of 1.995 Mg/m^3 and a dry density of 1.740 Mg/m^3) and moisture content (natural in-situ moisture content of 25%).

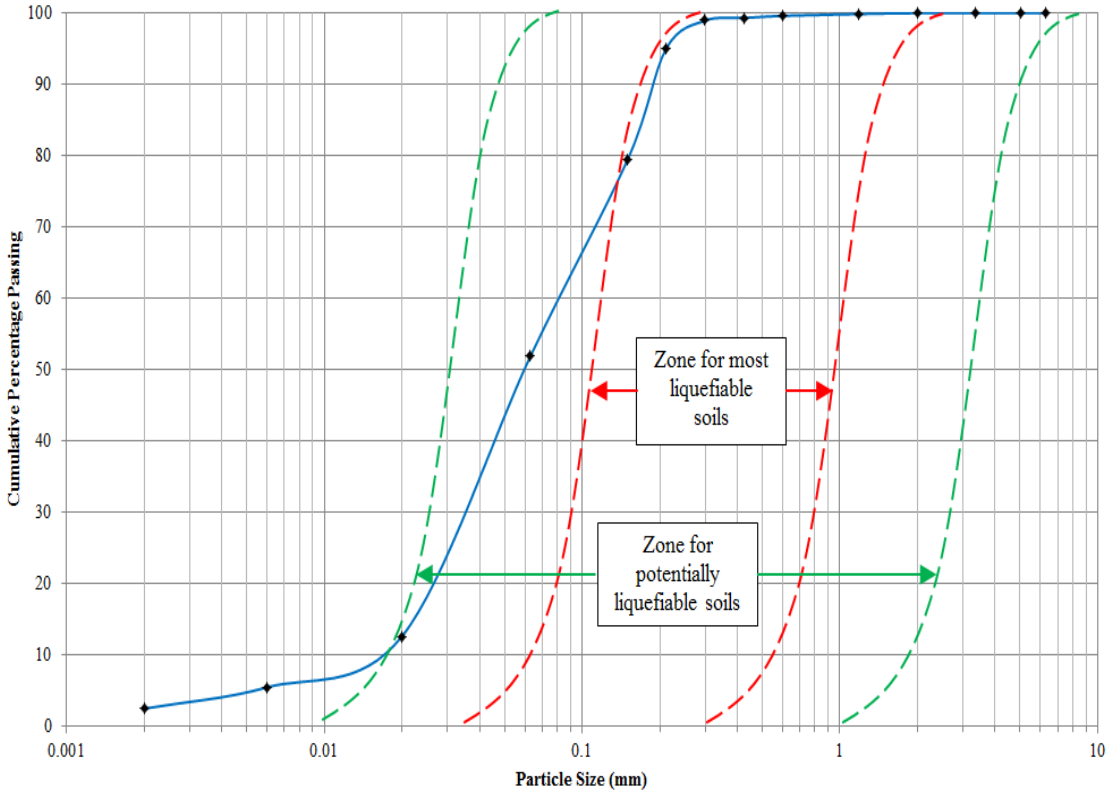

Figure 5.4: PSD curve for Lanton alluvium soil with Tsuchida (1970) liquefaction criteria superimposed.

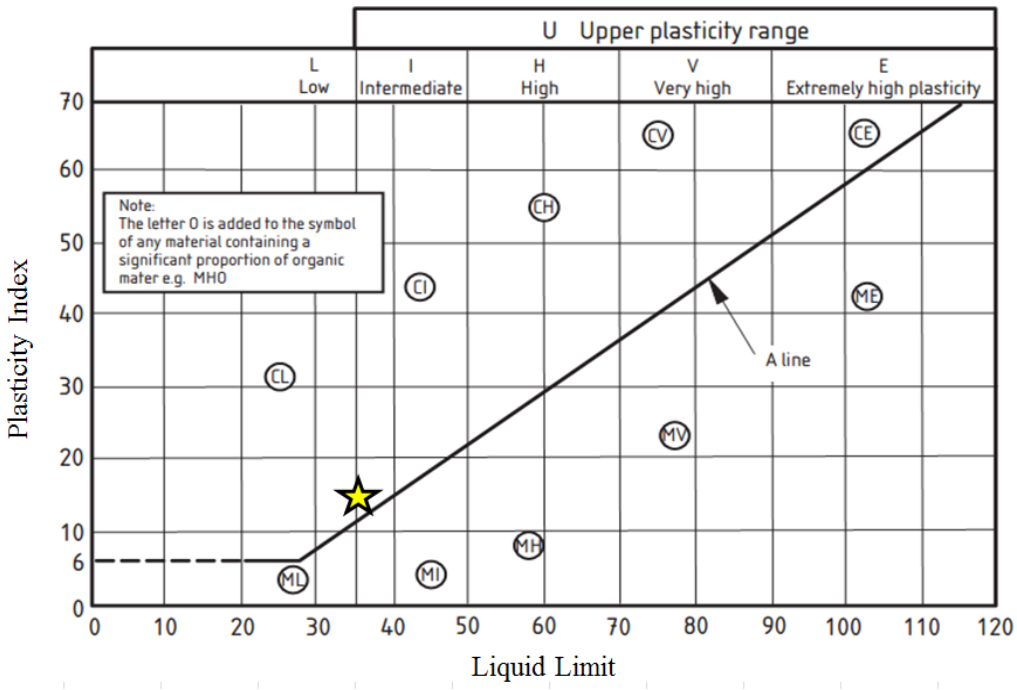

Figure 5.5: BS5930 Atterberg limits classification for Lanton alluvium; an intermediate plasticity clay soil.

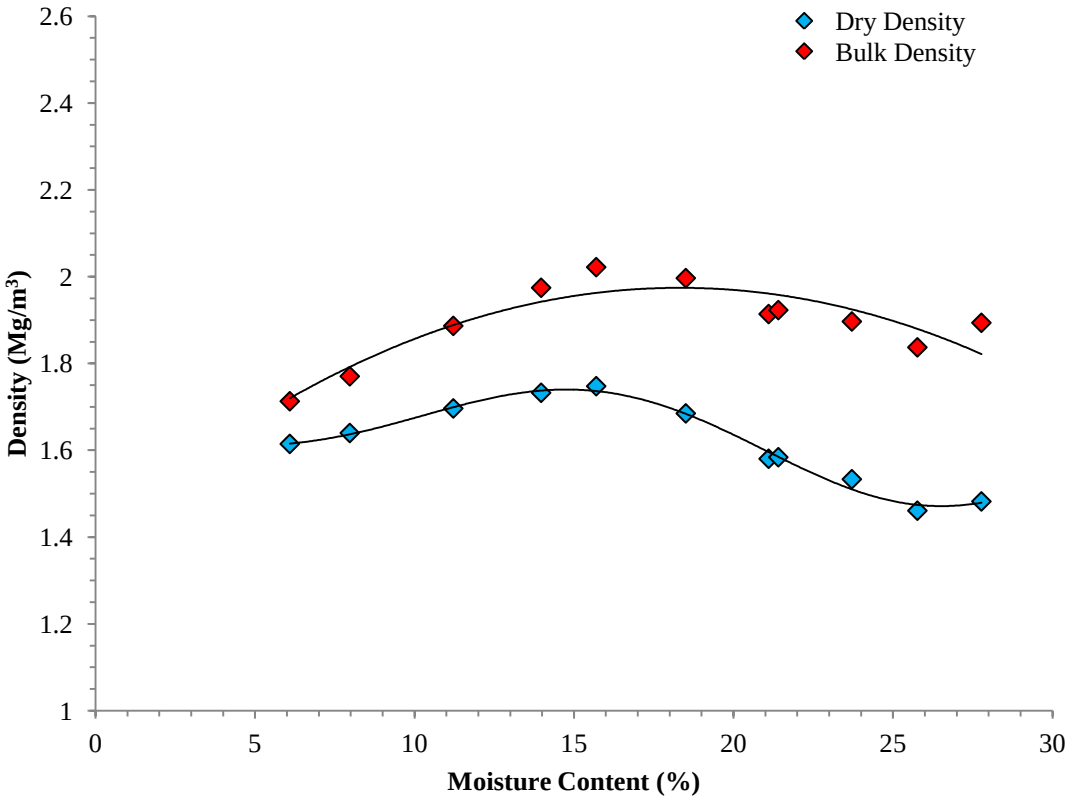

Figure 5.6: Relationship between dry and bulk density and moisture content for Lanton alluvium.

The soil can therefore be categorised as a silty SAND in terms of dry density, according to criteria stated by BS 5930 (1999) and Tomlinson (2001). Per criteria stated by Tsuchida (1970), the PSD curve in Figure 5.4 for Lanton alluvium lies within the zone for soils which may potentially liquefy during earthquakes or when dynamically loaded by anthropogenic activity. This raises concerns about the strength of the soil and therefore emphasises the need for treatment for any engineering development founded upon this soil.

As with the artificial alluvium, Lanton alluvium was also tested to determine its CEC and σ_{CEC} according to BS 7755. The soil was found to have an average CEC of 11.45 cmol/kg and σ_{CEC} of 0.0019. From these values, the CEC for Lanton alluvium is an order of magnitude higher than that measured for the artificial alluvium. Based on general criteria stated by Cooper (2009), it appears Lanton alluvium is a soil characterised by low to medium organic matter contents. Additionally, the soil has lower sand and clay contents than the artificial alluvium; but a higher silt content. BET surface area testing revealed that Lanton alluvium had an average surface area value of 6.454 m^2/g, almost three times higher than that obtained for the artificial alluvium.

Based on these higher CEC and surface area results, it is postulated that Lanton alluvium is a more favourable soil compared with the artificial silty sand alluvium examined in the previous chapter for soil stabilisation, as there is a lower sand content and therefore more cation exchange sites available within for cementitious bond formation. However, it should be reiterated that Lanton alluvium still has what would be considered to be low-medium CEC and low surface area values, owing to its low clay and relatively high silt content.

Besides the CEC and BET surface area testing, given that Lanton alluvium is a natural soil, it was also subjected to total organic carbon, total organic content and sulphate content testing. It was determined that Lanton alluvium had low total organic carbon and total organic contents of 0.42% and 0.76%, respectively. For sulphate content testing, the equipment used was the Dionex Ion-Chromatography ICS-1000, which determined a very low sulphate content of 49 mg per kg of soil.

Finally, 100 mm diameter samples of Lanton alluvium were placed in a triaxial cell under consolidated conditions to determine values for its coefficient of permeability (k_v) in the vertical direction for both its natural undisturbed and remoulded states. The

procedure and subsequent calculations were per BS 1377 (BSI, 1990). At a laboratory temperature of 22^{o}C, the k_v values obtained for the soil in its undisturbed and remoulded states were 1.41 x 10^{-8} m/s and 5.58 x 10^{-9} m/s, respectively.

5.2.2.1 Sample preparation

Further to section 3.3.2.2 for preparing stabilised samples, based on the optimum compaction characteristics (Figure 5.6) and the in-situ moisture content of Lanton alluvium, all samples were prepared with a bulk density of 1.9 Mg/m^3.

5.2.3 Results

5.2.3.1 Compressive strength and stiffness

The GGBS-NaOH-Na_2SiO_3 binder mixture used to treat the artificial alluvium in the previous chapter produced impressive compressive strengths of around 6 MPa after 28 days curing. Observations from the previous chapter's UCS testing showed that such high strength stabilised soils may be liable to experience a highly brittle failure upon dynamic loading. Although there will be some engineering specifications which will require high strengths and stiffnesses, there are also engineering scenarios such as foundations for high speed rail lines where dynamic loading of the ground caused by passing train traffic may require lower stiffnesses to prevent brittle failure of the ground. Hence, one of the main aims for the strength testing on stabilised Lanton alluvium was to achieve strengths and stiffnesses which were slightly lower than those recorded for the GGBS-NaOH-Na_2SiO_3 stabilised artificial alluvium in the previous chapter, but sufficiently high to still be considered acceptable for engineering applications involving static and dynamic loading on soft soils. Most deep/shallow soil mixing scenarios require 28 day UCS values which typically range between 0.3–3.0 MPa (EuroSoilStab, 2002; Horpibulsuk et al., 2011); whereby the strength required for a site will be location and application specific.

A summary of the average maximum compressive strengths achieved by the activated and non-activated IBP - Lanton mixtures are presented in Figure 5.7, along with those achieved by samples which had either been untreated or stabilised with CEM-I and lime for comparative purposes. With a few exceptions, it is evident that sample strength increased over the 28 day curing period for all the binder mixtures tested. However, the degree of strength development observed within samples varies significantly between binder types. In general, using a binder dosage of 2.5 or 5% for any binder type proved unsuccessful in producing UCS values required by EuroSoilStab (2002) after 28 days. The UCS values for samples stabilised with 10% PFA were very disappointing, as they failed to surpass 50 kPa over the 56 day testing period even when using the higher dosage. When activated with NaOH, a slight increase in strength up to 95 kPa was observed after 56 days. In general, all such samples were characterised by ductile behaviour upon failure. Therefore, based on the natural UCS performance of Lanton alluvium, there appears to be no benefit in using PFA in stabilising the soil, even when activated with NaOH.

The strengths recorded for 5 and 10% GGBS in its non-activated state were also fairly low, reaching maximum values of 74 kPa after 28 days and 157 kPa after 56 days; both failing to match the strengths achieved by either lime or CEM-I using the same dosages for the same curing periods. In addition, these samples were characterised by highly ductile behaviour at failure. Hence, as similarly seen for GGBS stabilised artificial alluvium in the previous chapter, alkali activation was clearly necessary to produce any considerable strength development. Given the impressive performance of NaOH as an alkali activator in the previous chapter and its widely known ability to raise soil pH, four dosages (2.5, 5, 7.5 and 10%) of GGBS-NaOH were assessed to identify the most sustainable and optimum dosage in terms of strength gain. Based on the results in Figure 5.7, there was no advantage in using either the 2.5 or 5% activated GGBS dosages due to the strengths achieved for each curing period (70 kPa after 28 days) closely resembling the performance of untreated Lanton alluvium (63 kPa after 28 days). The 10% GGBS-NaOH samples exhibited the highest and most rapid strength enhancements with curing over the 56 day testing period, with the effects of the NaOH in activating the GGBS first being seen after 14 days curing. After 28 and 56 days curing, impressive UCS values of 2.08 and 2.73 MPa were recorded respectively.

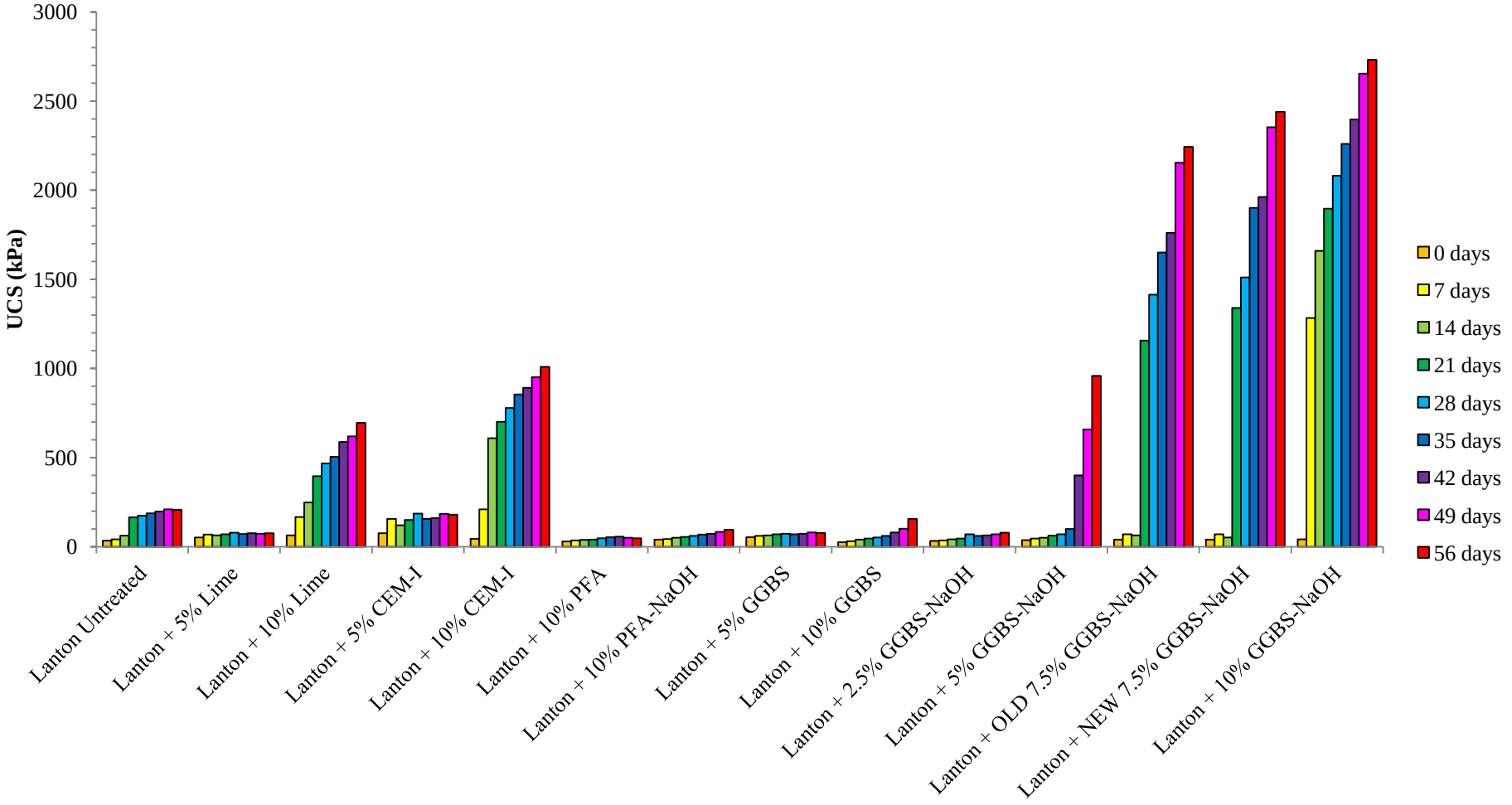

Figure 5.7: Unconfined compressive strength performances for all binder mixtures and dosages used to stabilise Lanton alluvium after all curing periods. Note that the maximum strengths achieved by strongest mixture (10% GGBS-NaOH) after 56 days is approximately half those observed in Figures 4.4 and 4.6.

Although the 7.5% GGBS-NaOH binder dosage produced significantly lower strengths than the 10% dosage after 0, 7 and 14 days; significant strength enhancements initiated after 21 days curing, producing UCS values of 1.3–1.4 MPa. The strength values obtained for the 7.5% GGBS-NaOH dosages (using either the old or new batches of GGBS) both easily exceeded the 28 day strengths of 10% lime and 10% CEM-I samples by factors of 3 and 2, respectively. The strengths also met the minimum 28 day strength requirements of EuroSoilStab (2002).

The behaviour of the GGBS-NaOH samples at dosages of 7.5 and 10% after 28 days curing was brittle upon failure. The 10% GGBS-NaOH samples exhibited higher levels of brittle behaviour due to their higher strength, even after 7 days curing. This behaviour contrasts with the less brittle and more ductile behaviour observed for all the other stabilised mixtures tested, whose strengths failed to surpass those of Lanton alluvium when untreated or stabilised with lime and CEM-I.

Based on the similar strengths achieved by samples with 7.5% binder dosage using new and old batches of GGBS, there appears to be little merit in using one over the other when attempting to achieve strength gains that match or exceed those exhibited by lime or CEM-I. This therefore suggests that the effectiveness of the older GGBS in stabilising Lanton alluvium once activated was not greatly influenced by age or variations in storage temperatures and humidity conditions, which are typically experienced in geotechnical laboratories.

5.2.3.2 Durability testing

5.2.3.2.1 Wetting-Drying

All the aforementioned stabilised and untreated Lanton alluvium sample mixtures were subjected to wetting-drying durability testing to determine soil-cement loss and changes in moisture content and sample volume due to wetting and drying cycles per ASTM D559. The durability performance of the aforementioned binders is a very important factor to consider in determining the most suitable binder for treating Lanton alluvium, given that the UK is characterised by a temperate maritime climate

where rainfall is experienced all year round. Given the silty and sandy nature of the alluvium, any surface water will percolate through the soil mass and potentially cause shrinkage and swelling during dry and wet periods, respectively. Hence, it is very important that the IBP binders being considered can cope with such frequent wetting and drying cycles in order to prevent the disintegration of DSM columns both prior to and after being subjected to any overlying static or dynamic loads.

Results from the wetting-drying testing programme are displayed in Figures 5.8 and 5.9. For the traditional binders, a minimum dosage of 10% was required to achieve optimum performance. Samples stabilised with CEM-I survived the entire 12 cycle (24 day) testing period with a gradual reduction in volume, whereas 10% lime samples only survived 3 cycles and exhibited larger volumetric losses. For the IBP-based binders, it is evident that most non-activated samples failed after the first cycle, the only exceptions being the 5 and 10% GGBS samples which survived 2 and 3 cycles respectively. PFA based samples displayed significant volumetric reductions during preceding cycles, particularly those which had either been un-activated. Activating the PFA with NaOH was effective in ensuring that the material survived all 12 cycles, although a volumetric reduction of almost 50% was observed. Although the addition of fines in the form of PFA would act towards reducing the soil's permeability, the dosage used was still insufficient and ultimately had no effect on enhancing durability.

The use of GGBS-NaOH at dosages of 2.5 and 5% displayed similarly disappointing performances to those observed for non-activated PFA and GGBS samples. However, very impressive performances were recorded for specimens containing a dosage of 7.5 or 10%, as they displayed negligible changes in volume or moisture content over the 12 cycle testing period.

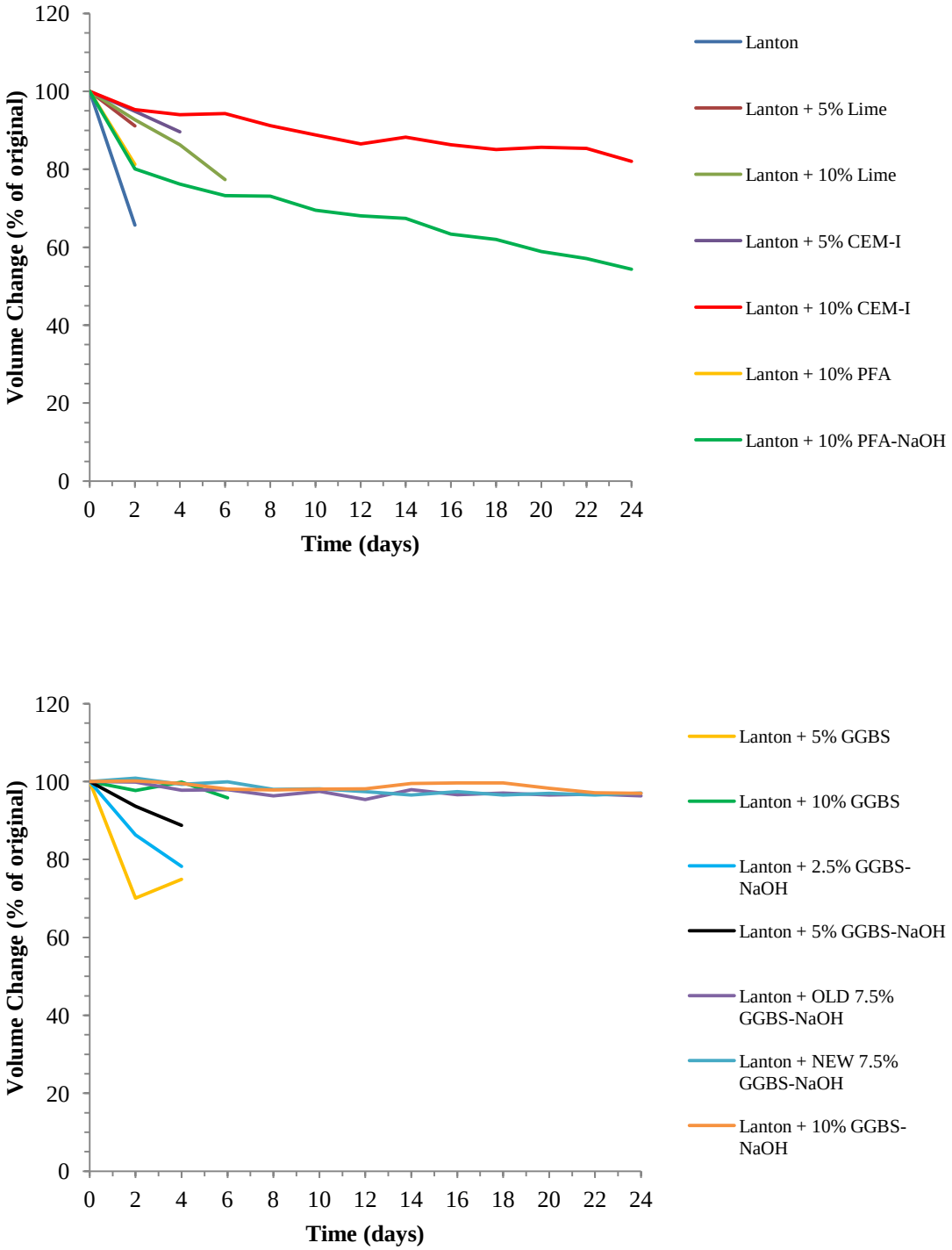

Figure 5.8: Volumetric changes experienced by samples during wetting-drying testing.

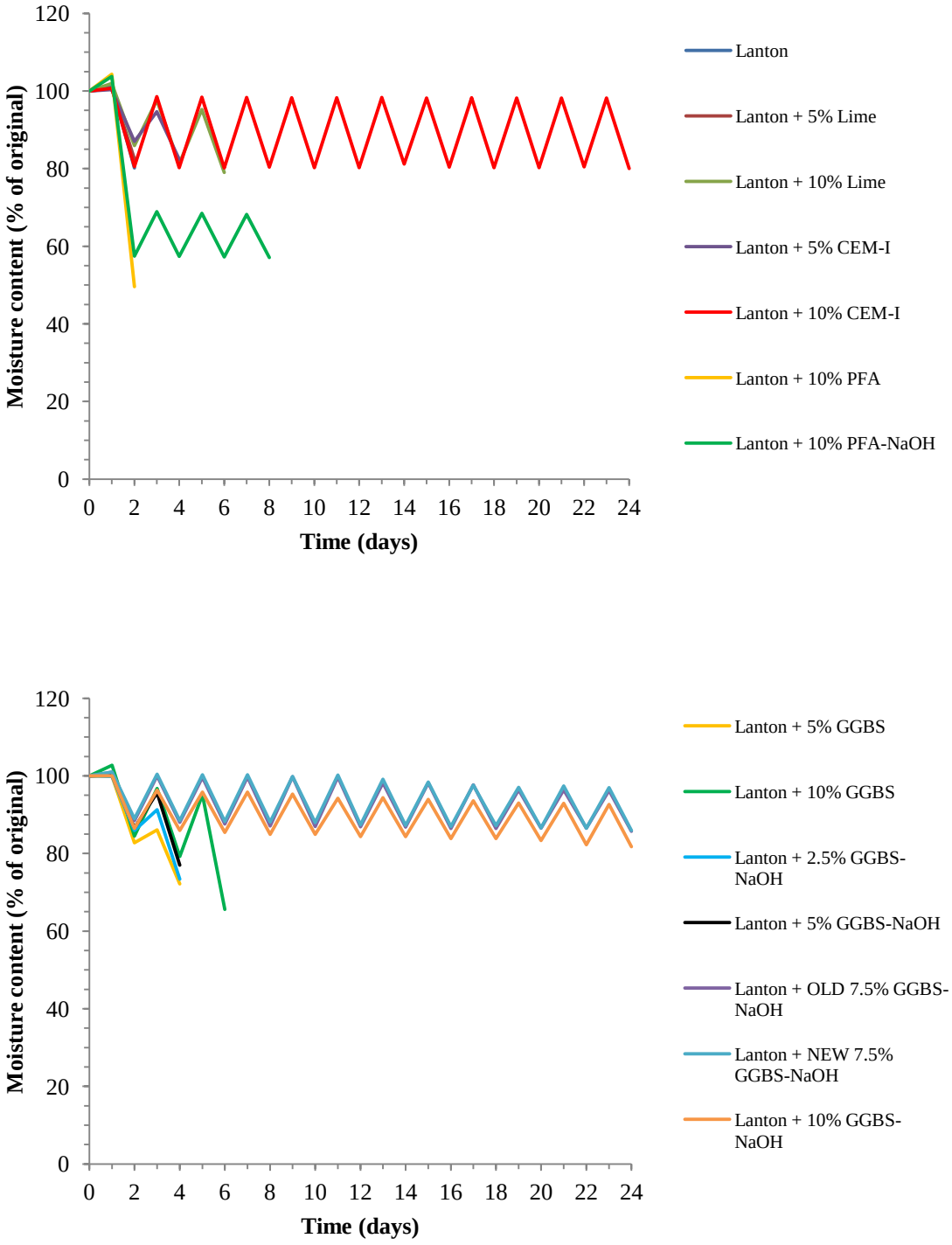

Figure 5.9: Moisture content changes experienced by samples during wetting-drying testing.

5.2.3.2.2 Freezing-Thawing

The freezing-thawing testing programme was conducted to assess the ability of the various IBP binder mixtures to cope with repeated freezing-thawing cycles by measuring changes in sample volume, moisture content and soil-cement losses. As previously stated, the UK possesses a temperate maritime climate, which means freeze-thaw processes are likely to occur up to depths of 2 metres during the winter months. Given the grading of Lanton alluvium and that water may easily percolate through the soil, shrinkage, swelling and physical weathering is likely to occur within the shallow sub-surface. This in turn raises concerns when DSM columns are to be installed, as the binder within the columns must be able to resist such shrinkage and swelling. Albeit the testing procedure stated in ASTM D560 may be considered a little extreme for simulating typical freeze-thaw conditions in the UK, the results will prove useful when assessing similar alluvial soils in other countries whose climates are characterised by colder winter weather. Results from the freezing-thawing testing are presented in Figures 5.10–5.11.

As for the wetting-drying results, using a dosage of 5% for lime and CEM-I was too low to produce any marked strength or durability enhancements, as samples failed after their first immersion. Although the 10% lime specimens only survived 2 cycles with a significant volumetric reduction, the 10% CEM-I samples survived all 12 cycles. However, the samples did experience a volumetric reduction of up to 60%. As observed for the wetting-drying results, non-activated PFA displayed a very poor performance as it failed after the first cycle and activation was clearly required to produce an improved performance. NaOH activation of PFA was not as effective in resisting freeze-thaw cycles compared with wet-dry cycles as the material only survived 3 cycles instead of 12.

The alkali activation of GGBS was essential to ensure that samples survived beyond 3–10 cycles. As previously demonstrated in both the UCS and wetting-drying durability testing results, adding NaOH to GGBS is required in order to promote pozzolanic conditions and subsequent strength gains. This behaviour continued for the freeze-thaw testing when using a dosage ≥7.5%; whereby such samples survived all 12 cycles with negligible volumetric reductions or moisture content variations until the

end of the testing period. The 10% GGBS-NaOH binder mixture was once again the most effective binders tested, followed closely by the 7.5 % dosage, as the binders provided high levels of resistance to harsh freezing-thawing cycles.

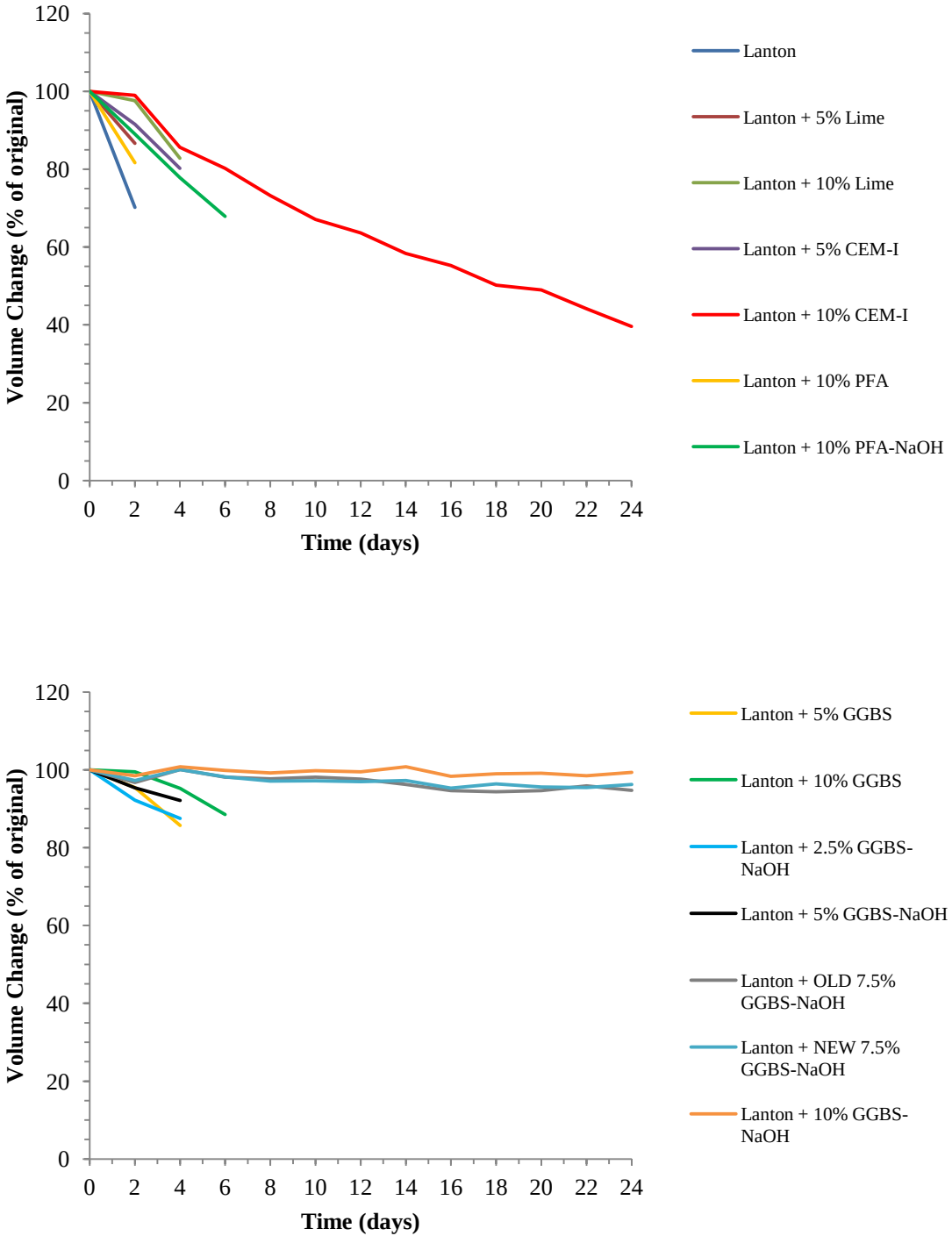

Figure 5.10: Volumetric changes experienced by samples during freezing-thawing testing.

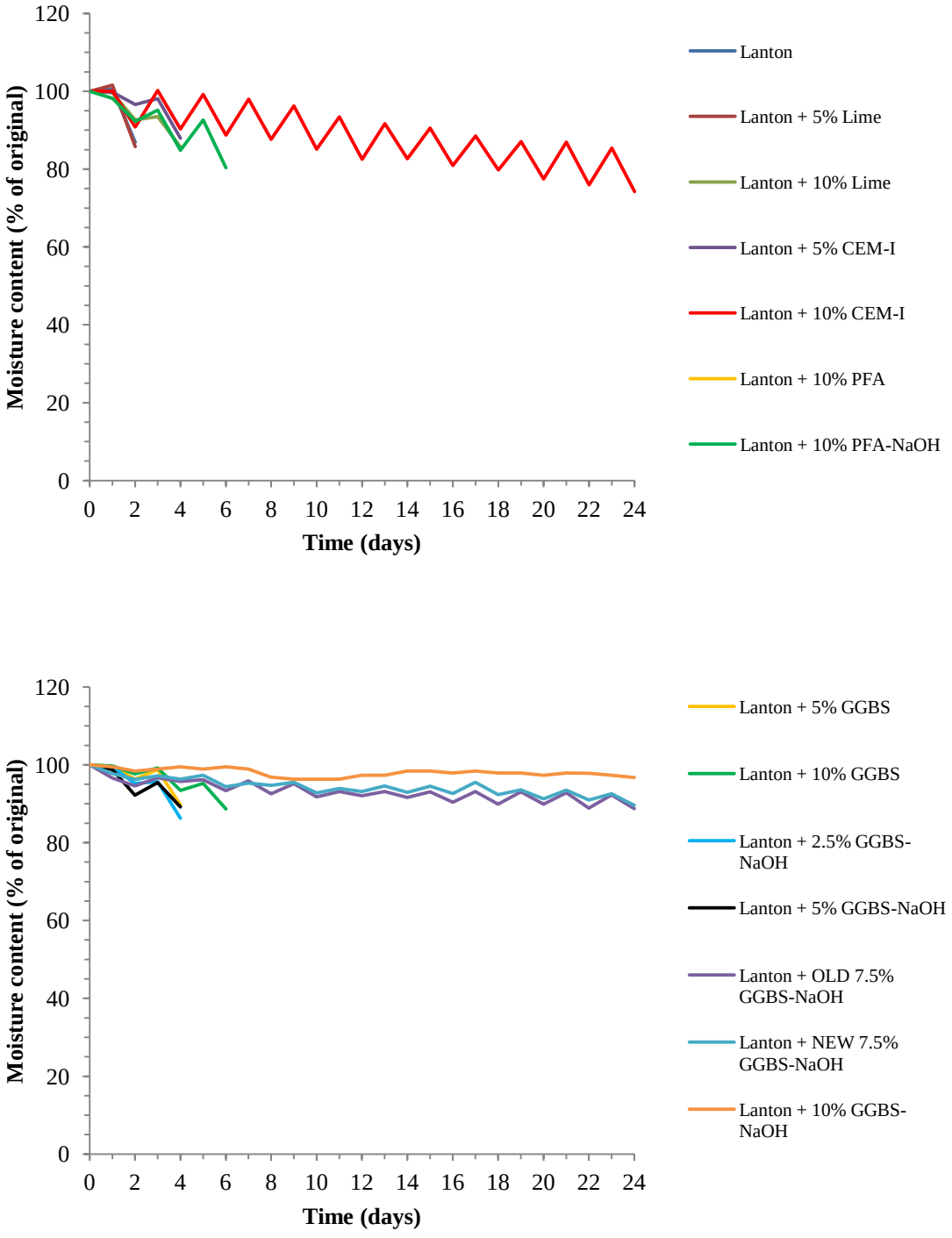

Figure 5.11: Moisture content changes experienced by samples during freezing-thawing testing.

5.2.3.3 Water content testing

As with stabilised artificial alluvium specimens in the previous chapter, sub-samples were retained promptly after UCS testing to assess whether samples contained adequate supplies of water to allow for continued hydration and cementitious bond formation. Water content determination was conducted according to BS 1377: Part 2 (BSI, 1990) by oven drying samples at a temperature of 110 ^{o}C for 24 hours.

Table 5.1: Average changes in water content observed over 28 days curing for all untreated and stabilised Lanton alluvium mixtures.

Soil – Binder Mixture	Water content (%) with increasing curing time		Reduction in water content (%)
	0 days	28 days	
Lanton	24.63	23.89	0.74
Lanton + 5% Lime	24.08	23.32	0.76
Lanton + 10% Lime	25.07	21.62	3.45
Lanton + 5% CEM-I	24.15	22.68	1.47
Lanton + 10% CEM-I	24.51	19.26	5.25
Lanton + 10% PFA	26.37	25.47	0.90
Lanton + 10% PFA-NaOH	25.92	25.32	0.60
Lanton + 5% GGBS	24.81	24.12	0.69
Lanton + 10% GGBS	24.99	24.58	0.41
Lanton + 2.5% GGBS-NaOH	24.55	23.52	1.03
Lanton + 5% GGBS-NaOH	25.57	24.48	1.09
Lanton + OLD 7.5% GGBS-NaOH	25.08	23.68	1.40
Lanton + NEW 7.5% GGBS-NaOH	25.09	23.64	1.45
Lanton + 10% GGBS-NaOH	24.72	22.94	1.78

Based on the results in Table 5.1, it is clear most samples had water contents of 22–25%. Each mixture showed slight reductions in moisture content over 28 days curing. Negligible moisture content reductions were recorded within all non-activated samples. For samples containing GGBS-NaOH binder, moisture content reductions ranged between 1 and 1.8%; whereby reductions >1.4% were observed for samples containing a dosage >7.5%. The most significant reductions in moisture content (up to 5.25%) were observed in samples stabilised with a 10% dosage of the traditional binders (lime and CEM-I). To summarise, moisture content reductions >1% correspond with samples which achieved high UCS values and pleasing durability

performances; thereby suggesting that cementitious bonds were forming through hydration and pozzolanic reactions. This indicates that there was plenty of water within all samples for such reactions to occur beyond 28 days, which is proven in the UCS results by the increasing strengths observed for "higher strength" samples between 28 and 56 days curing.

5.2.3.4 pH Testing

Further to findings by Hughes et al. (2011) that low pH can result in low strength development within stabilised soils, the primary aim of measuring the pH of all the aforementioned stabilised Lanton alluvium mixtures is to determine whether they reach a minimum value of 10.5, which is a necessary requirement for promoting pozzolanic conditions and subsequent strength developments through cementitious gel formation. Per previous pH tests, sub-samples were retained after compressive strength testing at 28 days and tested according to BS 1377: Part 3 (BSI, 1990). All pH results are displayed in Figure 5.12.

Average pH values recorded for untreated Lanton alluvium ranged between 6.7 and 7.2 over the 56 day curing period, thereby indicating the need for either an alkali activator or a high alkaline binder in order to promote pozzolanic conditions. Stabilisation using CEM-I or lime at dosages of 5 or 10% all produced pH values which comfortably surpassed the minimum value of 10.5 (i.e. >11.2); and were sustained for the entire 56 day curing period. Average pH values recorded for non-activated PFA or GGBS samples were all <10, thereby highlighting the need for both PFA and GGBS to be activated to promote pozzolanic conditions. Using NaOH was very effective in raising soil pH to at least 12 in PFA and GGBS based samples; albeit a factor other than pH is clearly responsible for the relatively poor strength performance of PFA-NaOH specimens. Finally for GGBS-based specimens activated using NaOH, all four dosages successfully raised soil pH to a minimum value of 11.7 - even the 2.5% dosage. The maximum pH values recorded ranged between 12.6 for the 7.5% dosage and 12.9 for the 10% dosage. Each of these values were comparable with the high pH values recorded for samples stabilised with either 10% lime or 10% CEM-I; thereby confirming that pH conditions within the soil were ideal for pozzolanic reactions and cementitious bonding to take place.

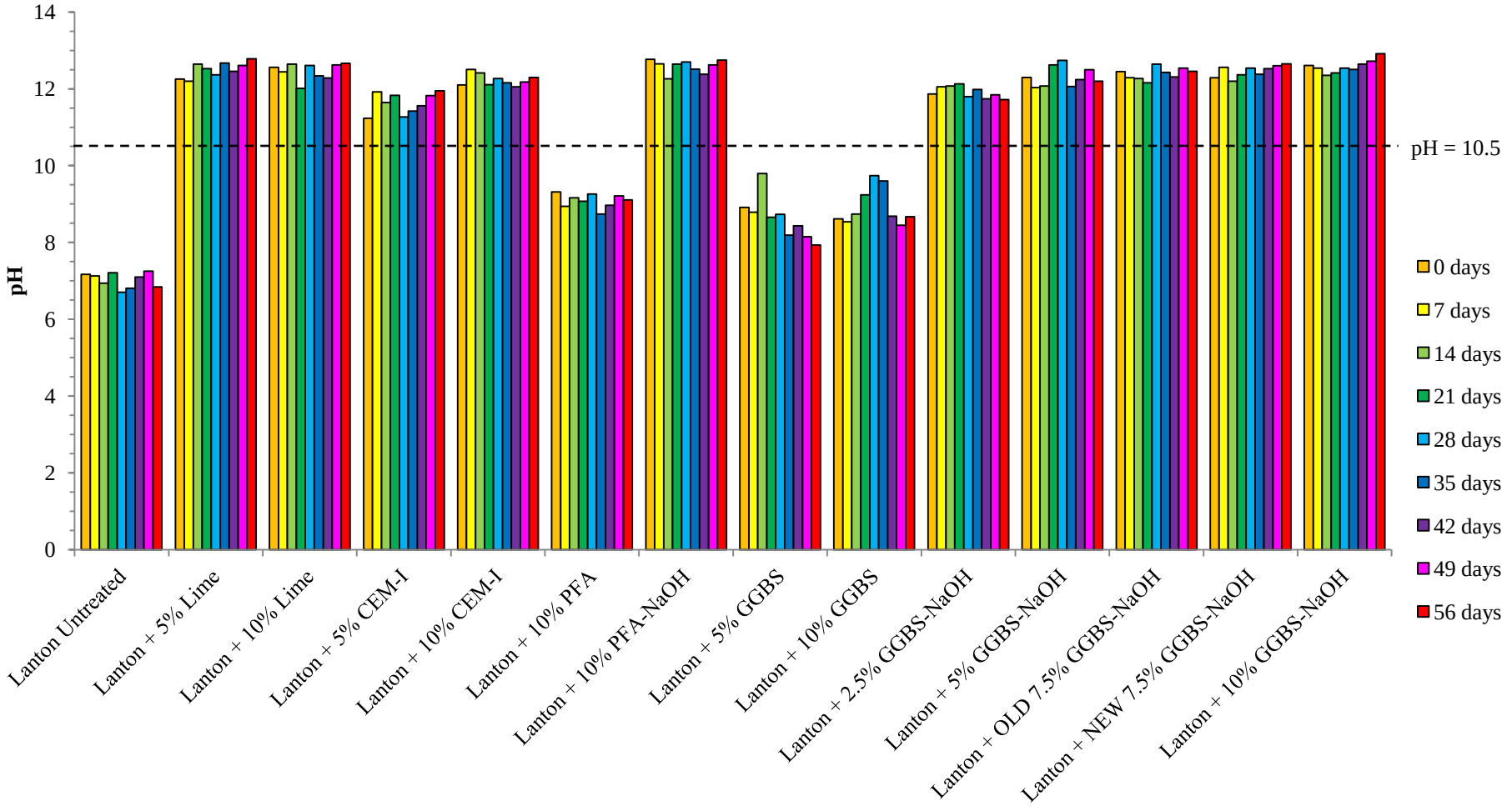

Figure 5.12: Bar charts presenting the average pH values obtained by all stabilised and non-treated Lanton alluvium samples after all curing periods.

5.3 Binder dosage trial results discussion

5.3.1 Strength

Compressive strength testing has proved that using lime or NaOH activators within GGBS at dosages ≥7.5% was necessary for cementitious bonds to form and produce significant strength gains. Although the compressive strengths recorded for GGBS-NaOH stabilised Lanton alluvium were up to three times lower than those recorded for the GGBS-NaOH-Na_2SiO_3 stabilised artificial alluvium from the previous chapter, the 28 day strengths achieved by using at least 7.5% GGBS-NaOH met EuroSoilStab (2002) criteria. After 21 days curing, the strengths achieved by using 7.5% GGBS-NaOH exceeded those for samples stabilised with 10% lime or CEM-I by factors of 3 and 2, respectively. The same binder at 10% dosage produced even more impressive strength developments after just 7 days. Poor strength performances were recorded for all curing periods when using a 2.5% dosage; as similarly observed for the 5% dosage until 42 days curing, after which strength development commenced – reaching comparable 56 day strengths to 10% CEM-I. However, such delayed strength gains would be unacceptable in industry, as construction specifications tend to require such strength enhancements after 28 days (Hansson et al., 2001).

Stabilised samples containing PFA displayed very disappointing strength developments and ductile behaviour with progressive shearing during UCS testing. PFA has been known to retard cementitious bond development and that pozzolanic reactions can take weeks to initiate (Fraay et al., 1989). Additionally, the lower UCS values recorded for PFA-based binders may also be attributed to type F PFA's low silica to alumina ratio (Rowles and O'Connor, 2003) and low CaO content (Shi et al., 2006). Hence, the use of type F PFA in stabilising Lanton alluvium is ill advised given its poor cementitious properties.

For NaOH activated GGBS-based samples, increases in strength with curing also resulted in higher levels of stiffness. Using a GGBS-NaOH dosage >7.5% within Lanton alluvium produced brittle failures. As previously mentioned, this behaviour could be potentially unfavourable under dynamic loading conditions; such as those

presented by passing rail traffic and earthquakes. However, the strengths achieved by the 7.5 and 10% GGBS-NaOH dosages were lower than those recorded for the GGBS-NaOH-Na_2SiO_3 stabilised artificial alluvium, suggestive of being more favourable for dynamic loading applications.

Based on the higher CEC and surface area values measured for Lanton alluvium compared with those for the artificial alluvium from the previous chapter, it is logical to suggest that higher strengths would be achieved after 28 days when Lanton alluvium is stabilised with alkali activated GGBS, due to the higher number of sites for cementitious bonds to form. However, the results show that this is not the case, as strengths using the GGBS-NaOH binder at a dosage of 10% were nearly three times lower than those achieved by the artificial alluvium stabilised with NaOH-Na_2SiO_3 activated GGBS. This could be attributed to numerous factors. Firstly, the lower moisture content of the artificial alluvium (15%) and hence its higher calcium concentration due to the GGBS would result in any available water within the soil being utilised at a faster rate to form cementitious gels and therefore achieving higher strength gains over 28 days compared with Lanton alluvium. Also, based on the higher moisture content of Lanton alluvium and that pozzolanic reactions are known to occur over periods of months and years (Tutumluer, 2012), it is possible that strength gains develop at a much slower rate when using lower GGBS-NaOH dosages, as demonstrated for the 5% dosage.

Another contributing factor which has been attributed by Consoli et al. (2011) to influence strength development within cemented soils is the porosity of the original soil. Whilst a soil's moisture content influences the strengths achieved by altering its structure, Consoli et al. (2011) state that porosity influences the strengths achieved by modifying the number of contact points between soil particles. For more porous soils, it is anticipated that delayed strength gains are likely due to the higher number of larger pore spaces which must be filled with cementitious growths to ultimately increase inter-particle contacts and achieve strength gains. Hence, given that the artificial alluvium has a significantly higher clay content than the Lanton alluvium, the porosity of the former is likely to be lower than for the latter. This suggests that any delays in strength development or comparably lower strength values are likely to be observed within stabilised Lanton alluvium samples. The influence of porosity on strength will be investigated and quantified below in section 5.4.3.

Tutumluer (2012) states numerous criteria of a soil's natural properties are normally required for lime and cement stabilisation to work effectively; namely low organic matter content (<1%), low sulphate contents (<0.3%) and clay contents of 10–50%. The low clay content of Lanton alluvium may therefore partly explain why lime and CEM-I stabilised samples had relatively low compressive strengths. With that said, the artificial alluvium's higher clay content solely consisted of Kaolinite, whereas the clay mineralogy of Lanton alluvium is not yet known. The typical surface areas of Kaolinite, Illite and Smectite are 15, 100 and 800 m^2/g, respectively (Tutumluer, 2012). Hence, mineralogical analyses are required to determine which types of clay minerals are present within Lanton alluvium. It is possible that although the clay content for Lanton alluvium was significantly lower than the artificial alluvium, the Lanton soil contains high surface area clay minerals such as Illite and Smectite, which would compensate to allow strength developments to occur. The author forwards the reader to the next chapter which presents findings from mineralogical analysis work.

According to the k_v values documented by Terzaghi et al. (1996), which may be expected for most soils; Lanton alluvium is considered to be of poor permeability in its natural undisturbed state and practically impervious when remoulded. As the soil contains a mixture of sand, silt and clay particles, it is thought there are two major factors explaining why such impressive strength gains have been achieved within such a low permeability soil. Firstly, the activated GGBS binder was thoroughly mixed into the soil to achieve the highest level of homogeneity possible. This allowed hydration and pozzolanic reactions to occur throughout soil samples and therefore a wide distribution of cementitious gel formation. Albeit Lanton alluvium has a low permeability; impressive strength gains within alkali activated samples may also be attributed to the even distribution of water throughout samples. This is owed in part to the high quality of mixing during sample preparation in addition to the soil's particle size distribution; namely the sand and silt fractions which provide hydration reactions with better access to water for cementitious gel formation compared with soils containing higher clay contents.

5.3.2 Durability

As similarly determined from the UCS testing programme, adding GGBS-NaOH at dosages >7.5% (particularly 10%) to Lanton alluvium produced the most impressive durability performances, both for wetting-drying and freezing-thawing. Their performances surpassed those of other "high strength" binders which survived all 12 cycles (10% GGBS-lime and 10% CEM-I), given their negligible reductions in volume or moisture content. Specimens comprising PFA were the least durable, disintegrating after the first wet-dry or freeze-thaw cycle.

Per the durability testing programme from the previous chapter, the alkali activation of GGBS with NaOH proved very effective in producing dense high strength samples, which were also characterised by low permeabilities and thereby less likely to experience water absorption and subsequent sample deterioration through shrinkage, swelling and physical weathering.

For any of the binder mixtures tested during this study, a binder dosage of <7.5% is strongly advised against given the natural chemical and geotechnical properties of Lanton alluvium, along with the aggressiveness of the ASTM's wetting-drying and freezing-thawing cycles testing programme, which may occur regularly in some countries. Further research is required into the viability of PFA as an IBP binder in the DSM treatment of alluvial soils, as their future potential seems precarious, given the results presented from both this and the previous chapter.

5.3.3 Water content

It is important for stabilised samples to contain sufficient volumes of water to ensure binders hydrate and produce cementitious gels. When each of the samples tested in this study were initially prepared, their moisture contents were recorded as approximately 25%. For each curing period up to 56 days, the moisture contents of samples were measured after UCS testing. Overall, the water contents of all samples decreased over the 56 day period by a maximum of 3.45%. However, most samples only experienced moisture content reductions of 0.4–1.8%. The smallest moisture

content reductions were observed for low strength samples (e.g. PFA) where strength reactions had not occurred. This implies that all the sample mixtures contained ample volumes of water for hydration and cementitious bonding reactions to occur during and beyond the 56 day curing period tested.

In line with the findings presented in the previous chapter and those documented by Duxson et al. (2007), there is evidence to suggest that a relationship exists between decreasing moisture content and strength enhancement when Lanton alluvium is stabilised with lime or NaOH activated GGBS. As water within soils is consumed during the dissolution of geopolymeric reactions and solid aluminosilicates break down to give silicate and aluminate species through alkaline hydrolysis (Duxson et al. (2007); it comes as no surprise that NaOH activated GGBS samples showed greater reductions in water content compared with non-activated GGBS.

Albeit very small water content reductions were observed across the 56 day testing period for the GGBS-NaOH samples, significant strength enhancements were recorded when using a binder dosage ≥7.5%. Considering that Lanton alluvium has a natural water content of 25%, this would initially suggest that there is plenty of scope for further hydration and pozzolanic reactions to occur, and therefore further water consumption and cementitious gel development within the stabilised soil's matrix post-56 days. Although GGBS-AA stabilised artificial alluvium samples from the previous chapter achieved higher strengths with a lower water content than stabilised Lanton alluvium samples; research by Locat et al. (1990) suggests that in the long term, it is plausible that Lanton alluvium stabilised with binder dosages <7.5% may outperform the strength performances of stabilised soils containing lower water contents. Locat et al. (1990) attributed this behaviour to solutes being able to migrate through the soil's pore spaces more easily. This process may be apparent for the 5% GGBS-NaOH sample, which started to display encouraging strength developments after 42 days. Mechanical and physical conceptual models published by Locat et al. (1990) on how strength develops within lime stabilised clayey soils of high and low water contents is presented in Figure 5.13.

Per Locat et al.'s (1990) mechanical conceptual model, stabilised soils tend to go through three phases of strength development; phase 1 denotes the initial period of chemical reaction initiation and the development of cementitious gels. Any mechanical

strength enhancements of the material are due to the formation of cementitious gel coatings or bonding between soil particles.

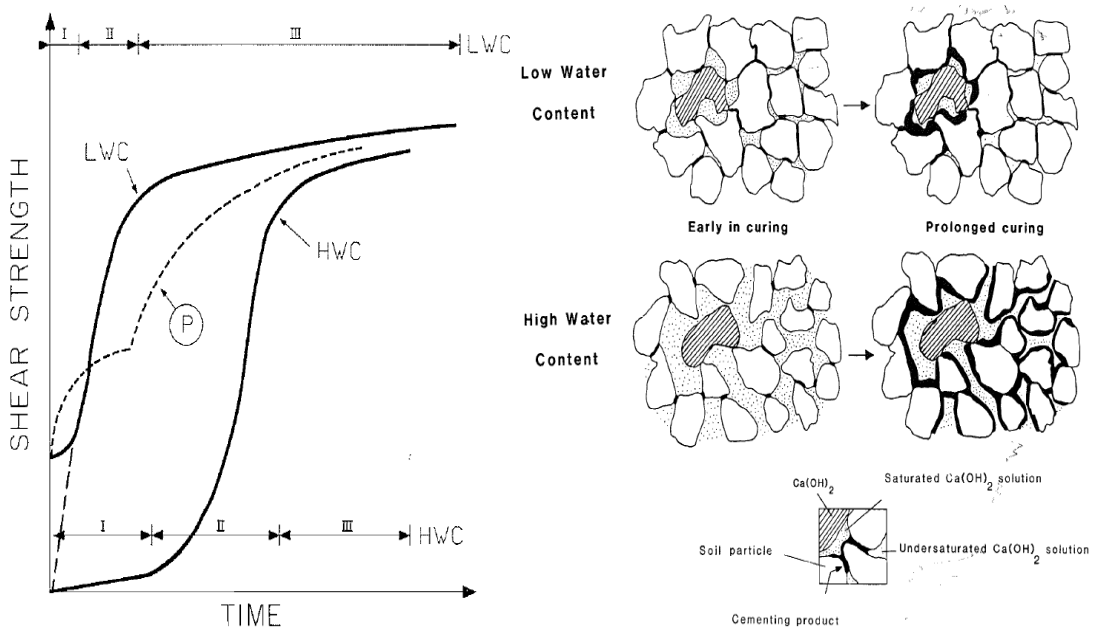

Figure 5.13: Mechanical and physical conceptual models of strength development for lime stabilised clayey soils containing high and low water contents. Courtesy of Locat et al. (1990).

Phase 2 involves further development of cementitious gels due to pozzolanic reactions; whereby considerable strength enhancements tend to be exhibited. Finally, phase 3 is characterised by a marked decrease in strength development rates and/or a plateauing of strength development. Locat et al. (1990) believed that phase 3's characteristics can be a result of a combination of: 1) the exhaustion of the binder and therefore completion of pozzolanic reactions; 2) pozzolanic reactions may still be occurring but solute migration within the material may be retarded by the newly cemented soil matrix, and 3) cementitious gels may still be forming but their effects are not as noticeable compared with phase 2.

Locat et al.'s (1990) research implies that stabilising Lanton alluvium with a dosage of 10% GGBS-NaOH closely resembles the strength-time curve shown for low water contents on Figure 5.13. Phase 1 lasted only for a couple of days before entering phase 2 after 7 days where considerable compressive strengths of 1.3 MPa were recorded. Using a dosage of 7.5% showed a slower rate of strength development, with strengths of 1.3 MPa being achieved after only 28 days. When comparing the behaviour of this

dosage with Locat et al.'s (1990) mechanical conceptual model, this behaviour seems to correspond well with the strength-time curve for soils with high water contents; whereby the material was in phase 1 up to at least 14 days and entered phase 2 at 21 days. For GGBS-NaOH samples containing a dosage of 5%, negligible strength developments were observed until 42 days, at which point the material went from phase 1 to phase 2 of strength development. These findings prove that further study is required over a longer period of time (i.e. 365 days) to gain a better understanding of the progressive strength development of GGBS-NaOH stabilised Lanton alluvium; specifically in terms of defining the length of time taken by different dosages to complete the three phases defined by Locat et al. (1990).

In addition to the influence of higher water content in retarding strength development within GGBS-NaOH stabilised Lanton alluvium compared with GGBS-AA stabilised artificial alluvium from Chapter 4, the concentration of calcium within the mixture is also likely to be a major influencing factor. Given the lower moisture content of 15% for the artificial alluvium compared with 25% for Lanton alluvium, the calcium concentration was higher for the former to produce new calcium-based cementitious gels, even when identical binder dosages of 10% were used for treating both soils. This would therefore also account for the observed lower strengths and rates of strength development within GGBS-NaOH stabilised Lanton alluvium.

Based on the sample preparation method adopted for producing UCS samples, it is possible that suction was generated within samples during preparation. This may have consequently resulted in slightly higher sample strengths than may be expected. Although the clay contents within soils are required to be 10–20% for any marked improvements in engineering performance to be experienced through DSM treatment, higher clay contents inherently lower the soil's permeability; as does the addition of a dry granulated binder. It is therefore postulated that attempting to stabilise soils containing clay contents >20% will not be as successful compared with soils containing <20% clay, given that it would reduce the volume of water which hydration and pozzolanic reactions could utilise to form C-S-H/C-A-H gels (Hughes et al., 2011).

5.3.4 pH

Strength development of stabilised soils can be greatly influenced by their pH, as alkali activation is clearly required to raise soil pH to ≥10.5 to promote pozzolanic conditions and subsequent high UCS values. This was evident in this study for Lanton alluvium which had been stabilised either with 10% GGBS or 10% PFA; whereby the sample's pH was <10.5 and showed poor engineering performances compared with sample mixtures which had been activated with either NaOH or lime.

Whilst stabilisation using lime and CEM-I at a dosage of 5% was successful in raising and maintaining a soil of pH >10.5 for 56 days, poor compressive strength and durability performances were recorded for these sample mixtures. Therefore, should lime or CEM-I be used for mixing within Lanton alluvium or similar soils, a dosage of at least 10% is strongly recommended to achieve improved mechanical strength and durability performances. A similar observation was made for the 2.5% GGBS-NaOH sample, although this occurrence may simply be attributed to a combination of: 1) mixing insufficient binder into the soil; 2) the soil's relatively high water content and 3) potentially an insufficient amount of time for cementitious gels to start forming.

Should oxidising reactions and subsequent pH reductions be allowed to occur within stabilised samples, hydration and pozzolanic reactions may become inhibited and therefore result in either poor or severely delayed strength developments. Thus it is essential to assess the quantities of alkali activator which are required within samples to ensure that pH values >10.5 are maintained for the long-term. Finally, in relation to the use of the old and fresh batches of GGBS, the close similarity of the pH values recorded suggests that the shelf life of the old GGBS had not been exceeded.

5.3.5 Surface area and CEC

Soils containing higher clay contents are more favourable for soil stabilisation when attempting to achieve high strength gains, due to their higher surface area and therefore cation exchange characteristics. When using lime or cement, Tutumluer (2012) stated that an optimum clay content of 18–50%, low organic (<1%) and

sulphate (<0.3%) contents are necessary to observe any considerable improvements in engineering performance. However, Lanton alluvium is characterised by a low clay content (<10%) and a relatively higher surface area and CEC values compared with the artificial alluvium from the previous chapter, which may partly explain why lime and CEM-I stabilised samples had relatively low compressive strengths.

Based on the above, it is possible that binders of lower reactivity (i.e. type F PFA) are more suitable for stabilising soils containing higher clay contents than that for Lanton alluvium. Regarding GGBS-NaOH stabilised mixtures, it is possible that after 56 days a large proportion of the reactive CEC sites on the soil's clay particles have already been used to form cementitious bonds. Thus, it is plausible to suggest that any strength enhancements within these samples after 56 days using a dosage of ≥7.5% will not be as significant as those observed between 7 and 28 days curing and would be attributed to the increase in strength of current bonds, rather than the development of new bonds on silica-based sand/silt particles. To provide firmer conclusions regarding the mineralogy of Lanton alluvium in its untreated and treated states, XRD and SEM-EDX analyses are essential (please see next chapter).

5.3.6 Alkali activator

A study by Habert et al. (2011) revealed that the use of Na_2SiO_3 solution within binders for use in geopolymers was environmentally unsustainable and financially expensive. Additionally, the Na_2SiO_3 used in the previous chapter came in the form of a solution, which is not practical for use in DDSM treatments. Hence, NaOH was used without Na_2SiO_3 as an alkali activator when added to GGBS. Using solid NaOH flakes as an alkali activator also made the GGBS-based binder more commercially viable and more practical to use on sites.

Results demonstrated that NaOH was the most effective activator in raising soil pH up to at least 11.8 when combined with GGBS. Although the carbon footprint associated with the manufacture and transport of NaOH look much more favourable over Na_2SiO_3 amongst other alkali materials, there are a few potential health and safety issues which require acknowledgement and would need addressing should NaOH be used on a commercial scale. According to the Health Protection Agency (HPA, 2010),

inhalation of NaOH can cause irritation to the eyes and nose, causing common symptoms such as sore throats and headaches. If NaOH is ingested, it can burn the lining of the mouth, throat and stomach; which in turn can cause side effects such as abdominal pain and vomiting. Direct dermal contact with NaOH should be avoided by using rubber gloves as it tends to cause burns, inflammation and dermatitis. Thus, strict and thorough health and safety protection schemes need to be put in place for all DSM sites which use binders containing an NaOH component. In addition to wearing all basic pieces of personal protection equipment, all site workers are recommended to wear full body protection overalls, safety glasses, masks and thick rubber gloves.

5.4 Oedometer characterisation

Having identified that GGBS-NaOH was the most effective binder mixture in producing the most impressive engineering performances after various curing periods, the compressibility characteristics of Lanton alluvium in its untreated state and when stabilised using 2.5, 5, 7.5 and 10% GGBS-NaOH after 0 and 28 days curing will now be investigated.

Oedometer testing was conducted according to BS 1377: Part 5 (BSI, 1990). Coefficients of volume compressibility (Mv) were calculated to gain an understanding into the compressible nature of Lanton alluvium when untreated and stabilised after 28 days curing. Triplicate samples for each sample mixture and curing period were subject to two loading-unloading loops; whereby the first loop followed the loading sequence of 5, 10, 20, 25, 50, 100, 200 and 400 kPa, after which samples were unloaded back to 5 kPa using the same vertical stresses. For the second loop, samples were reloaded back to 400 kPa using the same loading sequence and were subject to higher stresses of 800 and 1600 kPa, before being unloaded incrementally back to 5 kPa. The compression (Cc') and swelling (Cs') indices were then derived from the loading and unloading paths, respectively.

5.4.1 Untreated Lanton alluvium results

Raw compression curves for the remoulded and undisturbed Lanton alluvium are displayed in Figure 5.14. The compression curves demonstrate the effect of removing sedimentation structure (typical of normally consolidated soils) within the soil due to disturbance. The remoulded Lanton alluvium (red curve) has a significantly lower initial void ratio compared with that recorded for the soil in its undisturbed state (blue curve). Additionally, the reduction in void ratio during compression was lower for the soil in its remoulded state compared with its undisturbed state. The undisturbed soil has a preconsolidation pressure (σ'_c) of 40 kPa. As the sample was obtained from 2.3 metres depth and the unit weight of the soil was 17.52 kN/m^3, the undisturbed soil's in-situ effective stress was also 40 kPa. This provides an overconsolidation ratio (OCR) of 1, thereby confirming that Lanton alluvium is a normally consolidated soil.

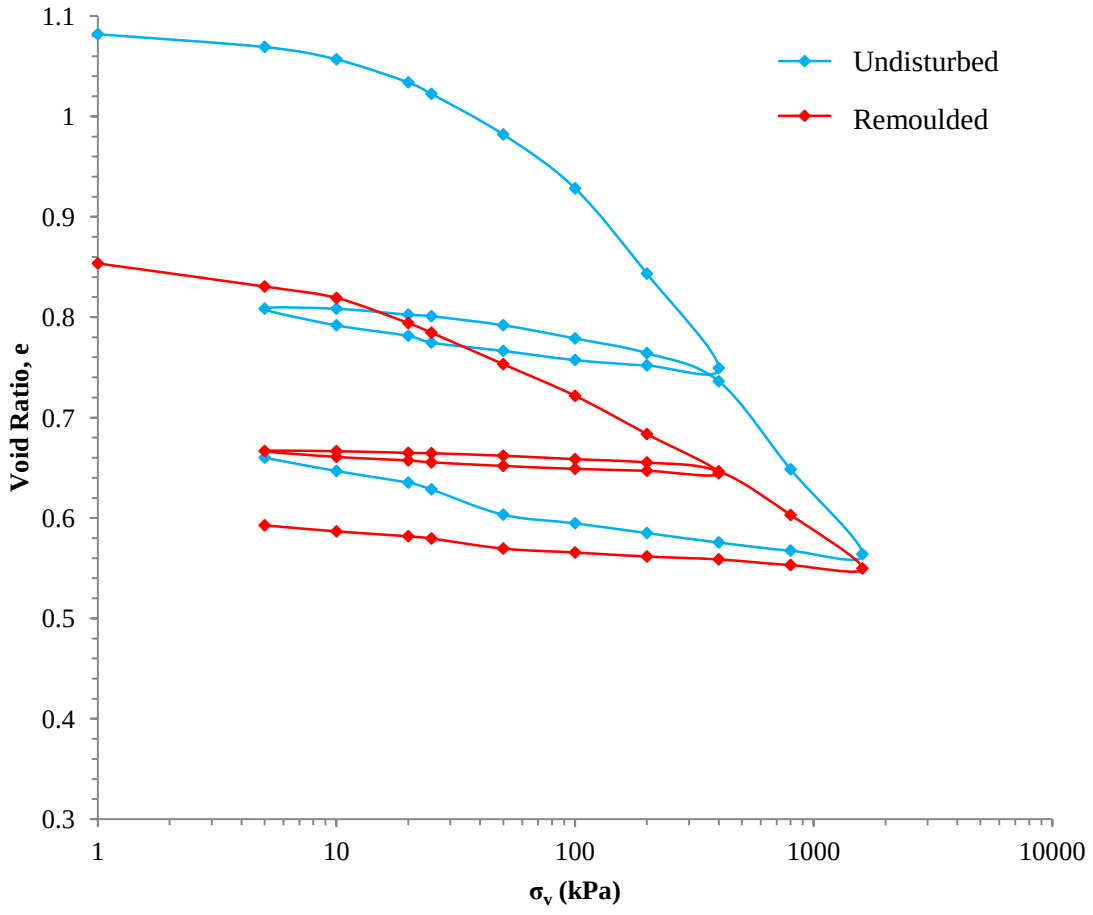

Figure 5.14: Raw oedometer compression curves for non-treated Lanton alluvium in both its undisturbed (blue curve) and remoulded (red curve) states.

The Cc' values obtained for undisturbed Lanton alluvium samples ranged around 0.309, indicating high compressibility behaviour. Remoulded Lanton alluvium samples had lower Cc' values of approximately 0.132; thereby classifying them as silts of medium compressibility per criteria stated by Reeves et al. (2006). The markedly lower Cc' and Cs' values recorded for the remoulded samples indicate a stiffer response to loading compared with undisturbed samples. This may be attributed to the reduction in void ratio as a consequence of compaction during sample preparation and also sample loading during the oedometer testing.

In terms of defining the level of structure within the Lanton alluvium according to criteria defined by Gasparre and Coop (2008), Figure 5.16 below illustrates the derivation of values for YSR and S_σ. The intrinsic compression line (ICL) has been derived directly from the compression path - a.k.a. the virgin compression line (VCL) taken by the remoulded Lanton alluvium, as observed in Figure 5.14. Per Figure 5.15, a YSR value of 40 and S_σ value of 6.06 have been derived. Unlike overconsolidated soils, the gross σ'_y value is fairly well defined for Lanton alluvium; whereby in comparison to a stiff overconsolidated clay, the destructuration processes occurred relatively quickly with compression. Gasparre and Coop (2008) also noted that as soil structure is lost, the swelling (unloading) line of the undisturbed material steepens towards the same gradient of the swelling line for the reconstituted soil. However, this behaviour was not apparent for Lanton alluvium, based on Figure 5.14.

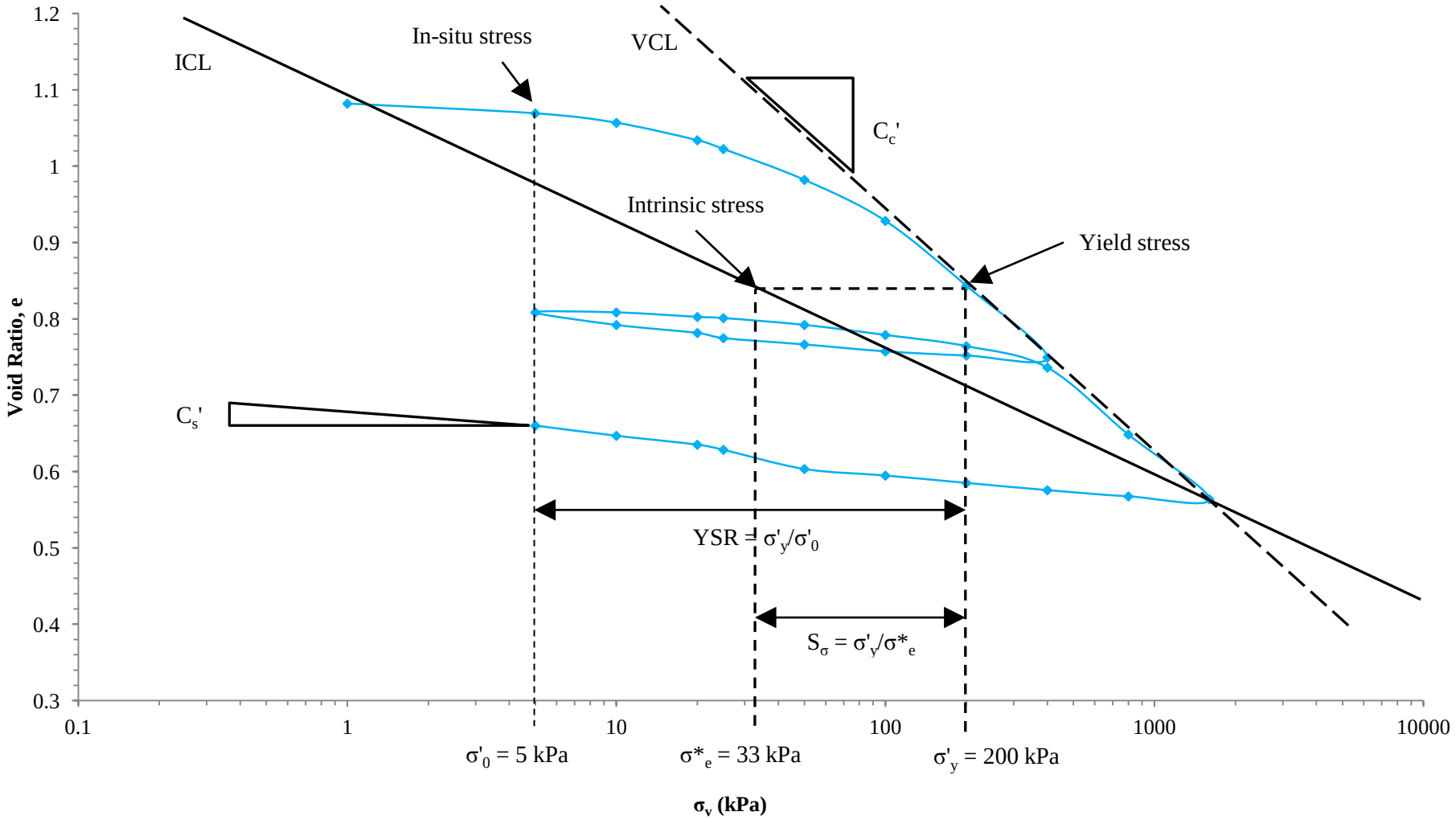

Figure 5.15: Normal compression and swelling curve for undisturbed Lanton alluvium, relative to the soil's ICL and VCL in order to define its initial degree of structure.

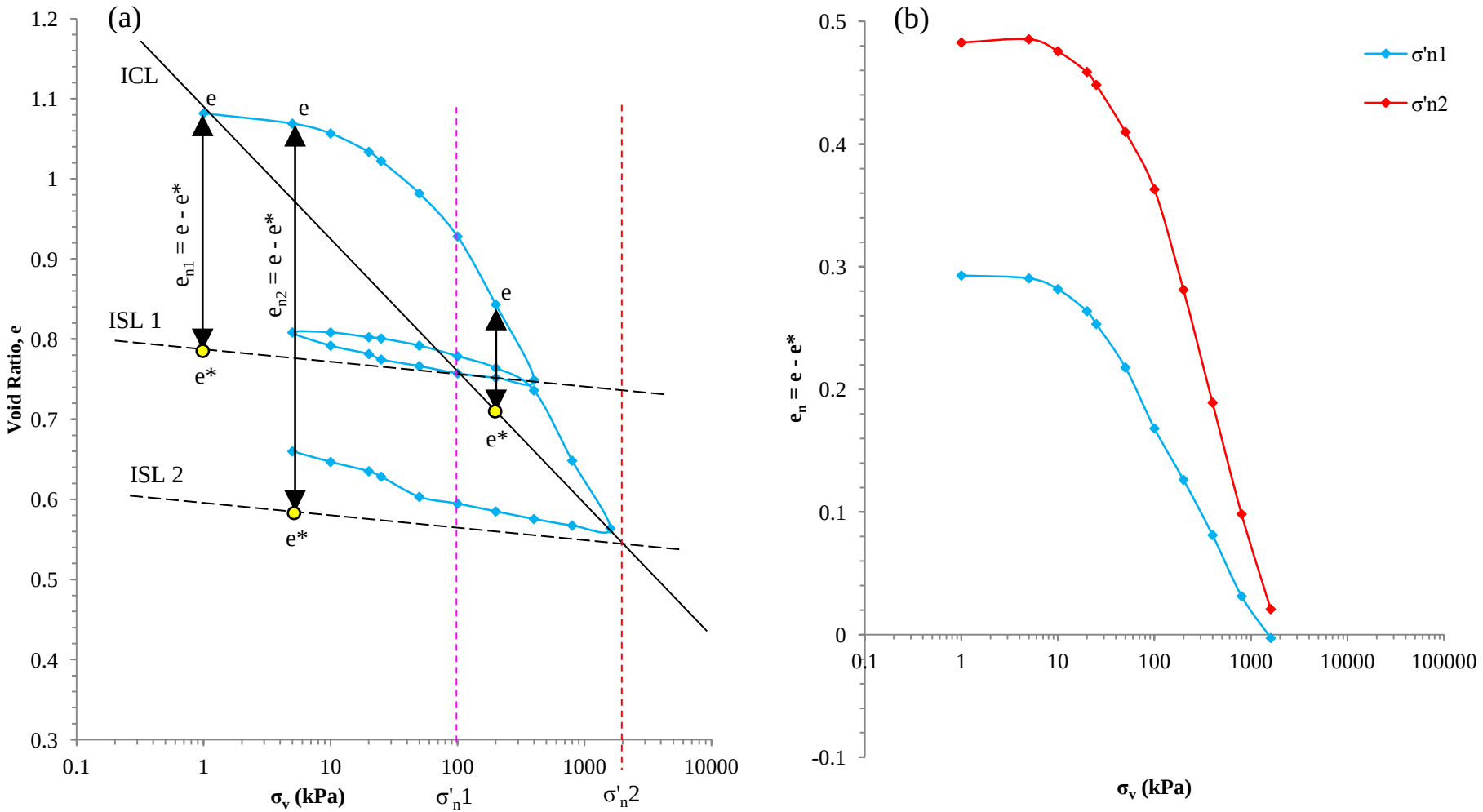

Figure 5.16: (a) Visualisation of applying Gasparre and Coop's (2008) normalisation technique to undisturbed Lanton alluvium; (b) Normalised oedometer data for Lanton alluvium, using both σ'_n1 and σ'_n2 for determining e* and e_n values.

Figure 5.16a shows a schematic following the application of Gasparre and Coop's (2008) normalisation technique to undisturbed Lanton alluvium oedometer data, whereas Figure 5.16b presents the normalised data. There are two possible positions for taking σ'_n based on the position of the two ISL's from unloading stages conducted during testing. Given the soft and normally consolidated nature of Lanton alluvium and the maximum capacity of the oedometer equipment used, using σ'_n2 was unable to consider conditions where $\sigma'_v > \sigma'_n$. A comparative study was conducted whereby both σ'_n1 and σ'_n2 were used to define e* and therefore e_n values. The results from this comparison are presented in Figure 5.16b.

Per Figure 5.16b, there is a considerably higher initial e_n value of 0.48 achieved when using σ'_n2 compared with the initial e_n value of 0.29 when using σ'_n1, which accounts for a considerable degree of initial sedimentation structure. However, given that Gasparre and Coop (2008) took the ISL which was produced upon the final unloading of samples (rather than an unload-reload loop conducted mid-way through testing), ISL 2 on Figure 5.16a should be used for calculating e* and e_n values, in order to allow for direct comparisons.

The red curve in Figure 5.16b displays evidence of rapid structure loss, given its steep gradient once it had passed the gross-yield point. The vertical stresses at which destructuration occurred were much lower than those required to overcome the effects of structure within much stiffer overconsolidated clays such as London Clay (Figure 5.17). In Gasparre and Coop's (2008) study, the initial e_n values recorded for London Clay at shallower depths (<28 m) and greater depths (35–51m) ranged between 0.18–0.25 and 0.36–0.38, respectively. Based on the shape of the compression path once it first crosses the ICL, the structure within the soil can be predominantly attributed to inter-particle bonding rather than fabric (Coop, 2014), as demonstrated in Figure 5.18 below.

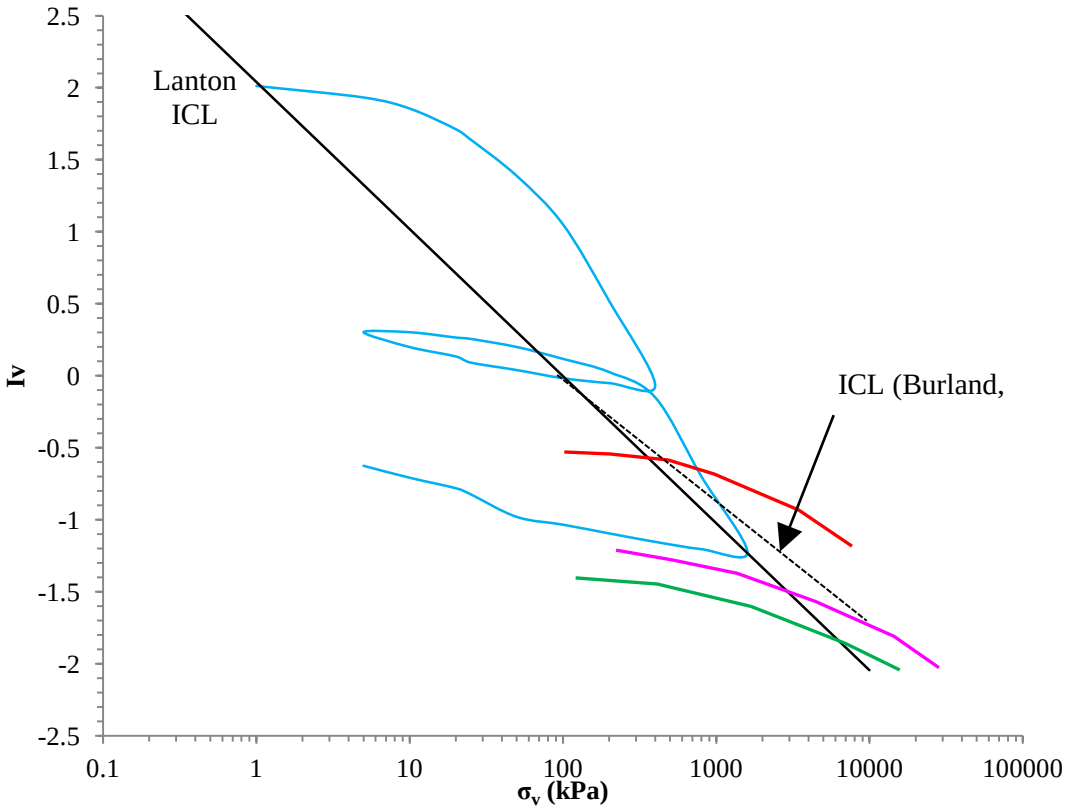

Figure 5.17: Compressional behaviour of undisturbed Lanton alluvium (blue) within the Iv – log σ_v plane. For comparison purposes, approximate compressional curves for London Clay (red), Oxford Clay (pink) and Gault Clay (green) are superimposed, as is their corresponding ICL from Burland (1990) (taken from Coop, 2014).

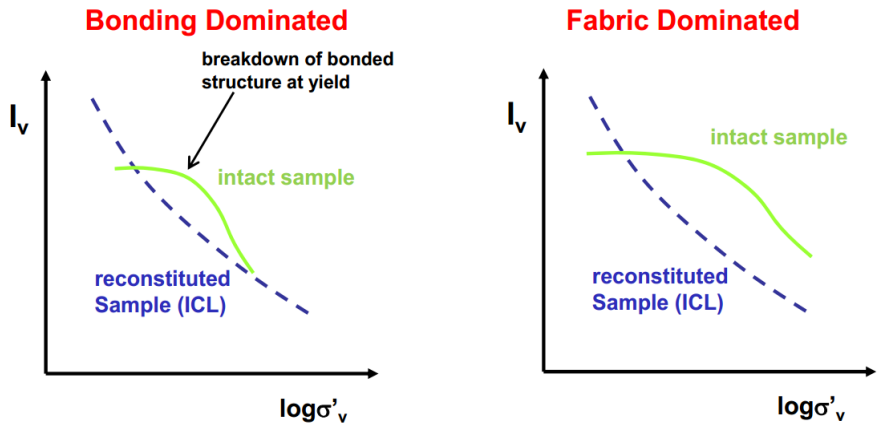

Figure 5.18: Effect of bonding or fabric dominated structure on soil compressional behaviour. Taken from Coop (2014).

In contrast to the lower e_n values for London Clay and the difficulty experienced by Gasparre and Coop (2008) in overcoming the post-sedimentation structure within deeper samples, which may be attributed to the soil's stiff overconsolidated state and high clay content; the undisturbed Lanton alluvium appeared to have a higher degree of initial natural structure. However, the soil's structure was much more easily lost upon disturbance using much lower vertical stresses than those used by Gasparre and Coop (2008). This may be attributed to numerous factors including Lanton alluvium's higher silt and sand contents, predominantly bonding-based structure rather than fabric based, relatively high in-situ moisture content and ultimately higher sensitivity to loading.

5.4.2 GGBS-NaOH treated Lanton alluvium results

Compression curves for the various GGBS-NaOH treated Lanton alluvium mixtures after 0 and 28 days curing are displayed in Figure 5.19. A summary of the Mv values obtained for each sample after 0 and 28 days curing is given in Figure 5.20. The compression curves all demonstrate that all stabilised mixtures exhibited much stiffer responses after only 0 days curing compared with untreated Lanton alluvium, both in its undisturbed and remoulded states. After 0 days, all stabilised mixtures experienced void ratio reductions of only 0.1, which contrasts with untreated samples whose void ratios decreased by 0.25 and 0.4 for remoulded and undisturbed samples, respectively. Given that introducing a binder via deep mixing disturbs the soil, it is not surprising that the initial void ratios of stabilised samples were relatively similar to the remoulded Lanton alluvium.

After 28 days curing, samples containing 2.5 and 5% GGBS-NaOH exhibited slightly improved consolidation behaviour compared with that observed after 0 days curing, as proven by the Cc' and Cs' values in Table 5.2.

Table 5.2: Summary of the compression and swelling indices recorded for treated and untreated Lanton alluvium oedometer samples after 0 and 28 days curing.

Soil – Binder Mixture	Compression index (Cc')		Swelling index (Cs')	
	0 days	28 days	0 days	28 days
Lanton remoulded	0.132		0.013	
Lanton undisturbed	0.309		0.030	
Lanton + 2.5% GGBS-NaOH	0.065	0.039	0.015	0.004
Lanton + 5% GGBS-NaOH	0.087	0.034	0.011	0.004
Lanton + 7.5% GGBS-NaOH	0.077	0.016	0.011	0.004
Lanton + 10% GGBS-NaOH	0.055	0.014	0.009	0.003

Figure 5.19b shows that samples containing a GGBS-NaOH dosage of 7.5 or 10% displayed a significantly stiffer response to consolidation after 28 days. Cc' values for these sample mixtures decreased considerably compared with their 0 day values. Cs' values for all four binder dosages were almost identical. Cc' values for 7.5 and 10% dosage samples are at least one third of the values obtained for samples containing 2.5 or 5% binder, 9 and 20 times smaller than the Cc' values obtained for the remoulded and undisturbed Lanton alluvium, respectively.

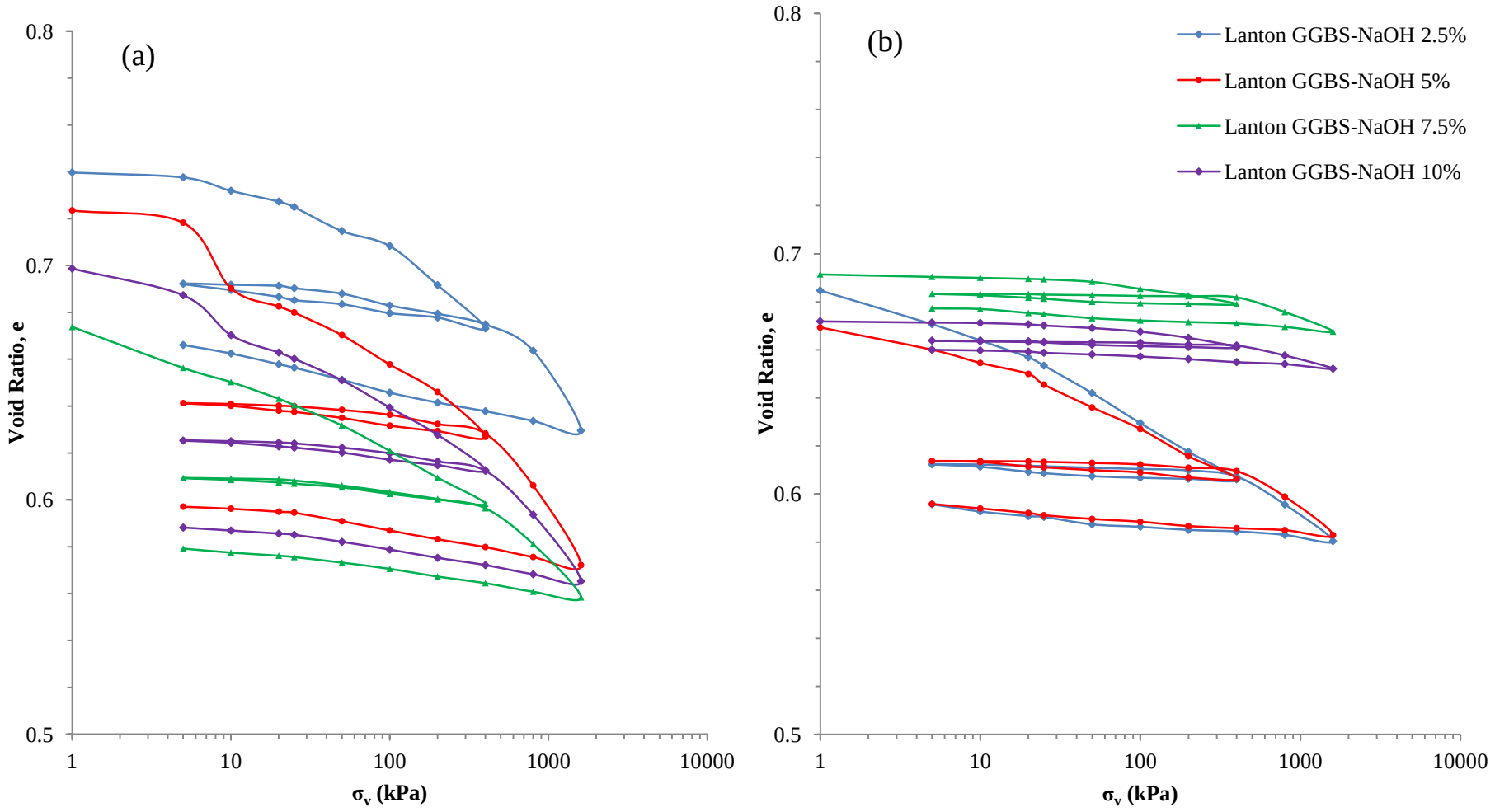

Figure 5.19: Oedometer compression curves of the GGBS-NaOH stabilised Lanton alluvium samples after: (a) 0 days and (b) 28 days curing. Note: the curves produced are based on averages taken from triplicate testing.

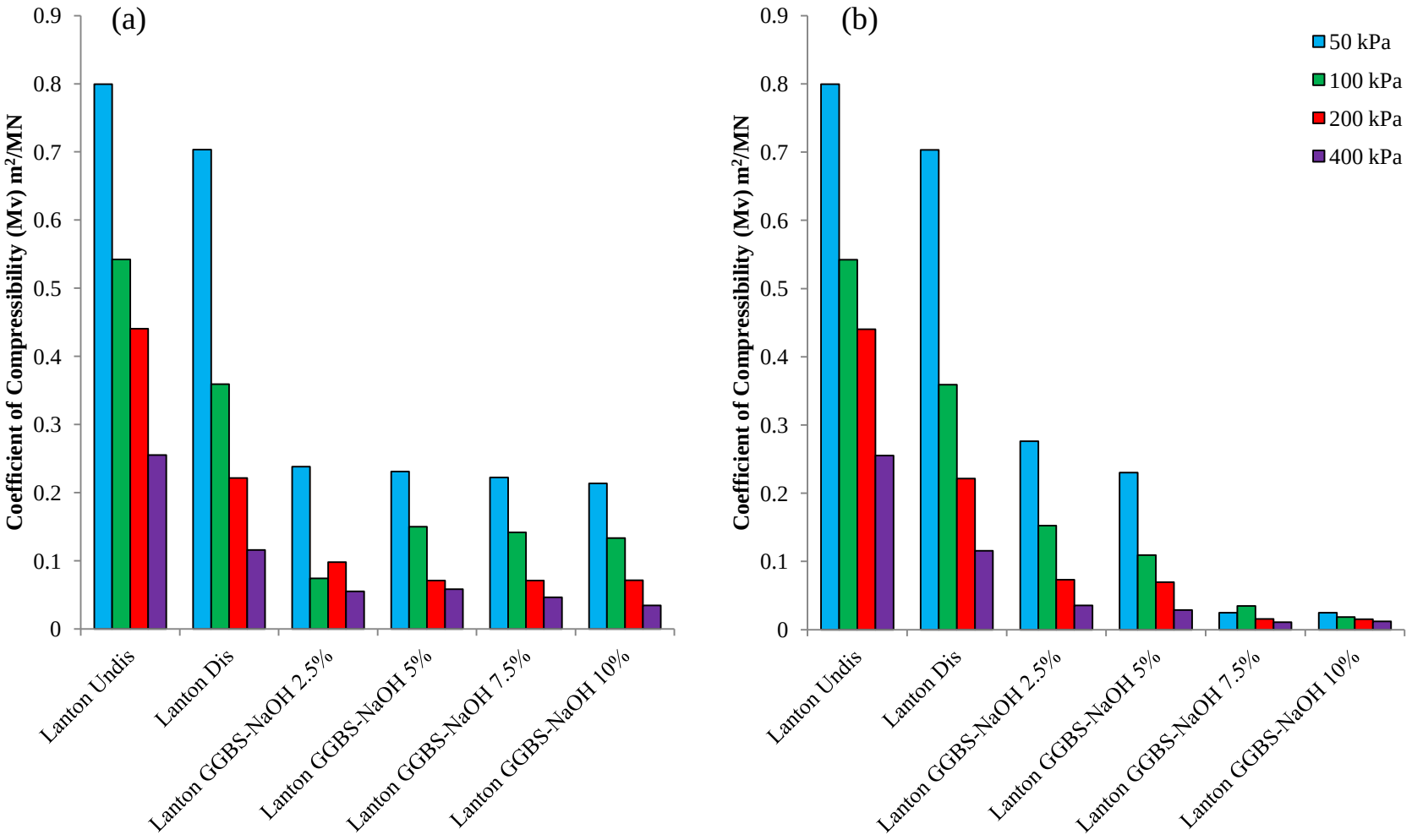

Figure 5.20: Summary of the M_v values (m^2/MN) calculated from oedometer tests on stabilised Lanton alluvium samples after: (a) 0 days and (b) 28 days curing.

The M_v results in Figure 5.20 well complement the compression curves in Figure 5.19; whereby all of the binder dosages reduced the compressibility of the untreated Lanton alluvium after just 0 days. The initial M_v values of the untreated undisturbed and disturbed alluvium were calculated to range between 0.7 and 0.8 m^2/MN, which according to Tomlinson (2001) and Reeves et al. (2006) is typical of normally consolidated alluvial clays and therefore highly compressible. The 0 day M_v values for each binder dosage ranged between 0.21 m^2/MN for σ_v = 50 kPa and 0.03 m^2/MN for σ_v = 400 kPa. Per Tomlinson (2001) and Reeves et al. (2006), these values indicate that each of the stabilised mixtures had a medium to very low compressibility. For dosages of 2.5 and 5%, there were negligible changes in the M_v values achieved after 0 and 28 days curing. However, there was a significant reduction in M_v values after 28 days for samples containing 7.5 or 10% GGBS-NaOH, where the effect of cementation within the stabilised material is apparent. Considerably lower M_v values of 0.01–0.03m^2/MN and 0.01–0.02m^2/MN were calculated for samples containing 7.5 and 10% binder dosages, respectively; and are deemed materials of very low compressibility per Tomlinson (2001).

These results suggest that the most effective dosage of the GGBS-NaOH binder in reducing the initially high compressibility of untreated Lanton alluvium was 10%. However, using the 7.5% GGBS-NaOH dosage appeared to be equally as effective in producing very low M_v values when samples were subjected to σ_v values >200 kPa. Hence, based on these observations there appears to be relatively little merit in using a dosage of 10% over 7.5%, given their close similarity in terms of very small reductions in void ratio after two loading-unloading cycles. Therefore, based on the impressive performances presented above and financial/environmental criteria, the final component of characterising the compressibility of GGBS-NaOH stabilised Lanton alluvium will now aim to examine the degree of structure created within the 7.5% GGBS-NaOH sample mixture due to cementation. The same Gasparre and Coop (2008) technique as conducted for normalising untreated Lanton alluvium is followed for the cemented soil.

Although the same loading-unloading sequence was applied to the stabilised samples, the material's very high stiffness required very high σ_v values to be applied during oedometer testing to produce a compression curve that sufficiently captures the yield point and post-yielding behaviour towards ICL convergence. However, this was not

possible during this study as the oedometer's maximum loading capacity of 1600 kPa was reached shortly after the Lanton + 7.5% GGBS-NaOH sample underwent yielding. Clearly, further research on the oedometer characterisation of this sample mixture is required to produce a more complete compression curve and gain more reliable insights into the material's cemented structure and rate of collapse. However, from the compression curve in Figure 5.21, it can be seen that at σ_v values ≥400 kPa, the gradient of the compression curve starts to show signs of steepening. Based on the knowledge gained from the UCS results presented earlier in this chapter for this cemented material, an assumed compression path for σ_v> 1600 kPa has been extrapolated (denoted by the green dashed line in Figure 5.21) to provide a provisional quantification of the material's cemented structure. Given the brittle nature of the soil when stabilised with 7.5% GGBS-NaOH, once the critical yielding strength has been reached and surpassed it is likely that the majority of the material's cemented structure will have completely degraded. This would therefore suggest that the compression curve would bend downwards and converge with the ICL (as drawn on Figure 5.21), rather than following a path parallel to the ICL which would indicate the presence of a stable structure that does not degrade with progressive straining (Gasparre and Coop, 2008).

By using the same in-situ stress of 5 kPa as the undisturbed untreated Lanton alluvium, a possible yield stress of approximately 13000 kPa has been assumed, thus providing a YSR value of 2600 and a S_σ value of 4.64. The YSR value for this stabilised material is nearly two orders of magnitude higher than that recorded for the undisturbed Lanton alluvium. However, the value recorded for the cemented material's stress sensitivity was lower by 1.42. Per Gasparre and Coop (2008), S_σ quantifies the amount of spacing between the cemented soil's compression curve and the ICL for Lanton alluvium; whereby its value can vary with increasing stress and is also influenced by the shape and position of the compression curve post-yielding. This highlights the need for further high pressure oedometer testing. Figure 5.22a shows a schematic following the application of Gasparre and Coop's (2008) normalisation technique to GGBS-NaOH stabilised Lanton alluvium oedometer data; and Figure 5.22b presents the normalised data.

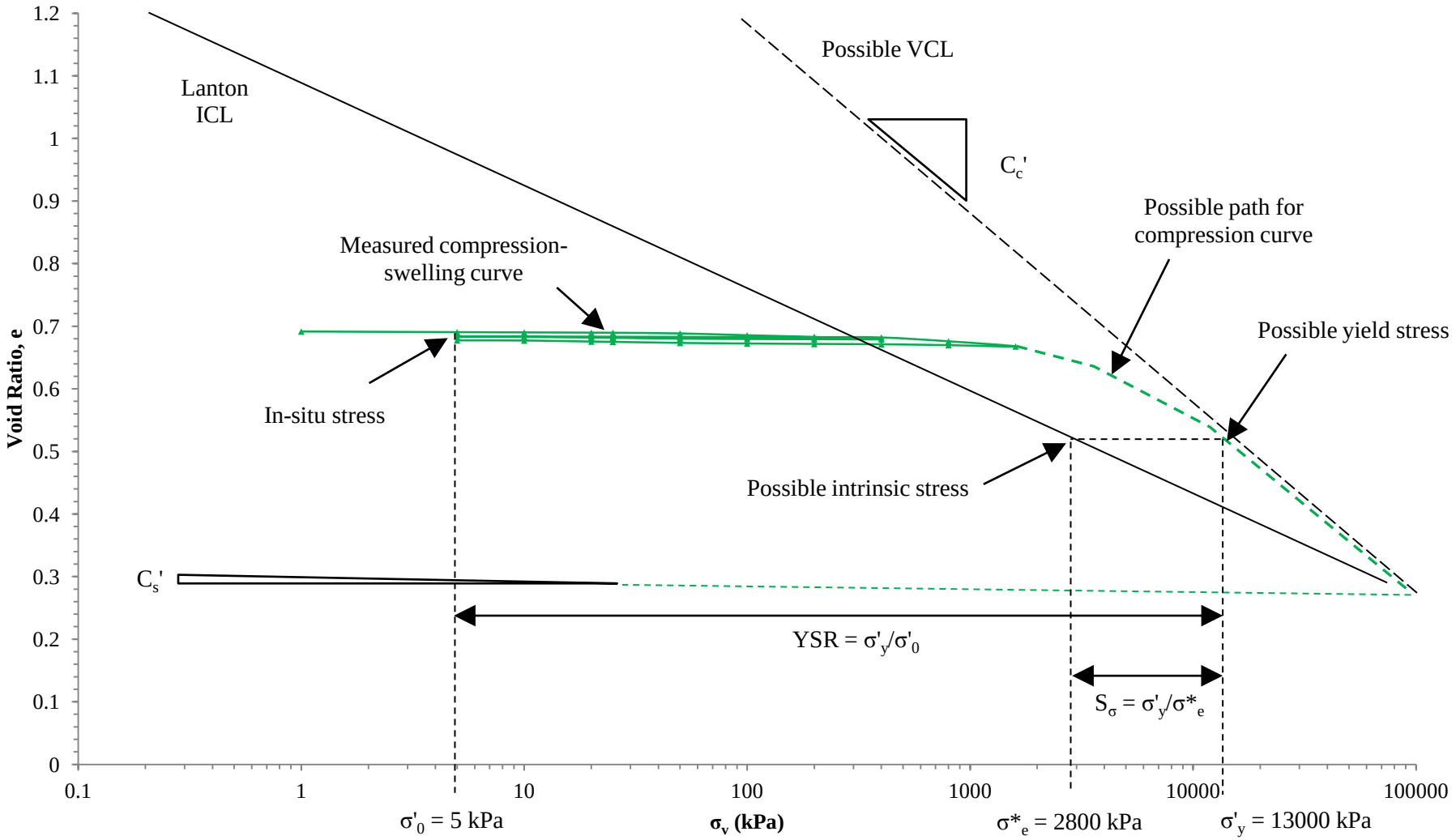

Figure 5.21: Possible normal compression and swelling curve for 7.5% GGBS-NaOH stabilised Lanton alluvium, relative to its possible VCL and the Lanton alluvium ICL in order to define the degree of structure caused by cementation.

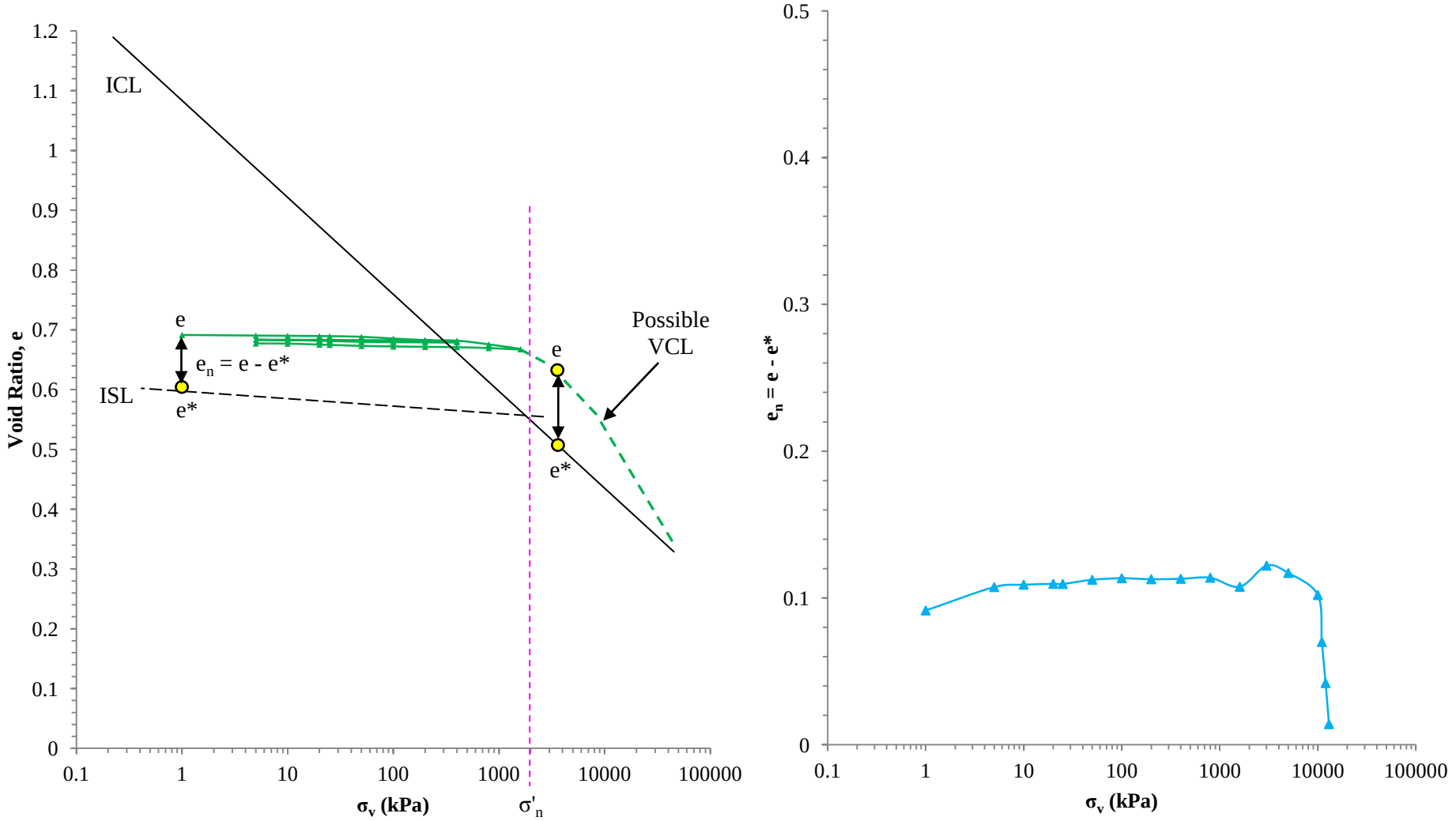

Figure 5.22: (a) Visualisation of applying Gasparre and Coop's (2008) normalisation technique to 7.5% GGBS-NaOH stabilised Lanton alluvium; (b) Normalised oedometer data for the stabilised material for determining e* and e_n values.

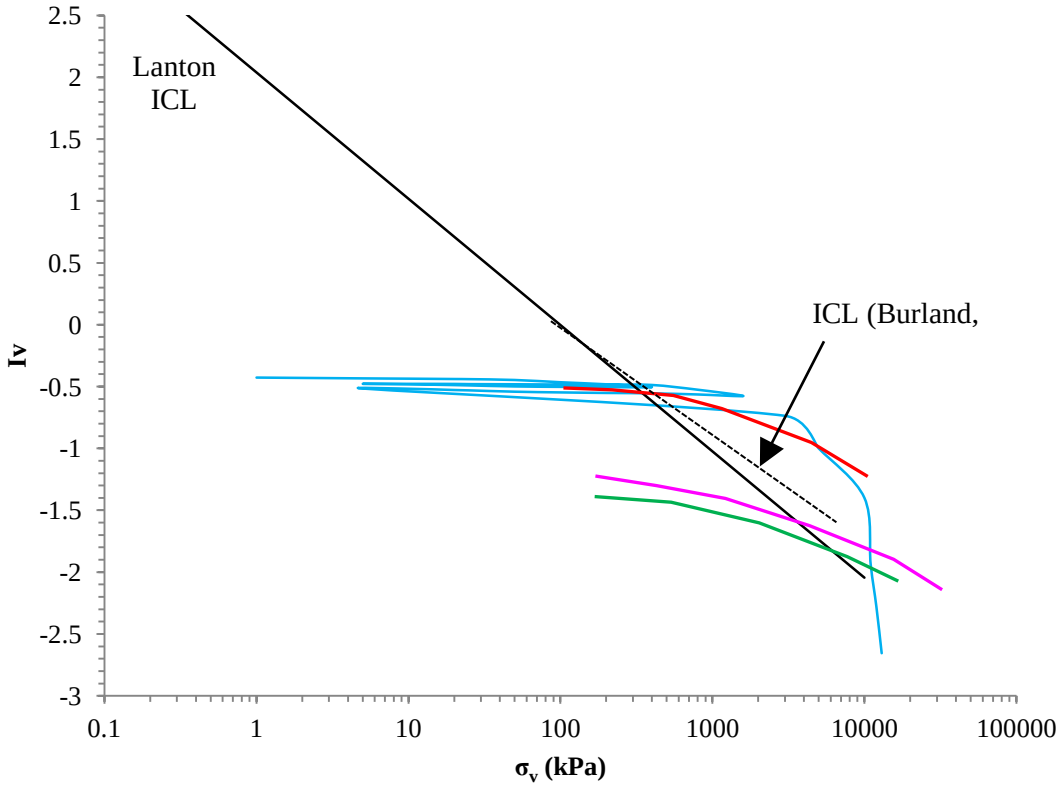

Figure 5.23: Compressional behaviour of 28 day 7.5% GGBS-NaOH treated Lanton alluvium (blue) within the Iv – log σ_v plane. Approximate compressional curves for London Clay (red), Oxford Clay (pink) and Gault Clay (green) are superimposed as well as their corresponding ICL from Burland (1990) (taken from Coop, 2014).

In contrast to undisturbed untreated Lanton alluvium, the calculation of e_n values for the cemented soil required using both the ISL when $\sigma_v < \sigma'_n$ and the ICL when $\sigma_v > \sigma'_n$. For the cemented soil, a considerably lower initial e_n value of 0.09 was obtained (Figure 5.22) compared with that measured for undisturbed Lanton alluvium. The material's initially low e_n values are even lower than those recorded by Gasparre and Coop (2008) for shallow depth London Clay samples, indicating an even stiffer initial response of stabilised Lanton soil when loaded. One feature to note is the sudden downward bending of the compression curve at σ_v = 10000 kPa, which can be attributed to the material's rapid strength reduction post-yielding. Although very high stresses are required to break down the structure of both stiff London Clay and cemented Lanton alluvium, the structure for the latter breaks down almost entirely at a much faster rate compared with London Clay whose structure has still not fully broken down at stresses >10000 kPa (Figure 5.23). Additionally, the structure of the cemented

Lanton alluvium arguably breaks down slightly more rapidly than the destructuration of the undisturbed untreated soil. This implies that both materials are much more susceptible to experiencing sudden and dramatic structure loss once they have passed their yield points, compared with stiff overconsolidated clays.

As similarly observed by Gasparre and Coop (2008) with their normalised data, it is apparent that there is a slight increase in en values up to σ_v = 1000 kPa for cemented Lanton soil, implying that the effect of structure is initially increasing. According to Gasparre and Coop (2008) this is unlikely, as such occurrences may be the result of simplifications involved in the normalisation of the data; specifically when normalising with respect to a line which changes suddenly from using the ISL to using the ICL at σ'_n.

5.4.3 Compressibility results discussion

Testing results signify that Lanton alluvium in its undisturbed state possessed a fairly high level of sedimentation structure. However, only the slightest disturbance or increase in loading up to 50 – 100 kPa resulted in a sudden and considerable reduction in void ratio, and therefore a significant degree of destructuration. This clearly highlighted that treatment was required to improve the soil's initially high levels of compressibility. At 0 days, the introduction of each GGBS-NaOH binder dosage produced very similar performances in significantly reducing Lanton alluvium's originally high compressibility, down to medium-low levels of compressibility. After 28 days curing, a significant improvement in compressibility was observed for stabilised specimens containing a GGBS-NaOH binder dosage of 7.5 or 10%. Such samples exhibited very similar behaviour to each other, whereby M_v values decreased down to <0.03m^2/MN with increasing σ_v, indicating very low levels of compressibility per Tomlinson (2001).

As mentioned in section 5.3.1, in addition to moisture content and cement dosage, porosity is also considered to have a marked influence on the strengths achieved within cement stabilised soils. This has been observed by Consoli et al. (2011) on a CEM-III stabilised silt, who defined relationships between compressive strength, porosity, cement content and moisture content. On this basis, the porosity and

saturation ratio values of the unstabilised artificial alluvium (Chapter 4) and Lanton alluvium were quantitatively defined from oedometer testing data; the results from which are presented in Table 5.3.

Table 5.3: Summary of the void ratio, porosity and saturation ratios recorded from oedometer testing for the artificial alluvium and Lanton alluvium.

Soil	Void ratio, e	Porosity, n (%)	Saturation ratio, Sr (%)
Artificial alluvium	0.416	29.4	94.6
Lanton alluvium (remoulded)	0.853	46.0	76.3
Lanton alluvium (undisturbed)	1.082	52.0	60.2

Based on the above figures, these suggest that the remoulded Lanton alluvium has a porosity that is 39 % higher than the artificial alluvium, whereas the undisturbed Lanton alluvium is 77 % higher. These significantly higher porosity values certainly assist in clarifying why lower strengths and slight delayed strength gains were observed within GGBS-NaOH stabilised Lanton alluvium compared with GGBS-NaOH-Na_2SiO_3 stabilised artificial alluvium, particularly when using binder dosages <7.5 %.

In line with works conducted by Consoli et al. (2011), the 28 day cured UCS values achieved by the four GGBS-NaOH dosages used to stabilise Lanton alluvium have been plotted on Figure 5.24 as a function of their porosity and cement (i.e. GGBS-NaOH) dosages for their initial moisture content of 25 %. As similarly observed by Consoli et al. (2011), a power law function may be used to define the relationship between UCS and the porosity-cement dosage ratio, achieving an R^2 value of 75 %. Whilst this R^2 value is encouraging, it is not as high as the values (0.83 – 0.90) determined by Consoli et al. (2011). This may be attributed to the slight degree of data scatter, which may be improved by conducting further oedometer tests on stabilised Lanton alluvium for more GGBS-NaOH dosages between 0 and 10 %.

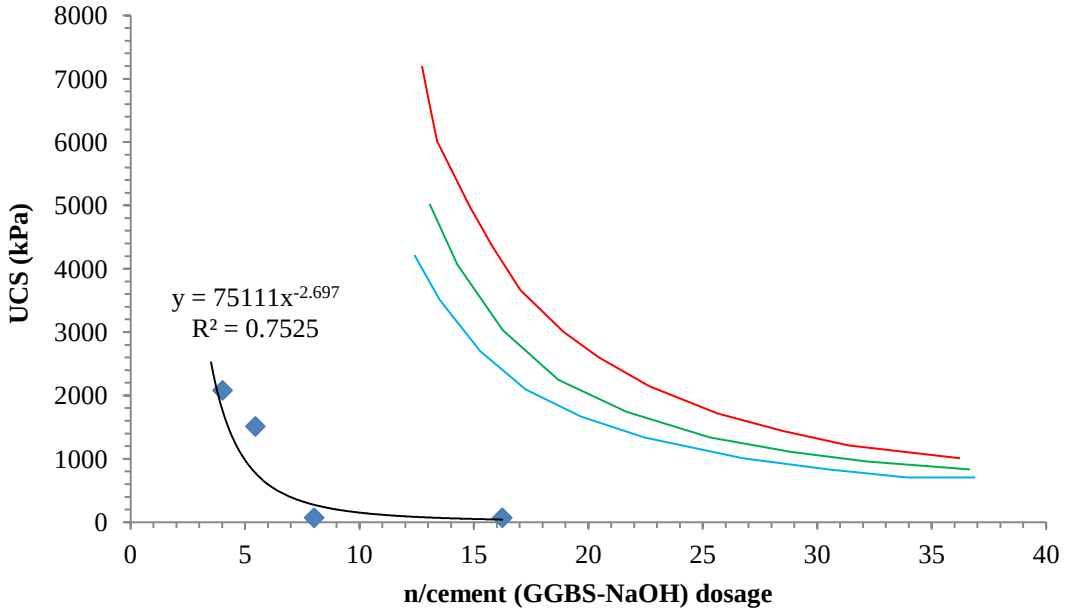

Figure 5.24: Relationship between 28 day UCS and porosity/cement dosage ratio for the GGBS-NaOH stabilised Lanton alluvium (black curve) for a moisture content of 25 %. Superimposed are the power law relationships defined by Consoli et al. (2011) for CEM-III stabilised silt at moisture contents of 17 % (blue curve), 20 % (green curve) and 23 % (red curve).

Using Gasparre and Coop's (2008) technique for normalising the oedometer data for Lanton alluvium in both its undisturbed and treated states enabled a more effective assessment of the effects of structure on the compressional behaviour of samples compared with using the Iv parameter. Initial increases in e_n values during tests should not be considered as representing increasing effects of structure, but as a consequence of making certain simplifications during the normalisation process.

Regarding the assumed extrapolation used by the author in Figure 5.21 to provide initial estimations of the GGBS-NaOH stabilised soil's behaviour under vertical stresses >1600 kPa, this is not a truly accurate representation of the material's one-dimensional consolidation behaviour. Inherently, this assumption potentially impacts the normalised results presented in Figure 5.22 and therefore the quantification of the cemented structure within the material. Should the material have a lower or higher yield stress than that assumed, this in turn would shift the point at which e_n values start to markedly decrease in Figure 5.22 to the left or right of its current position, respectively.

Additionally, should degradation of the cemented structure (a.k.a. structure collapse) occur at a rate different from that assumed, this would result in a variation of the rate e_n values decrease with increasing σ_v in Figure 5.22. The more rapidly degradation occurs within the material, the more rapidly e_n values decrease. According to Medero et al. (2009), the collapse potential of cement stabilised soils increases with increasing cement content; whereby stiffer samples containing higher cement dosages will exhibit highly brittle failures. This behaviour was observed during the UCS testing conducted in sections 4.2.3.1 and 5.2.3.1. Similar to natural collapsible soils, cemented soils undergo increasing collapse with increasing vertical stress up to a maximum value, which is then subsequently followed by a reduction in the degree of collapse as vertical stress continues to be applied (Medero et al., 2009). As the vertical stresses increase, the degree of cemented structure collapse which occurs decreases due to the progressive breakage of cementitious bonds between soil particles and hence the stabilised soil's skeleton (Medero et al., 2009). Thus, at very high stresses (i.e. >3 MPa), it is anticipated that the material's cemented structure will have mostly degraded through compression; whereby the application of further stress would result in further void ratio reductions. However, Medero et al. (2009) state that the degree of collapse experienced would be almost imperceivable.

Albeit the compressive strength and compressibility testing results complement each other, there is a slight concern regarding the reliability of some of the 28 day compressibility results for high-strength samples containing either a 7.5 or 10% dosage of GGBS-NaOH. All the samples were prepared within an oedometer ring, wrapped in cling film and left to cure within a sealed container. Once testing had been completed, the samples could not be simply removed from their oedometer rings; rather they required breaking out using several firm blows with a hammer (see Figure 5.25).

Figure 5.25: Photograph showing the removal of an oedometer sample comprising Lanton alluvium with 7.5% binder dosage.

Upon inspecting the oedometer rings, their inner surfaces showed a degree of discolouration. It is assumed this was a result of the alkali activated specimens reacting with the oedometer ring during curing and testing to produce a form of cementitious bonding between the oedometer rings and the samples. If this was the case, it may be plausible to suggest that at least a small proportion of the high stiffness/very low compressibility behaviour recorded for these high-strength samples may be attributed to the stiffness of the oedometer ring. One possible recommendation for future oedometer studies on GGBS-NaOH activated Lanton alluvium is to use an alternative methodology for curing the samples that is similar to that used for curing UCS samples within wax sealed PVC moulds. However, following this methodology will present the risk of sample shrinkage during curing; thereby leaving a gap between the outer edge of the sample and the oedometer ring. If such a situation were to arise, an option could be to carefully infill the gap with a stiff and preferably non-reactive/cementitious material, to ensure that the stabilised sample does not move during testing.

5.5 Chapter summary and conclusions

Further to the results and conclusions made from the previous chapter on phase 1 of testing, the IBP's of interest for use as a binder in stabilising Lanton alluvium were GGBS and PFA. Detailed binder dosage trials were then conducted on Lanton alluvium to determine the most appropriate IBP binder mixture for use as a binder in deep dry soil mixing. Results from a comprehensive suite of compressive strength, moisture content, pH, durability and oedometer tests revealed that by using NaOH to activate GGBS at an optimum dosage of 7.5% by dry weight produced the most impressive engineering performances. The strengths achieved overcompensated for any destructuration within the soil which would be observed during soil mixing. In addition, the strengths comfortably met engineering performance requirements stated by Hansson et al. (2001) and EuroSoilStab (2002) for deep mixed soils after 28 days. The binder's performance also surpassed those of lime and CEM-I. The 28 day UCS values of >1.5 MPa were lower than those presented for GGBS-AA samples from the previous chapter, although such lower strengths and stiffnesses were recommended as it would ensure that the stabilised soil mixtures would become less prone to experiencing sudden brittle failures when subjected to dynamic loads. Hence, the remainder of this thesis will solely focus on using the GGBS-NaOH binder at a dosage of 7.5% for stabilising Lanton alluvium.

Although the combination of NaOH flakes and Na_2SiO_3 solution proved very effective as an alkali activator in the previous chapter, the practicality in using Na_2SiO_3 solution for deep dry soil mixing becomes problematic. Additionally, the environmental and economic costs associated with Na_2SiO_3 solution production and usage is high. Hence, substituting Na_2SiO_3 with an alternative alkali activator for future binder mixtures would be preferable. However, the sole use of NaOH as an alkali activator was more than sufficient in raising soil pH to promote pozzolanic conditions and subsequent cementitious gel formation.

Based on findings from this chapter and the literature, at least three factors significantly influence the rate of strength gain and strength values achieved by cement stabilised soils; namely cement content, moisture content and porosity. Whilst both the artificial alluvium and Lanton soils had sufficiently high moisture contents to allow hydration and pozzolanic reactions to occur, the moisture content of Lanton

alluvium was 10% higher than that of the artificial alluvium. This contributed towards the slower rate of strength development within samples, particularly those containing GGBS-NaOH, lime or CEM-I at dosages <7.5%, whereby the higher water content caused greater changes in soil structure (Consoli et al., 2011) compared with that experienced by the artificial alluvium. The relatively high porosity of the Lanton alluvium also played a role in the rates at which strengths were achieved. Slower rates of strength development and lower strengths for samples stabilised with GGBS-NaOH dosages <7.5 % were attributed to fewer soil inter-particle contacts and hence longer time periods required for cementitious gels to grow within pore spaces and strengthen the soil matrix. Higher dosages of the GGBS-NaOH binder within Lanton alluvium resulted in higher concentrations of calcium within the stabilised mixture, thereby resulting in accelerated rates of strength gain through hydration and pozzolanic reactions with subsequent higher strengths achieved with curing. Ultimately, it may be suggested that the relatively high porosity of the Lanton alluvium may have been counteracted by higher GGBS-NaOH dosages (i.e. >7.5 %) in terms of the strengths achieved for each curing period assessed. Despite the similar qualitative effect of delayed strength development, it should be emphasised that the mechanisms by which higher moisture contents, GGBS-NaOH dosages and porosities influence hydration rates within stabilised Lanton alluvium mixtures are notably different from each other.

The application of Gasparre and Coop's (2008) normalisation technique to oedometer data collected for the untreated and stabilised Lanton alluvium proved very useful in quantifying the level of structure within these materials; particularly in understanding the rate at which destructuration occurs post yield stress within the Lanton alluvium. The technique also enabled useful comparisons to be made with other soils, such as London Clay (Gasparre and Coop, 2008) whose initial degrees of structure and collapse behaviour contrast with those observed for natural and GGBS-NaOH stabilised Lanton alluvium.

An assumed extrapolation of the material's compression curve was required to derive the necessary parameters required for Gasparre and Coop's (2008) normalisation. However, the extrapolation may not be fully accurate and therefore presents difficulties in accurately defining the material's true yield point and post-yielding collapse behaviour. Post-yield, any residual strength within stabilised soils is lost more rapidly compared with untreated soils; thereby resulting in more sudden brittle

failures. Overestimating the yield stress and underestimating the rate of collapse are likely to have severe geotechnical design implications; whereby unexpected brittle material failure and consequent damage to surrounding soils, infrastructure and geotechnical structures in the field may occur. Hence, this highlights the need for future high-pressure oedometer testing to understand the complete one dimensional compression behaviour and structure characteristics of 7.5% GGBS-NaOH stabilised Lanton alluvium. However, given the high stiffnesses observed for the material during UCS and oedometer testing, the extrapolation and subsequent normalisation results in Figure 5.22 do not detract from the conclusion that the strength of the material met the 28 day performance criteria defined by EuroSoilStab (2002) and exceeded those exhibited by lime and CEM-I stabilised samples.

Finally, Lanton alluvium had higher CEC and specific surface area values compared with the artificial alluvium; thereby making it theoretically more favourable for soil stabilisation, even though the artificial alluvium had a higher clay content. Therefore, it is essential to determine any mineralogical changes experienced by stabilised samples to quantify the impressive strength enhancements achieved by using the 7.5% dosage of GGBS-NaOH. It would also be prudent to search for any unfavourable minerals which may have formed within the stabilised samples during curing, such as Ettringite which can potentially cause structural problems within calcium-based stabilised soil matrices (Little et al., 2005). The mineralogical characterisation of Lanton alluvium in both its untreated and stabilised states is addressed in the next chapter as part of the final testing phase of this research.

Chapter 6:

Phase 3: Mineralogical and Microstructural Analyses

6.1 Introduction

Using NaOH activated GGBS at a dosage of 7.5% by dry weight has been determined as the optimum binder mixture from all the alternative IBP's and alkali activators tested for stabilising the soft Lanton alluvium. Significant mechanical strength and durability performances have been observed using this binder mixture after 21 days curing. Hitherto, Lanton alluvium's naturally high moisture content of 25% has been attributed to any initial slow developments in mechanical strength, per Locat et al.'s (1990) model. The soil's low-medium CEC and low surface area values are attributable to its low clay and relatively high silt content. Per Wilkinson et al. (2010a), a soil's mineralogy and organic contents potentially adversely effects the progression of metastable cementitious reactions during curing. Testing results from chapter 5 showed that Lanton alluvium had low total organic carbon and total organic contents of 0.42% and 0.76%, respectively and a very low sulphate content of 49 mg per kg (ppm) of soil. Per criteria stated by Nair and Little (2009), soils with soluble sulphate concentrations <3000 ppm are considered at low risk of ettringite formation. Therefore, it is anticipated that such material characteristics will not play a significant role in inhibiting cementitious reactions or causing ettringite formation within GGBS-NaOH stabilised Lanton alluvium.

This chapter presents a series of SEM micrographs, EDX and XRD spectra for untreated Lanton alluvium, the GGBS binder and GGBS-NaOH stabilised Lanton soil after 28 and 56 days curing. The results are anticipated to provide insights into the mineralogical and microstructural changes within Lanton alluvium when stabilised with GGBS-NaOH at a dosage of 7.5%. It is also hoped these findings will provide good visual insights into the identification of cementitious reactions and new minerals formed within the material. Spectra from SEM-EDX and XRD analyses provide useful information in determining Lanton alluvium's clay mineralogy to explain its higher surface area and CEC values compared with the artificial silty sand which was stabilised in chapter 4. Additionally, SEM-EDX spectra are anticipated to play a fundamental role in establishing an understanding of the cementitious (physico-chemical) reactions occurring within the GGBS-NaOH stabilised alluvium after long curing periods, ultimately clarifying the material's improved geotechnical performances presented in the previous chapter.

6.2 Mineralogical X-ray diffractometry analyses

6.2.1 Lanton alluvium

Multiple qualitative XRD scans were conducted on a bulk sample of Lanton alluvium to determine the soil's clay mineralogy by increasing the peak to background ratio as much as possible. Figure 6.1 displays an XRD spectra recorded for the soil after a high resolution scan. Quartz was the most dominant mineral phase present. Per the ICDD database, undissolvable minerals including Orthoclase (K) and Albite (Na) Feldspars were detected within the soil. Dolomite, Chlorite amongst other clay minerals including Illite, Vermiculite and Na-Montmorillonite (i.e. Smectite) were also identified. However, given the nature of the bulk sample, the precise clay mineral phases did not show up particularly well as their low angle peaks were fairly small and hard to resolve.

The bulk scan has provided an indication of the soil's clay mineralogy and that the clay minerals present are characterised by higher surface areas than Kaolinite; thereby explaining the soil's higher surface area compared with the artificial silty sand from chapter 4. Although these findings provided sufficient information for this study, further XRD work on Lanton alluvium would be required to state convincingly which clay minerals were present within the soil. It is recommended that rather than analysing a bulk sample, the <2 μm clay-sized fraction of the soil (in slurry form) be tested. To recover this fraction, sedimentation/disaggregation testing would be required; whereby as much of the soil's <2 μm clay-sized fraction is recovered with a

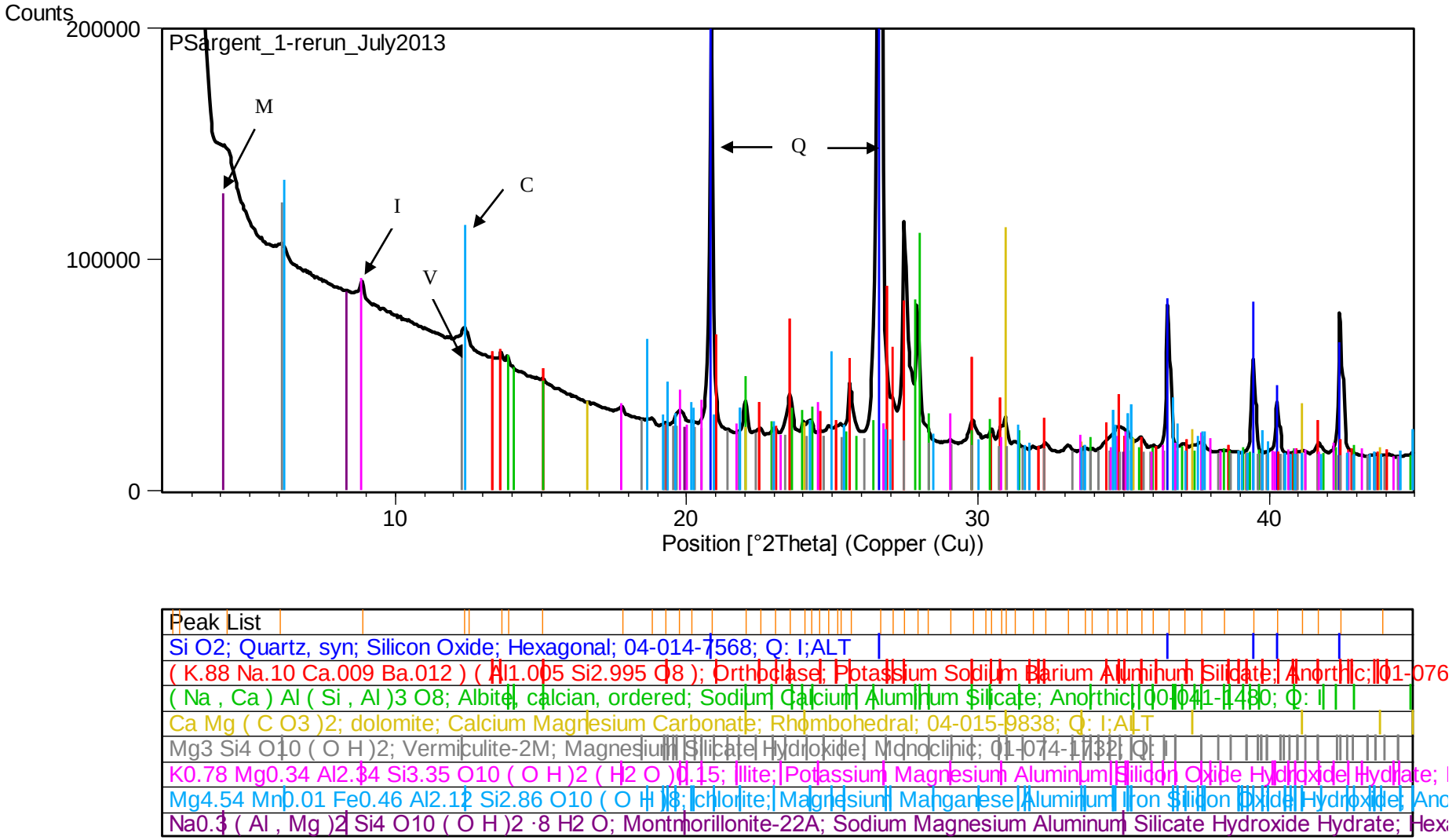

Figure 6.1: XRD scan of Lanton alluvium soil (abbreviations: M = Na-Montmorillonite, I = Illite, V = Vermiculite, C = Chlorite, Q = Quartz).

syringe. Subsequently, samples would need to be centrifuged to ensure that the <2 μm fraction settles out. Once complete and when most of the supernatant has been decanted off, the remaining slurry would then be used to make an oriented mount, which would be ideal for observing low clay peaks at higher resolutions without interference on the XRD scan from other larger minerals (e.g. quartz and carbonates).

6.2.2 7.5% GGBS-NaOH stabilised Lanton alluvium

Several qualitative XRD scans were also conducted on bulk samples of GGBS-NaOH stabilised Lanton alluvium after both 28 and 56 days curing, in an attempt to identify any mineralogical changes occurring within the soil with curing; and ultimately explain the strength gains observed within the material. Figures 6.2 and 6.3 present high resolution XRD spectra for the stabilised soil after 28 days and 56 days curing, respectively.

Based on the magnitude of the peaks observed within both samples, quartz was the dominant mineral phase present due to the relatively high silt and sand contents of natural Lanton alluvium. When comparing the XRD spectra for the two stabilised samples with that presented in Figure 6.1 for natural Lanton soil, there are numerous similarities in composition. Both the 28 and 56 day cured stabilised samples contained traces of Illite, Vermiculite, Orthoclase and Albite feldspar minerals. Montmorillonite, Chlorite or Dolomite minerals could not be traced with confidence within either of the stabilised samples. Given the similar peak positions for Illite and Dolomite on XRD spectra, it is possible that the X'Pert PANalytical High Score Plus analytical programme had difficulty in distinguishing between the two minerals. However, it is also likely that the Dolomite and Chlorite have been utilised and digested to form new cementitious gels during cementation reactions, given Dolomite's calcium and Chlorite's aluminium and silica contents.

Although the presence of the alumina-silicate clay minerals was still clear within both the 28 and 56 day cured samples, the intensity of their peaks was lower than those observed within untreated Lanton alluvium. This suggests that such clay minerals had not undergone total dissolution into forming new cementitious gel phases (Cristelo et al., 2011). In contrast to findings by Hughes and Glendinning (2004), Wilkinson et al.

(2010a) suggest it is possible to use XRD to identify new cementitious mineral phases within stabilised soil samples, albeit their hydrated amorphous nature presents difficulties in identification.

However, based on the XRD spectra in Figures 6.2 and 6.3 for the 28 and 56 day cured stabilised samples respectively, no traces of any new cementitious minerals were detected. One possible explanation behind Wilkinson et al. (2010a) identifying C-S-H and C_4AH_{13} minerals in XRD spectra is associated with the freeze-drying technique used to prepare samples for analysis. Freeze-drying essentially removed any excess moisture, preserved neoformed cement mineral phases for their identification and also reduced the influence of quartz within the samples (Wilkinson et al., 2010a). Future XRD analyses on GGBS-NaOH stabilised Lanton soil could therefore consider using Wilkinson et al.'s (2010a) freeze-drying sample preparation technique.

The mineralogical results presented below strongly suggest that using XRD alone is unwise when trying to accurately determine the presence and composition of cementitious minerals/gels within stabilised soils. This highlights the need to use both XRD and SEM-EDX techniques in mineralogical analyses of cemented soils/geopolymers, as SEM-EDX has fewer difficulties in determining the chemical composition of cementitious mineral phases.

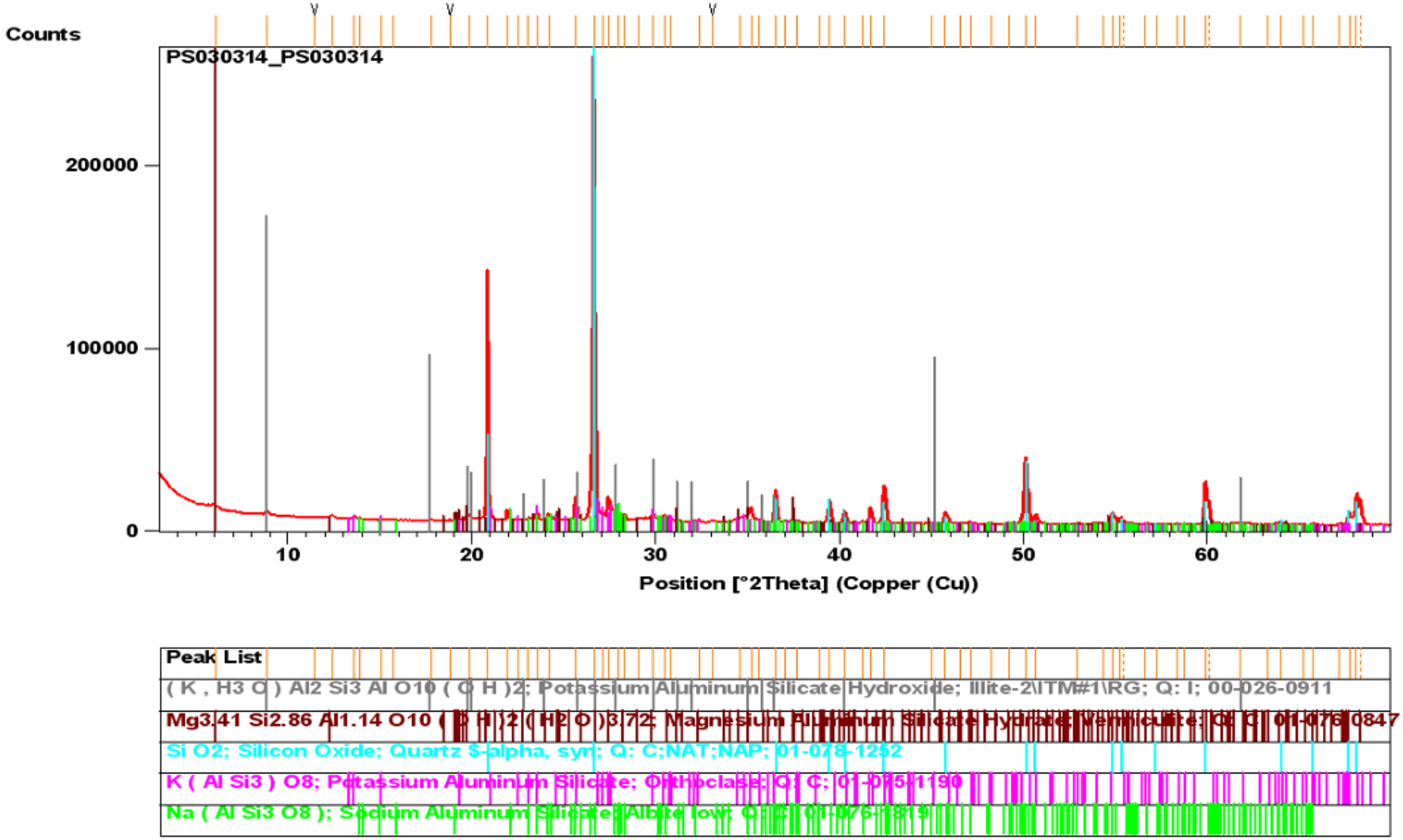

Figure 6.2: XRD spectra for GGBS-NaOH stabilised Lanton alluvium after 28 days.

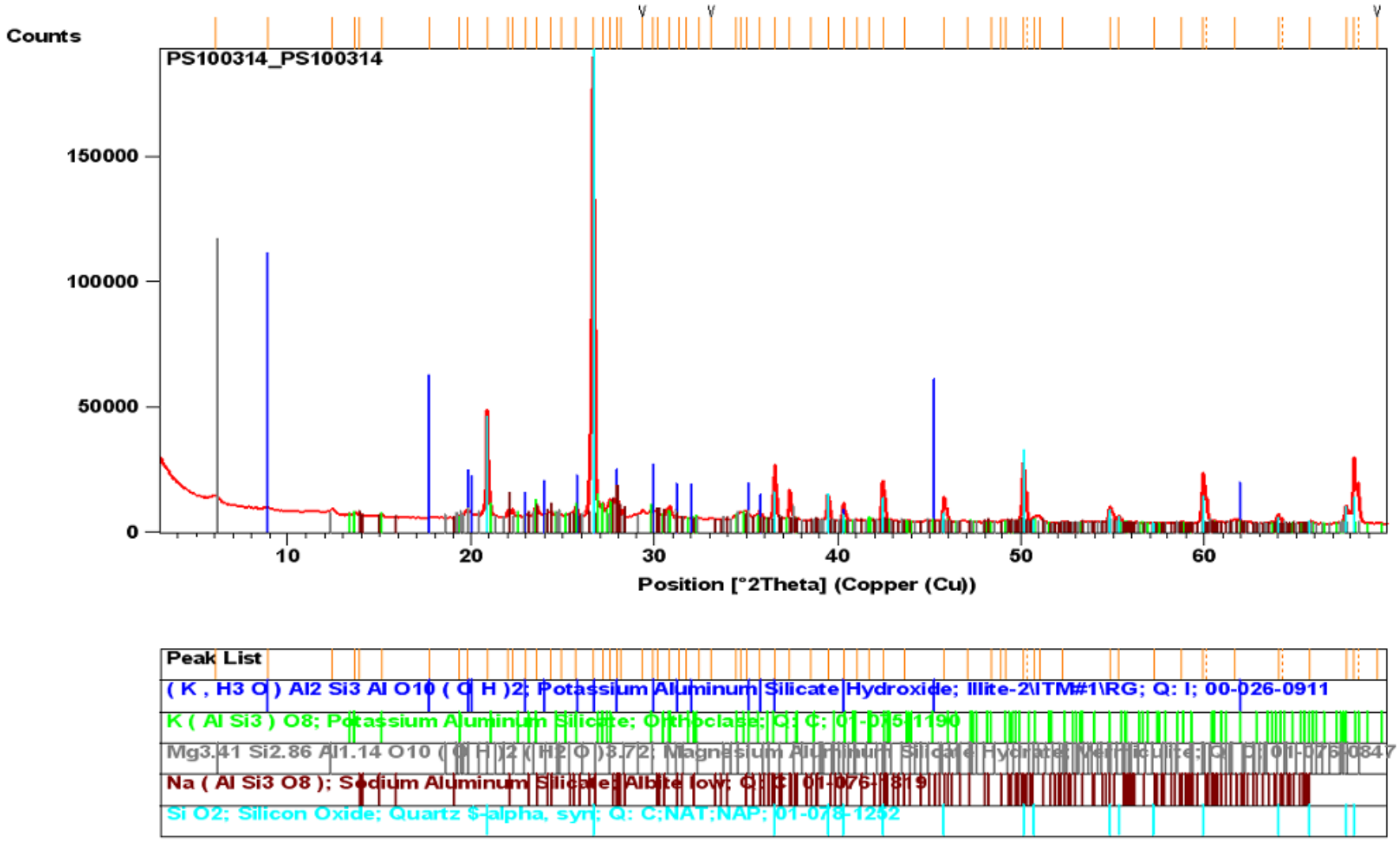

Figure 6.3: XRD spectra for GGBS-NaOH stabilised Lanton alluvium after 56 days.

6.3 Mineralogical and microstructural scanning electron microscopy analyses

6.3.1 Lanton alluvium

As defined in chapter 5, Lanton alluvium's geotechnical characterisation is a silty SAND with <10% clays (BS 5930, BSI 1999) with a low sulphate, TOM and TOC contents. XRD analyses suggest that the soil's relatively high surface area and CEC values (with respect to sandy alluvial soils in general) are attributed to its Illite content. The SEM micrographs in Figures 6.4 and 6.5 show the dominant presence of dark grey-coloured coarse grained (sub-angular) sand and silt (quartz) particles, the majority of which form either inter-particle edge-to-edge or edge-to-face contacts. Overall, the sand and silt particles within the soil fail to show any evidence of a predominant orientation.

Observations from Figure 6.4 show that the smaller lightly coloured Illite clay platelets are widely distributed throughout the soil and tend to occupy pore spaces between grains of silt and sand. Additionally, it can be seen that smaller Illite grains/platelets (i.e. <10 μm) can be found partially coating the surfaces of some larger sand and silt particles (area encircled on Figure 6.5). Given the loose powdered state of the soil when being analysed within the ESEM chamber, Illite minerals were occasionally observed to migrate across the field of view, making it difficult to capture high definition images of the morphology of Illite platelets. However, towards the top (centre) of the micrograph in Figure 6.5, an Illite platelet and its morphology are clearly seen.

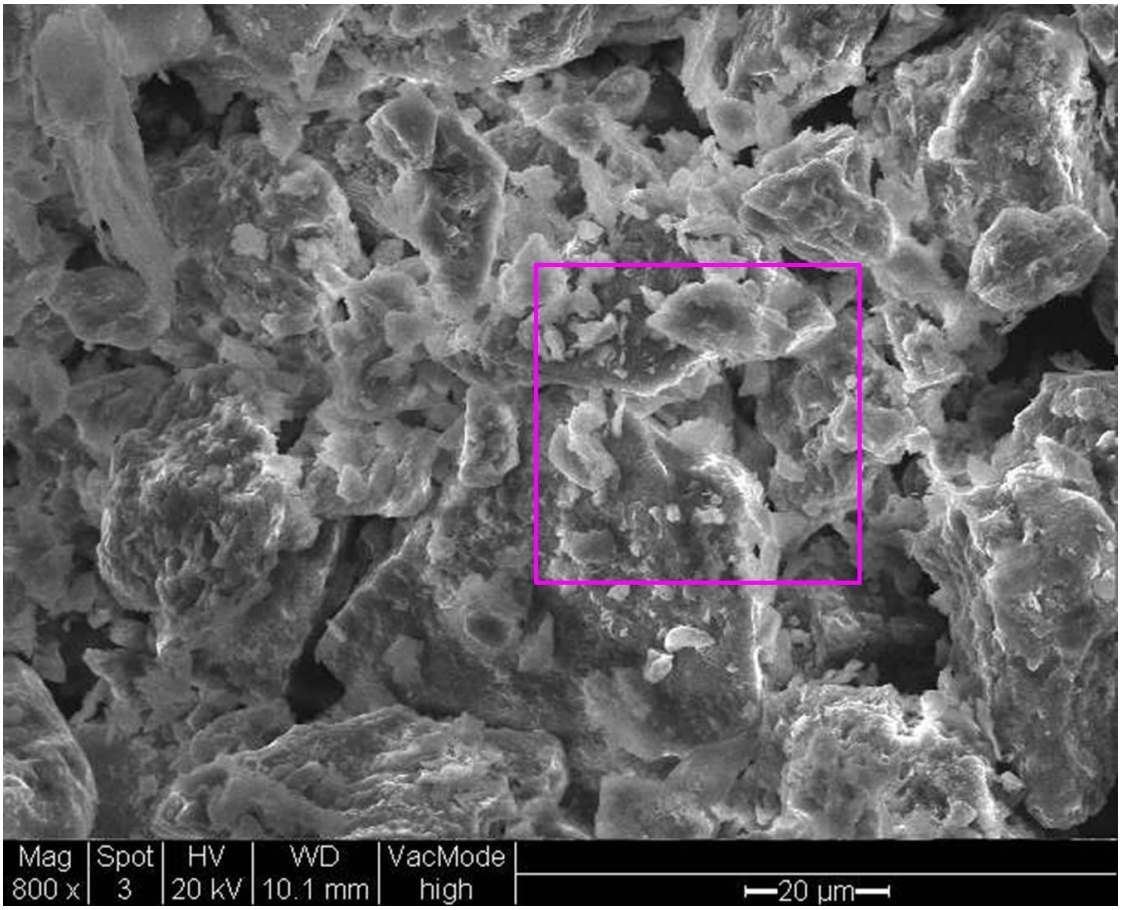

Figure 6.4: SEM micrograph of Lanton alluvium soil at x800 magnification. Area of focus (pink) is shown at a higher magnification in Figure 6.5.

Regarding the surfaces and edges of the sand, silt and clay particle, all appear to be relatively clean and well defined. This implies they are free of any evidence of physical bonding. This observation will prove useful when comparing the particle morphology and overall sample microstructure of cemented specimens presented later in this chapter.

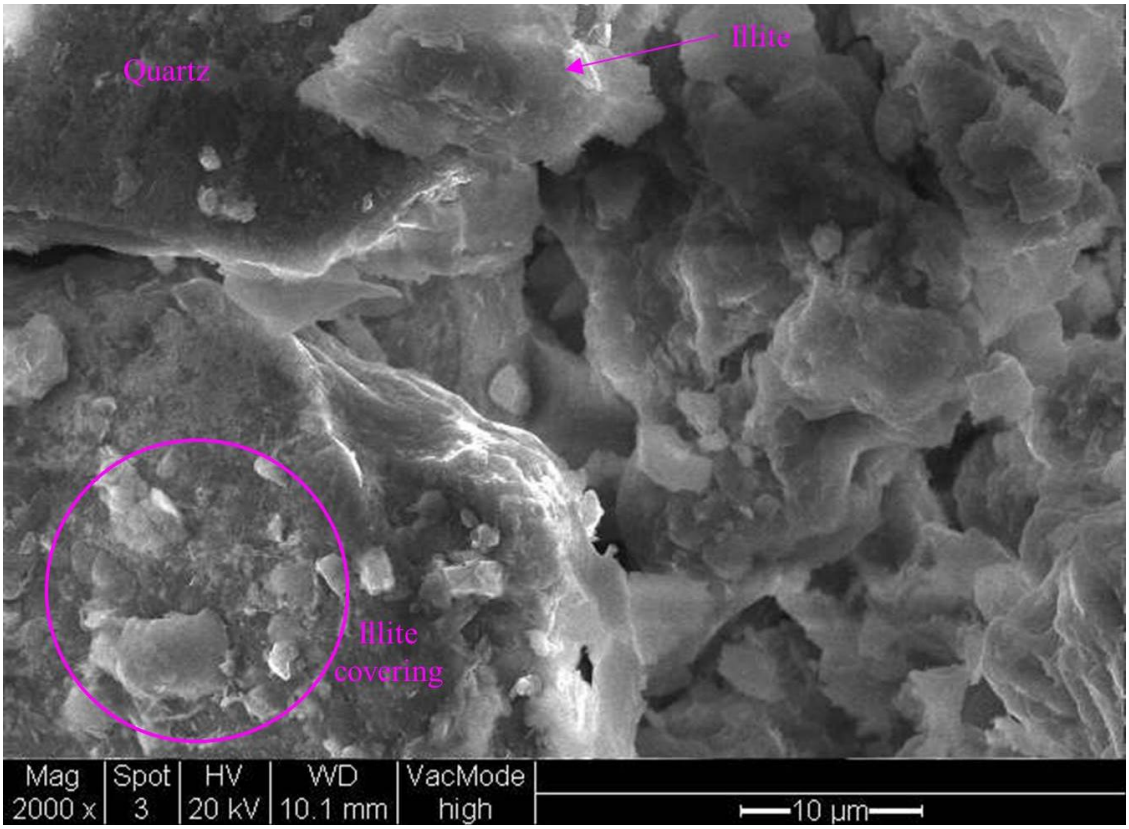

Figure 6.5: SEM micrograph of particle boundaries and Illite morphology within Lanton alluvium soil at x2000 magnification.

Once Lanton alluvium's microstructure had been examined, an EDX elemental analysis was conducted on the entire soil sample to make a comparison with the XRD data in Figure 6.1. The EDX spectra produced for Lanton alluvium is presented in Figure 6.6. It is clear that the dominant elemental peaks were for silica (approx. 1.75 keV) and oxygen (approx. 0.5 keV), which corresponds to the soil's high quartz (i.e. silt and sand) content. The relatively high potassium peak at approximately 3.25 keV would explain the soil's Orthoclase feldspar and Illite contents, as would the high aluminium peak at approximately 1.45 keV. The low magnesium trace in Figure 6.6 at 1.25 keV may explain the identification of Vermiculite and Illite, whereas the calcium peak may be attributed to the presence of Albite feldspar. At approximately 6.35 keV, there is a peak for iron, which is of a similar magnitude to those for calcium and magnesium. The most plausible explanation behind the presence of this peak is the presence of Chlorite within the soil, albeit in very low quantities. The quantitative elemental composition of the soil is per Table 6.1.

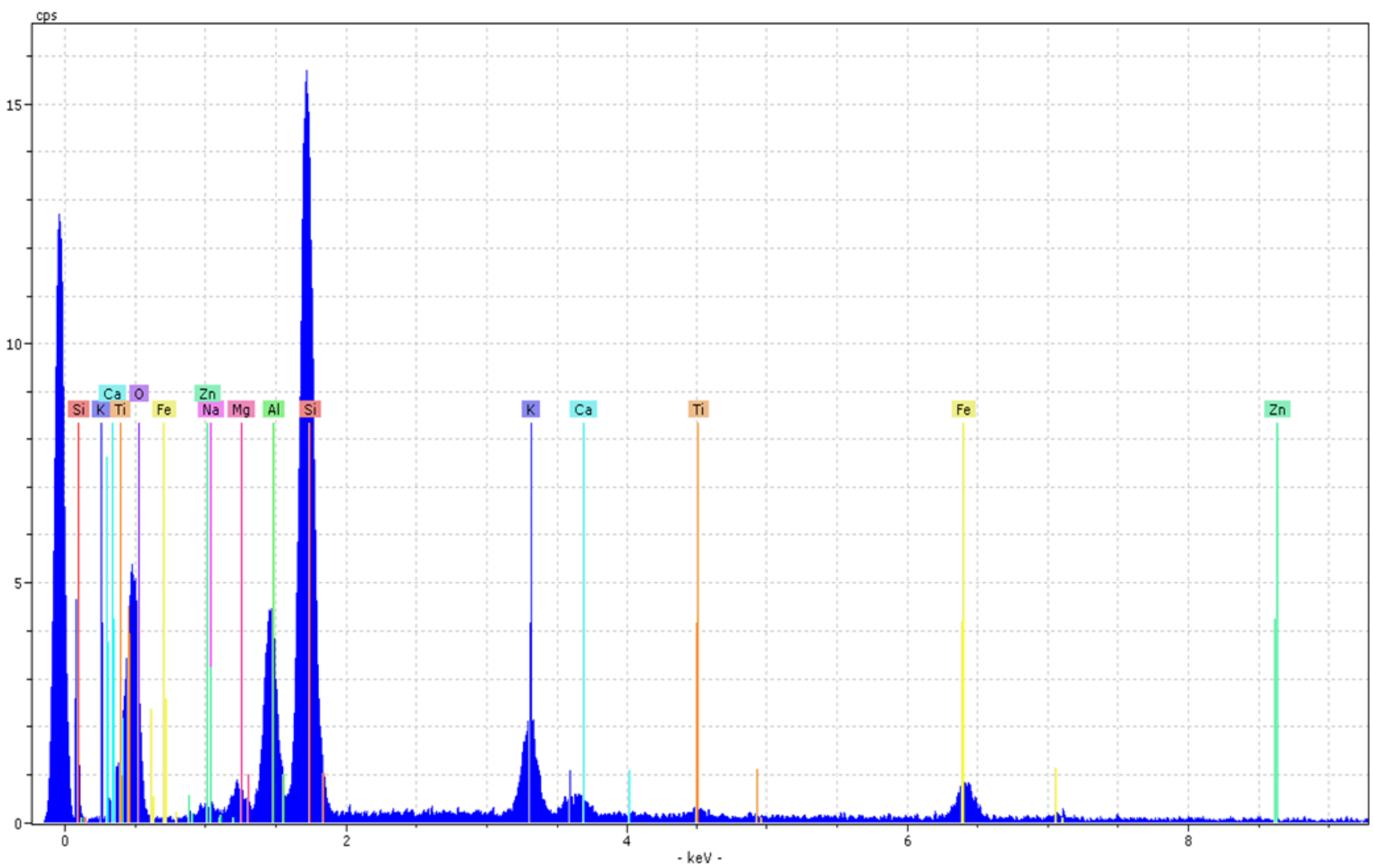

Figure 6.6: EDX spectra for Lanton alluvium, with elemental data superimposed.

Table 6.1: Quantitative elemental composition of Lanton alluvium from EDX spectra analysis.

Element	Series	Net	Unn. C (wt.%)	Norm. C (wt.%)	Atom. C (at.%)
Si	K	17436	24.27	31.41	24.41
Al	K	4651	6.48	8.39	6.78
K	K	2888	4.60	5.95	3.32
Ca	K	424	0.71	0.92	0.50
Na	K	1	0.00	0.00	0.00
Fe	K	1314	4.15	5.38	2.10
Ti	K	282	0.58	0.75	0.34
Zn	K	186	1.07	1.39	0.46
O	K	2245	34.71	44.91	61.26
Mg	K	418	0.70	0.91	0.82
		Total:	77.30%		

6.3.2 Ground granulated blast furnace slag

In contrast to PFA particles (characterised by highly spherical morphologies), the morphology of the glassy GGBS particles in Figure 6.7 is generally highly angular and irregular in shape and size. Although not as clear for smaller particles (<10 μm), there is a significantly larger GGBS particle at the centre of the image exhibiting a well-defined edge (arrowed) and angled surfaces. Per Wan et al. (2004), GGBS powders containing such a variety of particle shapes and particle morphologies characterised by edges and angled surfaces tend to be produced when slags are processed within a ball mill.

An EDX elemental analysis was conducted on the GGBS powder to gain an insight into how the chemical composition of Lanton alluvium would change after mixing in the GGBS binder. Establishing a knowledge regarding the elemental composition of both the soil and GGBS proved very useful in determining which types of cementitious minerals are likely to have formed during the curing process. The EDX spectra and quantitative elemental composition for the GGBS are shown in Figure 6.8 and Table 6.2, respectively.

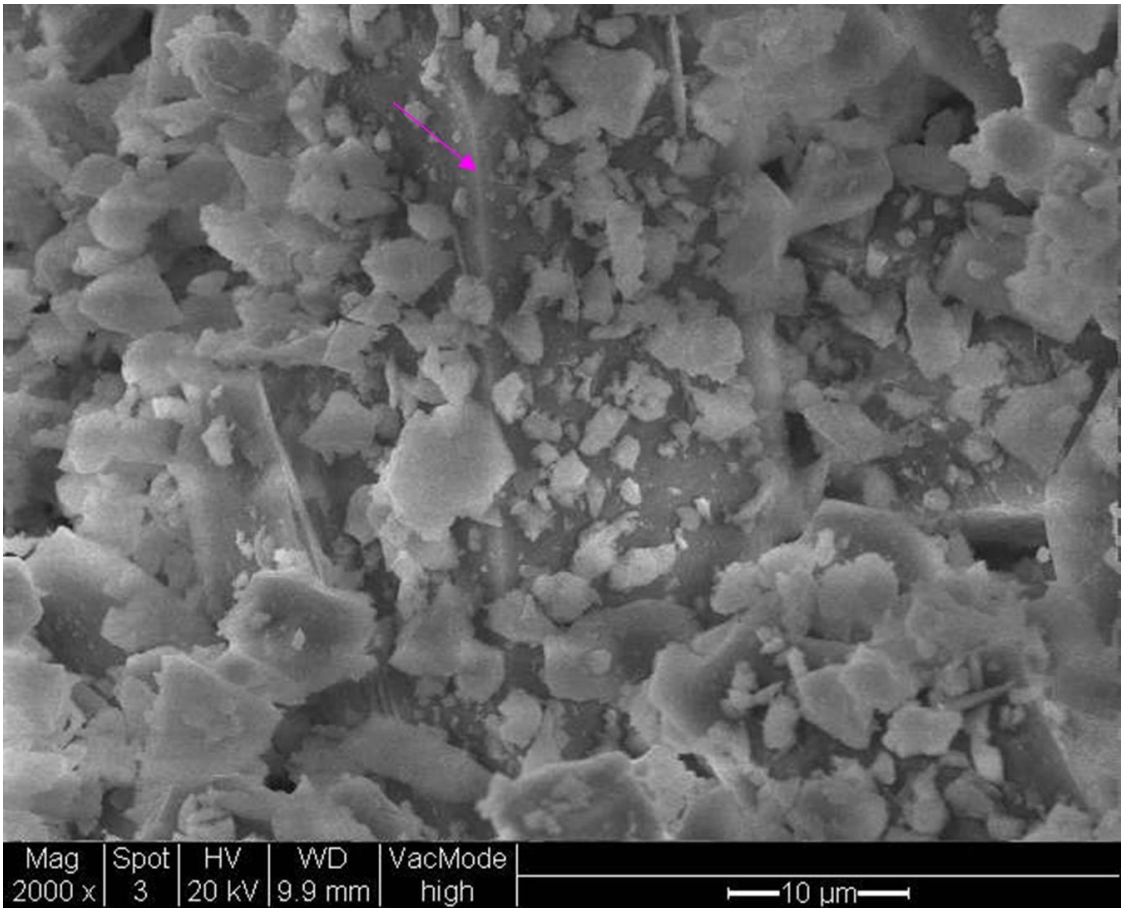

Figure 6.7: SEM micrograph of the raw GGBS binder at x2000 magnification.

Table 6.2: Quantitative elemental composition of GGBS from EDX spectra analysis.

Element	Series	Net	Unn. C (wt.%)	Norm. C (wt.%)	Atom. C (at.%)
O	K	1220	25.25	32.30	50.33
Si	K	10695	12.96	16.53	14.72
Al	K	3582	4.70	5.99	5.55
K	K	703	0.86	1.09	0.70
Fe	K	183	0.54	0.68	0.31
Zn	K	210	1.19	1.52	058
Ca	K	20456	28.81	36.73	22.92
Mg	K	1895	2.92	3.72	3.83
Na	K	1	0.00	0.00	0.00
Ti	K	213	0.43	0.55	0.29
S	K	593	0.78	0.99	0.77
		Total:	78.4%		

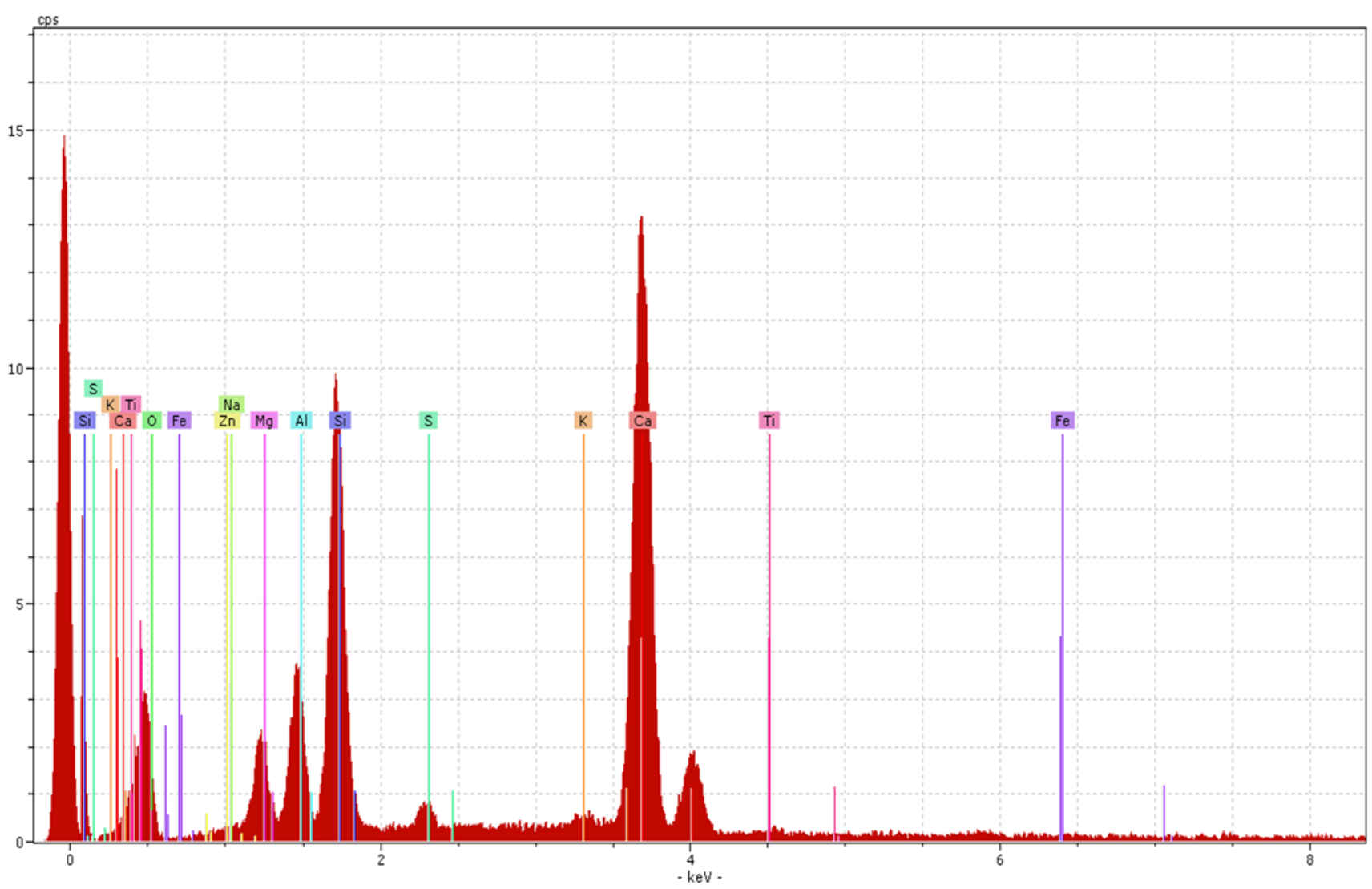

Figure 6.8: EDX spectra for raw GGBS, with elemental data superimposed.

The composition of blast furnace slags does vary slightly between all iron manufacturing plants (Shi et al., 2006). However, Figure 6.8 and Table 6.2 demonstrate that the composition of the GGBS powder used in this study generally resembles that of most GGBS powders, as it contains high quantities of silica, calcium and aluminium with lower quantities of magnesium (Scott et al., 1986). Hence, the GGBS would provide the necessary calcium and additional aluminium and silica to produce AFm and C-S-H-based cementitious mineral phases within stabilised Lanton alluvium. However, based on the results obtained from compressive strength and oedometer testing in chapter 5 and findings from Haha et al. (2011), the alkali activation of GGBS using NaOH would be necessary to observe the formation and development of any cementitious mineral phases and subsequent strength gains.

6.3.3 GGBS-NaOH stabilised Lanton alluvium

Based on these mineralogical and microstructural results and findings within the academic literature involving using alkali activated (NaOH) GGBS in geopolymer mixes (Hughes et al., 2010; Wilkinson et al., 2010a; Haha et al., 2011, Myers et al., 2013), examples of hydrated cementitious mineral phases potentially forming within stabilised Lanton soil include C_3S/C_2S (Manning, 1995), sodium rich C-S-H and C-A-H, C-N-A-S-H and C-H. The possibility of other less favourable Aft minerals forming (e.g. ettringite) isnot considered likely, as the growth of such minerals require soils characterised by both high moisture and sulphate contents (Nair and Little, 2009b) and Lanton alluvium has high moisture but low sulphate contents. Per a recent study on the hydration kinetics, assemblages and microstructural development of NaOH activated GGBS by Haha et al. (2011); ettringite may not form within GGBS-NaOH stabilised Lanton alluvium. Nonetheless, a thorough microstructural and mineralogical analysis of stabilised Lanton alluvium after 28 and 56 days curing now follows.

For both the 28 and 56 day cured samples, it is anticipated that the microstructure will exhibit evidence of cementitious mineral/gel growths both coating surfaces of soil and GGBS particles and bonding them together. Numerous SEM micrographs were taken of the stabilised soil at a minimum magnification of x2000 to gain detailed visualisations of microstructural features within the material, possibly attributable to

the high strength gains achieved during curing. Once the material's microstructure had been sufficiently classified, point elemental EDX measurements were taken to help identify which cementitious mineral phases had formed within the stabilised soil.

6.3.3.1 28 days curing

6.3.3.1.1 Sample microstructure

Upon inspecting 28 day cured stabilised Lanton alluvium, the material's higher level of complexity compared with the soil in its untreated state immediately became apparent per Figure6.9. Pore space aperture between particles was either very narrow or negligible, due to the dense packing of the GGBS and soil particles, the infilling of pore spaces either by clay minerals or new growths, or a combination of the two factors. Soil and GGBS particles also showed a variety of face-to-face, edge-to-edge and edge-to-face inter particle contacts. These factors combined indicate that the material had a much denser microstructure and therefore lower permeability compared with Lanton alluvium in its untreated state.

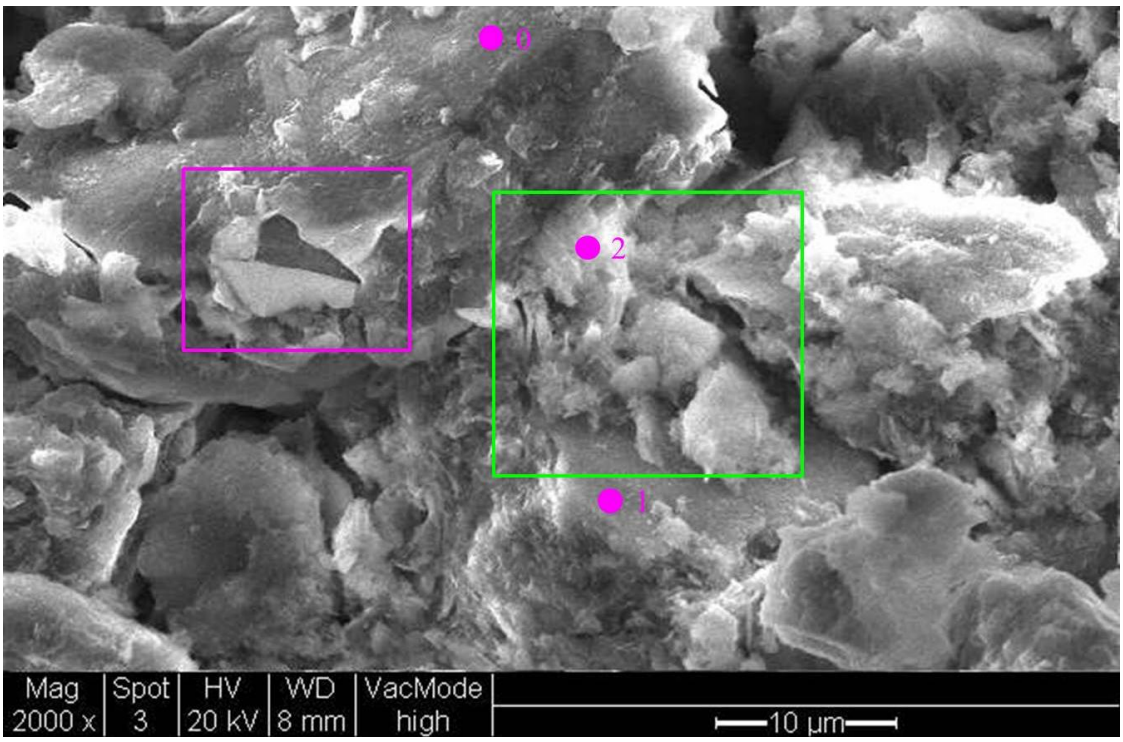

Figure 6.9: SEM micrograph of the 28 day cured Lanton alluvium at x2000 magnification. Areas of interest and points taken for EDX analysis are labelled.

Unlike when the untreated soil was analysed in the ESEM and Illite clay platelets were occasionally observed to migrate across the field of view, no such observations were made within the 28 day cured sample, indicating higher levels of material density (packing), cementation and therefore sample strength. Features of key interest within the stabilised material were the light grey/white coloured amorphous growths, which were seen to stem mainly from GGBS particle surfaces and growing towards neighbouring GGBS or silt/sand soil particles. An example of such a growth is evident at the centre of the micrograph in Figure 6.9 (labelled 2) and appears to have stemmed from the large (GGBS) particle (labelled 0) and grown to infill pore space and bond with the neighbouring particle (labelled 3). However, these growths appear to be clustered in one area rather than distributed evenly around the particles, as seen within the green square on Figure 6.9 and in more detail in Figure 6.10.

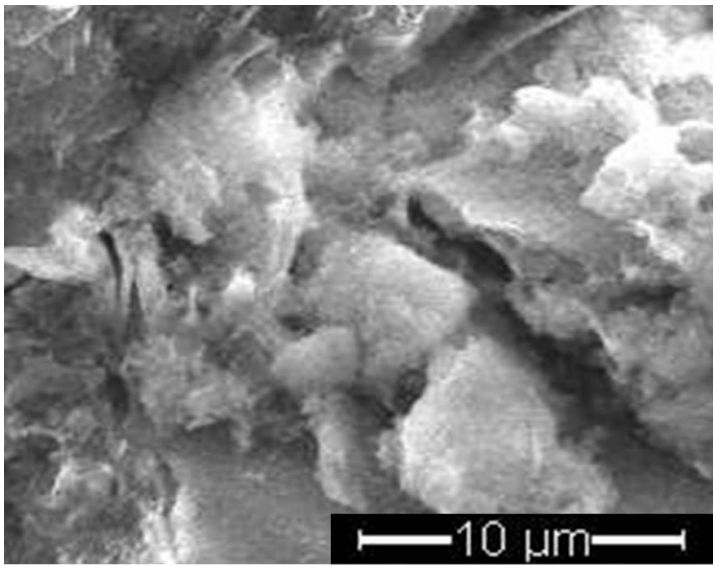

Figure 6.10: Magnified view of green area in Figure 6.9, showing cluster of cementitious growths.

According to Haha et al. (2011), when GGBS particles are activated with an alkali such as NaOH, this process creates a series of layered C-S-H-related coatings around the GGBS particle. Darker inner zones are formed during the later hydration stages; whereas a lighter outer zone forms during the first few days of hydration. Evidence can be found within the pink square on Figure 6.9 and in Figure 6.11, whereby a small segment of the outer early hydration material has peeled away (pink arrow), exposing a darker surface of more recent hydration products (green arrow).

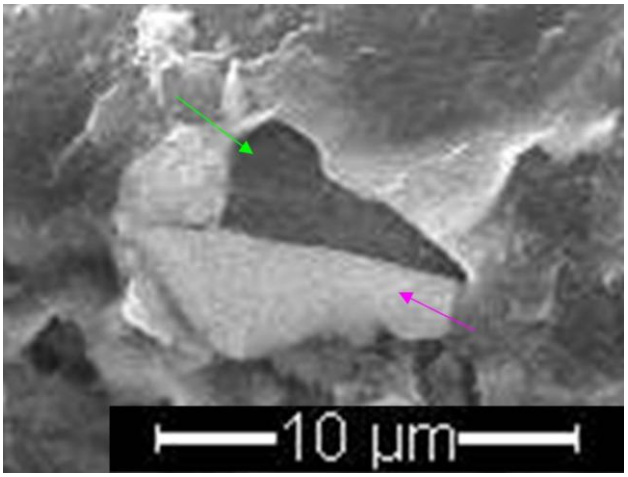

Figure 6.11: Magnified view of pink area in Figure 6.9, showing exposed surface of recent hydration.

At another location within this sample, another SEM micrograph was taken of similar light grey/white coloured cluster of amorphous growths at the base of a larger silt-sand sized (GGBS or soil) particle (green area in Figure 6.12). Scattered across the GGBS or soil particle's surface are several either small clay platelets or cementitious growths in their early stages of development.

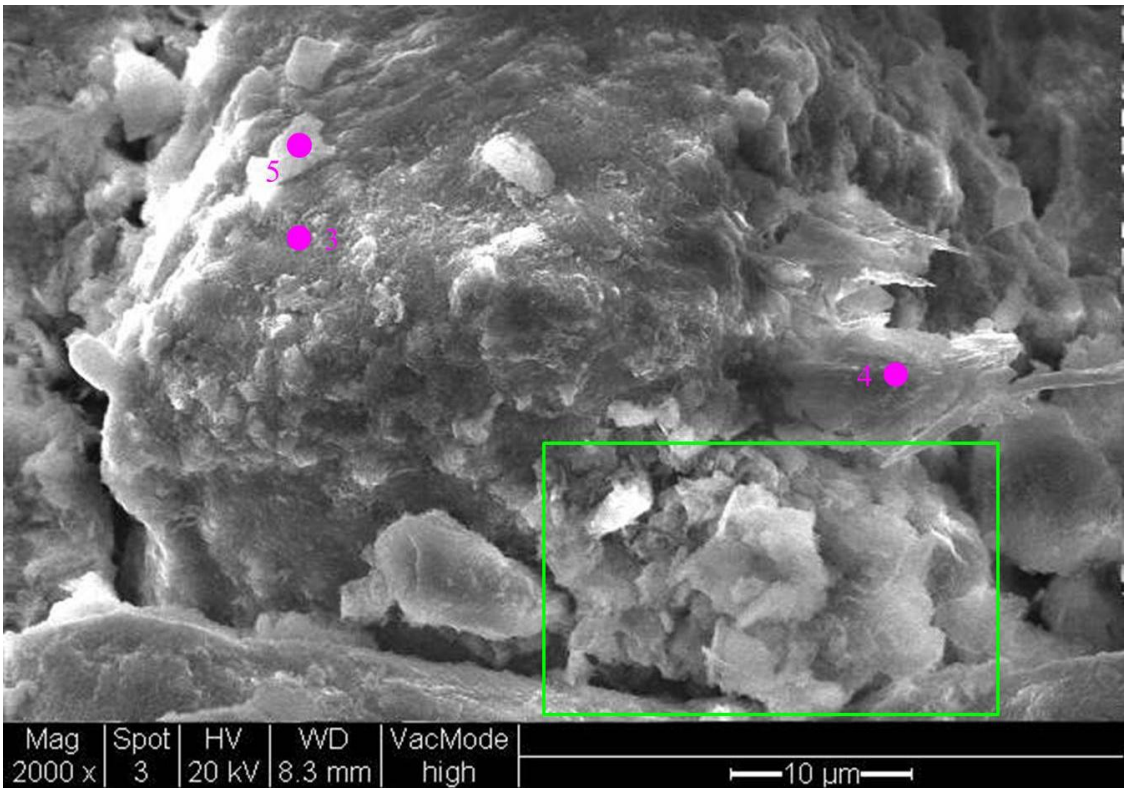

Figure 6.12: SEM micrograph of a large GGBS particle within 28 day cured Lanton alluvium at x2000 magnification, showing cementitious coating and growths between neighbouring particles. Points taken for EDX analysis are labelled.

As more clearly seen in Figure 6.13, this amorphous material (arrowed in green) appears to be combining and reacting with small clay platelets (arrowed in pink) in filling the void space between several neighbouring large particles and ultimately cementing the soil matrix together.

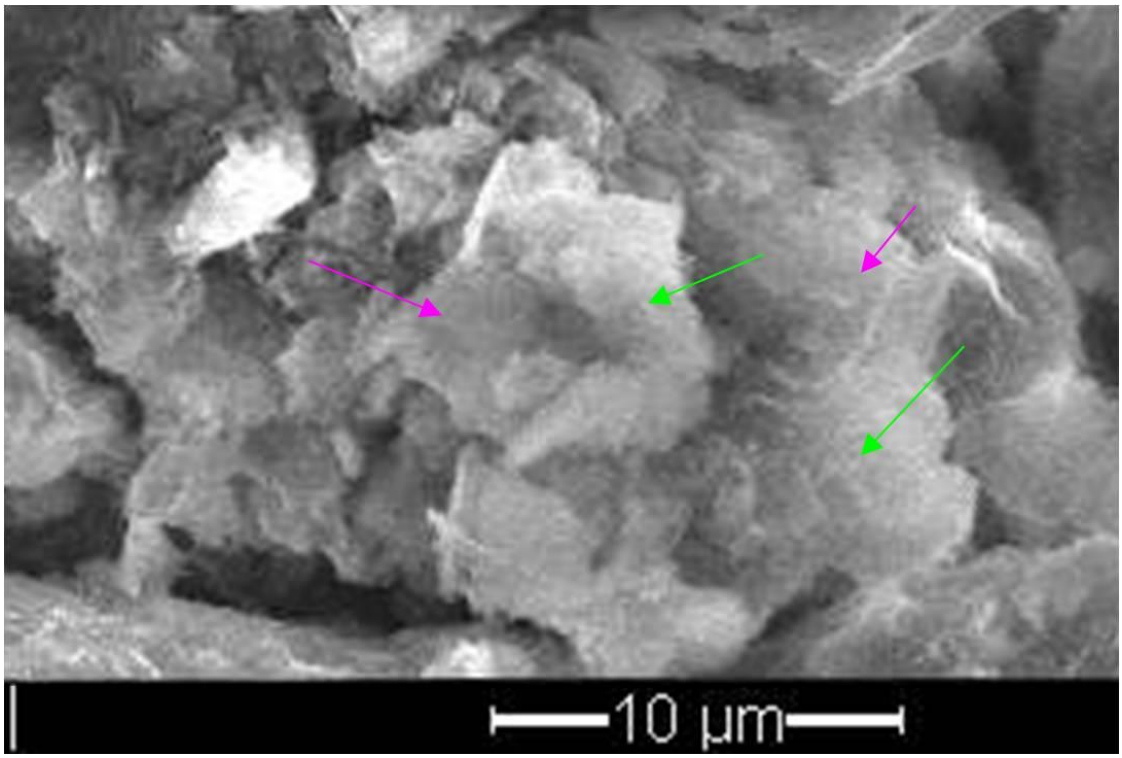

Figure 6.13: Magnified view of green area in Figure 6.12, showing the reaction between clay platelets and the amorphous cementitious gel in infilling pore spaces.

6.3.3.1.2 Sample mineralogy

Post-microstructural analysis, the chemical composition of the overall stabilised material was analysed quantitatively using EDX spectra. This enabled comparisons with the XRD spectra obtained for the material in order to start determining the nature of mineralogical changes within the soil through GGBS-NaOH stabilisation. The quantitative elemental composition for the material is shown in Table 6.3 and the corresponding EDX spectrum is presented in Figure 6.14.

Table 6.3: Quantitative elemental composition of stabilised Lanton alluvium after 28 days curing from EDX spectra analysis.

Element	Series	Net	Unn. C (wt.%)	Norm. C (wt.%)	Atom. C (at.%)
O	K	3998	46.89	63.78	77.37
Si	K	13614	14.91	20.28	14.02
Al	K	3577	4.16	5.66	4.07
K	K	1791	2.21	3.01	1.49
Fe	K	758	2.18	2.96	1.03
Zn	K	178	1.06	1.44	0.43
Ca	K	1024	1.32	1.80	0.87
Mg	K	367	0.53	0.72	0.58
Ti	K	156	0.25	0.34	0.14
Na	K	1	0.00	0.00	0.00
		Total:	73.50%		

For comparison purposes, the EDX spectra for untreated Lanton alluvium is also superimposed on Figure 6.14 in order to observe any discernible differences between the two materials. The chemical composition of the two materials is relatively similar, with significant peaks observed for silica, aluminium, potassium, iron and oxygen. However, there are a few notable differences, probably attributable to adding GGBS-NaOH and subsequent reactions. The three main differences are the larger peaks for sodium/zinc, calcium and sulphur within the 28 day stabilised material. The higher calcium and sulphur peaks are caused by adding GGBS, which per Figure 6.8 has a high concentration of calcium. Additionally, the production of hydrated cementitious gels were calcium based, which would also contribute towards the higher calcium peak.

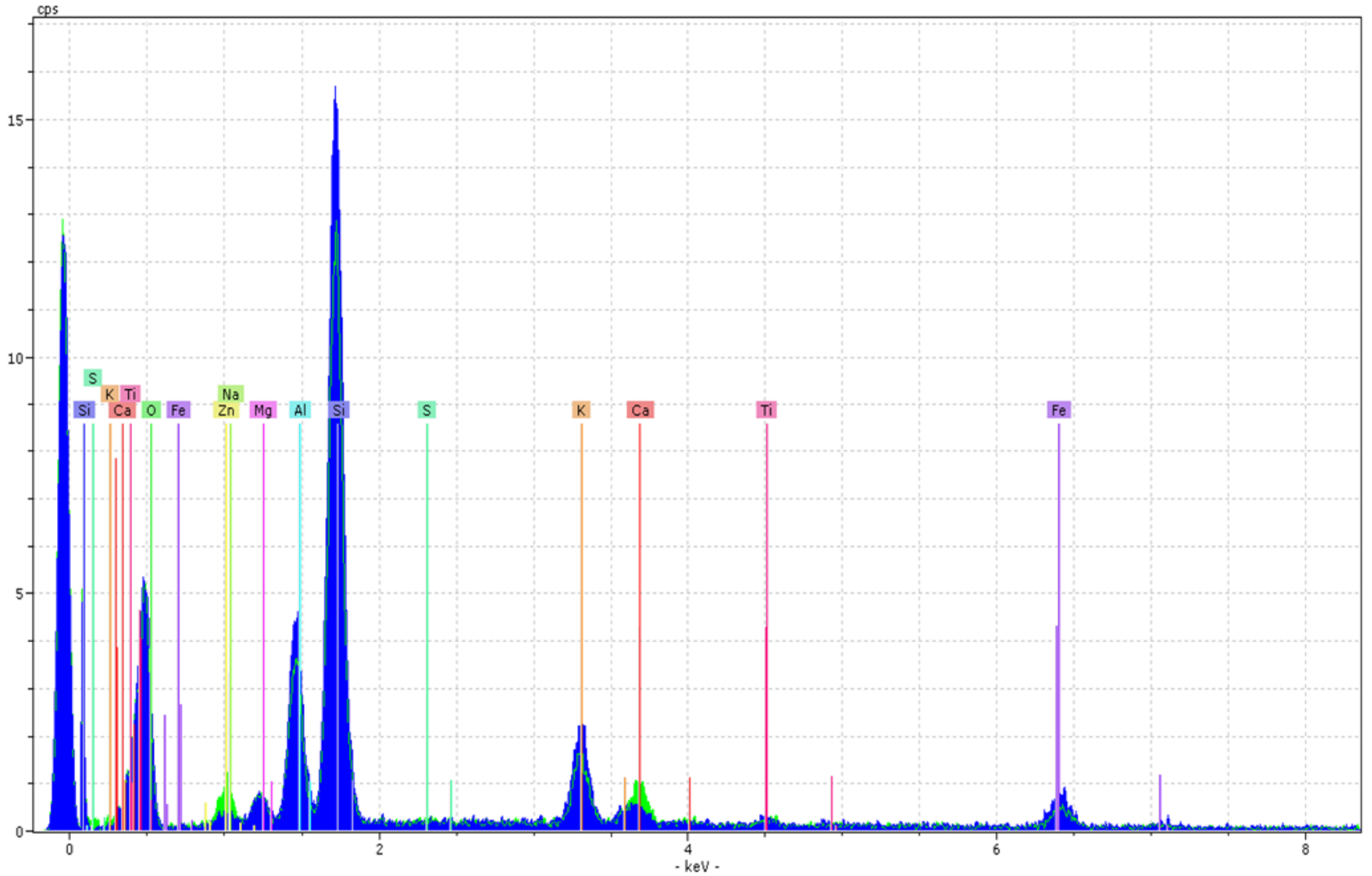

Figure 6.14: EDX spectra for Lanton alluvium in its natural state (blue) and when stabilised with 7.5% GGBS-NaOH after 28 days curing (green), with elemental data superimposed.

Regarding the higher sodium/zinc peak at approximately 1 keV, the EDX software used to determine which elements were present within the sample appears to have experienced difficulties in determining whether this peak was due to the presence of sodium or zinc. According to Barker and Fournelle (1996), there is an inherent problem in EDX/EDS analysis whereby the separation between some elemental peaks is very poor and can therefore cause a degree of overlap. Such a problem is commonly observed for sodium and zinc, whereby their characteristic X-ray keV values are 1.041 and 1.012, respectively. Given the absence of zinc within any minerals identified from all of the XRD analyses conducted on Lanton alluvium in both its untreated and treated states, the fact that sodium is known to be present within the stabilised material due to adding NaOH activator; instances where a sodium/zinc peak is observed within EDX spectra is very likely to be sodium. However, the EDX software may have determined very small traces for zinc in all samples due to zinc being used to produce the SEM micrographs.

6.3.3.1.3 EDX point element analyses

The EDX spectra obtained for the overall 28 day stabilised material in Figure 6.14 cannot provide accurate information on the chemical composition of the cementitious material clearly observed within the material. To gain better insights into the nature of the amorphous cementitious gels/minerals, a series of EDX point elemental analyses is essential. Numerous points for analysis were selected within the field of views within Figures 6.9 and 6.12 to determine the chemical nature of the cementitious gels. Points on neighbouring coarser grained particles were also selected for elemental analyses to confirm whether the cementitious gels originally stem from activated GGBS particle surfaces and grow towards other neighbouring GGBS and soil (quartz and Illite) particles.

The EDX spectra and quantitative analyses of the three points labelled in both Figure 6.9 and 6.12 are hereby presented. For comparisons to be made between the chemical data obtained for each of the points analysed, the EDX spectra for points 0-2 are superimposed on top of each other in Figure 6.18 and points 3-5 are superimposed in Figure 6.22.

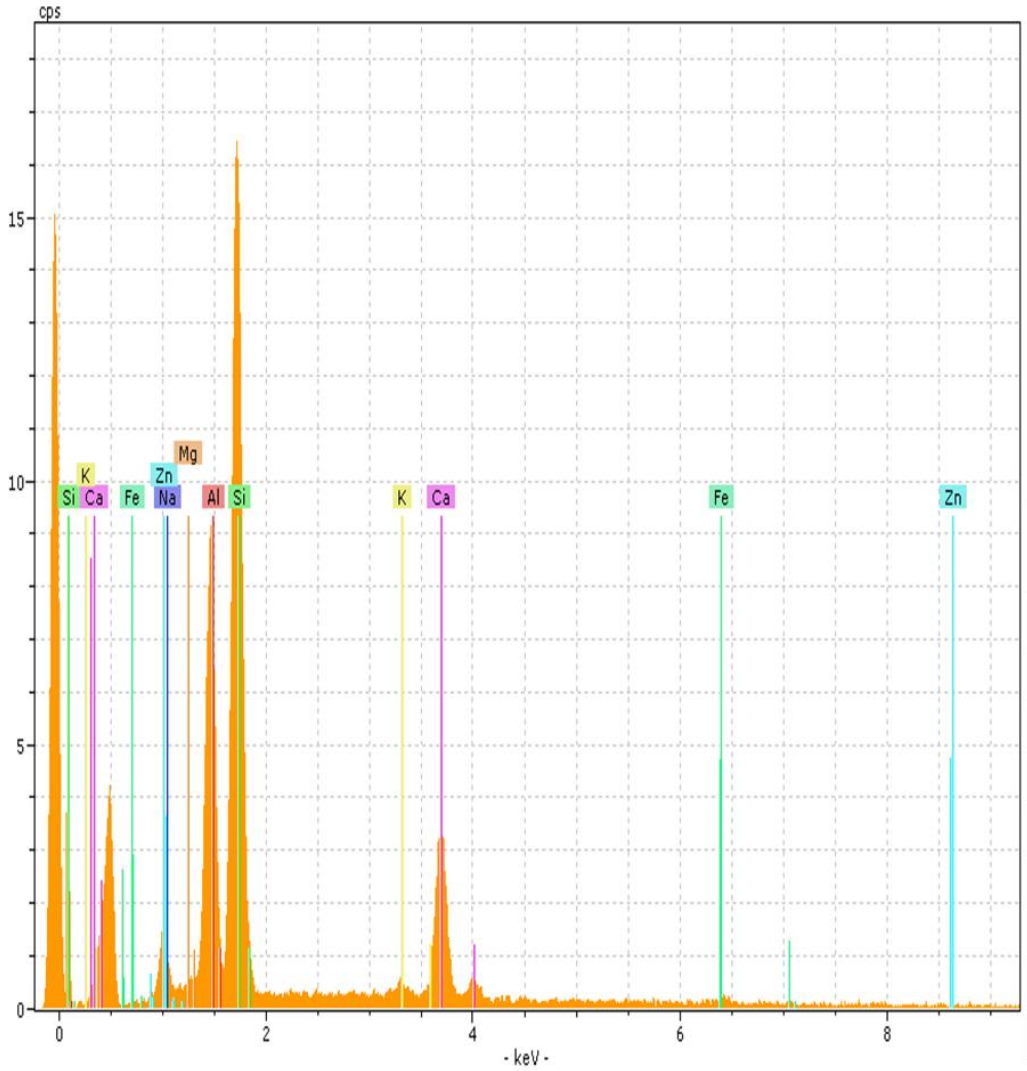

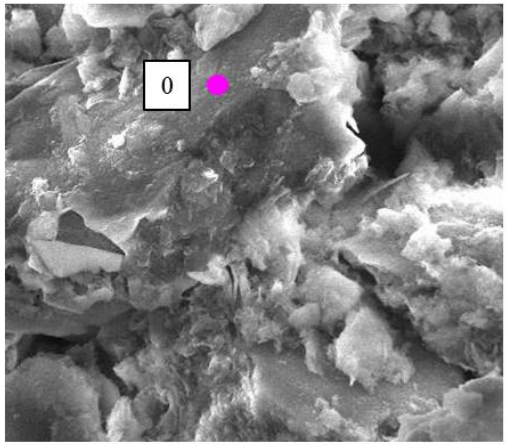

Element	Series	Net	Unn. C (wt.%)	Norm. C (wt.%)	Atom. C (at.%)
Al	K	9775	13.31	21.70	24.30
Si	K	19101	33.76	55.06	59.22
Na	K	1	0.00	0.00	0.00
Zn	K	181	1.47	2.40	1.11
Ca	K	4884	9.74	15.89	11.98
K	K	723	1.36	2.27	1.75
Mg	K	113	0.17	0.28	0.34
Fe	K	369	1.47	2.39	1.29
		Total:	61.3 %		

Figure 6.15: Point elemental spectra analysis of Point 0 within 28 day cured 7.5% GGBS-NaOH treated Lanton alluvium.

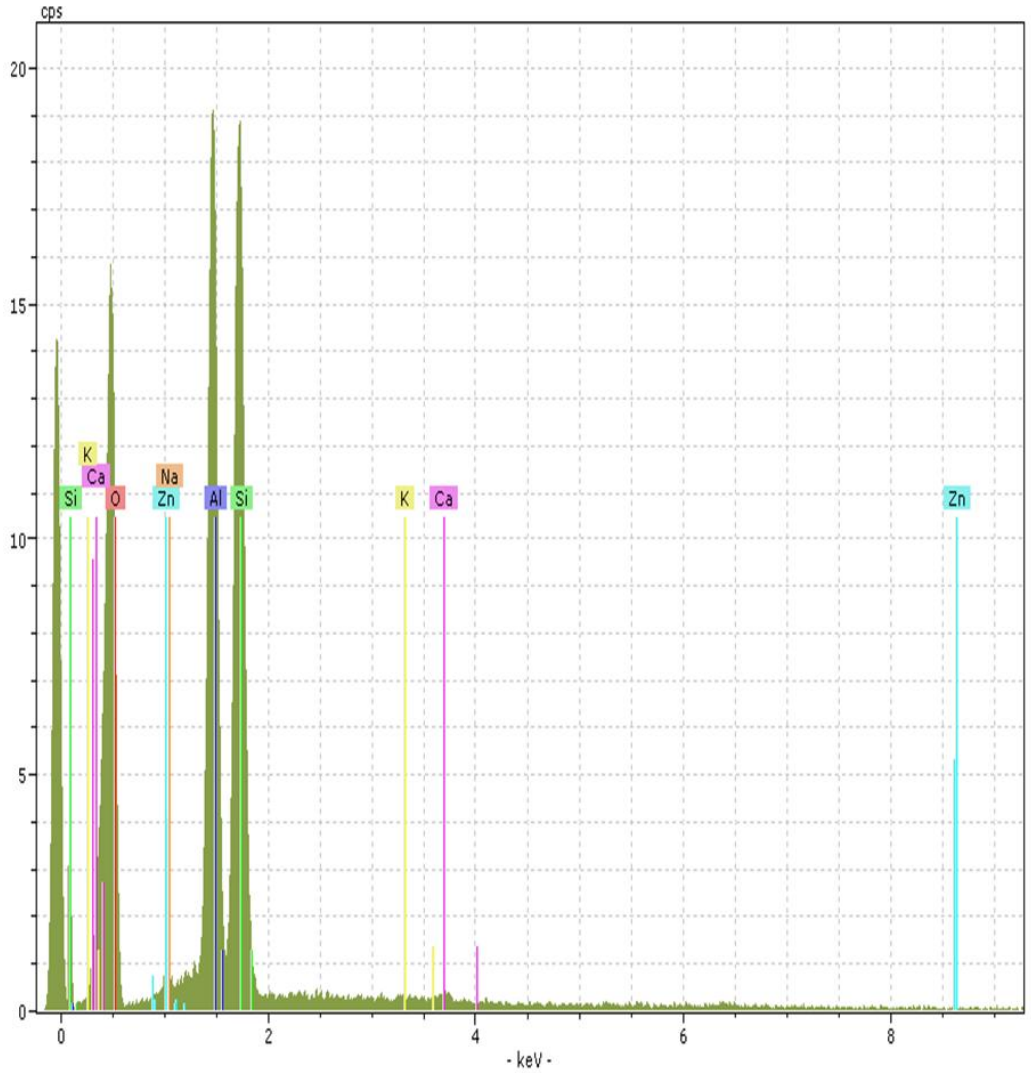

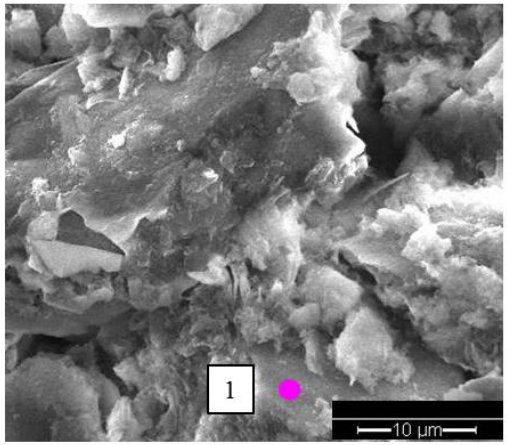

Element	Series	Net	Unn. C (wt.%)	Norm. C (wt.%)	Atom. C (at.%)
Ca	K	393	0.48	0.46	0.22
K	K	201	0.23	0.21	0.11
Si	K	22003	21.40	20.23	13.91
Al	K	22358	18.81	17.79	12.73
Na	K	1	0.00	0.00	0.00
Zn	K	197	1.09	1.03	0.30
O	K	19544	63.73	60.27	72.73
		Total:	105.7 %		

Figure 6.16: Point elemental spectra analysis of Point 1 within 28 day cured 7.5% GGBS-NaOH treated Lanton alluvium.

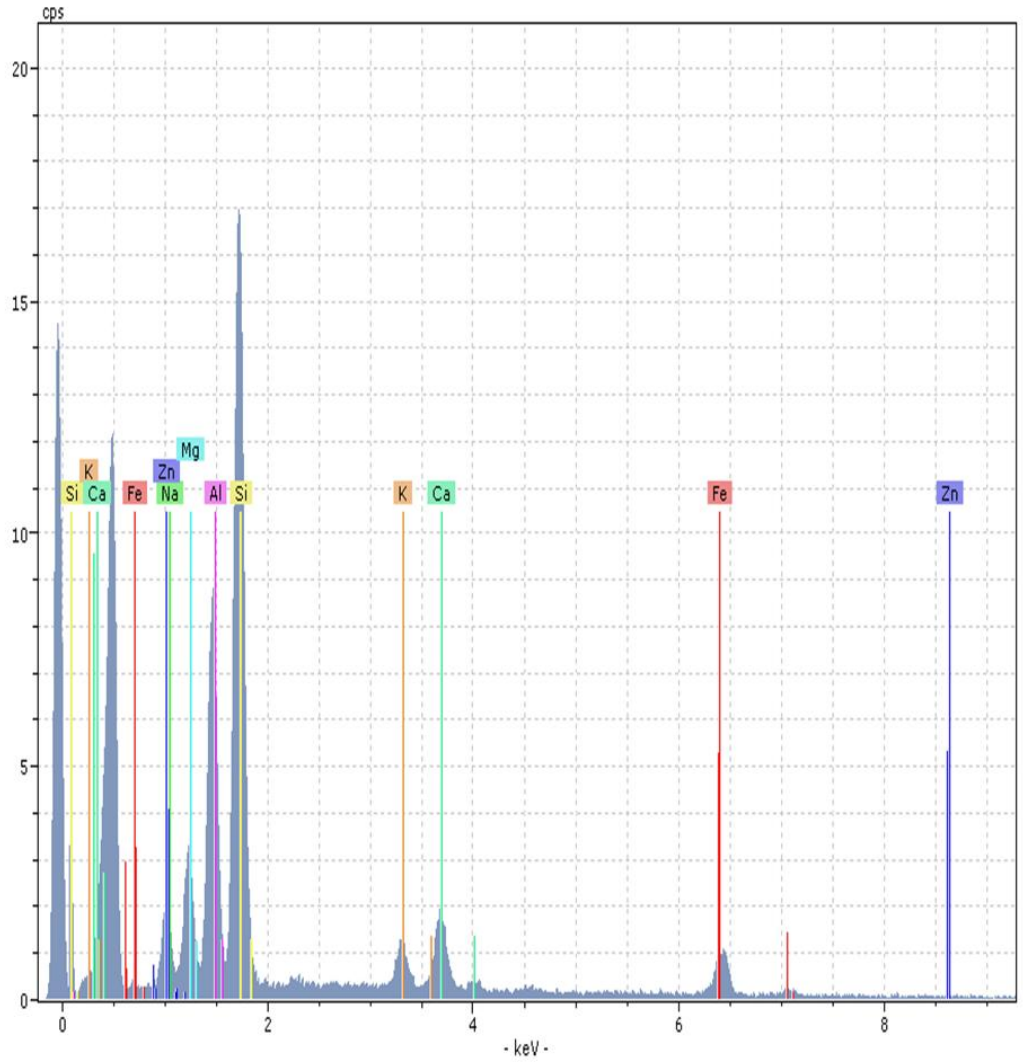

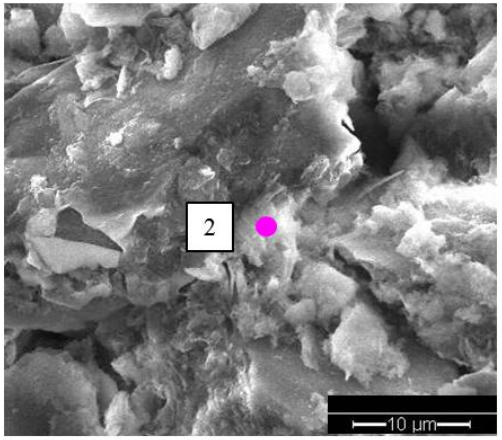

Element	Series	Net	Unn. C (wt.%)	Norm. C (wt.%)	Atom. C (at.%)
Fe	K	1885	6.33	9.85	5.36
Na	K	1	0.00	0.00	0.00
Zn	K	192	1.36	2.12	0.98
Mg	K	3067	4.19	6.52	8.15
Al	K	9689	12.99	20.22	22.78
Si	K	20091	32.08	49.94	54.04
K	K	1736	2.81	4.37	3.40
Ca	K	2689	4.48	6.98	5.29
		Total:	64.2 %		

Figure 6.17: Point elemental spectra analysis of Point 2 within 28 day cured 7.5% GGBS-NaOH treated Lanton alluvium.

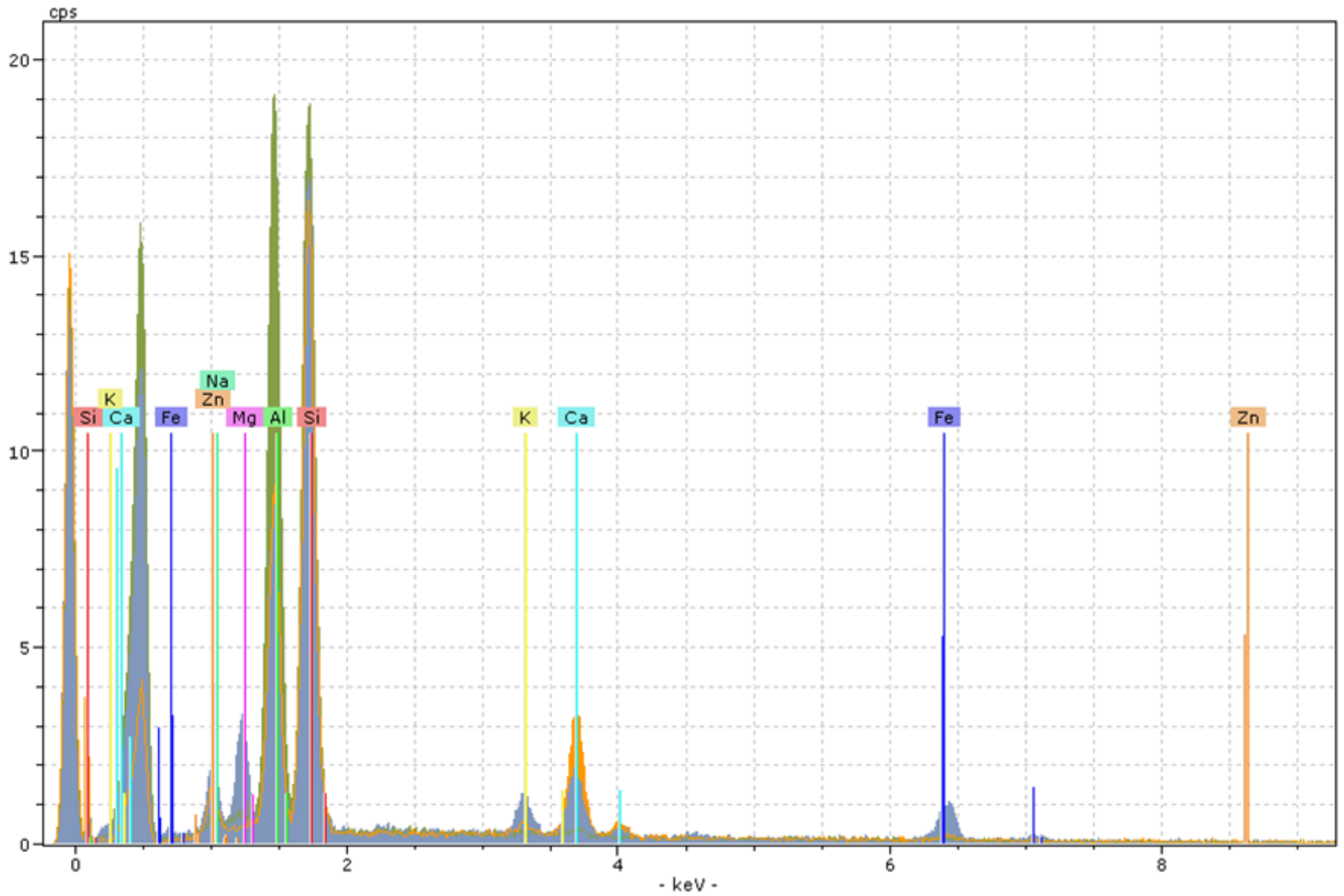

Figure 6.18: Superposition of EDX spectra obtained for points 0 (orange), 1 (green) and 2 (blue) for 28 day cured Lanton + 7.5% GGBS-NaOH sample.

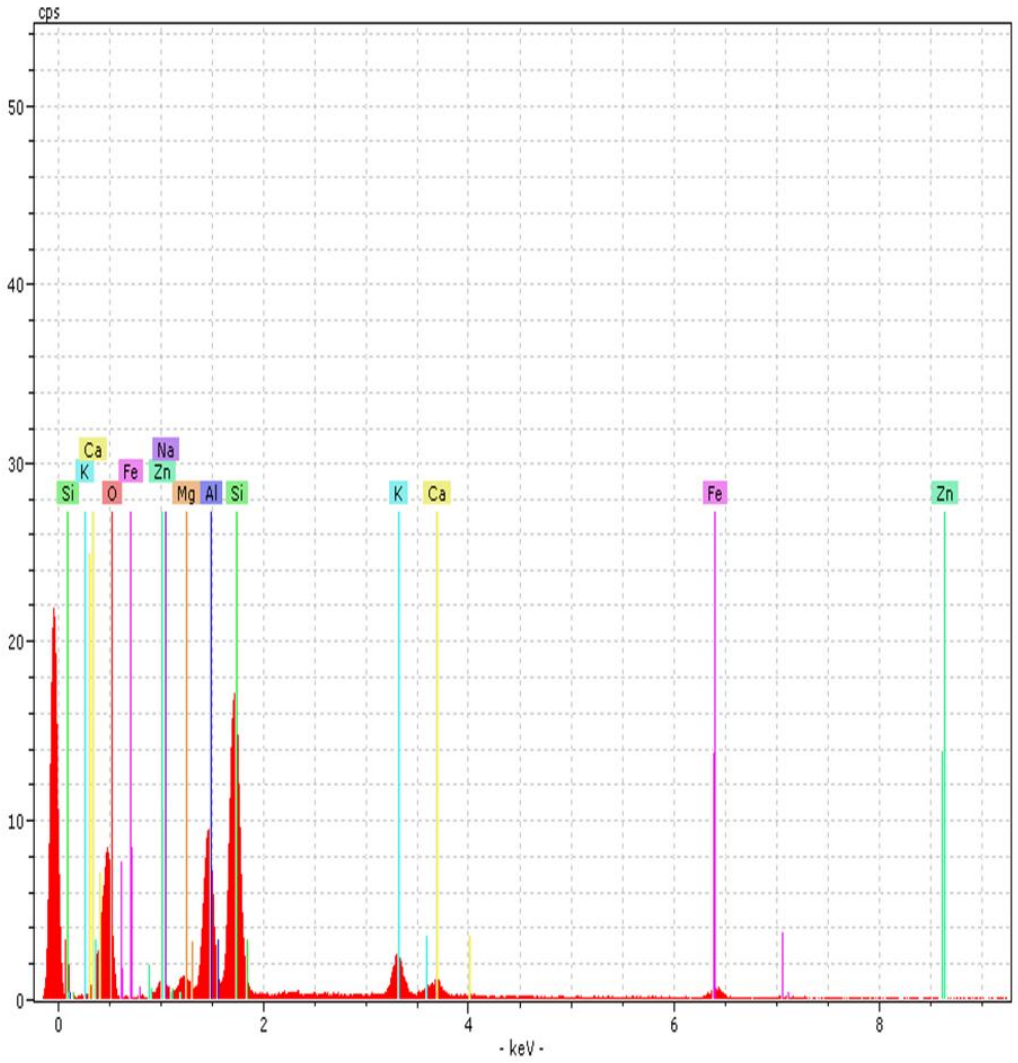

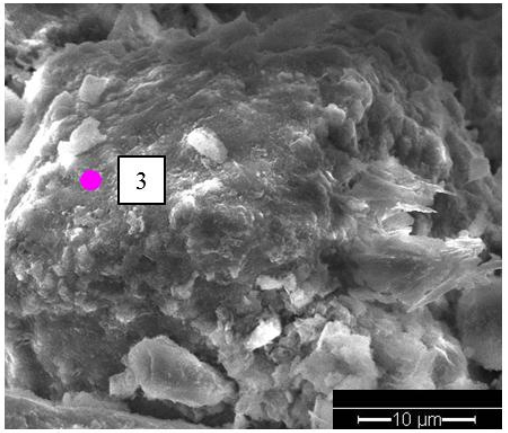

Element	Series	Net	Unn. C (wt.%)	Norm. C (wt.%)	Atom. C (at.%)
Al	K	11004	11.75	12.71	9.71
Si	K	20531	23.36	25.25	18.54
Mg	K	1170	1.46	1.58	1.34
Na	K	1	0.00	0.00	0.00
Zn	K	186	1.00	1.08	0.34
K	K	3510	4.27	4.62	2.44
Ca	K	1176	1.50	1.62	0.83
Fe	K	809	1.72	1.86	0.69
O	K	7199	47.45	51.28	66.11
		Total:	92.5 %		

Figure 6.19: Point elemental spectra analysis of Point 3 within 28 day cured 7.5% GGBS-NaOH treated Lanton alluvium.

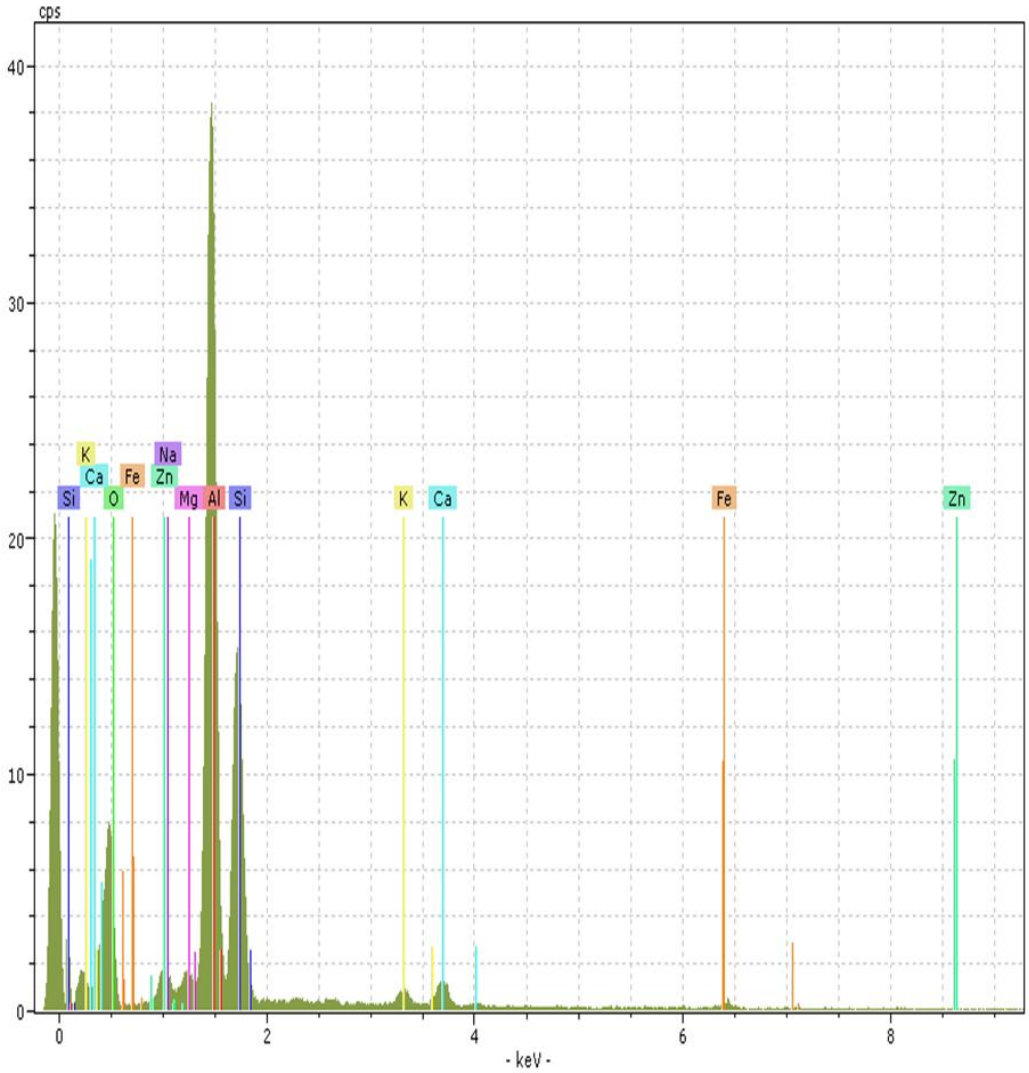

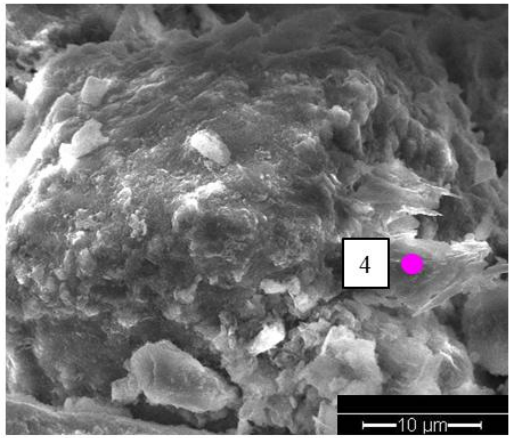

Element	Series	Net	Unn. C (wt.%)	Norm. C (wt.%)	Atom. C (at.%)
Al	K	46355	47.16	36.61	30.51
Si	K	19378	30.84	23.94	19.16
O	K	7126	42.50	33.00	46.37
K	K	1174	1.53	1.18	0.68
Ca	K	1740	2.31	1.79	1.00
Na	K	1	0.00	0.00	0.00
Mg	K	2062	2.24	1.74	1.61
Zn	K	178	0.92	0.71	0.25
Fe	K	506	1.33	1.03	0.41
		Total:	128.8 %		

Figure 6.20: Point elemental spectra analysis of Point 4 within 28 day cured 7.5% GGBS-NaOH treated Lanton alluvium.

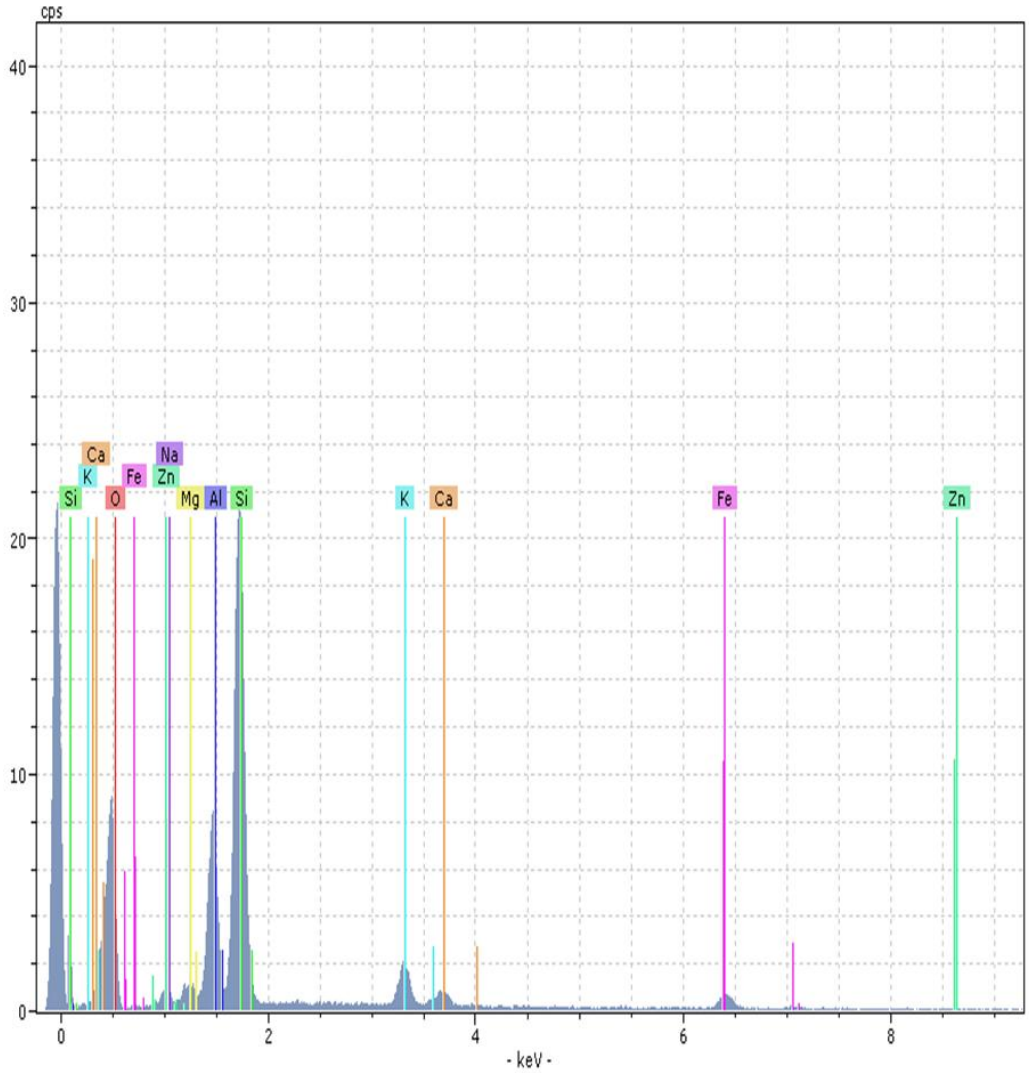

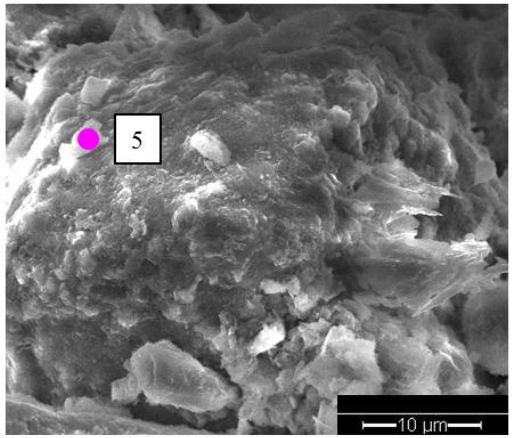

Element	Series	Net	Unn. C (wt.%)	Norm. C (wt.%)	Atom. C (at.%)
Si	K	24805	27.58	29.09	21.35
Al	K	9317	9.99	10.53	8.05
K	K	2892	3.58	3.78	1.99
Ca	K	944	1.22	1.28	0.66
Na	K	1	0.00	0.00	0.00
Mg	K	1005	1.27	1.34	1.13
Zn	K	144	0.76	0.80	0.25
Fe	K	938	2.02	2.13	0.79
O	K	7442	48.40	51.05	65.77
		Total:	94.8 %		

Figure 6.21: Point elemental spectra analysis of Point 5 within 28 day cured 7.5% GGBS-NaOH treated Lanton alluvium.

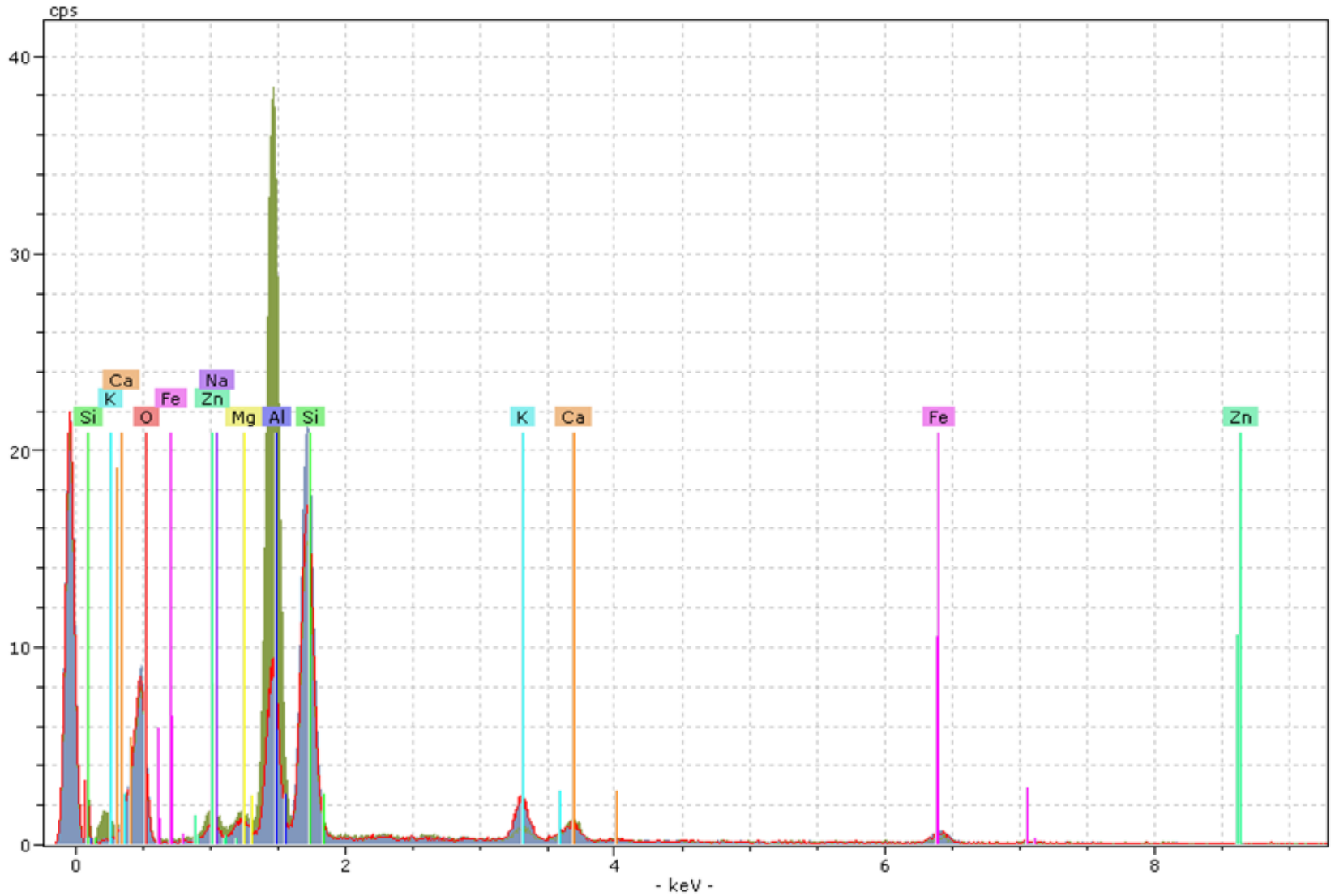

Figure 6.22: Superposition of EDX spectra obtained for points 3 (red), 4 (green) and 5 (blue) for 28 day cured Lanton + 7.5% GGBS-NaOH sample.

From Figure 6.15, the elemental analysis for point 0 shows that the large particle has fairly high concentrations of silica, aluminium, oxygen and calcium, with a small peak for sodium. These peaks strongly suggest the particle is an NaOH activated GGBS grain. This corresponds well with findings in Figure 6.11 where a small segment of early hydration material has peeled away and exposed an inner more recent hydration surface. The elemental analysis obtained for point 1 is rather different. Even though there are still very high peaks for silica and oxygen, the peak for aluminium is much higher and there are no peaks for either calcium or sodium. The strong peaks for silica and oxygen suggest that the mineral is quartz and therefore a soil particle. In general, quartz is a very pure mineral. There are two possible explanations for this. Firstly, if point elemental EDX analyses are conducted on uneven rough sample surfaces, it is possible that closely neighbouring particles can have an influence on the quantitative elemental data obtained for the particle of interest; with X-ray bouncing off other particle surfaces and providing additional (unwanted) elemental peaks. The other possible explanation is that the quartz grain may contain traces of aluminium. Per Nacke (2007), quartz can form within aluminium-saturated environments. The resulting aluminium content can be used as an indicator of the temperature conditions under which it formed.

The elemental data obtained for point 2 closely resembles that for the activated GGBS particle (point 0); whereby high silica, oxygen and aluminium peaks were observed along with smaller calcium and sodium peaks. This data suggests the formation of C-(N)-S-H and/or C-(N)-A-H minerals. However, the element spectra presented in Figure 6.17 also shows evidence for three smaller peaks for magnesium, iron and potassium. Based on the chemical composition of minerals known to be present within the stabilised soil from XRD data (Figure 6.2), the traces of potassium and magnesium may be attributed to the presence of reacting Illite platelets within the cementitious cluster identified in Figure 6.13. The trace of iron may stem from the original presence of a chlorite mineral, which also contains magnesium, aluminium, silica and oxygen. However, no traces of manganese (a major component of chlorite's chemical structure) were identified within the EDX spectrum.

Similar to point 2, the point elemental data obtained for point 3 on the surface of the large particle at the centre of Figure 6.19 shows that the dominant elements present were silica, aluminium, oxygen and potassium, with smaller peaks for magnesium,

sodium, calcium and iron. Based on the high silica and aluminium peaks, along with the presence of calcium and magnesium, it is likely that the large particle is GGBS. By examining the overall particle, surfaces which are not in direct or close contact with another neighbouring GGBS or soil particle are covered with many small protruding growths of amorphous material. This can be seen in Figure 6.23, taken just to the left of the field of view in Figure 6.13.

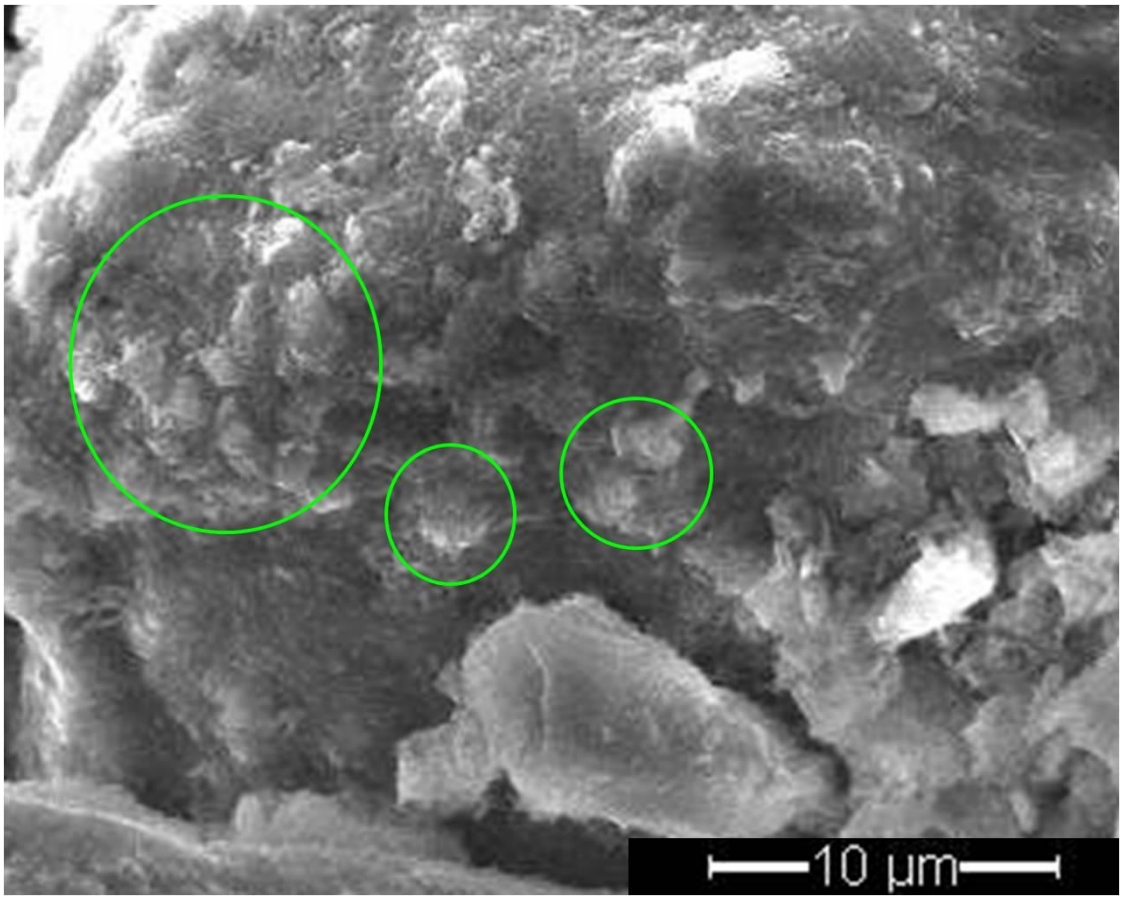

Figure 6.23: Small protruding amorphous cementitious growths (encircled in green) on the surface of a GGBS particle.

Based on this observation and that such small growths occur around point 3, the detection of sodium indicates that the surface of the particle has undergone activation with NaOH and formed a C-N-A-S-H surface coating. However, the detection of potassium or iron cannot be attributed to the initial composition of the GGBS. Located very close to point 3 in the field of view in Figure 6.12 is a platelet mineral adhered to the surface of the NaOH activated GGBS particle. The platelet was subjected to point

elemental analysis (point 5). The results are displayed in Figure 6.21. Due to the common aluminosilicate composition, the presence of potassium and negligible sodium content; the platelet is likely to be either Illite or Orthoclase feldspar. Hence, given the close proximity of the platelet and that X-rays are likely to bounce off other neighbouring particles due to the irregular rough surface of the sample, the potassium trace in point 3 could be caused by interference by the Illite/Orthoclase platelet. However, the platelet still cannot explain the iron trace detected for point 3. Based on the XRD analyses and EDX spectra obtained for untreated and GGBS-NaOH stabilised Lanton alluvium, any iron content may only be attributed to the mineralogy of the natural soil; namely the presence of Chlorite in Figure 6.1. It is therefore possible that a nearby Chlorite mineral has interfered with the spectra presented for points 3 and 5.

The final elemental analysis conducted on the 28 day stabilised sample was for point 4. The results are shown in Figure 6.20. The mineral from which the elemental analysis was taken has a definite morphology. It is platelet-like comprising numerous individual sheets with an irregular shape. Its morphology closely resembles that observed for the Illite mineral observed in Figure 6.5 within natural Lanton alluvium. The very high aluminium peak, high silica and oxide traces along with the smaller traces of potassium and magnesium would collectively suggest that the mineral was an Illite. Other low magnitude elemental traces such as calcium and sodium may have been caused by 1) interference from the neighbouring NaOH activated GGBS particle and 2) the X-ray passing through thinner sections of the Illite mineral, thereby picking up elemental data from minerals/particles located behind the Illite.

6.3.3.1.4 Sample summary

The microstructure of 7.5% GGBS-NaOH stabilised Lanton alluvium is significantly more dense and complicated compared with natural Lanton soil. Mineralogical changes were abundant within the material, due to the NaOH activated GGBS. Adding NaOH caused GGBS particles to hydrate, whose surfaces were now characterised by layers of hydrated material and small cementitious growths. Where soil and NaOH-activated GGBS particles were observed to be in close/direct contact with each other,

clusters of cementitious growths were observed to stem from the GGBS particle and grow towards neighbouring GGBS and soil particles; thereby creating a structural bond. These cementitious gels also reacted with smaller Illite clay minerals and were found to be infilling void spaces and increasing inter-particle contacts. From point elemental analyses, the majority of the cementitious gels within the stabilised soil are predominantly thought to be sodium rich C-S-H (C-N-S-H), sodium rich C-A-H (C-N-A-H) and C-N-A-S-H. The branching typically associated with C-S-H gels (Wilkinson et al., 2010a) was not observed within the sample. However, the presence of the cementitious hydrate products could not be fully confirmed as the ESEM equipment utilised was not calibrated to detect hydrogen. Finally, no evidence was found to suggest that any structurally unfavourable needle-like AFt minerals had formed within the stabilised material over the 28 day curing period.

6.3.3.2 56 days curing

Having examined the mineralogical and microstructural characteristics of the 28 day cured sample, it was anticipated that the mineralogy and microstructure of the 56 day cured sample would be even more complex per findings in chapter 5 where higher UCS values were achieved for the material after 56 days compared with 28 days.

6.3.3.2.1 Sample microstructure

As anticipated, SEM micrographs demonstrated that the microstructure of 56 day cured GGBS-NaOH Lanton alluvium was more complex than its 28 day counterpart and significantly more complex compared with untreated Lanton alluvium. Void spaces within the stabilised material had become increasingly filled due to a combination of the level of compaction used to prepare the material and the further development of cementitious mineral/gel growths; thereby contributing towards the material's even lower permeability and porosity compared with after 28 days curing.

Similar to the 28 day sample, the soil and GGBS particles displayed a range of face-to-face, edge-to-edge and edge-to-face inter particle contacts. However, given the

additional 28 days of curing and further development of light grey/white coloured cementitious gels, GGBS particles generally showed higher degrees of cementitious surface coatings, as can be seen in the lower right quadrant of Figure 6.24. Generally, no darker inner hydrated GGBS surfaces were exposed.

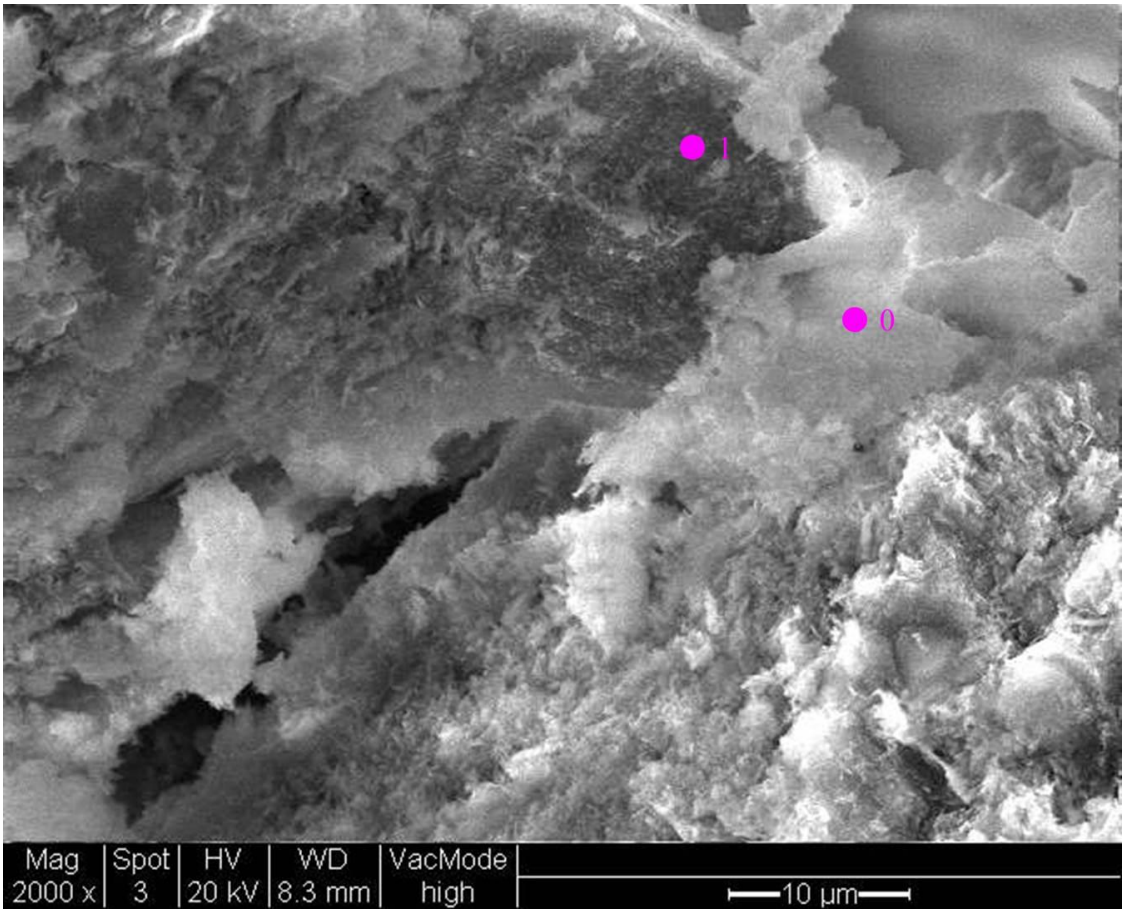

Figure 6.24: SEM micrograph of cementitious surface coating and bonding between soil particles within 56 day cured Lanton alluvium at x2000 magnification. Points taken for EDX analysis are labelled.

Small clay minerals are seen scattered across GGBS and soil particle surfaces, but are not as clearly seen in SEM micrographs due to the extensive cementitious reactions occurring along their edges and the gel/mineral growths surrounding them. Bearing in mind the x2000 magnification of the SEM micrograph in Figure 6.24 is the same as that for Figures 6.9 and 6.12, the number of cementitious growths on particle surfaces were not only more extensive and branch-like (typical of C-S-H) but also larger and more protrusive (Figure 6.25).

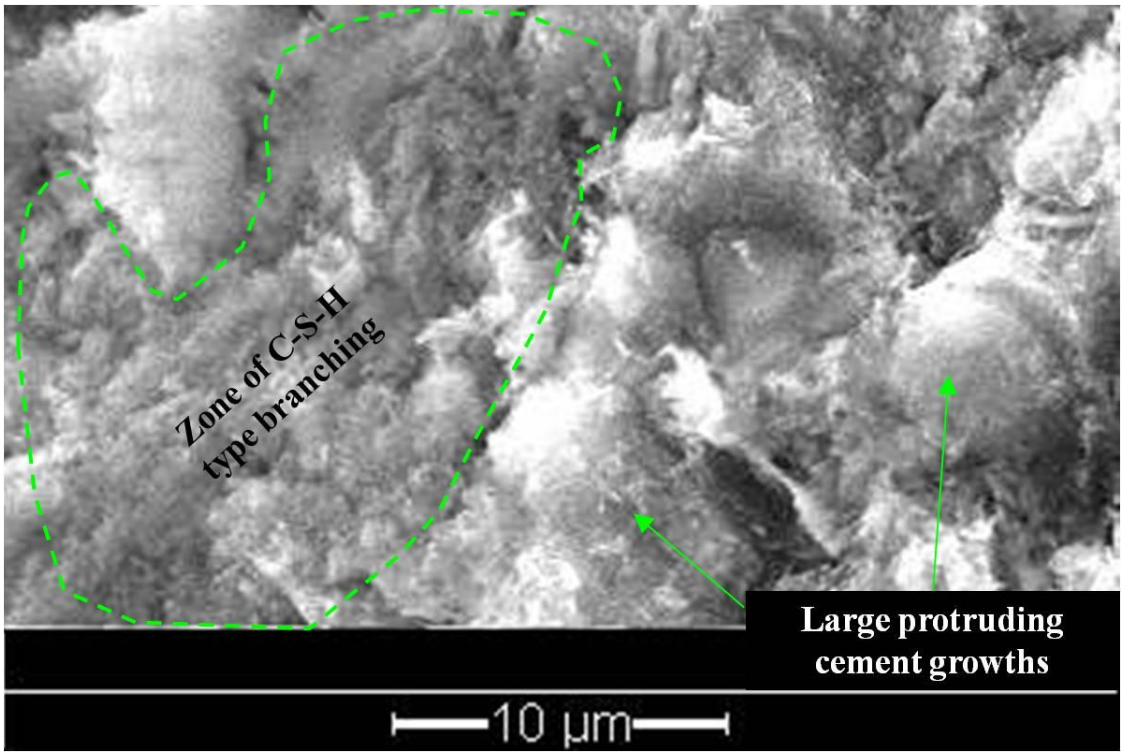

Figure 6.25: SEM micrograph of C-S-H type branching (green area) and large protruding cement growths on the surface of a GGBS particle.

The degree of inter-particle contacts and bonding within the sample due to the development of cementitious clusters between GGBS and neighbouring soil particles was much higher than observed within the 28 day cured sample. In contrast to the nature of the cementitious clusters within the 28 day sample which tended to contain some Illite clay minerals, the 56 day cured material contained more cement clusters that were both solely characterised by cement and occurred more frequently throughout the sample. An example of such a pure cement growth that has developed a firm structural bond between a soil and GGBS particle and simultaneously infilled some void space can be observed at point 0 on Figure 6.24 and within the green area on Figure 6.26.

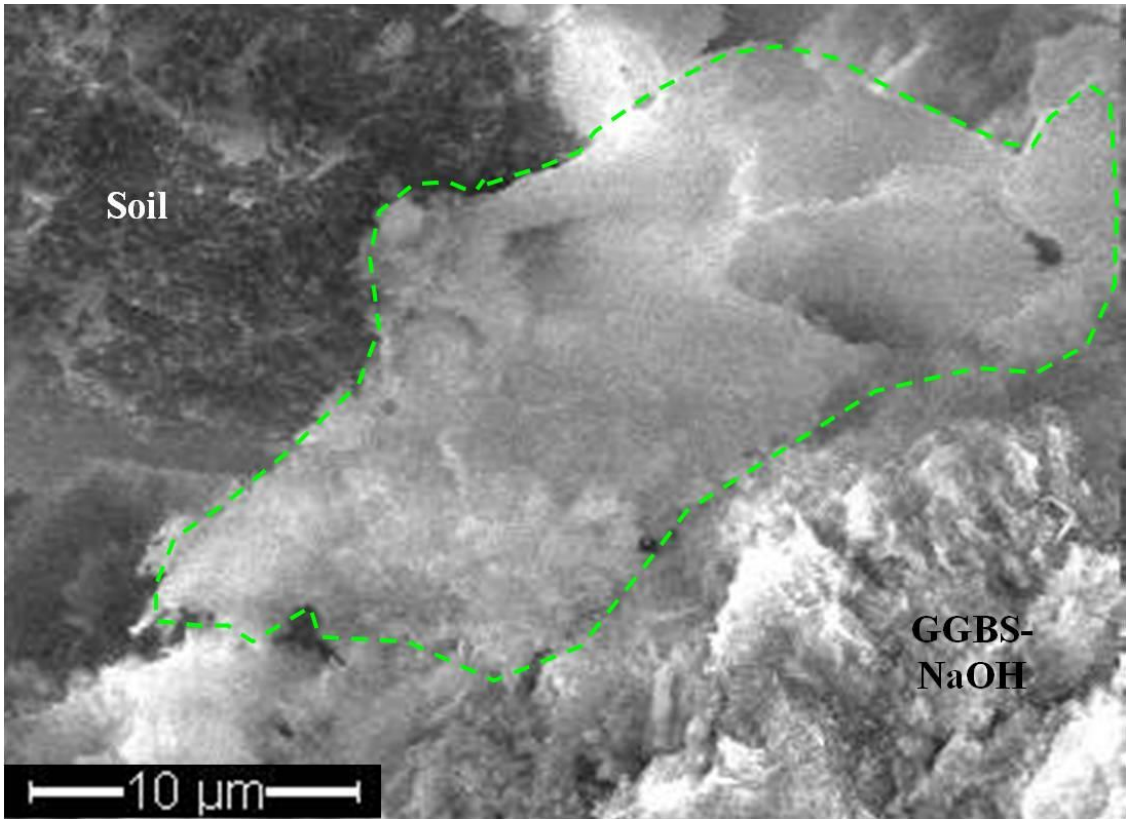

Figure 6.26: SEM micrograph of a substantial cementitious bond (green area) between a soil and NaOH activated GGBS particle within 56 day cured stabilised Lanton alluvium.

6.3.3.2.2 Sample mineralogy

The overall chemical composition of the 56 day cured stabilised material was analysed quantitatively using EDX spectra, which allowed for mineralogical comparisons to be made with the material's associated XRD spectrum, along with the XRD and EDX spectra obtained for the untreated and 28 day cured material through GGBS-NaOH stabilisation. Table 6.4 presents the quantitative elemental composition for the material and Figure 6.27 displays the corresponding EDX spectrum. Per Figures 6.27–6.28, the chemical composition of the 56 day cured material is similarly different to untreated Lanton alluvium as the 28 day cured material. Similar sized peaks were observed for silica, aluminium, potassium, iron and oxygen, due to the presence of non-dissolvable soil minerals such as Quartz and Orthoclase/Albite Feldspars in addition to the Illite and Vermiculite clay minerals. However, two main differences were noted; these being the larger sodium/zinc and calcium peaks due to the addition of the GGBS-NaOH binder and subsequent cementitious reactions.

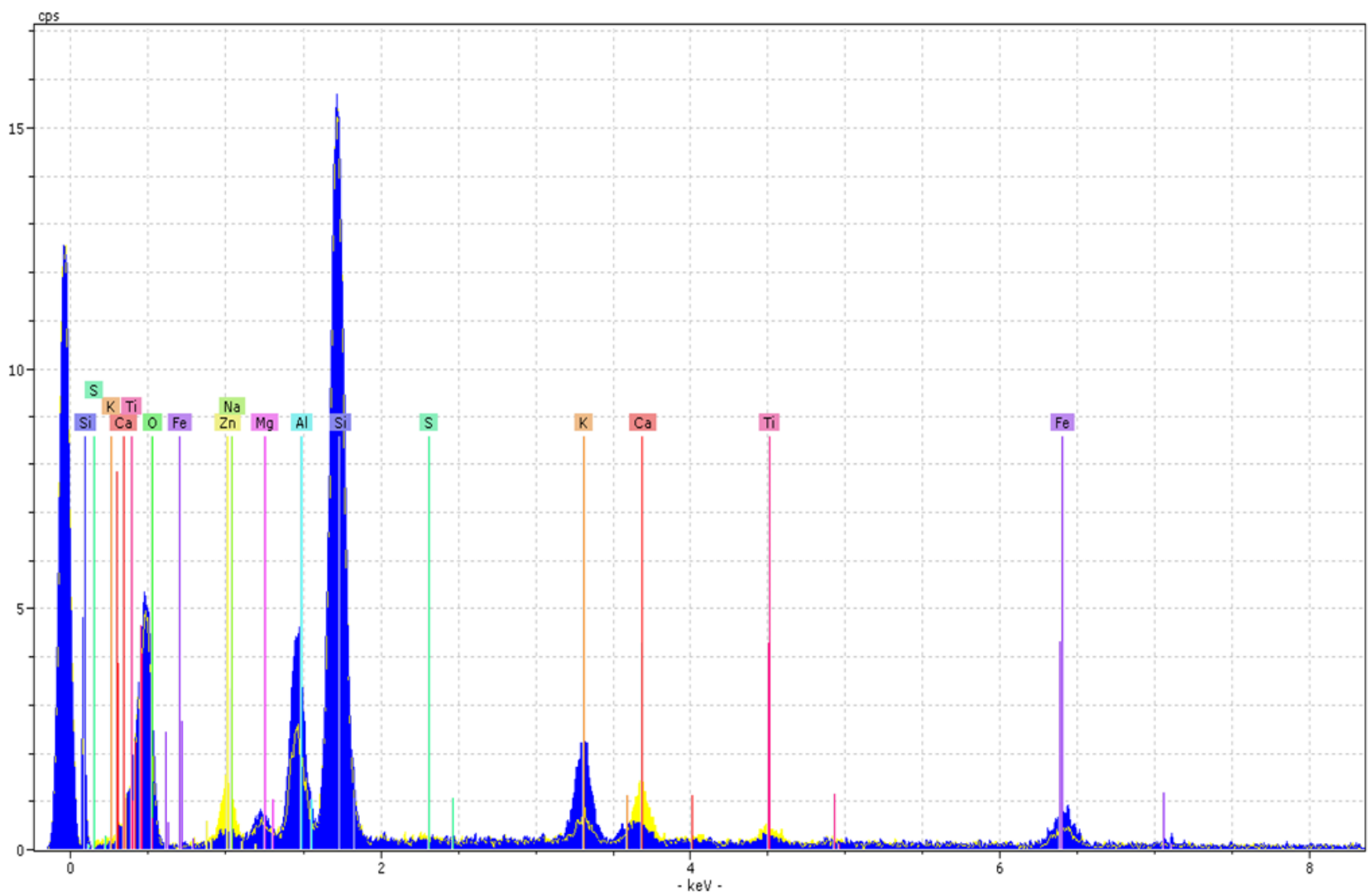

Figure 6.27: EDX spectra for Lanton alluvium in its natural state (blue) and when stabilised with 7.5% GGBS-NaOH after 56 days curing (yellow), with elemental data superimposed.

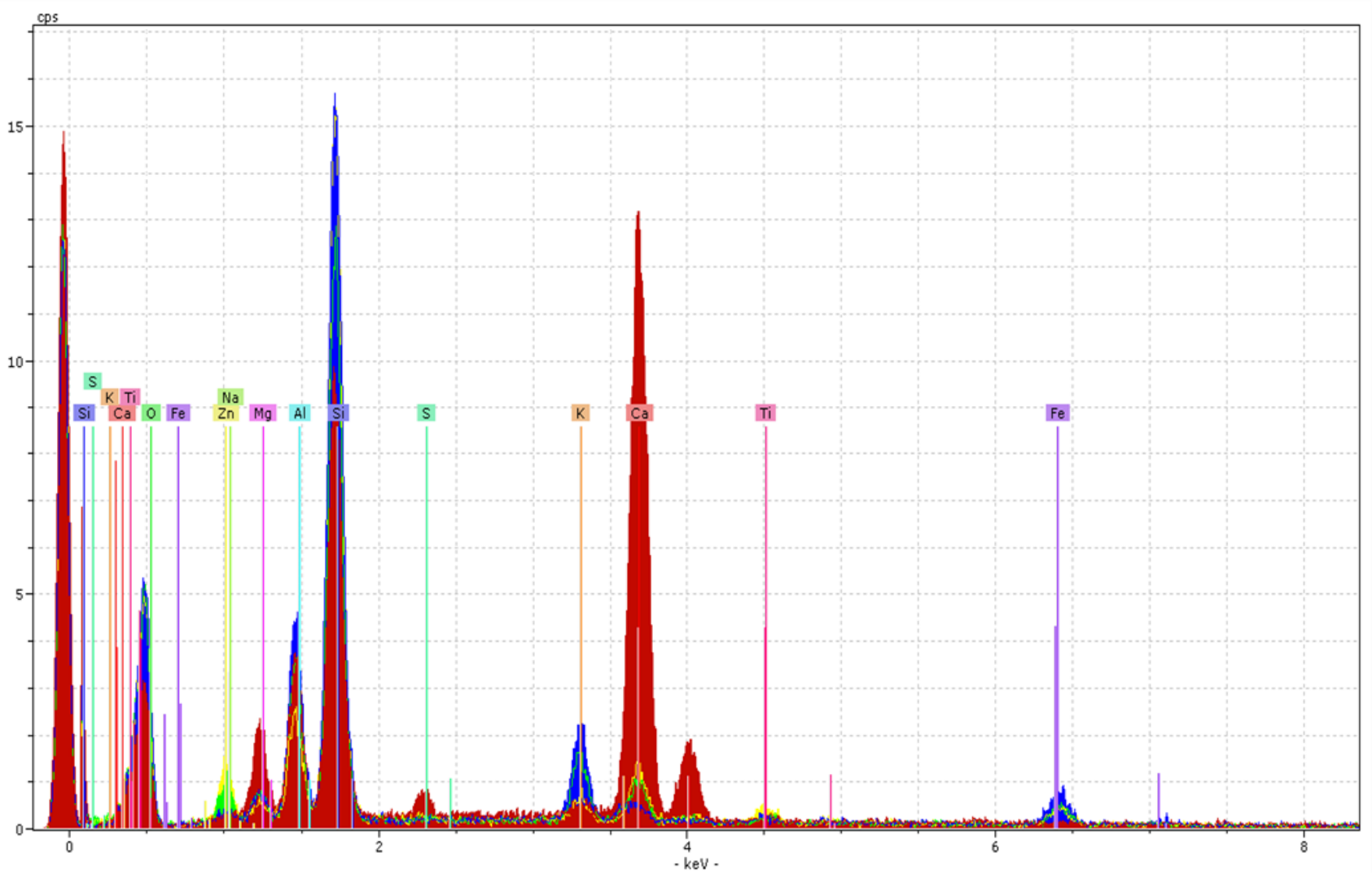

Figure 6.28: Superimposed sample EDX spectra for Lanton alluvium (blue), 28 day cured Lanton + 7.5% GGBS-NaOH (green), 56 day cured Lanton + 7.5% GGBS-NaOH (yellow) and the raw GGBS (red).

Table 6.4: Quantitative elemental composition of stabilised Lanton alluvium after 56 days curing from EDX spectra analysis.

Element	Series	Net	Unn. C (wt.%)	Norm. C (wt.%)	Atom. C (at.%)
O	K	1987	37.30	50.12	66.04
Si	K	16863	23.78	31.95	23.98
Al	K	2515	3.72	5.00	3.91
K	K	690	1.15	1.55	0.84
Fe	K	741	2.47	3.32	1.25
Zn	K	165	1.05	1.41	0.45
Ca	K	1694	2.93	3.94	2.07
Mg	K	251	0.45	0.61	0.53
Ti	K	710	1.56	2.09	0.92
Na	K	1	0.00	0.00	0.00
		Total:	74.4%		

The small sulphur peak observed within the GGBS sample's EDX spectrum (Figure 6.8) was not detected in this material. This may be due to the further development of thicker NaOH activated cementitious coatings on GGBS particle surfaces, which in turn may have masked the presence of sulphur within the unreacted zone of GGBS particles. The same sodium/zinc peak identification problem encountered for the 28 day cured material was also encountered within the 56 day material. Based on the poor separation between the sodium and zinc peaks due to their similar characteristic X-ray keV values, none of the minerals identified in the XRD analyses contain zinc. However, sodium is known to be present. Thus, a sodium/zinc peak observed within EDX spectra is considered to be sodium.

6.3.3.2.3 EDX point element analyses

As for the 28 day cured material, the EDX spectrum for the 56 day stabilised material in Figure 6.27 fails to provide definitive information regarding the chemical composition of cementitious material observed within the stabilised soil. Using EDX point elemental analyses facilitates the determination of the chemical composition of such cementitious gels. Numerous points for elemental analysis were selected

throughout the sample, particularly in key interest areas where highly coated particle surfaces and/or physical bonding was observed between two or more particles. Excellent examples of such cementitious surface coatings and physical bonding are displayed in Figure 6.24. Points 0 and 1 labelled on Figure 6.24 were selected for elemental analyses to determine: 1) the composition of the cementitious gels formed and 2) to confirm whether they grew from activated GGBS particle surfaces to bond with neighbouring soil and GGBS particles. The EDX spectra and quantitative analyses for points 0 and 1 are shown in Figures 6.29–6.31.

The quantitative elemental results presented for point 0 within Figure 6.29 demonstrate that the lightly-coloured amorphous growth seen to be bridging two larger particles is characterised by strong peaks for silica, aluminium and oxygen and slightly lower magnitude (but still pronounced) peaks for calcium, sodium, magnesium and iron. The spectrum also bears a close resemblance to that in Figure 6.18 for a similar amorphous growth within the 28 day cured sample. These findings suggest that the amorphous growth observed in Figures 6.24 and 6.26 is cementitious and is likely to be C-(N)-A-H and/or C-(N)-S-H. The peak recorded for potassium is probably attributable to the conversion of Illite clay mineral(s) to form the cementitious gel, which also contains aluminium, silica and oxygen. Regarding the origins of the magnesium and iron traces recorded within the cementitious growth, these are likely to have come from Vermiculite and/or Chlorite minerals, which have either been partially or completely converted during the reaction process.

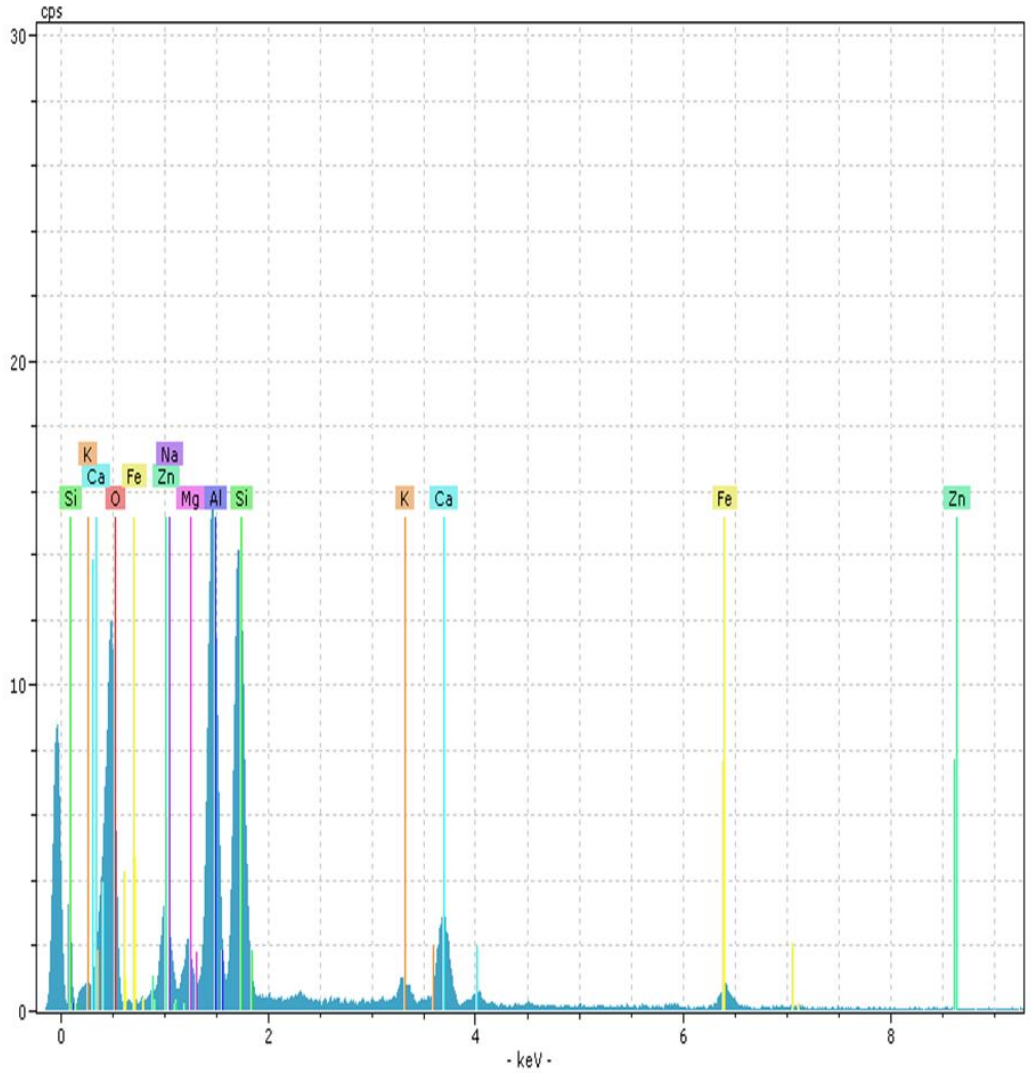

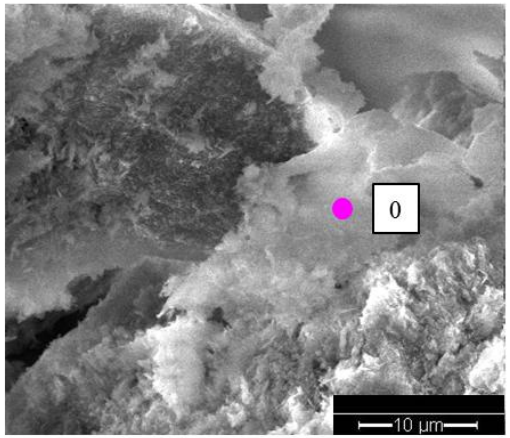

Element	Series	Net	Unn. C (wt.%)	Norm. C (wt.%)	Atom. C (at.%)
Si	K	17348	23.63	21.49	16.18
Al	K	18358	21.38	19.44	15.24
Mg	K	2148	2.83	2.57	2.24
Na	K	1	0.00	0.00	0.00
Zn	K	189	0.96	0.88	0.28
Ca	K	4419	6.03	5.49	2.89
K	K	1430	1.87	1.70	0.92
Fe	K	958	2.08	1.89	0.72
O	K	10457	51.17	46.54	61.52
		Total:	110.0 %		

Figure 6.29: Point elemental spectra analysis of Point 0 within 56 day cured 7.5% GGBS-NaOH treated Lanton alluvium.

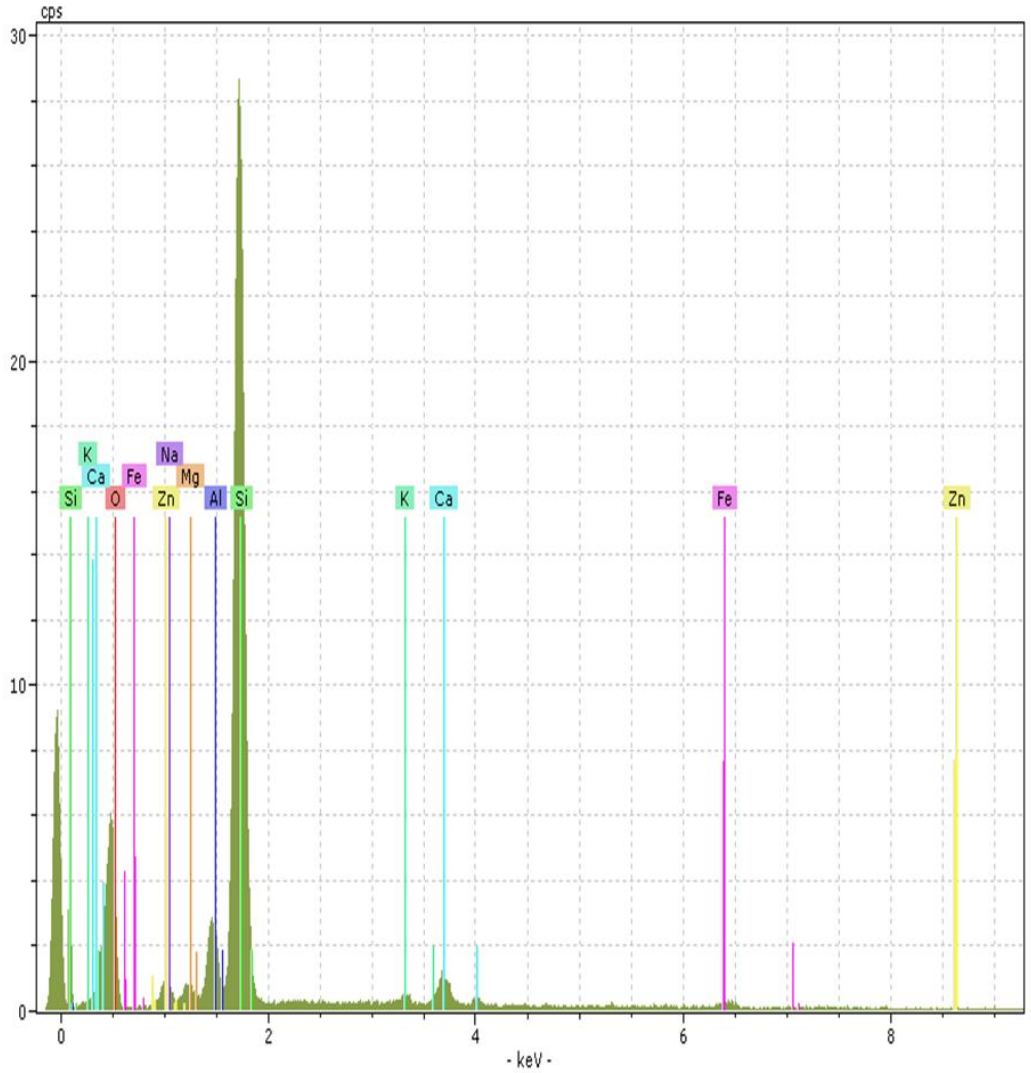

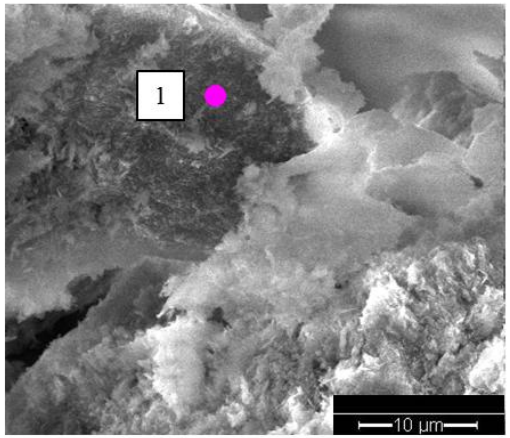

Element	Series	Net	Unn. C (wt.%)	Norm. C (wt.%)	Atom. C (at.%)
Si	K	32953	33.20	38.15	28.00
Al	K	3077	3.25	3.74	2.86
Na	K	1	0.00	0.00	0.00
K	K	405	0.53	0.61	0.32
Ca	K	1578	2.17	2.49	1.28
Mg	K	519	0.66	0.76	0.64
O	K	5121	44.45	51.07	65.80
Zn	K	208	1.18	1.36	0.43
Fe	K	549	1.58	1.81	0.67
		Total:	87.0 %		

Figure 6.30: Point elemental spectra analysis of Point 0 within 56 day cured 7.5% GGBS-NaOH treated Lanton alluvium.

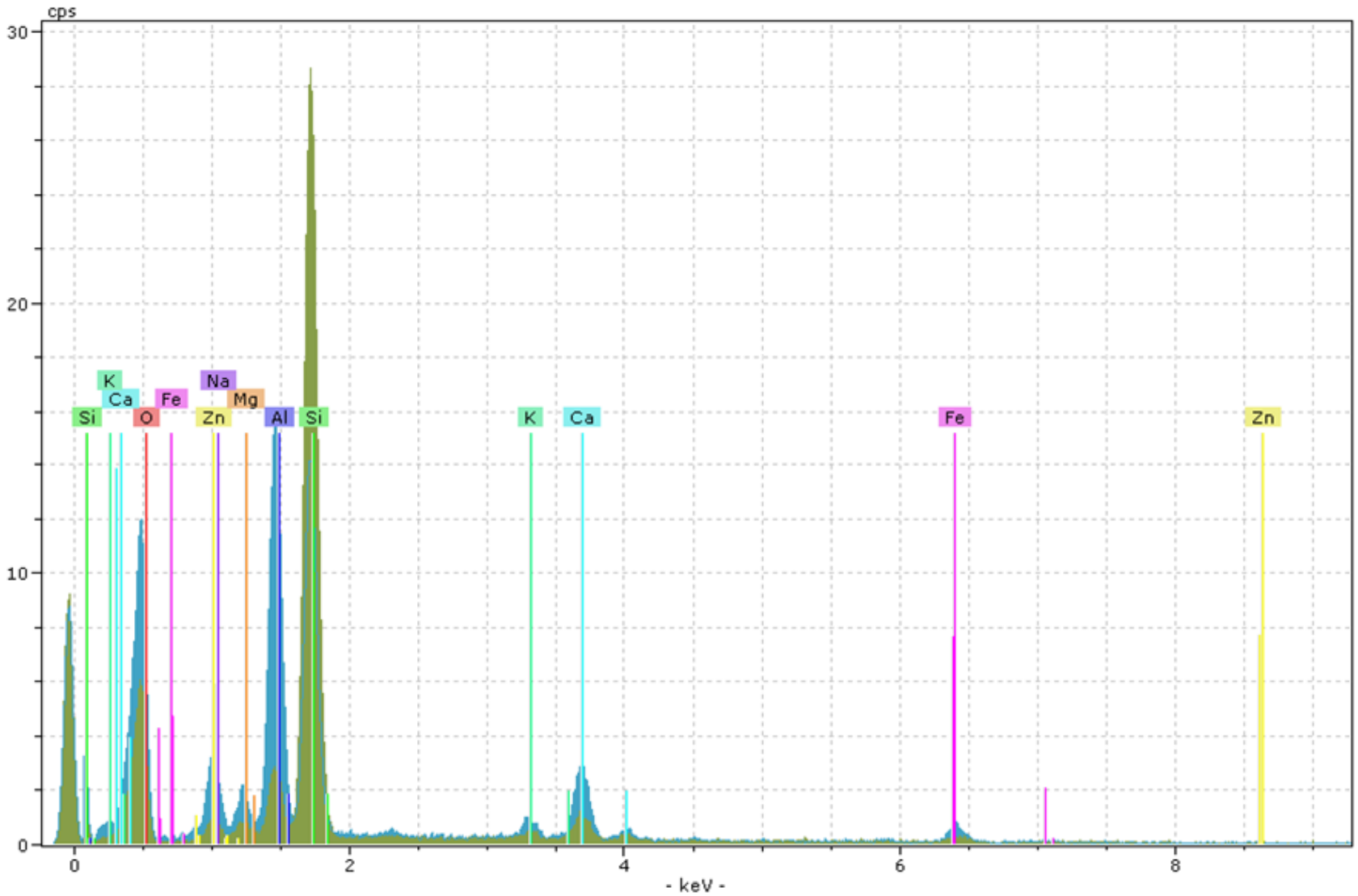

Figure 6.31: Superposition of EDX spectra obtained for points 0 (blue) and 1 (green) for 56 day cured Lanton + 7.5% GGBS-NaOH sample.

Finally, the point elemental data obtained for point 1 within Figure 6.30 is clearly different to that presented for point 0 (Figure 6.31), which shows that the dominant element present was silica, followed closely by oxygen and aluminium. Much smaller secondary peaks of calcium, potassium, magnesium, sodium and iron are apparent. Based on the high silica and oxygen peaks, the EDX analysis strongly suggests that the particle is a Quartz silt/fine sand grain sized soil particle. The lower peak for aluminium could be caused by one or a combination of three factors; 1) traces of aluminium present within the Quartz grain and 2) the slight influence of small cementitious reactions occurring elsewhere on the Quartz grain or from closely neighbouring larger cementitious growths containing aluminium. This will be due to X-rays bouncing off the sample's uneven surface and may also explain the small potassium, iron and magnesium peaks within the spectrum for point 1.

6.3.3.2.4 Sample summary

As predicted, the microstructure of 7.5% GGBS-NaOH stabilised Lanton alluvium after 56 days curing was even denser and more complex compared with the 28 day cured sample. There was abundant evidence to suggest mineralogical changes occurred within the material; whereby NaOH activated GGBS particles had reached more advanced stages of hydration processes. Activated GGBS particle surfaces showed higher degrees of cementitious layer coverage, ultimately contributing towards the formation of much larger cementitious growths stemming from their surfaces. Such growths tended to occur as clusters within the material and were observed to increase levels of inter-particle bonding and providing a means of structural bonding with neighbouring GGBS and Quartz soil particles throughout the microstructure. These cementitious gels were also seen to be further filling void spaces and thereby considerably reducing the stabilised material's permeability and porosity compared with 28 days curing.

Clay minerals such as Illite and Vermiculite were less easily identified within the material; thereby suggesting that they had experienced a higher degree of conversion during cementitious reactions to produce cementitious gels compared with 28 days curing. Results from point elemental analyses strongly suggest that the cementitious

gels present within the stabilised soil would predominantly be sodium rich calcium aluminosilicate hydrates; namely C-N-S-H, C-N-A-H and C-N-A-S-H. The typical branching morphology associated with C-S-H formation was occasionally observed on surfaces of NaOH-activated GGBS particles. However, the ESEM equipment used was not calibrated to detect hydrogen; therefore full confirmation regarding the presence of these minerals was not possible. Finally, no convincing evidence was observed to suggest that unfavourable ettringite or thaumasite minerals had formed over the 56 day curing period, given the absence of distinct needle-like minerals within the material's microstructure.

6.4 Chapter summary and conclusions

NaOH activated GGBS was added to the soft Lanton alluvium at a dosage of 7.5% by dry weight. Results in chapter 5 proved that this binder and dosage produce increased geotechnical performances after 21 days of curing. To explain these improvements in strength and durability, XRD and SEM-EDX analyses were conducted on Lanton alluvium before and after treatment with the GGBS-NaOH binder after 28 and 56 days curing to identify the cementitious reactions and the resulting new cementitious gels within the soil's matrix.

SEM successfully demonstrated that the microstructure of Lanton alluvium experienced considerable modifications upon stabilisation using a NaOH-activated GGBS binder with increasing curing time. NaOH was successful in activating GGBS particles. Layered cementitious surface coatings and protruding growths were clearly observed to stem from GGBS particle surfaces and increased inter-particle contacts between other GGBS and soil particles. Additionally, the continued development of cementitious growths and layered surface coatings also made a considerable contribution in reducing the permeability and porosity of the material by infilling pore spaces.

According to qualitative XRD results, the mineralogy of Lanton alluvium in its natural state predominantly comprised Quartz with smaller amounts of Illite, Vermiculite, Dolomite, Chlorite, Orthoclase and Albite Feldspars. Possible traces of Na-

Montmorillonite were also observed. Further analysis of the soil's <2 μm fraction would be required to confirm this, which would remove any interference from larger minerals. The XRD spectra produced for both the 28 and 56 day cured stabilised samples were very similar; whereby both contained considerable quantities of Quartz, Illite, Vermiculite, Orthoclase and Albite Feldspars. However, traces for Chlorite and Dolomite were no longer present, suggesting that their aluminium, silica and calcium contents had been fully consumed to produce cementitious gels. Some of the soil's original Illite and Vermiculite contents had yet to be altered. Future quantitative XRD analyses would be required to accurately determine the volume of unaltered Illite and Vermiculite remaining within the stabilised material.

Based on the high calcium, aluminium and silica contents recorded within GGBS-NaOH stabilised Lanton soil from EDX analyses, the formation of cementitious products including C-S-H and C-A-H was likely. However, given the introduction of the NaOH activator, more complex types of cementitious gels have also formed; namely C-N-A-H, C-N-S-H and C-N-A-S-H. Table 6.5 summarises the minerals identified within untreated and treated samples of Lanton alluvium, along with the cementitious minerals which are likely to have formed, based on EDX spectra analyses. Per Myers et al. (2013), the structural models used to define calcium alumina-silicate hydrate gels have previously been based on non-cross-linked tobermorite (C-S-H) structures. This does not apply for C-(N)-A-S-H gels; whereby a mixture of cross-linked and non-cross-linked tobermorite-based structures are considered more appropriate, particularly when describing the material's density and spectroscopic characteristics (Myers et al., 2013).

Per Tutumluer (2012), clay contents of 10–50% and therefore fairly high surface area (SA) and CEC values are required for lime and cement stabilisation to work effectively. XRD results revealed that the low clay content of Lanton alluvium (10%) comprised Illite and Vermiculite; whereas the higher clay content of the artificial alluvium tested in chapter 4 (30%) solely comprised Kaolinite. Given the significantly higher SA and CEC values of Illite (SA = 100 m^2/g, CEC = 0.2-0.3 meq/100g) and Vermiculite (SA = 700 m^2/g; CEC = 100-150 meq/g) compared with Kaolinite (SA = 15 m^2/g; CEC = 0.03 – 0.1 meq/100g) (Terzaghi et al., 1996;Tutumluer, 2012), the smaller quantities of Illite and Vermiculite within Lanton alluvium have compensated to allow strength developments to occur within the stabilised material.

Table 6.5: Summary of identified and likely mineral phases within 28 day cured 7.5% GGBS-NaOH stabilised Lanton alluvium from XRD and SEM-EDX analyses.

	Minerals identified (XRD)	**Elements identified (SEM-EDX)**	**Likely cement minerals (SEM-EDX)**
Natural Lanton alluvium	Quartz Orthoclase Feldspar Albite Feldspar Dolomite Vermiculite Illite Chlorite Na-Montmorillonite (possible)	Silica Oxygen Aluminium Potassium Magnesium Calcium Iron	N/A
28 day cured Lanton alluvium + 7.5% GGBS-NaOH	Quartz Orthoclase Feldspar Albite Feldspar Vermiculite Illite	Silica Oxygen Aluminium Potassium Calcium Sodium Magnesium Iron	C-(N)-S-H C-(N)-A-H C-N-A-S-H
56 day cured Lanton alluvium + 7.5% GGBS-NaOH	Quartz Orthoclase Feldspar Albite Feldspar Vermiculite Illite	Silica Oxygen Aluminium Potassium Calcium Sodium Magnesium Iron	C-(N)-S-H C-(N)-A-H C-N-A-S-H

As observed in SEM micrographs of the stabilised soil after 28 and 56 days, the vast majority of cementitious bonds between activated GGBS and soil particles grew in the form of clusters at edge-to-edge or edge-to-face particle contacts, rather than growing throughout the soil's entire void space and establishing bonds along all face-to-face/edge-to-edge/edge-to-face contacts. This may be explained by the relatively low abundance and scattered distribution of clay particles throughout the soil matrix; whereby cementitious bonding clusters occurred in similar locations as clusters of Illite, Vermiculite and Chlorite platelets between neighbouring activated GGBS and Quartz (silt/sand) particles (Figure 6.32).

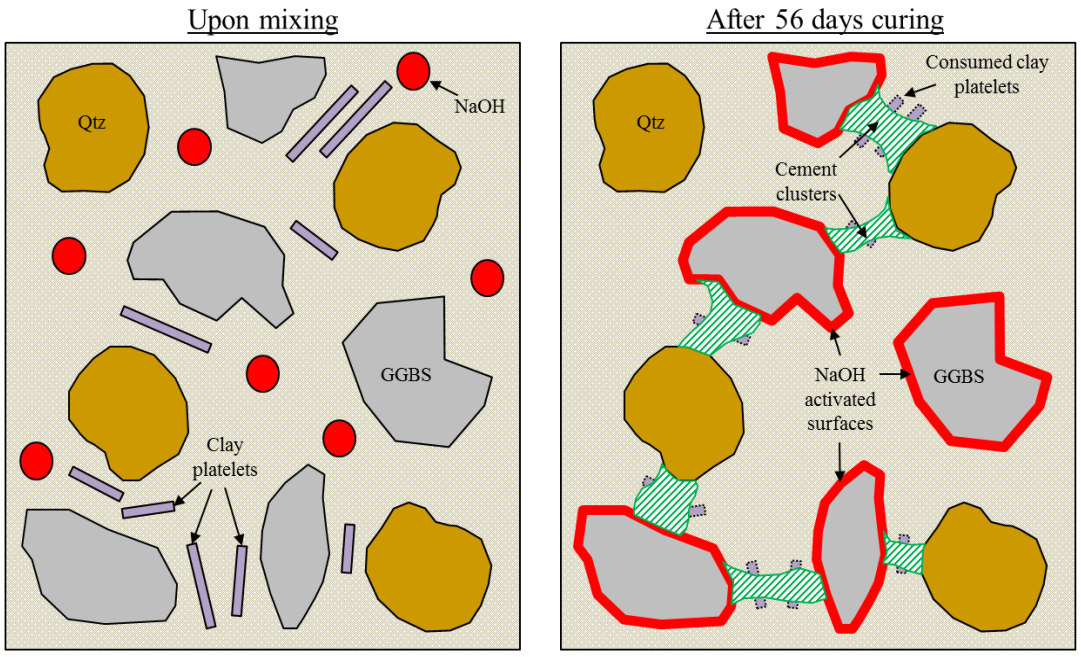

Figure 6.32: Illustration showing the importance of clay minerals in forming cementitious clusters within GGBS-NaOH stabilised Lanton alluvium's matrix. (Qtz = quartz, GGBS = ground granulated blast furnace slag).

Given the relatively low clay content of Lanton alluvium, it is possible that a large proportion of the clay minerals have already been used to form cementitious bonds after 56 days curing. Thus, any further strength enhancements within the material are not anticipated to be as significant as those observed between 21 and 56 days curing, unless a higher dosage of GGBS-NaOH is utilised. Should another natural soil with a higher clay fraction and water content of around 25% be stabilised with the GGBS-NaOH binder, it is anticipated that higher strength gains would be observed over 28 days curing and that pozzolanic reactions would continue for a longer period of time.

The very low TOC/TOM and sulphate contents of natural Lanton alluvium did not appear to interfere with cementitious reactions and therefore the subsequent formation and growth of cementitious bonds when stabilised with NaOH activated GGBS. Although, the soil's high moisture content appeared to influence the time taken for strength gains to be achieved and would be a major influencing factor in ettringite formation, no such minerals were observed within the stabilised soil after 28 or 56 days. This complements the impressive durability performances of the material in chapter 5; whereby the presence of AFt minerals would be apparent as they would

cause considerable levels of swelling within samples and consequently lead to their premature failure.

Although AFt mineral phases have not yet been observed within 7.5% GGBS-NaOH stabilised Lanton alluvium, future mineralogical and microstructural studies ought to be conducted to assess whether such minerals form after much longer curing periods (i.e. years). For such future studies, carefully prepared (polished) sections of stabilised samples should be analysed in order to take more detailed SEM micrographs of the internal structure of activated GGBS particles and cementitious mineral/gel growths. Polished section analyses would also provide better insights into the nature of pore spaces changes with curing (i.e. the nature of inter-particle contacts and the extent to which reaction products are infilling voids). Based on a recent study by Haha et al. (2011) on the hydration kinetics, associated mineral assemblages and microstructural development of NaOH activated GGBS, the formation of unfavourable AFt minerals is considered unlikely within Lanton alluvium, given its negligible sulphate content of 46 ppm.

Should the NaOH activated GGBS binder be used at the same dosage to stabilise other soils characterised by higher clay contents, it is likely that the binder will produce even higher strengths than those observed in this research for stabilised Lanton alluvium. More complex and denser microstructures would also be anticipated due to more extensive cementitious gel growths through the higher abundance of clay minerals available for reactions, thereby giving lower permeabilities and porosities. However, using the 7.5% GGBS-NaOH binder to stabilise soils containing even smaller quantities of clay (especially if the clay mineralogy is Kaolinite) compared with Lanton alluvium are unlikely to produce improved engineering performances that surpass those presented in this research. The dosage of the GGBS-NaOH to be used should take into consideration the organic, sulphate and moisture contents of the soil.

Chapter 7:

Phase 3: Monotonic and dynamic triaxial testing of Lanton alluvium

7.1 Introduction

Based on oedometer results in chapter 5, Lanton alluvium soil in its undisturbed state is characterised by a degree of initial (sedimentation) structure. However, the soil is considered fairly sensitive, as most of the soil's structure was lost when subjected to relatively low strains. It is likely that considerable reductions in initial structure and stiffness within Lanton alluvium will be observed if subjected to disturbances caused by deep soil mixing (DSM) processes and dynamic loading cycles typically associated with frequent high-speed train (HST) traffic. It should also be noted that the higher the frequency at which such disturbing processes/dynamic loads occur, the more sensitive any underlying soils are likely to be. Given the nature of Lanton alluvium, a comprehensive knowledge and understanding of the stiffness degradation, stress-strain and volume change behaviour of the untreated Lanton alluvium soil is required. This may be achieved through using conventional triaxial testing techniques under both monotonic and dynamic loading conditions.

This chapter investigates the behaviour of both reconstituted and undisturbed samples of Lanton alluvium under various drainage and mean effective stress conditions, by using conventional monotonic triaxial testing techniques at Newcastle University. It is hoped that the results obtained from these tests will complement oedometer testing results in defining the extent to which initial structure and higher levels of stiffness are lost within the soil through disturbances caused by DSM or static loads. Additionally, the response of Lanton alluvium when subjected to dynamic loads typically presented by an HST is also examined by using conventional dynamic triaxial testing techniques. The results obtained from all of these tests will provide useful insights into the magnitude of displacements, which may be experienced by high-speed railway tracks when founded over soft and potentially sensitive foundation soils similar to Lanton alluvium.

The findings from this chapter will provide useful comparisons to those in the next chapter for triaxial tests conducted on Lanton alluvium stabilised with a GGBS-NaOH binder. This will allow the influence of cementation on shearing behaviour at large and small strains to be investigated in detail.

7.1.1 Testing schedule and nomenclature

Triaxial samples were named in such a manner to easily determine the drainage conditions of tests, whether the sample was reconstituted or undisturbed and finally whether the test was dynamic or static. Below is a list of the letters and abbreviations used to name samples:

dyn = dynamic test

dis = disturbed/reconstituted sample

undis = undisturbed sample

l = normal loading test

l-u-r = loading-unloading-reloading loop test

The triaxial testing schedule followed during this research programme is summarised in Tables 3.5–3.7.

7.2 Monotonic results

The triaxial testing results on undisturbed and reconstituted Lanton alluvium obtained from Newcastle are hereby discussed. Small strain triaxial testing was also conducted on undisturbed Lanton alluvium at Bristol University, which involved the use of local strain and bender element measurements. For the results obtained from these tests, the reader is directed to Appendix 5.

7.2.1 Reconstituted samples

7.2.1.1 Shearing behaviour

The deviatoric stress response of reconstituted samples under undrained conditions with increasing axial strain are presented in Figures 7.1–7.2; whereas the deviatoric stress response of samples under drained conditions are shown in Figures 7.3–7.4. Figures 7.2 and 7.4 also show a series of unload-reload loops conducted during triaxial tests. It is clear from Figures 7.1–7.4 that the majority of samples sheared at p'_0 values of 50 and 150 kPa displayed clear evidence of work hardening behaviour between small and large strains up to failure. However, samples which were consolidated to p'_0 values of 200–250 kPa started to show signs of strain softening at larger strains (>6% for undrained tests and >10% for drained tests).

The average drained and undrained shear strengths obtained for the reconstituted Lanton alluvium at p'_0 = 50 kPa were 65 kPa and 29 kPa, respectively. Young's modulus measurements were taken for all undrained and drained triaxial tests using both the tangential and secant methods. For undrained samples consolidated to a p'_0 = 50 kPa, secant and tangential E_u values of 7.10 and 11.67 MPa were recorded respectively; whereas for drained tests consolidated to a p'_0 = 50 kPa, secant and tangential E' values of 3.28 and 10.79 MPa were obtained. Per the literature (Atkinson, 2000) and analytical results from this testing programme, using the secant method for determining Young's modulus along with bulk and shear moduli is preferred over the tangential method. This is because the secant method provides much better quality, tighter fitting stiffness-strain curves and that higher, more representative stiffness values are obtained.

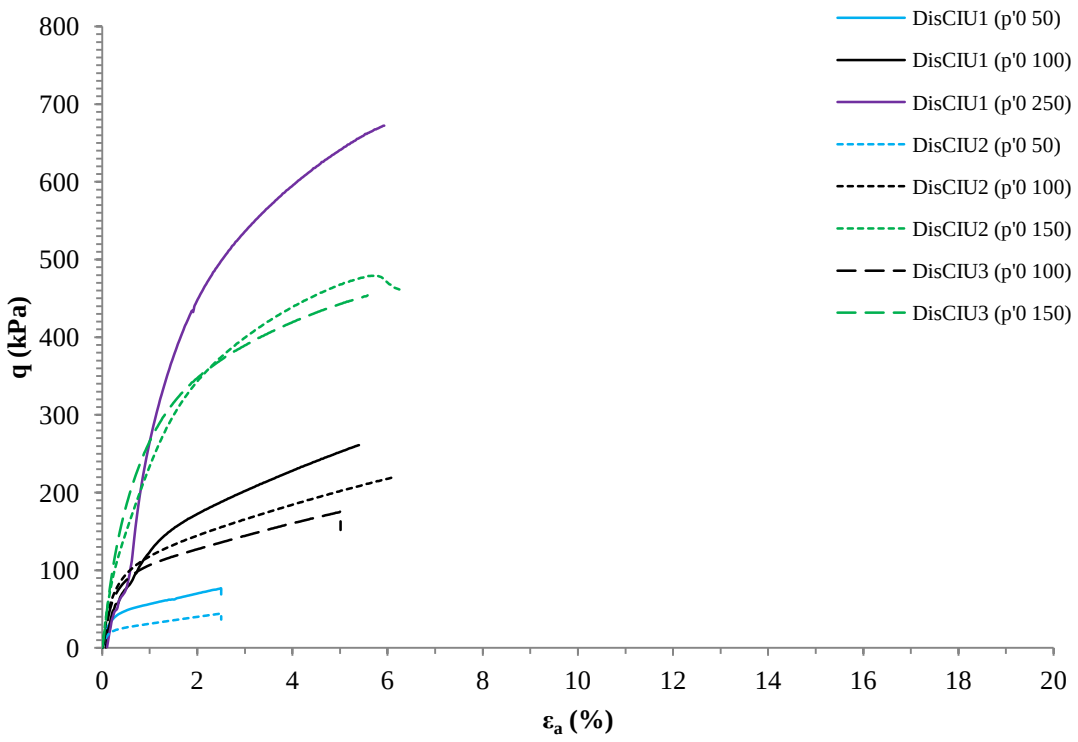

Figure 7.1: Deviatoric stress-strain behaviour of undrained reconstituted samples of Lanton alluvium.

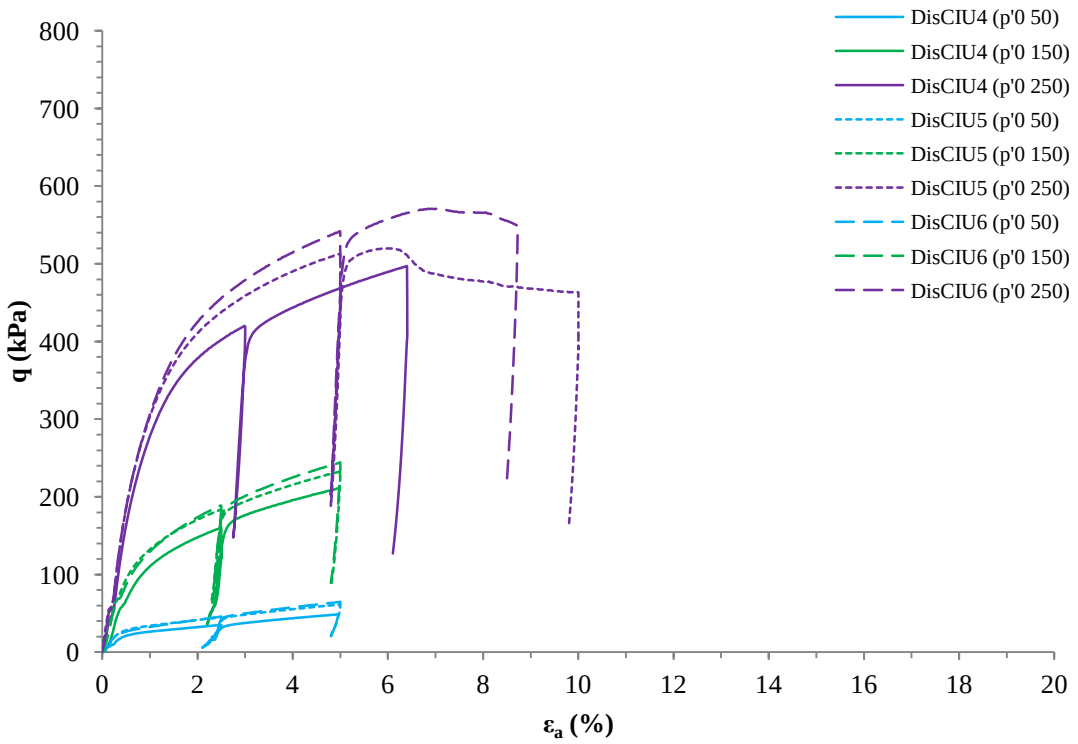

Figure 7.2: Unload-reload deviatoric stress-strain behaviour of undrained reconstituted samples of Lanton alluvium.

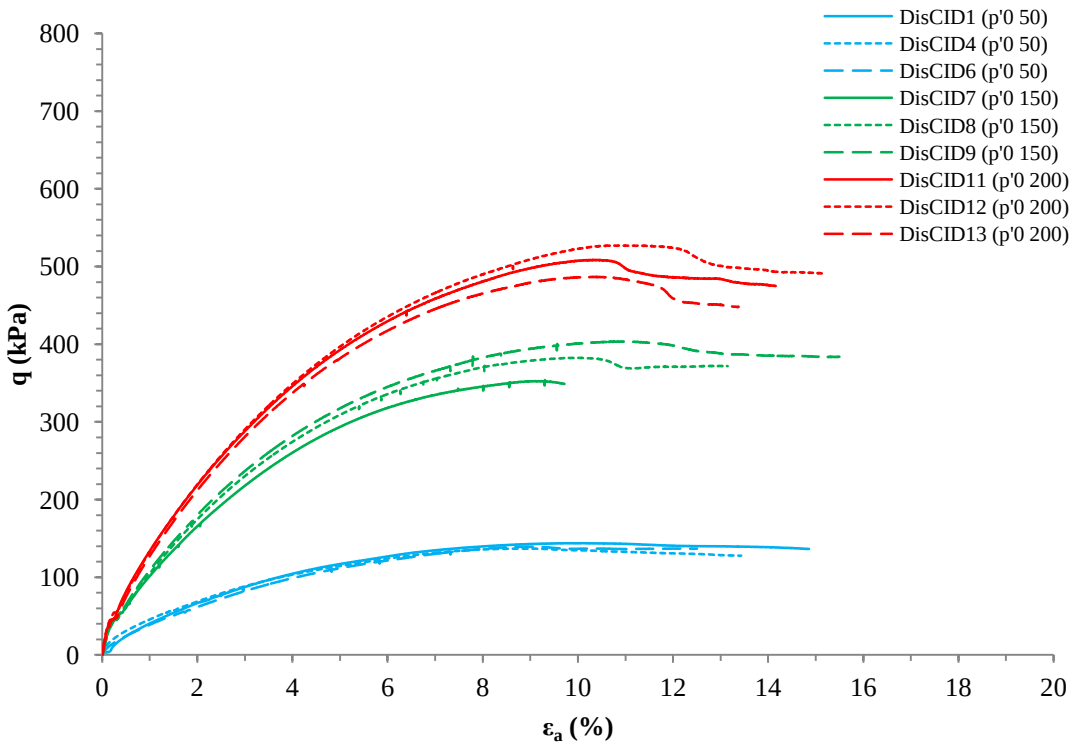

Figure 7.3: Deviatoric stress-strain behaviour of drained reconstituted samples of Lanton alluvium.

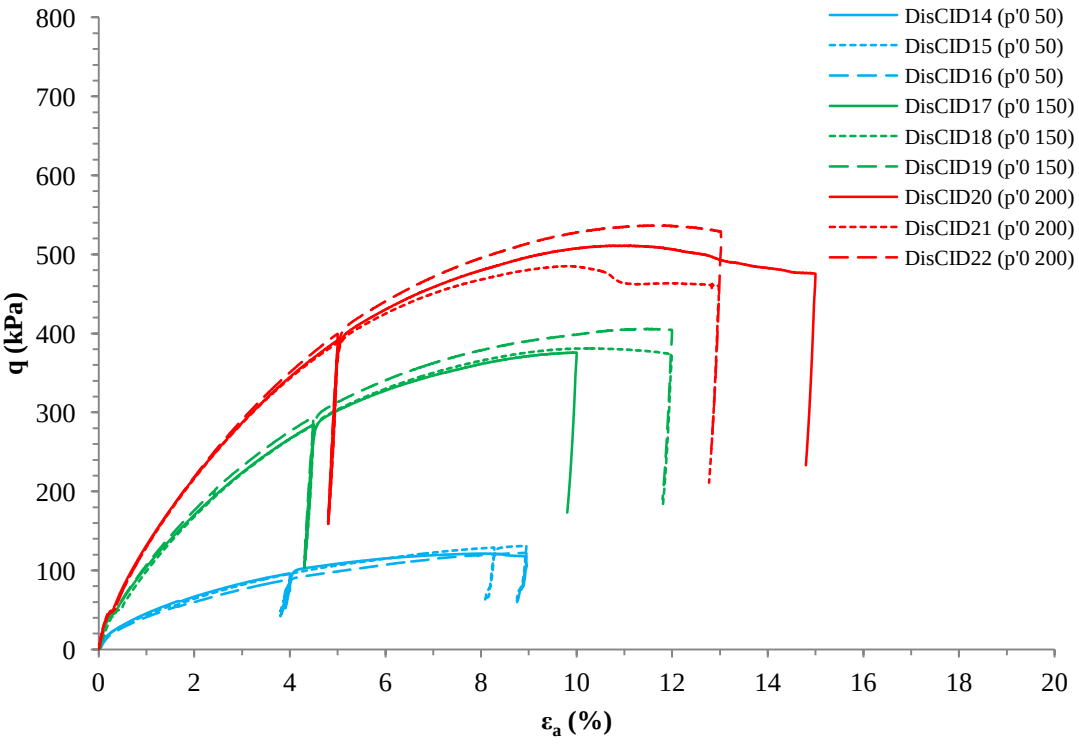

Figure 7.4: Unload-reload deviatoric stress-strain behaviour of drained reconstituted samples of Lanton alluvium.

The differences between the E' and E_u values may be explained by the strain rates used during these tests. For undrained tests a strain rate of 0.05 mm/min was used, whereas for drained tests the rate was 0.01 mm/min. The faster rate of loading for samples during undrained tests inherently resulted in higher apparent stiffnesses being calculated compared with those for drained tests.

The pore pressure response of samples when sheared under undrained conditions is displayed in Figure 7.5. For tests conducted at p'_0 values of 50 kPa, the pore pressures within the samples increased up to 20–40 kPa at axial strains of 1%; at which point the pore pressures remained fairly constant with further straining until sample failure. In contrast, pore pressure development within undrained samples tested at p'_0 values of 100–250 kPa were characterised by reaching a distinct peak at 2% axial strain of 50 kPa for tests conducted at p'_0 = 100–150 kPa, and 90 kPa for tests using a p'_0 = 250 kPa. With increased straining, a gradual reduction in pore pressure of 30–50 kPa was then observed within these samples until failure.

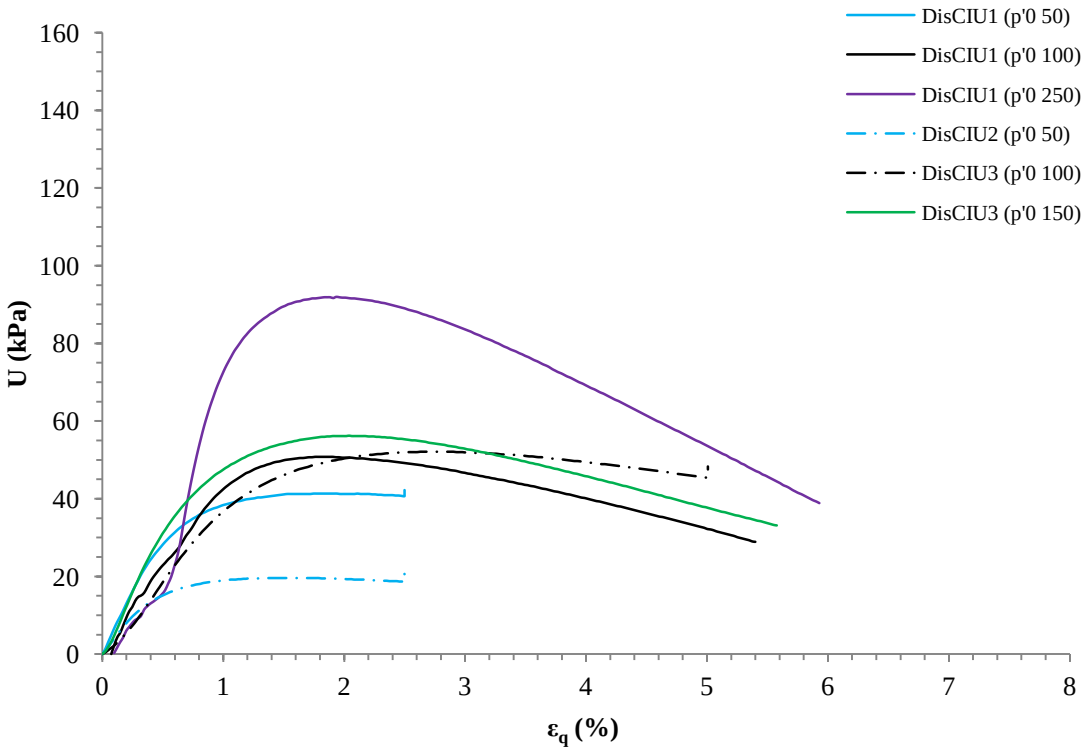

Figure 7.5: Pore pressure behaviour of undrained reconstituted samples of Lanton alluvium.

Along with the clear contractional normally consolidated behaviour observed for the reconstituted Lanton alluvium samples, there is some evidence for dilation at larger strains, as observed in Figure 7.6b for drained tests. Albeit samples did not dilate to the extent that negative volumetric strains were measured, the degree of dilation experienced by samples may be attributed to their void ratio characteristics, whereby samples with lower void ratios (0.5–0.6) experienced more dilation than those with higher void ratios (0.7). In general, higher degrees of dilation were also observed within samples which were tested at lower p'_0 values. The lower effective confining pressure allowed particle rearrangement to occur more easily compared with higher effective confining pressures.

Regarding accurately identifying the point at which dilation occurs within samples, Figures 7.6a and 7.6b show that for tests conducted at p'_0 values of 50, 150 and 200 kPa, the onset of dilation was observed at shear strains of 5, 6.5 and 7.5%, respectively. It is at these points when the samples almost reached their peak deviatoric strengths; thereby implying that the sample's stress paths were close to reaching the critical state line. Upon reaching an approximate shear strain of 10%, most of the samples in Figure 7.6b showed evidence of dilation becoming suppressed, which also corresponds with most of the samples reaching their maximum deviatoric stress values. This indicates at 10% shear strain, most of the reconstituted samples had probably reached their critical state, at which point no further significant volumetric changes are expected to occur with further straining. However, zero volumetric strain was not observed within any of the samples tested during this testing programme. Also, strain localisation and the development of shear planes were generally not recorded within any reconstituted samples.

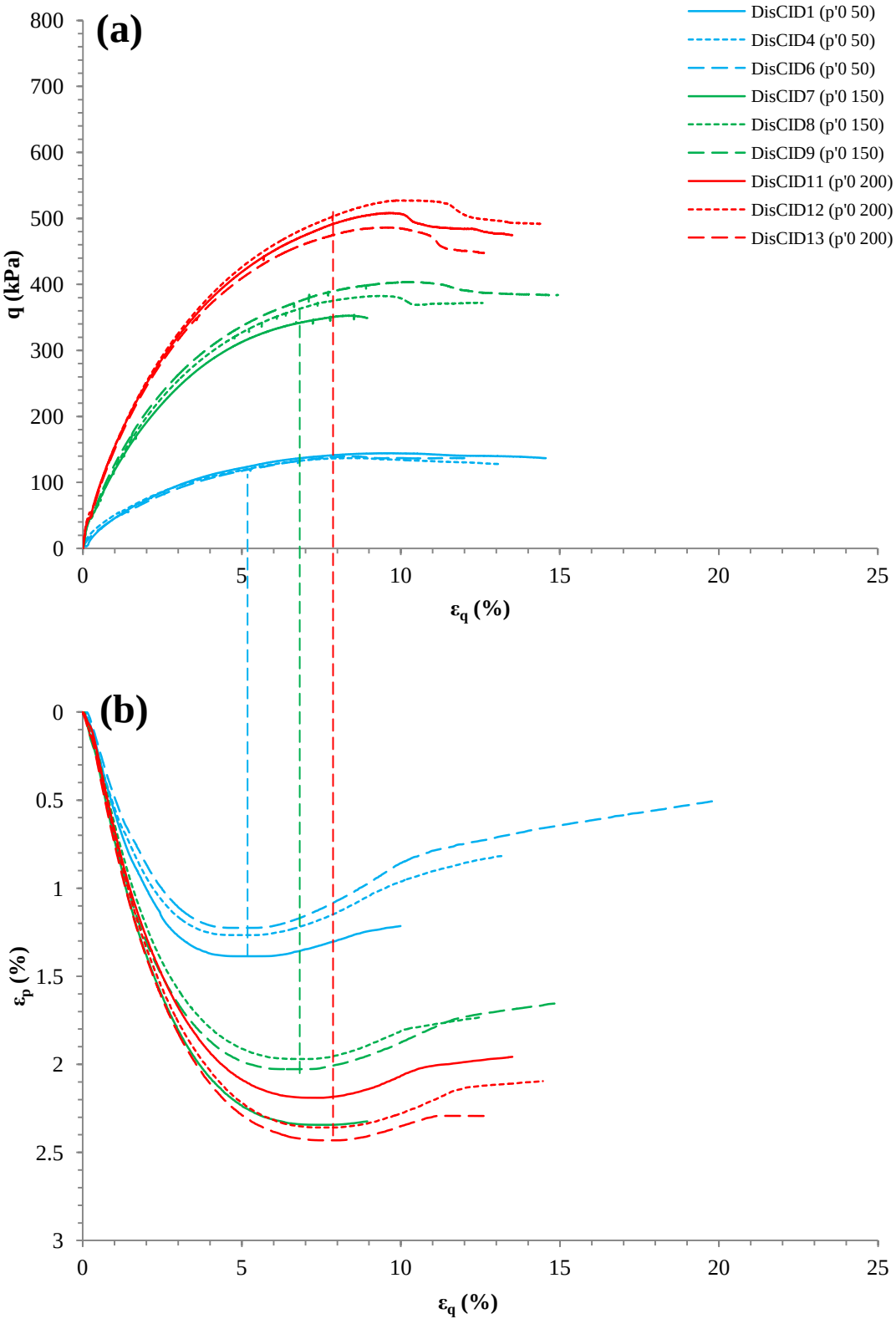

Figure 7.6: (a) Deviatoric stress and (b) volumetric strain response drained reconstituted Lanton alluvium samples with increasing shear strain.

7.2.1.2 Stress dilatancy

The stress dilatancy behaviour of reconstituted Lanton alluvium samples is displayed in Figure 7.7, whereby all samples appear to display frictional behaviour. They compress to ultimately reach similar critical state M values ranging between 1.3 and 1.4. No dilation behaviour is observed within any samples until an M value of approximately 0.7 is reached. As implied in Figure 7.6b, samples tested at p'_0 values of 150 and 200 kPa experienced smaller degrees of dilation with increasing shear strain compared with samples tested at a p'_0 of 50 kPa.

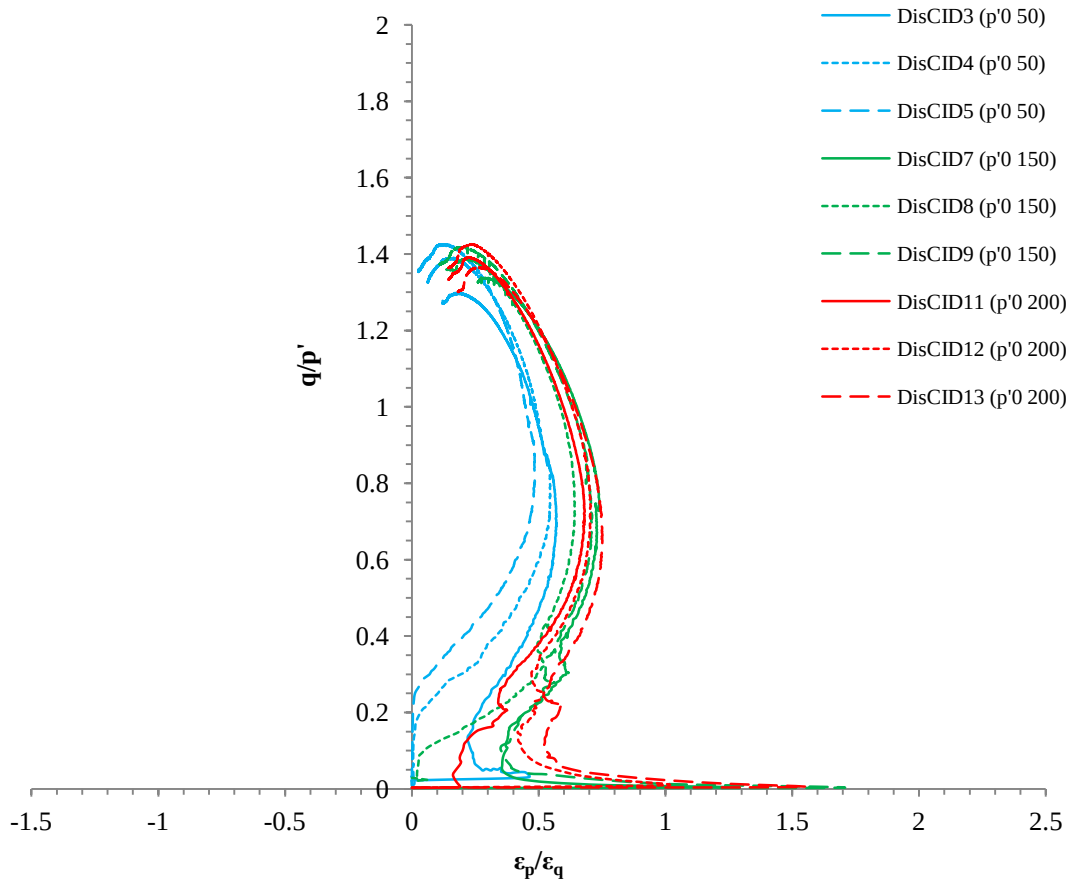

Figure 7.7: Stress-dilatancy behaviour of drained reconstituted samples of Lanton alluvium.

Shear strains of approximately 10% marked the end of samples' peak rates of dilation, after which a degree of suppression in the amount of dilation experienced was

observed along with a slight reduction in stress ratio. By taking the slope (M*) of the dilation segments of the volumetric-shear strain curves in Figure 7.6b, a dilation angle (ψ) for the reconstituted Lanton alluvium may be calculated through the use of Equation 3.43.

Generally for non-cohesive (sandy) soils, ψ may be calculated by subtracting 30^o from the friction angle (φ'); whereas for cohesive (clayey) soils, $\psi \approx 0$. Values for the material's dilation angle generally fell within the range of 1.0–1.5^o; whereby higher dilation angles were generally observed for samples tested at lower p'_0 values. Higher dilation angles of up to 2.3^o were also recorded for a few samples tested at p'_0 values of 50, 150 and 200 kPa. Such high dilation angles are attributable to the slight density variations to which samples were compacted.

7.2.1.3 Failure envelopes

Based on the silt and sand content of Lanton alluvium, the soil was expected to behave as a frictional granular material. The Mohr-Coulomb failure envelopes for the drained and undrained samples are shown in Figure 7.8, along with the maximum τ values recorded for each sample (Mohr circle) tested.

The failure envelopes for the undrained and drained tests are very close to each other. Hence, reconstituted samples were characterised by an average effective cohesion (c') value of 2.35 kPa and an average effective friction angle (φ') of 34.1^o.

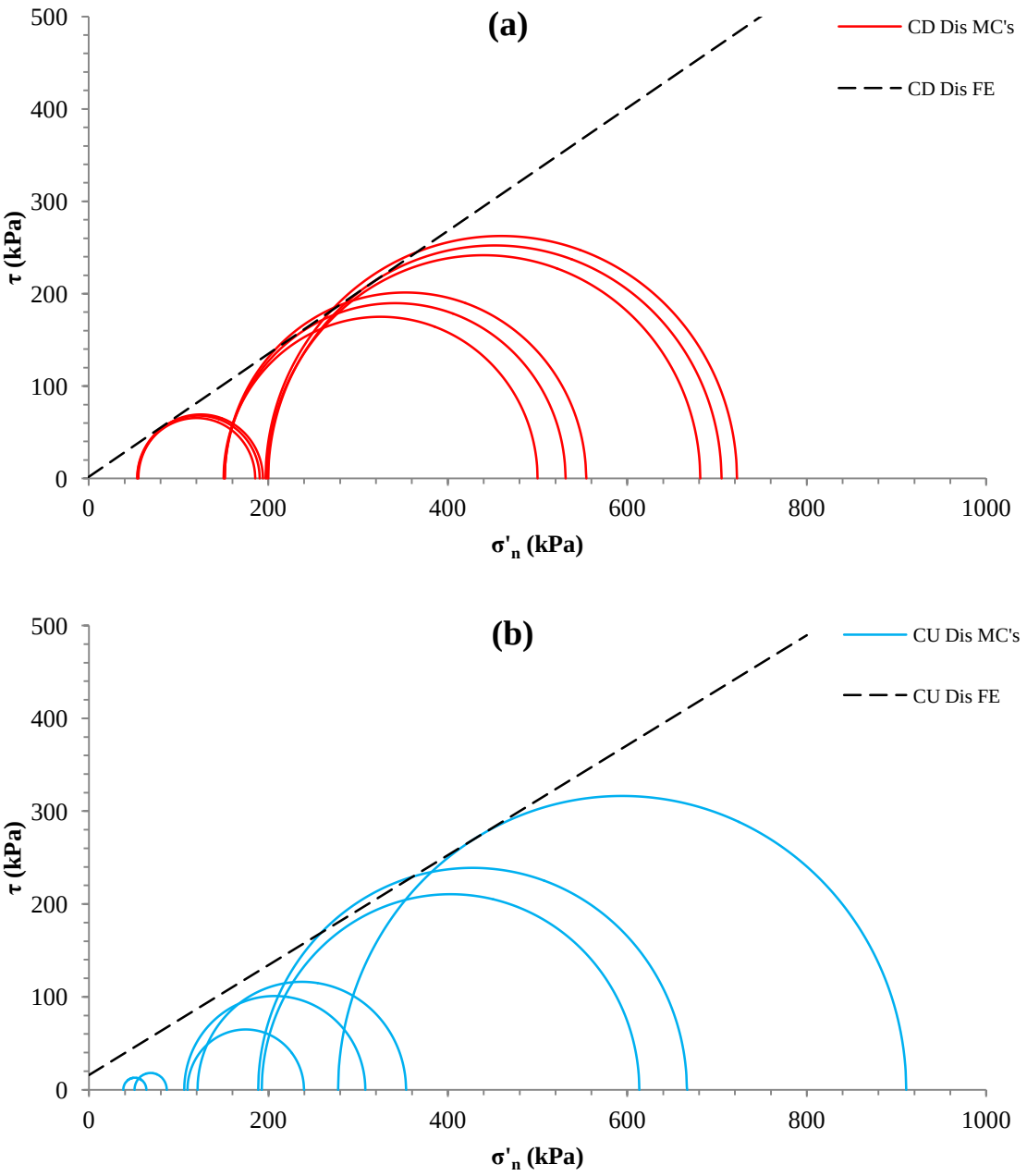

Figure 7.8: Mohr-Coulomb failure envelopes (FE) and peak τ-σ'$_n$ values obtained from (a) drained and (b) undrained reconstituted samples of Lanton alluvium.

Within q-p' stress space (Figure 7.9), the shape of the undrained stress paths demonstrate the soil experienced strain hardening with very limited softening; and drained paths exhibited the 1:3 slope typically expected for all drained triaxial tests. Per Muir Wood (1990), the Cam Clay model states that stress paths for normally consolidated soils such as Lanton alluvium end up touching and following the critical state line (CSL); whereby their critical state conditions coincide with the maximum

deviatoric stresses experienced, i.e. the soil's failure envelope. The CSL almost passes through the origin, as would typically be expected for frictional granular soils. Based on all of the undrained tests conducted on the reconstituted Lanton alluvium, an average M value (slope of CSL) of 1.45 was obtained for the CSL; whereas an average M value of 1.39 was obtained for the CSL based on drained triaxial tests.

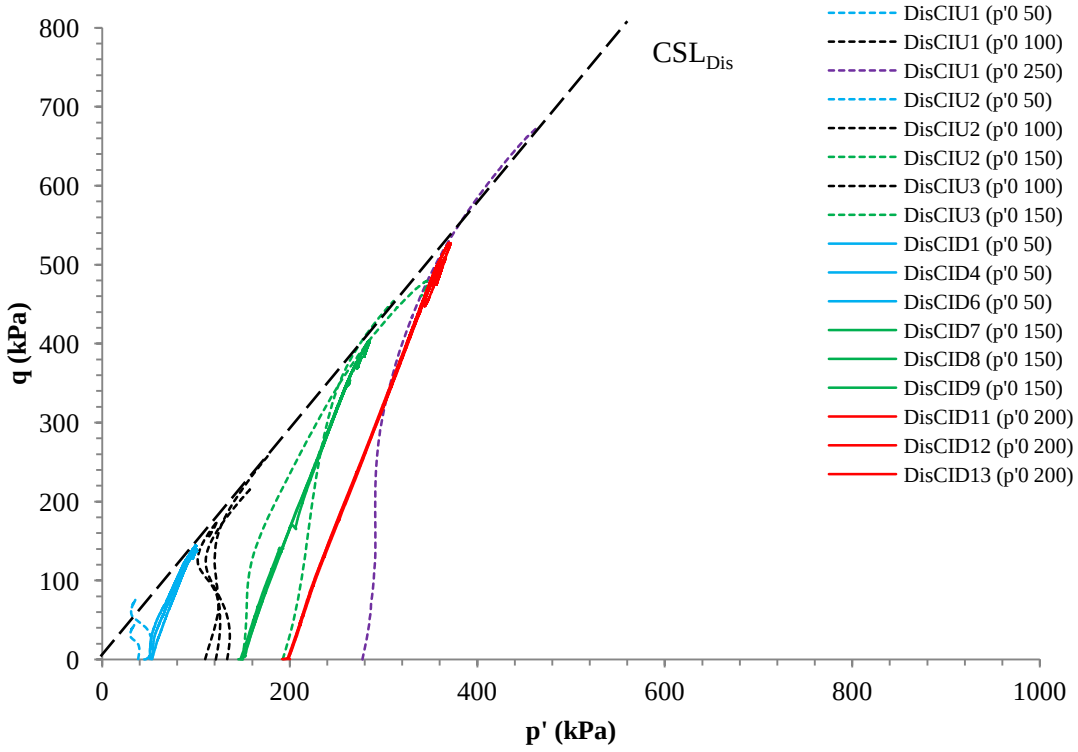

Figure 7.9: Drained and undrained stress paths and CSL within the q-p' stress plane for all reconstituted Lanton alluvium samples.

By using the average of these M values (1.42), an average φ' value of 35.04^{o} was obtained via the following formula taken from Muir Wood (1990):

Effective friction angle: $$sin\phi' = \frac{3M}{6+M}$$ **(Equation 7.1)**

In order to calculate the c' value for the reconstituted Lanton alluvium from the CSL and φ' data, the following equation (taken from Muir Wood ,1990) may be used:

Effective cohesion: $$c' = \frac{3-sin\phi'}{6cos\phi'}$$ **(Equation 7.2)**

whereby an average c' value of 0.5 kPa was calculated. Figures 7.10 and 7.11 display all the monotonically loaded undrained and drained effective stress paths obtained for the reconstituted Lanton alluvium. All the stress paths have been normalised by their respective p'_0 values.

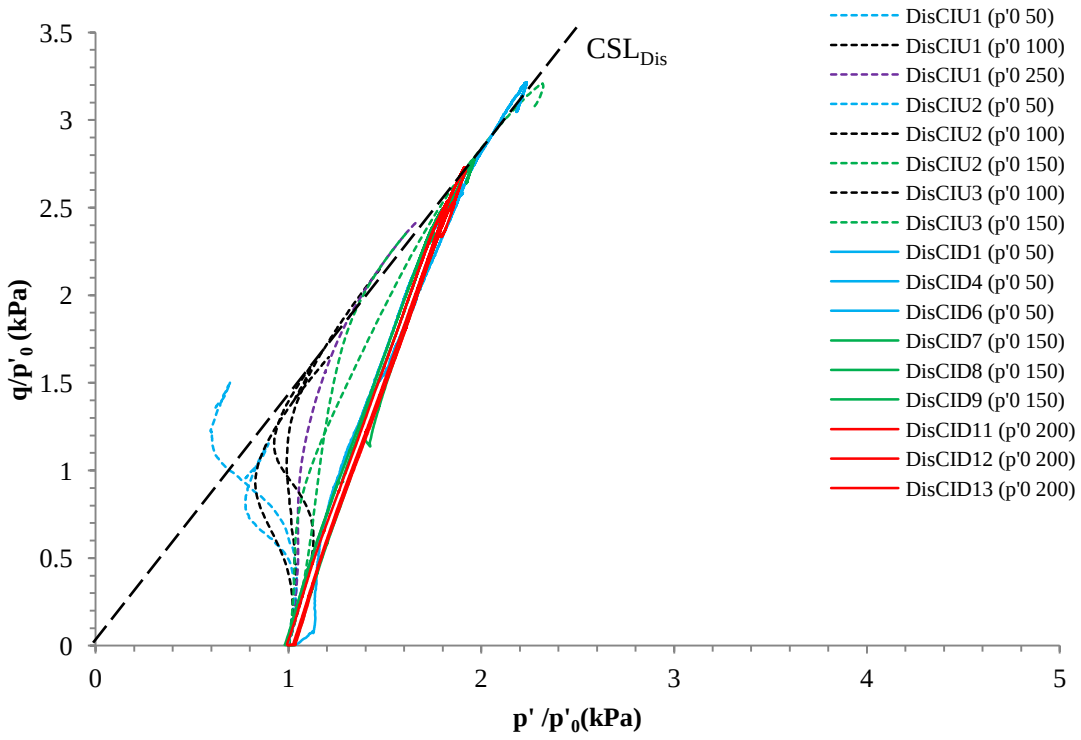

Figure 7.10: Drained and undrained stress paths for reconstituted Lanton alluvium samples within the q/p'_0-p'/p'_0 stress plane, normalised by their corresponding p'_0 values.

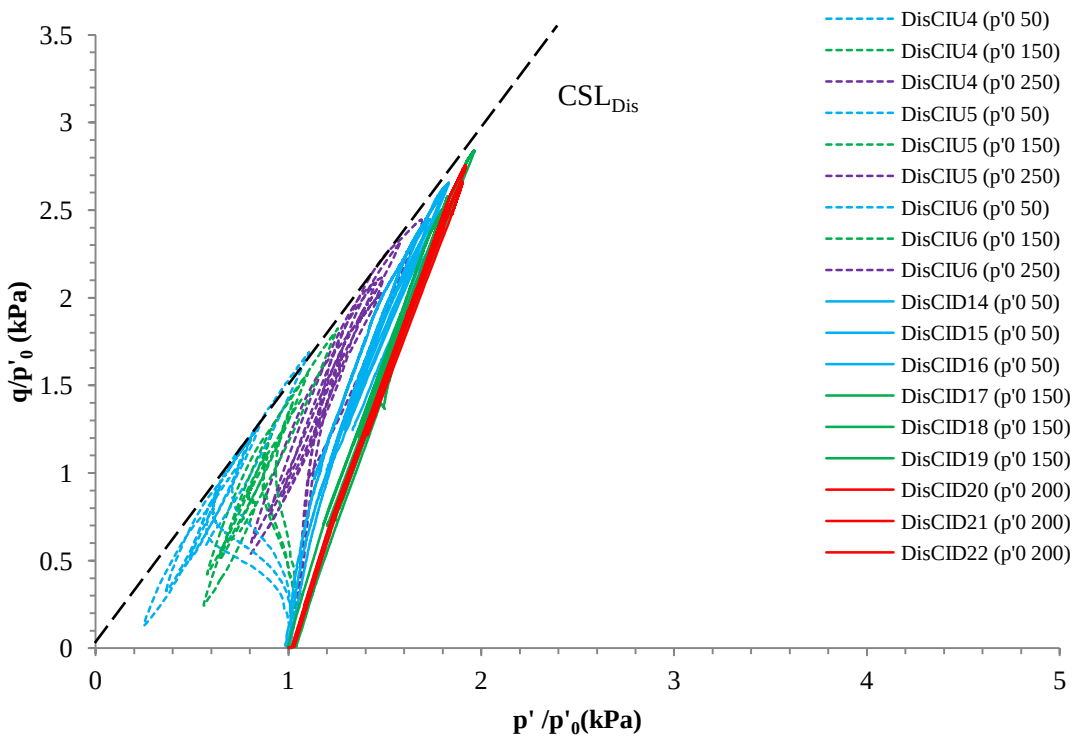

Figure 7.11: Drained and undrained unload-reload stress paths for reconstituted Lanton alluvium samples within the q/p'_0-p'/p'_0 stress plane, normalised by their corresponding p'_0 values.

The figures demonstrate the effect of mean effective stress to which the samples were consolidated on the maximum q values achieved during testing, with higher p'_0 states producing higher q values up to failure. Making the q and p' axes non-dimensional through normalising by p'_0 also allows the loci of points of peak deviatoric strength for each undrained and drained sample tested to form a single locus within the q/p'_0-p'/p'_0 plane (Muir Wood, 1990).

The failure envelope and hence CSL for reconstituted Lanton alluvium was also determined by producing compression curves from drained triaxial data within the specific volume (v) – p' compression plane. Per Muir Wood (1990), under isotropic compression the (virgin) compression curves/lines (VCL) for a given soil within the compression plane ultimately converge to define a normal compression line (NCL). The VCL's recorded from drained triaxial tests conducted on the reconstituted soil are shown to define a potential CSL and NCL in Figure 7.12.

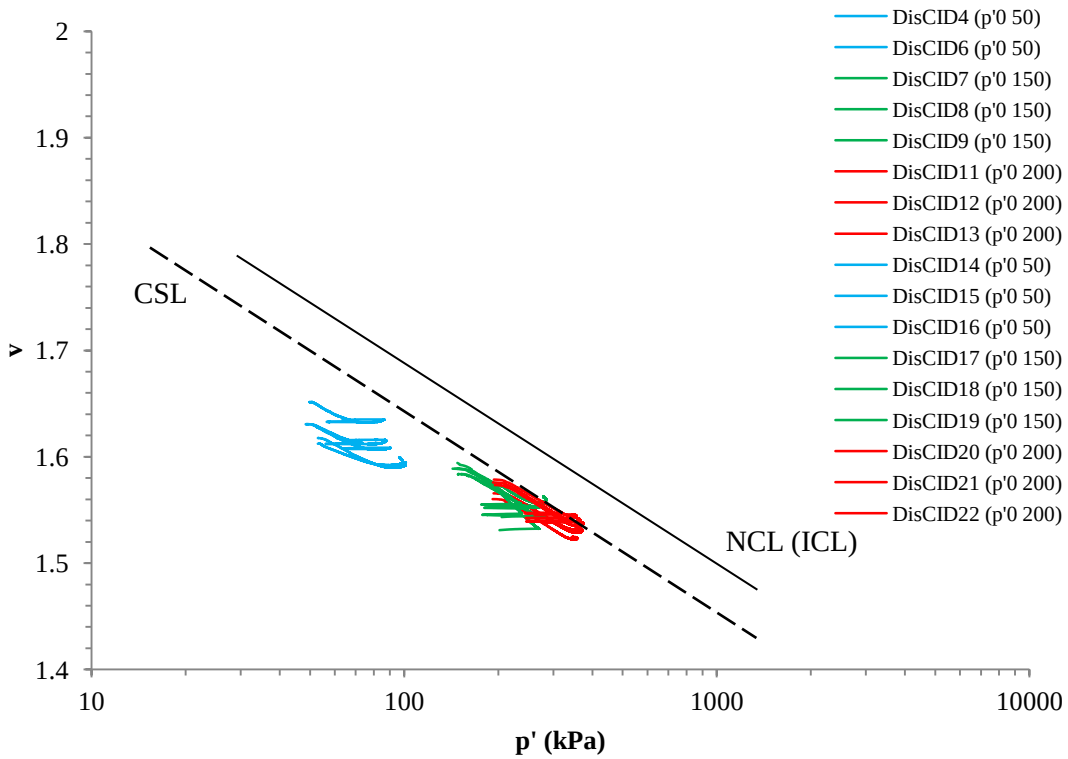

Figure 7.12: CSL and ICL within the υ – ln p' stress plane, obtained from drained reconstituted Lanton alluvium samples.

Given that these VCL paths and possible NCL correspond to the reconstituted Lanton alluvium, the NCL may be defined as the soil's intrinsic normal compression line (ICL). The ICL defined in Figure 7.12 is used later in this chapter to quantify the initial degree of sedimentation structure within the undisturbed Lanton alluvium, by comparing the relative positions of the ICL with the NCL. Note: the ICL defined from triaxial tests in Figure 7.12 is different to that defined in Figure 5.15 from oedometer testing and should not be confused. The VCL's produced from triaxial testing involve a direct measurement of volume change during sample compression, whereas no such measurements are taken during oedometer tests. Hence, although the two laboratory tests are able to define the Lanton alluvium's ICL, it is the author's opinion that triaxial testing be the preferred method for defining the soil's ICL in the compression plane.

7.2.1.4 Stiffness degradation

As previously mentioned, the secant method was used to calculate how the shear and bulk stiffnesses of Lanton alluvium degrade with progressive shear straining. Figure 7.13 shows the G_{sec} degradation of all undrained reconstituted samples tested.

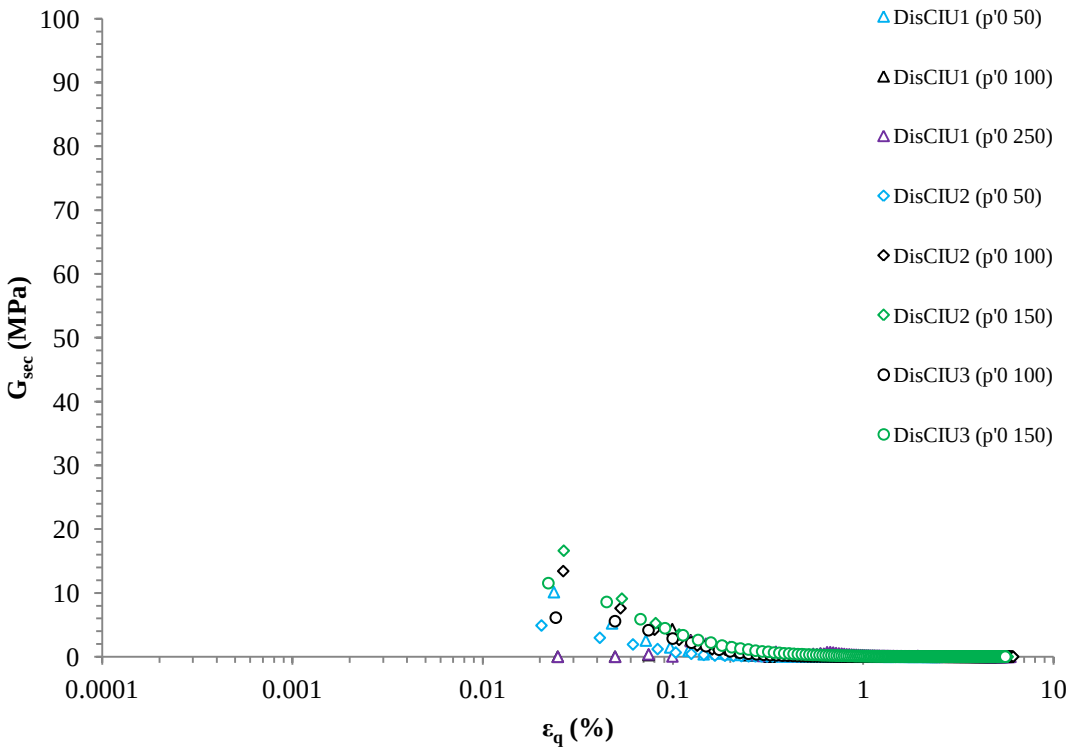

Figure 7.13: Secant shear stiffness degradation behaviour for undrained reconstituted Lanton alluvium samples.

From Figure 7.13, no G_{sec} values could be calculated at shear strains smaller than 0.02%. This highlights the lower resolution of stiffness and strain data obtained from using global rather than local strain measurements. Hence, the soil's initial shear stiffness (G_{max}) at the start of shearing and its subsequent degradation behaviour within the very small and small strain ranges unfortunately has not been captured. Further to the methodologies chapter, such small strain data is essential in geotechnical design as strains around geotechnical structures are also small. The results obtained at Bristol University (see Appendix 5) were of higher resolution than

the shear stiffness degradation data presented above and therefore provide better insights into the shear stiffness degradation behaviour of Lanton alluvium within the very small and small strain ranges.

In general, Figure 7.13 illustrates that the shear stiffnesses of the samples at shear strains <0.1% were considerably higher than those at shear strains >0.1%. Once samples had experienced shear strains >1%, their shear stiffnesses were negligible and remained so until either sample failure or cessation of testing. Another significant observation from the data in Figure 7.13 is that even though the secant method was used to calculate changing shear stiffnesses during testing, there is considerable data scatter. This may be attributed to the different tests being consolidated to different p'_0 values. Hence, the shear stiffness data has been normalised, with a view to fitting all of the results from the tests to a much tighter, better correlated curve. Normalised results are given in Figure 7.14.

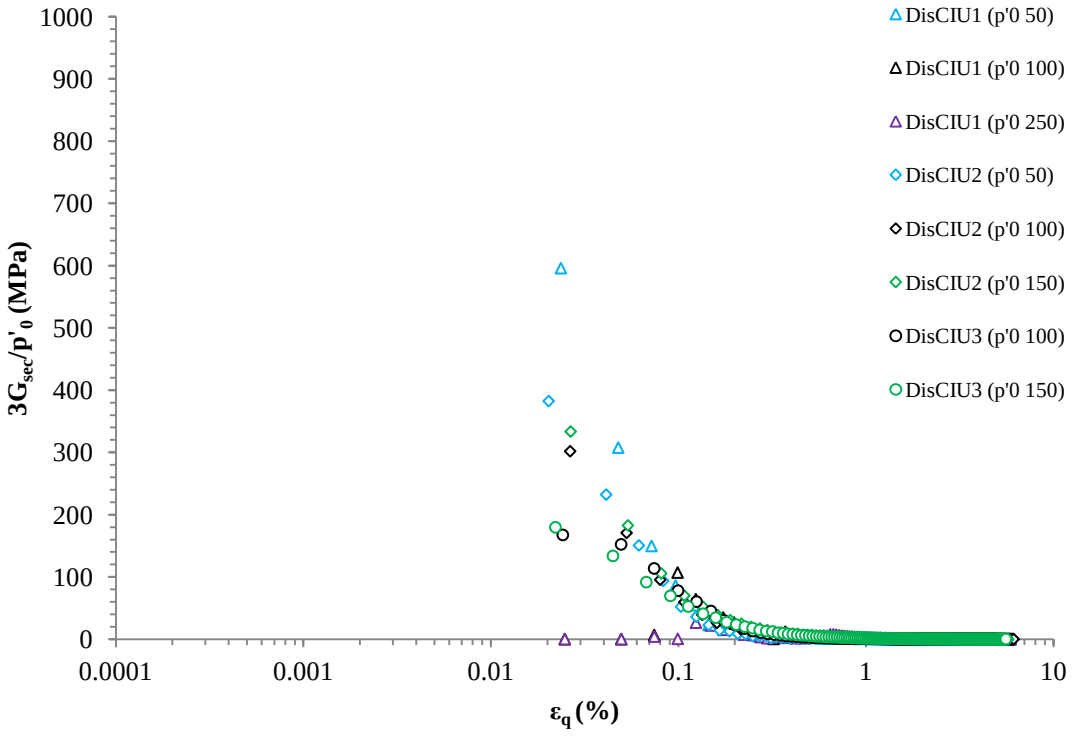

Figure 7.14: Secant shear stiffness degradation behaviour for undrained reconstituted Lanton alluvium samples, normalised by their corresponding p'_0 values.

Figure 7.14 demonstrates that normalisation has been moderately successful in producing a tighter fitting curve. However, there are still instances where normalisation was less successful - particularly for the DisCIU1 (p'0 250) sample and for all other samples at shear strains <0.06%. Shear stiffness degradation plots obtained for drained tests using non-normalised and normalised G_{sec} values are displayed in Figures 7.15–7.16, respectively.

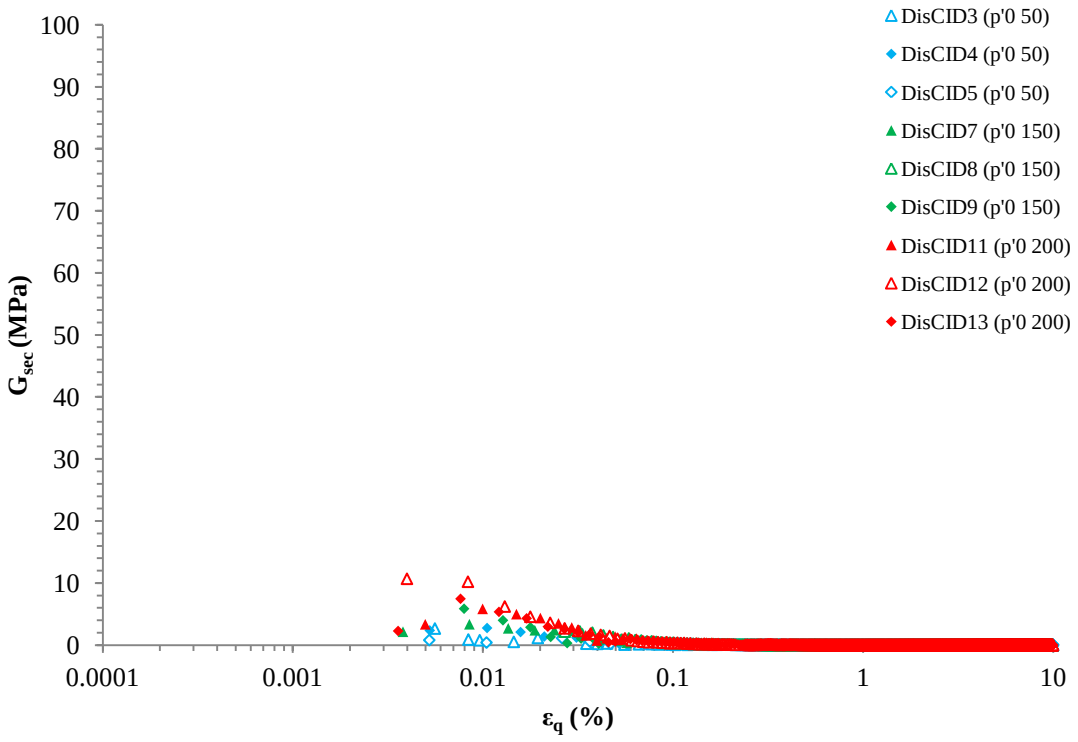

Figure 7.15: Secant shear stiffness degradation behaviour for drained reconstituted Lanton alluvium samples.

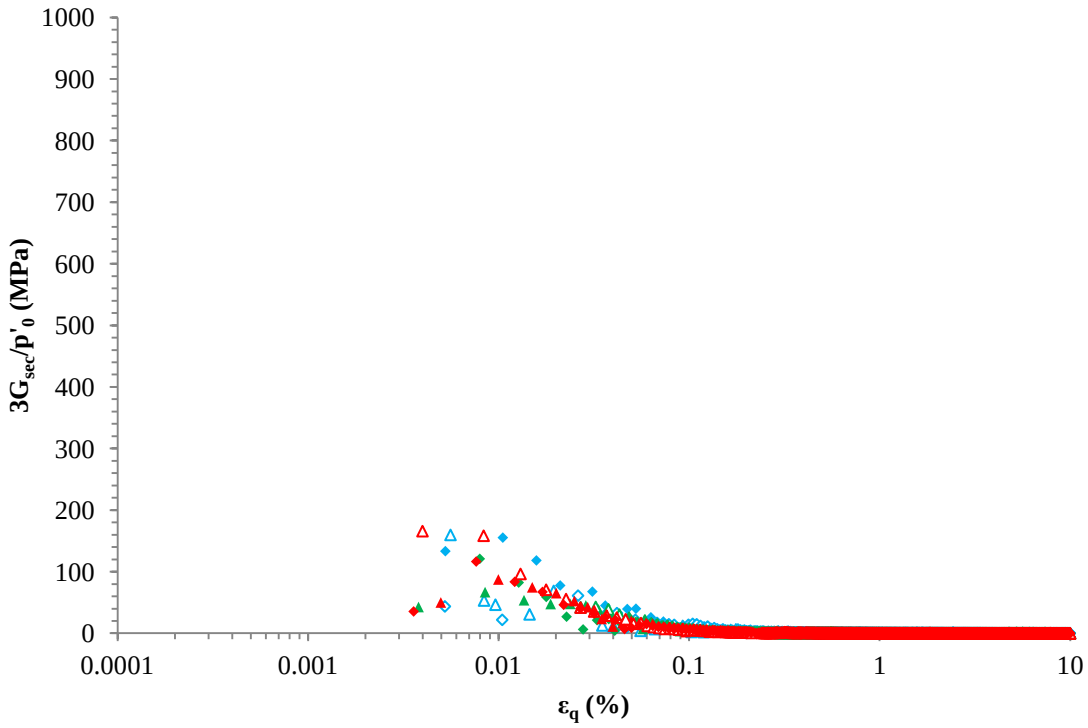

Figure 7.16: Secant shear stiffness degradation behaviour for drained reconstituted Lanton alluvium samples, normalised by their corresponding p'_0 values.

Similar observations may be made for the drained shear stiffness degradation plots, whereby normalisation produces a slightly tighter fitting curve. However, a degree of scatter is still apparent within the data for shear strains <0.02%, particularly for samples consolidated to a p'_0 value of 50 kPa.

The measured degradation in bulk stiffness for samples during drained tests is shown in Figure 7.17. One major difference with this data compared with that in the drained shear stiffness degradation plot (Figure 7.15) is the much larger spread of data across the small strain range. The bulk stiffness data plotted within the very small – small strain ranges in Figure 7.17 should not be considered completely reliable in defining the true bulk stiffness behaviour of reconstituted Lanton alluvium. This is because the ELDYN apparatus at Newcastle University only used global strain measurements.

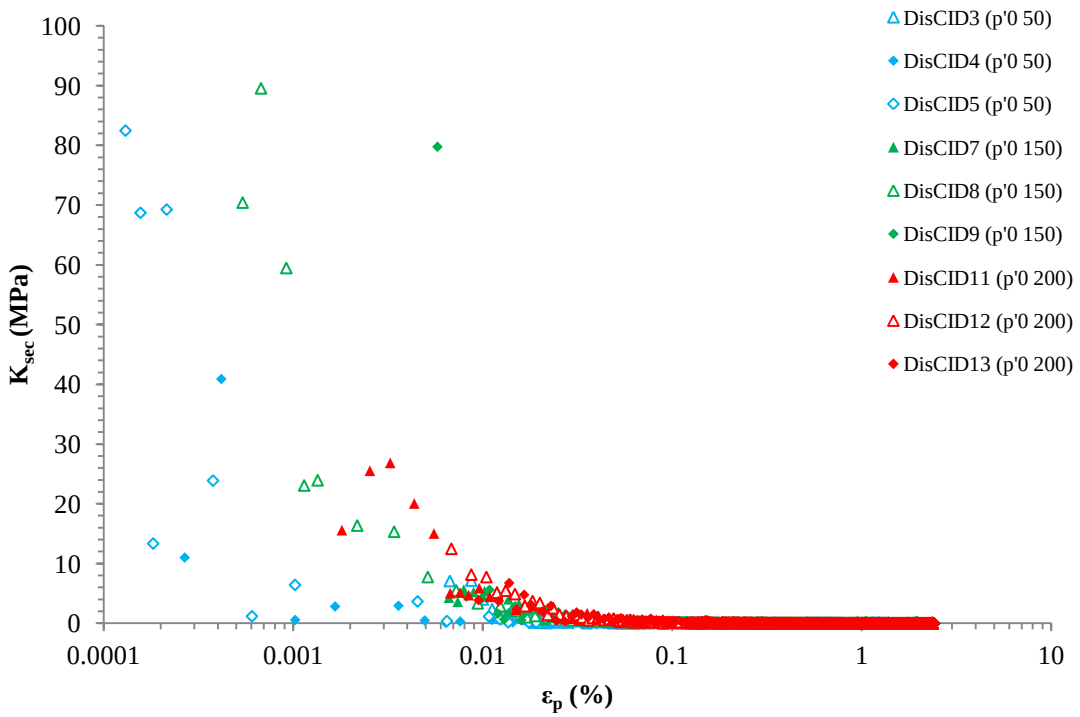

Figure 7.17: Secant bulk stiffness degradation behaviour for drained reconstituted Lanton alluvium samples.

The reasoning behind the presence of the apparent bulk stiffness data within the small strain ranges may be associated with the method used to calculated secant bulk stiffnesses. Whilst the normalised bulk stiffness data in Figure 7.18 brings the data towards a tighter fitting curve at volumetric strains <0.01%, normalisation appears to have had no effect on resolving the data scatter at small strains.

Although Jardine et al. (1986), Rouili (2007) and Simpson and Rouainia (2012) demonstrated that normalising shear and bulk stiffnesses by their initial p'_0 values produces tighter fitting curves (whereby the higher the p'_0 value, the stiffer the soil during testing), this normalisation technique was not as successful when applied to bulk and shear stiffness data sets obtained from this testing programme. Varying degrees of data scatter were still apparent – especially for bulk stiffness degradation plots.

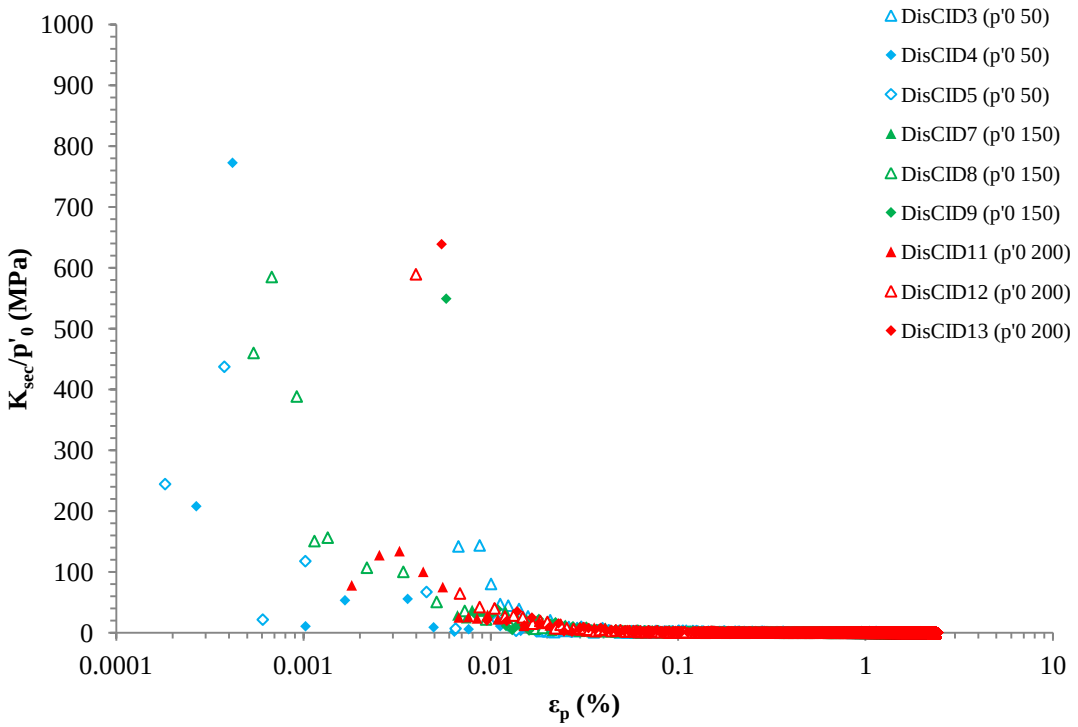

Figure 7.18: Secant bulk stiffness degradation behaviour for drained reconstituted Lanton alluvium samples, normalised by their corresponding p'_0 values.

If all tests were conducted on highly comparable samples of similar high quality, any scatter within the data sets ought to be corrected for by normalisation. However, as this scatter still exists after normalisation, factors other than p'_0 must also play a role in the bulk and shear stiffnesses of the soil samples tested. Slight variations associated with sample quality due to the sample preparation technique adopted may be a contributing factor. Per Lee et al. (2004), slight variations in the fines content of silty sand soils can cause considerable variations in strength and stiffness. Hence, whilst a general PSD curve has been produced for the soil in chapter 5, it is possible that the various reconstituted samples tested had slightly different soil grading curves to each other. Finally, the amount of time taken by samples to consolidate prior to shearing may also have had an effect, as longer consolidation times tend to produce stiffer samples.

7.2.2 Undisturbed samples

7.2.2.1 Shearing behaviour

Figures 7.19–7.20 present the deviatoric-strain responses of undisturbed Lanton alluvium samples during undrained and drained tests, respectively. Like undrained reconstituted samples, undisturbed samples which were consolidated to p'_0 values of 50 and 150 kPa displayed work hardening behaviour up to failure (Figure 7.19), whereas undrained samples consolidated to p'_0 values of 250 kPa experienced strain softening at larger strains >7%. Work hardening was predominantly observed during drained tests conducted on undisturbed samples. However, for undisturbed samples consolidated to a p'_0 of 50–150 kPa, higher degrees of strain softening were experienced (Figure 7.20) compared with their reconstituted counterparts. The UndisCID3 (p'0 200) sample was the only exception, as it displayed no signs of softening even when sheared to very large strains.

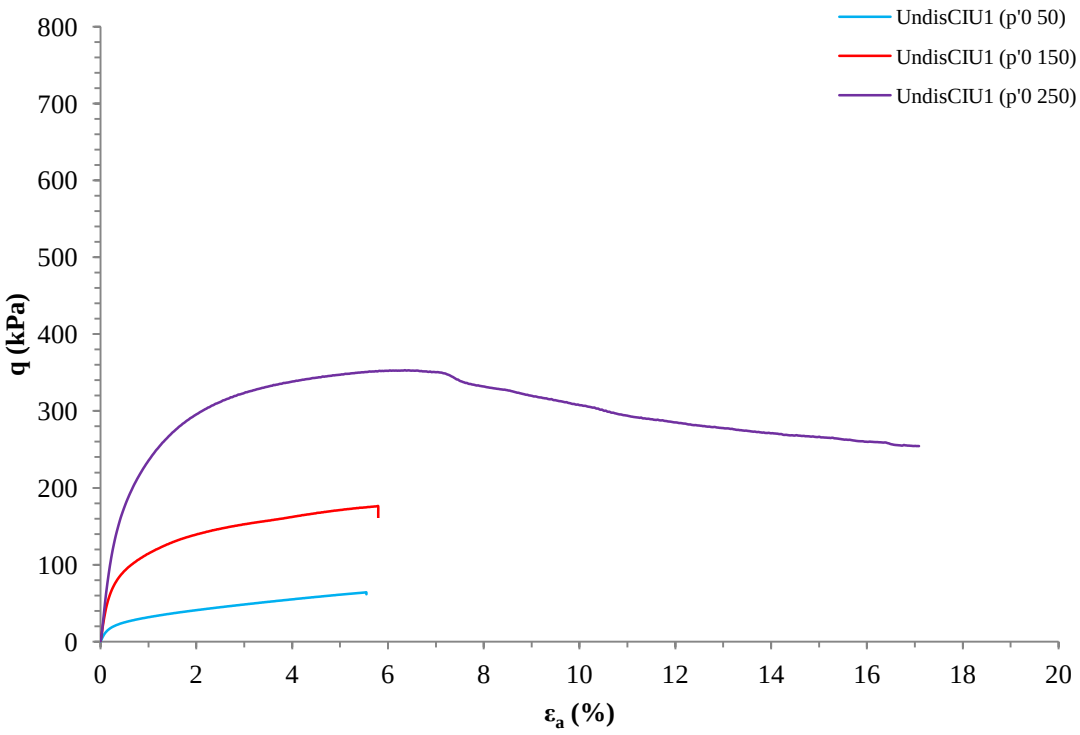

Figure 7.19: Deviatoric stress-strain behaviour of undrained undisturbed samples of Lanton alluvium.

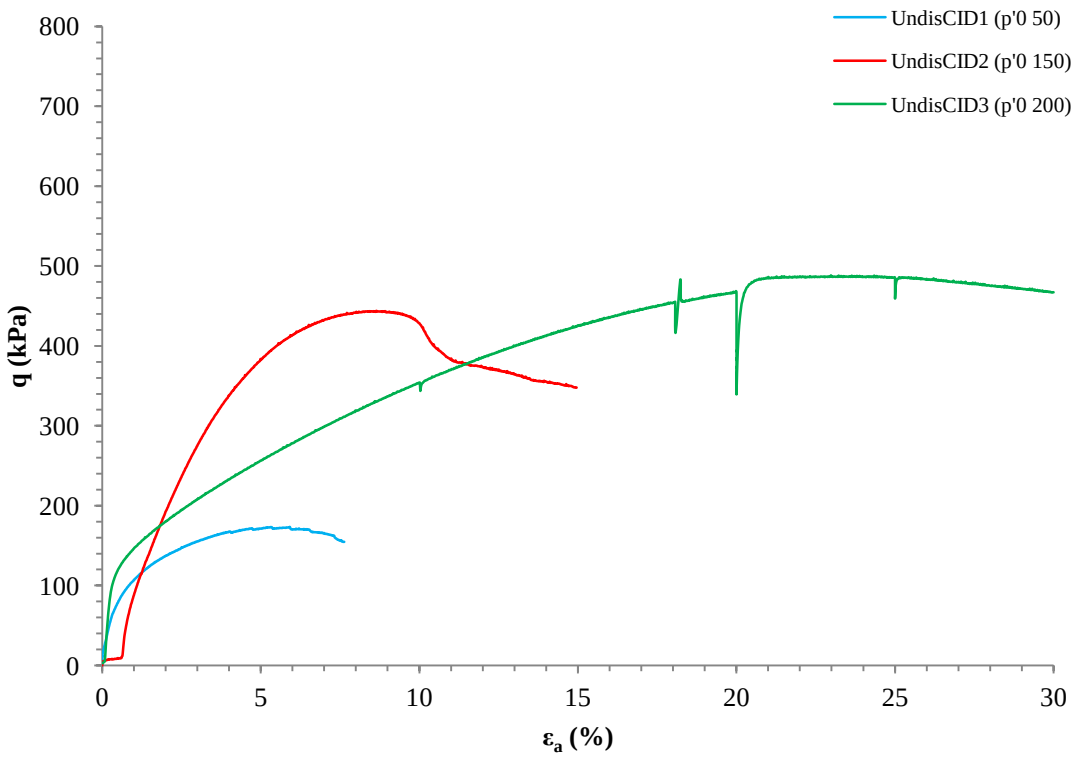

Figure 7.20: Deviatoric stress-strain behaviour of drained undisturbed samples of Lanton alluvium.

Other significant differences between the behaviour of reconstituted and undisturbed samples include the undisturbed samples reaching higher yield stresses at smaller strains for each test and displaying higher levels of stiffness within the elastic range (i.e. higher Young's moduli values). The average drained and undrained shear strengths obtained for the undisturbed Lanton alluvium at p'_0 = 50 kPa were 87 kPa and 31 kPa, respectively; and secant E_u and E' values of 14.89 and 15 MPa. Additionally, strain localisation and the development of shear planes were observed within all undisturbed samples.

Soils exhibiting hardening behaviour prior to yield/peak strength and softening post-yield tend to be overconsolidated in nature. However, based on the OCR value of 1 obtained from the oedometer characterisation of the undisturbed Lanton alluvium (see chapter 5), the soil is certainly deemed to be normally consolidated. Considering the higher yield stresses and elastic stiffnesses of Lanton alluvium in its undisturbed rather than reconstituted state, the softening behaviour of the undisturbed soil post-yield can

be attributed to the degradation of sedimentation structure within the material. The analysis of oedometer testing results demonstrated that in its undisturbed state, Lanton alluvium has a bonding-based structure. However, a considerable difference in the deformational behaviour of the soil may be observed upon destructuration, achievable with relative ease given the soil's sensitivity. During drained tests on samples UndisCID1 and UndisCID2, their higher strengths compared with reconstituted samples due to their internal structure would have caused dilation, ultimately leading to a peak deviatoric stress. Once the peak deviatoric stress had been overcome through continued shearing, the sample's natural resistance to shearing reduced – i.e. softened.

Samples' pore pressure responses during undrained tests are given in Figure 7.21; whereby for samples consolidated to a p'_0 of 150–250 kPa, their pore pressures peaked at axial strains of approximately 3%. For the sample consolidated to a p'_0 of 50 kPa, pore pressures peaked at slightly lower axial strains of 1–2%. Once all the samples reached their peak pore pressures, further straining resulted in a slow decrease in their pore pressures until failure. However, this was not apparent for the sample consolidated to a p'_0 of 250 kPa, whereby at 7.2% shear strain the pore pressure slowly increased towards 120 kPa, at which point it then remained fairly constant with further straining. This slow rise in pore pressure coincides with the onset of strain localisation and softening behaviour (Figure 7.19).

Volumetrically, negligible amounts of contraction were observed within drained samples with p'_0 values of 50 kPa. Figure 7.22 shows that the sample's behaviour was predominantly dilational at most strain levels, with only a small degree of contractional behaviour recorded during the initial stages of the test at small strain levels.

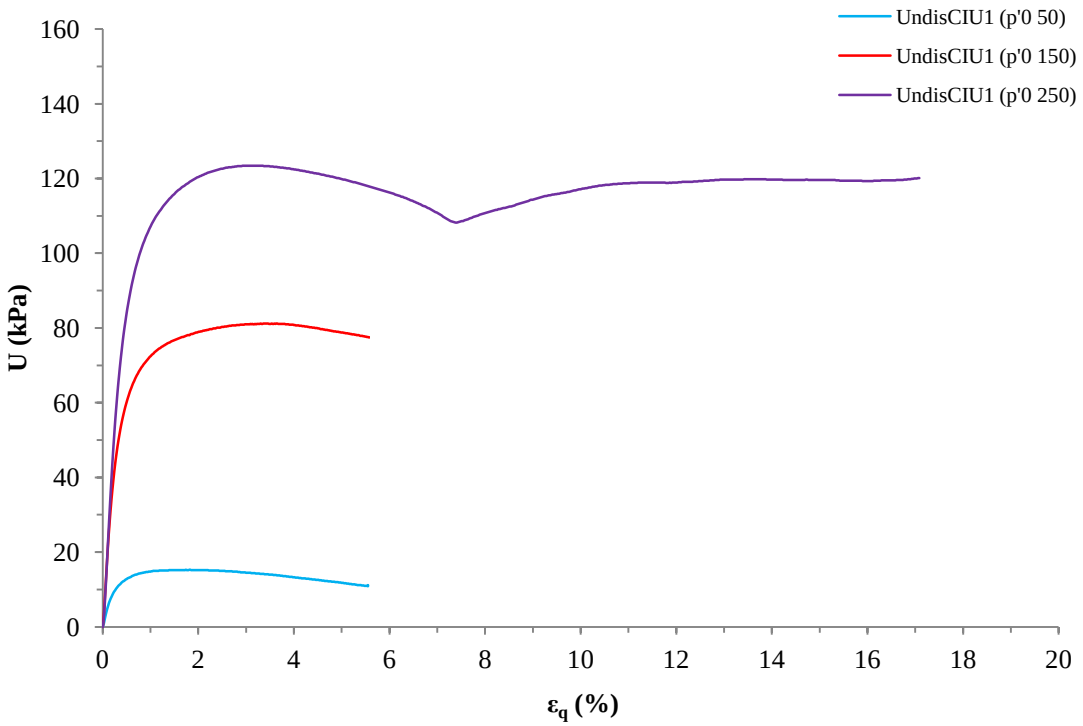

Figure 7.21: Pore pressure behaviour of undrained undisturbed samples of Lanton alluvium.

Until reaching approximately 1.3% shear strain, the sample consolidated to a p'_0 of 150 kPa demonstrating contractional behaviour. Although the sample started to dilate for shear strains >1.3%, positive dilation (i.e. negative volumetric strain) was not observed. Contrastingly, for the sample which was consolidated to a p'_0 of 200 kPa, purely contractional behaviour was recorded throughout the test. This conforms with the pure work hardening behaviour observed for the sample in Figure 7.20. As for the reconstituted samples, higher degrees of dilation were observed within samples which had been consolidated to lower p'_0 values; where particle rearrangement more easily occurred due to lower effective confining pressures.

Figure 7.22 shows that for tests conducted at p'_0 values of 50 and 150 kPa, dilation initiated at much smaller shear strains of 0.3 and 1.2% respectively, compared with reconstituted samples. At these points, the samples were generally within 1% shear strain of reaching their yielding points, indicating that the samples' stress paths were close to reaching the CSL. The sample tested at p'_0 = 50 kPa was considered to have reached maximum effective stress ratio and therefore failure at a shear strain of 3%. However, the test was stopped before any evidence of dilation suppression could be observed, indicating that the sample had not quite reached its critical state.

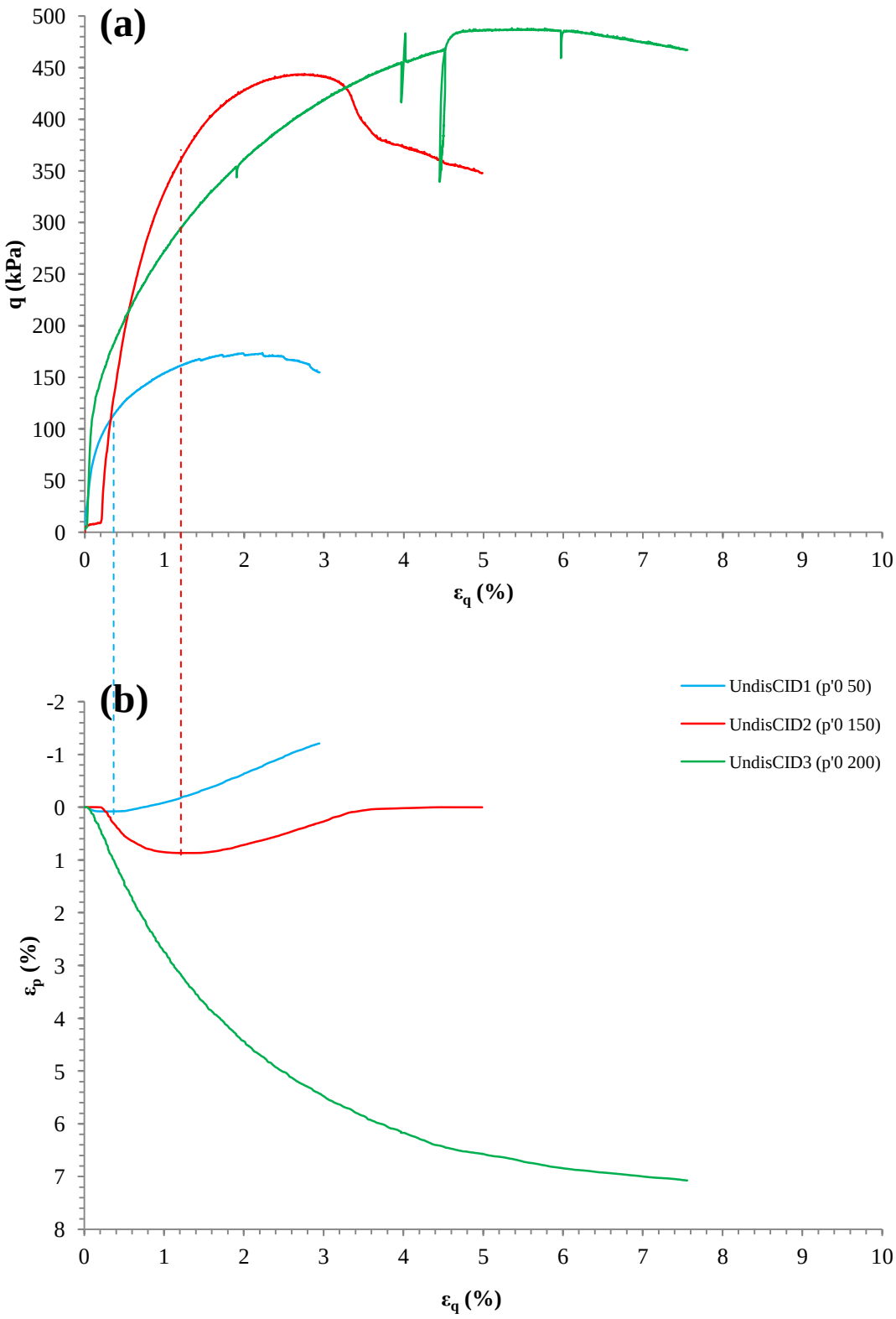

Figure 7.22: (a) Deviatoric stress and (b) volumetric strain response drained undisturbed Lanton alluvium samples with increasing shear strain.

Samples tested at p'_0 values of 150 and 200 kPa were recorded as having reached critical state, as demonstrated in Figure 7.22b whereby the dilation rate of sample UndisCID2 (p'0 150) significantly decreased at a shear strain of 3.3%. Also, the contraction experienced by sample UndisCID3 (p'0 200) became negligible with further straining at shear strains >6%. The dilational behaviour coupled with the loss of structure may explain the observed post-yielding softening behaviour for samples UndisCID1 (p'0 50) and UndisCID2 (p'0 150) (Obrzud, 2010). Finally, as found for reconstituted samples, zero volumetric strain was not observed for any undisturbed samples even upon reaching their critical states.

7.2.2.2 Stress dilatancy

Further to the volumetric strain response of drained undisturbed Lanton alluvium in Figure 7.22b, the frictional stress dilatancy behaviour of these samples is shown in Figure 7.23. Although all samples experience compression, samples UndisCID1 (p'0 50) and UndisCID2 (p'0 150) experience dilation, particularly for the former where a negative $\varepsilon_p/\varepsilon_q$ ratio was recorded during the latter stages of testing.

All samples reached critical state M values ranging between 1.35 and 1.5; although in contrast to reconstituted samples, none of the undisturbed samples reached a similar $\varepsilon_p/\varepsilon_q$ ratio at the end of their testing. Samples generally experienced a transition from contraction to dilational/reduced contractional behaviour when M values ranged between 0.8 and 1.

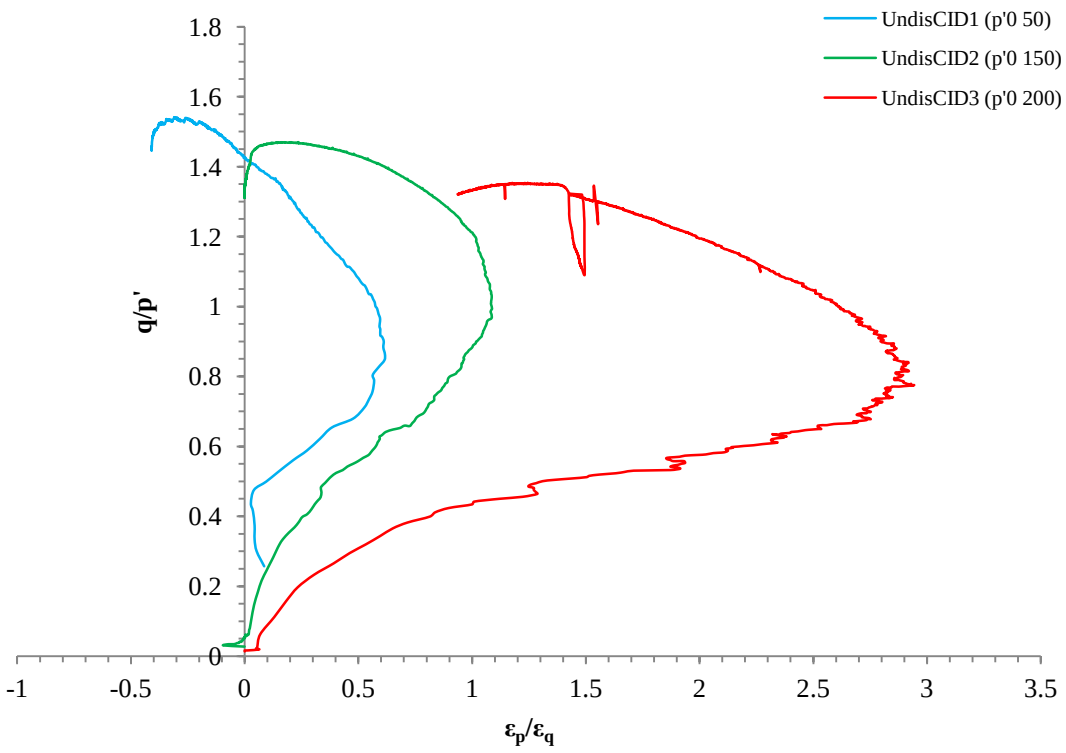

Figure 7.23: Stress-dilatancy behaviour of drained undisturbed samples of Lanton alluvium.

A direct ψ measurement was not possible for the UndisCID3 (p'0 200) sample due to its purely contractional behaviour during testing. However, ψ angles calculated from the other two drained specimens were 6.8° for UndisCID2 (p'0 150) and 13.6° for UndisCID1 (p'0 50). The variation in these undisturbed ψ angles confirms that higher p'_0 values make it harder for soil particles to rearrange. However, these dilation angles are too high for a silty sandy soil like Lanton alluvium, regardless of the presence of natural bonding structure within the material and the associated peak and softening behaviour. Further testing is required to define an accurate dilation angle for the undisturbed soil. Therefore, dilatancy angles for the undisturbed soil were calculated based on φ' values per the next section.

7.2.2.3 Failure envelopes

Within Figure 7.24, the position of the Mohr Coulomb failure envelope for the undrained undisturbed soil was considerably lower than that for the reconstituted

sample Although a relatively similar c' value of 5.03 kPa was recorded for the undisturbed material, its φ' value of 30° was up to 5° lower than that for the undisturbed drained and reconstituted drained and undrained counterparts.

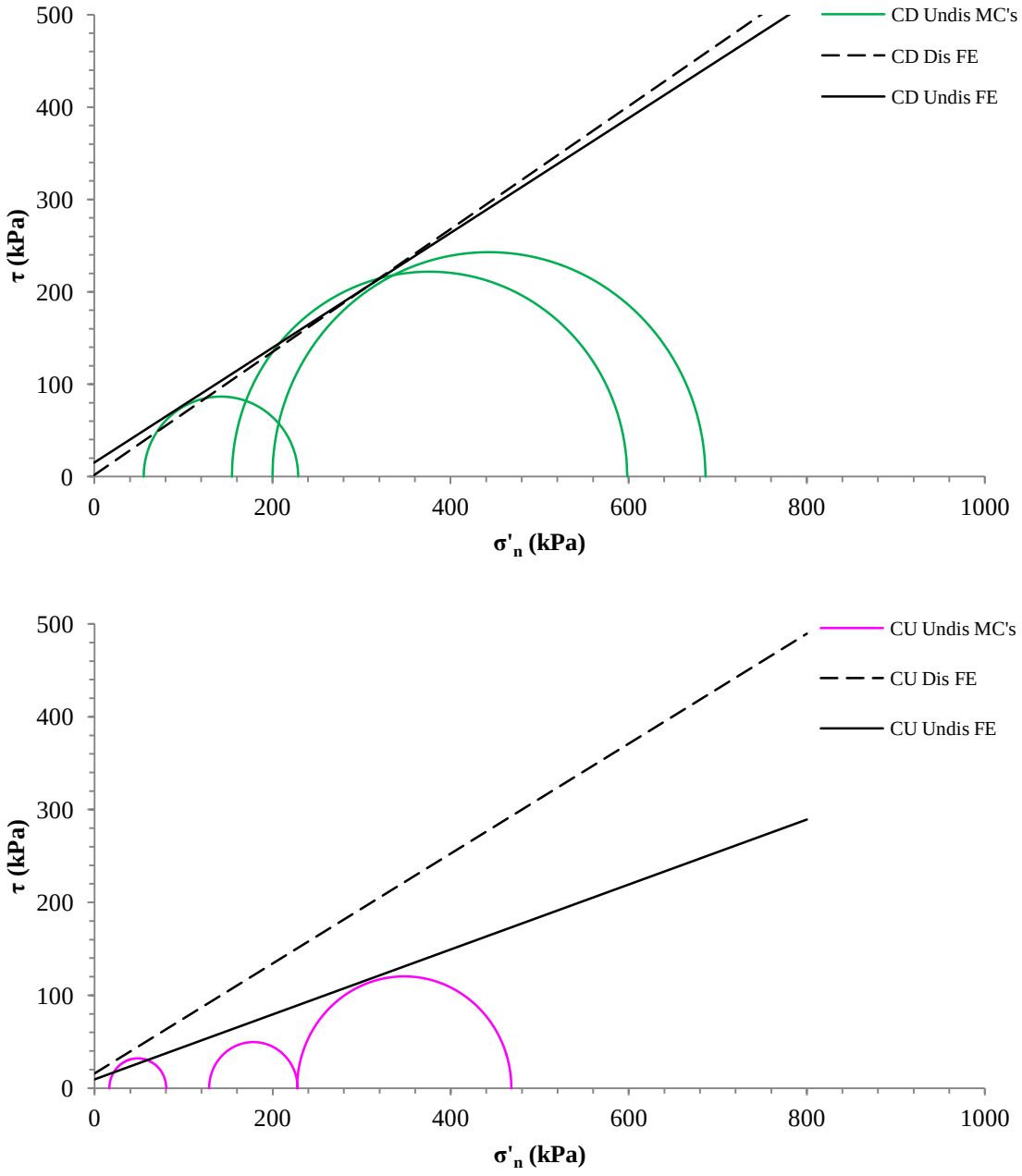

Figure 7.24: Mohr-Coulomb failure envelopes (FE) and peak τ-σ'$_n$ values obtained from (a) drained and (b) undrained undisturbed samples of Lanton alluvium. FE's for reconstituted samples are superimposed for comparison.

For the drained undisturbed samples, c' and φ' values of 12.1 kPa and 31.7^{o} were recorded. The effect of structure within the undisturbed samples compared with the reconstituted samples is apparent, given their higher levels of initial effective cohesion. Theoretically, the soil in its undisturbed state ought to possess higher shear strength properties compared with its reconstituted state, due to the presence of inter-particle bonding within the soil structure. However, Figure 7.24 shows the inverse of this expected theoretical behaviour, which appears to be particularly emphasised for undrained tests. Considering that the peak deviatoric stresses encountered during undrained tests are generally lower in magnitude compared with those recorded during drained tests under identical confining stress conditions, the apparent higher strength of reconstituted Lanton alluvium may be attributed to the over-compaction of such samples during their preparation prior to testing. Additionally, given the levels of sensitivity observed for the soil during oedometer tests conducted in Chapter 5, some of the soil's bonding-based structure may have collapsed during transport from in-situ to the laboratory and consequently caused a degree of strength reduction. This ultimately calls for in-situ testing (e.g. pressuremeter) and improved sample preservation during transport from the field.

Similar to the shape of the q-p' stress paths for the reconstituted samples, the shape of the undrained stress paths for the undisturbed samples displays evidence of strain hardening with little softening (Figure 7.25); whereas the drained paths exhibited the typical 1:3 slope. Additionally, the failure envelope for the undisturbed soil almost coincides with its critical state line (CSL_{Undis}). The position of the CSL_{Undis} is only slightly higher than that for the CSL_{Dis}; whereby the CSL_{Undis} passes through the origin at a higher q value of 19.34 kPa. This signifies the effect of structure within the soil. The average M value obtained for the undisturbed CSL's was 1.37, which then produced a φ' value of 33.87^{o}. By using this φ' value, a c' value of 6.68 kPa was derived. All the monotonically loaded undrained and drained effective stress paths for the undisturbed Lanton alluvium are shown in Figure 7.25, which have also been normalised by their p'_0 value in Figure 7.26.

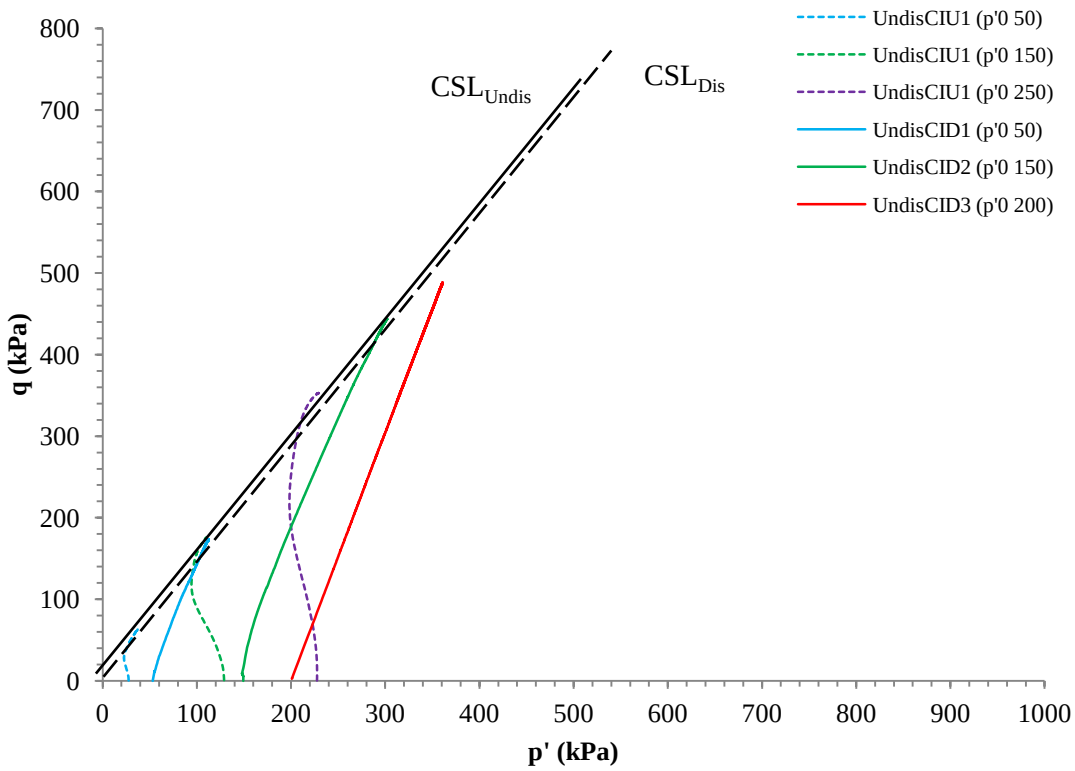

Figure 7.25: Drained and undrained stress paths and CSL (CSL_{Undis}) within the q-p' stress plane for all undisturbed Lanton alluvium samples. The CSL for reconstituted samples (CSL_{Dis}) is superimposed for comparison.

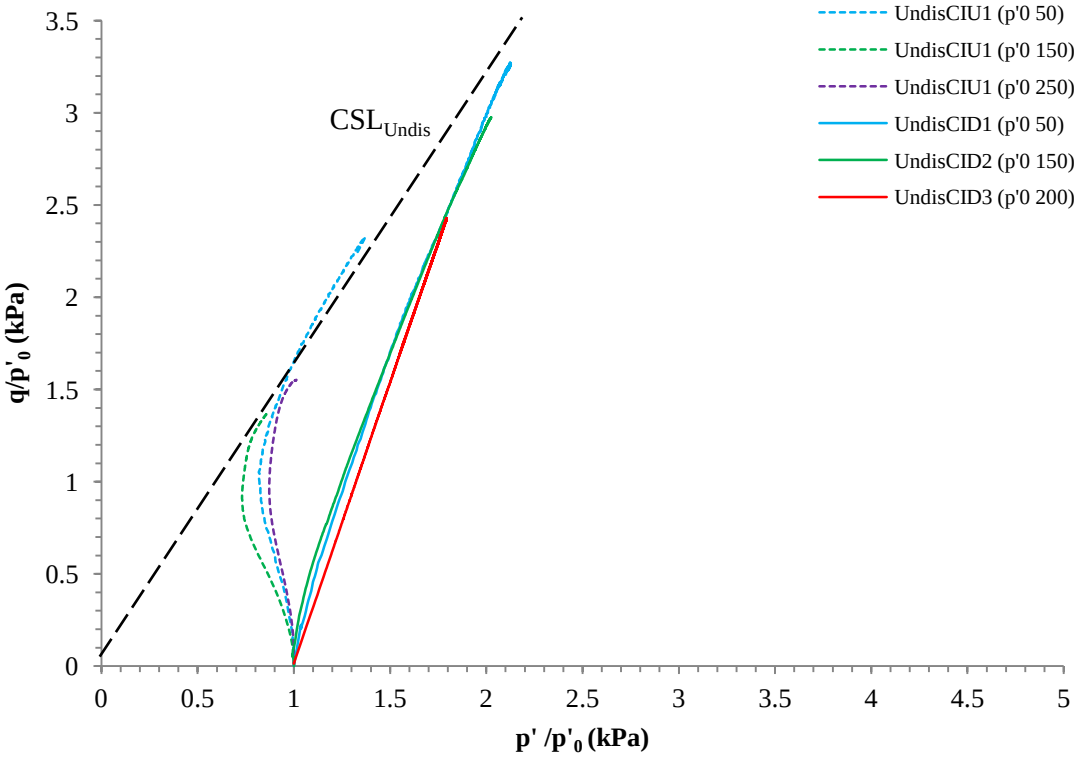

Figure 7.26: Drained and undrained stress paths for undisturbed Lanton alluvium samples within the q/p'_0-p'/p'_0 stress plane, normalised by their corresponding p'_0 values.

As for the reconstituted samples, the influence of p'_0 to which the undisturbed samples were consolidated on the maximum q values achieved during tests is clear. Higher p'_0 states produce higher q values up to failure for both drained and undrained samples. Normalisation also proved successful in bringing all the stress paths together in defining a single locus within the q/p'_0-p'/p'_0 plane.

Compression curves from drained undisturbed samples within the specific volume (v) – p' compression plane are presented in Figure 7.28. A possible NCL for the undisturbed soil is defined based on the curve for the test consolidated to a p'_0 value of 200 kPa. The position of Lanton alluvium's ICL is superimposed on Figure 7.28 has a smaller gradient and lies beneath the CSL_{Undis}. At a specific volume of 1.47 and a mean effective stress of 850 kPa, the ICL and CSL_{Undis} converge. To quantify the degree of initial structure (r_0) within the undisturbed Lanton alluvium, the structure degradation law developed by Rouainia and Muir Wood (2000) and as used by Callisto and Rampello (2004) will be adopted (Figure 7.27).

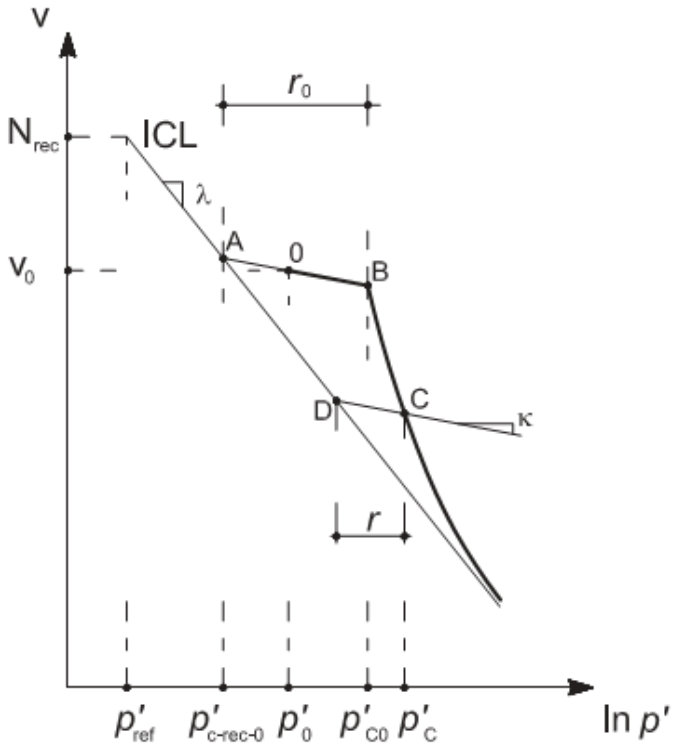

Figure 7.27: Quantification of structure per Rouainia and Muir Wood (2000). Taken from Callisto and Rampello (2004).

Values for r_0 may be derived via the following equation:

Initial degree of structure: $$r_0 = \frac{p'_{c\,Undis}}{p'_{c\,Dis}}$$ (**Equation 7.3**)

where p'_{cUndis} is the mean effective stress at which the compression curve for the Undisturbed Lanton alluvium starts to turn downwards to ultimately meet the soil's CSL_{Undis}; whereas p'_{cDis} is the mean effective stress of the undisturbed soil when the sample's initial specific volume meets the ICL. The undisturbed compression line (UCL) is a hypothetical compression line which the undisturbed Lanton alluvium is likely to follow if no destructuration within the material occurred during compression (Callisto and Rampello, 2004). According to Callisto and Rampello (2004), the UCL is assumed to have the same slope as the ICL, and in this case is synonymous with the position of the NCL. Based on the readings for p'_{cUndis} and p'_{cDis} values from Figure 7.28, a very high r_0 value of 78 is achieved. Such an r_0 value is considerably higher than that recorded by Callisto and Rampello (2004) for Pisa Clay, whose r_0 was 9. Lanton alluvium's high r_0 value from triaxial testing corresponds with the high degree of structure implied from oedometer testing results in chapter 5, according to the normalisation procedure defined by Gasparre and Coop (2008). However, as observed within the oedometer testing results, the structure of Lanton alluvium was observed to be more easily lost compared with London Clay and Pisa Clay during drained triaxial testing, due to its silt content and therefore sensitivity to loading disturbance. This contrasts to the compressional behaviour of the London and Pisa Clays, whereby the structure within these soils is retained for much longer when subjected to higher p' conditions.

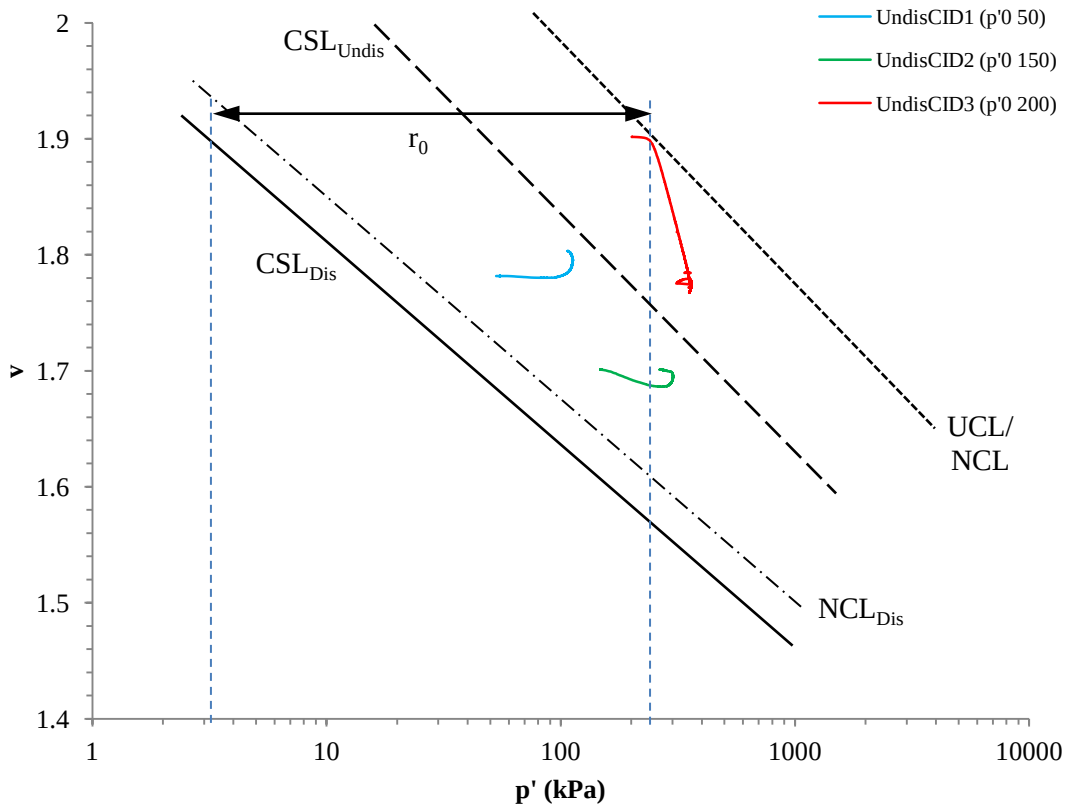

Figure 7.28: NCL/UCL and CSL_{Undis} within the υ – ln p' stress plane, obtained from drained undisturbed Lanton alluvium samples.

Whilst all of the compression paths for reconstituted samples in Figure 7.12 were located beneath the CSL (i.e. on its "dry" side) and therefore all exhibited dilation during shearing (as also confirmed in Figure 7.6), compression paths in Figure 7.28 are observed above ("wet" side) and below the CSL_{Undis}. This implies that the UndisCID3 (p'0 200) sample had a moisture content that was higher than the critical moisture content and that the soil experienced compression rather than dilation during shear, whereas vice versa applies for the UndisCID1(p'0 50) and UndisCID2 (p'0 150) samples. These observations are consistent with the volumetric-shear strain behaviour shown in Figure 7.22 and those made by Parry (1958) (Muir Wood, 1990).

7.2.2.4 Stiffness degradation

The secant shear stiffness degradation behaviour of undisturbed Lanton alluvium samples under undrained conditions is displayed in Figure 7.29. No G_{sec} values are

presented for shear strains smaller than 0.02%, due to the lower resolution of stiffness and strain data from global rather than strain measurements. These stiffness results will be combined with the higher resolution data from testing at Bristol University to gain a crucial understanding into the soil's stiffness degradation behaviour at very small to small strains.

The undrained shear stiffnesses of samples at shear strains <0.1% were markedly higher than those at >0.2%, beyond which secant shear stiffnesses had reached their lowest values and remained constant until sample failure or when the test had been stopped. As with reconstituted samples, higher G_{sec} values were recorded for samples which were consolidated to p'_0 values of 200 kPa compared with those consolidated to a p'_0 of 50 kPa. Considerably less data scatter is observed for the shear stiffness values calculated for each sample at larger strains, although there is a distinct separation between the three stiffness degradation curves. Normalising the data sets with respect to their p'_0 values was fairly successful in producing much tighter, better correlated curves (Figure 7.30).

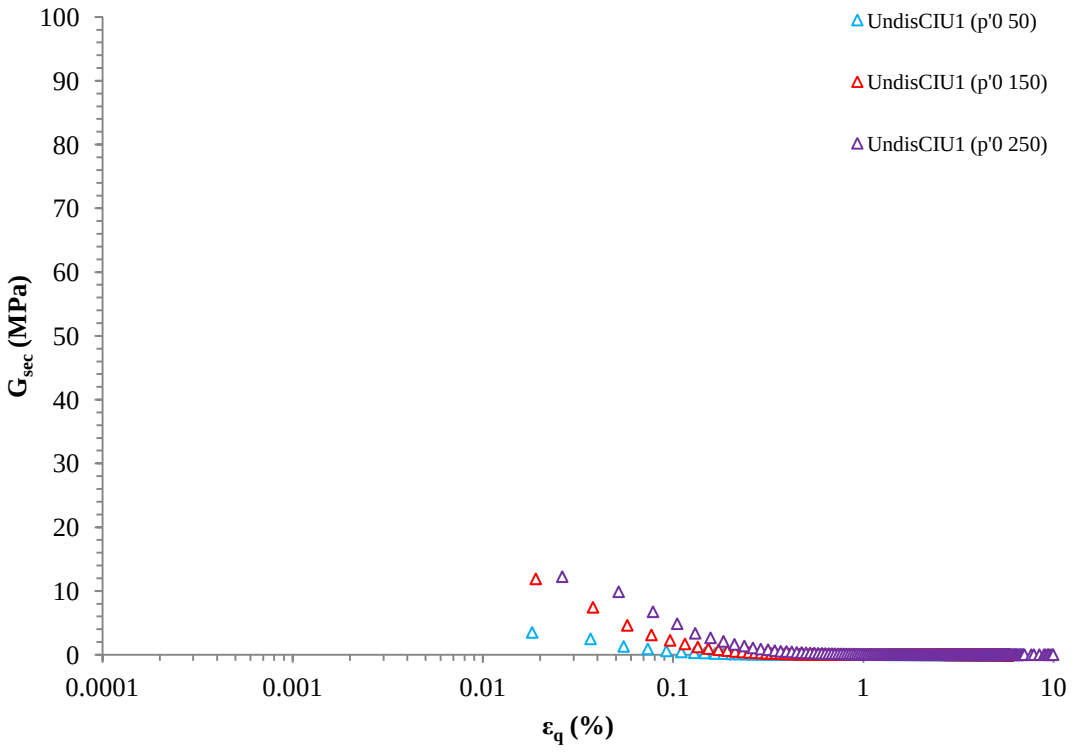

Figure 7.29: Secant shear stiffness degradation behaviour for undrained undisturbed Lanton alluvium samples.

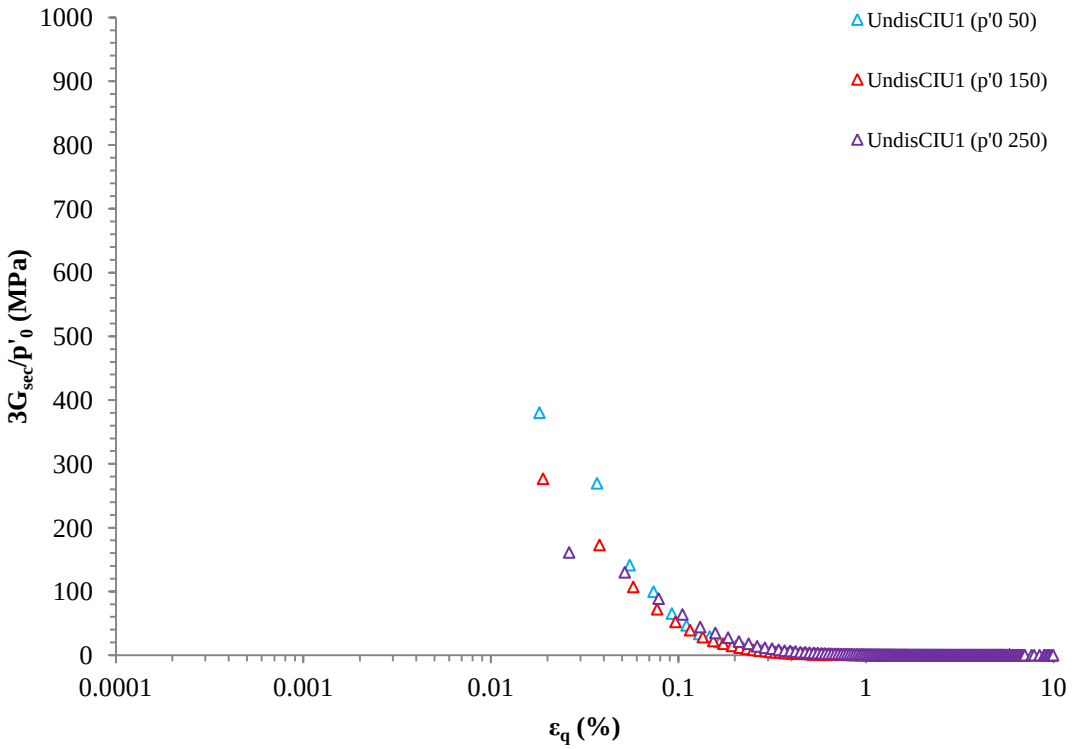

Figure 7.30: Secant shear stiffness degradation behaviour for undrained undisturbed Lanton alluvium samples, normalised by their corresponding p'_0 values.

However, at shear strains <0.07%, the amount of data scatter starts to increase and the curves become less tightly fitted with the curve for UndisCIU1 (p'0 50) showing the highest level of deviation away from the other two curves. Non-normalised and normalised shear stiffness degradation plots for drained tests are displayed in Figures 7.31–7.32, respectively.

Although there are some similarities between the stiffness degradation behaviour for undrained and drained samples, (e.g. higher p'_0 values generally produced higher G_{sec} values); there are also several differences. Firstly, per Figure 7.31, drained samples' lowest shear stiffnesses were achieved at smaller shear strains of >0.08% compared with undrained samples.

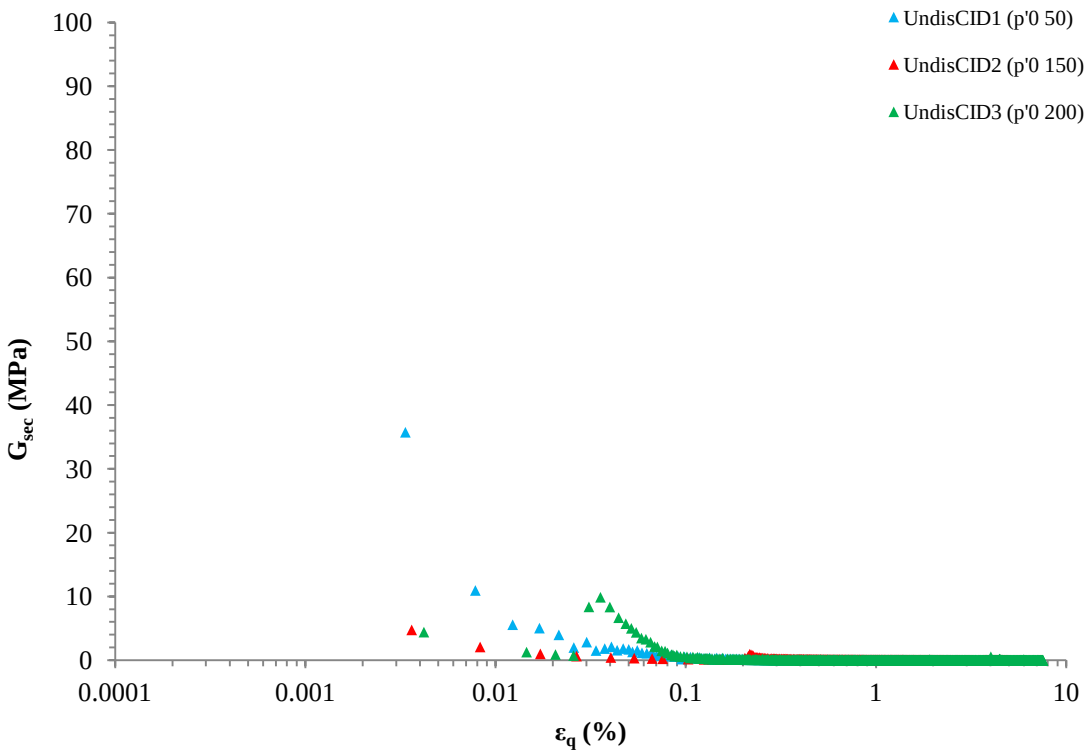

Figure 7.31: Secant shear stiffness degradation behaviour for drained undisturbed Lanton alluvium samples.

Secondly, a larger degree of data scatter was produced at shear strains <0.03%; although such data points ought to be disregarded, given the relatively low resolution of globally measured strains compared with local strain measurements. Greater separation also exists between the three shear stiffness degradation curves, whereby higher G_{sec} values were recorded for the UndisCID1 (p'0 50) sample compared with UndisCID2 (p'0 150). Such an unexpected occurrence may be attributed to the sample's initial quality. Slight disturbances during sample preparation may have inadvertently removed considerable elements of the soils high structure, thereby producing lower G_{sec} values. Figure 7.32 presents the drained shear stiffness degradation plots, which have been normalised with respect to their initial p'_0 value.

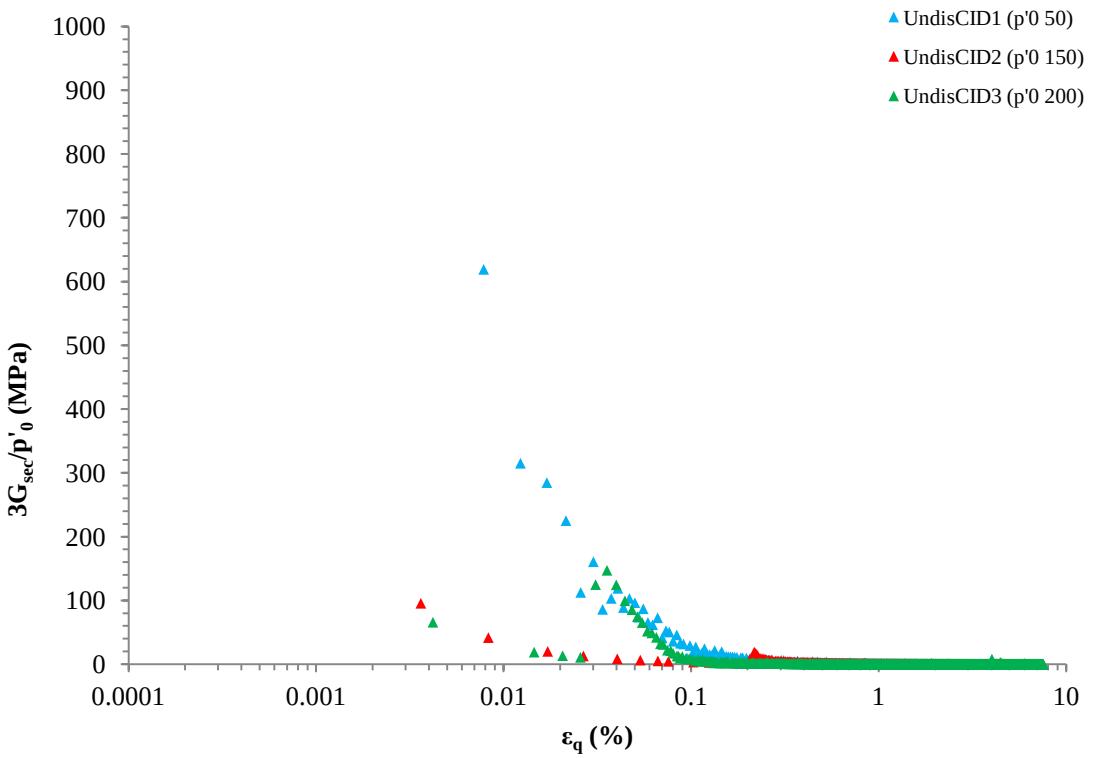

Figure 7.32: Secant shear stiffness degradation behaviour for drained undisturbed Lanton alluvium samples, normalised by their corresponding p'_0 values.

From Figure 7.32, the effect of normalising the data has proved to be moderately successful in bringing the stiffness degradation data for UndisCID1 and UndisCID3 much closer together and producing a much tighter curve. However, the UndisCID2 curve still lies considerably lower than the other two curves. This highlights that factors in addition to initial p'_0, such as initial sample quality are responsible for this occurrence. Further testing is required to fully determine the major influencing factor.

The bulk stiffness degradation behaviour observed for drained samples is presented Figure 7.33. Although the data for the UndisCID3 sample produces a well-defined curve between large strains and 0.01% shear strain, much data scatter can be observed for the UndisCID1 and UndisCID2 samples for shear strains <0.03%. Such data scatter is likely to be the result of a combination of initial sample quality and the calculation method used to determine secant bulk stiffnesses; whereby a higher resolution of volumetric and shear strain measurement is required. Hence, bulk stiffnesses at shear strains <0.01% should not be considered as representative values for the undisturbed Lanton alluvium.

Referring to Figure 7.34, normalising the bulk stiffness data in Figure 7.33 appears to have been successful in bringing the data from samples UndisCID1 and UndisCID3 towards a tighter fitting curve at volumetric strains <0.01%, albeit there is considerably more scatter at smaller strain levels. However, normalisation had a negligible effect on resolving the data scatter observed for the UndisCID2 sample at both small and large shear strains.

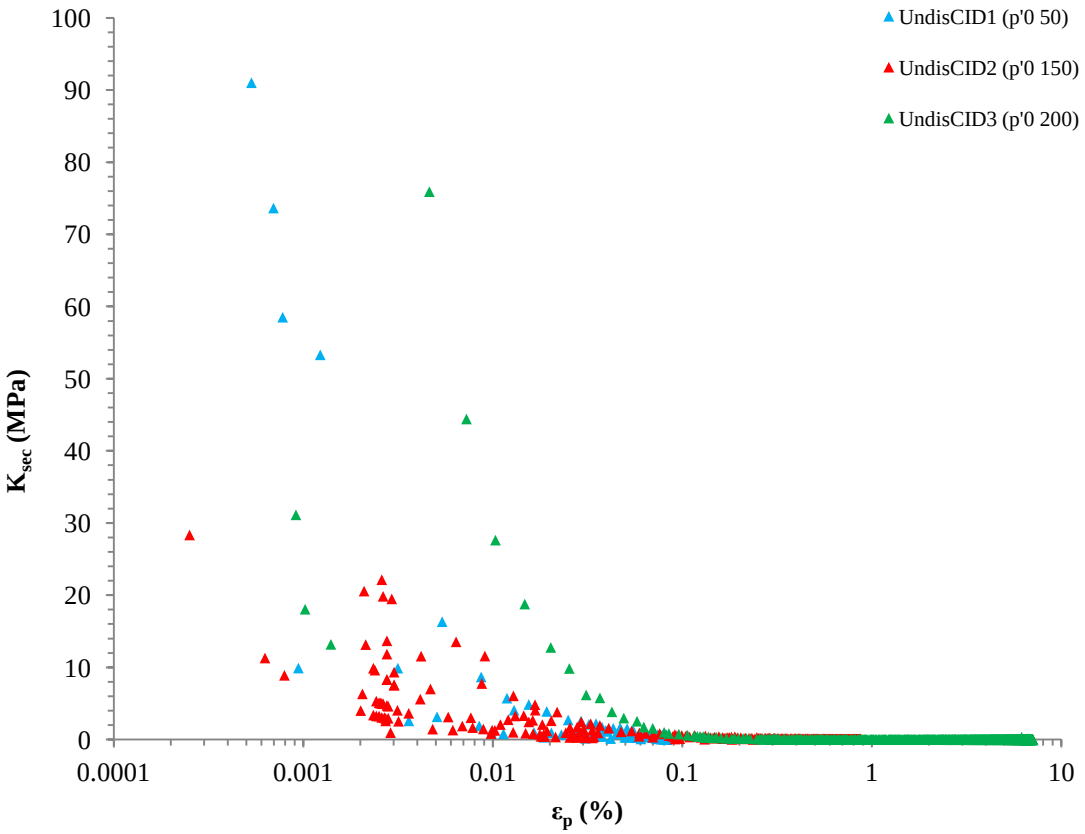

Figure 7.33: Secant bulk stiffness degradation behaviour for drained undisturbed Lanton alluvium samples.

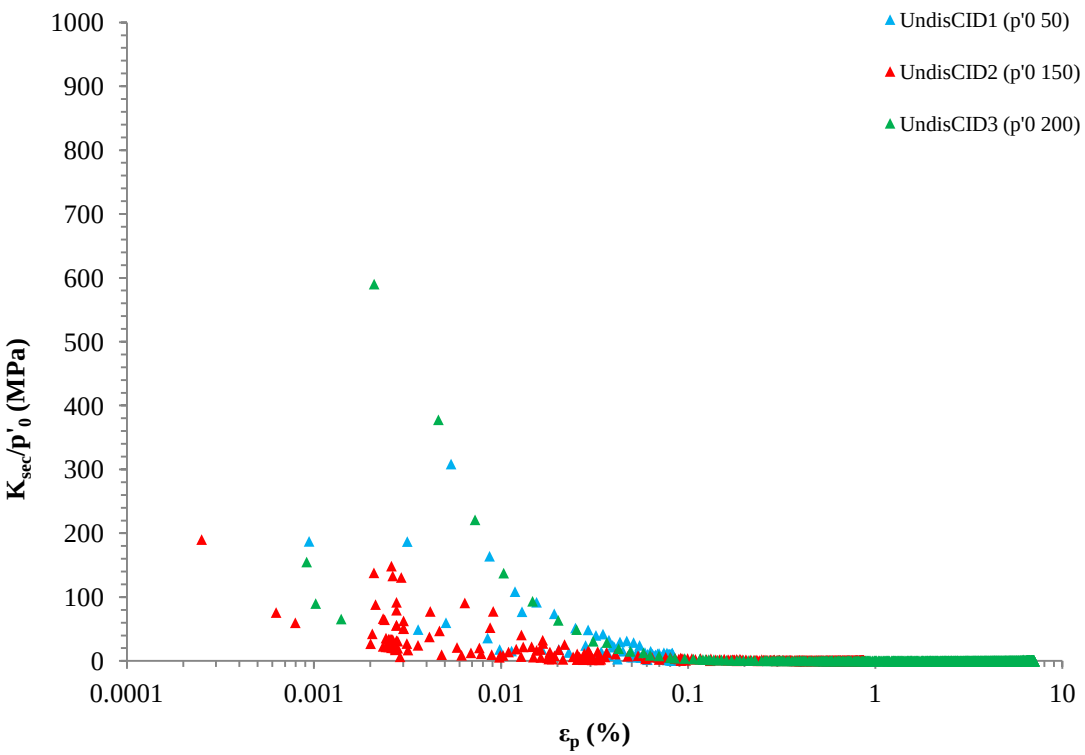

Figure 7.34: Secant bulk stiffness degradation behaviour for drained undisturbed Lanton alluvium samples, normalised by their corresponding p'_0 values.

Although normalising shear stiffnesses with respect to their initial p'_0 values proved to be particularly useful in producing tighter fitting curves, this method of normalisation was not as successful in producing tighter fitting curves of better correlation for bulk stiffnesses, as high degrees of data scatter were still apparent. Alternative factors need to be investigated for normalising bulk stiffness data sets, such as silt and sand contents (Lee et al., 2004), given Lanton alluvium's relatively high level of sensitivity to disturbances compared with stiffer clay-based soils.

7.3 Dynamic results

Oedometer and monotonic triaxial testing results have confirmed the presence of a relatively high degree of initial structure within the undisturbed Lanton alluvium, which may be lost with relative ease at small strains due to the soil's high silt content and therefore sensitive behaviour. A dynamic triaxial testing programme was conducted at Newcastle using the conventional GDS ELDYN apparatus, in order to investigate the response of the alluvium when subjected to dynamic loads associated with a passing HST, whilst paying attention towards whether the soil is likely to liquefy under such conditions. [Note that the aim of the dynamic testing programme was not to determine the cyclic stress ratio (CSR) required to produce double amplitude axial strains of 5% and ultimately, liquefaction; as this study is not liquefaction focussed.] Although the monotonic testing results above highlighted the importance of using local strain and bender element measurements in calculating soil stiffnesses, which would be of particular importance during dynamic loading events, no small strain equipment was available at the time of testing. One-way dynamic tests were conducted on both reconstituted and undisturbed samples of Lanton alluvium under undrained conditions at mean effective stresses (p'_0) of 60 (-3 m), 108.65 (-7.5 m) and 147.48 kPa (-12 m). The dynamic loading conditions to which samples were subjected simulated the passing of one HST at a speed of 125 mph. Due to the maximum capacity of the triaxial apparatus, the loading frequency used (2.794 Hz) was ten times slower than the true frequency associated with HST's. Triplicate tests were conducted for the three aforementioned effective confining stress conditions; the results from which are hereby presented.

7.3.1 Reconstituted samples

The average seat loads and cyclic loading conditions applied to reconstituted samples for the three effective confining stress conditions tested are provided in Figure 7.35. Cycle 1 corresponds to the initial passage of the HST's Class 43 locomotive; cycle 2 corresponds to the passage of nine Mark 3 passenger coaches, which was finally

followed by cycle 3, corresponding to the passage of the rear Class 43 locomotive/brake car. Table 7.1 below summarises the average cyclic stress ratio (CSR) conditions subjected to testing samples consolidated to p'_0 values of 60, 108.65 and 147.48 kPa, which correspond to the dynamic loading conditions exerted by the passing of a Class 43 locomotive, nine Mark 3 coaches and finally a Class 43 brake car.

Table 7.1: Summary of CSR conditions used during dynamic testing on reconstituted samples.

	CSR		
	p'_0 = 60 kPa	***p'_0 = 108.65***	***p'_0 = 147.48***
Load cycle 1 (1 x Class 43 locomotive)	0.67	0.24	0.13
Load cycle 2 (9 x Mark 3 coaches)	0.41	0.18	0.11
Load cycle 3 (1 x Class 43 brake car)	0.67	0.25	0.13

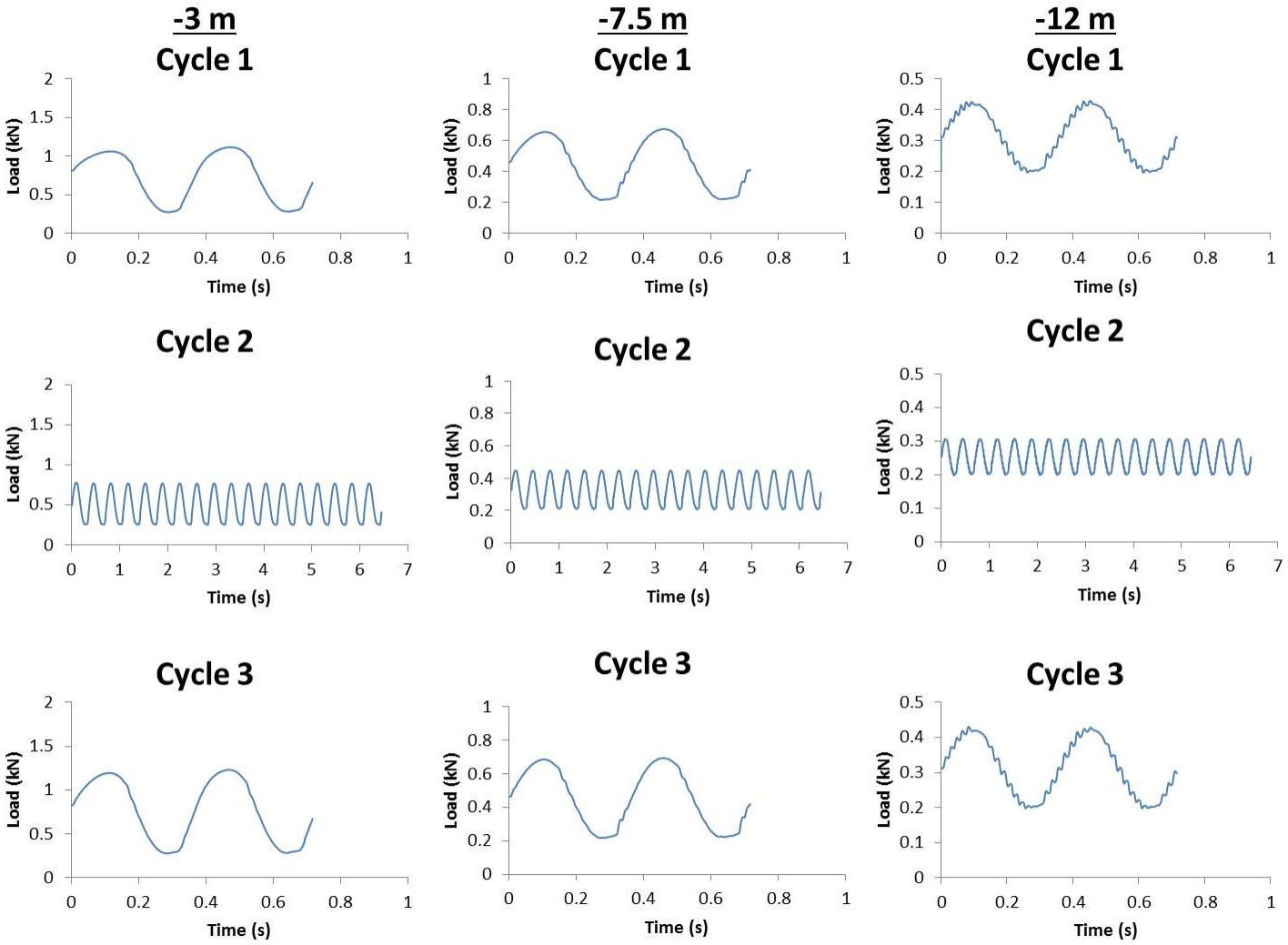

Figure 7.35: Summary of loading patterns observed for dynamic tests conducted at effective confining stresses replicating 3, 7.5 and 12 metres depth.

The deviatoric stress – axial strain and deviatoric stress – cyclic shear strain behaviour of the reconstituted Lanton alluvium samples are presented in Figures 7.36 and 7.37. Given the soft nature of the reconstituted soil compared with its undisturbed state, Figures 7.36 and 7.37 both demonstrate that a considerable amount of axial strain was experienced by samples to reach the seat load required for one-way loading tests conducted at p'_0 = 60 kPa. Once the samples were under their required seat load, almost 2% strain was experienced by the samples after cycle 1, due to the high load associated with the Class 43 locomotive. Further axial strains of 0.5% were experienced after cycle 2 and between 1–1.3% after cycle 3. Hence, negating the amount of strain required to place samples under their necessary seat loads, at 3 metres depth the passing of one HST configuration at 125 mph typically caused axial/cyclic shear strain accumulations of 4–6%. These plastic strain accumulations are considerable. Based on small strain stiffness measurements from the monotonic testing results above; such dynamic loading disturbances would inevitably result in the soil's initial sedimentation structure being completely removed and considerable ground surface settlements.

As hypothesised, the effect of increasing the effective confining stress on the samples resulted in considerably smaller axial and cyclic shear strains being accumulated during dynamic loading. The strains accumulated during tests conducted at p'_0 = 108.65 kPa were still considered within the large strain range (>0.1%) per criteria stated by Atkinson (2000). However, the axial strains recorded during tests conducted at effective confining stresses of 147.48 kPa (0.02 – 0.095%) were considered to be within the small strain range. Based on the oedometer and monotonic triaxial experimental findings already presented for Lanton alluvium, further plastic strains are likely to accumulate within the soil when subjected to further dynamic loading events associated with passing HST traffic.

The generation of excess pore pressure with increasing axial strain within reconstituted samples in response to the three loading cycles is shown in Figure 7.38. Particularly during cycle 2 (passage of nine Mark 3 coaches) for tests conducted at p'_0 = 60 and 108.65 kPa, pore pressure ratcheting can be observed with increasing numbers of load pulses (N).

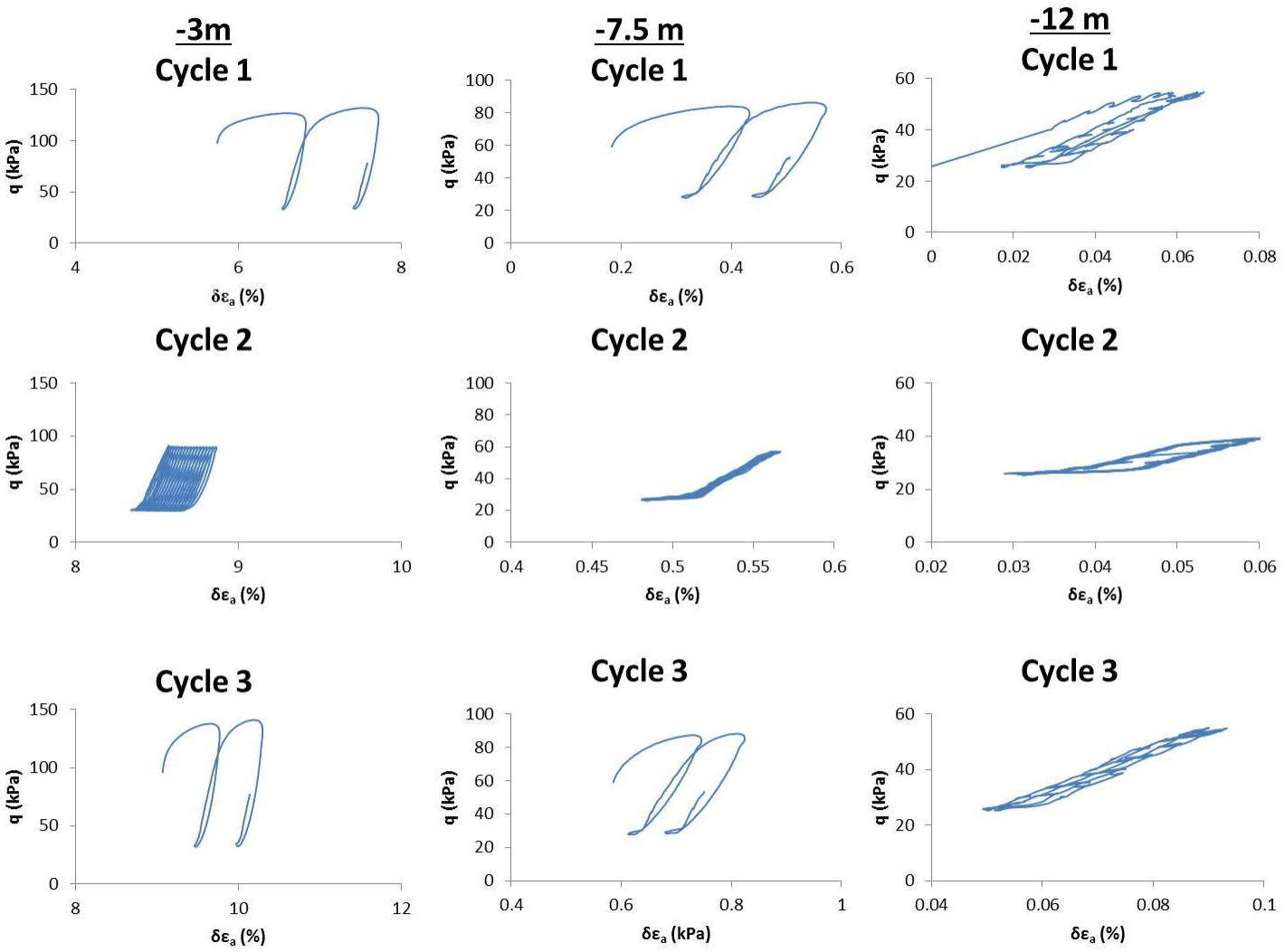

Figure 7.36: Summary of deviatoric stress-axial strain relationships during dynamic tests conducted at effective confining stresses corresponding to 3, 7.5 and 12 m depth.

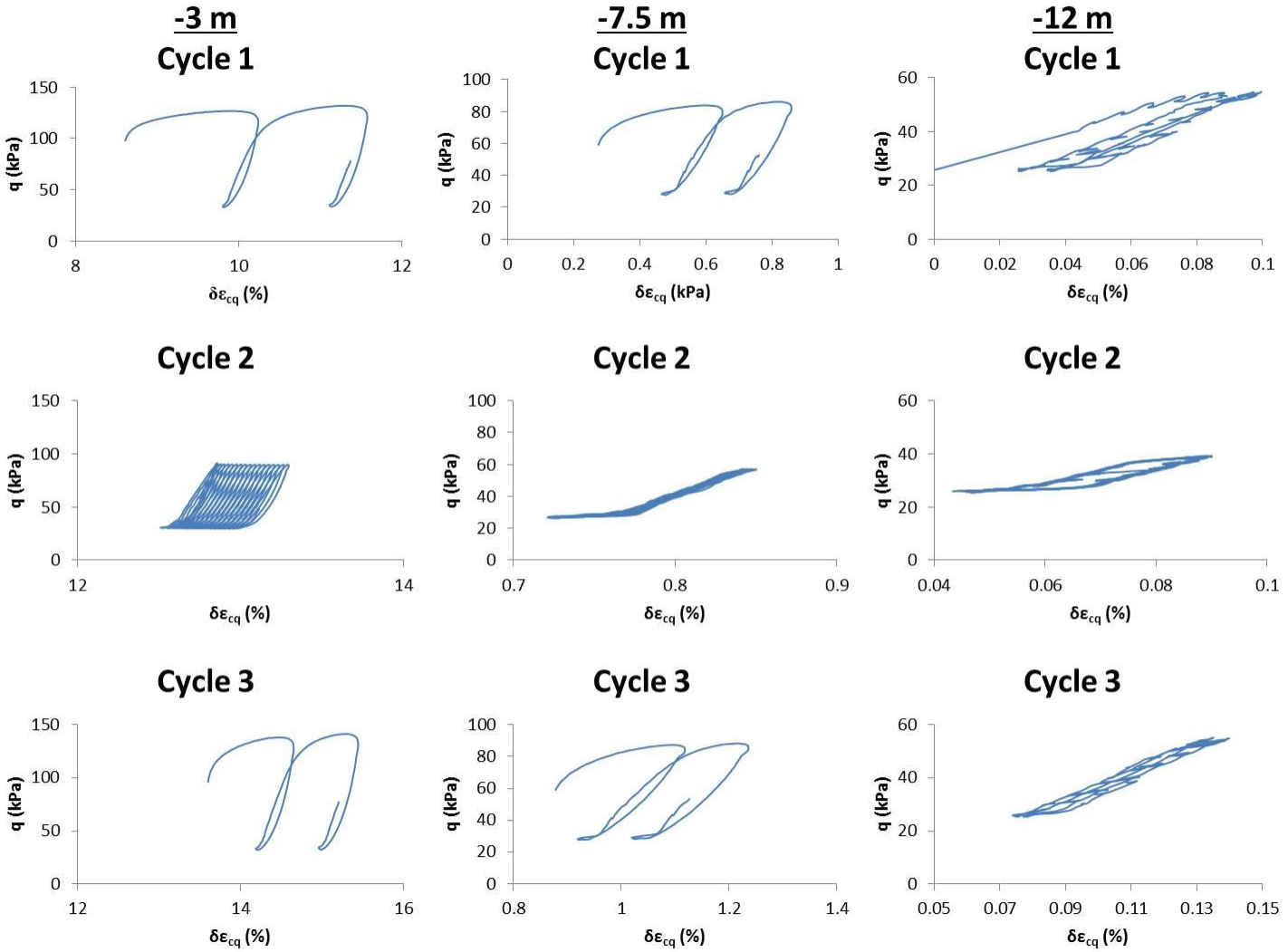

Figure 7.37: Deviatoric stress-cyclic shear strain relationships during dynamic tests conducted at effective confining stresses corresponding to 3, 7.5 and 12 m depth.

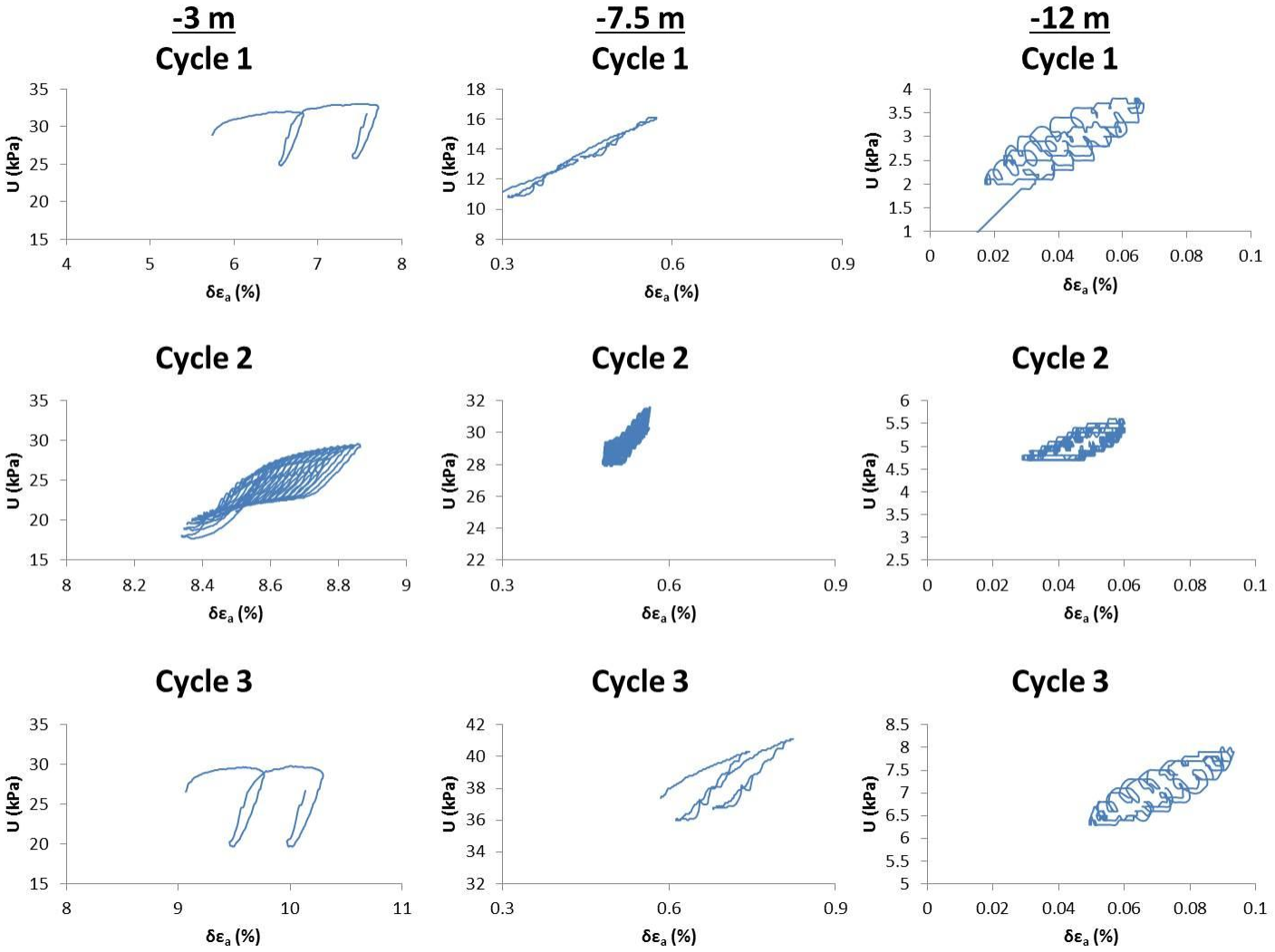

Figure 7.38: Pore pressure response of reconstituted samples during dynamic tests conducted at effective confining stresses corresponding to 3, 7.5 and 12 m depth.

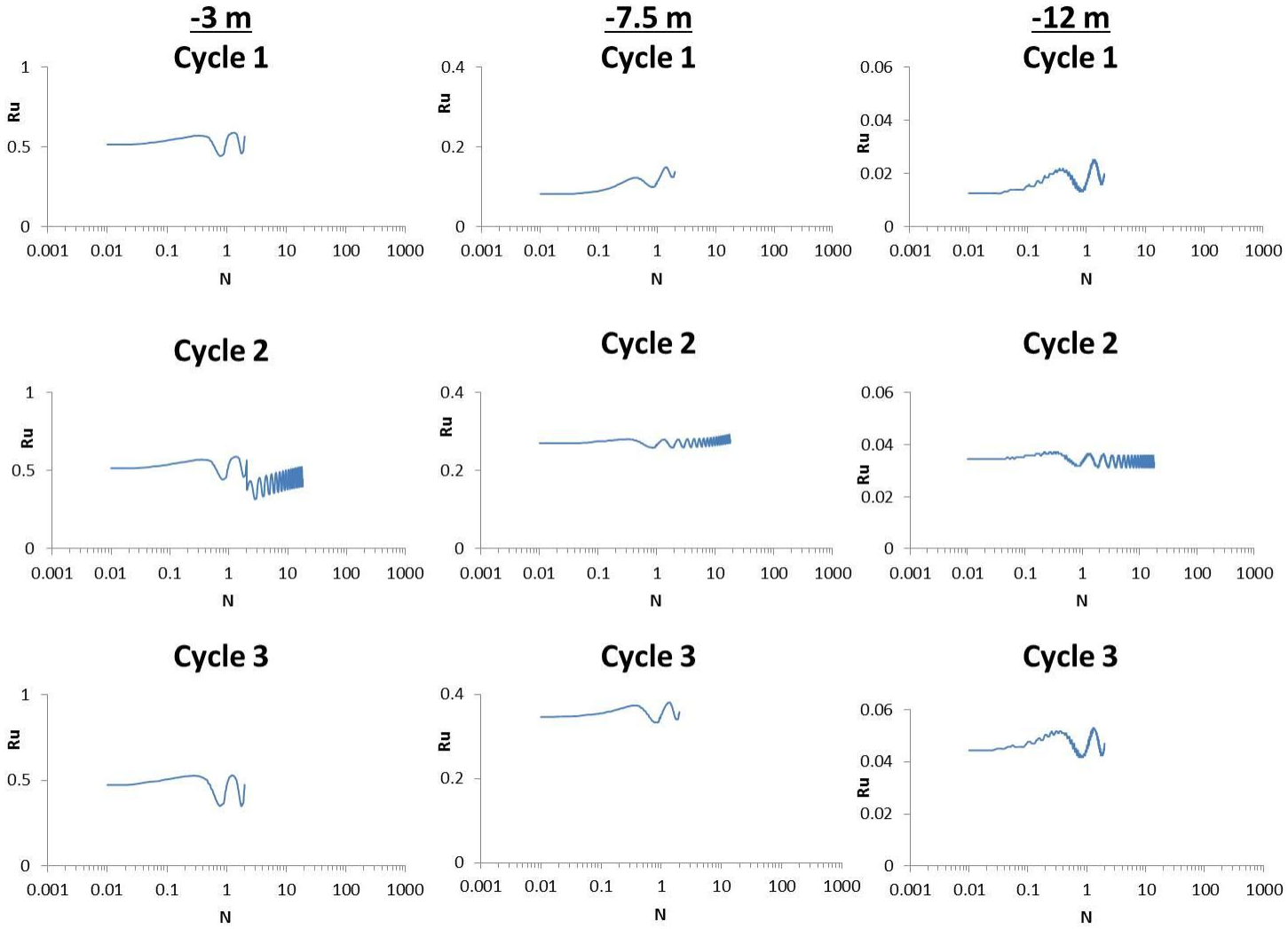

Figure 7.39: Variations in pore pressure ratio observed for reconstituted samples during dynamic tests.

For tests conducted at p'_0 = 147.48 kPa, no ratcheting was observed at such small strain levels. The excess pore pressures simply cycled between a single maximum and minimum value for their respective loading cycles. A widely used criteria in defining whether liquefaction, or cyclic mobility (softening) has occurred within a soil is when pore pressures ratchet towards the value of the effective confining stress used during the triaxial test; i.e. achieving an R_u value of 1 (Ishihara, 1993). Figure 7.39 presents data showing how the R_u value of samples changed during dynamic testing. It can be seen that the highest R_u values ranging between 0.5 and 0.6 were recorded for tests conducted at p'_0 = 60 kPa, when excess pore pressures had reached 30–40 kPa.

Regarding Lanton alluvium's liquefaction potential, its PSD curve lies within the range of potentially liquefiable soils, as defined by Tsuchida (1970). Per criteria stated by Seed et al. (2003), Lanton alluvium's plasticity index (14.95) and liquid limit at 20 mm penetration (35.66) plot within the zone of soils potentially susceptible to classic cyclically induced liquefaction if the water content is >80% of the liquid limit. However, the in-situ moisture content of the soil used for all testing in this research was 25%, which implies the soil probably would not liquefy. Per characteristics of liquefiable soils during monotonic triaxial compression defined by Kramer (1996) (Figure 7.40), the pore pressure – strain, deviatoric stress – strain and effective stress path behaviour of the reconstituted Lanton alluvium (Figures 7.2, 7.5 and 7.9) closely resembles the behaviour of soils with limited liquefaction and dilation.

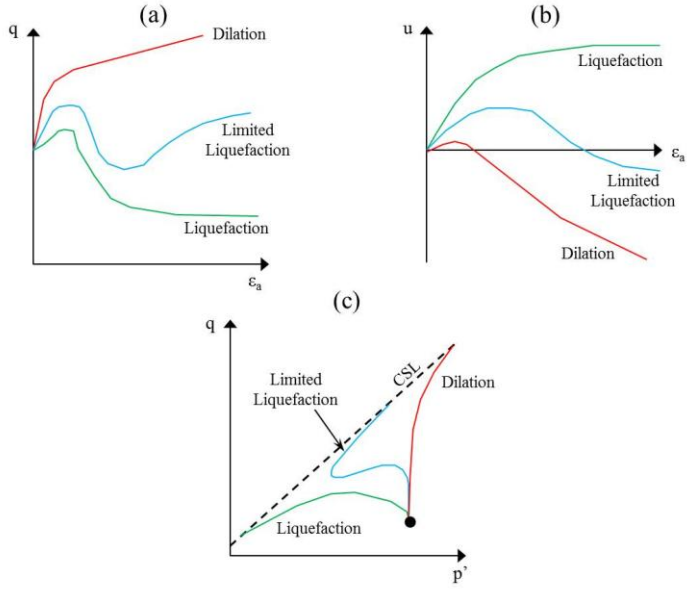

Figure 7.40: (a) Deviatoric stress–strain; (b) pore pressure–strain and (c) effective stress path behaviour of soils likely to experience dilation, limited and total liquefaction. Adapted from Kramer (1996).

The R_u values in Figure 7.39 suggest that liquefaction did not occur within any of the reconstituted samples during tests conducted at p'_0 values of 60, 108.65 or 147.48 kPa, although R_u values were not observed to stabilise by the end of any of the three loading cycle events. It is therefore possible that further Class 43 locomotive or Mark 3 coach loading cycles would cause R_u values to increase further, although whether an R_u value of 1 would be achieved is unknown based on these results. The total amount of axial strain accumulated by samples tested at 60 kPa effective confining stress over the course of the three loading cycles ranged between 4 and 6%. Per criteria defined by Ishihara (1993), such high strain accumulations contrastingly suggest that cyclic mobility may have occurred within samples. At the stress state where R_u = 1 and liquefaction is achieved, a double amplitude axial strain of 5% is commonly observed and is therefore used as a criteria for defining the onset of cyclic mobility. Another means of observing whether liquefaction occurred is by verifying the positions of the effective stress paths recorded for Lanton alluvium within q-p' stress space, relative to the reconstituted soil's CSL, which was defined from monotonic triaxial testing (Figure 7.41).

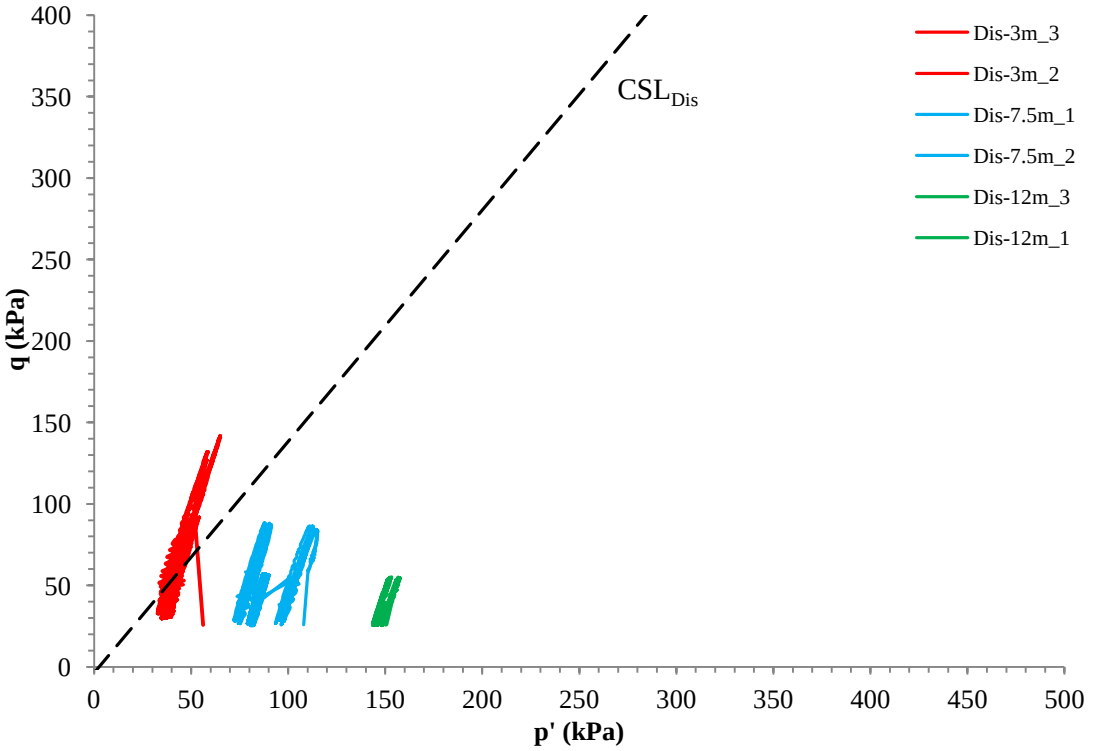

Figure 7.41: Dynamic stress paths for reconstituted Lanton alluvium samples within q-p' stress space, with the soil's CSL_{Dis} superimposed.

Figure 7.41 illustrates that no stress reversals were observed for any of the samples tested, as two-way dynamic loading was not possible. Stress reversals (i.e. behaviour in tension) may only be expected during two-way tests, whereby samples are cyclically loaded about q = 0 kPa as the datum; and allowed to experience tension. Although the combination of the three loading cycle events these samples were subjected to during dynamic testing reduced their mean effective stress states, samples tested at effective confining stresses of 108.65 and 147.48 kPa did not touch Lanton alluvium's CSL_{Dis} line. However, for samples tested at p'_0 conditions of 60 kPa, the cyclic stress paths seen in Figure 7.41 migrate across the CSL_{Dis} line. Unlike the dynamic/cyclic behaviour displayed by other soils in the literature, the "butterfly effect" was not observed for Lanton alluvium when the stress state of the soil reached the CSL. The butterfly effect is the direct result of continued loading at very low mean effective stresses, where the stress state of the soil will move up and down the CSL until it stabilises. Figure 7.42 summarises the peak dynamic stresses applied to samples compared with the reconstituted soil's monotonic peak deviatoric stress for the three dynamic load cycle events at p'_0 conditions of 60, 108.65 and 147.48 kPa. For tests conducted at p'_0 = 60 kPa, the applied cyclic deviatoric stress far exceeded the monotonic deviatoric strength of the soil (Figure 7.42a). This occurrence was not observed for samples tested at p'_0 = 108.65 kPa (Figure 7.42b) or 147.48 kPa (Figure 7.42c) as the applied cyclic deviatoric stresses were less than the monotonic deviatoric strengths.

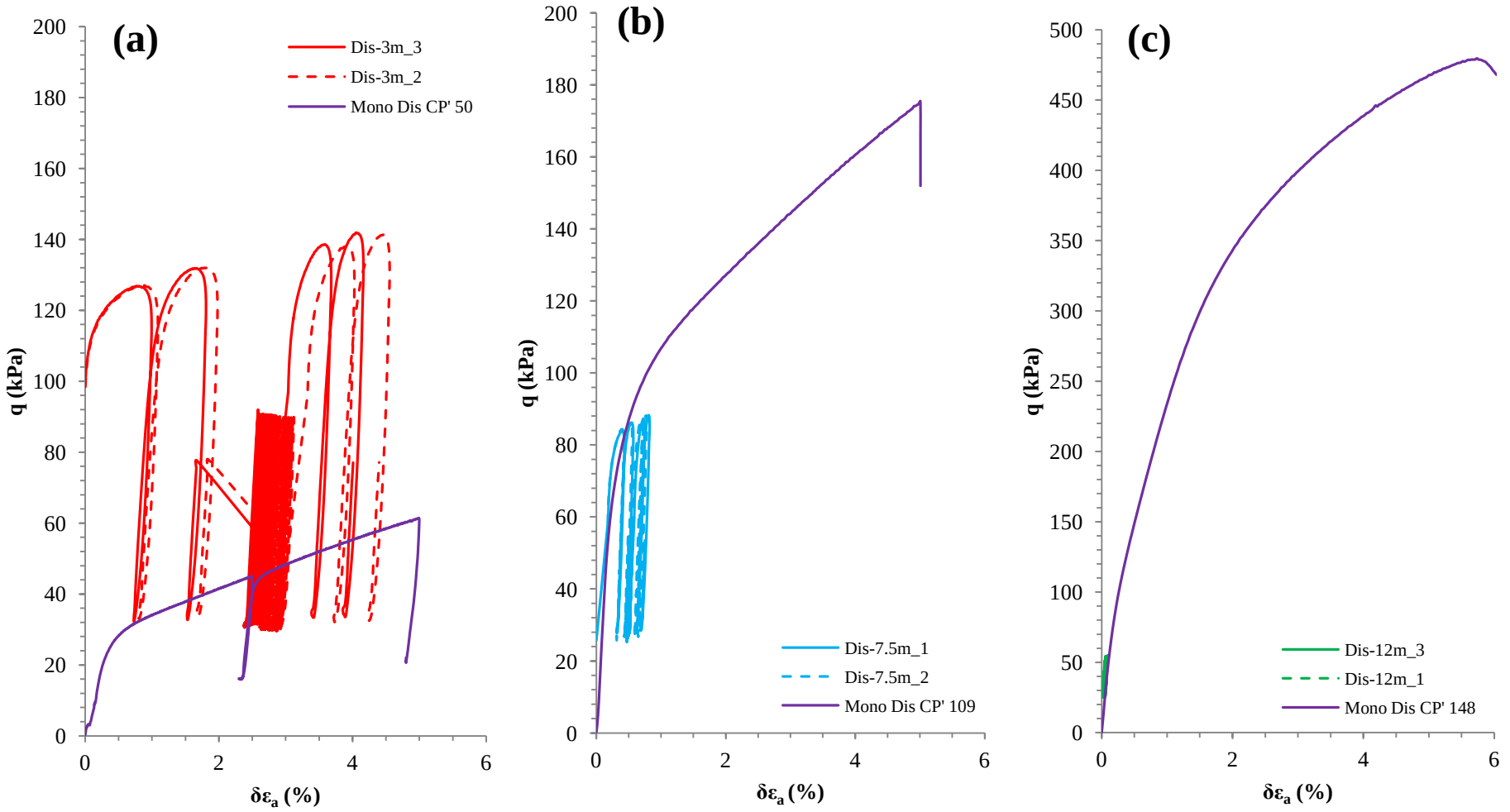

Figure 7.42: One-way compressive loading with peak cyclic deviatoric stress compared with monotonic deviatoric strength for reconstituted samples at p'_0 stress conditions of: (a) 60 kPa, (b) 108.65 kPa and (c) 147.48 kPa.

Regardless of whether the peak cyclic deviatoric stress applied to samples during tests exceeded or remained below the monotonic deviatoric strength, accumulations of plastic strains were observed. However, the amplitude of plastic strain accumulation experienced by samples tested at p'_0 conditions of 108.65 and 147.48 kPa per loading pulse for each of the three loading cycle events was smaller; as similarly observed by Yilmaz et al. (2004) on low plasticity silt-clay alluvium mixtures from Adapazari, Turkey. The behaviour exhibited by samples tested under p'_0 conditions of 60 kPa, (when the cyclic dynamic stresses applied pass through and above the reconstituted soil's CSL and exceed its monotonic strength) is unusual for such a silty cohesive soil. According to Yilmaz et al. (2004), these observations may be explained by the soil's pronounced viscous response to the high loading frequency. Hence, at shallow depths where effective confining pressures are ≤60 kPa, viscous behaviour dictates the deviatoric strength and accumulation of plastic axial/cyclic shear strains of these soils when subjected to high-frequency dynamic loads associated with passing HST traffic.

Figure 7.43 shows the relationship experienced by reconstituted samples between cyclic shear strain and the number of loading pulses for the three loading cycle events. Cyclic shear strain is seen to increase in a ratcheting manner with the number of pulses, particularly for samples which had been consolidated to a p'_0 of 60 kPa. For load cycles 1 and 3, cyclic shear strains of 3 and 2% were recorded respectively. Lower cyclic shear strains of 0.75–1% were recorded for load cycle 2; thereby indicating that the liquefaction initiation criteria of 5% double amplitude strain was exceeded after the passage of an HST. For tests conducted at p'_0 = 108.65 and 147.48 kPa, total cyclic shear strains of approximately 1 and 0.12% were recorded, respectively. Whilst the amount of cyclic shear strain was observed to slowly increase with increasing number of pulses for the tests conducted at p'_0 = 108.65 kPa, such ratcheting cyclic shear strains were less apparent during tests conducted at p'_0 = 147.48 kPa.

Figure 7.44 shows the relationship between mean effective stress and cyclic shear strain. Displayed in Figure 7.38, the pore pressure within all samples increased due to the application of the three dynamic loading cycles, resulting in reductions in mean effective stresses. This behaviour was more pronounced for samples consolidated to p'_0 = 60 kPa, compared with those consolidated to 108.65 or 147.48 kPa; particularly during load cycles 1 and 3, representing the passage of the Class 43 locomotive.

During the cyclic loading of soils, there is a critical cyclic shear strain level at which an excessive increase in shear strain occurs within samples, known as the cyclic yield shear strain level. However, due to the low number of pulses experienced by samples during the three loading cycles and the relatively high loading frequency used, the cyclic yield shear strain level for reconstituted Lanton alluvium could not be derived. Further longer term cyclic testing at various frequencies would be required to define the critical strain level. Per Terzaghi et al. (1996), the cyclic yield shear strength for reconstituted soils is generally expected to be lower than for undisturbed soils, primarily due to the absence of structure. This infers that the cyclic yield shear strains for reconstituted soils are expected to be smaller than those for their undisturbed equivalents. This behaviour has been observed for Lanton alluvium during oedometer testing (see chapter 5). However, there may be instances particularly within silt and sand based soils where reconstituted soils with higher levels of compaction and relative densities are characterised by higher cyclic yield shear strengths than their undisturbed counterparts.

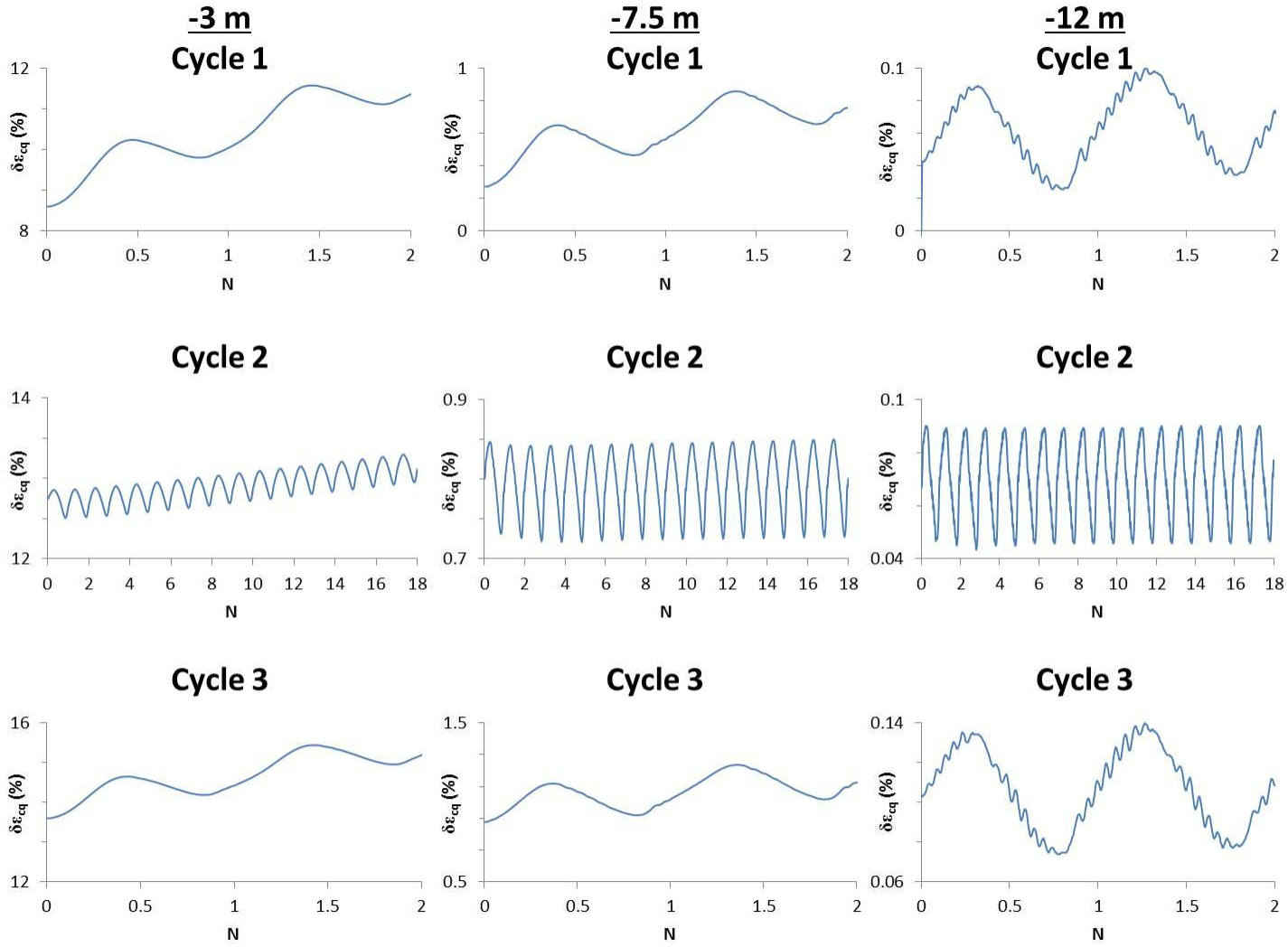

Figure 7.43: Relationship between cyclic shear strain and number of loading pulses experienced by reconstituted samples during the three dynamic loading events.

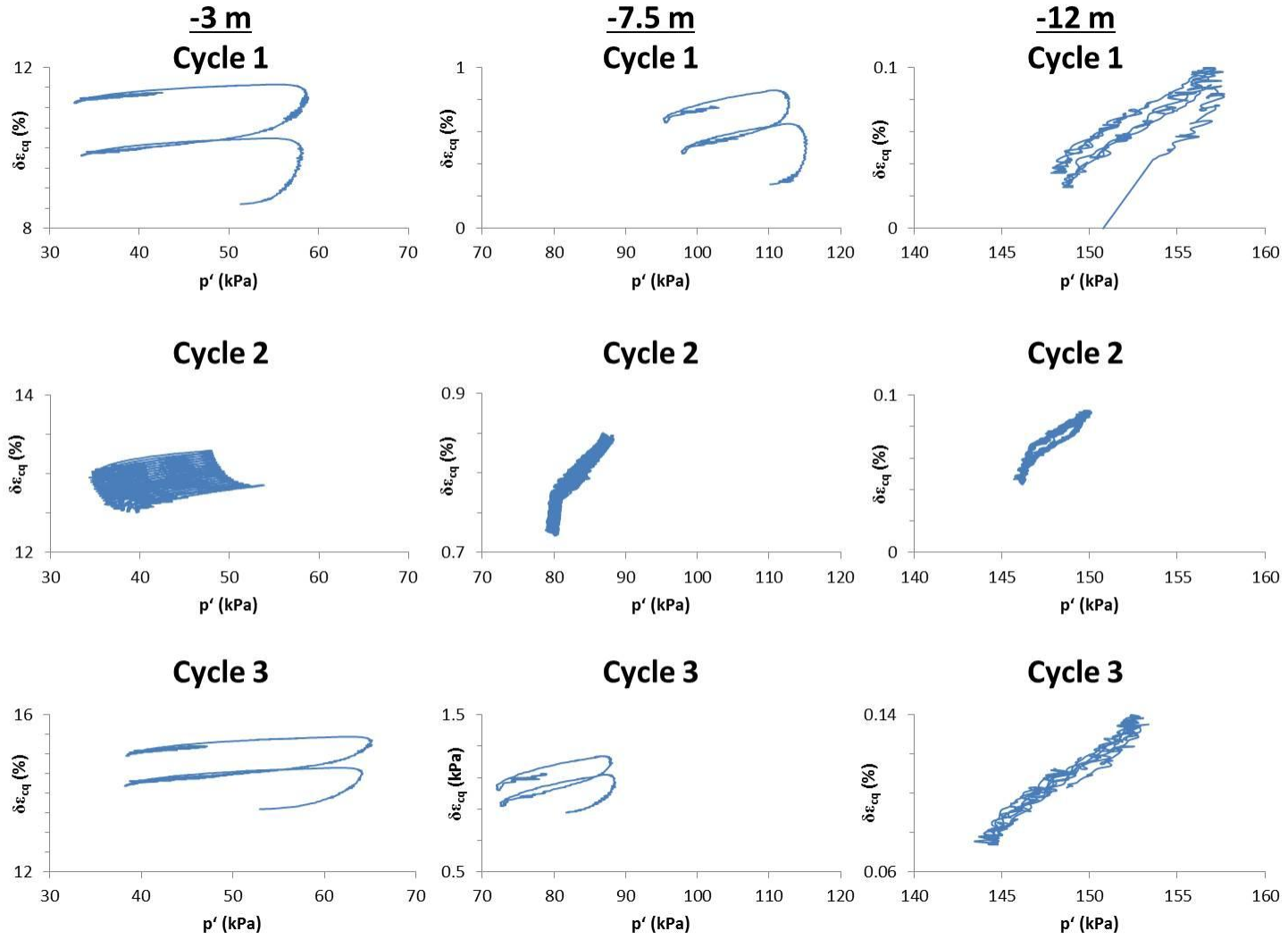

Figure 7.44: Relationship between cyclic shear strain and mean effective stress for reconstituted samples during dynamic tests.

Figure 7.45 presents the Resilient modulus (M_r) values recorded by samples after each locomotive and coach loading cycle. In general, higher M_r values were recorded for locomotive loading cycles compared with coach loading cycles, due to the higher dynamic loading experienced on relatively densely compacted reconstituted samples of Lanton alluvium. As considerably less permanent plastic strain was experienced by samples tested at higher p'_0 conditions, the stiffness of the reconstituted soil was a little higher than those measured at lower p'_0 conditions. With increasing numbers of pulses for all three loading cycle events, the M_r values recorded for the soil were observed to remain fairly constant after the second pulse. This may be explained by the sample's reconstituted states; whereby no pre-existing structure (i.e. high initial stiffness) was present within the soil, indicating that any marked stiffness degradation had taken place prior to dynamic loading. Reconstituted samples were prepared by means of compaction, which had also undergone isotropic consolidation; thereby suggesting all the reconstituted samples were characterised by a relatively dense state during dynamic testing.

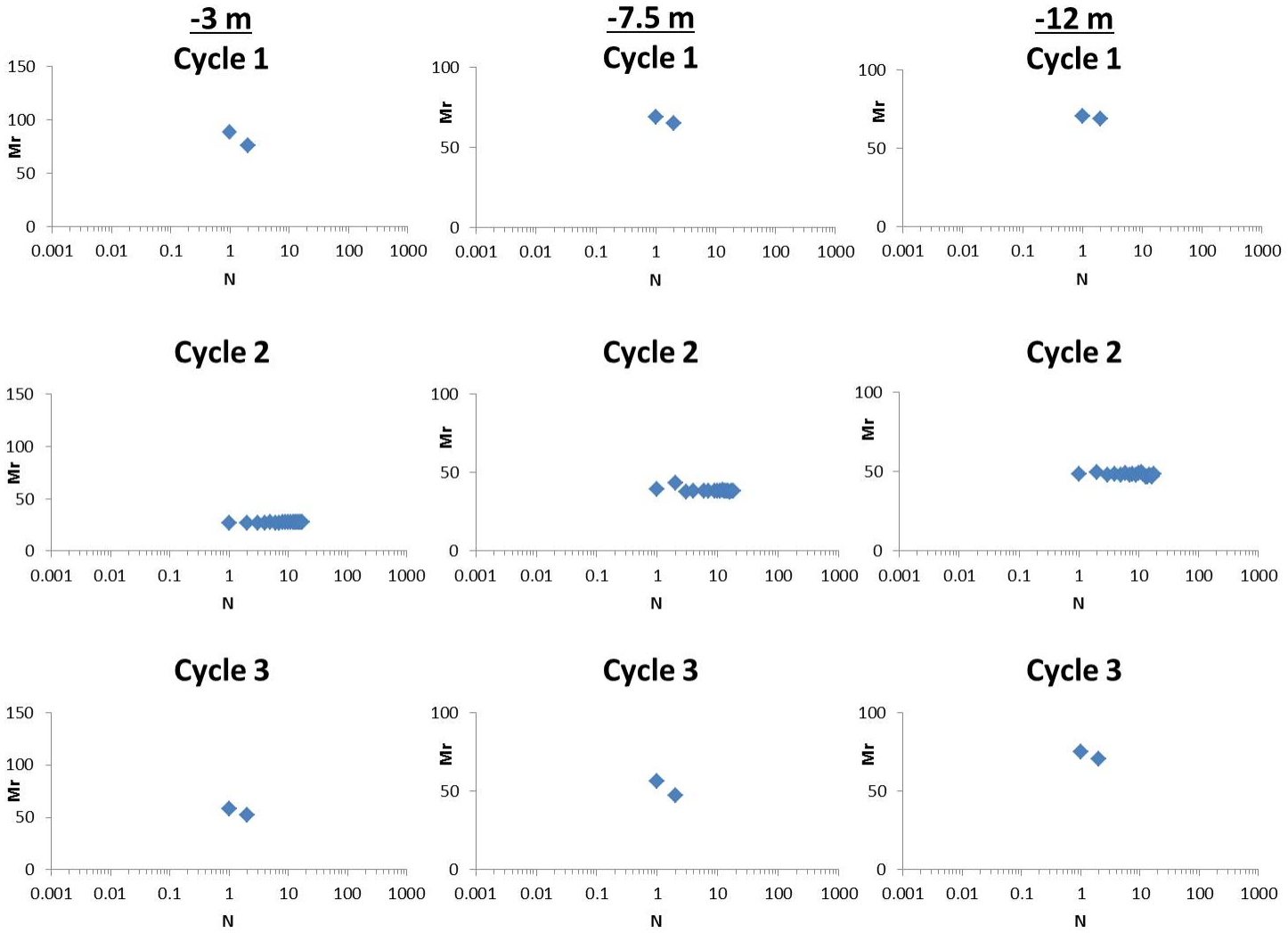

Figure 7.45: Variations in resilient modulus (Mr) observed with increasing number of cycles for reconstituted samples during dynamic tests.

7.3.2 Undisturbed samples

Figure 7.46 presents a summary of the seat load and dynamic loading conditions applied to undisturbed samples for the three p'_0 states used to represent a passing HST during dynamic tests. The corresponding cyclic stress ratio values are given in Table 7.2. As with dynamic tests on reconstituted samples, tests used the one-way loading technique. Figures 7.47–7.48 present the deviatoric stress – axial strain and deviatoric stress – cyclic shear strain behaviour of the undisturbed Lanton alluvium samples, whereas Figure 7.49 presents the relationship between cyclic shear strains with increasing numbers of loading pulses for the three dynamic loading cycle events. As with reconstituted samples, axial and cyclic shear strains within samples were generally seen to exhibit ratcheting behaviour with increasing numbers of pulses, particularly at lower effective confining pressures. For tests conducted at p'_0 = 60 kPa, the most significant axial strains recorded were caused by the dynamic loads associated with load cycle events 1 (0.75%) and 3 (0.55%), due to the passing Class 43 locomotive and brake car, respectively. Considerably smaller axial strains of 0.25% were recorded during load cycle event 2 for the passing of nine Mark 3 coaches. Hence, after the passing HST loading event, total unrecoverable axial strain accumulations of approximately 1.4% were recorded (excluding the amount of strain induced in placing samples under their required seat loads). Although such axial strains were smaller than those observed for reconstituted samples due to the presence of an inter-particle bonding based structure, they are still considered to be significant and potentially cause unfavourable ground surface displacements.

For tests conducted at p'_0 conditions of 108.65 and 147.48 kPa, the cyclic strains experienced during the three dynamic load cycle events were smaller compared with samples tested at p'_0 = 60 kPa. As expected, higher cyclic strain ranges and plastic strain accumulations occurred in response to the simulated Class 43 locomotive and brake car loadings, due to their higher magnitude dynamic stresses than those for nine Mark 3 coaches. The total accumulated plastic shear strains measured for samples tested at p'_0 states of 108.65 and 147.48 kPa were 0.09 and 0.025%, respectively; much lower than the values for samples tested at p'_0 = 60 kPa (1.09%).

According to the small strain stiffness behaviour of undisturbed Lanton alluvium from the monotonic testing results in Appendix 5, approximately 75% of the soil's initially high shear stiffness due to structure is degraded after 0.002% shear strain has been experienced. The magnitude of plastic shear strain accumulations recorded within all samples at each effective confining pressure were outside the small strain range, even at higher effective confining pressures when lower deviator stresses of 15–30 kPa were applied. This confirms Lanton alluvium's sensitivity to monotonic and dynamic loading disturbances; whereby the passing of a single HST at 125 mph would result in considerable plastic strain accumulations and therefore unfavourable settlements at the ground surface.

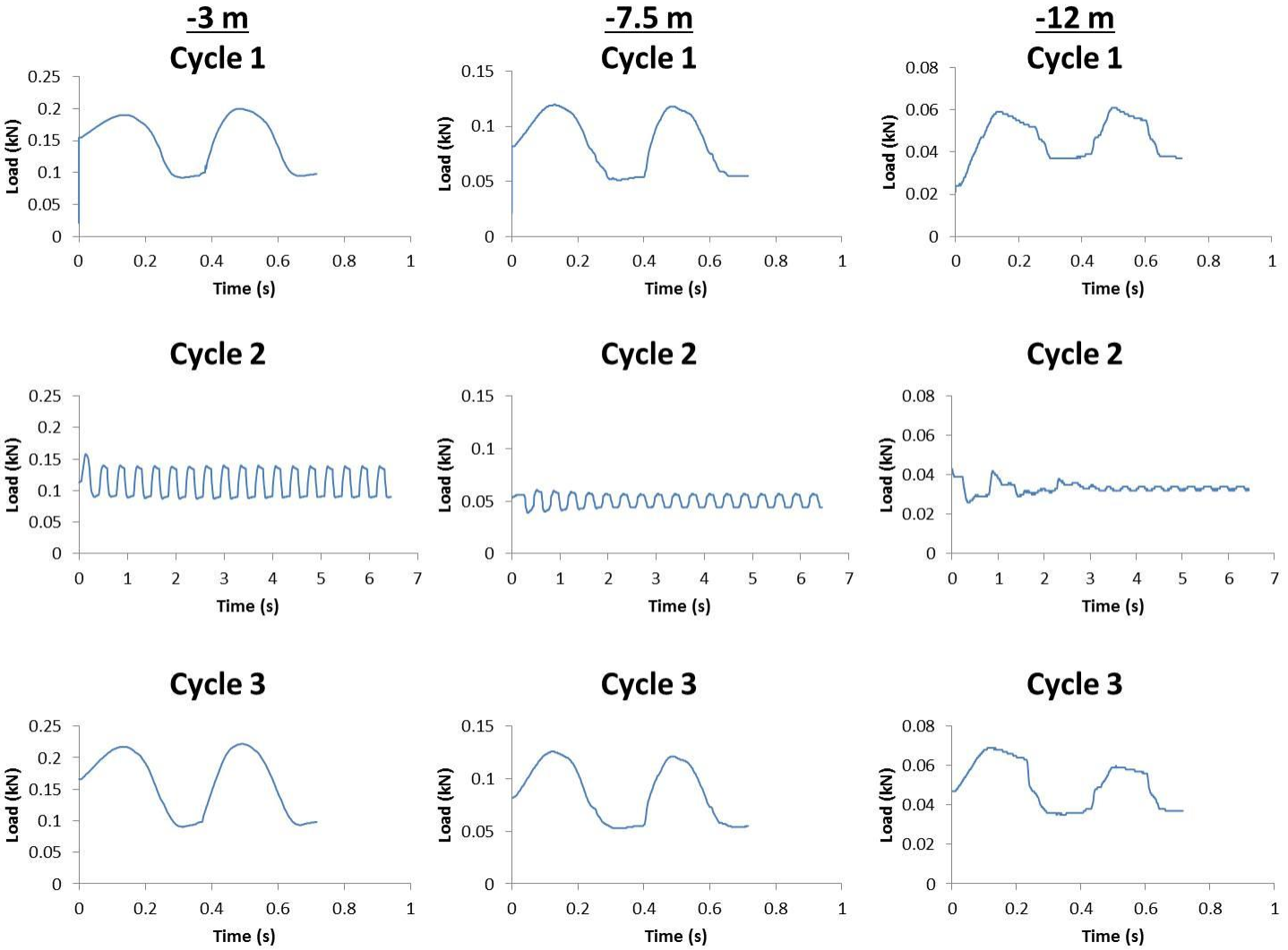

Figure 7.46: Summary of loading patterns observed for dynamic tests conducted on undisturbed samples at three effective confining stresses.

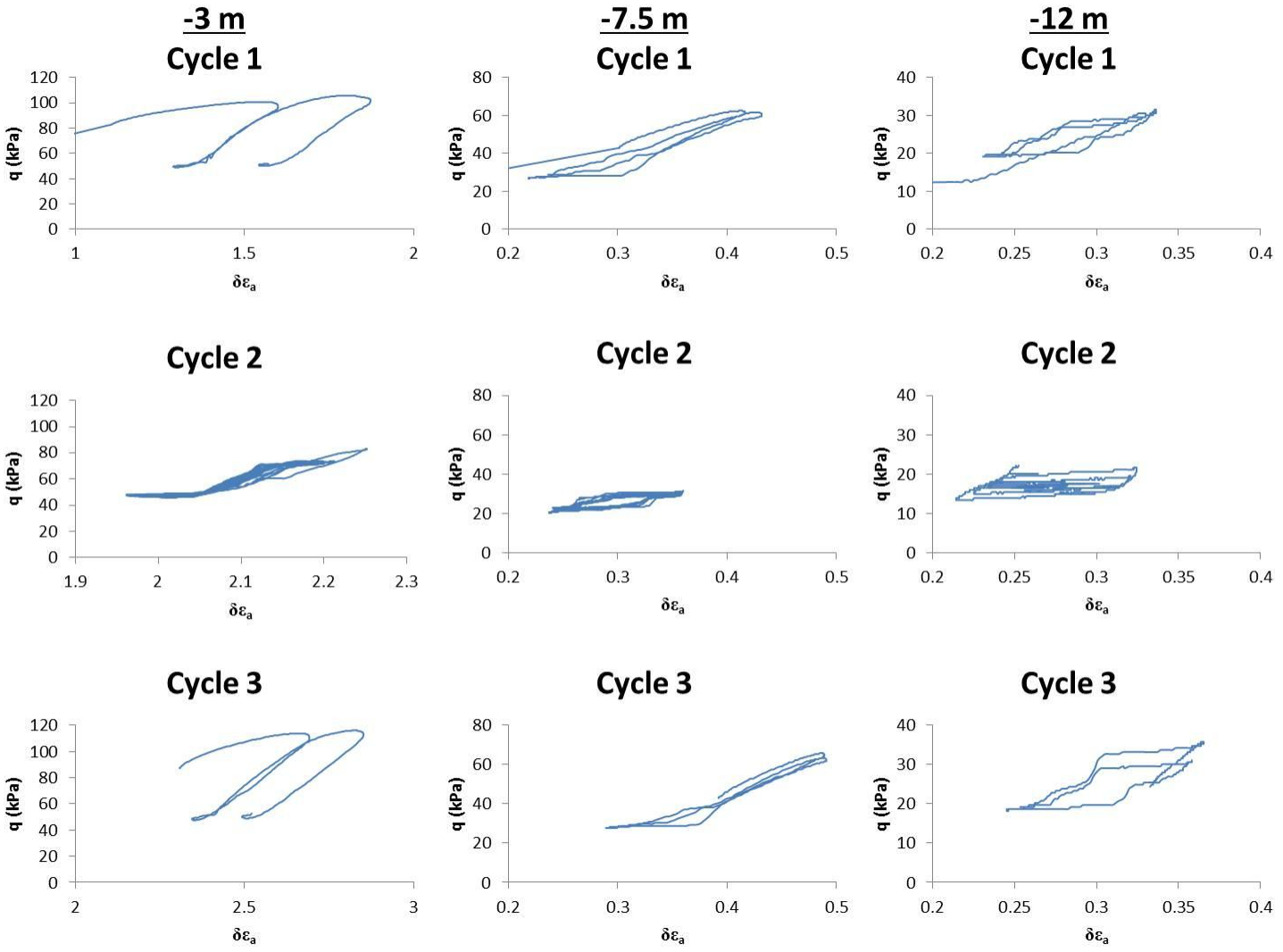

Figure 7.47: Summary of deviatoric stress-axial strain relationships during dynamic tests conducted on undisturbed samples at three effective confining stresses.

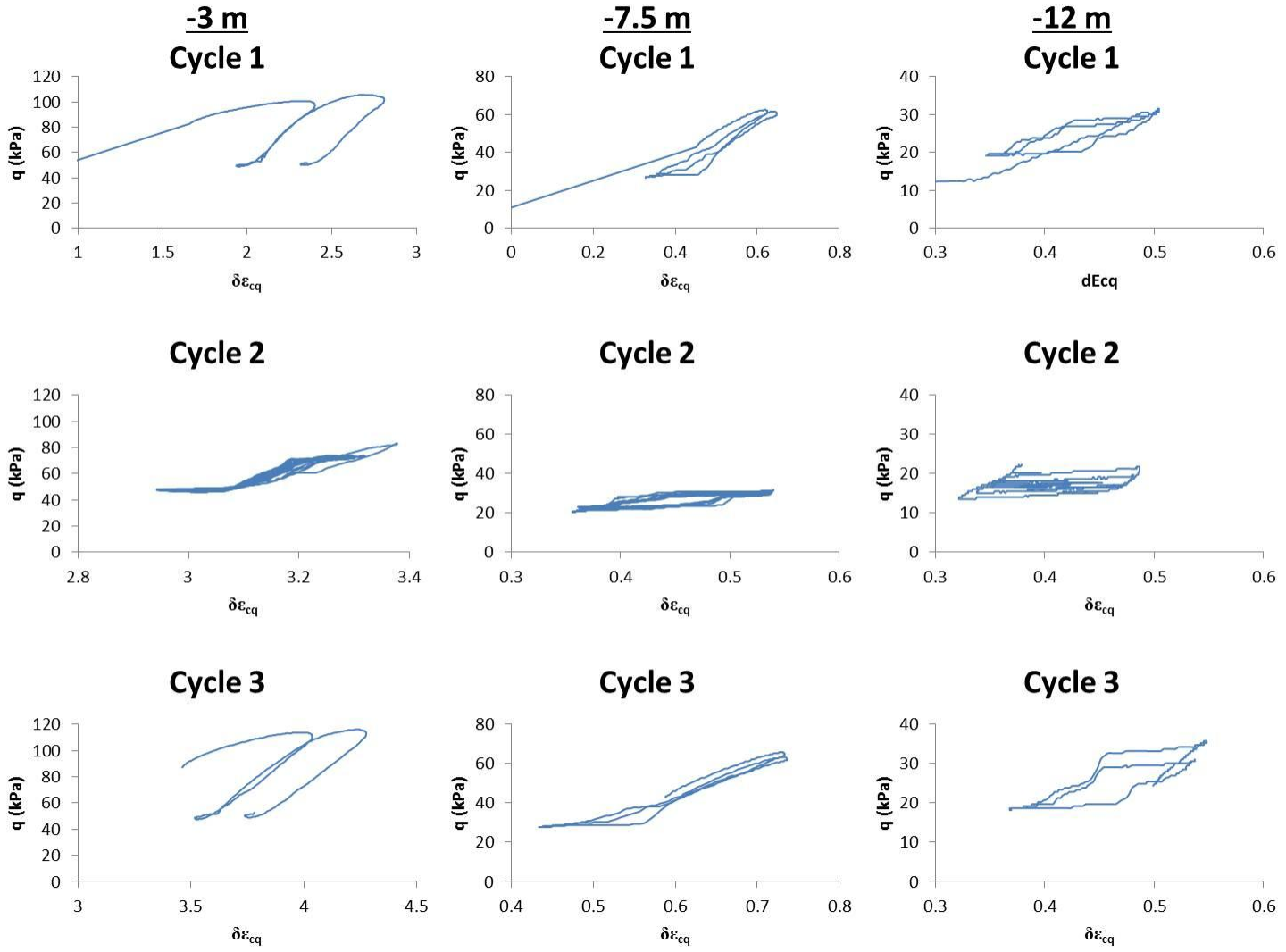

Figure 7.48: Summary of deviatoric stress-cyclic shear strain relationships during dynamic tests conducted on undisturbed samples at three effective confining stresses.

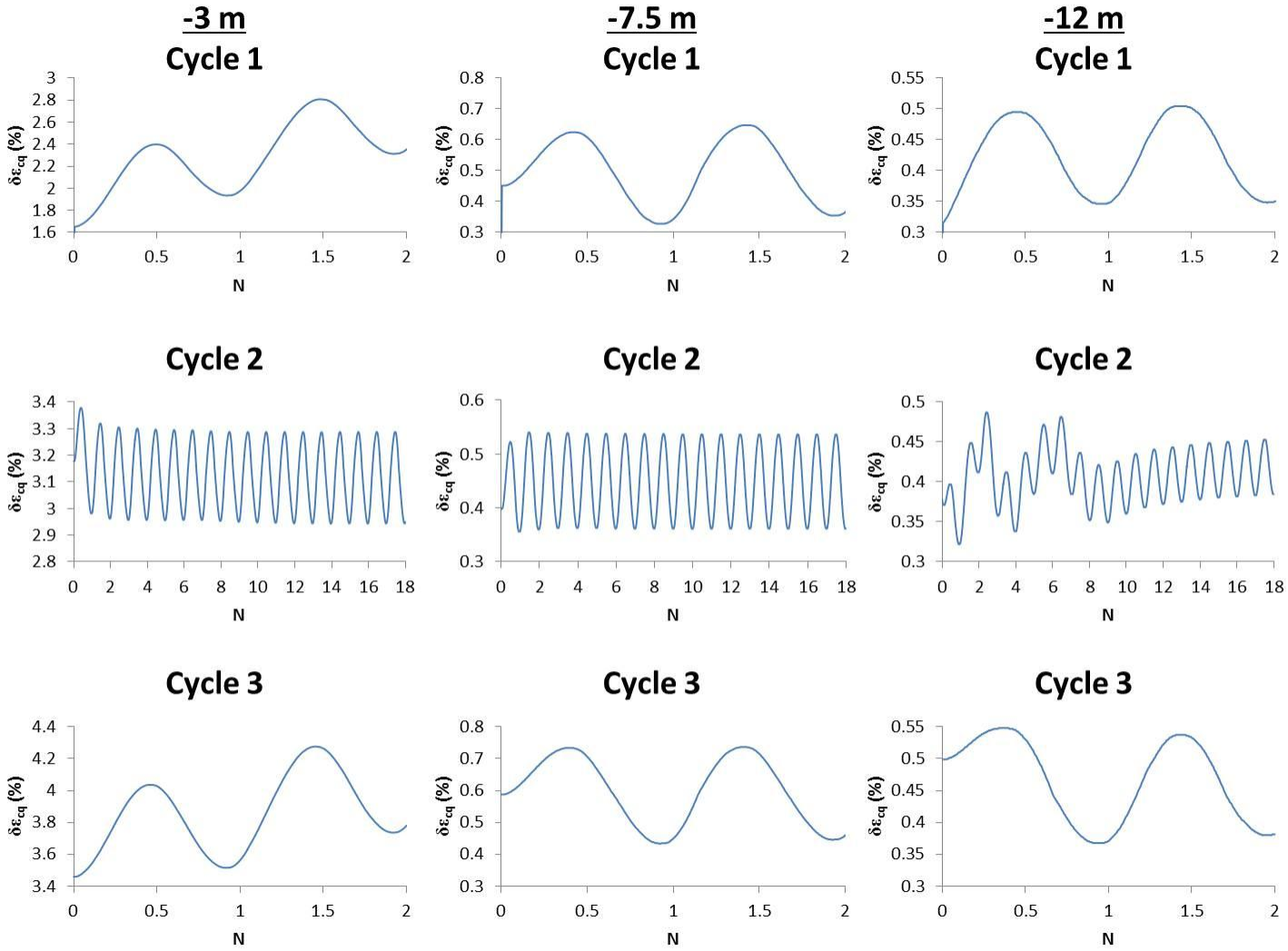

Figure 7.49: Cyclic shear strain behaviour of undisturbed Lanton alluvium with increasing number of cycles.

Table 7.2: Summary of CSR conditions used during dynamic testing on undisturbed samples.

	CSR		
	p'$_0$ = 60 kPa	***p'$_0$ = 108.65***	***p'$_0$ = 147.48***
Load cycle 1 (1 x Class 43 locomotive)	0.43	0.13	0.07
Load cycle 2 (9 x Mark 3 coaches)	0.41	0.11	0.05
Load cycle 3 (1 x Class 43 brake car)	0.44	0.13	0.07

Pore pressures within the undisturbed samples were recorded to increase in response to the dynamic loads being applied during each loading cycle event (Figure 7.50). At a stress state of p'_0 = 60 kPa, maximum excess pore pressures of 10–12 kPa developed within samples; whereas at p'_0 = 147.48 kPa, lower excess pore pressures of 0.5–4 kPa were seen to develop. Figure 7.50 demonstrates that pore pressure and axial/cyclic shear strain ratcheting occurred in tandem with increasing numbers of load pulses. The degree of ratcheting experienced depended upon the p'_0 conditions and the magnitude of the dynamic loads exerted. Generally, higher degrees of pore pressure ratcheting were observed for load cycle events corresponding to the passing of the Class 43 locomotive and brake car at lower effective confining stresses of 60 kPa. For samples tested under p'_0 conditions of 147.48 kPa, negligible ratcheting was observed at smaller strain levels.

The changing pore pressure ratio state of undisturbed Lanton alluvium samples during dynamic testing is shown in Figure 7.51. In general, the R_u value for samples steadily increased as dynamic loading progressed and that lower R_u values were recorded for samples tested at higher p'_0 stress conditions. As similarly noted for reconstituted samples, the highest R_u values ranged between 0.3 and 0.4 for tests conducted at p'_0 = 60 kPa. Considerably lower final R_u values were recorded for samples tested under p'_0 conditions of 108.65 and 147.48 kPa; whereby average final R_u values of 0.17 and 0.05 were recorded, respectively. Hence, per criteria stated by Ishihara (1993), liquefaction was not observed within the undisturbed Lanton alluvium as $R_u<1$.

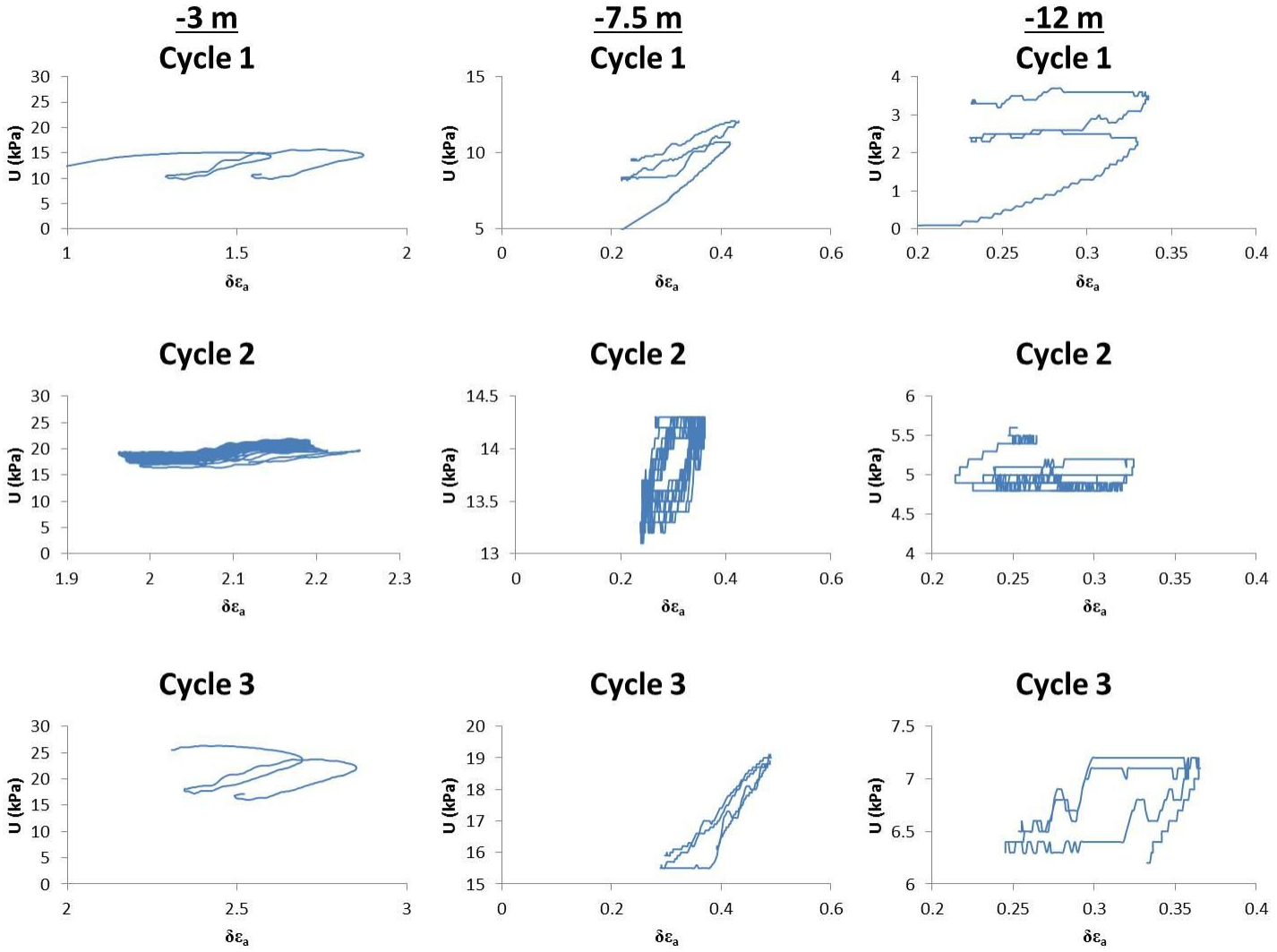

Figure 7.50: Pore pressure response during dynamic tests conducted on undisturbed samples at three effective confining stresses.

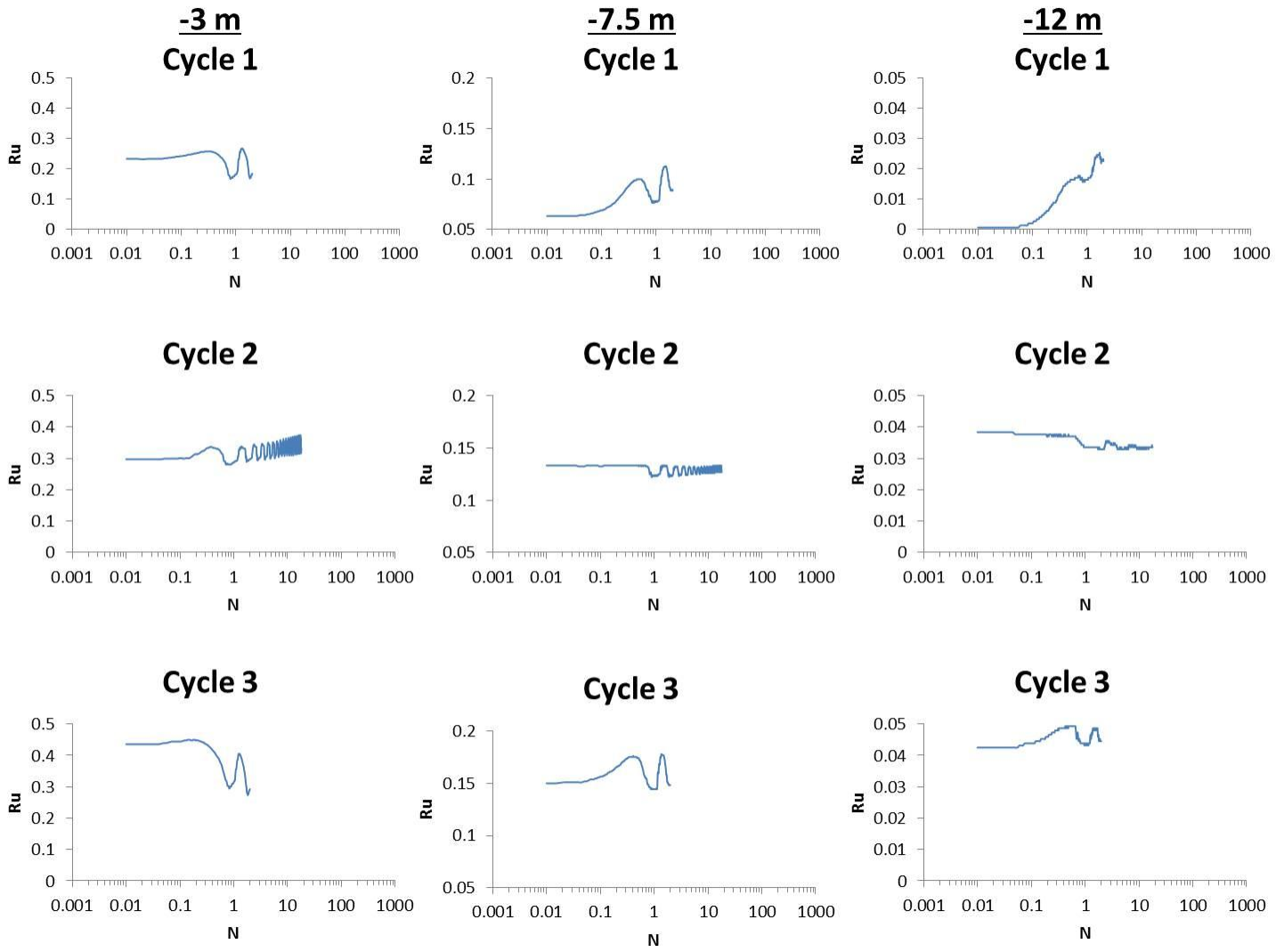

Figure 7.51: Variations in the pore pressure ratio with increasing number of cycles during dynamic tests conducted on undisturbed samples.

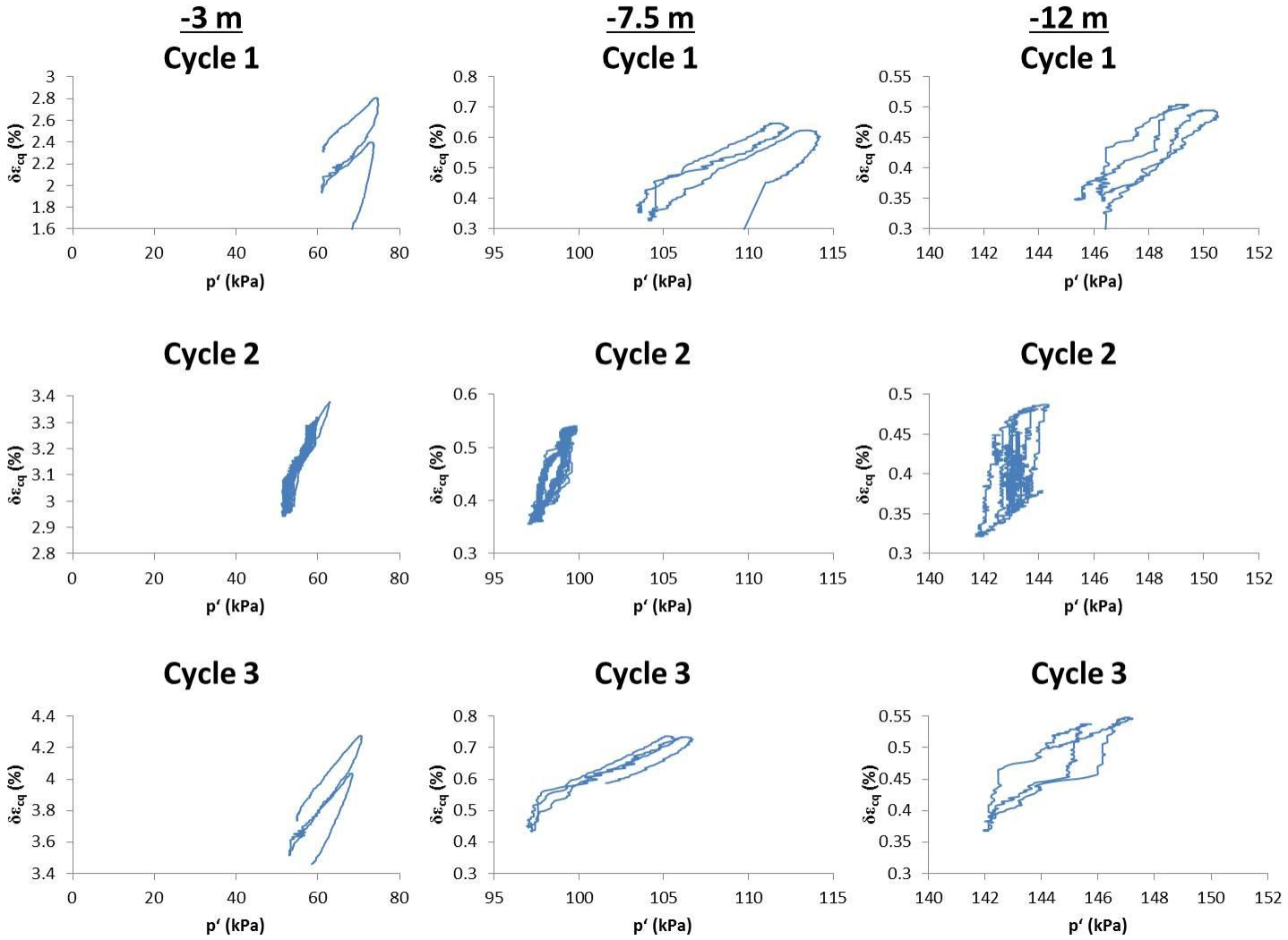

Figure 7.52: Cyclic shear strain versus mean effective stress relationship under dynamic loading for undisturbed Lanton alluvium.

The relationship between mean effective stress and cyclic shear strain for undisturbed samples under the three aforementioned p'_0 stress conditions is shown in Figure 7.52. The observed ratcheting in pore pressures within samples due to the dynamic loading conditions presented by the Class 43 locomotive, brake car and Mark 3 coaches has consequently caused the mean effective stresses to decrease as dynamic loading progressed. On average, total mean effective stress reductions of 15, 8 and 4 kPa occurred after the three dynamic loading events for tests conducted at p'_0 conditions of 60, 108.65 and 147.48 kPa, respectively. Greater reductions in mean effective stress occurred during tests when samples were subjected to loads corresponding to the Class 43 locomotive and brake car and/or lower p'_0 values (i.e. 60 kPa). The p' reductions measured for undisturbed samples were approximately half the magnitude of those measured for reconstituted samples over the course of the three loading cycle events. Given the relatively low number of pulses and high loading frequency used during the dynamic loading testing programme, the precise measurement of the undisturbed soil's cyclic yield shear strain level could not to be defined. Based on monotonic triaxial and oedometer testing results for the reconstituted and undisturbed Lanton alluvium, the cyclic yield shear strain for the soil in its undisturbed state is assumed to be higher than that for undisturbed natural soils, due to the soil's bonding-based structure. Future testing involving a higher number of loading pulses for each loading cycle event, lower loading frequencies and local strain measurements on samples is therefore highly recommended.

Resilient modulus values measured for samples after each locomotive, brake car and coach loading cycle are given in Figure 7.53. Although the undisturbed Lanton alluvium possesses internal structure and would therefore be anticipated to have higher elastic stiffnesses upon dynamic loading compared with reconstituted samples, in general lower M_r values were recorded for all three loading cycle events compared with those measured for reconstituted samples. This may be attributed to the higher relative densities of the reconstituted samples (Terzaghi et al., 1996), due to their compaction-based preparation. Additionally, the effect of increasing the p'_0 stress conditions during testing reduced the M_r values after each loading cycle event and that marked degradations in stiffness were observed with increasing number of pulses. This behaviour was particularly pronounced during loading cycle 2, due to the high number of loading pulses compared with cycles 1 and 3; whereby the soil's structure and

initial high stiffnesses degraded from 20–30 MPa down to 5–10 MPa at the end of the loading cycle, due to repeated dynamic loading.

Although the R_u = 1 and 5% double amplitude axial/cyclic shear strain criteria required for soil liquefaction were not met by the undisturbed soil, the position and shape of the dynamic effective stress paths taken by all undisturbed samples in q-p' stress space relative to Lanton alluvium's CSL_{Undis} should also be considered (Figure 7.54). Due to the one-way loading technique used for dynamic testing, no stress reversals into extension or "butterfly" behaviour were observed for any samples. As also displayed in Figure 7.52, the stress paths taken by samples for each p'_0 condition are observed to migrate steadily towards the left of the q-p' plot, indicating reductions in mean effective stress.

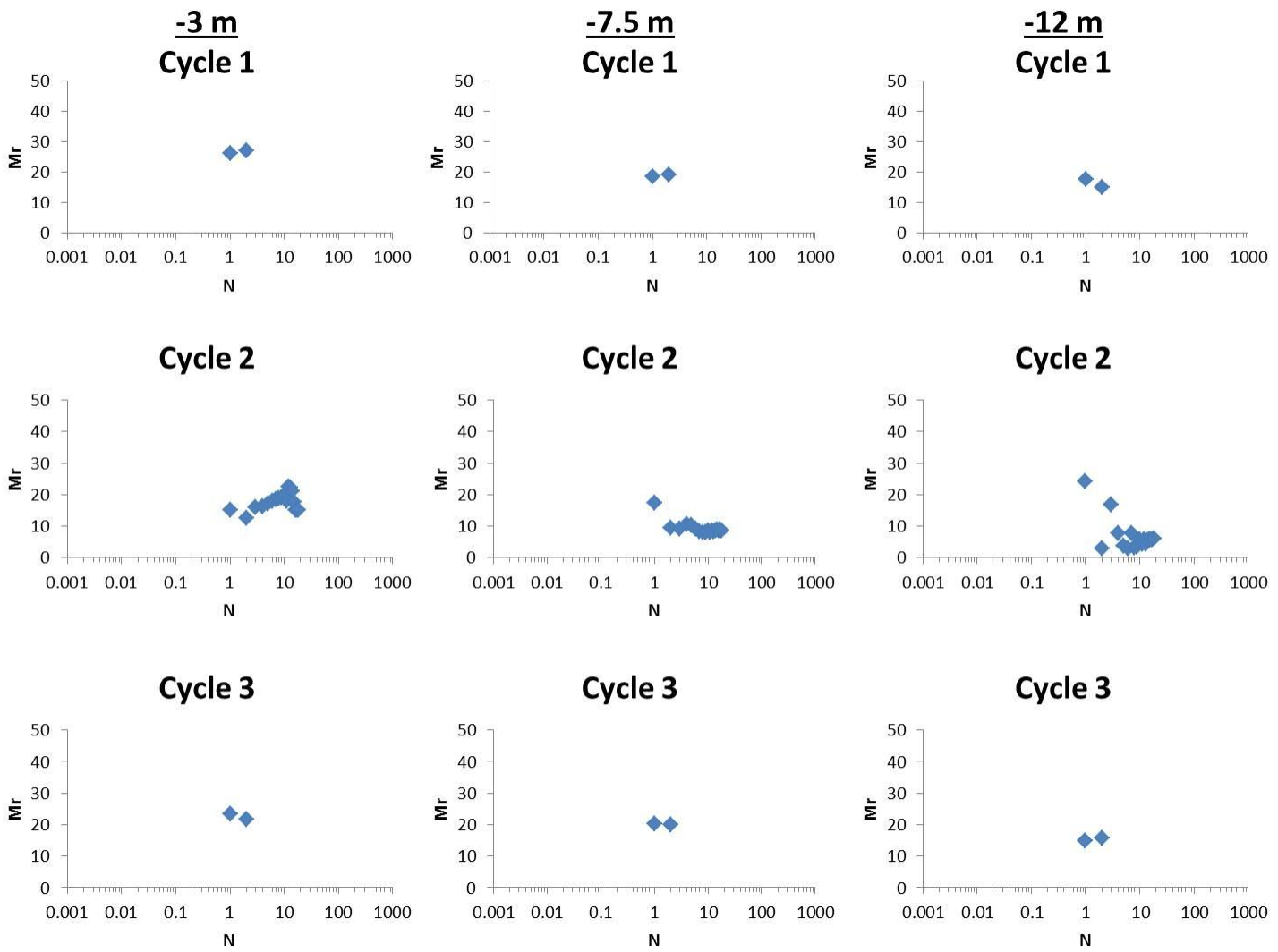

Figure 7.53: Variations in resilient modulus values observed for undisturbed samples with increasing number of pulses during dynamic tests.

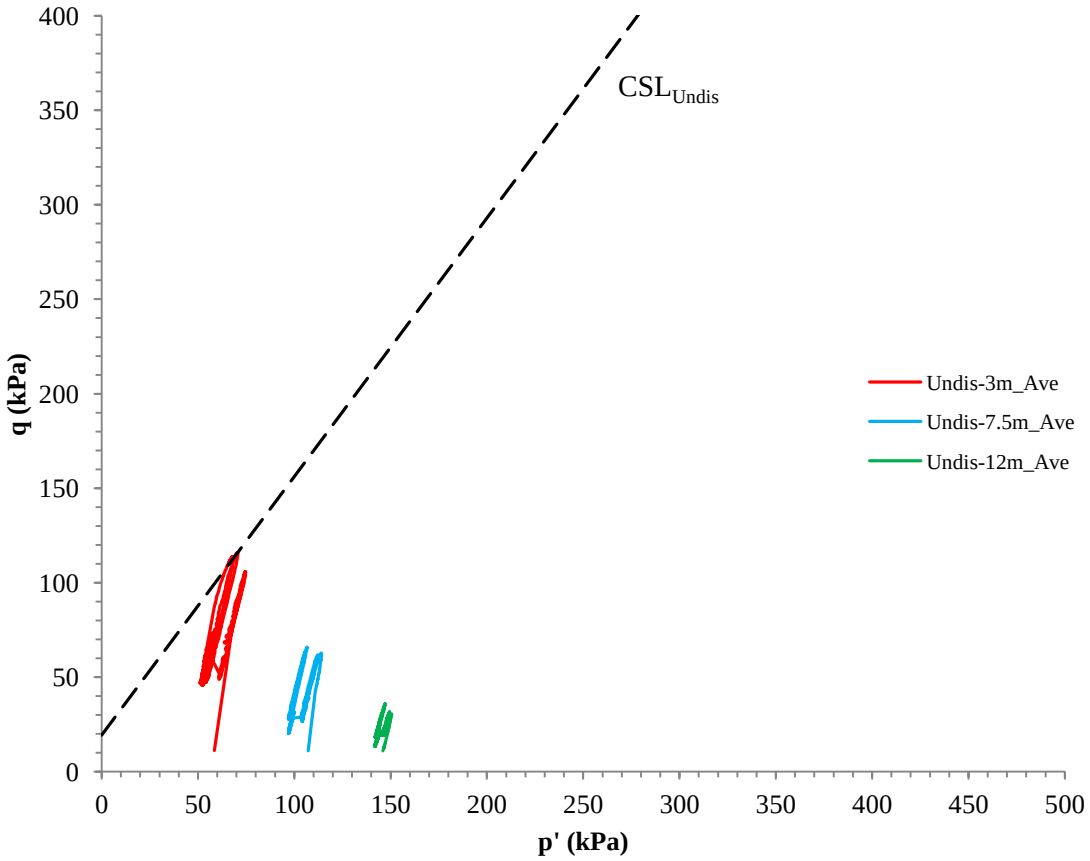

Figure 7.54: Dynamic stress paths for undisturbed Lanton alluvium samples within q-p' stress space, with the soil's CSL_{Undis} superimposed.

As with reconstituted samples, undisturbed samples tested at effective confining stresses of 108.65 and 147.48 kPa did not touch Lanton alluvium's CSL_{Dis} line; thereby suggesting these samples did not liquefy. Regarding undisturbed samples which were dynamically tested at p'_0 = 60 kPa, their cyclic stress paths appear to touch the CSL_{Undis} line, suggesting liquefaction occurred during testing. This finding contradicts the R_u and accumulated plastic strain results. Figure 7.55 displays a comparison between the peak stresses applied to undisturbed samples during dynamic tests conducted under the three aforementioned p'_0 conditions and the corresponding monotonic peak deviatoric strengths.

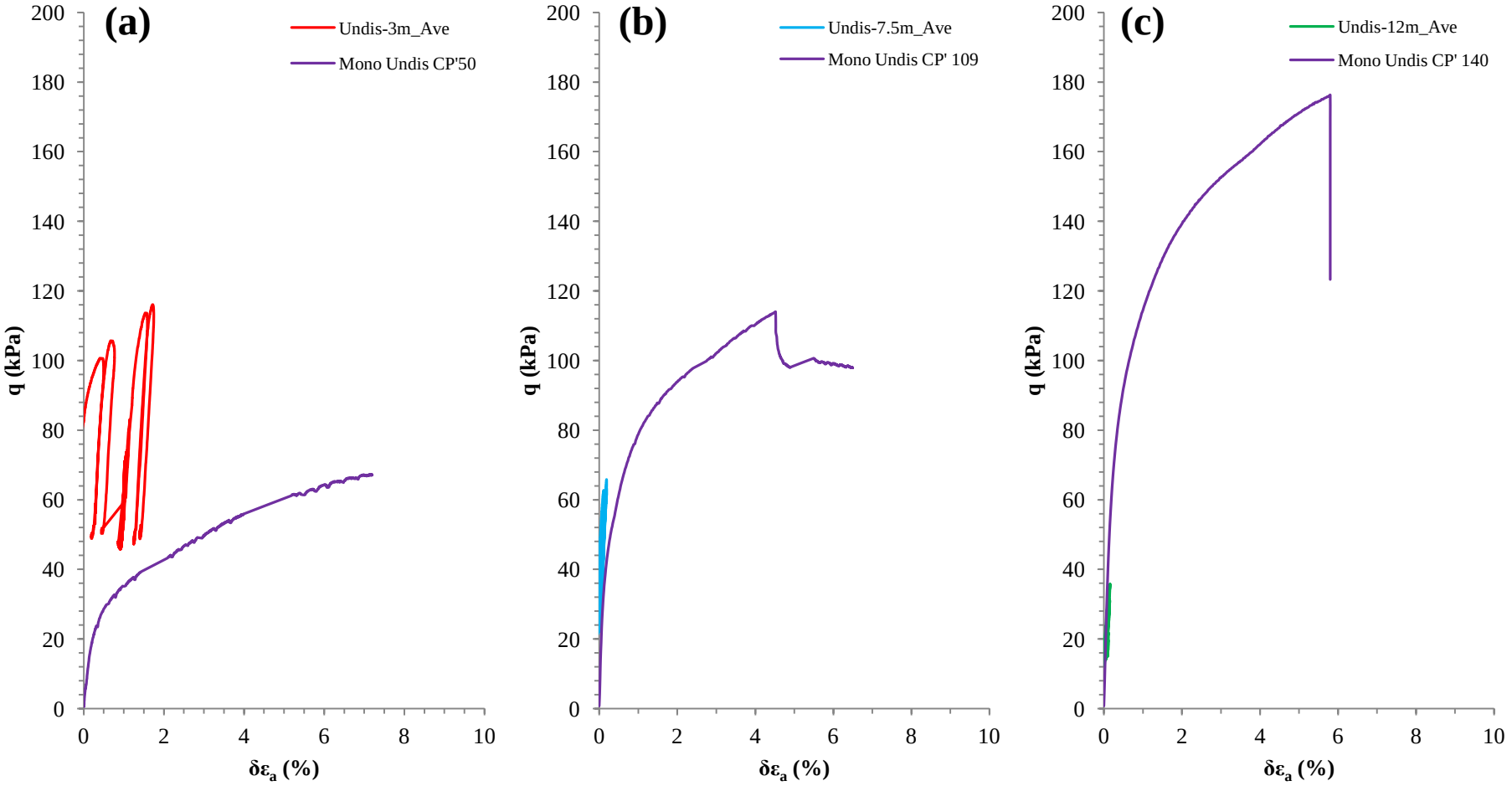

Figure 7.55: One-way compressive loading with peak cyclic deviatoric stress compared with monotonic deviatoric strength for undisturbed samples at p'_0 stress conditions of: (a) 60 kPa, (b) 108.65 kPa and (c) 147.48 kPa.

Although the peak of the cyclic effective stress paths taken by samples under effective stresses of 60 kPa just touch the CSL_{Undis}, the applied cyclic deviatoric stress exceeded the corresponding monotonic deviatoric strength (Figure 7.55a). Unlike the behaviour observed for reconstituted samples, the peak cyclic deviatoric stresses recorded by undisturbed samples during tests conducted at p'_0 = 108.65 kPa also exceeded the monotonic deviatoric strength (Figure 7.55b). However, Figure 7.55c shows that the applied cyclic deviatoric stresses recorded for samples during tests conducted at p'_0 = 147.48 kPa were less than their respective monotonic deviatoric strengths. Accumulations of non-recoverable strains were observed within all samples tested, as illustrated in Figures 7.52 and 7.55; whereby the amount of strain accumulation measured by samples after the passage of an HST was greatest for those tested at p'_0 conditions of 60 kPa.

The unconventional behaviour of undisturbed samples tested at p'_0 conditions of 60 and 108.65 kPa in q-p' stress space was similar to that noted for reconstituted samples at p'0 = 60 kPa, with the material exhibiting viscous behaviour under a relatively high loading frequency. This resulted in the cyclic deviatoric stresses applied to samples being greater than their monotonic deviatoric strengths. Thus, the soil's viscosity response to HST loadings and frequencies dictated its behaviour at effective confining pressures of 60 and 108.65 kPa regarding strength and plastic strain accumulations. As the testing conducted involved one-way loading, further testing on the frequency dependence of the butterfly effect for Lanton alluvium is highly recommended by using the two-way loading technique and a vylastic sleeve top cap fitting.

7.4 Chapter summary

The results from the monotonic triaxial testing programme indicate that Lanton alluvium is predominantly characterised by normally consolidated behaviour both in its reconstituted and natural undisturbed states. Regarding deviatoric stress – strain behaviour, work hardening was mainly observed. Undisturbed samples generally achieved higher deviatoric strengths than reconstituted samples for both drained and undrained tests; although there were some instances where some reconstituted samples had been over compacted - thereby making them stiffer than undisturbed samples.

However, some undisturbed samples exhibited both work hardening, softening and peak behaviour. These samples also displayed clear evidence of dilation during drained tests when p'_0 <150 kPa, compared with the predominantly contractional behaviour observed for most reconstituted samples and undisturbed samples tested where p'_0 >200 kPa. These behavioural differences between the undisturbed and reconstituted samples signify that the undisturbed Lanton alluvium possesses a degree of sedimentation structure, which according to oedometer tests is bonding rather than fabric based. This was confirmed by shear stiffness degradation curves, although given the silty nature of the soil and therefore its sensitivity, the initially high shear stiffness and structure of the undisturbed soil degrades fairly rapidly after only small strains are applied.

Albeit the monotonic tests conducted at Newcastle on the conventional GDS ELDYN triaxial apparatus were of the highest quality possible for strain ranges down to 0.01%, the results were of relatively low resolution compared with those obtained at Bristol (see Appendix 5), which captured small strain behaviour down to 0.0001%. This highlights the need for testing to use local strain measurements and bender elements during triaxial tests to gain true insights into a soil's mechanical behaviour, particularly when using such stiffness parameters in geotechnical designs around structures such as railway embankments. Using mid-height pore pressure probes would also be valuable in gaining a better understanding of the distribution of pore pressures throughout samples during testing. Based on the author's personal experience, future high-quality triaxial testing on sensitive soils such as Lanton alluvium ought to use computer controlled electro-mechanical triaxial frames with computer controlled air/water pressure controllers. This is primarily due to their higher levels of accuracy and operating capacities compared with Bishop-Wesley triaxial cells and simple air/water bladder pressure controlled systems. However, such advanced triaxial systems along with small strain measurements are essential in defining Lanton alluvium's small strain kinematic and elastic yield surfaces.

Accumulating cyclic plastic shear strains, increasing excess pore pressures and resulting reductions in mean effective strength were observed within all reconstituted and undisturbed samples when subjected to dynamic loading conditions associated with an HST. The axial and cyclic shear strains experienced by samples during tests conducted under p'_0 conditions of 60 kPa were significant, especially for reconstituted

samples; whereby the slightly smaller strains experienced by undisturbed samples are owed to the soil's degree of structure. These results imply that considerable surface settlements would occur after just a single HST loading event.

Certainly for effective confining pressures of <60 kPa, the dynamic stresses which reconstituted and undisturbed samples were subjected to by an HST exceeded both the soil's respective monotonic strength and CSL. These considerable increases in the apparent strength of the reconstituted and undisturbed soil during dynamic loading are thought to be owed to the material's viscous behaviour under an HST's high loading frequency of 2.794 Hz. The resilient modulus of the reconstituted soil remained relatively constant during all tests as dynamic loads were applied; as the soil's internal structure had already been removed. Although reductions in resilient modulus were observed with increasing numbers of loading cycles for undisturbed samples due to the degradation of structure, the resilient modulus values for undisturbed samples were lower than those measured for undisturbed samples. This was attributed to the reconstituted samples' higher relative densities due to the compaction induced during sample preparation, along with the added effects of isotropic consolidation prior to dynamic testing.

There are causes for concern regarding the soil's potential to undergo liquefaction, particularly at p'_0 conditions ≤60 kPa, based on 5% double amplitude cyclic shear strains being experienced by reconstituted samples after the passage of one HST, in addition to the dynamic effective stress paths of the reconstituted and undisturbed soil passing through the reconstituted soil's CSL. However, the measured R_u values for the soil in its reconstituted or undisturbed states did not reach the critical value of 1.

Based on the behavioural characteristics of liquefiable soils defined by Tsuchida (1970), Kramer (1996) and Seed et al. (2003), Lanton alluvium's Atterberg limits, in-situ moisture content and monotonic triaxial compression behaviour, the soil is considered to have the potential to liquefy under dynamic loading conditions typically associated with HSTs. However, further more detailed dynamic testing is required to determine how many HST cycles would be required to cause cyclic mobility and liquefaction. As the testing conducted involved only one-way loading, two-way loading testing involving the use of a vylastic sleeve top cap fitting is highly recommended in order to examine the behaviour of Lanton alluvium in extension, determine the soil's cyclic yield shear strain and the frequency dependence of the

butterfly effect for the soil. Future dynamic tests should also involve using local strain measurements to record higher resolution data. Alluvial soils can be highly variable within close geographical proximities; namely variations in plastic fines contents. According to Erken and Ulker (2007), such variations in plasticity and fines content can strongly influence the CSR, the number of loading pulses required to reach 5% double amplitude shear strain and the critical cyclic yield shear strain at which shear strains rapidly increase (Figure 7.56), thereby identifying the onset of liquefaction. Hence, future dynamic testing should also aim to examine the content and influence of plastic fines within Lanton alluvium.

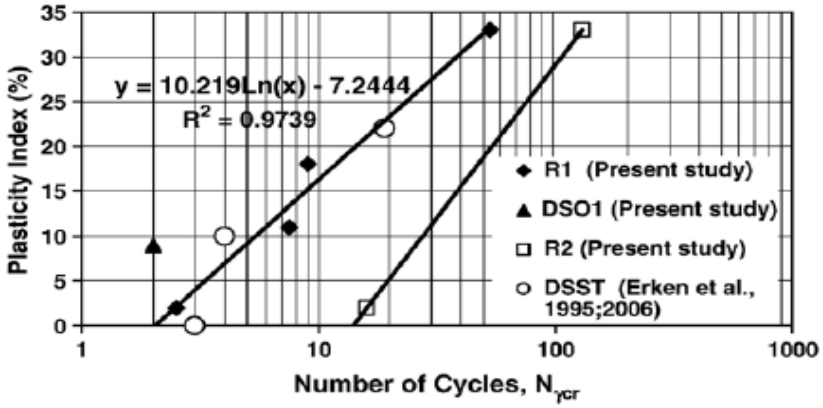

Figure 7.56: Relationship between a soil's plasticity and the number of loading cycles required to reach its cyclic yield shear strain (R1 = reconstituted, DSO1 = undisturbed). Taken from Erken and Ulker (2007).

Based on Lanton alluvium's sensitive mechanical behaviour under monotonic and dynamic loading, along with the significant plastic axial strains which would be induced by dynamic loads typical of HSTs; there is a clear necessity for the soil to be stabilised to ensure that it is mechanically able to cope with long-term HST traffic. The monotonic and dynamic results presented in this chapter will act as a control with regards to the results presented in the next chapter on the monotonic and dynamic testing of Lanton alluvium stabilised with 7.5% GGBS-NaOH binder after 28 days curing.

Chapter 8:

Phase 3: Monotonic and dynamic triaxial testing of stabilised Lanton alluvium

8.1 Introduction

The oedometer, monotonic and dynamic triaxial characterisation of Lanton alluvium from chapters 5 and 7 showed that the soil is normally consolidated and has a relatively high degree of initial bonding-based sedimentation structure in its undisturbed state. Due to the soil's high level of sensitivity to monotonic and dynamic loading, its structure and associated high initial shear stiffnesses is mostly degraded after just 0.002% strain. Pore pressure ratcheting, reductions in mean effective strength and considerable axial/cyclic shear strain accumulations were measured within the reconstituted and undisturbed Lanton alluvium when dynamically loaded, using the typical loads and loading frequencies for a single high-speed InterCity 125 train (HST) travelling at 125 mph. At low effective confining pressures corresponding to ≤3m depth, the dynamic stresses experienced by samples exceeded the soil's monotonic strength and CSL and the soil's viscous behaviour was thought to control its mechanical behaviour under high-frequency dynamic loads. Although not necessarily observed after the passage of one HST, it is thought that after multiple passing HST's the Lanton alluvium is likely to liquefy; based on the dynamic testing results presented in chapter 7 and the soil's index properties and monotonic characteristics (please refer to chapters 5 and 7) closely resembling those of potentially liquefiable soils (Tsuchida, 1970; Kramer, 1996; Seed et al., 2003).

To mitigate against any liquefaction phenomena and significant ground settlements occurring within Lanton alluvium due to monotonic and dynamic loads associated with high-speed railway embankments and regular HST's, ground improvement via soil stabilisation is essential. This chapter investigates the small, medium and large strain behaviour of Lanton alluvium stabilised with the GGBS-NaOH binder at a dosage of 7.5% by dry weight, which has been cured for 28 days. The monotonic and dynamic behaviour of stabilised samples was examined at Newcastle and Bristol Universities using the same sets of triaxial apparatus and similar monotonic/dynamic loading, drainage and mean effective stress conditions to those used in the previous chapter on the untreated Lanton alluvium. Based on the significant performance results for this binder and dosage in stabilising Lanton alluvium in chapter 5, it is anticipated that the effect of cementation within the stabilised soil will produce considerably

higher monotonic and dynamic deviatoric strengths and stiffnesses compared with those for the untreated soil. It is also hoped that far smaller axial/cyclic shear strains will accumulate within the stabilised material when subjected to the complex loading conditions presented by a high-speed railway embankment.

8.2 Monotonic results

Monotonic triaxial testing was carried out at using the GDS ELDYN triaxial equipment. The results from triaxial tests are hereby presented and discussed in turn.

8.2.1 Shearing behaviour

8.2.1.1 Deviatoric stress – axial strain

The undrained and drained deviatoric stress responses of each stabilised sample with increasing axial strain are displayed in Figures 8.1 and 8.3, respectively. Figures 8.2 and 8.4 show the average deviatoric stress – axial strain behaviour demonstrated during undrained and drained tests, respectively. Immediately upon the onset of loading, all undrained and drained samples exhibited non-linear elastic hardening behaviour. In general, most samples reached a peak deviatoric strength, followed by slow rates of strain softening. However, the peak deviatoric strength behaviour appeared to become suppressed and less pronounced with increasing effective confining stress conditions; particularly for p'_0 conditions ≥400 kPa. The strain levels at which yielding and therefore peak strength occurs within samples also increases with increasing effective confining stresses. For undrained tests, peak deviatoric strengths tended to occur at axial strains of approximately 2% for samples tested at p'_0 = 50 and 100 kPa, and 3% for samples tested at p'_0 = 200, 400 and 600 kPa. Secant elastic stiffnesses for undrained (E_u) and drained (E') samples were derived and found

to increase with effective confining pressure; whereby at p'_0 = 200 kPa, average values of 141 and 199 MPa were recorded for E_u and E', respectively.

The level of effective confining pressure applied to samples during testing appeared to have an effect on their deviatoric stress – strain relationships. For samples tested at effective confining pressures ≤200 kPa, the peak deviatoric strengths and corresponding strains were remarkably similar. However, for samples tested under effective confining stresses of 400 and 600 kPa, the maximum deviatoric stresses recorded by samples and their corresponding axial strains both increased. This behaviour was similarly observed by Ahnberg (2006). The effect of stabilisation using the GGBS-NaOH binder produced undrained and drained shear strengths which were four times higher than those measured for reconstituted Lanton alluvium at effective confining stresses of 200 kPa. Given the significantly higher strength of the stabilised Lanton alluvium compared with the untreated soil, brittle behaviour was evident upon failure, due to strain localisation and the development of shear planes (Figure 8.3).

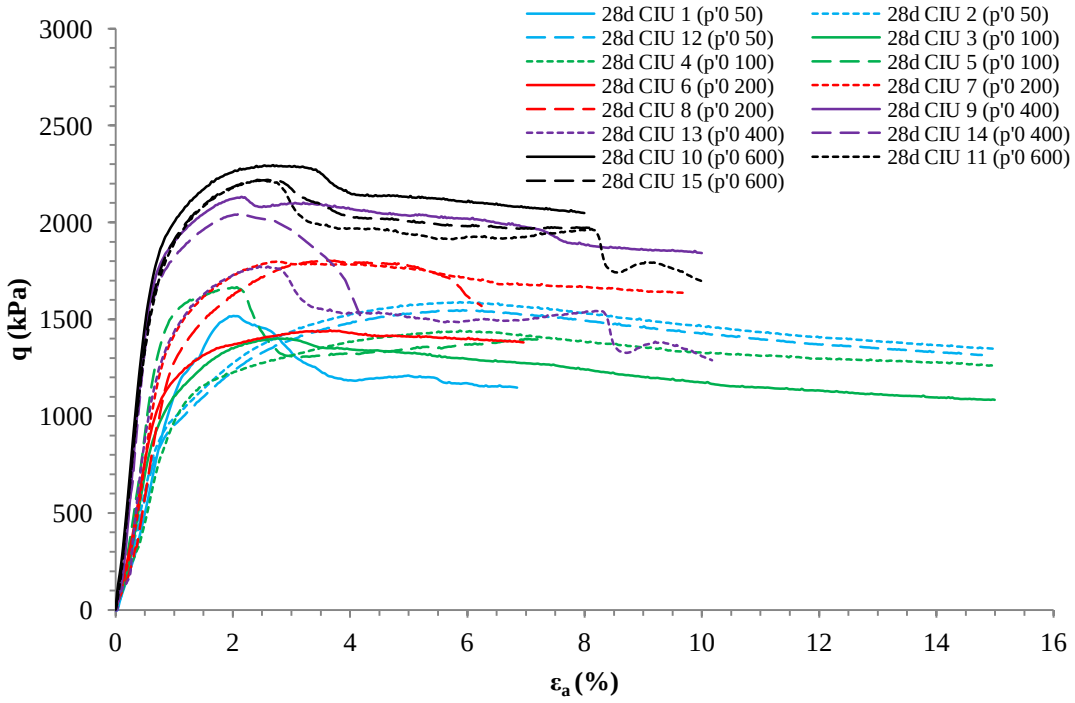

Figure 8.1a: Deviatoric stress-strain behaviour of all undrained GGBS-NaOH stabilised samples of Lanton alluvium.

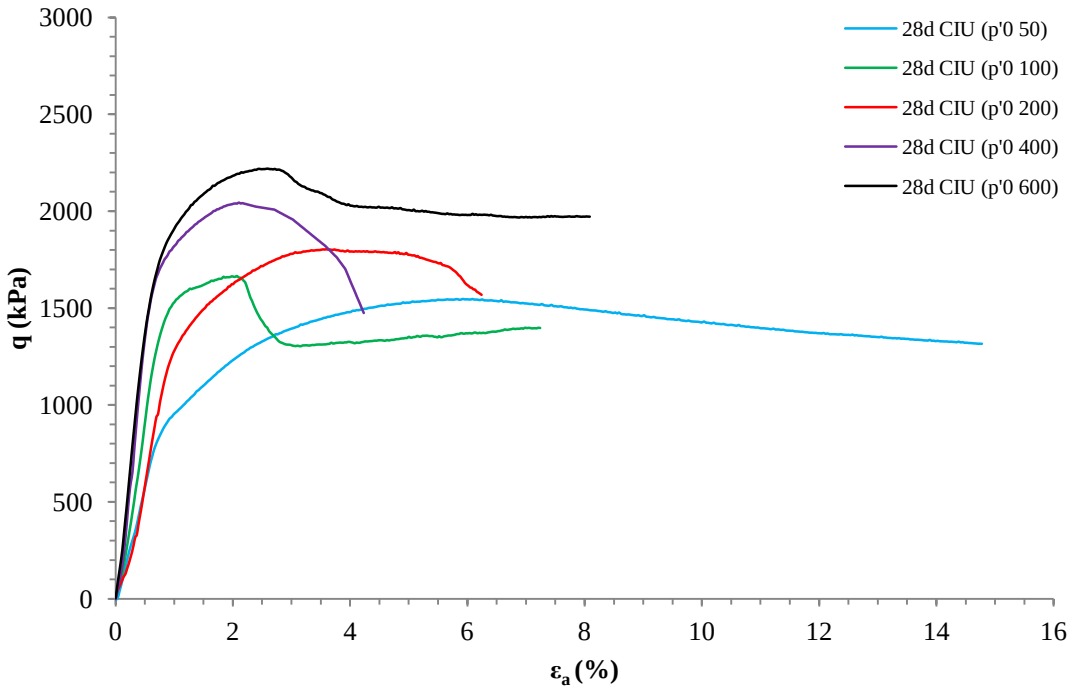

Figure 8.1b: Average deviatoric stress-strain behaviour of undrained GGBS-NaOH stabilised samples of Lanton alluvium.

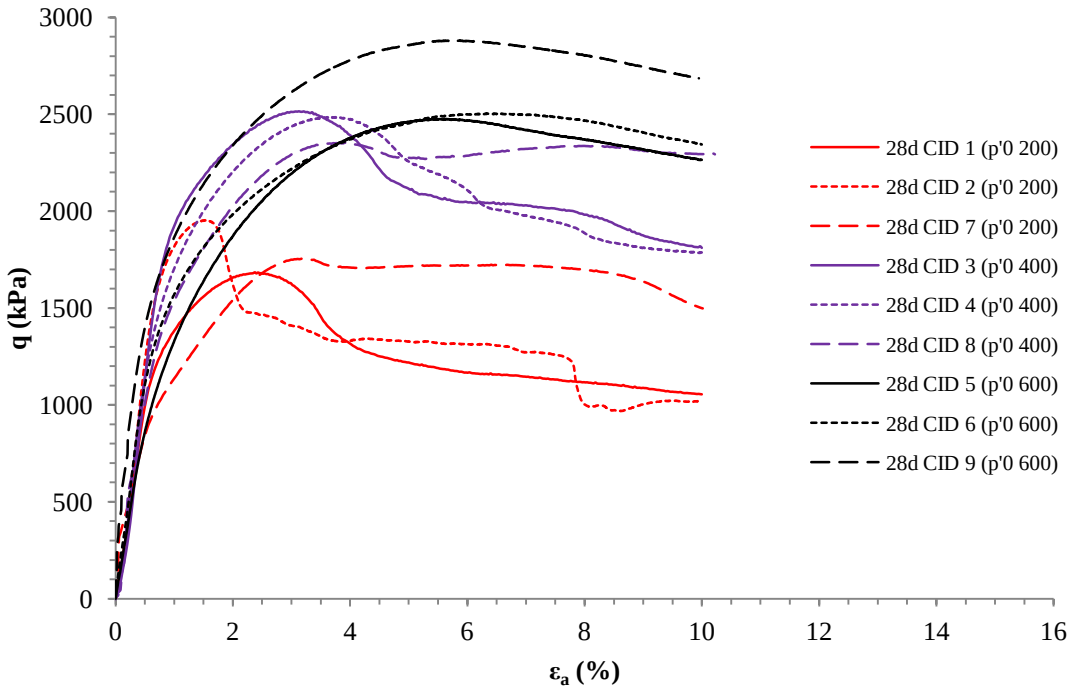

Figure 8.2a: Deviatoric stress-strain behaviour of all drained GGBS-NaOH stabilised samples of Lanton alluvium.

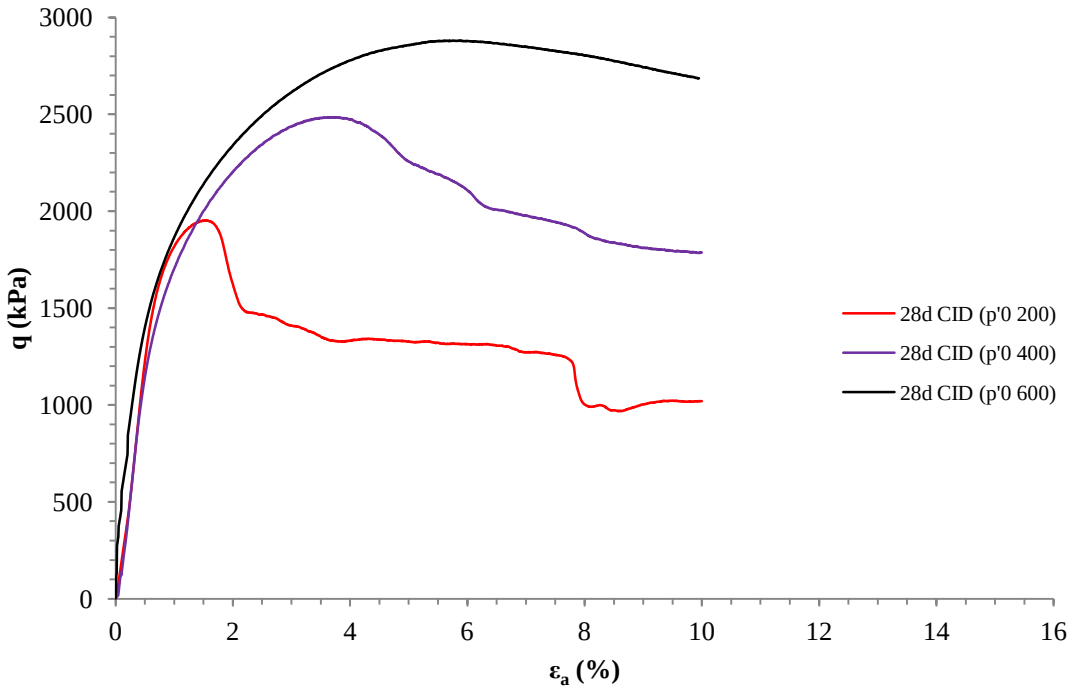

Figure 8.2b: Average deviatoric stress-strain behaviour of drained GGBS-NaOH stabilised samples of Lanton alluvium.

Figure 8.3: Development of a shear plane within the 100mm diameter 28d CIU 1 (CP' 50) - Bristol sample via strain localisation.

8.2.1.2 Pore pressures

The response of undrained sample's pore pressures are presented in Figure 8.4. For all the samples tested at each of the five different effective confining stress states, pore pressures were observed to peak as the samples started to experience yielding. After reaching a peak, pore pressures then started to reduce to more stable values as the deviatoric stresses continued to increase towards sample failure at shear strains >3%. This pore pressure behaviour is characteristic of densely cemented soils; whereby for less dense cemented soils, pore pressures keep increasing towards a steady state (Rios et al., 2014).

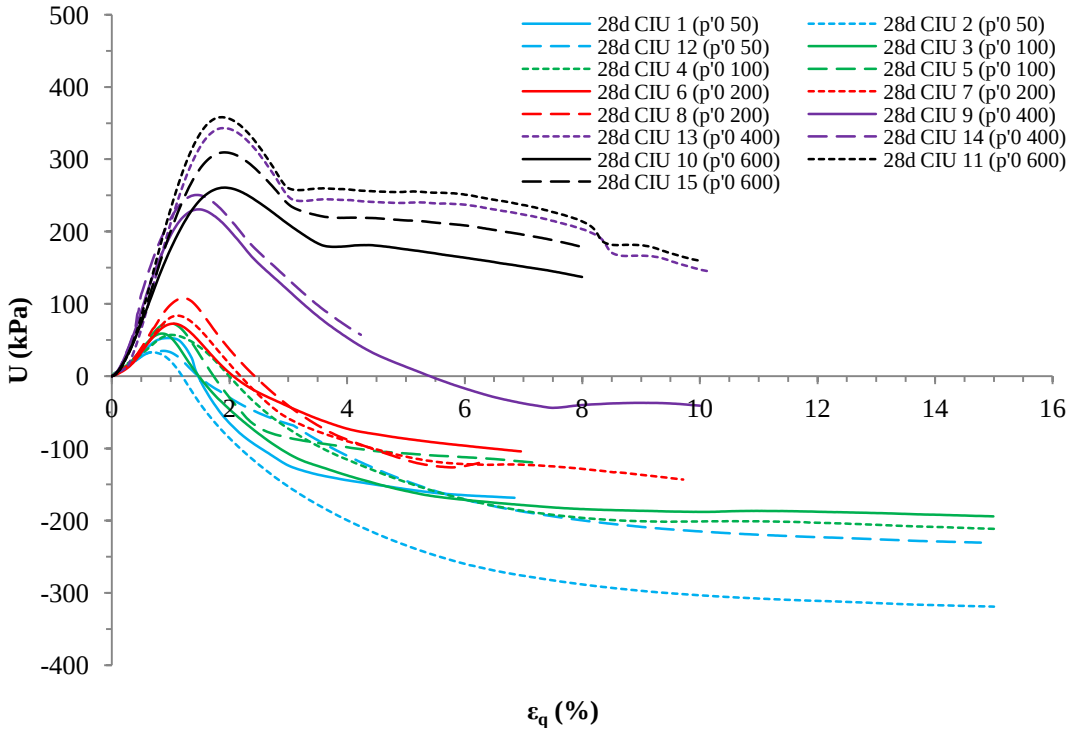

Figure 8.4: Pore pressure behaviour of undrained GGBS-NaOH stabilised samples of Lanton alluvium.

A distinct feature evident in Figure 8.3 for samples tested at lower p'_0 conditions <200 kPa is that once their pore pressures had peaked and started to reduce, they continued to decrease such that negative pore pressures were eventually observed. Although this behaviour was not observed by Rios et al. (2014) on an artificially cemented silty sand, it was recorded by Ahnberg (2007) for cemented post-glacial Swedish clays.

This behaviour is commonly observed within dense rocks, whereby the generation of negative pore pressures tends to occur near to the point of rupture when a sample starts to dilate (Mesri et al., 1972). This reduction in pore pressure ultimately increased the effective confining stresses being imposed on samples and therefore their strengths.

8.2.1.3 Volumetric strains

Evidence for stabilised Lanton alluvium's dilative behaviour during shearing is shown in Figure 8.5. Volumetrically, samples experienced a combination of contractional and dilational behaviour. Those which were characterised by more dilation than contraction were samples tested under p'_0 conditions of 200 kPa. The onset of dilation within such samples occurred at shear strains of 1.7%, where negative volumetric strain was achieved at shear strains ranging between 3 and 3.5%. Such pronounced dilational behaviour corresponds with the softening behaviour exhibited by samples tested at p'_0 = 200 kPa, due to the degradation of cementitious bonding structure throughout the material.

For samples consolidated to p'_0stress conditions of 400 and 600 kPa, their behaviour was predominantly contractional. This again demonstrates how the effective confining pressure applied to stabilised Lanton alluvium influences its behaviour during shearing. However, at larger shear strains of 3–5%, the stabilised samples started to experience varying degrees of dilation; albeit no negative volumetric strains were recorded. This behaviour complements the suppressed peak and softening behaviour observed in deviatoric stress – strain plots in Figure 8.2; whereby work hardening behaviour becomes more dominant; particularly for samples tested at higher p'_0 conditions of 600 kPa. Under such high mean effective stress conditions, particle rearrangement within samples was less permissible compared with samples tested at lower effective confining pressures of 200 kPa. Once soils have failed and reached their critical state, no further volumetric strains are anticipated as they continue to be sheared. Zero volumetric strains were not observed during any drained tests, although significantly smaller/negligible volumetric strains can be observed within most samples after shear strains exceed 5%. This implicates that some samples may not have reached their critical state during testing.

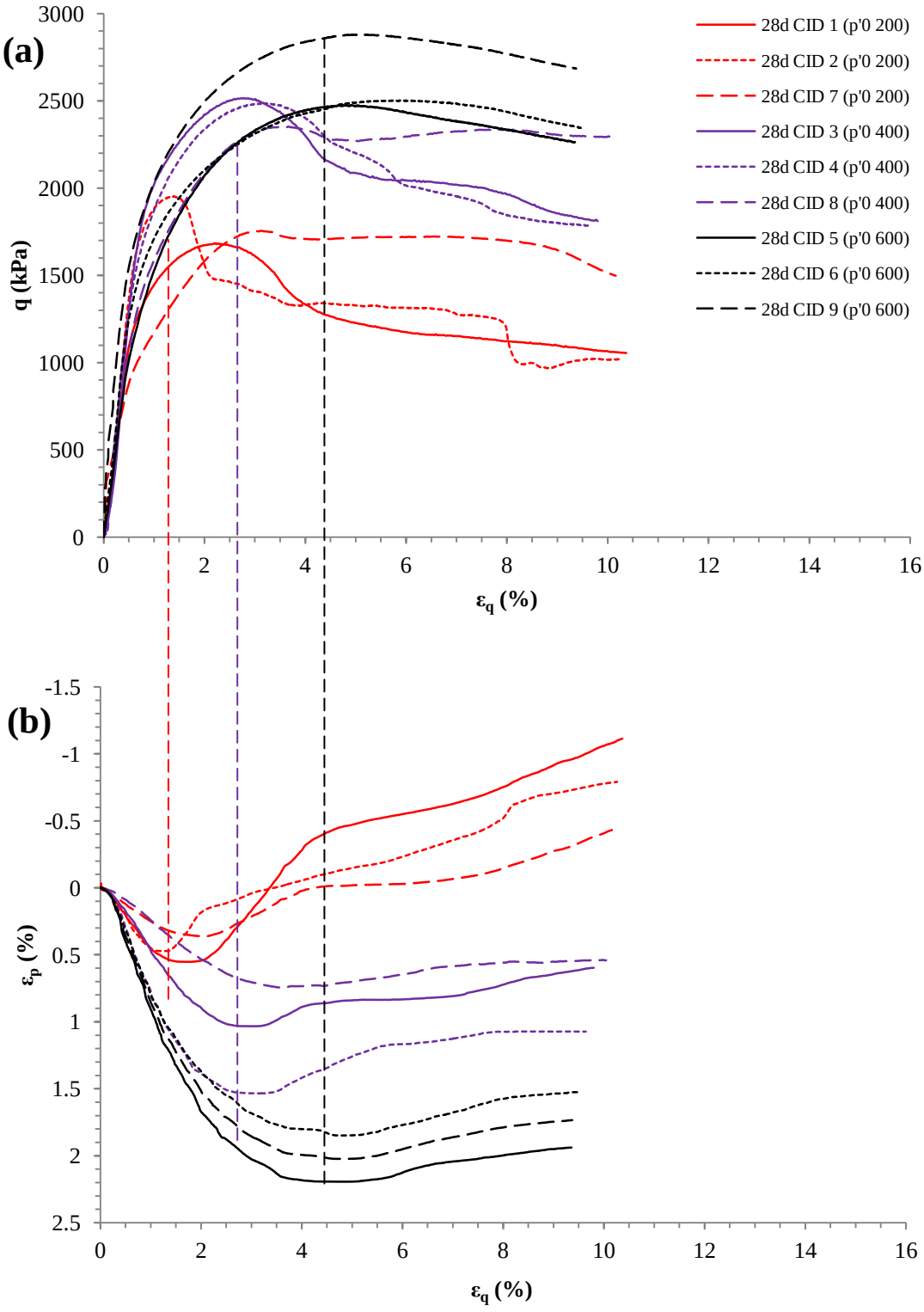

Figure 8.5: (a) Deviatoric stress and (b) volumetric strain response of all drained GGBS-NaOH stabilised Lanton alluvium samples with increasing shear strain.

8.2.1.4 Stress dilatancy

Further to the volumetric strain – shear strain response of stabilised Lanton alluvium under drained conditions, the relationship between stress ratio (M = q/p') and dilatancy for these samples is presented in Figure 8.6. As expected, all the samples exhibit frictional behaviour. In contrast to the behaviour observed by Rios et al. (2014) for samples prior to reaching their maximum M value, contractional volumetric strains were observed for stabilised Lanton alluvium samples.

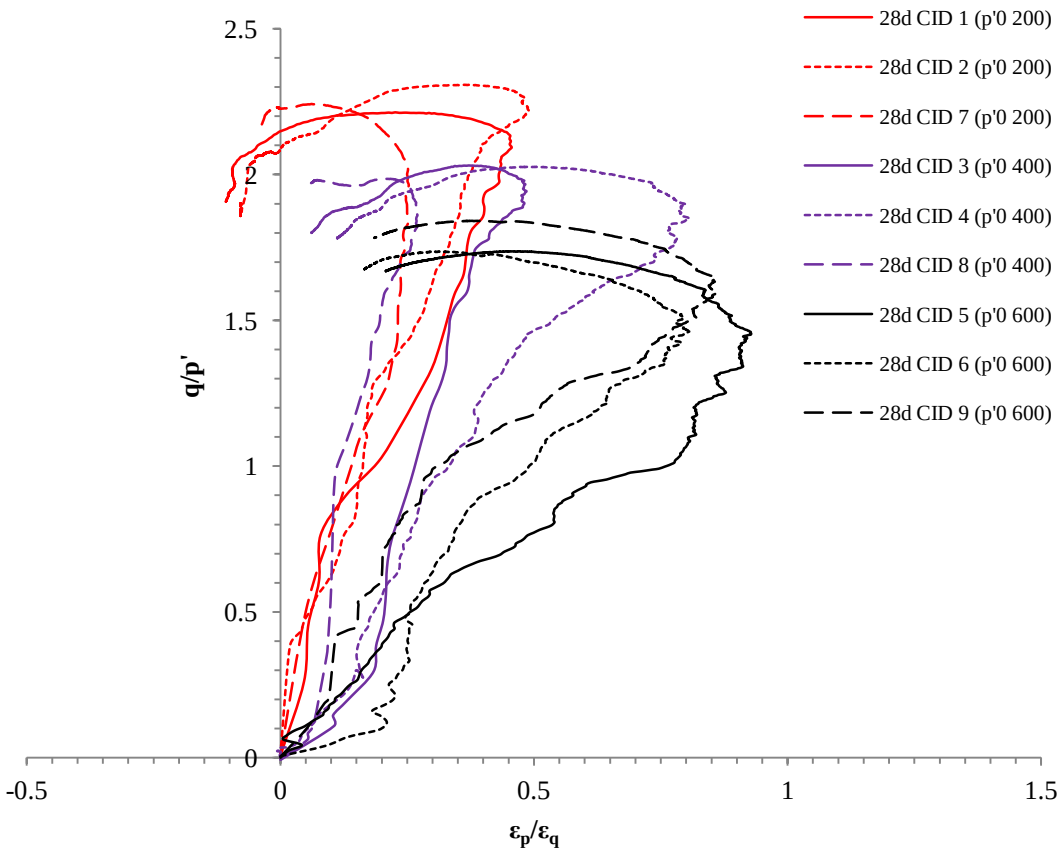

Figure 8.6: Stress-dilatancy behaviour of drained GGBS-NaOH stabilised samples of Lanton alluvium.

Dilation angles (ψ) for the material ranged between 1.2 and 3.5°, with higher ψ values obtained for samples tested at lower effective stress conditions. Samples achieving their maximum effective stress ratios marked the onset of dilational behaviour. Particularly for samples tested at p'_0 conditions of 200 kPa, once the peak dilation rate

had finished at shear strains of approximately 5%, the degree of dilation and the effective stress ratio reduced.

A notable contrast between the stress-dilatancy results in the previous chapter for untreated Lanton alluvium and those in Figure 8.6 for the stabilised soil is that for the latter, the effect of increasing effective confining stresses on samples reduced their maximum effective stress ratios. Rios et al. (2014) observed that once cemented soils reach the state where their minimum $\delta\varepsilon_p/\delta\varepsilon_q$ and maximum M values are recorded, strain localisation causes the material's dilation rate to decrease at an accelerated rate compared with that at which M is decreasing; thereby bringing the material's stress path inside the frictional envelope. However, Figure 8.6 demonstrates that even after strain localisation occurred for all the drained samples tested, only slight reductions in their M values were observed and there was no evidence of $\delta\varepsilon_p/\delta\varepsilon_q$ values increasing again. To potentially capture the behaviour noted by Rios et al. (2014) for stabilised Lanton alluvium, future testing would be required; and samples would need to be tested to higher levels of shear strain (i.e. 20%).

8.2.2 Failure envelopes

In contrast to untreated Lanton alluvium which behaved as a typical frictional granular material, the behavioural characteristics of stabilised Lanton alluvium will be controlled by its cement content. As previously mentioned, strain localisation and the development of shear failure planes occurred during triaxial compression when stress conditions closely approached their peak. The maximum stresses which acted on the samples' shear planes were calculated by constructing Mohr circles. The peak shear stresses from each of the undrained and drained tests are presented in Figure 8.7, along with their corresponding Mohr-Coulomb failure envelopes (FE).

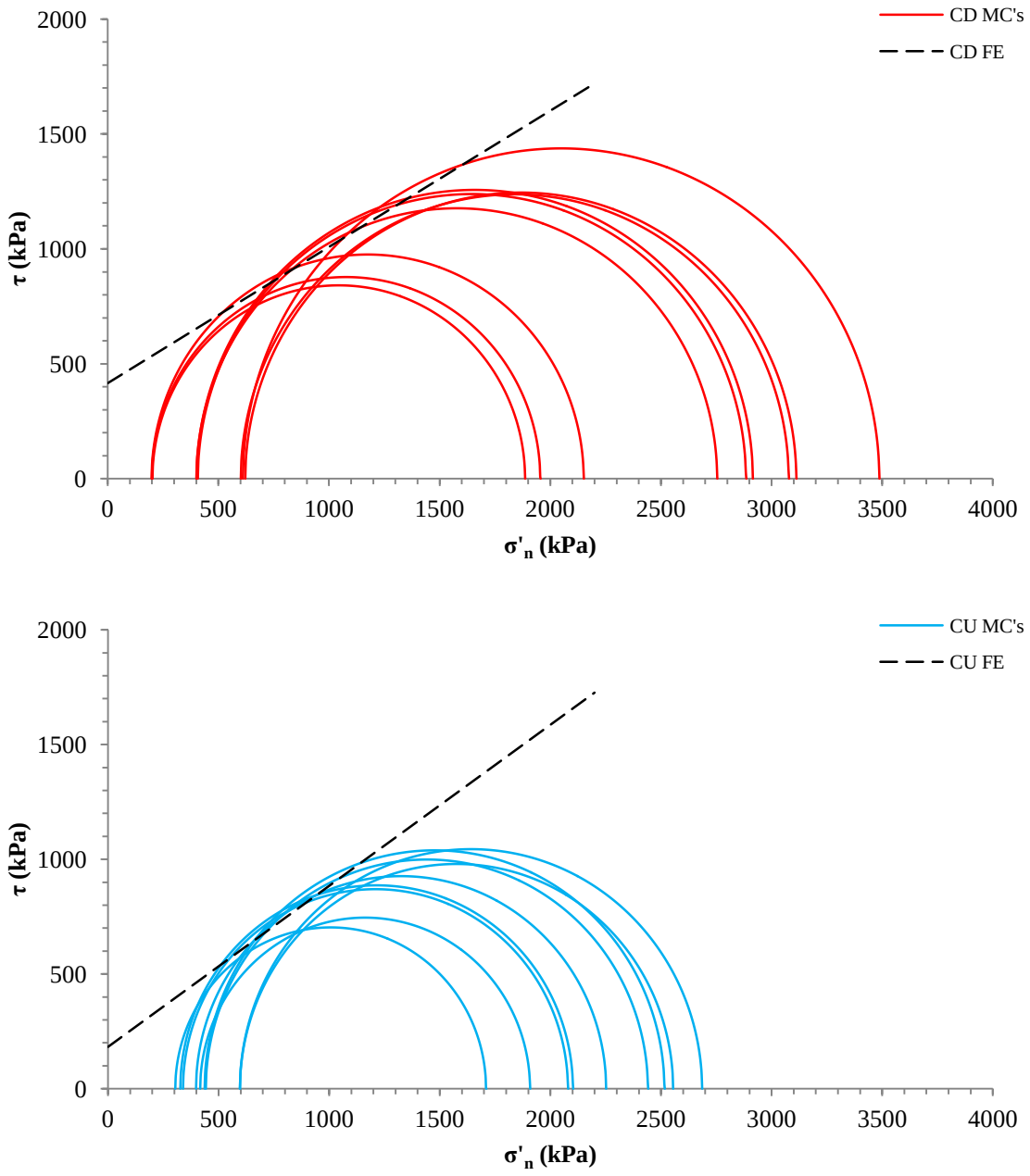

Figure 8.7: Mohr-Coulomb failure envelopes (FE) and peak τ-σ'$_n$ values obtained from (a) drained and (b) undrained GGBS-NaOH stabilised samples of Lanton alluvium.

At lower effective confining pressures, there appears to be a larger degree of separation between the undrained and drained Mohr-Coulomb failure envelopes. However, at higher effective confining pressures where samples experience σ'$_n$ values >2000 kPa, the undrained and drained failure envelopes converge. Values for the effective shear strength parameters for the stabilised Lanton alluvium showed some variation, with φ' ranging between 30 – 44.5^o and c' varying between 351 – 370 kPa.

Such degrees of variation may be attributed to slight variations in sample quality. Hence, average values for φ' and c' were 37.25° and 360.5 kPa. The level of engineering improvement provided by mixing the GGBS-NaOH binder within Lanton alluvium is per the Mohr-Coulomb failure envelopes for untreated and stabilised Lanton alluvium presented in Figure 8.8.

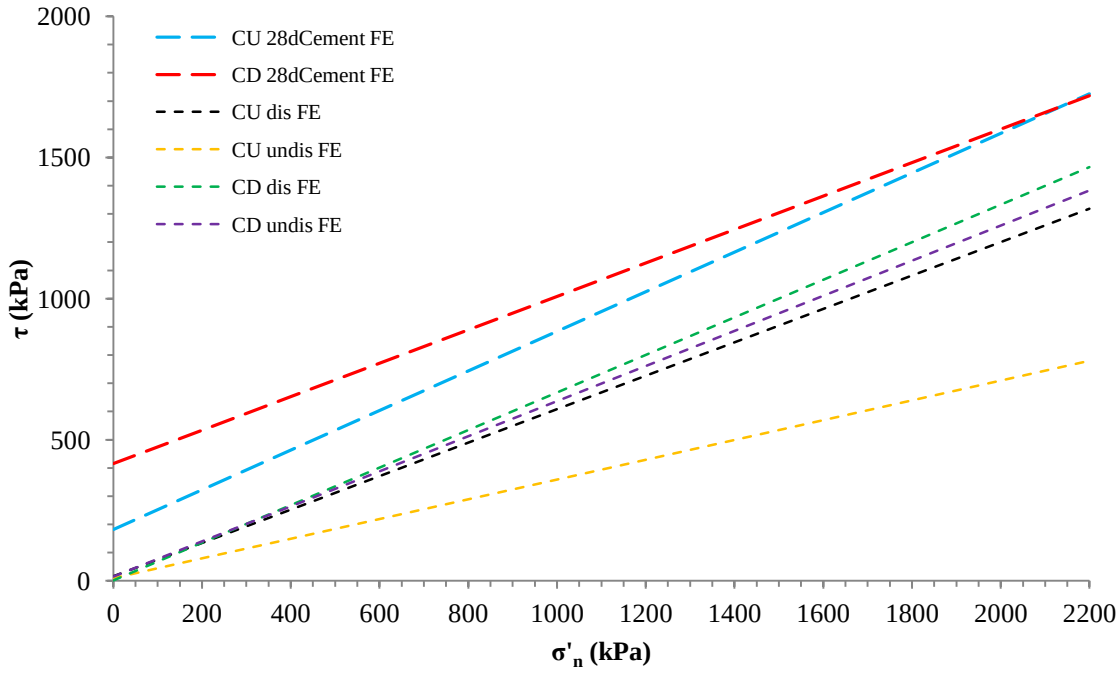

Figure 8.8: Mohr-Coulomb failure envelopes (FE) for drained and undrained triaxial tests conducted on untreated Lanton alluvium (in both reconstituted and undisturbed states) and GGBS-NaOH stabilised Lanton alluvium after 28 days curing.

Within q-p' effective stress space, the drained stress paths taken by the stabilised material were characterised by a 1:3 slope until they touched the failure envelopes (Figure 8.9). Once drained samples reached their critical state, they generally retraced their loading stress paths towards the CSL. However, the shapes of samples' undrained stress paths varied according to the level of effective confining pressures used during testing. For samples tested at p'_0 conditions of ≤200 kPa, undrained stress paths followed a 1:3 slope similar to drained samples until they reached their yielding point when a sharp phase transformation occurred. The stress paths then followed the failure envelope until sample rupture and failure occurred. Regarding stress paths taken by samples during undrained tests conducted at $p'_0 \geq 400$ kPa, their shapes bore a much

closer resemblance to those typically expected for soils which predominantly experience work hardening with limited softening. Once these samples started to reach advanced stages of yielding and their corresponding stress paths had reached their failure envelopes, a phase transformation occurred. Mean effective stresses started to increase whilst deviatoric stresses started to stabilise. Once the stress paths reached their peak deviatoric strength (i.e. defining the failure envelope), deviatoric stresses started to decrease. This caused the direction of the stress paths to come down onto the CSL. However, the stress paths did not sit on the CSL for long, as the deviatoric stress often suddenly decreased due to brittle rupturing within the samples.

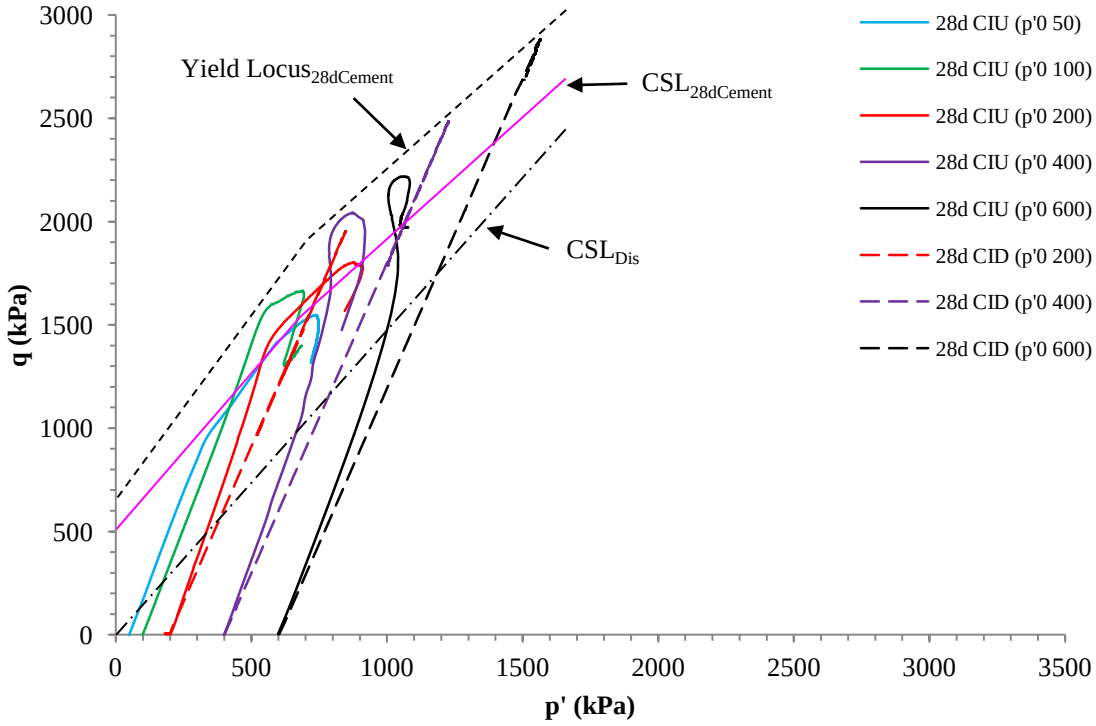

Figure 8.9: Average drained and undrained stress paths, yield locus and CSL within the q-p' stress plane for all 28 day cured GGBS-NaOH stabilised Lanton alluvium samples. CSL for reconstituted untreated Lanton alluvium (CSL_{Dis}) superimposed for comparison.

As previously mentioned, the shearing behaviour and therefore the strength of stabilised Lanton alluvium is significantly influenced by the effective confining stress conditions samples are subjected to. Hence, to observe this effect more clearly, the effective stress paths in Figure 8.9 were normalised with respect to their corresponding p'_0 conditions. The normalised data is presented in Figure 8.10. The normalised

effective stress paths show that samples consolidated to higher p'_0 values achieved higher peak deviatoric strengths. Additionally, this normalisation procedure outlined by Muir Wood (1990) proved useful in bringing all the drained and undrained effective stress paths for stabilised Lanton alluvium together in defining a single locus within the q/p'_0 - p'/p'_0 plane. However, it is worth noting that the normalisation of elastic moduli data with respect to effective confining pressure is unlikely to be significant over larger ranges of moduli, given the underlying assumption of linear dependence will not apply as the cemented alluvium behaves non-linearly.

These findings have demonstrated that the failure envelope and CSL for stabilised Lanton alluvium does not coincide with each other. According to critical state soil mechanics theory, a soil's CSL and failure envelope do not have to coincide, as was observed in the previous chapter for untreated normally consolidated Lanton alluvium. The stabilised alluvium demonstrated overconsolidated behaviour; whereby the peak deviatoric stress of overconsolidated geomaterials is generally followed by a sudden reduction in deviatoric stress towards the critical state. Hence, for materials such as stabilised Lanton alluvium, the material's yield locus is above the CSL within q-p' stress space (Muir Wood, 1990). Per Muir Wood (1990), for more heavily overconsolidated geomaterials, peak deviatoric stresses are achieved at the intersection of the effective stress path with the initial yield locus at lower q-p' stress states.

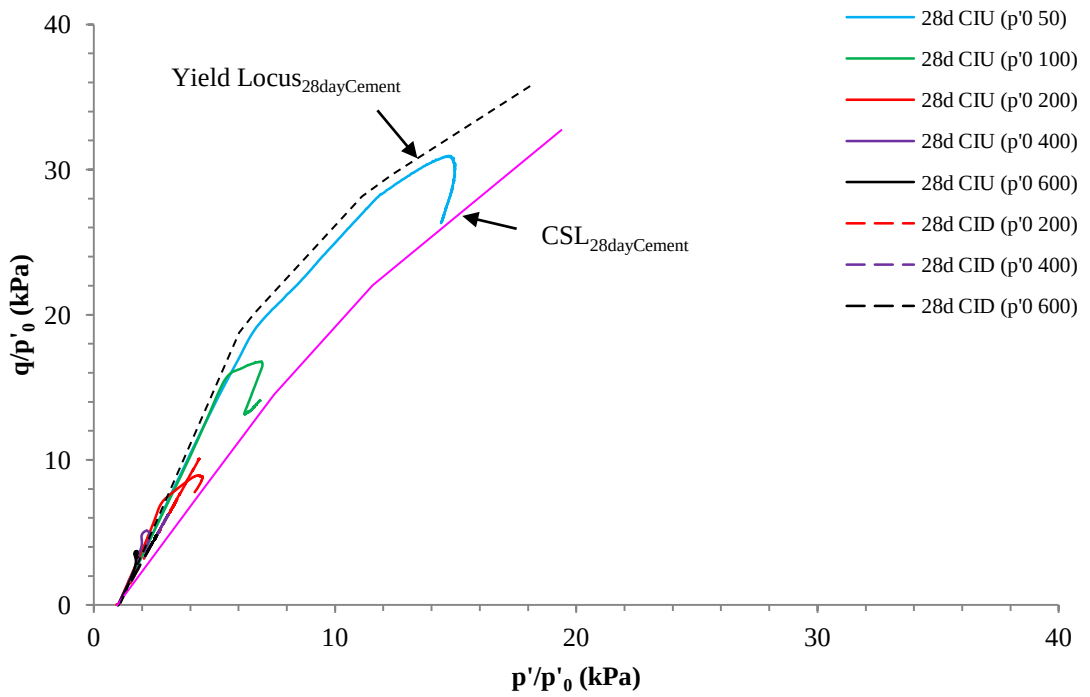

Figure 8.10: Average drained and undrained stress paths for GGBS-NaOH stabilised Lanton alluvium samples within the q/p'_0-p'/p'_0 stress plane, normalised by their corresponding p'_0 values.

In defining the stabilised alluvium's CSL and yield locus, it is possible to suggest that they are not perfectly linear within q-p' stress space. By examining the stress path data in Figure 8.9, the CSL and yield locus appear to have a steeper gradient (M) at lower mean effective stresses up to approximately 750 kPa; after which their M values decrease to a stable value for higher mean effective stress conditions. However, for simplicity; and per the Cam clay model, an average M value of 1.22 was obtained for the material from undrained and drained tests. Effective shear strength parameters were derived from undrained and drained tests separately based on their M values; with 360 kPa and 37.5^o being measured for c' and φ', respectively.

Further to the volumetric behaviour of stabilised Lanton alluvium shown in Figures 8.5–8.6, compression curves derived from drained testing results are presented within the specific volume (v) – p' compression plane (Figure 8.11).

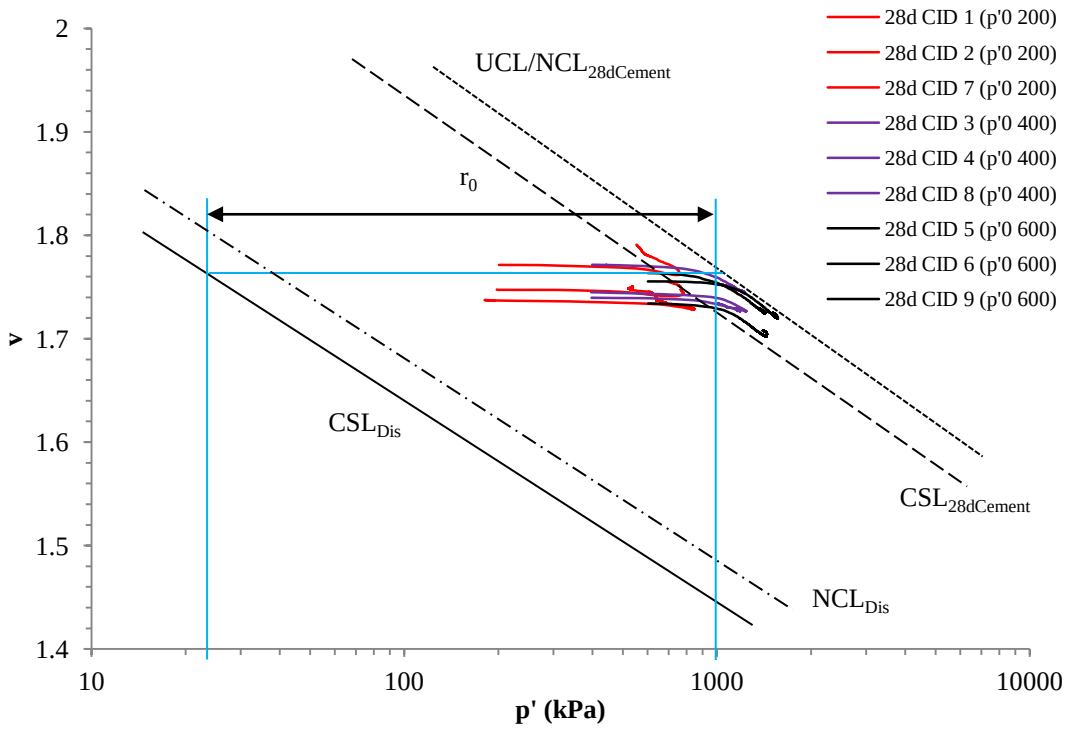

Figure 8.11: NCL/UCL and $CSL_{28dCement}$ within the υ – ln p' stress plane, obtained from drained GGBS-NaOH stabilised Lanton alluvium samples. The NCL and CSL_{Undis} for the reconstituted Lanton alluvium samples are superimposed for comparison.

Per the compression paths displayed in Figure 8.11, samples tested under p'_0 conditions of 400 and 600 kPa start to turn downwards due to decreasing specific volumes and therefore dilation at mean effective stresses of approximately 1000 kPa. With increased shearing, these paths appeared to follow the same stress path at a fairly constant gradient. Hence, a possible location for stabilised Lanton alluvium's CSL was defined within the v-p' compression plane. For comparison, the NCL_{Dis} (i.e. ICL_{Dis}) and CSL_{Dis} representing untreated Lanton alluvium in its reconstituted state are also displayed on Figure 8.11. Given the bonding-based structure within stabilised Lanton alluvium, it is hypothesised that the compression paths will eventually steepen with further straining to ultimately converge with the NCL_{Dis}. However, further drained triaxial testing involving higher strains and effective confining pressures would be required to define under what specific volume and mean effective stress conditions convergence would occur.

To quantitatively determine the contribution of the GGBS-NaOH cement towards enhancing Lanton alluvium's initial degree of structure (r_0), the structure degradation

law developed by Rouainia and Muir Wood (2000) was used. Per Figure 8.11, the effect of cementation within the material created an impressive r_0 value of approximately 45. Although this r_0 value appears to be lower than that recorded for undisturbed Lanton alluvium in the previous chapter, it ought to be noted that the untreated soil is very sensitive and its natural structure is easily lost after experiencing only very small strains. However, oedometer testing results and Figure 8.11 demonstrate that much higher stresses are required to start significantly breaking down the stabilised soil's cemented structure.

8.2.3 Stiffness degradation

A key area of interest regarding GGBS-NaOH stabilised Lanton alluvium's improved mechanical behaviour over that of the untreated soil is its stiffness degradation behaviour with increasing shear strain. Secant bulk and shear stiffnesses of the material were calculated. The G_{sec} degradation of 28 day cured stabilised Lanton alluvium with increasing strain under undrained conditions is per Figure 8.12.

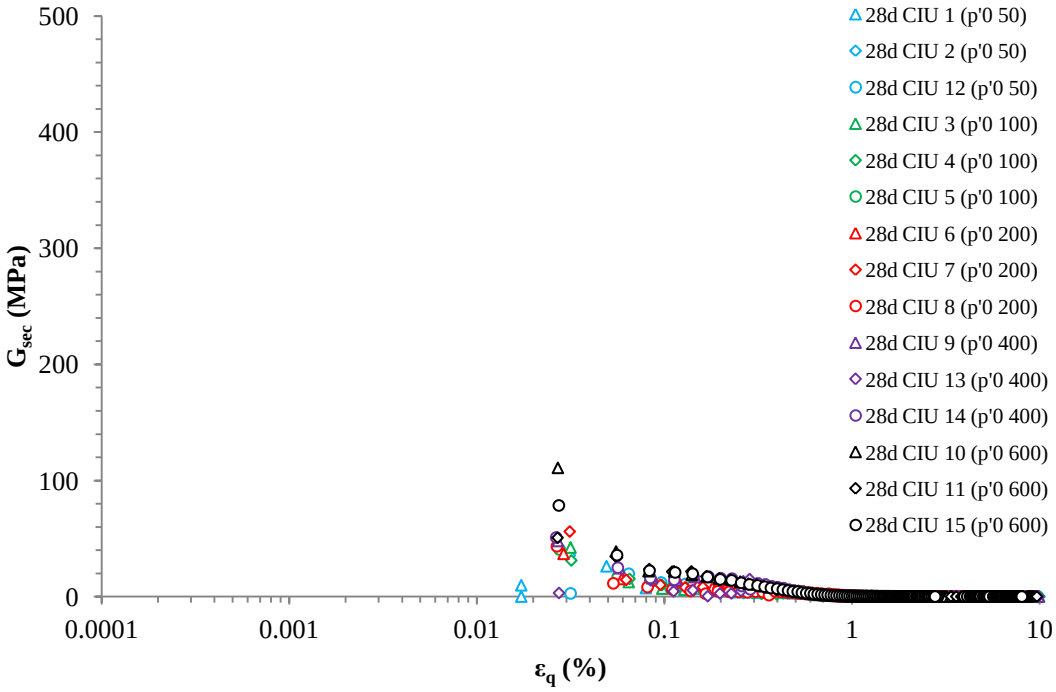

Figure 8.12: Secant shear stiffness degradation behaviour for undrained GGBS-NaOH stabilised Lanton alluvium samples.

As recorded for untreated Lanton alluvium tested at Newcastle, no G_{sec} values could be recorded for shear strains <0.02%. Per chapter 3, this degree of low resolution within the stiffness data can be attributed to using global strain rather than local strain measurements. The small strain behaviour of stabilised Lanton alluvium was studied at Bristol. The results are presented later in Appendix 5. It can generally be seen in Figure 8.12 that the shear stiffnesses of stabilised alluvium at strains levels of 0.02–0.1% were considerably higher (50–100 MPa) than those recorded for untreated Lanton alluvium (6–16 MPa). Similar to most geomaterials, the shear stiffnesses for the undrained stabilised soil samples reached their minimum values once shear strains >1% were achieved.

To remove the effects of samples' initial p'_0 conditions on their stiffness values obtained during tests, the data sets were normalised with respect to their p'_0 values. Figure 8.13 presents the normalised shear stiffness degradation data for undrained tests.

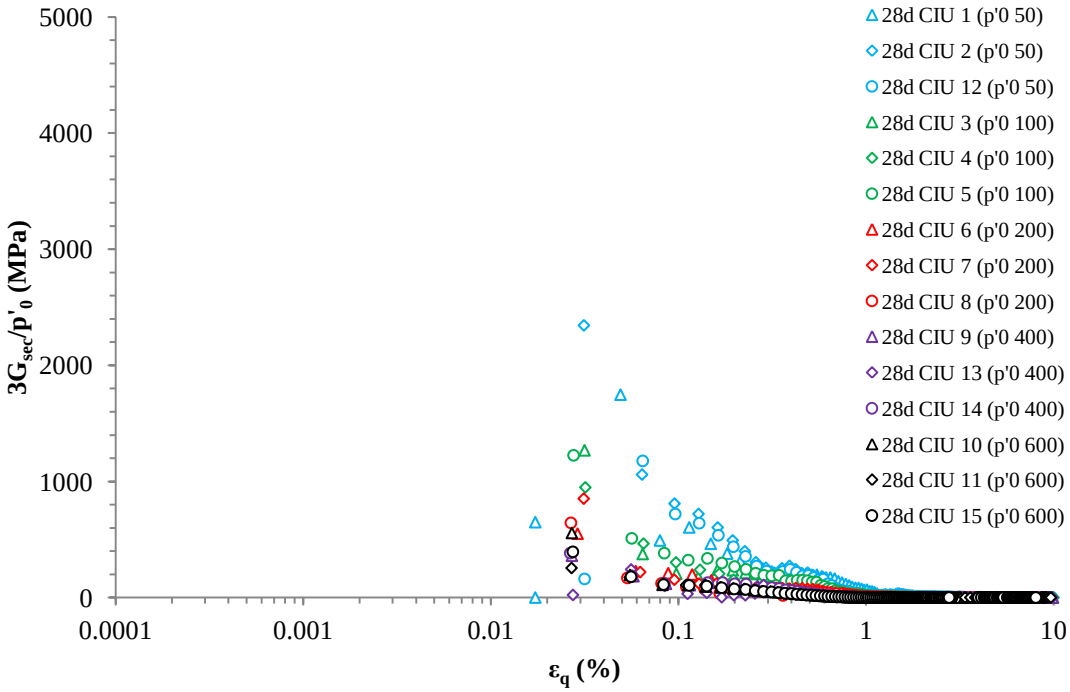

Figure 8.13: Secant shear stiffness degradation behaviour for undrained GGBS-NaOH stabilised Lanton alluvium samples, normalised by their corresponding p'_0 values.

Unlike the observations made for untreated Lanton alluvium's normalised shear stiffness data, normalisation of stabilised Lanton alluvium's shear stiffness measurements was unsuccessful in bringing all the stiffness degradation curves closer together to produce a tighter better correlated curve. In fact this normalisation technique, successfully used by Jardine et al. (1986), Rouili (2007) and Simpson and Rouainia (2012); appeared to produce more data scatter and increased the separation between the stiffness degradation curves. The shear stiffness degradation data obtained from drained triaxial tests both in their raw and normalised states are shown in Figures 8.14 and 8.15, respectively.

Two of the main observations from the drained shear stiffness degradation curves are that there is more data scatter and that stiffness values at 0.01% shear strain are generally a little lower (<50 MPa) than those from undrained tests.

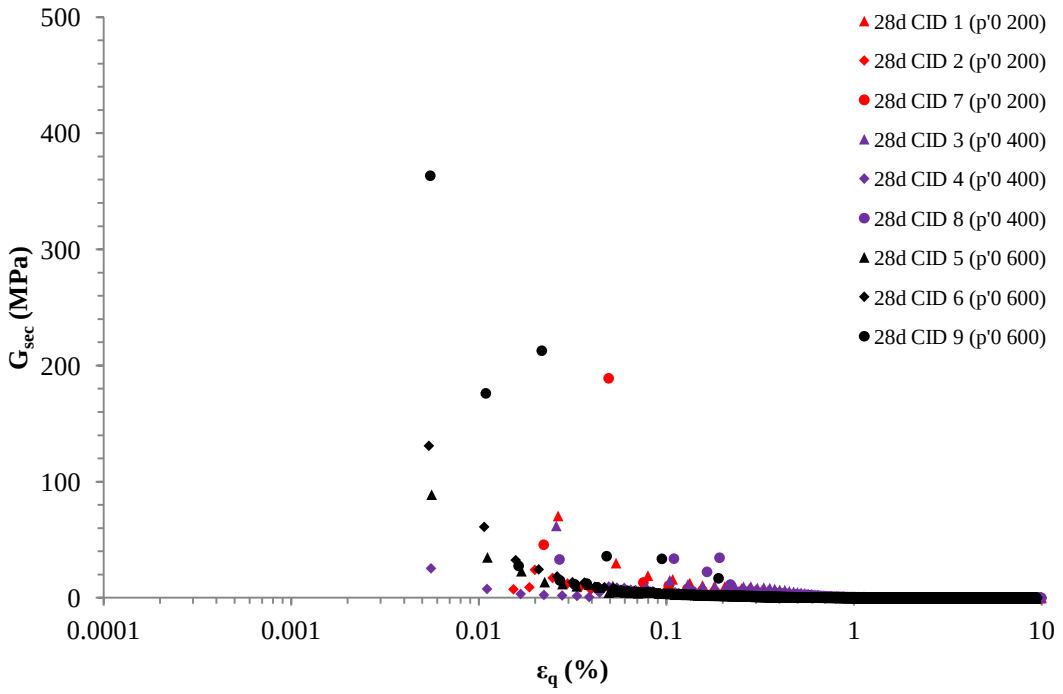

Figure 8.14: Secant shear stiffness degradation behaviour for drained GGBS-NaOH stabilised Lanton alluvium samples.

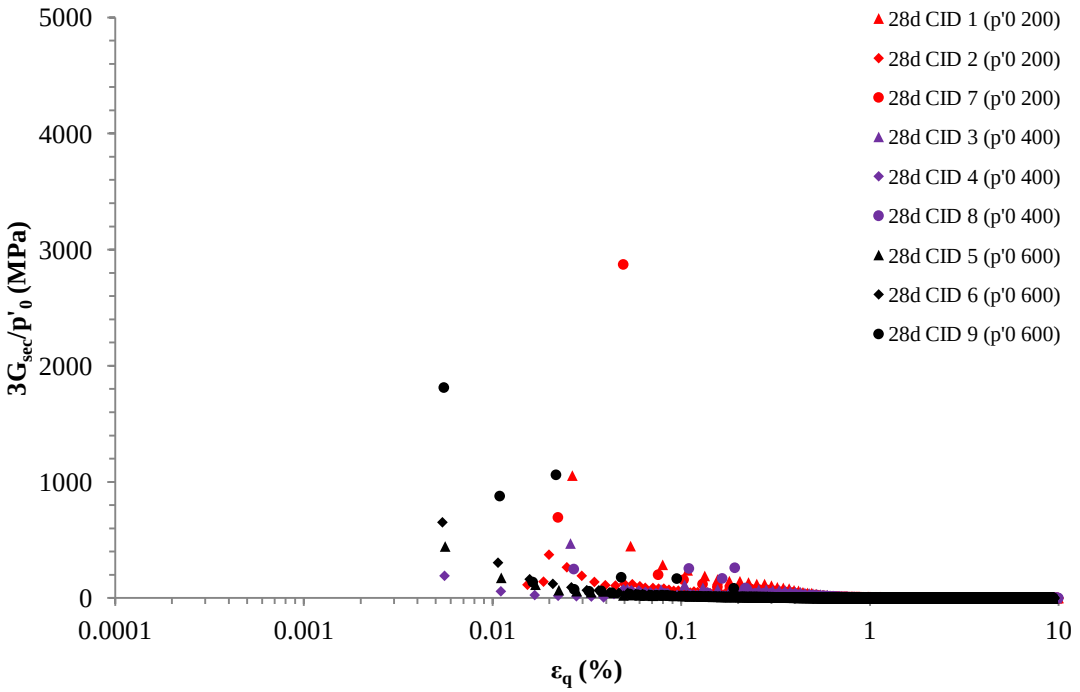

Figure 8.15: Secant shear stiffness degradation behaviour for drained GGBS-NaOH stabilised Lanton alluvium samples, normalised by their corresponding p'$_0$ values.

The likely reasoning behind such lower G_{sec} values is that drained tests were carried out at a strain rate five times slower (0.01 mm/min) compared with that used for undrained tests, with higher apparent stiffnesses resulting from faster rates of sample loading.

Changes in secant bulk stiffnesses within samples due to increasing shear strain during drained tests are apparent in Figure 8.16. Although degradation curves can be defined from each of the data sets, much data scatter can be seen in Figure 8.16; particularly at volumetric strain levels <0.02%. Based on the relatively low resolution of volumetric strain data obtained, K_{sec} values plotted for samples on Figure 8.16 for volumetric strain levels <0.01% should not be considered as accurate representations of stabilised Lanton alluvium's volumetric stiffness/strain behaviour.

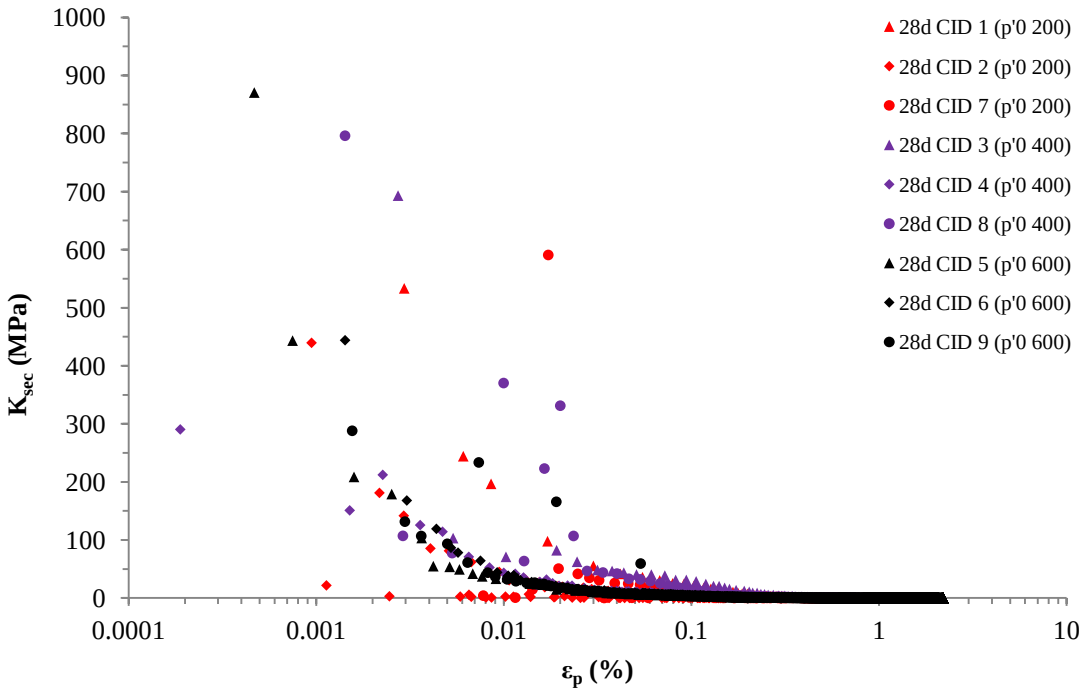

Figure 8.16: Secant bulk stiffness degradation behaviour for drained GGBS-NaOH stabilised Lanton alluvium samples.

As per the shear stiffness data sets, the bulk stiffnesses recorded for samples were normalised with respect to their post-consolidation mean effective stress conditions to produce a tighter fitting, better correlated bulk stiffness degradation curve. However, this normalisation procedure was also relatively unsuccessful in producing such a tighter fitting curve as further data scatter and curve separation was observed instead.

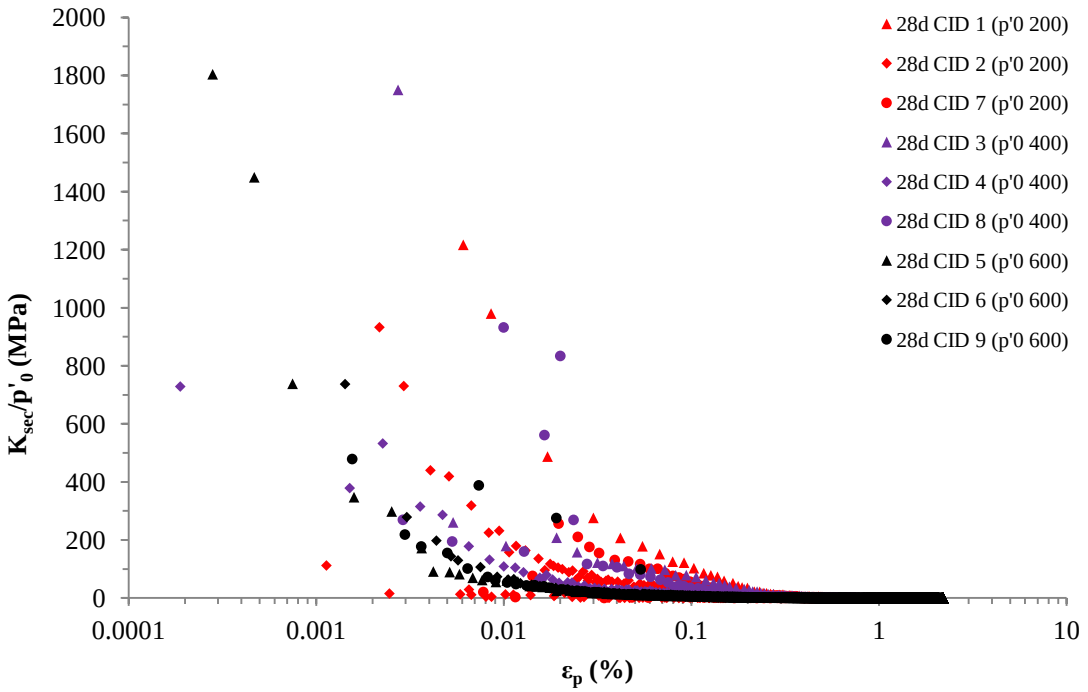

Figure 8.17: Secant bulk stiffness degradation behaviour for drained GGBS-NaOH stabilised Lanton alluvium samples, normalised by their corresponding p'_0 values.

Clearly the normalisation technique used by Jardine et al. (1986), Rouili (2007) and Simpson and Rouainia (2012) has limited applicability for normalising shear and bulk stiffness data sets obtained for relatively high-strength GGBS-NaOH stabilised Lanton alluvium after 28 days curing. Special care was taken to ensure that stabilised samples were of the same high quality. Had there been any significant variations in sample quality, normalisation would have corrected for this and produced tighter fitting curves. Thus, individual sample quality is not considered by the author as a major contributing factor behind the post-normalisation data scatter.

Per Figures 8.12 and 8.13 for the G_{sec} results, normalisation resulted in the stiffness degradation curves for samples tested at p'_0 = 50 and 100 kPa being positioned on top of those for samples tested at higher p'_0 stress conditions. Also, there was considerable separation between samples tested at p'_0 = 50 kPa and those tested at p'_0>200 kPa. However, certainly for undrained tests, normalisation appeared to be relatively successful in bringing shear stiffness degradation curves obtained for samples tested at p'_0>200 kPa much closer together. This suggests that although the effective confining stresses samples are subjected to at the start of shearing do have an effect on the shear

stiffnesses produced, they appear to have less of an effect at effective confining stresses ≤200 kPa. This corresponds well with the q-p' effective stress path behaviour observed for stabilised Lanton alluvium samples in Figure 8.9. The peak deviatoric strengths for undrained samples were fairly similar at effective confining stresses 50 and 100 kPa. For undrained tests conducted at p'_0>400 kPa, increases in sample's peak deviatoric strengths and a change in shape of the undrained effective stress paths taken by samples were observed.

8.3 Dynamic results

The inclusion of the GGBS-NaOH binder within reconstituted Lanton alluvium and the 28 day curing period has proved very successful in improving the original soil's monotonic strength. The level of cementation within the stabilised soil more than compensated for the loss of natural sedimentation structure within the natural soil, which was lost very easily upon the application of relatively low stresses, due to the soil's high level of sensitivity. The accumulations of plastic cyclic shear strains and developments in pore pressures observed within untreated Lanton alluvium due to the application of a dynamic loading cyclic simulating a single HST travelling at 125 mph, were significant. At shallow depths beneath the surface of a high-speed railway embankment, the peak cyclic deviatoric stress applied to the soil due to the high frequency dynamic loading exceeded the soil's monotonic strength. As similarly observed for silt-clay mixtures by Yilmaz et al. (2004), the strength and stiffness of the soil became dictated by its viscosity, due to the relatively high frequency at which the train loads were applied to soil samples. Collectively, all these findings raised serious concerns that the soil could potentially liquefy after just a few HST cycles were applied to the soil; thereby highlighting the need for soil stabilisation.

Thus, the following dynamic triaxial testing programme investigates the behavioural response of GGBS-NaOH stabilised Lanton alluvium after 28 days curing when subjected to the same dynamic high-frequency (2.794 Hz) train loading conditions and effective confining stresses (60, 180.65 and 147.48 kPa) as those experienced by untreated Lanton alluvium. Triplicate one-way dynamic loading tests were conducted for these three effective confining stress conditions. Although small strain and bender

element measurements would be an essential requirement during the dynamic testing of stabilised Lanton alluvium in calculating dynamic stiffnesses at small strains, no such equipment was available at the time of testing. The inclusion of this high strength performance binder is postulated to provide an effective means of mitigating any significant developments in pore pressure, accumulations in plastic cyclic shear strains and ultimately liquefaction. The stabilised soil has considerably higher stiffnesses than the untreated soil and is therefore more likely to experience brittle failure upon dynamic loading. Thus, the potential for the development and propagation of small/large brittle fractures within the stabilised alluvium, along with any consequential damage to the overlying railway embankment is an important factor to consider when assessing the GGBS-NaOH binder's suitability in stabilising Lanton alluvium when subjected to frequent HST loading.

The average seat loads and dynamic HST loads applied to stabilised samples for tests conducted at effective confining stresses of 60, 108.65 and 147.48 kPa are shown in Figure 8.18. The corresponding cyclic stress ratio values for these dynamic loading conditions are presented in Table 8.1.

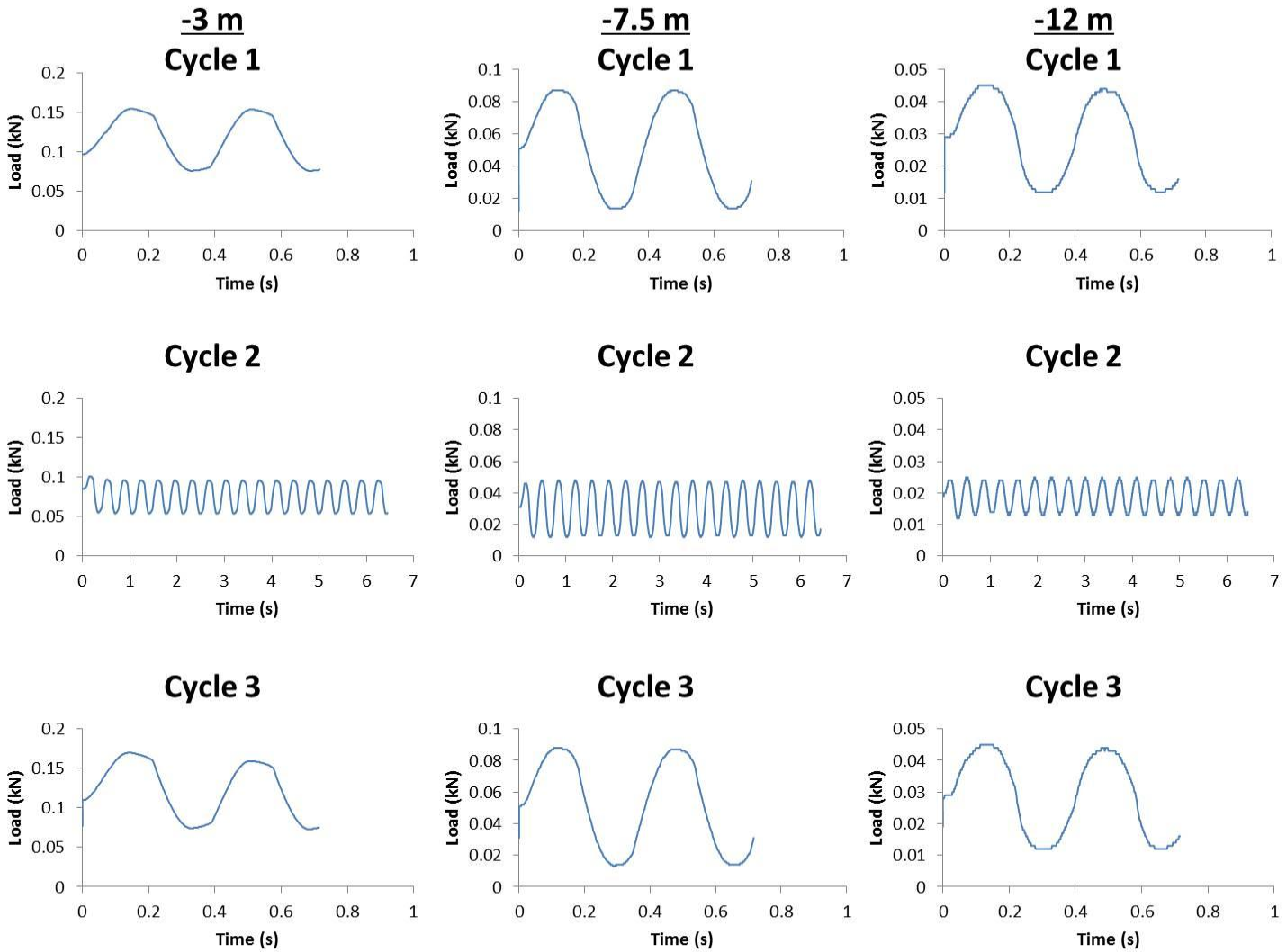

Figure 8.18: Summary of loading patterns observed for dynamic tests conducted at effective confining stresses replicating 3, 7.5 and 12 metres depth.

Table 8.1: Summary of CSR conditions used during dynamic testing on GGBS-NaOH stabilised Lanton alluvium samples.

	CSR		
	p'$_0$ = 60 kPa	***p'$_0$ = 108.65***	***p'$_0$ = 147.48***
Load cycle 1 (1 x Class 43 locomotive)	0.50	0.11	0.05
Load cycle 2 (9 x Mark 3 coaches)	0.35	0.07	0.04
Load cycle 3 (1 x Class 43 brake car)	0.49	0.11	0.05

Figures 8.19–8.20 show the deviatoric stress – axial/cyclic shear strain behaviour of stabilised Lanton alluvium. The roughness of the hysteretic loops in the aforementioned figures is due to global strain measurements being taken, rather than local measurements, thereby highlighting the need for future dynamic tests on this material to use local LVDT's and bender elements. It can generally be seen that the amount of strain experienced by the material over the course of the three dynamic loading cycle events (corresponding to a Class 43 locomotive, nine Mark 3 coaches and a Class 43 brake car) was one to two orders of magnitude smaller than that experienced by untreated reconstituted Lanton alluvium. The amount of axial strain applied to the material at p'_0 = 60 kPa due to the dynamic loads subjected by both the Class 43 locomotive and brake car was 0.1%; and 0.075% due to the Mark 3 coaches. Only small plastic axial strain accumulations were observed within the material at 3 metres depth due to these dynamic loads, whereby a maximum of 0.055% was measured after all three dynamic loading cycles had been applied. Under p'_0 conditions of 108.65 kPa, the total amount of accumulated plastic axial strain experienced by stabilised Lanton alluvium after the passage of one HST appeared to be within the small strain range of up to 0.002%. For p'_0 conditions of 147.48 kPa, the stabilised soil demonstrated impressive stress-strain memory as the shape of the dynamic stress-strain loops were identical and that very small (≈0.0001) to negligible strains were incurred due to the material. This suggests that at this effective confining pressure, the material behaved in an almost perfectly linear elastic manner.

The response of pore pressures within samples due to the HST dynamic loading cycle is displayed in Figure 8.21. Under effective confining stresses of 60 kPa, the peak

dynamic loads applied by the Class 43 locomotive and brake car generated excess pore pressures of 1.5 kPa and only 1 kPa for the Mark 3 coaches. Negligible degrees of pore pressure ratcheting were measured with increasing number of loading pulses during the three dynamic load cycle events; namely 0.1–0.2 kPa. Slightly larger developments of 2–5 kPa and 0.5–1.5 kPa in pore pressure due to dynamic loading were observed for samples tested at p'_0 states of 108.65 and 147.48 kPa, respectively. Although slightly higher pore pressures developed during tests conducted at p'_0 = 108.65 compared with those conducted at p'_0 states of 60 or 147.48 kPa (possibly due to natural variations in sample's moisture contents); negligible to no pore pressure ratcheting was observed with increased numbers of Class 43 locomotive/brake car or Mark 3 coaches loading pulses (N) within samples tested at the higher p'_0 states of 108.65 or 147.48 kPa (Figure 8.22).

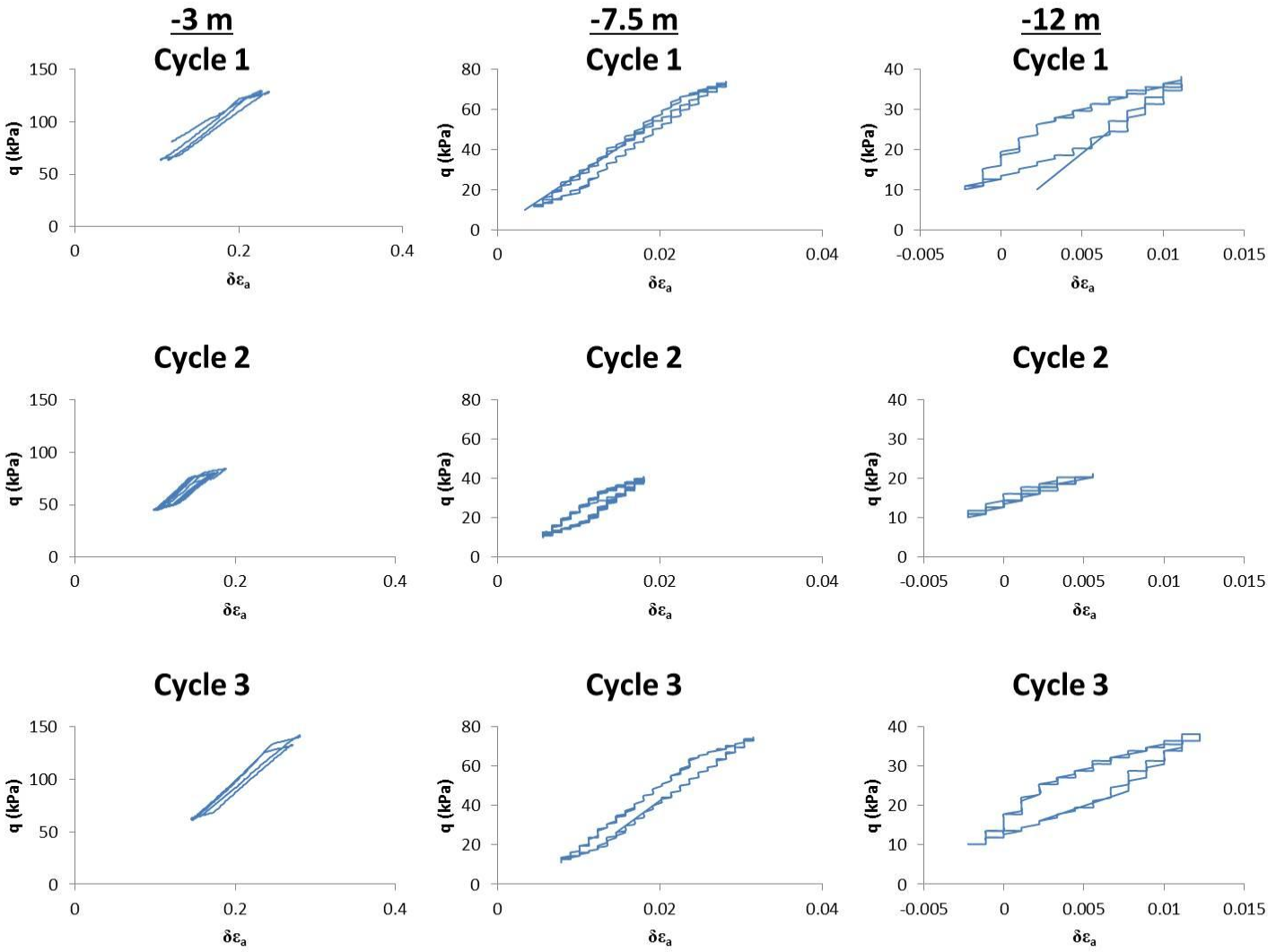

Figure 8.19: Summary of deviatoric stress-axial strain relationships during dynamic tests conducted at effective confining stresses corresponding to 3, 7.5 and 12 m depth.

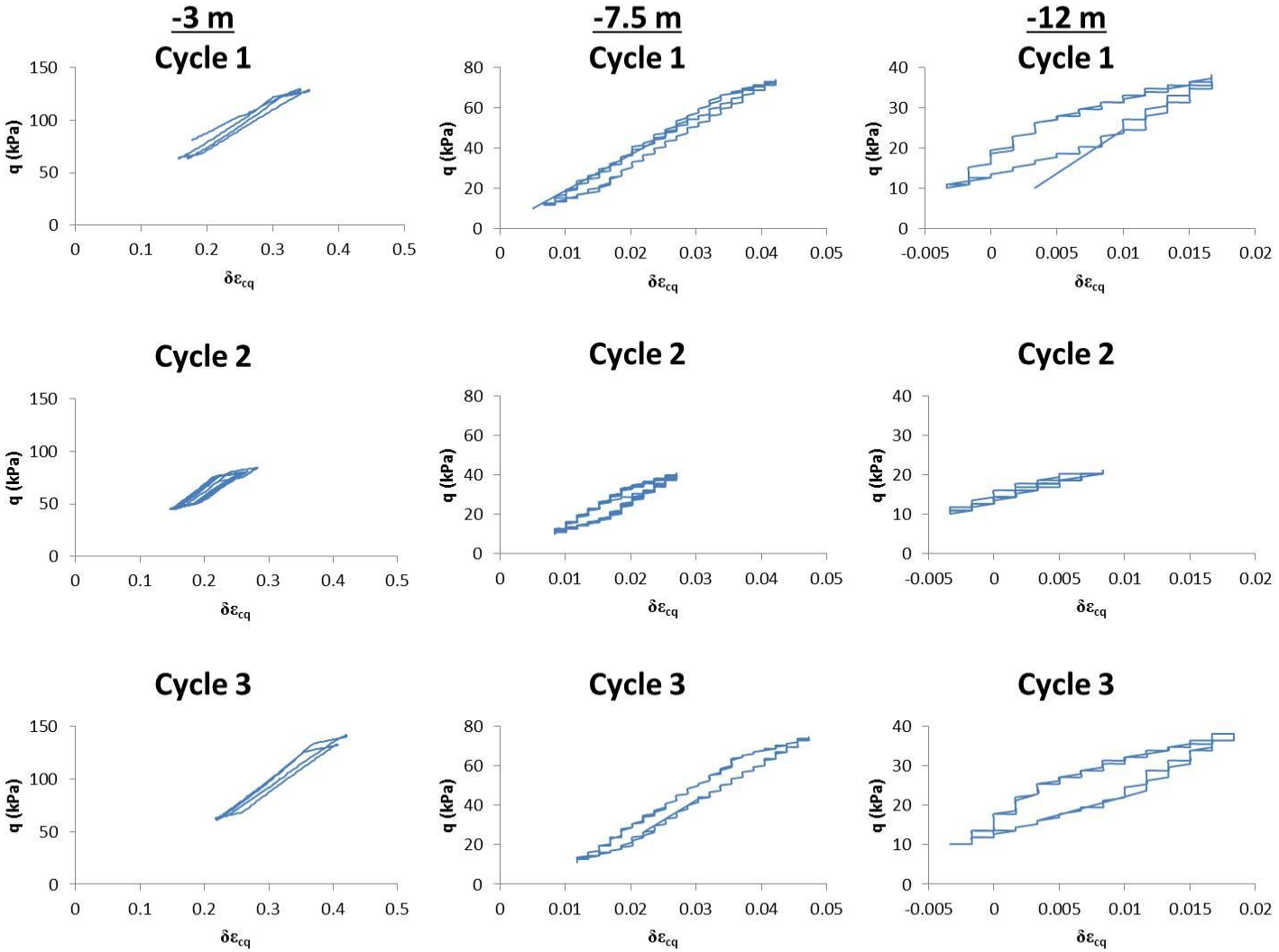

Figure 8.20: Deviatoric stress-cyclic shear strain relationships during dynamic tests conducted at effective confining stresses corresponding to 3, 7.5 and 12 m depth.

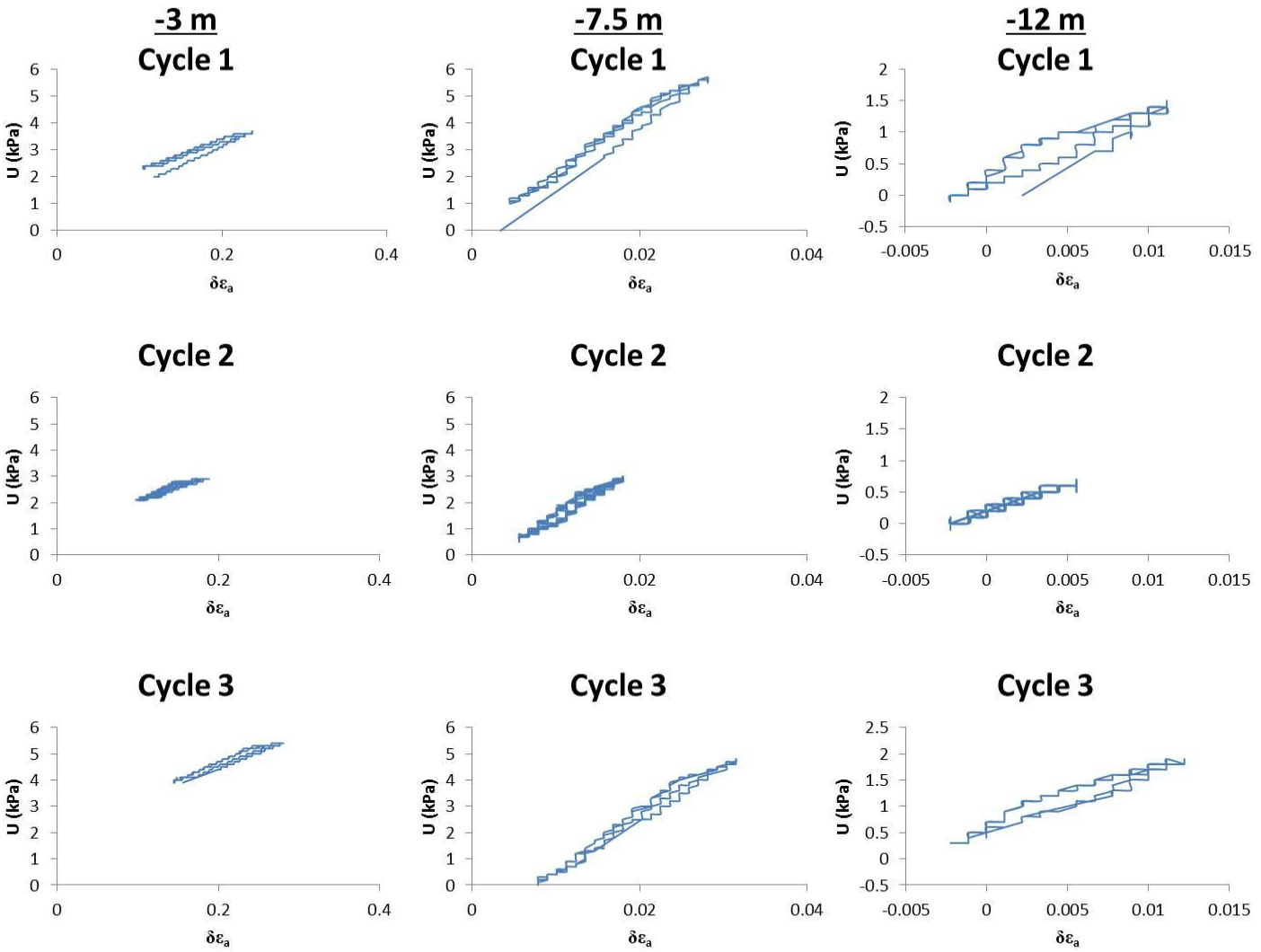

Figure 8.21: Pore pressure response of stabilised samples during dynamic tests conducted at effective confining stresses corresponding to 3, 7.5 and 12 m depth.

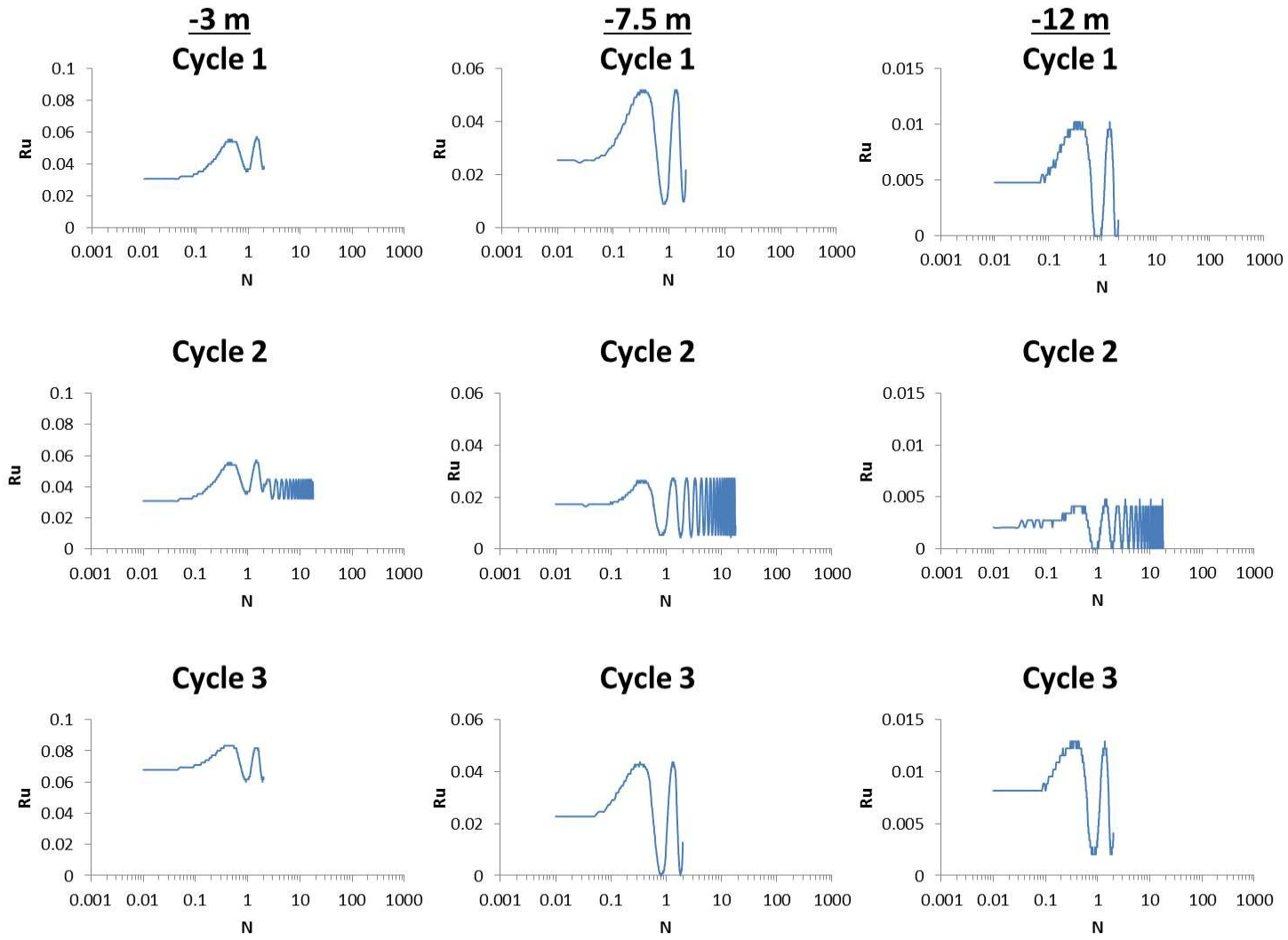

Figure 8.22: Variations in pore pressure ratio (R_u) with increasing number of loading pulses for stabilised samples during dynamic tests.

Further to the pore pressure data sets in Figure 8.21, the changes in samples' pore pressure ratio (R_u) are shown in Figure 8.22. From the data, it is clear that none of the sample's R_u values met Ishihara's (1993) liquefaction criterion of $R_u = 1$, as R_u values didnot exceed 0.08 for any of the p'_0 or dynamic loading conditions samples were subjected to. Additionally, during each of the three dynamic load cycle events, the Ru values remained constant with increasing numbers of loading pulses. Albeit the observed ratcheting of pore pressures within samples tested at $p'_0 = 60$ kPa were only small, this inherently caused slight reductions (1–3 kPa) in their mean effective strength (p') with increasing number of loading pulses and thus axial/dynamic shear strain (Figure 8.23). However, negligible to no reductions in samples' mean effective strengths occurred when dynamically tested at higher effective confining pressures ≥ 108.65 kPa.

The very small amounts of plastic cyclic shear strain accumulations recorded within samples at all three p'_0 conditions (Figure 8.24) may be attributed to stabilised Lanton alluvium's high stiffness after 28 days curing and the relatively low deviatoric stresses applied due to the HST event. Although the strains measured by the ELDYN apparatus for stabilised Lanton alluvium due to dynamic loading were small, it is possible that the strains developed were within the small strain range; based on the stiffness-strain behaviour observed from monotonic testing. This highlights the need to use local strain measurements for dynamic testing programmes on such high-stiffness geomaterials. The cyclic yield shear strain at which stabilised Lanton alluvium's cemented structure breaks down and results in excessive increases in shear strain couldn't be captured after the passage of just one HST loading event. Further longer term testing involving larger numbers of dynamic load pulses, small strain measurments, various loading frequencies and effective confining pressures would therefore be required to accurately define this parameter for the stabilised soil.

The resilient modulus (M_r) results from all dynamic tests is presented in Figure 8.25. The M_r values obtained for samples tested at $p'_0 = 60$ kPa compared well with those recorded for untreated reconstituted Lanton alluvium (40–100 MPa); although the stabilised soil's M_r values at higher p'_0 states of 108.65 and 147.48 kPa were at least three to four times higher (>150–300 MPa) than those measured for the untreated soil. With increasing numbers of loading pulses during the Class 43 locomotive/brake car and Mark 3 coaches dynamic loading events, the M_r values measured for GGBS-

NaOH stabilised Lanton alluvium remained relatively constant. This implies that negligible or no reductions in the material's stiffness occurred due to a passing HST. It is assumed the material's cemented soil matrix remained intact under such relatively low dynamic stresses. However, it is emphasised that local strain measurements would be required to calculate higher resolution more accurate M_r values for the material during dynamic testing.

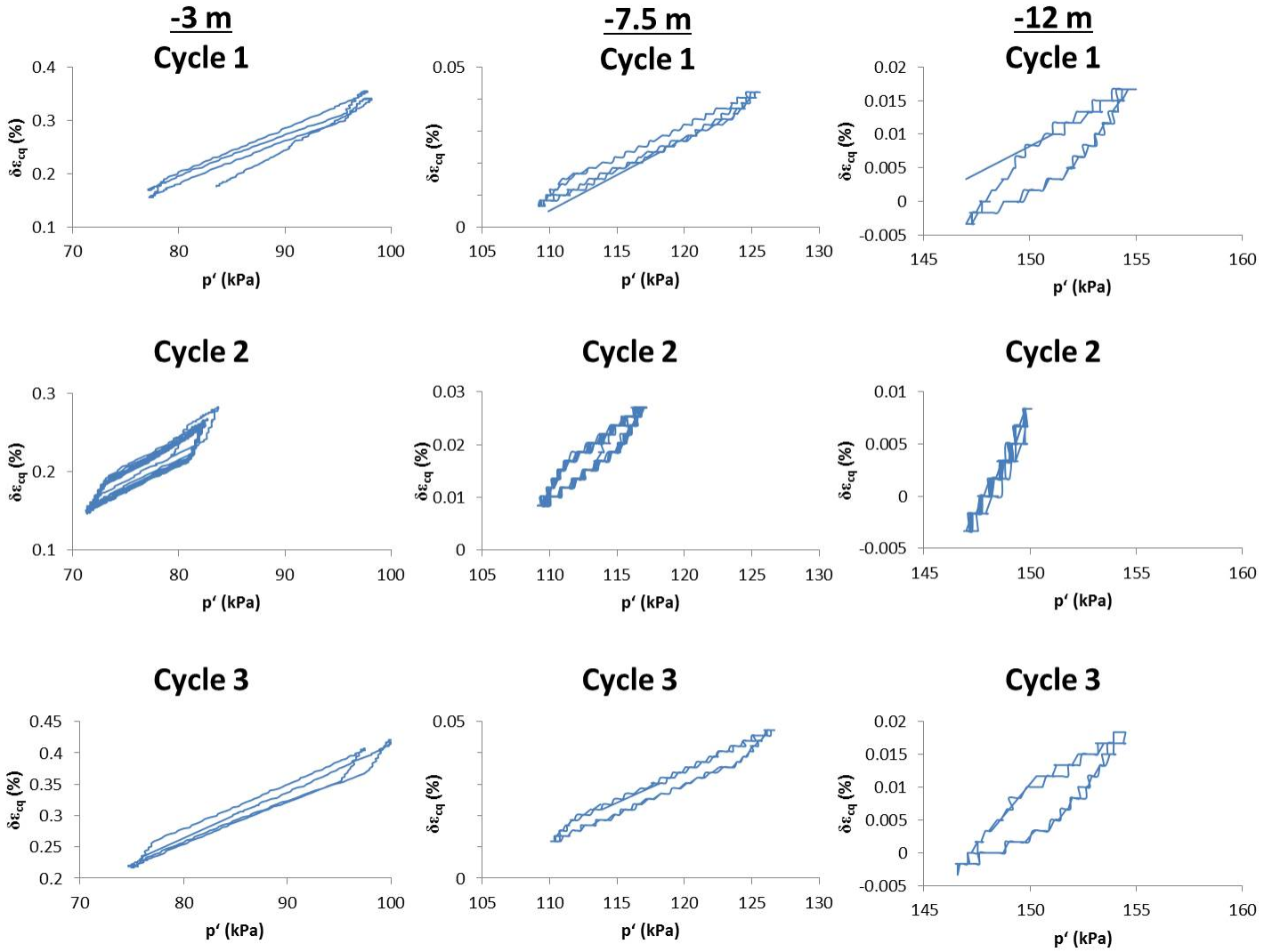

Figure 8.23: Relationship between cyclic shear strain and mean effective stress for stabilised samples during dynamic tests.

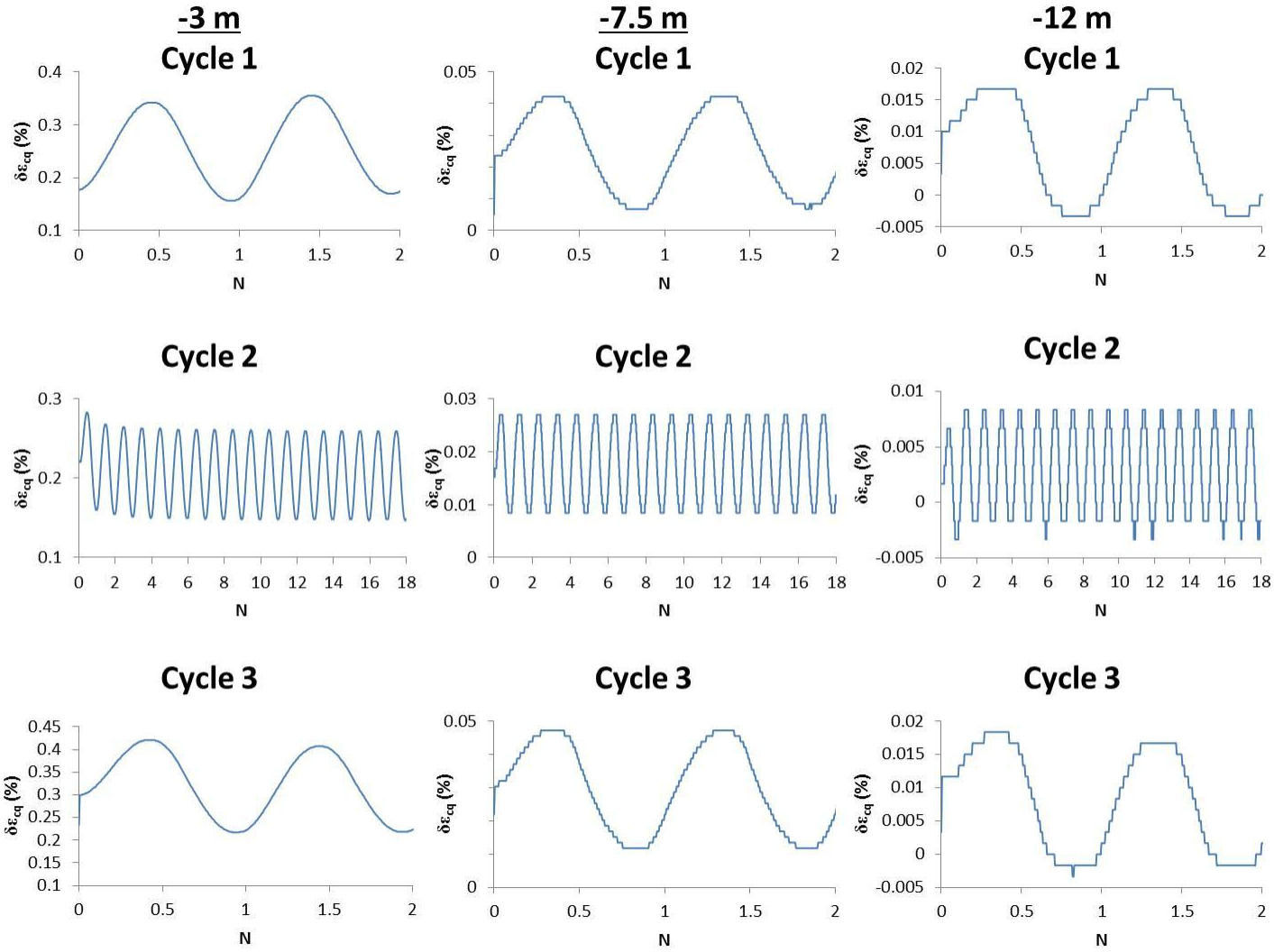

Figure 8.24: Relationship between cyclic shear strain and number of loading pulses experienced by stabilised samples during the three dynamic loading events.

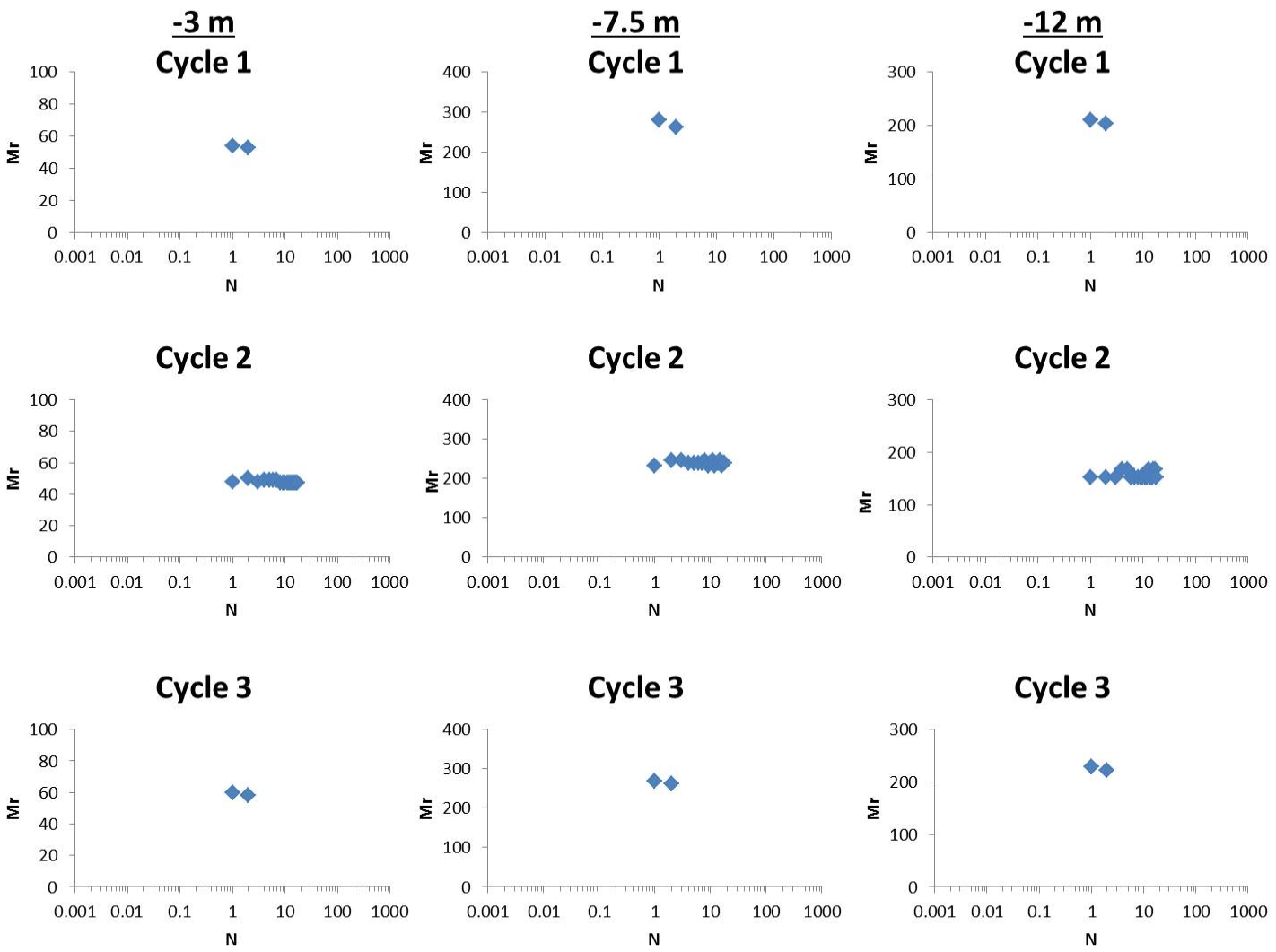

Figure 8.25: Variations in resilient modulus (M_r) observed with increasing number of loading pulses for stabilised samples during dynamic tests.

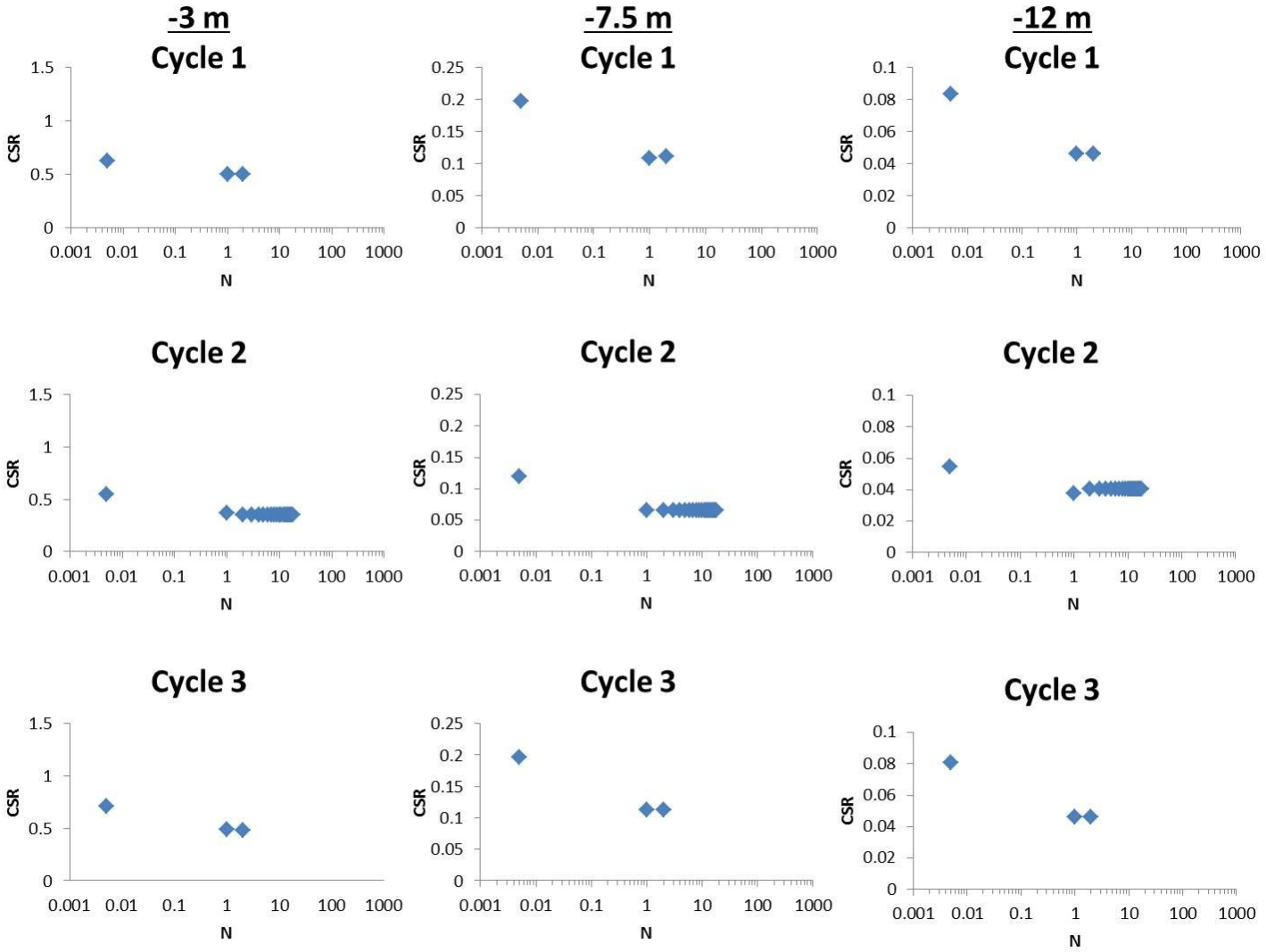

Figure 8.26: Variations in cyclic stress ratio (CSR) observed with increasing number of loading pulses for stabilised samples during dynamic tests.

The cyclic effective stress paths taken by all samples within q-p' stress space are shown Figure 8.27. Further to the data in Figure 8.23, a marked feature regarding the behaviour of stabilised Lanton alluvium samples compared with untreated reconstituted samples is their much lower degree of migration towards lower p' stress states with increasing numbers of loading pulses.

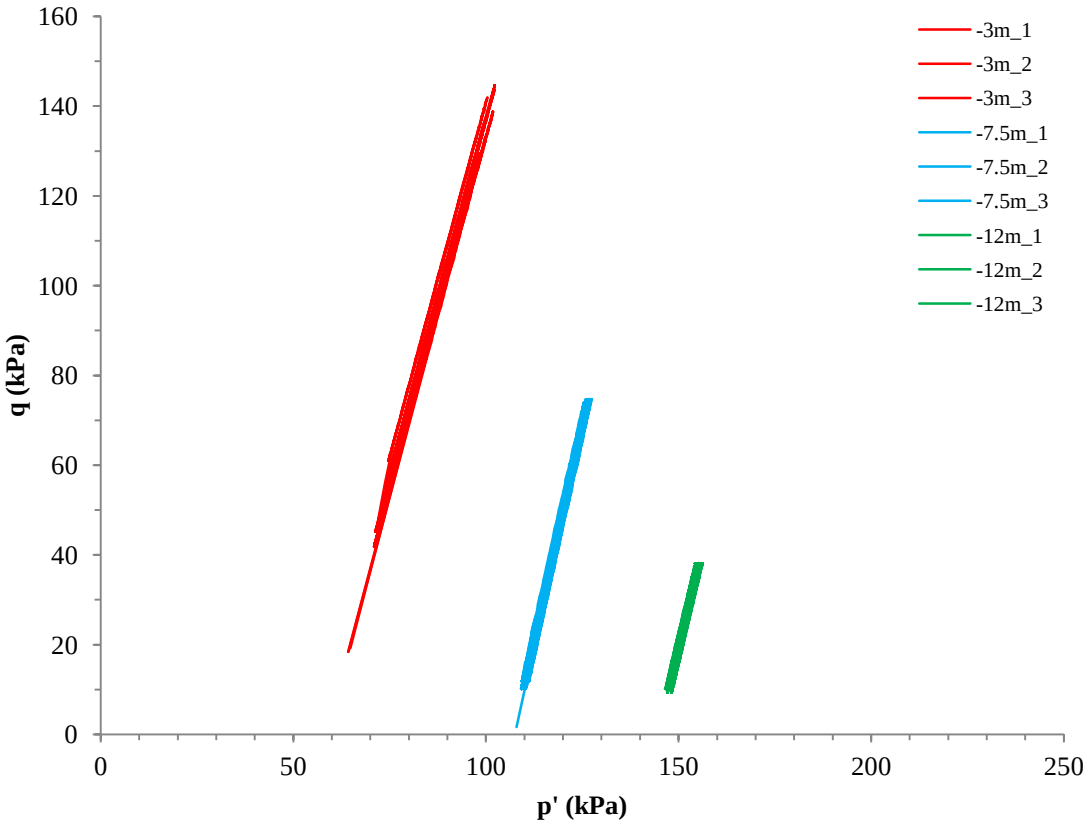

Figure 8.27: Dynamic stress paths for all GGBS-NaOH stabilised Lanton alluvium samples within q-p' stress space.

When comparing the relative positions of the samples' dynamic effective stress paths with the stabilised material's critical state line ($CSL_{28dCement}$), derived from monotonic testing (Figure 8.28); it is clear that the dynamic stress paths are at a considerable distance from the $CSL_{28dCement}$. In Figure 8.29, the deviatoric stress – axial strain response of samples when subjected to HST dynamic loading at the three different p'_0 conditions is compared with the monotonic deviatoric stress – strain behaviour for the material at very similar p'_0 conditions. According to Figure 8.29, in contrast to the

behaviour of untreated reconstituted Lanton alluvium, where the peak dynamic stresses exceeded the monotonic strength; the dynamic stresses experienced by stabilised samples were all significantly lower than their respective monotonic deviatoric strengths.

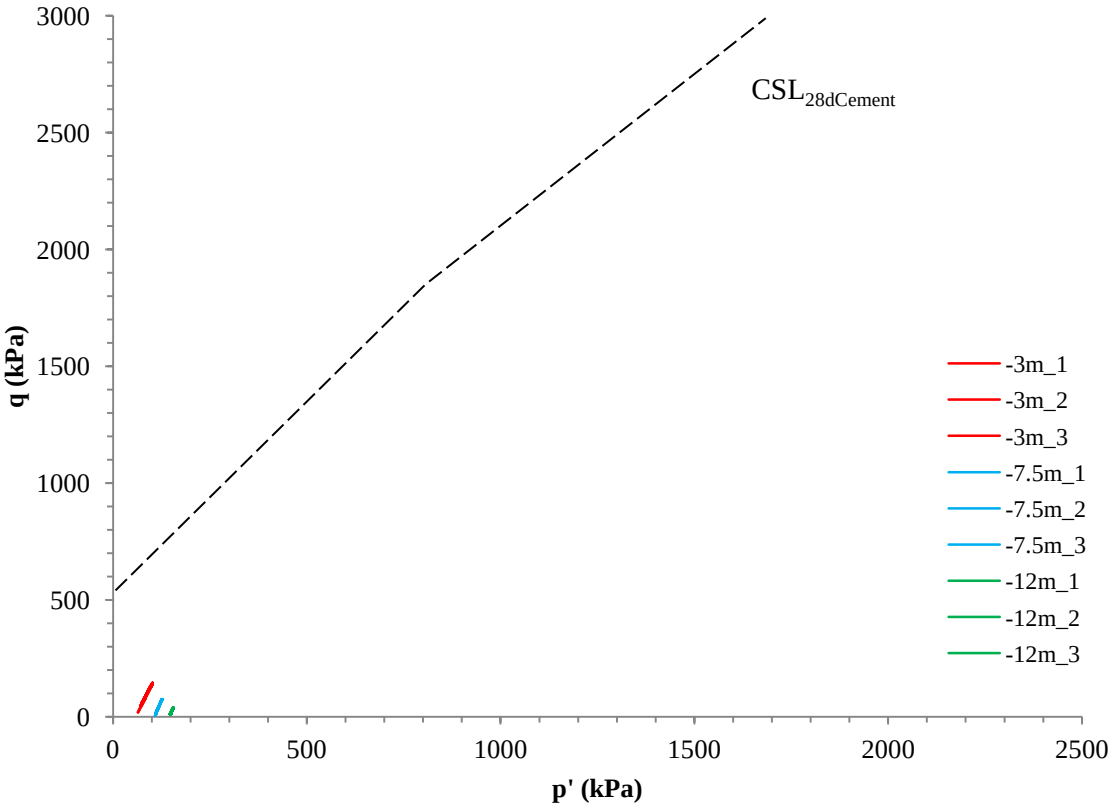

Figure 8.28: Dynamic stress paths for GGBS-NaOH stabilised Lanton alluvium samples within q-p' stress space, with the stabilised soil's $CSL_{28dCement}$ superimposed.

Collectively, these findings suggest that stabilising Lanton alluvium with GGBS-NaOH at a dosage of 7.5% and cured for 28 days has been successful in mitigating significant developments in pore pressures, axial/cyclic shear strains and therefore liquefaction phenomena. No reductions in pore pressure were observed with increasing numbers of loading pulses, which if observed would have implied the breakdown of cementitious bonds within the stabilised material and therefore the onset of dilation. The effect of stabilisation and 28 days curing has caused a major transformation in the mechanical behaviour of the soil during high-frequency dynamic train loading. Lanton alluvium's strength and plastic deformation accumulation response changed from

being controlled by its viscosity characteristics to its cement content and bonded internal structure. Upon inspecting each sample after being subjected to dynamic load testing under the three different effective confining pressures used, there was no visual evidence to suggest that the stabilised material had developed any small or large scale brittle fracturing.

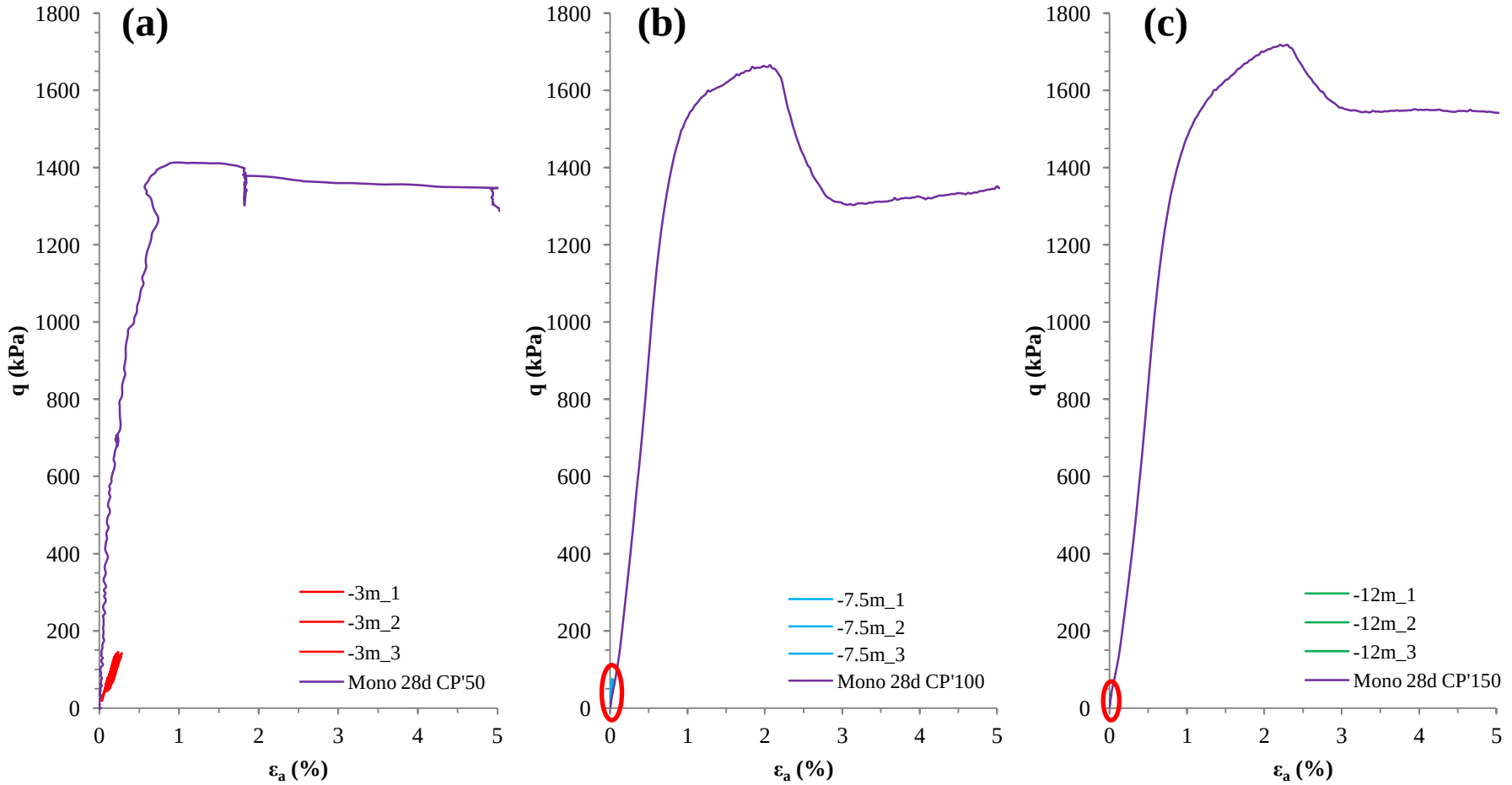

Figure 8.29: One-way compressive loading with peak cyclic deviatoric stress compared with monotonic deviatoric strength for GGBS-NaOH stabilised Lanton alluvium samples at p'_0 stress conditions of: (a) 60 kPa, (b) 108.65 kPa and (c) 147.48 kPa. Areas encircled show the positions of the dynamic effective stress paths.

8.4 Chapter Summary

The improved monotonic and dynamic strength of Lanton alluvium due to stabilisation with GGBS-NaOH is impressive. The introduction of the binder has more than compensated for the loss of the soil's natural structure. Due to the stabilised alluvium being considerably stiffer compared with its untreated counterpart during monotonic loading, it exhibits overconsolidated behaviour. Akin to soft rocks, once stabilised Lanton alluvium started to yield and eventually fail, dilation and negative pore pressure behaviour was observed within the material during drained conditions. Although the effect of increasing effective confining stress conditions increases deviatoric strength was observed, such effects were much less pronounced at lower effective confining pressures of ≤200 kPa. Hence, the normalisation technique used by Jardine et al. (1986) and Rouili (2007) was only successful in producing tighter fitting, better correlated stiffness degradation curves for samples tested at p'_0 conditions ≥400 kPa. The threshold shear strain at which stabilised Lanton alluvium's initially high shear stiffness starts to degrade is higher compared with that measured for the untreated soil. Although untreated undisturbed Lanton alluvium is considered to have relatively high sensitivity and its initial sedimentation structure is lost fairly quickly, once the cemented structure within the stabilised soil starts to break down, its shear stiffnesses has been observed to degrade at an accelerated rate compared with that for the untreated undisturbed soil.

The initial elastic and shear stiffnesses obtained from tests at Newcastle and Bristol differed from each other considerably. Tests conducted at Newcastle only captured shearing behaviour for strain ranges no smaller than 0.01% (due to the lack of local strain measurements); at which point the undrained shear stiffnesses were measured between 50 and 110 MPa. Contrastingly, the test conducted at Bristol (see Appendix 5) captured behaviour down to 0.0001% strain. Bender elements determined a G_{max} of 1385 MPa and local strain measurements identified that the materials shear stiffness had reached its minimum steady state at shear strains an order of magnitude smaller than that suggested by Newcastle monotonic triaxial tests.

Dynamic testing results showed that mixing the GGBS-NaOH binder at a 7.5% dosage within Lanton alluvium and allowing to cure for 28 days significantly reduced the

amount of accumulating plastic shear strains, excess pore pressure generation, mean effective strength and resilient modulus reductions observed when subjected to loading conditions typically presented by an HST travelling at 125 mph. Per global strain measurements, stabilised samples experienced axial and cyclic shear strains at least an order of magnitude smaller than those observed by the untreated soil at all three effective confining stresses. Encouragingly, no evidence was found to suggest that any small or large fractures formed within samples during dynamic loading at effective confining pressures up to 147.48 kPa. Although further testing is required, the strains experienced by stabilised samples were either close to or within the small strain range. In contrast with the viscosity controlled stiffness and plastic strain accumulation behaviour of untreated reconstituted Lanton alluvium (per chapter 7), stabilisation has resulted in the soil's stiffness and strain behaviour becoming controlled by its structure. Based on the findings from the dynamic testing programme, stabilisation has been successful in significantly reducing the likelihood of liquefaction phenomena when the soil is subjected to HST loading.

Although the results from the monotonic and dynamic testing programmes are encouraging in terms of highlighting the GGBS-NaOH's potential as a useful binder for stabilising soils which are to experience monotonic and frequent dynamic loads, there remains a need for future testing. As railway embankments are subject to dynamic loads from frequently passing railway traffic for many years, the performance of GGBS-NaOH stabilised Lanton alluvium when subjected to such long-term dynamic loading conditions should be investigated by using much larger numbers of high-frequency dynamic loading cycles. Given the complexity of HST loads, the stabilised soil must be able to provide sufficiently high dynamic and monotonic stiffnesses that will not be exceeded by the peak monotonic and dynamic stresses applied by the embankment and passing rail traffic. Concurrently, it is also important that the stabilised soil does not possess too high a stiffness, as the material would be more prone to brittle failures at smaller strains. The stabilised soil should possess sufficiently high levels of elasticity, whereby the dynamic loads to be applied should fall within this range to either prevent any plastic strain accumulations or keeping them to a minimum within an acceptable design range, which will not compromise the long term strength of the material and therefore the structural integrity of the railway embankment.

Regarding equipment, future dynamic and monotonic tests should use local axial and radial strain measurements (as utilised by Viana da Fonseca et al., 2013) plus bender element measurements to more accurately define the stabilised soil's changing stiffnesses and its monotonic/cyclic yield shear strains. These are critical in the design of high-speed railway embankments. The monotonic and dynamic tests have predominantly measured changing pore pressures within samples from their base. To gain a better understanding about the distribution of pore pressures throughout stabilised Lanton alluvium during monotonic and dynamic testing, future tests ought to use a mid-height pore pressure probe. Rather than using simple air/water bladder pressure controlled triaxial systems, future tests should also make use of much higher precision computer controlled air/water pressure controllers to more accurately regulate the back and cell pressures during testing; and to allow stress path testing to define stabilised Lanton alluvium's small strain kinematic and elastic yield surfaces.

Chapter 9:

Discussion

The testing results obtained from the dosage trials, mineralogical and microstructural studies, monotonic and dynamic triaxial testing programmes are discussed in detail within their respective chapters. The aim of this chapter is to summarise the discussions presented in the five results chapters, relate them with existing literature where possible and address the key themes which emerge.

9.1 Engineering performance

9.1.1 Development of a new binder

The strength and stiffness performances for a variety of controlled and alkali activated IBP's, including GGBS, PFA and RG were investigated to assess their potential for stabilising soft alluvial soils typically found in the UK, rather than using traditional binders such as lime and CEM-I. The primary strength criteria used to assess these binders included undrained shear strength requirements of 50 – 150 kPa, as defined by EuroSoilStab (2002) after 28 days curing (Hanson et al., 2001); and that the strengths of the IBP binders should meet or surpass the strengths achieved by CEM-I and lime.

Initial dosage trials conducted on a laboratory produced silty sand demonstrated that GGBS and GGBS-PFA activated with sodium silicate solution and sodium hydroxide flakes at a dosage of 10% by dry weight exhibited the most impressive engineering performances when added to the soil after 28 days curing. RG exhibited poor engineering performances, which may be attributed to its non-pozzolanic nature and weakened microstructure through the evaporation of water when converting the material from its initial filter cake form to a dry powder. Regarding the poor performance of PFA samples, it is thought there were insufficient cation exchange sites within the silty sand, due to its relatively high sand/silt – low clay contents. The NaOH flakes – sodium silicate solution activator proved very effective in raising soil pH to promote pozzolanicity. However, using sodium silicate solution in deep dry soil mixing is impractical and the environmental and financial costs associated with its manufacture are considerable (Habert et al., 2011). Hence, its continued use in this research was impractical and unsustainable. Therefore, the NaOH flakes was selected

as the sole alkali activator for the remainder of this research; as it was able to raise soil pH to at least the required minimum value of 10.5.

9.1.2 Stabilising a Northumberland alluvium

9.1.2.1 Untreated soil behaviour

Oedometer testing results suggested that the Lanton alluvium had unfavourably high coefficients of compressibility. A considerable difference in the void ratio reduction during compression between the reconstituted and undisturbed soil pointed towards the presence of structure within the undisturbed soil, which was bonding-dominated. Normalising oedometer data according to a technique defined by Gasparre and Coop (2008) revealed that the soil possessed high degrees of structure. However, due to the soil's relatively high level of sensitivity, attributable to its high silt and in-situ moisture contents; the structure was easily lost upon applying relatively low vertical stresses and small strains. Monotonic triaxial testing on the reconstituted and undisturbed soil indicated that it was normally consolidated; whereby slightly higher deviatoric strengths were achieved for undisturbed samples compared with reconstituted samples. Table 9.1 summarises the effective strength parameters derived from CIU triaxial tests for the reconstituted and undisturbed Lanton alluvium. The soil's initially high degree of structure was also quantified from triaxial results according to the method developed by Rouainia and Muir Wood (2000). These findings correlated well with the degree of structure defined from oedometer testing.

The high silt and moisture content, high compressibility and relatively low stiffness characteristics of the Lanton alluvium indicate difficult ground conditions for construction purposes; particularly regarding bearing capacity. The soil's low levels of cohesion in both its dry and wet states may potentially result in wall collapses within excavations and slope instabilities. Such ground conditions are common across the UK, particularly on floodplains within river valleys where housing and industrial developments are concentrated. The UK government's plans to improve the UK's high-speed rail network between northern and southern England with the development

of HS2 and HS3. The poor mechanical strength properties of the Lanton alluvium highlight the need for its stabilisation to make it suitable for engineering projects characterised by complex monotonic and high-frequency dynamic loading conditions, such as high-speed railway embankments.

9.1.2.2 Effects of stabilisation

9.1.2.2.1 Strength, stiffness and compressibility

The UCS, triaxial and oedometer testing results demonstrated that the most effective binder mixture in producing the most impressive strength improvements and reductions in compressibility within the Lanton alluvium was GGBS activated with NaOH. The binder was mixed into the soil at four dosages (2.5, 5, 7.5 and 10% by dry weight) with a view to identifying the most optimum dosage in terms of engineering performance, whilst meeting EuroSoilStab (2002) 28 day strength criteria and achieving performances which met or surpassed those of the more traditional CEM-I and lime binders.

9.1.2.2.1.1 Compressive strength

The structural integrity and strengths provided by deep mixed soil columns must have a design life that compares with that for the overlying engineering structure - typically 50-100 years for a railway embankment. For geopolymers, although a large proportion of their improved strengths are achieved after a couple of weeks–months due to hydration, for soil's with pH conditions >10.5 their strength further develops within the material through pozzolanic reactions (Davidson et al., 1965). Such reactions occur over periods of years. Thus after installation and 28 days curing, the strength of deep mixed columns is likely to be sustained and then increase. The degree of any long-term strength enhancement due to pozzolanic reactions will be largely dependent on the soil's physico-chemical properties and the binder's mineralogy. For the 7.5%

GGBS-NaOH stabilised Lanton alluvium, its compressive strengths continued to develop from 1.5 MPa after 28 days to 2.4 MPa after 56 days; although the rate of strength increase appeared to start decreasing after 49 days.

The improved engineering performances observed for the 7.5% GGBS-NaOH stabilised Lanton alluvium after 28 days at the optimum dosage were impressive. Relatively poor engineering performances within this stabilised mixture were observed up to 21 days curing, after which strength improvements started to develop. The soil's relatively low cation exchange capacity and surface area due to its low clay content are suggestive of a limited number of sites within the soil from which cementitious bonds could develop. Per Tutumluer (2012), clay contents of 10–50% are usually required for soil stabilisation to work effectively. However, strength enhancements within the stabilised Lanton were observed even when the soil's clay content was <10%.

The soil's high moisture content also contributed to the observed delays in initial strength development, which complies with a mechanical conceptual model developed by Locat et al. (1990) for stabilised soils with high moisture contents. Contrastingly, the soil's high moisture content ensured that cementation reactions had good access to water to form bonds. Additionally, the soil's relatively high sand/silt fractions provided a higher number of larger pore spaces for cementitious bonds to form between soil and GGBS particles, compared with clay soils. This higher porosity inherently resulted in delayed strength gains, due to the longer amount of time required for cementitious bonds to infill pore spaces, create a well cemented matrix and produce higher strengths. Using the porosity/cement index previously investigated by Consoli et al. (2011) and Rios et al. (2012), a power law relationship was identified between 28 day unconfined compressive strengths and the porosity/cement index for 2.5, 5, 7.5 and 10% GGBS-NaOH stabilised Lanton alluvium for a moisture content of 25%. This relationship was in agreement with that observed by Consoli et al. (2011) for a cemented silty soil, whereby the untreated soil may be considered akin to the artificial and Lanton alluvium soils examined in this research.

From the UCS results presented in Figure 5.7, as GGBS-NaOH dosage increased, the yield stresses also increased. Using GGBS-NaOH dosages ≥7.5% successfully produced strengths which surpassed those achieved by all other traditional and IBP binders and EuroSoilStab (2002) criteria. However, vice versa was observed for

GGBS-NaOH dosages ≤5%. From these results, whilst the optimum GGBS-NaOH dosage appears to be 7.5% (i.e. 107 kg m^{-3}), this may not be the true optimum dosage

Whilst further testing is required to more definitively identify the most optimum dosage for use in stabilising Lanton alluvium, Figure 9.1 uses the strength results achieved with increasing curing time for the four GGBS-NaOH dosages in an attempt to approximate an optimum dosage. The performance of this new binder also surpassed that for the more traditional CEM-I and lime binders. According to the 28 day strength development trendline presented in Figure 9.1, there is an indication that the GGBS-NaOH dosage which satisfies the EuroSoilStab (2002) strength criterion would be approximately 5.5%. However, this dosage would be insufficient to produce the 28 day strength of 778 kPa recorded for 10% CEM-I; whereby an approximate GGBS-NaOH dosage of 6.5% would be required. Thus, to satisfy both strength criteria, an optimum GGBS-NaOH dosage of 6.5% would be envisaged for inclusion within the Lanton alluvium.

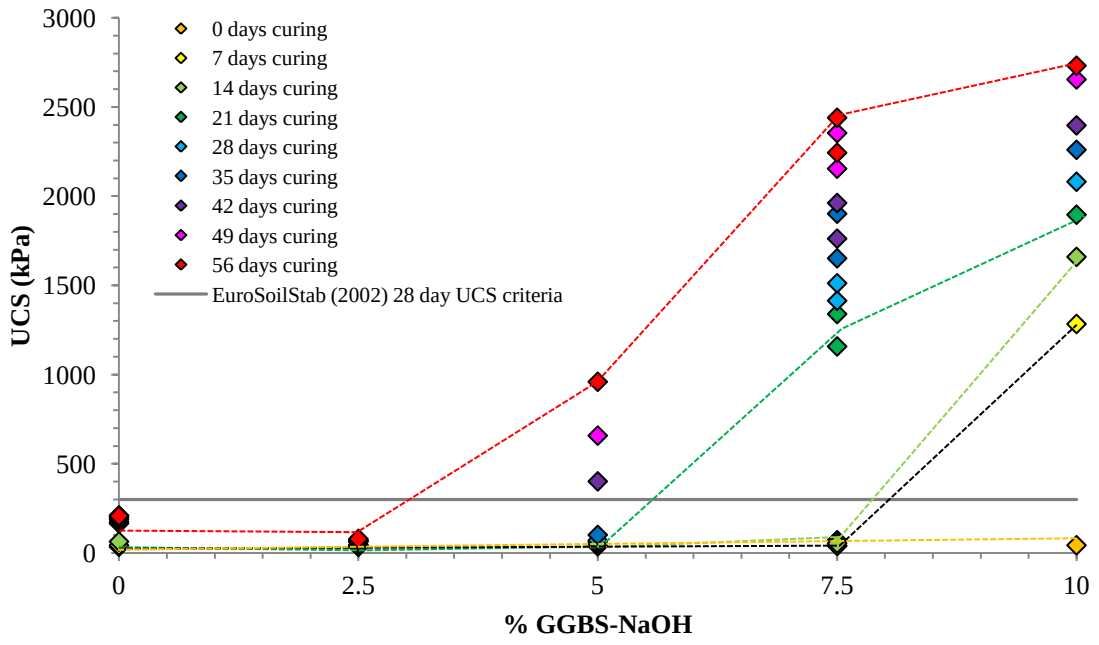

Figure 9.1: Relationship between unconfined compressive strength and GGBS-NaOH dosage, with trendlines shown for 0 (yellow), 7 (black), 14 (light green), 28 (dark green) and 56 (red) days curing.

9.1.2.2.1.2 Compressibility

After 28 days curing, the compressibility of the 7.5% GGBS-NaOH stabilised Lanton alluvium due to the formation of cementitious bonds was significantly reduced to very low levels of compressibility, according to criteria defined by Tomlinson (2001). Relatively little research is available within the literature on the oedometer characterisation of cemented soils, especially in terms of defining levels of cemented structure and post-yield collapse behaviour. Per Medero et al. (2009), cement stabilised soils are more prone to experiencing rapid structural collapse post-yield and highly brittle failures with increasing cement content; whereby as the vertical stresses applied to samples increase, the degree of collapse which occurs decreases due to the progressive breakage of cementitious bonds between soil particles. According to an oedometer study conducted by Rao and Shivananda (2005) on artificially cemented soils, compression curves are typically characterised by an initial region where no axial strains are experienced upon loading, which is subsequently followed by an initial yield stress - at which point some axial strain occurs but is considered to be elastic. Following the initial yield, a more significant "secondary" yield occurs where larger non-recoverable strains (up to 15%) occur due to the breakdown of cementitious bonds. Figure 9.2 compares the axial strains experienced during oedometer testing by the 7.5% GGBS-NaOH stabilised Lanton alluvium with those experienced by 4, 7 and 10% lime stabilised clay tested by Rao and Shivananda (2005).

One of the most marked differences between the four materials is that the 7.5% GGBS-NaOH stabilised Lanton soil is considerably stiffer; whereby at 1600 kPa the axial strains experienced were less than half the values experienced by the three lime-clay samples. However, a comparison in terms of the axial strains induced under vertical stresses of 3200 kPa could not be made due to equipment capacity limitations at Newcastle University. Whilst the 7.5% GGBS-NaOH sample could not be loaded up to 3.2 MPa vertical stress; it had experienced similar degrees of axial strain and appears to have undergone the initial and secondary yielding described by Rao and Shivananda (2005).

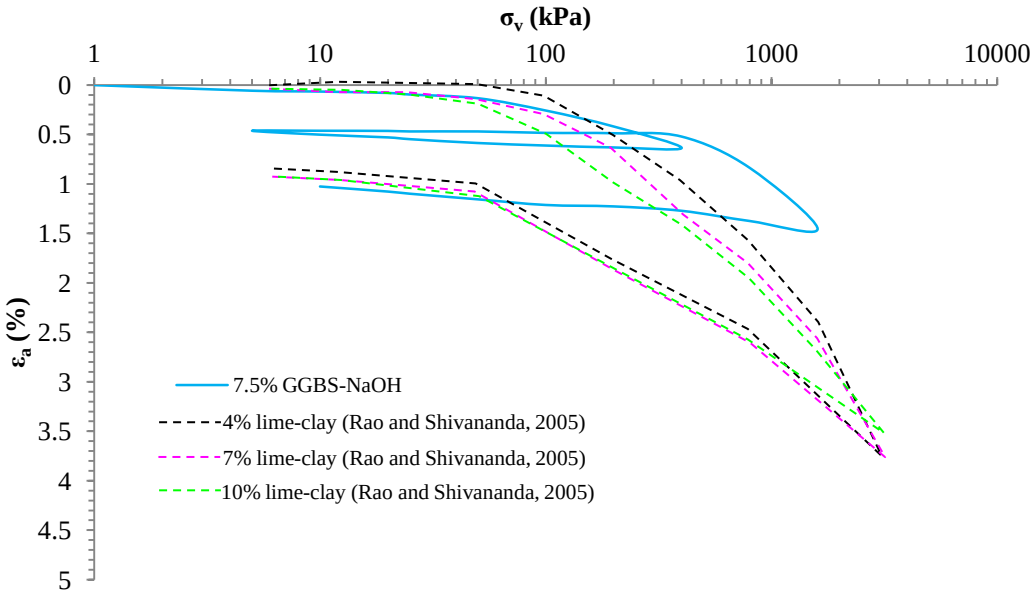

Figure 9.2: Axial strain behaviour experienced for 7.5% GGBS-NaOH stabilised Lanton alluvium during oedometer testing, compared with that recorded by Rao and Shivananda (2005) for 4, 7 and 10% lime stabilised clay.

However, although the stress regime applied to the 7.5% GGBS-NaOH stabilised Lanton alluvium was high enough to capture the two phases of yielding, they were insufficiently high to either fully define both the material's level of initial cemented structure according to Gasparre and Coop's (2008) normalisation technique or the rate at which post-yielding collapse occurs.

As observed in Figure 5.14 for the untreated Lanton alluvium, the compression curves for the undisturbed and reconstituted (ICL) ultimately converge at higher stresses, specifically at 1600 kPa. However, the stresses applied during oedometer testing were insufficiently high to observe the convergence of the 7.5% GGBS-NaOH stabilised Lanton alluvium and the ICL and thus the stress at which the stabilised Lanton alluvium loses all of its cemented structure. Solely based on the position of the ICL and the extrapolated compression curve for the 7.5% GGBS-NaOH stabilised Lanton alluvium on Figure 5.23, an initial estimate of the stress at which the material's cemented structure is lost is approximately 10 MPa.

Based on the above, these therefore highlight the need for future oedometer testing to be conducted on GGBS-NaOH stabilised Lanton alluvium up to higher stresses of at

least 3.2 MPa, but preferably up to stress values where the convergence of the VCL and ICL can be defined. It is anticipated that the information gained from such high pressure oedometer testing will prove valuable in geotechnical design and in the further development and validation of new constitutive models for stabilised soils, such as that developed by Horpibulsuk et al. (2010), which was based on the structured modified Cam clay model. One of the behavioural features which Horpibulsuk et al. (2010) stated as being characteristic of cement stabilised soils is that they sustain higher void ratios than their associated untreated or reconstituted equivalents. However, based on the findings presented in Chapter 5 and by Rao and Shivananda (2005), this may not be accurate for all cement stabilised soils. Once a soil has been stabilised with a cementitious binder and undergoes curing, cementitious gels grow within pore spaces. Hence, the volume of voids within the material decreases with progressive curing, as does the material's void ratio. Therefore, future work should focus on reassessing whether Horpibulsuk et al.'s (2010) structured modified Cam clay model is able to capture compression behaviour for stabilised soils with lower initial void ratios than reconstituted soils.

9.1.2.2.1.3 Triaxial characterisation

The maximum deviatoric stresses achieved during undrained triaxial tests for the 28 day cured 7.5% GGBS-NaOH stabilised Lanton alluvium were over 20 times higher than those measured for the undisturbed untreated Lanton alluvium, as seen in Figure 9.3. A summary of the effective strength parameters derived from undrained triaxial tests on the stabilised Lanton alluvium is provided in Table 9.1. Under an effective confining stress of 50 kPa, the laboratory undrained shear strength of 758.50 kPa for the 28 day 7.5% GGBS-NaOH stabilised Lanton alluvium comfortably achieved and surpassed the required 28 day strength criteria per EuroSoilStab (2002). This proves the potential of GGBS-NaOH as a binder in improving soft alluvial soils when used at the aforementioned dosage.

Table 9.1: Summary of the effective monotonic strength parameters for the untreated reconstituted and undisturbed Lanton alluvium and the 28 day cured GGBS-NaOH stabilised Lanton alluvium at effective confining stresses of 50 kPa.

Material		Effective shear strength parameters (undrained)		
		c' (kPa)	***φ' (degrees)***	***Cu (kPa)***
Untreated Lanton alluvium	Reconstituted	3.73	34.05	28.50
	Undisturbed	5.03	30.52	31
28 day cured GGBS-NaOH stabilised Lanton alluvium (107 kg m^{-3} dosage)		369.54	44.55	758.50

Based on the effective undrained stress path behaviour shown in Figure 8.9 and the normalised shear stiffness degradation behaviour in Figure 8.13 observed for the stabilised alluvium, both appeared to be independent of initial mean effective stress conditions (p'_0) up to 400 kPa.

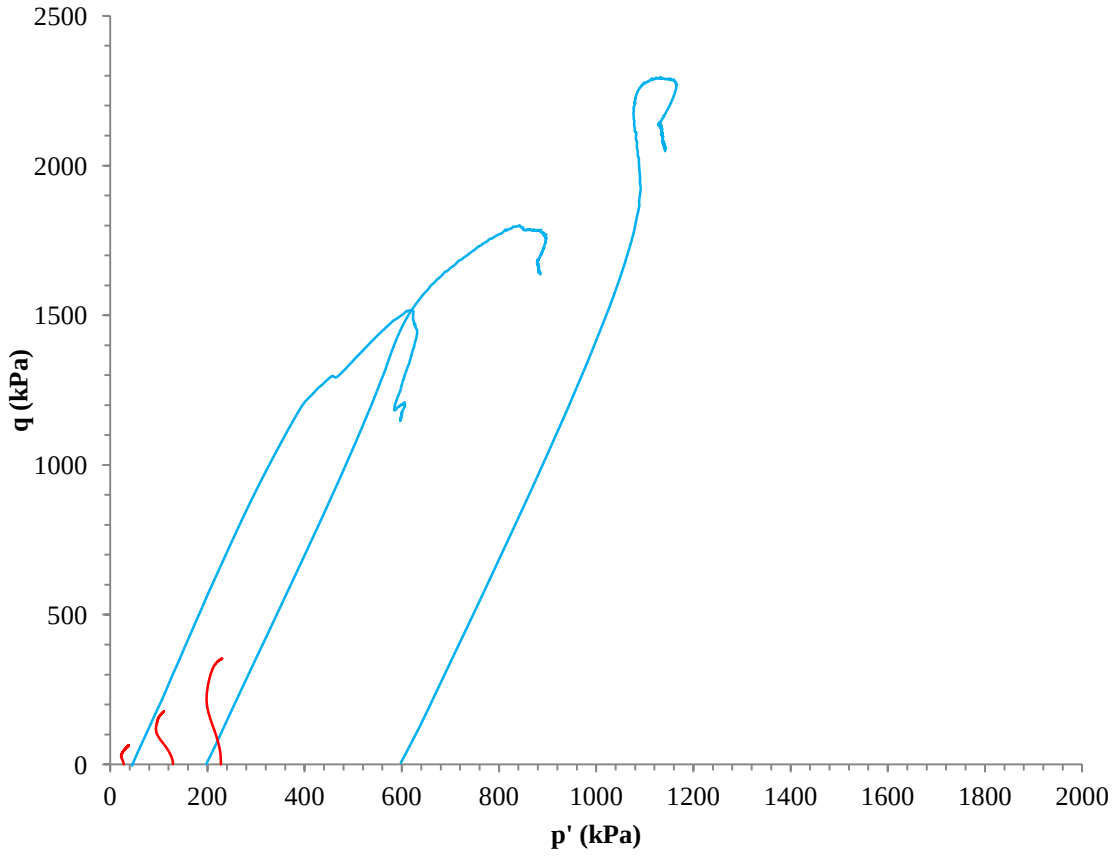

Figure 9.3: Effective stress paths for the undisturbed untreated Lanton alluvium (red) and the 28 day cured GGBS-NaOH stabilised Lanton alluvium (blue).

The maximum deviatoric strengths and shear moduli were observed to increase with p'_0 (i.e. effective confining pressure) values >400 kPa, which is more in line with the behaviour typically observed for most uncemented soils such as the Lanton alluvium, where stiffness is dependent on effective confining pressures. This behaviour for the GGBS-NaOH stabilised Lanton alluvium appears to be in line with literature review findings and triaxial testing conducted by Trhlikova et al. (2012), whereby the shear stiffness of cemented sandy soils is independent of mean effective stress and dependent on cementation until it reaches a "threshold stress" corresponding to the onset of cement structure collapse. However, the behaviour of GGBS-NaOH stabilised Lanton alluvium is also in partial agreement with that observed for cemented clay soils, where stiffness is controlled by cementation below isotropic or vertical yield stress and becomes dependent on p'_0 at higher stresses (Trhlikova et al., 2012). Hence, given that the Lanton alluvium comprises sand, silt and clay (please refer to the soil's PSD curve in Figure 5.4), the behaviour of 7.5% GGBS-NaOH stabilised Lanton alluvium appears to be slightly complex; whereby it is characterised by typical cemented sand behaviour under p'_0 conditions <400 kPa and by typical cemented clay behaviour for p'_0 conditions>400 kPa.

Trhlikova et al. (2012) conducted small strain triaxial testing on 4% CEM-I stabilised kaolin clay involving the use of bender elements, in order to measure the effect of mean effective stress on the initial small strain shear stiffness (G_0). An equation developed by Viggiani and Atkinson (1995) to define the influence of effective stress state and stress history on G_0 was modified by Trhlikova et al. (2012) to incorporate the effect of cemented structure. Trhlikova et al. (2012) found there to be a high level of agreement between small strain triaxial testing results and their equation (Figure 9.4); whereby after yielding, the development of G_0 was interpreted to be dependent on the rate of cementation collapse.

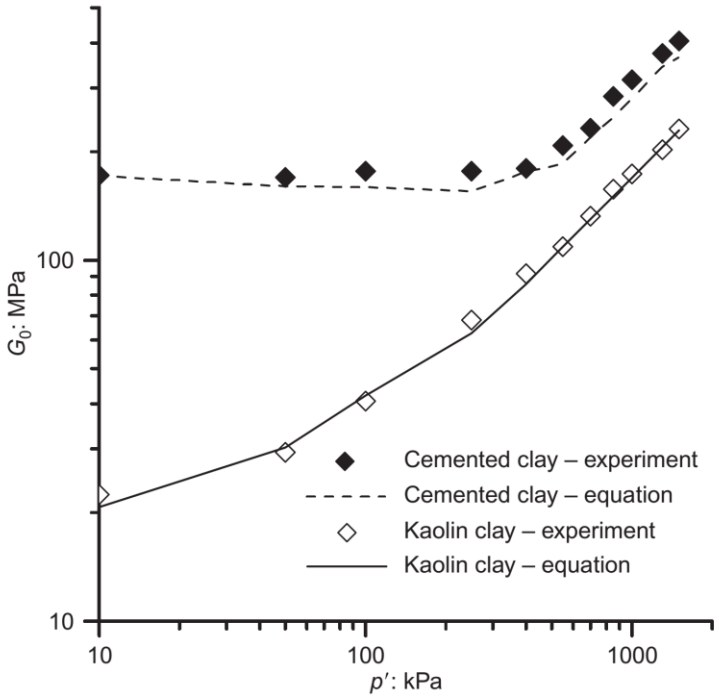

Figure 9.4: Relationship observed by Trhlikova et al. (2012) between small strain shear modulus and mean effective stress for uncemented and CEM-I stabilised kaolin clay. Taken from Trhlikova et al. (2012).

Small strain bender element measurements were unable to be taken during the triaxial testing conducted at Newcastle University, due to equipment availability limitations. Such measurements would be required to gain better insights into the influence of mean effective stress on the G_0 and shear stiffness degradation behaviour of GGBS-NaOH stabilised Lanton alluvium, in addition to its small-large strain compressional behaviour. This information would prove valuable in the development of constitutive cemented soil models and ultimately in geotechnical design. The strain levels which generally occur around geotechnical structures are small - i.e. 10^{-3} % (Clayton, 2011); whereby at such small strains, the stiffness of natural and cemented soils have been found to be much higher than previously estimated, through the use of higher resolution local LVDT and bender element measurements rather than lower resolution global LVDT measurements. Given the research conducted by Verastegui Flores and Van Impe (2009) and Trhlikova et al. (2012), in addition to most modern triaxial testing research involving local strain and bender element measurements; this highlights the need for small strain monotonic triaxial testing to be conducted on

Lanton alluvium in both its untreated and GGBS-NaOH stabilised states, with a view to defining their mechanical behaviour at higher levels of precision.

The author conducted two small strain triaxial tests on the undisturbed untreated and 28 day cured 7.5% GGBS-NaOH stabilised Lanton alluvium at Bristol University to gain some initial insights into the small strain mechanical behaviour of these materials and the data interpretation techniques required. The reader is invited to refer to Appendix 5 for the findings taken from this provisional study, which are intended to form the basis of future work in this area of research.

The strength improvements observed in the field from soil stabilisation are generally lower than those observed in the laboratory. For deep mixed column stabilisation, EuroSoilStab (2002) state that the expected undrained shear strengths for treated soils is 20–50% of those recorded for laboratory test samples. Even if the field strength of the GGBS-NaOH stabilised alluvium only reaches 20% of its laboratory strength, the resultant figure of 151.70 kPa, would still exceed the EuroSoilStab (2002) criterion of 50–150 kPa.

9.1.2.2.1.4 Mineralogical changes

The qualification of the impressive strength gains observed within the GGBS-NaOH stabilised Lanton alluvium came from mineralogical and microstructural analyses. XRD analyses detected clear differences between the mineralogy of the untreated and the stabilised soil; whereby the aluminium and silica contents of Dolomite and Chlorite minerals within the soil were consumed during cementation reactions to form new cementitious gels within the soil's matrix. SEM imaging analysis on the stabilised Lanton alluvium revealed new cementitious growths within the soil's microstructure generally developed as clusters between activated GGBS and silt/sand particles. The distribution of these new clusters coincided with the distribution of Illite and Vermiculite minerals, whose calcium and aluminium contents would have been consumed to produce the cementitious growths. Energy dispersive X-ray point elemental analyses indicated that complex minerals including C-N-A-H, C-N-S-H and C-N-A-S-H were anticipated to be the predominant cementitious phases present (Figure 9.5). No visual evidence for the formation of AFt minerals such as ettringite

was observed within the GGBS-NaOH stabilised Lanton alluvium. This complements the soil's low organic carbon/matter and sulphate contents, the material's impressive durability performance and findings from a study conducted by Haha et al. (2011) on the hydration kinetics, mineral assemblages and microstructural evolution of NaOH activated GGBS.

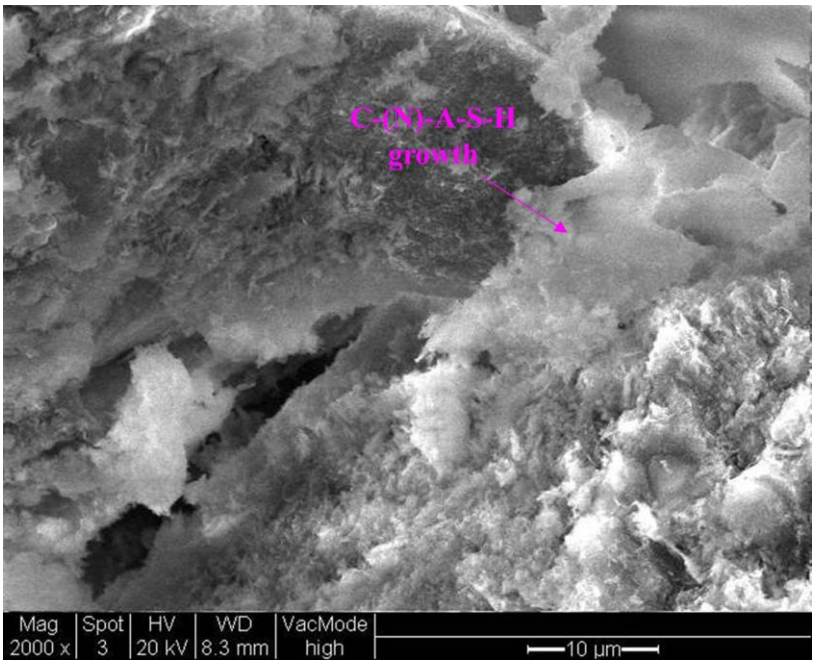

Figure 9.5: SEM micrograph of a likely C-(N)-A-S-H bond (arrowed) within the GGBS-NaOH stabilised Lanton alluvium.

The performance of the GGBS-NaOH binder is dependent on its microstructural properties. Per Richardson et al. (1994) and Shi et al. (2008), high-calcium bearing binders such as GGBS tend to produce cementitious gels such as C-A-S-H, which are low-calcium C-S-H structures with a large distribution of aluminium; whereas low-calcium bearing binders such as PFA produce N-A-S-H. According to Global Cement (2011) and Duxson et al. (2005), the difference between microstructures of C-A-S-H and N-A-S-H is that the latter does not incorporate water into a hydrate structure. Instead, the molecular water stays within the gel. Thus, the microstructure of N-A-S-H is less effective in producing tightly space filling cementitious bonds/gels; whereas C-A-S-H incorporates water into its structure during hydration (Global Cement, 2011). Given the high calcium content of the GGBS-NaOH binder and its impressive strength

and durability performances, the formation of N-A-S-H within the stabilised material was unlikely. SEM-EDX analyses suggested that the much more favourable C-A-S-H mineral phase was present within the stabilised soil, in addition to the slightly more complex C-(N)-A-S-H mineral phase due to the presence of the NaOH activator within the binder.

9.1.2.2.2 Durability

During the life of deep mixed soil columns, they will be subjected to long-term wetting-drying cycles and to freezing-thawing cycles; depending on local climates. Natural soft soils such as alluvium and soft clays with high in-situ moisture contents are prone to experience significant amounts of volumetric shrinkage and swelling due to the effects of wetting-drying and freezing-thawing cycles. Stabilised soils experiencing such volumetric changes would present a severe risk of deep mixed column failure. The likely consequence would be the partial or complete failure of any overlying engineering structures.

The durability results of all 28 day cured alkali activated IBP stabilised artificial silty sand and Lanton alluvium correlated well with their respective strength results; whereby samples stabilised with NaOH flakes and/or sodium silicate solution activated GGBS-based binders exhibited the most resistance towards volumetric shrinkage and swelling during wetting-drying and freezing-thawing cycles over all other activated IBP and traditional binders. Figures 9.6a and 9.6b below show the performance of the four GGBS-NaOH dosages in terms of sample's volumetric changes in relation to their initial dry weight after each cycle of wetting-drying and freeze-thaw testing respectively (whereby 1 cycle takes 2 days to complete). As confirmed by Figures 5.8 and 5.10, significantly higher volumetric changes were experienced by samples stabilised with GGBS-NaOH dosages ≤5% compared with samples containing dosages ≥7.5%. In addition, samples with 0, 2.5 and 5% GGBS-NaOH failed to survive more than 2 cycles during wetting-drying testing or 3 cycles during freeze-thaw testing. Whereas, samples containing 7.5 or 10% GGBS-NaOH lasted the entirety of the wetting-drying and freezing-thawing testing periods.

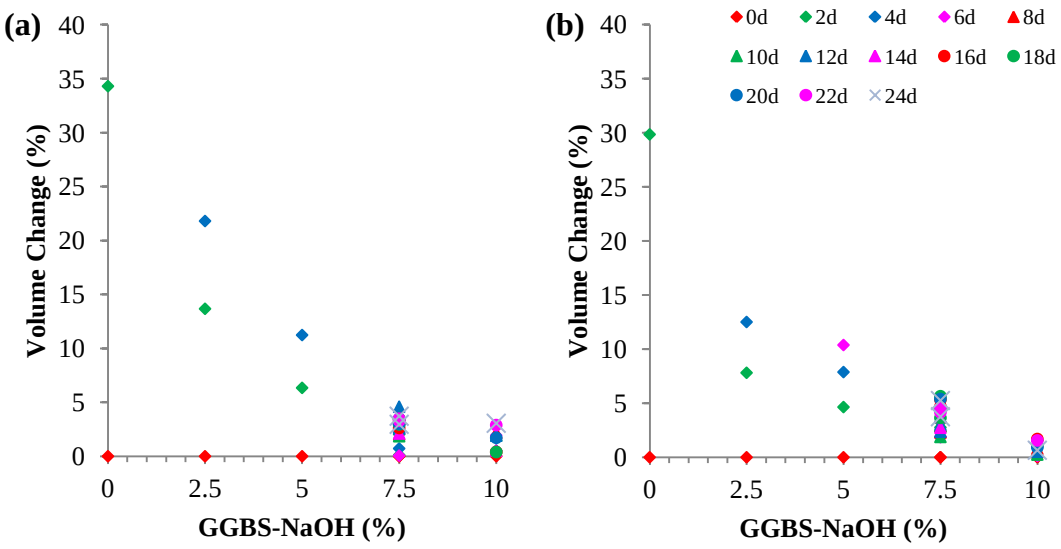

Figure 9.6: Volumetric changes experienced by 28 day cured GGBS-NaOH stabilised Lanton alluvium samples during: (a) wetting-drying and (b) freeze-thaw durability testing.

One of the most notable observations from Figure 9.6 is that significantly smaller volumetric changes were encountered by samples containing higher GGBS-NaOH dosages. Such behaviour was similarly observed by Zhang and Tao (2008) for a cement stabilised low plastic silty clay from Louisiana, USA. In terms of defining a relationship between the degree of volumetric change experienced by samples and their GGBS-NaOH content, Figure 9.7 below shows that based on the distribution of data points, an exponential relationship is likely.

Based on the R^2 values presented for the entire data sets, there appears to be a stronger exponential relationship between volume change and GGBS-NaOH dosage for freeze-thaw behaviour (0.68) compared with wetting-drying behaviour (0.39). However, these R^2 values are insufficiently high to say with confidence that there is a definite exponential relationship, compared with the R^2 value of 0.97 observed by Zhang and Tao (2008). It should be noted that only four dosages of GGBS-NaOH were considered in an attempt to define a relationship, whereas Zhang and Tao (2008) considered at least six dosages over a wider range of cement content.

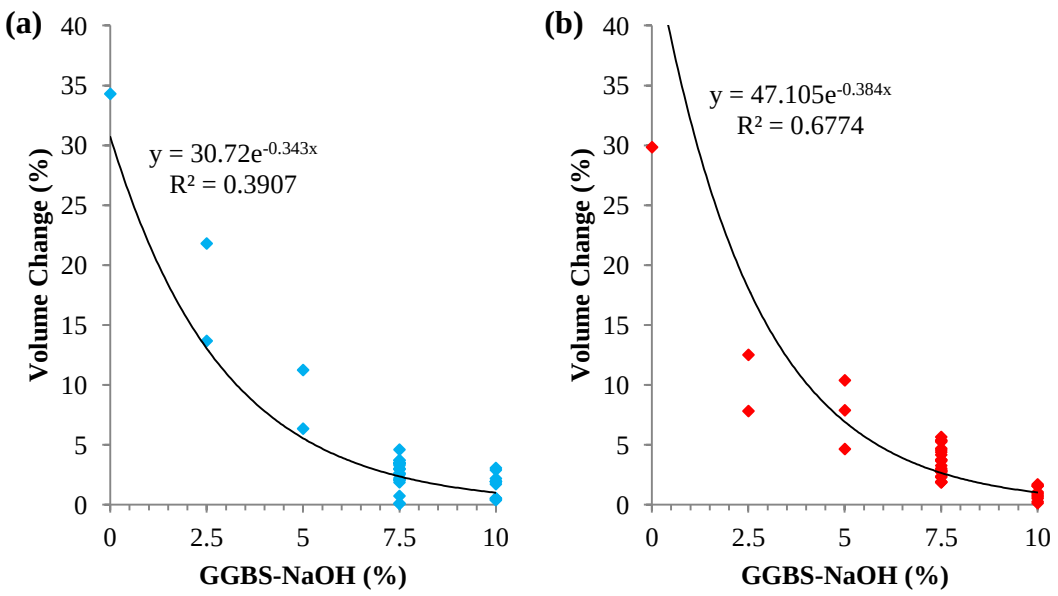

Figure 9.7: Relationship between GGBS-NaOH dosage and volume changes experienced by 28 day cured GGBS-NaOH stabilised Lanton alluvium samples during: (a) wetting-drying and (b) freeze-thaw durability testing.

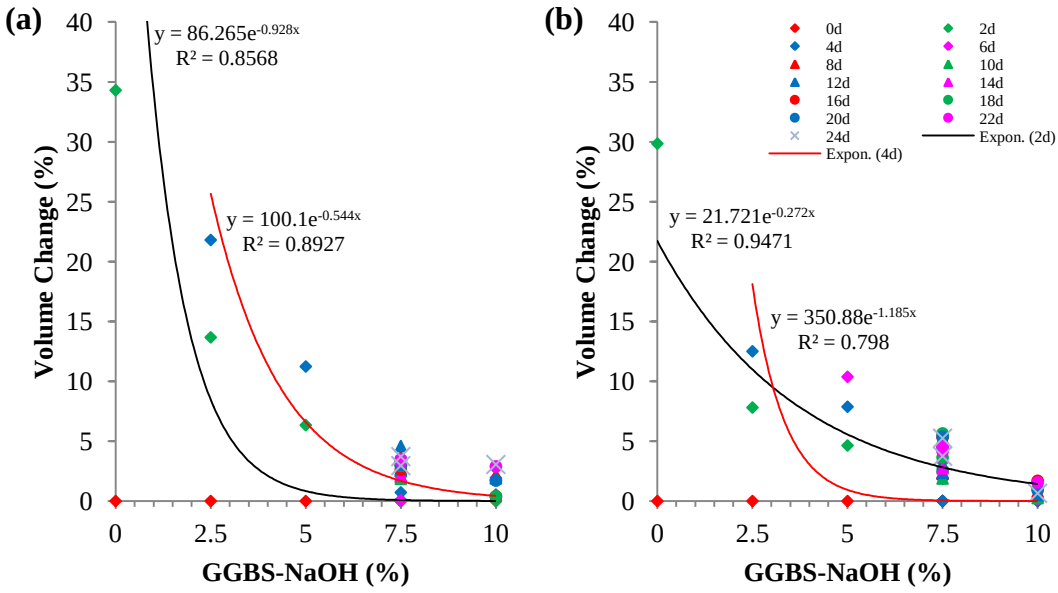

Figure 9.8: Relationship between GGBS-NaOH dosage and volume changes experienced after 1 (2 days) and 2 cycles (4 days) by 28 day cured GGBS-NaOH stabilised Lanton alluvium samples during: (a) wetting-drying and (b) freeze-thaw durability testing.

Although this highlights the need for further durability testing to be conducted, it should be noted that when considering the volume changes encountered by the untreated and four GGBS-NaOH stabilised Lanton alluvium mixtures during the first and second cycles of freeze-thaw and wetting-drying testing, strong exponential relationships were observed based on the high R^2 ranges of 0.87-0.89 and 0.80-0.95 obtained for wetting-drying and freeze-thaw respectively (Figure 9.8).

Given that the ASTM standards for such durability tests are considered to be extreme in terms of representing typical climatic conditions in the UK, the impressive durability performance of the GGBS-NaOH binder at a dosage of 7.5% (i.e. 107 kg m^{-3}) promotes itself for potential use in other countries, where climatic conditions are more representative of ASTM standard procedures.

9.1.3 Engineering practicality

A key factor to consider in assessing the potential for the GGBS-NaOH binder to be used instead of lime or CEM-I for future DDSM projects is engineering practicality. The application of chemical treatment in stabilising soft soils is generally limited to those whose mineralogies/chemical compositions are characterised by low organic and sulphate contents and relatively high clay contents. These criteria have been defined to ensure that cation exchange and long term cementitious reactions occur within the stabilised material. Although the Lanton alluvium possessed unfavourably high moisture and silt-sand contents, the 7.5% GGBS-NaOH binder proved very effective in producing high levels of strength and durability within the soil post 21 days curing. The enhanced mechanical performances of the GGBS-NaOH stabilised Lanton soil were at least 2 – 3 times better than those observed for samples mixed with traditional binders, whilst meeting strength criteria defined by EuroSoilStab (2002).

Another component which needs to be considered in assessing the engineering practicality of the GGBS-NaOH binder for use in DDSM is whether any modifications to existing plant and equipment would be required. GGBS comes in the form of a dried fine powder and that NaOH pellets/flakes are solid particulates. Hence, it is anticipated that the GGBS-NaOH binder could be substituted for CEM-I and lime with relative ease; whereby only minimal plant and equipment modifications would be

required to ensure that the efficiency of binder delivery during deep mixing is maintained.

Based on the aforementioned factors, the GGBS-NaOH binder potentially has an impressive level of engineering practicality, exceeding that of lime, CEM-I and other waste-based binders. In addition to being used as a binder to stabilise soils, it may also be used as a partial/total substitute to CEM-I in concrete mixtures. However, the binder's engineering practicality in terms of soil stabilisation requires further research; whereby the performance of the GGBS-NaOH binder needs to be assessed when incorporated within soils characterised by higher organic and sulphate contents compared with Lanton alluvium.

9.2 Sustainability

Besides the engineering performance consideration of the GGBS-NaOH binder, it is also essential to consider its financial and environmental sustainability before attempting to utilise it on a commercial scale. Detailed knowledge exists for geopolymers regarding their chemistry, impressive strength gaining mechanisms and long-term durability in the laboratory. It is more challenging to produce similar performances in the field (EuroSoilStab, 2002; Global Cement, 2011). The UK's civil engineering industry tends to use traditional materials and processes wherever possible, as they are better known and proven. Ultimately, new geopolymers must demonstrate commercial and practical viability as alternatives to CEM-I and lime. Per Global Cement (2011), the demonstration of GGBS-NaOH for use in soil stabilisation on a relevant industrial field scale in the UK is essential to proving its practicality: and for developing knowledge regarding the cost implications of non-equitable economies of scale. Assurance of this binder's potential for commercialisation should be taken from the fairly recent commercialisation of relatively similar alkali activated GGBS/PFA-based geopolymer concretes ("E-Crete") in Australia (Global Cement, 2011).

9.2.1 Environmental impact

Cement and lime production impose large carbon footprints. Cement production contributes up to 7% of the world's CO_2 emissions (McLellan et al., 2011), mainly through the quarrying/processing of limestone and the combustion of fossil fuels in the production plants. Although the use and practicality of these binder materials is well proven in soil stabilisation, their continued usage is environmentally unsustainable. The cement and civil engineering industries are under significant pressure to reduce CO_2 permissions and to contribute towards the capture and storage of atmospheric carbon (CCS).

Using industrial waste products as alternatives or partial replacements to CEM-I or lime has real potential for reducing the environmental impact of using cements. According to Hanson (2014), GGBS has impressive environmental sustainability credentials. Compared to the production of lime and CEM-I, it reduces embodied CO_2 emissions by 2 million tons per annum (i.e. reduction by >900 kg per ton of CEM-I), reduces primary energy usage during manufacture/processing by 2000 million kWh, saves 3 million tons of quarrying and also reduces landfill by almost 2 million tons. Per Connell (2014), using GGBS as partial replacements to CEM-I has advantages over other IBP's such as PFA, due to the quantity of CEM-I which it can replace within a given concrete or stabilised soil, whilst achieving strengths and durability performances comparable with pure CEM-I. Typically, 50–70% of CEM-I may be replaced by GGBS (depending on the requirements of the intended concrete or stabilised soil); whereas only 20–25% of CEM-I may be replaced by PFA (Connell, 2014). Additionally, mixing high-calcium binders such as GGBS and SS within urban soils has recently proved to have excellent atmospheric CO_2 sequestration potential in the UK (Sanna et al., 2012). This was demonstrated by Washbourne et al. (2012) on the Science Central site in Newcastle upon Tyne.

However, based on the testing results presented in chapters 4 and 5, strength gains within GGBS-stabilised soft alluvial soils require alkali activation. Most alkali materials for industrial purposes are synthetically sourced with high costs and negative environmental impacts. Although the use of NaOH in this research was successful in promoting pozzolanic conditions and impressive strength gains within the GGBS

stabilised Lanton alluvium, its production involves the electrolysis of brine, which is very energy intensive and produces considerable CO_2 emissions. During its production, there is also the risk of NaOH being released into local aquatic environments, which can have a negative impact on aquatic wild life. However, a more sustainable source could be the NaOH produced as a by-product from existing chlor-alkali plants (Kumar et al., 2012). Encouragingly, NaOH appears to show some carbonation potential. When the alkali NaOH reacts with CO_2 (an acid gas), they essentially cancel each other out to become neutral and forms sodium bicarbonate minerals, although such bicarbonate minerals are more soluble than calcium carbonates produced during the carbonation of CEM-I; and may inherently act as an alkali sink (Global Cement, 2011).

According to a sustainability study conducted by McLellan et al. (2011) on the potential use of Australian geopolymers over more traditional cements, significant CO_2 emission reductions of 44–64% were estimated compared with CEM-I. Albeit the impressive environmentally sustainability credentials for GGBS are apparent, there are carbon footprint implications associated with the brine electrolysis (membrane) technique used to produce NaOH. However, the quantities of NaOH required in this research to activate the GGBS and produce strength gains within the Lanton alluvium were very small. The GGBS CO_2 reductions far outweigh the carbon footprint produced by the NaOH's manufacture. There is also potential for both the GGBS and NaOH to sequester atmospheric carbon within the stabilised soil, which also helps to drive the GGBS-NaOH binder towards commercialisation. However, much further work needs to be conducted on the effects of carbonation on the long-term durability, strength and mineralogical development of soft soils such as the stabilised Lanton alluvium and on how much atmospheric CO_2 such stabilised soil mixtures are able to capture.

9.2.2 Financial costs

The final major factor to consider in using the GGBS-NaOH binder is financial cost; specifically in terms of market price, cost of production and transport. Although the engineering performances observed in this research meet EuroSoilStab (2002) strength

criteria and surpass the performances exhibited by CEM-I and lime, it is also crucial to demonstrate to the cement and civil engineering industries that the overall cost of GGBS-NaOH binder is financially competitive.

Hanson Cements UK is one of the UK's leading producers of GGBS (a.k.a. Regen). There are considerable stockpiles of GGBS in the UK, based on the country's active pig iron and steel manufacturing industry. This therefore makes GGBS sustainable in the UK with regards to sourcing it for use in geopolymers; as stockpiles are continuously being replenished and thus avoids sourcing from overseas, which would incur high costs. GGBS requires little post-production processing to make it suitable for mixing into cements and concrete, namely ground granulation to produce a fine powder. As already stated, GGBS has some impressive sustainability credentials over using CEM-I (Hanson, 2014). Additionally, GGBS also has sustainability advantages over other IBP's which tend to be used in geopolymers, such as PFA. The amount of cement replaceable by GGBS whilst still achieving comparable strength and durability performances can be up to 50%; whereas for PFA, the figure is only 20–25%.

When examining the commercial potential of the 7.5% GGBS-NaOH binder mixture, this rather depends on whether a best or worst case scenario viewpoint is taken by the reviewer. Worst case scenarios for GGBS and NaOH prices are based on current pricing regimes adopted by the UK's main suppliers of these materials; whereas best case scenarios are based on world market prices according to Alibaba.

Worst case scenario

At the time of writing, the UK's market price of GGBS (including delivery to site) is approximately £60 per ton (Connell, 2014). Encouragingly, this market price is £10 cheaper than that for CEM-I. Regarding the solid NaOH activator, it is available in the form of flakes, pellets or pearls. However, NaOH is no longer produced in the UK due to lower levels of demand over the last ten years. According to Gould (2014), most of the world's NaOH is produced in China and Russia. Based in Runcorn (Cheshire, UK), ReAgent is one of the UK's main suppliers of NaOH pellets. In general, NaOH is commercially available in two forms; the first is in its raw bulk production form and the second is in its scientific form. The key difference between them is that the scientific NaOH has had any impurities removed from its raw bulk production state.

On this basis, the overall cost of scientific NaOH is much higher. However, in terms of their effectiveness as an alkali activator, both forms of NaOH are deemed equally good. For laboratory studies involving various chemicals and materials, the use of the scientific NaOH is highly recommended as it is in a much purer form. For large scale applications of NaOH, such as an activator for use within geopolymers mixtures, the use of raw bulk production NaOH is much more financially feasible. Based on deliveries up to 5 tons, the current market UK price for NaOH pellets is approximately £0.55 per kilogram (£550 per ton) plus a £50 transport fee per 1 ton pallet (Gould, 2014).

Based on the above quotations and that the binder composition (66.67% GGBS and 33.33% NaOH), the price for the binder to treat 1 m^3 of soil at a dosage of 107 kg m^{-3} is £23.90. Therefore, the price of the GGBS-NaOH binder is £223.33 per ton, which is three times higher than the price per ton for CEM-I (£70 per ton). This high price for the binder seriously questions its financial sustainability, and therefore its ability to compete in the UK and international market places. However, the manufacture of CEM-I is energy intensive and its production costs are expensive; whereby according to Madlool et al. (2011) the amount of electrical energy consumed per ton of CEM-I produced is 75 kWh as compared with the much lower electrical energy consumption figure of 1.285 kWh required to produce 1 ton of NaOH.

Thus, whilst the UK market price of the GGBS-NaOH binder is three times higher than that of CEM-I, significant savings in production costs can be made with the use of the GGBS-NaOH binder over CEM-I. This would therefore advocate that the GGBS-NaOH binder is indeed a financially more sustainable alternative to CEM-I. McLellan et al.'s (2011) study demonstrated that for a number of NaOH-bearing geopolymers developed in Australia, the total financial cost of these mixtures was not much greater than that for CEM-I. However their transportation costs were considerably higher than those associated with CEM-I, due to the great transportation distances between binder source and the treatment site. However, no such transportation distances would be experienced in the UK when sourcing the components for the GGBS-NaOH binder; thereby making the GGBS-NaOH binder more financially sustainable.

Best case scenario

By taking an optimistic view of GGBS and NaOH prices, the international market prices of these materials was considered; whereby the source of these prices was Alibaba. At the time of writing (July, 2014), taking into account US$:£ currency exchange rates; the price of GGBS varied between £25 - 60 per ton whereas NaOH pellets was available for £175 per ton (Alibaba, 2014). Hence, by taking the price of £25 per ton for GGBS, this therefore produces a significantly lower price for the GGBS-NaOH binder when using the 66.67% GGBS : 33.33% NaOH ratio, namely £75 per ton. This price is therefore only marginally more expensive per ton compared with CEM-I; whereby in order to make the GGBS-NaOH break even and become a direct competitor with CEM-I, the price of GGBS-NaOH would only need reducing by 7%.

Theoretically, whilst maintaining the same GGBS : NaOH ratio as that used in this research, reducing the GGBS-NaOH dosage within the Lanton alluvium from 7.5 to 5.5% would correspond to a price reduction of 7%. Although further research would be clearly essential to determine whether 5.5% GGBS-NaOH would produce 28 day compressive strengths within the Lanton alluvium which meet EuroSoilStab (2002) criteria, provisional indications from Figure 9.1 suggest that a dosage of at least 6% would be required to achieve acceptable 28 day compressive strengths. Hence, the best case price of stabilising $1m^3$ of Lanton alluvium with GGBS-NaOH at a dosage of 6% (85.6 kg/m^3) would cost approximately £6.50, which is only 50 pence more than using an equivalent dosage of CEM-I.

Turner and Collins (2013) stated that for an Australian geopolymer concrete comprising PFA, NaOH, sodium silicate and a superplasticiser, a carbon foot print reduction of 9% was measured against a comparable strength CEM-I concrete. There is clearly a confliction between the reduced carbon footprint estimates provided by McLellan et al. (2011) and Turner and Collins (2013). However, the geopolymers mixture assessed by Turner and Collins (2013) contained a considerable quantity of sodium silicate, which is expensive and has significant negative environmental impacts (Habert et al., 2011). Thus, the reductions in the GGBS-NaOH carbon

footprint compared with CEM-I is more in line with the estimates provided by McLellan et al. (2011) rather than those provided by Turner and Collins (2013).

In summation, on the basis of all the available evidence, it is the opinion of the author that the GGBS-NaOH binder has a smaller carbon footprint and a lower overall financial cost compared with CEM-I; and highlights its excellent potential as a commercially viable and practical alternative to CEM-I. Further research into the 28 day strengths achieved by GGBS-NaOH binders using different GGBS : NaOH ratios (i.e. higher GGBS, lower NaOH) would be prudent in designing an optimum GGBS-NaOH mixture and dosage which would both be cheaper and produce better engineering performances than CEM-I, whilst meeting EuroSoilStab (2002) 28 day strength requirements.

9.3 Application to future engineering projects

Further to the literature review (chapter 2), chemical soil stabilisation has numerous engineering applications, given its ability to produce stiffer ground conditions and reduce soil permeability. One of the most common applications is for producing higher bearing capacities of soils for construction purposes; e.g. for supporting permanent overlying buildings and infrastructure. Other applications include stabilising natural and man-made slopes along road/railway embankments and cuttings against slip failures, levee creation and reducing active loads acting on retaining wall structures. For these types of applications where monotonic loading conditions predominate, the results presented in this thesis suggest that the GGBS-NaOH binder would be at least equally or even better suited than traditional binders for producing high levels of strength and stability. Since the 1990's, there has also been focus towards using chemical soil stabilisation to form a geohydrological cut-off wall for encapsulating and/or treating contaminated land. One of the most important criteria for such projects is that the stabilised soils have very low to negligible permeabilities, ensuring that any contaminants do not pollute surrounding groundwater and ecosystems. Drawing on the results taken from the triaxial, durability and microstructural analysis of the GGBS-NaOH stabilised Lanton alluvium, the binder proved successful in creating cementitious bonds throughout the soil, markedly

reduced the soil's permeability and significantly increased its durability performance. This therefore highlights the potential for using this binder for encapsulating contaminated land sites and levee construction. However, careful research must be undertaken for assessing the GGBS-NaOH's suitability for contaminated land applications; whereby contaminants within soils may interfere with the cementitious reactions and ultimately affect the material's final strength and permeability.

In addition to the aforementioned applications involving monotonic loading conditions, there are numerous complex engineering situations which involve a combination of monotonic and dynamic loading. For example, towns and cities situated in tectonically active zones (e.g. Japan and the Caribbean) are prone to experiencing regular earthquakes. Depending on the ground conditions present, such earthquakes can cause liquefaction at the surface and the consequences can be severe. Hence, where ground conditions are dominated by soft (sandy) low cohesive soils, deep mixing maybe used to encapsulate such liquefaction prone areas and mitigate against increases in pore pressure, significant ground surface settlements and any associated damage to local buildings and infrastructure. According to dynamic triaxial testing results presented in this thesis, the GGBS-NaOH binder proved effective in significantly reducing the displacements and pore pressure developments experienced by the Lanton alluvium when subjected to dynamic loads of higher frequency (>2 Hz) compared with those typical of earthquakes (1 Hz).

Another more common engineering situation which involves regular long-term dynamic loading is for railway embankments. Based on the nature of the dynamic triaxial testing conducted as part of this research, the application of DDSM and the GGBS-NaOH binder for stabilising high speed railway embankments forms the main focus of this section. Currently, there is great demand on the UK's railway network for higher axle loads and for trains to travel at faster speeds for both environmental reasons and to boost the economy. To compete economically with other continental European countries with well-established high-speed rail networks (e.g. France, Spain and Germany), the UK government has recently devised plans to improve the UK's high-speed rail network by introducing High Speed 2 (HS2), with a possible extension called High Speed 3 (HS3); with completion of HS2 proposed for 2026. The primary purpose of HS2 and HS3 is to significantly improve high-speed rail links between

major cities in northern and southern England (Figure 9.9); and hence to continental Europe.

It is almost certain that problematic ground conditions characterised by low levels of cohesion, poor bearing capacity and high settlements will be experienced along the proposed HS2 and HS3 routes (Figure 9.9). In addition to soft soils such as the Lanton alluvium, other soils which also present difficult ground conditions similar to those mentioned above include soft organic clays and peat soils

Figure 9.9: Map of proposed routes for HS2 (phase 1) and HS3 (phase 2). Taken from the BBC (2014).

The dynamic loading conditions presented by frequently passing HST traffic are much more complex than those presented by monotonic loads. Each passing train induces a series of considerable vibrations, which are transferred through the embankment to the underlying foundation soil. With increasing numbers of train loading cycles, the shear stiffness of the soil will degrade to very low values which are typically ≤25% of the soil's G_{max} at small strain levels (Holm et al., 2002). Track sleepers tend to deflect both upwards (heave) and downwards. Heave occurs in front of, between and after the passage of the bogey wheels (Holm et al., 2002). Figure 9.10 illustrates the typical relationship between increasing train speed and the resulting downward axial displacement of the railway track.

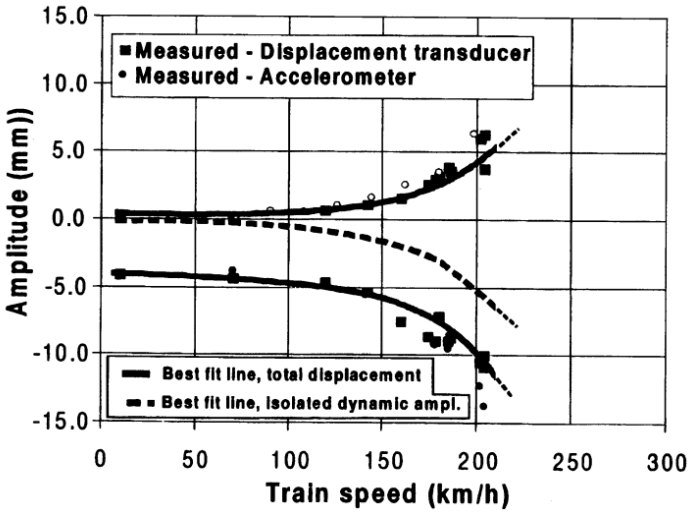

Figure 9.10: Relationship between downward axial displacements with increasing train speed. Taken from Holm et al. (2002).

It is very important that a railway embankment's foundation soil possesses the necessary strength, stiffness, bearing capacity and durability properties for it to cope with the long-term monotonic load presented by the railway embankment and other railway structures, as well as the long-term dynamic loads associated with high frequency high-speed train loading. Both pre-existing and proposed high-speed railway embankment sites experiencing problematic ground conditions require counter measures against excessive track displacement and embankment instability. Per Raju (2014), deep dry soil mixing is a suitable ground improvement technique for treating such problematic soils. Its effectiveness in stabilising railway embankments has been demonstrated the world over. The higher strengths and stiffnesses achieved by such stabilised soils significantly reduce the amount of axial and lateral displacement experienced by train tracks and railway embankments. Per Holm et al. (2002), the most important parameter in the design of stabilised soils intended for railway embankments is stiffness, which combined with the geometry and density of the deep mixed soil columns controls deflections and the critical speed of the stabilised soil mass.

Prime examples where deep dry soil mixing has been applied in railway embankment stabilisation include sections of the UK's Channel Tunnel Rail Link (CTRL – HS1, 2001) and the Vastkustbanan in Sweden (2000). Prior to treatment with lime-cement

mixed columns at a dosage of 150 kg m^{-3}, the section of interest along the Vastkustbanan in Ledsgard (Sweden) had experienced considerable settlements of up to 12 mm when subjected to passing train traffic at 160 km/h. This was attributed to the initial ground conditions being characterised by very soft organic soil ground conditions of low shear strengths (<15 kPa). Settlement measurements were taken for the lime-cement stabilised embankment up to 5 months post-treatment to determine the level of improvement achieved and the stabilised soil's response to train traffic travelling at 160 km/h. Vertical deflections of the track were reduced by a factor of 5 down to 0.8 mm at train speeds of 160 km/h and by factors of 15 – 20 for higher train speeds of up to 200 km/h. The successful effects of the treatment on track displacements at Ledsgard can be clearly seen in Figure 9.11.

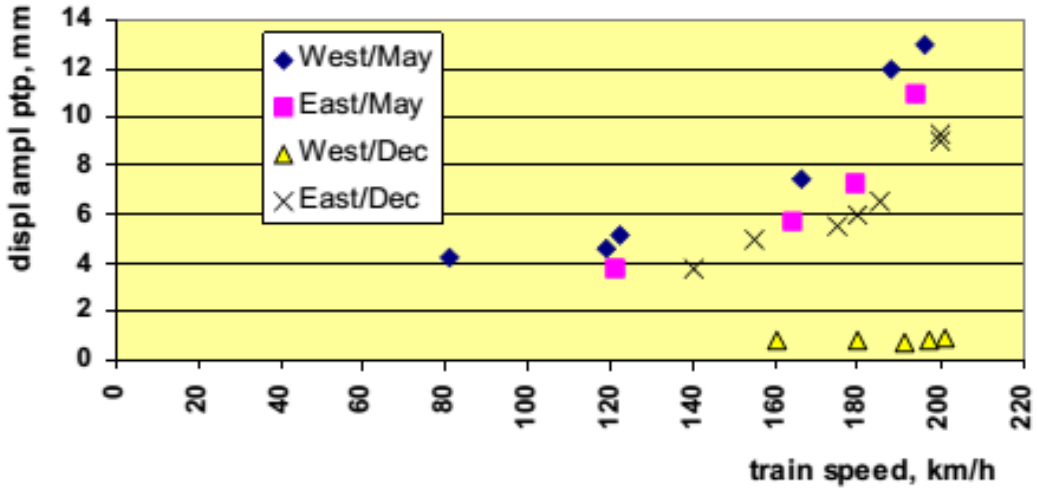

Figure 9.11: Vertical displacements measured within the track bed at Ledsgard prior to and post-treatment. Taken from Holm et al. (2002).

Holm et al. (2002) also observed that the amplitude of vertical track deflections decreased with increasing curing time, presumably due to ongoing strength developments as a result of pozzolanic reactions. The lime-cement deep mixed soil columns also had the added effects of reducing axial and lateral displacements within soils immediately adjacent to the railway embankment via a barrier effect; whereby the columns reduced train traffic induced vibrations on the reinforced track behind the columns.

The unfavourable ground conditions along a section of the CTRL near Sandling in Kent were characterised by low shear strength soft clays and peat soils. Hence the soils required stabilisation using deep dry soil mixing. The RLE contract specification for the project required stabilised soils to reach minimum 28 day undrained shear strength and Young's modulus values of 100 kPa and 10 MPa, respectively. This required 3000 tons of cement to treat 21000 m^3 of soil with a binder dosage of 200 kg m^{-3}. Hughes and Glendinning (2004) stabilised the soils with a GGBS-RG binder at a dosage of 250 kg m^{-3}, using a GGBS:RG ratio of 75:25. The in-situ SCPT undrained shear strengths achieved by the stabilised soil mixtures met the RLE contract strength requirements, with no evidence for AFt mineral formation. However, the GGBS-RG mixtures failed to reach the same strengths achieved by simply using CEM-I when using binder dosages <250 kg m^{-3}.

Hence, based on the required monotonic strength criteria and binder dosages for stabilising the Vastkustbanan and CTRL high-speed rail links, the strength of the GGBS-NaOH stabilised Lanton alluvium would be suitable to cope with the complex loading conditions typically presented by high-speed railway embankments and the associated high-frequency train traffic. In addition, the lower dosage of 107 kg m^{-3} required for the GGBS-NaOH makes it more cost effective compared with the 150 and 250 kg m^{-3} dosages required to stabilise the soft soils in Ledsgard and Sadling, according to Holm et al. (2002) and Hughes and Glendinning (2004). For thorough comparisons though, the performance of the GGBS-NaOH binder would need to be assessed when mixed into the Ledsgard and Sandling soft soils.

Until fairly recently, stabilised soil mixtures for incorporation within road and railway embankments have been designed based on their monotonic strength properties. This is clearly inaccurate given the complexity of dynamic loads and therefore requires a more advanced and realistic level of understanding through the use of dynamic testing. Such knowledge and understanding is crucial, because with increasing train speed, foundation soils become more sensitive to loading and more prone to experiencing larger axial displacements (Holm et al., 2002).

Research on the cyclic triaxial testing of CEM-I stabilised soils to be incorporated within a highway embankment has recently been conducted by Viana da Fonseca et al. (2013), which showed that cyclic yielding and significant plastic strain accumulations due to the breakdown of cementitious bonds started to initiate after 10000 cycles.

However, the loading frequency used by Viana da Fonseca et al. (2013) was 1 Hz, which is insufficiently high to accurately represent the typical dynamic loading frequencies that may be expected for high-speed trains on HS2 and HS3. The dynamic triaxial behaviour of the Lanton alluvium in its untreated and GGBS-NaOH stabilised states are considered more useful than monotonic tests and those conducted by Viana da Foseca et al. (2013) in designing stabilised soil mixtures for use within dynamic loading scenarios including earthquakes and high-speed railway embankments. This is because the dynamic tests conducted in this research programme more accurately simulate the high-frequency loadings typical of high-speed train sets travelling at high speeds of 125 mph. This in turn will provide a better understanding regarding the improved behavioural response of the soil due to stabilisation; specifically in terms of track and soil displacements.

The unfavourable viscosity-dominant behaviour of the untreated reconstituted Lanton alluvium soil under such high loading frequencies at low effective confining pressures, along with the associated accumulations of plastic axial strains, pore pressure ratcheting and mean effective strength reductions after the simulated passing of one InterCity 125 train raised concerns regarding instability. Although yet to be confirmed, given that the soil has been classified as having the potential to experience liquefaction according to criteria defined by Tsuchida (1970), Kramer (1996) and Seed et al. (2003), the soil may experience liquefaction after further high-frequency train loading cycles. This would consequently result in significant track displacements and potential railway embankment failure. However, upon stabilising the Lanton alluvium with the GGBS-NaOH binder and curing after 28 days, significant improvements in the material's behavioural response to dynamic loading were observed. The material's strength and deformation behaviour had become controlled by its cement content. At effective confining pressures representing 3 metres depth below the surface of the track, global strain measurements indicated that the peak deviatoric stresses imposed by the simulated passing InterCity 125 train produced maximum axial strains of 0.1%; whilst negligible strain accumulations (0.05%) were recorded. Although dynamic loading caused pore pressures to increase by up to 6 kPa during peak loading, no ratcheting behaviour occurred with increasing numbers of loading pulses. When comparing the peak dynamic deviatoric stresses with the stabilised soil's monotonic strength, the stresses applied during dynamic tests were well within the elastic range of

the material. Resilient modulus values recorded after each loading pulse remained constant throughout testing; thereby indicating that the stabilised soil's cemented structure had not broken down. This corresponds with visual inspections of the samples, whereby no evidence for small or large propagating brittle failures was observed.

Although, further testing involving the use of local small strain measurements is required to more accurately determine changing stiffnesses with much longer-term dynamic train loading of the GGBS-NaOH stabilised Lanton alluvium and to identify its critical cyclic yield shear strain; the binder has shown signs of great potential for application in stabilising high-speed railway embankments and potentially for other engineering applications where low permeability and high strength/bearing capacities are of paramount importance. The main factors justifying the binder's potential include the combined effects of the stabilised soil in significantly reducing track displacement and ground vibrations by increasing stiffness, along with its higher level of environmental and financial sustainability compared with CEM-I. However, the stiffness behaviour of the GGBS-NaOH stabilised Lanton alluvium should also be investigated with increasing curing time, on the basis that pozzolanic reactions and further strength gains continue beyond 28 days. If strengths and stiffnesses continue to develop, the risk of the stabilised soil experiencing brittle failure due to frequent dynamic loading increases. Hence, binder dosage and the GGBS-NaOH ratio used would need to be individually assessed according to the engineering project's strength requirements and the physico-chemical nature of the soils present on the site.

Chapter 10:

Conclusions and Recommendations

10.1 Conclusions

This research aimed to investigate the potential of using alkali activated IBP's as more environmentally and financially sustainable alternatives to CEM-I for use in DDSM, whether the strength and durability of such mixtures would be suitable for use in stabilising soft alluvial soils underlain by a high-speed railway embankment and finally to identify the mineralogical and microstructural changes within the stabilised soil which are responsible for its improved engineering performance. The following key conclusions arise from this research:

- Alkali activated IBP's show much potential for use as replacements for traditional binders such as CEM-I and lime. The strengths and stiffnesses achieved by the artificial silty sand and Lanton alluvium as seen in Figures 4.4, 4.6 and 5.7 significantly improved with increasing curing time through the addition of these new binders. Their performances comfortably met or surpassed those exhibited by samples stabilised with equivalent quantities of lime/CEM-I and met the 28 day strength criteria defined by EuroSoilStab (2002) (Figure 9.1).
- From all of the IBP binder mixtures tested within Lanton alluvium, which has not previously been characterised geotechnically or stabilised; Figure 5.7 illustrates that the new NaOH activated GGBS binder exhibited the highest strength gains of 2.7 MPa after 56 days when using a dosage of 10% by dry weight.
- Some engineering specifications require high strengths and stiffnesses and in these cases, using activated GGBS would be the most logical replacement for CEM-I or lime. However, there are engineering scenarios such as the deep mixed soil foundations for high-speed rail lines where the high-frequency dynamic loading of the ground caused by passing train traffic requires slightly lower stiffnesses to prevent brittle failures. In such cases, using the GGBS-NaOH binder at a lower dosage (i.e. $\leq$7.5%) would be preferred over higher dosages (>10%).

- With a dosage of 7.5% (i.e. 107 kg m^{-3}), the GGBS-NaOH binder proved successful in increasing the stiffness of the initially soft and very sensitive Lanton alluvium. As illustrated in Figures 8.24 and 8.28, the axial strains and reductions in resilient modulus measured during dynamic triaxial testing were negligible after the simulated passage of an InterCity 125 HST travelling at 125 mph. Such a dynamic triaxial characterisation of soils in their untreated or cemented states has not previously been investigated. The GGBS-NaOH stabilised Lanton alluvium showed at least comparably small axial displacements due to train loading to those recorded by lime-CEM-I columns used to stabilise sections of the UK's CTRL and Sweden's Vastkustbanan, as demonstrated in Figure 9.11. Thus, the GGBS-NaOH binder is likely to be suitable for stabilising problematic soils along the proposed routes for the UK's HS2/3 rail links.
- The mineralogies of the soil to be stabilised and the binder to be used must be carefully considered prior to treatment. Failure to do so will result in ineffective stabilisation and potentially worsen ground conditions in the long term. The strength, compressibility and durability performances of the GGBS-NaOH stabilised Lanton alluvium were attributed to the formation of some relatively complex cementitious mineral phases, most commonly C-(N)-A-S-H as observed in Figure 6.26. Figures 6.1 - 6.3 show that little mineralogical differences were observed between Lanton alluvium in its untreated and stabilised states; although chlorite, dolomite and vermiculite minerals originally recorded within the natural Lanton alluvium were either totally or partially consumed by cementation reactions during curing. No structurally unfavourable minerals such as ettringite were observed within the stabilised alluvium, given the hydration kinetics of GGBS-NaOH systems and this alluvium's very low sulphate content.
- Sodium hydroxide is very effective in activating GGBS and ultimately producing long term high strength gains. Whilst the sodium hydroxide-sodium silicate activator used during initial dosage trials proved effective in raising pH to a sufficient level within the samples (Figure 4.14), there will be difficulties in using it on site from a cost/practicality basis – specifically in terms of the sodium silicate solution. In addition, the production of sodium silicate is very

energy intensive and expensive. Substituting sodium silicate with a high alkalinity waste based powder would have clear advantages. However, the stabilisation work conducted on Lanton alluvium in chapter 5 solely used sodium hydroxide as the activator, which according to Figure 5.12 proved to be equally as effective as the sodium silicate-sodium hydroxide activator in raising soil pH, promoting pozzolanic conditions and long term strength gains.

- The GGBS based binders and solid sodium hydroxide activator pellets could be substituted for CEM-I and lime in the DDSM process with only minimal modification to pre-existing plant and equipment, or a reduction in the efficiency of the installation process.
- The use of the GGBS-NaOH binder in the UK is a more sustainable alternative than the continued use of lime and CEM-I; thereby promoting its commercialisation potential. Although the current UK market price for the GGBS-NaOH binder design is three times higher than that for CEM-I (£70 per tonne), the binder's international market price is more comparable at £75 per tonne. Should a worst case scenario be taken in terms of the GGBS-NaOH price, the financial costs in terms of raw materials, energy consumption, transport and the associated CO_2 emissions incurred by CEM-I production are still considered to outweigh those incurred by the GGBS-NaOH binder. However, the financial costs and CO_2 emissions incurred by the production and transport of this binder design may vary between different countries, due to the transport distances between binder source and the treatment site. Geopolymer components are commonly sourced from various locations, meaning that the distances between sourcing plants and the stabilisation site can be considerable. Given that modern transportation costs are high, careful planning must be conducted to keep the aforementioned distances down to a minimum. This will ensure that the use of geopolymers remains more sustainable and competitive.
- The dosage of the GGBS-NaOH binder for use within soils will differ between individual DDSM projects. For soils more problematic than Lanton alluvium, higher dosages (i.e. $\geq$10%) would be required to achieve high strengths. Additionally, the ratio between GGBS and NaOH within the binder will also require customisation for individual projects, whereby higher NaOH

concentrations would be required to effectively stabilise soils characterised by a low pH. Care must be taken in designing the GGBS-NaOH binder mixture for use in projects, as high concentrations of NaOH result in the binder becoming less environmentally and financially sustainable than demonstrated in this thesis.

Based on this thesis, four peer-reviewed publications have so far been produced: one Q1 Elsevier Engineering Geology journal paper (Sargent et al., 2013), two international geotechnical engineering conference papers (Sargent et al., 2012a and Sargent et al., 2012b) and finally a chapter for a handbook on alkali activated cements (Sargent, 2014). For convenience, copies of the journal and conference papers are provided in Appendices 1–4. All of the material used in the Sargent (2014) book chapter can be found in the literature review (chapter 2). Up to 3 further Q1 journal papers are planned, based on the findings in chapters 5 – 8. Paper 1 is intended to focus on the findings presented in chapter 5, which will focus on the engineering performance of Lanton alluvium when stabilised with the various IBP binder mixtures. Papers 2 and 3 will be based on the monotonic and dynamic triaxial characterisation of the untreated and GGBS-NaOH stabilised Lanton alluvium, respectively.

10.2 Recommendations for future study

Although a thorough research investigation was undertaken into the use of sustainable materials in soil stabilisation, several recommendations for future study are recommended:

- Although the engineering performance of the GGBS-NaOH binder at a dosage of 7.5% (107 kg m^{-3}) has proven to be very successful in the laboratory in stabilising Lanton alluvium, further stabilisation studies should be conducted involving the use of the binder at the same dosage within other UK problematic soils such as soft organic clays and peat.

- To improve existing oedometer data sets, further oedometer testing should be conducted on the GGBS-NaOH stabilised Lanton alluvium (particularly for dosages ≥7.5%), involving the application of higher vertical stresses (i.e. at least 3.2 MPa) to fully capture post-yielding behaviour up to stresses where the material's VCL and ICL converge. This will provide: (1) the information required to define the material's initial level of cemented structure through the use of Gasparre and Coop's (2008) technique; (2) a better understanding of the rate at which the material's cemented structure collapses with progressive compression and ultimately, (3) valuable experimental data for further developing existing constitutive cemented soil models which will be intended for use in geotechnical design.
- In addition to the suite of geotechnical laboratory tests already conducted on the various stabilised artificial alluvium and Lanton alluvium mixtures, another highly recommended engineering performance test which these mixtures should be subjected to is the leachability test. Recycling secondary aggregates such as GGBS and PFA as cementitious binders for stabilising soils raises concerns regarding the potential for any associated contaminants leaching out and polluting local ecosystems and water courses. The aggregate test defined in BS EN 1744-3 would be a suitable method for measuring leachability, which involves placing the stabilised soil on a tray surrounded by water that is continuously agitated. After 24 hours, the water would be sampled and chemically analysed to determine whether any water contamination has occurred.
- A site trial involving the GGBS-NaOH stabilisation of Lanton alluvium is strongly recommended. The primary purpose would be to determine the level of correspondence between laboratory strengths and field strengths; whereby according to EuroSoilStab (2002), a discrepancy is likely. The demonstration of the binder in the field would also be a crucial step in potentially driving forward its commercialisation within the UK as a practical and more sustainable alternative to CEM-I and lime. Hence, future laboratory and field studies in this research should involve research collaborations and liaison with cement manufacturers and ground improvement specialists within the civil engineering industry.

- For the monotonic and dynamic triaxial testing of the untreated and GGBS-NaOH stabilised Lanton alluvium, future tests should all involve small strain measurements of the materials involving the use of local LVDT's and bender elements under various loading, strain rate and effective confining stress conditions. This will ensure much more accurate stiffnesses measurements for these materials at all strain levels; particularly at small strains where stiffnesses are at their highest. It is within the small strain range that strains around geotechnical structures such as railway embankments occur. Given the results from this research, the effect of effective confining stress on the small strain stiffnesses of the GGBS-NaOH stabilised Lanton alluvium should be noted. Hence, knowledge of the small strain monotonic and dynamic behaviour of natural and stabilised soils will lead to future cost savings during the design and construction processes.
- Regarding monotonic triaxial testing on the GGBS-NaOH stabilised Lanton alluvium, besides bender elements and local axial/radial LVDT's, the testing equipment should incorporate highly accurate and sophisticated computer controlled water/air pressure controllers. This will enable the better definition of small bulk stiffnesses and volumetric strains during drained tests. Collectively, these pieces of advanced testing apparatus for triaxial tests will allow the elastic and kinematic yield surfaces to be defined via stress path testing for the untreated and GGBS-NaOH stabilised Lanton alluvium. This in turn will allow for more advanced constitutive material models to be developed for cemented soils and ultimately better capture their behaviour during (finite element) numerical analyses.
- Further to the previous two recommendations, the use of local strain instrumentation in future dynamic triaxial tests conducted on the untreated and GGBS-NaOH stabilised Lanton alluvium ought to focus on defining the critical cyclic yield strain for the material. This would necessitate conducting much longer term triaxial tests on the material by simulating frequent high-speed train traffic loading. To complement such long term dynamic triaxial data, it is also recommended that a full scale, fully instrumented field trial be conducted in order to measure axial/lateral displacements of the track and any long term accumulations of plastic strain within the stabilised soil. Instrumentation could

include high resolution LVDT's, remote video monitoring and geophones, as successfully demonstrated by Bowness et al. (2007).

- Until recently, cemented soils have been considered to exhibit linear elastic – perfectly plastic behaviour. Therefore, their behaviour has been modelled by geotechnical practitioners through the use of the rather simplistic Mohr-Coulomb model. However, based on the triaxial testing results presented in this thesis, stabilised soils exhibit more complex non-linear elasto-plastic behaviour. Therefore, the monotonic and dynamic triaxial data obtained from this thesis and that from future more advanced triaxial studies on the GGBS-NaOH stabilised Lanton alluvium will prove very valuable in the further development of cemented soil constitutive models and ultimately in more accurately modelling current and future geotechnical situations involving DDSM columns.

- Finally, given the individual carbon capture potential for GGBS and NaOH, this highlights the potential for the new binder to become a long term environmentally sustainable alternative for lime and CEM-I. Based on findings made by Manning et al. at Newcastle University over the past decade, using GGBS and NaOH in soil stabilisation could make a contribution in reducing global atmospheric CO_2 concentrations, slowing down the negative effects of climate change and potentially label the construction sector as a "greener" industry than at present. Further mineralogical and microstructure studies ought to investigate possible carbonation reactions within soils stabilised by the GGBS-NaOH binder, which according to the literature can inhibit cementitious gel formation and have detrimental effects on strength (Bargonza et al., 1987). Assessments should also be made as to whether any resulting carbonate mineral growths affect the material's long term engineering performance. Should such minerals be seen to make a marked contribution towards a stabilised soil's improved engineering properties in addition to that provided by C-(N)-A-S-H minerals, this would demonstrate the binders' potentially impressive level of overall sustainability. Based on mineralogical and geochemical testing results, estimates should then be provided regarding the storage capacity of such stabilised soils to capture atmospheric carbon.

References

Abu Bakar, B. H., Ramadhansyah, P. J. and Megat Azmi, M. J., 2011. Effect of rice husk ash fineness on the chemical and physical properties of concrete. Proceedings of the Institution of Civil Engineers, Magazine of Concrete Research. 65 (5), 313-320.Doi: 10.1680/macr.10.00019.

Adams, D., 2011. Keller Geotechnique, UK. Personal communication.

Ahnberg, H., Johansson, S.-E., Pihl, H. and Carlsson, T., 2003. Stabilising effects of different binders in some Swedish soils. Ground Improvement. 7, 9-23.

Ahnberg, H., 2006. Strength of stabilised soils – A laboratory study on clays and organic soils stabilised with different types of binder. Doctoral Thesis. Svensk Djupstabilisering: Swedish Deep Stabilization Research Centre – Report 16.

Ahnberg, H., 2007. On yield stresses and the influence of curing stresses on stress paths and strength measured in triaxial testing of stabilized soils. Canadian Geotechnical Journal. 44, 54-66.Doi: 10.1139/T06-096.

Alazigha, D. P., 2010. Using alkaline activation of waste materials as cement replacements. MSc Thesis, School of Civil Engineering and Geosciences, Newcastle University, UK.

Alibaba, 2014.International market prices for sodium hydroxide. [online]. Available at: <http://www.alibaba.com/premium/sodium_hydroxide.html?uptime=20140708&ptsid=1012000053229821&crea=47501223981&plac=&netw=s&device=c&ptscode=0110202010030001>. Last accessed: 19th July 2014.

Allen, P., 2007. Pollen analysis from Lanton Quarry, Northumberland. Archaeological Research Services (ARS) Ltd Report 2007/18, March 2007.

Al-Tabbaa, A. and Evans, C. W., 1998. Pilot in situ auger mixing treatment of a contaminated site – Part 1: treatability study. Proceedings of the Institution of Civil Engineers, Geotechnical Engineering. 131 Jan, 52-59.

Al-Tabbaa, A. and Evans, C. W., 1999. Laboratory-scale soil mixing of a contaminated site, Journal of Ground Improvement. 3, 119-134.

Al-Tabbaa, A., 2003. Soil mixing in the UK 1991 – 2000: state of practice report. Ground Improvement. 7, 117-126.

American Society for Testing and Materials (ASTM), 1996. Designation: D 559 – 89 Standard Test Methods for Wetting and Drying Compacted Soil-Cement Mixtures. Annual Book of ASTM Standards. 4.08, West Conshocken: Pa.

American Society for Testing and Materials (ASTM), 1996. Designation: D 560 – 96 Standard Test Methods for Freezing and Thawing Compacted Soil-Cement Mixtures. Annual Book of ASTM Standards. 4.08, West Conshocken: Pa.

American Society for Testing and Materials (ASTM), 2008. Designation: D 4543-08 Standard Practices for Preparing Rock Core as Cylindrical Test Specimens and Verifying Conformance to Dimensional and Shape Tolerances. Annual Book of ASTM Standards. 4.08, West Conshocken: Pa.

American Society for Testing and Materials (ASTM), 2012. Designation: D 5311-11. Standard Test Methods for Load Controlled Cyclic Triaxial Strength of Soil. Annual Book of ASTM Standards. 4.08, West Conshocken: Pa.

American Society for Testing and Materials (ASTM), 2012. C618-12a: Standard Specification for Coal Fly Ash and Raw or Calcined Natural Pozzolan for Use in Concrete. Developed by Subcommittee C09.24. Annual Book of ASTM Standards. 4.02, West Conshocken: Pa.

Arroyo, M., Pineda, J. A. and Romero, E., 2010. Shear wave measurements using bender elements in argillaceous rocks. Geotechnical Testing Journal. 3 (6), 1-11.

Atkinson, J. H., 2000. Non-linear soil stiffness in routine design. Geotechnique. 50 (5), 487-508.

Aursudkij, B., McDowell, G. R. and Collop, A. C., 2009. Cyclic loading of railway ballast under triaxial conditions and in a railway test facility. Granular matter. 11, 391-401. Doi: 10.1007/s10035-009-0144-4.

Bargonza, S., Peete, J. M., Freer-Hewish, R. and Newill, D., 1987. Carbonation of stabilised soil-cement and soil-lime mixtures. In: PTRC. Proc of Seminar H, PTRC Transport and Planning Summer Annual Meeting, University of Bath, 7-11 September 1987. London: PTRC Education and Research Services, 29-48.

Barker, W. and Fournelle, J., 1996. X-ray compositional microanalysis: EDS and WDS; chapter 9 in Electron Microscopy: Theory and Practice, 1996, UW Madison, Anatomy Department, Anatomy 660. [online] Available at <http://www.geology.wisc.edu/~johnf/660.html>. Last accessed 6th June 2014.

Bell, F. G., 1996, Lime stabilisation of clay minerals and soils. Engineering Geology. 42 (4), 223-237.

Beretka, J., Cioffi, R., Marroccoli, M. and Valenti, G., 1996. Energy-saving cements obtained from chemical gypsum and other industrial wastes. Waste Management. 16, 231-235.

Bergado, D. T., Anderson, L. R., Miura, N. and Balasubramaniam, A. S., 1996, "Soft Ground Improvement in Lowland and Other Environments", American Society of Civil Engineers – ASCE Press, ISBN 0-7844-0151-9.

Bishop, A. W. and Wesley, L. D., 1975. A hydraulic triaxial apparatus for controlled stress path testing. Geotechnique. 25 (4), 657-670.

Bowles, J. E., 1977. Foundation Analysis and Design. 2nd edition, McGraw-Hill, New York. ISBN 10: 0070067503.

Bowness, D., Lock, A. C., Powrie, W., Priest, J. A. and Richards, D. J., 2007. Monitoring the dynamic displacements of railway track. Proceedings of the Institution of Mechanical Engineers, Part F: Journal of Rail and Rapid Transit. 221 – special issue paper, 13-22. Doi: 10.1243/0954409JRRT51.

Briaud, J.-L., 2013. Geotechnical Engineering: Unsaturated and Saturated Soils. Wiley. ISBN: 978-0-470-94856-9.

British Broadcasting Corporation (BBC), 2014. BBC News: Stoke & Staffordshire. Stoke-on-Trent 'could be part of HS2'. [online] Available at: <http://www.bbc.co.uk/news/uk-england-stoke-staffordshire-26217552>. Last accessed: 10th July 2014.

Broms, B. B., 1984, "Stabilization of soft clay with lime columns", Proc. Seminar on Soil Improvement and Construction Techniques in Soft Ground, Nanyang Technological Institute, Singapore.

Brunauer, S., Emmett, P. H. and Teller, E., 1938. Adsorption of gases in multimolecular layers. Journal of the American Chemical Society. 60, 309-319.

BSI, 1990. BS: 1377, Incorporating Amendment No. 1, Methods of test for Soils for Civil Engineering Purposes. British Standards Institution, Milton Keynes.

BSI, 1996. BS: 7755-3.12, ISO 13536:1995. Soil Quality. Chemical methods. Determination of the potential cation exchange capacity and exchangeable cations using barium chloride solution buffered at pH = 8.1. British Standards Institution, Milton Keynes.

BSI, 1999. BS: 5930, Incorporating Amendment No. 1, Code of Practice for Site Investigations. British Standards Institution, Milton Keynes.

BSI, 2000. BS EN: 197-1 Incorporating Amendments No.1 and 2, Composition, Specifications and Conformity Criteria for Common Cements. British Standards Institution, Milton Keynes.

Burland, J. B., 1990. On the compressibility and shear strength of natural soils. Geotechnique. 40, 329-378.

Bye, G., 2011. Portland Cement. Third edition. Institute of Civil Engineers Publishing. ISBN: 978-0-7277-3611-6.

Callisto, L. and Rampello, S., 2004. An interpretation of structural degradation for three natural clays. Canadian Geotechnical journal. 41, 393-407.

Carter, J. P. and Liu, M. D., 2005. Review of the structure cam clay model. Soil constitutive models: evaluation, selection and calibration. ASCE; 2005 [Geotechnical special publication no.128. 99-132].

CDIT, Coastal Development Institute of Technology, 2002. The deep mixing method: principle, design and constructions. A. A. Balkema, The Netherlands.

CEN, 2004. EN 13286-7 Unbound and Hydraulically Bound Mixtures – Part 7: Cyclic Load Triaxial Test for Unbound Mixtures, Comite Europeen de Normalisation, Brussels.

Chan, C-M., 2012. On the interpretation of shear wave velocity from bender element tests. ACTA Technica Corviniensis – Bulletin of Engineering Tome V (Year 2012). Fascicule 1 (January – March). ISSN 2067-3809. 29-34.

Christopher, B. R., Schwartz, C. and Boudreau, R., 2006. Geotechnical Aspects of Pavements. National Highway Institute, Federal Highway Administration, U.S. Department of Transportation, Washington D.C. Publication No. FHWA NHI-05-037, May 2006.

Clarke, D. and Smethurst, J. A., 2010. Effects of climate change on cycles of wetting and drying in engineered clay slopes in England. Quarterly Journal of Engineering Geology and Hydrogeology. 43, 473-486.

Clayton, C. R. I., 2011. Stiffness at small strain: research and practice. Geotechnique. 61 (1), 5-37. Doi: 10.1680/geot.2011.61.1.5.

Connell, M., 2014. Hanson Cements, UK. Personal communication.

Consoli, N. C., Rosa, D. A., Cruz, R. C. and Rosa, A. D., 2011. Water content, porosity and cement content as parameters controlling strength of artificially cemented silty soil. Engineering Geology. 122, 328-333. Doi: 10.1016/j.enggeo.2011.05.017.

Coop, M. R., 2014. Influences of Geology on the mechanics of Soils. Presentation at City University of Hong Kong. [online]. Available at:<http://navier.enpc.fr/events/w(h)ydoc12/pdf/whydoc12_coop.pdf>. Last accessed: 4th June 2014.

Cooper, T. H., 2009. Unit 12 Chapter 2 – Cation exchange and cation exchange capacity. [online] Available at <http://www.swac.umn.edu/classes/soil2125/doc/s12ch2.htm> [Last accessed 20th June 2012].

Craig, R. F., 2004. Soil Mechanics. Seventh edition. Spon Press, Taylor & Francis Group, ISBN 978-0-415-32703-9.

Cristelo, N., Glendinning, S. and Teixeira Pinto, A., 2011. Deep soft soil improvement by alkaline activation. Proceedings of the Institution of Civil Engineers, Ground Improvement. 164 (2), 73-82. Doi: 10.1680/grim.900032.

Cuccovillo, T. and Coop, M. R., 1997. The measurements of local axial strains in triaxial tests using LVDT's. Geotechnique. 47 (1), 523-544.

Davidson, L. K., Demirel, T. and Handy, R. I., 1965. Soil Pulverization and Lime Migration in Soil Lime Stabilisation. Highway Research Record. 92, 103-126.

Delle Site, A., 2000. Factors affecting sorption of organic compounds in natural sorbent/water systems and sorption coefficients for selected pollutants. A review. J. Hys. Chem. Ref. Data. 30 (1), 187-439.

Diamond, S. and Kinter, E. B., 1965, "Mechanisms of soil-lime stabilization – An interpretative review", Highway Research Record No. 92, Highway Research Board, Washington, D. C., 83-102.

Dixon, M., 2009. Can alkaline activation enhance the performance of waste materials added to soft soils. MEng Thesis, School of Civil Engineering and Geosciences, Newcastle University, UK.

Dobereiner, L. and De Freitas, M. H., 1986. Geotechnical properties of weak sandstones. Geotechnique. 36 (1) March 1986, 79-94.

Duxson, P., Fernandez-Jimenez, A., Provis, J. L., Lukey, G. C., Palomo, A. and Deventer, J. S. J, 2007. Geopolymer technology: the current state of the art. Journal of Materials Science, Advances in Geopolymer Science and Technology. 42, 2917-2933.Doi: 10.1007/s10853-006-0637-z.

Edina (Geology) Digimap, 2013. [online]. Available at: <http://digimap.edina.ac.uk/digimap/home#>. Last accessed: 6th February 2012.

Erken, A. and Ulker, B. M. C., 2007. Effect of cyclic loading on monotonic shear strength of fine-grained soils. Engineering Geology. 89, 243-257.

Ersahin, S., Gunal, H., Kutlu, T., Yetgin, B. and Coban, S., 2006. Estimating specific surface area and cation exchange capacity in soils using fractal dimension of particle-size distribution. Geoderma. 136, 588-597.Doi: 10.1016/j.geoderma.2006.04.014.

EuroSoilStab, 2002. Development of design and construction methods to stabilise soft organic soils: Design guide soft soil stabilisation. CT97-0351. Project No.: BE 96-3177.

Fauziah, I., Zauyah, S. and Jamal, T., 1996. Characterization and land application of red gypsum: a waste product from the titanium dioxide industry. The Science of the Total Environment. 188, 243-251.

FHWA-RD-99-167, 2001. An introduction to the deep soil mixing methods as used in geotechnical applications: volume 3 – verification and properties of treated soil. Prepared by Geosystems (d. A. Bruce) for US Department of Transportation, Federal Highway Administration, 163.

Femern, A/S, 2011. Geotechnical properties for glacial deposits. Appendix GDR 00.1-001-C May 2011. Prepared by Rambøll Arup Joint Venture.

Federal Highway Administration – U.S. Department of Transportation (FHWA), 2012. User Guidelines for Waste and Byproduct Materials in Pavement Construction – Steel Slag. FHWA publication number: FHWA-RD-97-148. [online]. Available at: <http://www.fhwa.dot.gov/publications/research/infrastructure/structures/97148/ssal.cfm>. Last accessed: 6th February 2013.

Fraay, A. L. A., Bijen, J. M. and Haan, D. Y. M., 1989. The reaction of fly ash in concrete: a critical examination. Cement and Concrete Research. 19, 235-246.

Gasparre, A., 2005. Advanced laboratory characterisation of London Clay. PhD thesis. Department of Civil and Environmental Engineering, Imperial College London.

Gasparre, A. and Coop, M. R., 2008. Quantification of the effects of structure on the compression of a stiff clay. Canadian Geotechnical Journal. 45, 1324-1334.

Gazquez, M. J., Bolivar, J. P., Vaca, F., Garcia-Tenorio, R. and Caparros, A., 2013. Evaluation of the use of TiO_2 industry red gypsum waste in cement production. Cement & Concrete Composites. 37, 76-81.Doi: 10.1016/j.cemconcomp.2012.12.003.

GDS Ltd., 2014. GDS Bender elements system – User: GDS Instruments (internal product testing). [online] Available at <http://www.gdsinstruments.com/__assets__/webpages/000046/bender_elements_gds_testing.pdf> [Last accessed 29th April 2014].

Geo-Con., Inc., 1998. Promotional information.

Global Cement, 2011. Geopolymer concrete – A commercial reality (Wednesday 2nd February 2011). [online]. Available at: <http://www.globalcement.com/magazine/articles/316-geopolymer-concrete-a-commercial-reality>. Last accessed: 10th July 2014.

Gould, M., 2014. ReAgent, Cheshire, UK. Personal communication.

Greening, P. D. and Nash, D. F. T., 2004. Frequency determination of G_0 using bender elements. Geotechnical Testing Journal. 27 (3), 1-7.

Guimond-Barrett, A., Mosser, J. –Fr., Calon, N., Reiffsteck, Ph, Pantet, A. and Le Kouby, A., 2012. Deep mixing for reinforcement of railway platforms with a spreadable tool. ISSMGE – TC 211 International Symposium on Ground Improvement IS-GI Brussels, 31st May & 1st June 2012. Vol. 3, 169-178.

Habert, G., d'Espinose de Lacaillerie, J. B. and Roussel, N., 2011. An environmental evaluation of geopolymer based concrete production: reviewing current research trends. Journal of Cleaner Production. 19, 1229-1238.Doi: 10.1016/j.clepro.2011.03.012.

Haha, M. B., Le Saout, G., Winnefeld, F. and Lothenbach, B., 2011. Influence of activator type on hydration kinetics, hydrate assemblage and microstructural development of alkali activated blast-furnace slags. Cement and Concrete Research. 41, 301-310. Doi: 10.1016/j.cemconres.2010.11.016.

Han, J., Oztoprak, S., Parsons, R. L. and Huang, J., 2007. Numerical analysis of foundation columns to support widening of embankments. Computers and Geotechnics. 34, 435-448. Doi: 10.1016/j.compgeo.2007.01.006.

Hanson Cements (Heidelberg Cement Group), 2014.Regen GGBS. [online]. Available at:<http://www.heidelbergcement.com/uk/en/hanson/products/cements/ggbs_and_related_products/regen_ggbs.htm>. Last accessed: 10th July 2014.

Hansson, T., Parry, L., Graham, M., Troughton, V. and Eriksson, H., 2001. Limix: a deep dry mixing system used at Channel Tunnel Rail Contract 440. Proceedings of Underground Construction 2001 Symposium and Exhibition, London. Institute of Materials, Minerals and Mining, London.

Head, K, H., 1994. Manual of Soil Laboratory, Volume 2: Permeability, Shear Strength and Compressibility Tests. Second Edition. John Wiley & Sons, INC, New York – Toronto.

Health Protection Agency (HPA), 2010. Sodium Hydroxide: General Information. [online]. Available at: <http://www.hpa.org.uk/webc/hpawebfile/hpaweb_c/1287148061909>. Last accessed: 9th April 2013.

Holm, G., Andreasson, B., Bengtsson, P-E., Bodare, A. and Eriksson, H., 2002. Mitigation of track and ground vibrations by high speed trains at Ledsgard, Sweden. Svensk Djupstabilisering: Swedish Deep Stabilization Research Centre – Report 10.

Horpibulsuk, S., Rachan, R., Chinkulkijniwat, A., Raksachon, Y. and Suddeepong, A., 2010. Analysis of strength development in cement-stabilized silty clay from microstructural considerations. Construction and Building Materials. 24, 2011-2021.Doi: 10.1016/j.conbuildmat.2010.03.011.

Horpibulsuk, S. and Raksachon, Y., 2010. Fly ash as a dispersing material in cement stabilization. Ground improvement and geosynthetics, proceedings of sessions of Geoshanghai 2010. ASCE Geotechnical special publication no. 207. 137-142.

Horpibulsuk, S., Rachan, R. and Suddeepong, A., 2011. Assessment of strength development in blended cement admixed Bangkok clay. Construction and Building Materials. 25, 1521-1531.Doi: 10.1016/j.conbuildmat.2010.08.006.

Hossain, K. M. A., 2010. Development of stabilised soils for construction applications. Proceedings of the Institution of Civil Engineers, Ground Improvement. 163, 173-185.Doi: 10.1680/grim.2010.163.3.173.

HS2, 2014. [online]. Available at:< http://www.hs2.org.uk>. Last accessed: 10th July 2014.

Hughes, P. N. and Glendinning, S., 2004. Deep dry mix ground improvement of a soft peaty clay using blast furnace slag and red gypsum. Quarterly Journal of Engineering Geology and Hydrogeology. 37, 205-216.Doi: 10.1 144/1470-9236/04-003.

Hughes, P. N., 2005. The Use of Synthetic Red Gypsum as a Construction Material. PhD Thesis, School of Civil Engineering and Geosciences, Newcastle University, UK.

Hughes, P. N., Glendinning, S., Manning, D. A. C. and Noble, B. C., 2010. Production of ‘green’ concrete using red gypsum and waste. Proceedings of the Institution of Civil Engineers, Engineering Sustainability. 163, 137-146.Doi: 10.1680/ensu.2010.163.3.137.

Hughes, P. N., Glendinning, S., Manning, D. A. C. and White, M. L., 2011. Use of red gypsum in soil mixing engineering applications. Proceedings of the Institution of Civil Engineers, Geotechnical Engineering. 164, 223-234. Doi: 10.1680/geng.10.00061.

ICDD, 1999, The Powder Diffraction File: Database of the International Centre for Diffraction Data, Sets 1 – 49. ICDD, Newtown Square, PA.

Ishihara, K., 1993. Liquefaction and flow failure during earthquake. Geotechnique. 106 (3), 351-415.

Jardine, R. J., Potts, D. M., Fourie, A. B. and Burland, J. B., 1986. Studies of the influence of non-linear stress strain characteristics in soil-structure interaction. Geotechnique. 36 (3), 377-396.

Jegandan, S., Liska, M., Osman, A. A-M. and Al-Tabbaa, A., 2010. Sustainable binders for soil stabilisation. Proceedings of the Institution of Civil Engineers, Ground Improvement. 163, 53-61.Doi: 10.1680/grim.2010.163.1.53.

Kiattikomol, K., Jaturapitakhul, C., Songpiriyakij, S. and Chutubtim, S., 2001. A study of ground coarse fly ashes with different finenesses from various sources as pozzolanic materials. Cement and Concrete Composites. 23, 335-343.

King, H. L., 2010. Alkali activation and soil stabilisation. MEng Thesis, School of Civil Engineering and Geosciences, Newcastle University, UK.

Kramer, S. L., 1996. Geotechnical Earthquake Engineering. Prentice Hall. ISBN: 0133749436.

Kumar, S., Drozd, V. and Saxena, S. K., 2012. Catalytic studies of sodium hydroxide and carbon monoxide reaction. Catalysts. 2, 532-543. Doi: 10.3390/catal2040532.

Kurtis, K., 2007. Portland Cement Hydration; PowerPoint presentation from the School of Civil Engineering, Georgia Institute of Technology, Atlanta, Georgia. [online] Available at <people.ce.gatech.edu/~kk92/hyd07.pdf> [Last accessed 10th December 2013].

Larsson, R., 1977. Basic behaviour of Scandinavian soft clays. Report 4, Swedish Geotechnical Institute, Linkoping, Sweden.

Lee, J., Saldago, R. and Carraro, J. A. H., 2004. Stiffness degradation and shear strength of silty sands. Canadian Geotechnical Journal. Vol 41, 831-843. Doi: 10.1139/T04-034.

Lee, J-S. and Santamarina, J. C., 2005. Bender elements: performance and signal interpretation. Journal of Geotechnical and Geoenvironmental Engineering. American Society of Civil Engineers. September 2005. 1063-1070. Doi: 10.1061/(ASCE)1090-0241(2005)131:9(1063).

Lenart, S. and Vilhar, G., 2007. Dynamic and static liquefaction potential of a silty sand from Bostanj, Slovenia. 4th International Conference on Earthquake Geotechnical Engineering, Thessaloniki – Greece, June 25-28, 2007.

Leung, P. W. C. and Wong, H. D., 2010. Final report on durability and strength development of ground granulated blastfurnace slag concrete. Geo Report No. 258. Geotechnical Engineering Office, Civil Engineering and Development Department, The Government of the Hong Kong Special Administrative Region. [online]. Available at: <http://www.cedd.gov.hk/eng/publications/geo_reports/doc/er258/er258links.pdf>. Last accessed: 10th March 2014.

Little, D. N., Herbert, B. and Kunagalli, S. N., 2005. Ettringite Formation in Lime-Treated Soils: Establishing Thermodynamic Foundations for Engineering Practice. Transportation Research Record: Journal of the Transportation Research Board; Soil Mechanics 2005, Transportation Research Board of the National Academies. 1936, 51-59.

Little, D. N. and Nair, S., 2009. NCHRP web-only document 145: Recommended Practice for Stabilization of Sulfate Rich Subgrade Soils. Contractor's Final Task Report for NCHRP Project 20-07. National Co-operative Highway Research Program, Transportation Research Board of the National Academies.

Liu, M. D. and Carter, J. P., 2002. Structured cam clay model. Canadian Geotechnical Journal. 39 (6), 1313-1332.

Liu, J., Wang, T. and Tian, Y., 2010. Experimental study of the dynamic properties of cement- and lime-modified clay soils subjected to freeze-thaw cycles. Cold Regions Science and Technology. 61, 29-33. Doi: 10.1016/j.coldregions.2010.01.002.

Locat, J., Berube, M. A. and Choquette, M., 1990. Laboratory investigations on the lime stabilization of sensitive clays: shear strength development. Canadian Geotechnical Journal. 27, 294-304.

Madlool, N. A., Saidur, R., Hossain, M. S. and Rahim, N. A., 2011. A critical review on energy use and savings in the cement industries. Renewable and Sustainable Energy Reviews. 15, 2042-2060. Doi: 10.1016/j.rser.2011.01.005.

Manning, D. A. C., 1995. Introduction to Industrial Minerals. Chapman & Hall, London. ISBN: 0 412 5555 6.

Manning, D. A. C., Renforth, P., Lopez-Capel, E., Robertson, S. and Ghazireh, N., 2013. Carbonate precipitation in artificial soils produced from basaltic quarry fines and composts: An opportunity for passive carbon sequestration. International Journal of Greenhouse Gas Control. 17, 309-317. Doi: 10.1016/j.ijggc.2013.05.012.

Mayne, P. W., Coop, M. R., Springman, S. M., Huang, A-B. and Zornberg, J. G., 2009. Geomaterial behaviour and testing. Proceedings of the 17th International Conference on Soil Mechanics and Geotechnical Engineering. M. Hanza et al. (Eds.). 2009 IOS Press. 2777-2872. Doi: 10.3233/978-1-60750-031-5-2777.

McCarthy, G. J., Swanson, K. D., Keller, L. P. and Blatter, W. C., 1984. Mineralogy of Western fly ashes. Cement and Concrete Research. 14 (3), 471-478.

McGuire, M., Templeton, E. and Filz, G., 2012. Stability analyses of a floodwall with deep-mixed ground improvement at Orleans Avenue Canal, New Orleans. ISSMGE – TC 211 International Symposium on Ground Improvement IS-GI Brussels, 31st May & 1st June 2012. Vol. 2, 199-209.

McLellan, B. C., Williams, R. P., Lay, J., van Riessen, A. and Corder, G. D., 2011. Costs and carbon emissions for geopolymer pastes in comparison to ordinary portland cement. Journal of Cleaner Production. 19, 1080-1090. Doi: 10.1016/j.jclepro.2011.02.010.

Medero, G. M., Schnaid, F. and Gehling, W. Y. Y., 2009. Oedometer behaviour of an artificial cemented highly collapsible soil. Journal of Geotechnical and Geoenvironmental Engineering. American Society of Civil Engineers. June 2009, 840-843. Doi: 10.1061/(ASCE)1090-0241(2009)135:6(840).

Meunier, A., 2005. Clays, Springer Publishing - Berlin Heidelberg New York, ISBN 3-540-21667-7.

Mesri, G., Jones, R. A. and Adachi, K., 1972. Annual report on Influence of Pore Water Pressure on the Engineering Properties of Rock. Department of Civil Engineering, University of Illinois, Urbana, Illinois, USA. [online]. Available at: <http://www.dtic.mil/dtic/tr/fulltext/u2/740169.pdf>. Last accessed: 10th June 2014.

Mitchell, J. K., 1972. Innovations in Ground Stabilization. Chicago Soil mechanics Lecture Series, Innovations in Foundation Construction, Illinois Section.

Moranville-Regourd, M., 1998. Cements Made from Blast Furnace Slag. In Lea's Chemistry of Cement and Concrete (edited Hewlett). London: Arnold, 633-699.

Muir Wood, D., 1990. Soil Behaviour and Critical State Soil Mechanics. Cambridge University Press. ISBN: 0521332494.

Myers, R. J., Bernal, S. A., San Nicolas, R. and Provis, J. L., 2013. Generalized structural description of Calcium-Sodium Aluminosilicate hydrate gels: The cross-linked substituted Tobermorite model. Langmuir, American Chemical Society Publications. 29, 5294-5306. Doi:10.1021/la4000473.

Nacke, C., 2007. Aluminium in quartz as an indicator of the temperature of formation of agate. [online]. Available at:<http://www.geo.tu-freiberg.de/oberseminar/os06_07/ClaudiaNacke_Aluminium_in_Quartz.pdf>. Last accessed: 7th June 2014.

Nair, S. and Little, D. N., 2009. Water as the Key to Expansion of Ettringite in Cementitious Materials. Transportation Research Record: Journal of the Transportation Research Board, No. 2104, Transportation Research Board of the National Academies, Washington D.C., 55-62. Doi: 10.3141/2104-06.

Nash, D. and Diambra, A., 2013. University of Bristol – Department of Engineering. Personal communication.

Obrzud, R. F., 2010. On the use of the Hardening Soil Small Strain model in geotechnical practice, in Numerics in Geotechnics and Structures. Eds Zimmerman et al., Elmepress, Lausanne.

Onibonoje, A. A., 2009. The potential of alkaline-activated combined waste materials for soil stabilisation. MSc Thesis, School of Civil Engineering and Geosciences, Newcastle University, UK.

Palomo, A., Grutzeck, M. W. and Blanco, M. T., 1999. Alkali-activated fly ashes. A cement for the future. Cement and Concrete Research. 29, 1323-1329.

Parry, R. H. G., 1958. Correspondence: On the yielding of soils. Geotechnique. 8 (4), 183-186.

Porbaha, A., Zen, K. and Kobayashi, M., 1999. Deep mixing technology for liquefaction mitigation. ASCE Journal of Infrastructure Systems. March 1999, 21-34.

Potts, D. M. and Zdravkovic, L., 1999. Finite element analysis in geotechnical engineering – theory. Thomas Telford Ltd. ISBN: 0 7277 2753 2.

Powrie, W., Yang, L. A. and Clayton, C. R. I., 2007. Stress changes in the ground below ballasted railway track during train passage. Proceedings of the Institution of Mechanical Engineers, Part F: Journal of Rail and Rapid Transit. 221, 247-261.

Powrie, W., Jones, C. J. C., Priest, J. and Burrow, M., 2009. Interactions between the ground, track system and train. Eurailmag Business and Technology. 19, 130-134.

Puppala, A. J., Madhyannapu, R. S., Nazarian, S., Yuan, D. and Hoyos, L., 2008. Deep Soil Mixing Technology for Mitigation of Pavement Roughness. Texas Department of Transportation & Federal Highway Administration. Report No.: FHWA/TX-08/0-5179-1.

Quasthoff, P., 2012. State of the art in "Dry Soil Mixing" – Basics and case study. ISSMGE – TC 211 International Symposium on Ground Improvement IS-GI Brussels, 31st May & 1st June 2012. Vol. 3, 285-298.

Rahman, M. W., Ghataora, G. S., Chapman, D. N., Tyrer, M., Claisse, P. and Ganjian, E., 2008. Gypsum Waste Reduction through Stabilization for Trench Backfill. Proceedings of GeoCongress 2008: Geotechnics of Waste Management and Remediation. ASCE. 320-327.

Raju, V. R., 2014. Ground improvement techniques for railway embankments. Keller Grundau GmbH, Technical paper 10-59E. [online] Available at<http://www.kellerbrasil.com.br/images/10-59E.pdf>. Last accessed: 11th July 2014.

Rao, S. M. and Shivananda, P., 2005. Compressibility behaviour of lime-stabilized clay. Geotechnical and Geological Engineering. 23, 309-319. Doi: 10.1007/s10706-004-1608-2.

Rees, S., Le Compte, A. and Snelling, K., 2013. A new tool for the automated travel time analyses of bender element tests. Proceedings of the 18th International Conference on Soil Mechanics and Geotechnical Engineering, Paris 2013. Technical Committee 212. 2843-2846.

Reeves, G. M., Sims, I. and Cripps, J. C. (Eds.), 2006.Clay materials used in construction. Geological Society Engineering Geology Special Publication No. 21. Doi: 10.1144/GSL.ENG.2006.021.01.21.

Renforth, P., Manning, D. A. C. and Lopez-Capel, E., 2009. Carbonate precipitation in artificial soils as a sink for atmospheric carbon dioxide. Applied Geochemistry. 24 (2009), 1757-1764.

Richardson, I. G., Brough, A. R., Groves, G. W. and Dobson, C. M., 1994. The characterisation of hardened alkali-activated blast-furnace slag pastes and the nature of the calcium silicate hydrate (C-S-H) phase. Cement and Concrete Research. 24, 813-829.

Rios, S., Viana da Fonseca, A. and Baudet, B. A., 2012. Effect of the Porosity/Cement Ratio on the Compression of Cemented Soil. Journal of Geotechnical and Geoenvironmental Engineering, November 2012. 138, 1422-1426. Doi: 10.1061/(ASCE)GT.1943-5606.0000698.

Rios, S., Viana da Fonseca, A. and Baudet, B. A., 2014. On the shearing behaviour of an artificially cemented soil. Acta Geotechnica. 9, 215-226. Doi: 10.1007/s11440-013-0242-7.

Rodriguez-Navarro, C., Doehne, E. and Sebastian, E., 2000. How does sodium sulphate crystallised? Implications for the decay and testing of building materials. Cement and Concrete Research. 30, 1527-1534.

Rogers, C. D. F. and Glendinning, S., 1996. Modification of clay soils using lime, in: Dixon, N., Glendinning, S. and Rogers, C. D. F. (Eds.), Lime Stabilisation. Thomas Telford. London, 99-114.

Rogers, C. D. F. and Glendinning, S., 2000. Lime Requirement for Stabilization. Transportation Research Record 1721. Paper No. 00-0604, 9-18.

Rogers, C. D. F., Glendinning, S. and Holt, C. C., 2000. Slope stabilisation using lime piles – a case study. Proceedings of the Institution of Civil Engineers, Ground Improvement. 4, 165-176.

Rouainia, M. and Muir-Wood, D., 2000. A kinematic hardening constitutive model for natural clays with loss of structure. Geotechnique. 50 (2), 153-164.

Rouili, A., 2007. Stress history effect on the small strain behaviour of re-compacted clay. Twelfth International Colloquium on Structural and Geotechnical Engineering.

Rowles, M and O'Connor, B., 2003. Chemical composition of the compressive strength of aluminosilicate geopolymers synthesised by sodium silicate activation of metakaolinite. Journal of Materials Chemistry. 13, 1161-1165.

Salgado, R., Bandini, P. and Karim, A., 2000. Shear strength and stiffness of silty sand. Journal of Geotechnical and Geoenvironmental Engineering. May 2000. 126 (5), May 2000, 451-462.

Sanna, A., Dri, M, Hall, M. R. and Maroto-Valer, M., 2012. Waste materials for carbon capture and storage by mineralisation (CCSM) – A UK perspective. Applied Energy. 99 (2012), 545-554.

Sargent, P., 2009. The mineralogical health assessment of Mount Etna volcanic ash. Masters dissertation. Department of Earth Sciences, Durham University, UK.

Scott, P. W., Critchley, S. R. and Wilkinson, F. C. F., 1986. The chemistry and mineralogy of some granulated and pelletized blastfurnace slags. Mineralogical Magazine. March 1986, 50, 141-147.

Schanz, T., Vermeer, P. A. and Bonnier, P. G., 1999. The hardening soil model: Formulation and verification. In: Brinkgreve, R. B. J. (Ed.), Beyond 2000 in Computational Geotechnics: Ten Years of PLAXIS International. CRC Press. Balkema, Rotterdam, ISBN-10: 90 5809 040 X.

Seed, H. B., Cetin, K. O., Moss, R. E. S., Kammerer, A., Wu, J., Pestana, J., Riemer, M., Sancio, R. B., Bray, J. D., Kayen, R. E. and Faris, A., 2003. Recent advances in soil liquefaction engineering: A unified and consistent framework. Keynote presentation, 26th Annual ASCE Los Angeles Geotechnical Spring Seminar, Long Beach, CA.

Sherwood, P. T., 1993. Soil stabilisation with cement and lime – state of the art review. Transport Research Laboratory, Department of Transport. HMSO publications, ISBN 0-11-551171-7.

Shi, C., Krivenko, P. V. and Roy, D., 2006. Alkali-Activated Cements and Concretes. Taylor & Francis Publishing. ISBN 0-415-70004-3.

Simpson, D. and Rouainia, M., 2012. Non-linear small strain stiffness of glacial till. Annual Congress of the Geo-Institute of ASCE, Proceedings of the GeoCongress 2012 "State of the Art and Practice in Geotechnical Engineering", 25 – 29th March 2012, Oakland, CA, USA, 2234-2243.

Snelling, K., Sutton, J. and Mendes, J., 2011. Some recent developments in geotechnical laboratory testing. Proceedings of the Indian Geotechnical Conference, December 15-17 2011, Kochi. Paper No. A035.

Sumner, M. E. and Naidu, R., 1998. Sodic Soils. Oxford University Press, New York.

Supancic, K. and Obernberger, I., 2012. Wood ash utilization as a binder in soil stabilization for road construction – first results of large-scale tests. Proceedings of ASH 2012 conference, Stockholm, Sweden January 25-27, 2012.

Tanaka, N. and Stigson, B., 2009, "Cement Technology Roadmap 2009: Carbon emissions reductions up to 2050". A report by the World Business Council for Sustainable Development and the International Energy Agency. Atar Roto Presse SA printing, Switzerland, ISBN 978-3-940388-47-6.

Terzaghi, K., Peck, R. B. and Mesri, G., 1996. Soil Mechanics in Engineering Practice. Third edition. John Wiley & Sons, Inc Publishing. ISBN 0-471-08658-4.

Threadgold, L., 1996. Slope stabilisation using reinforced lime piles, in: Dixon, N., Glendinning, S. and Rogers, C. D. F. (Eds.), Lime Stabilisation. Thomas Telford, London, 176-183.

Tomlinson, M. J., 2001. Foundation Design and Construction. Seventh Edition. Pearson Education, Prentice Hall, ISBN 0-13-031180-4.

Topolnicki, M., 2004. In situ soil mixing. 331-428, within "Ground Improvement" 2nd edition, edited by Moseley, M. P. and Kirsch, K., Spon Press, ISBN 0-415-27455-9.

Topolnicki, M. and Pandrea, P., 2012. Design of in-situ soil mixing. ISSMGE – TC 211 International Symposium on Ground Improvement IS-GI Brussels, 31st May & 1st June 2012. Vol. 3, 309-316.

Treviicos, 2013. [online] Available at <http://www.treviicos.com/viewdoc.asp?co_id=1095>[Accessed 2nd May 2013].

Trhlikova, J., Masin, D. and Bohac, J., 2012. Small-strain behaviour of cemented soils. Geotechnique. 62, No. 10, 943-947. Doi: 10.1680/geot.9.P.100.

Tsuchida, H., 1970. Prediction and countermeasure against the liquefaction in sand deposits. Abstract of the seminar in the Port and Harbor Research Institute (in Japanese).

Turner, L. K. and Collins, F. G., 2013. Carbon dioxide equivalent (CO2-e) emissions: A comparison between geopolymers and OPC cement concrete. Construction and Building Materials. 43, 125-130. Doi: 10.1016/j.conbuildmat.2013.01.023.

Tutumluer, E., 2012. Short course notes for Geotechnical Aspects of Pavement Design and Construction – ASCE GeoCongress 2012 "State of the Art and Practice in Geotechnical Engineering", 25 – 29th March 2012, Oakland, CA, USA.

Van Impe, W. F. and Verastegui-Flores, F. D., 2006. Deep mixing in underwater conditions: a laboratory and field study. Ground Improvement. 10 (1), 15-22.

Vatsala, A., Nova, R. and Srinivasa Murthy, B. R., 2001. Elastoplastic model for cemented soils. ASCE Journal of Geotechnical and Geoenvironmental Engineering. August 2007, 679-687.

Verastegui Flores, R. D. and Van Impe, W. F., 2009. Stress-strain behaviour of artificially cemented Kaolin clay. Proceedings of the 17th International Conference on Soil Mechanics and Geotechnical Engineering, Hanza, M. et al. (Eds). 283-286.

Viana da Fonseca, A., Ferreira, C. and Fahey, M., 2008. A framework interpreting bender element tests, combining time-domain and frequency-domain methods. Geotechnical Testing Journal. 32 (2), 1-17.

Viana da Fonseca, A., Rios, S., Amaral, M. F. and Panico, F., 2013. Fatigue cyclic tests on artificially cemented soil. Geotechnical Testing Journal. 36 (2), 1-9. Doi: 10.1520/GTJ20120113.

Viggiani, G. and Atkinson, J. C., 1995. Stiffness of fine-grained soil at very small strains. Geotechnique. 45, No. 2, 245-265. Doi: http://dx.doi.org/ 10.1680/geot.1995.45.2.245.

Vilhar, G. and Jovicic, V., 2009. Measurement and interpretation of the small strain stiffness of Bostanjsilty sand. Acta Geotechnica Slovenica. 2009, 2. 57-75.

Wan, H., Shui, Z. and Lin, Z., 2004. Analysis of geometric characteristics of GGBS particles and their influences on cement properties. Cement and Concrete Research. 34, 133-137. Doi: 10.1016/S0008-8846(03)00252-7.

Washbourne, C.-L., Renforth, P. and Manning, D. A. C., 2012. Investigating carbonate formation in urban soils as a method for capture and storage of atmospheric carbon. Science of the Total Environment. 431 (2012), 166-175.

Weil, M., Dombrowski, K. and Buchwald, A., 2009. Life-cycle analysis of geopolymers. I: Provis, J. L. and Van Deventer, J. S. J. (Eds.), Geopolymers: Structures, Processing, Properties and Industrial Applications. Woodhead Publishing Limited, Cambridge, England, 194-210.

Werkmeister, S., Dawson, A. and Wellner, F., 2005. Permanent deformation behaviour of granular materials and the Shakedown concept. International Journal for Road Material Pavement Design. 6 (1), 32-52.

Wikipedia, 2012. InterCity 125 – Class 43 locomotive and Mark 3 coaches. [online] Available at: <http://en.wikipedia.org/wiki/InterCity_125>. Last accessed 10th December 2012.

Wild, S., Kinuthia, J. M., Jones, G. I. and Higgins, D. D., 1998. Effects of partial substitution of lime with ground granulated blast furnace slag (GGBS) on the strength properties of lime-stabilised sulphate bearing clay soils. Engineering Geology. 51, 37-53.

Wilkinson, A., Haque, A. and Kodikara, J., 2010a. Stabilisation of clayey soils with industrial by-products: part A. Proceedings of the Institution of Civil Engineers, Ground Improvement. 163, 149-163.

Wilkinson, A., Haque, A. and Kodikara, J., 2010b. Stabilisation of clayey soils with industrial by-products: part B. Proceedings of the Institution of Civil Engineers, Ground Improvement. 163, 165-172.

Wirtgen Group, 2014. Photograph of the Wirtgen 240 stabiliser, provided by Sarah Kaempf (sarah.kaempf@wirtgen.de) on 27th May 2014.

Yilmaz, M. T., Pekcan, O. And Bakir, B. S., 2004. Undrained cyclic shear and deformation behaviour of silt-clay mixtures of Adapazari, Turkey. Soil Dynamics and Earthquake Engineering. 24, 497-507. Doi: 10.1016/j.soildyn.2004.04.002.

Zain, M. F. M., Islam, M. N., Mahmud, F. and Jamil, M., 2011. Production of rice husk ash for use in concrete as a supplementary cementitious material. Construction and Building Materials. 25, 798-805.

Zhang, Z. and Tao, M., 2008. Durability of Cement Stabilized Low Plasticity Soils. Journal of Geotechnical and Geoenvironmental Engineering, February 2008. 134 (2), 203-213. Doi: 10.1061/(ASCE)1090-241(2008)134:2(203).

Zhang, M., Guo, H., El-Korchi, T., Zhang, G. and Tao, M., 2013. Experimental feasibility study of geopolymer as the next-generation soil stabilizer. Construction and Building Materials. 47, 1468-1478.

Appendix 1:

GeoCongress 2012

Conference Paper

Soil Stabilisation using Sustainable Industrial By-Product Binders and Alkali Activation

P. Sargent, P. N. Hughes, M. Rouainia and S. Glendinning

Drummond Building, School of Civil Engineering and Geosciences, Newcastle University, Newcastle upon Tyne, Tyne and Wear, NE1 7RU, United Kingdom.

E-mail: paul.sargent@newcastle.ac.uk

Abstract

This paper presents a laboratory study to assess the performance and feasibility of using various industrial-by-products and alkali activation in stabilising an artificial soft soil. Various geotechnical and mineralogical tests were conducted for curing periods up to 56 days. Comparisons with the performances of non-activated and CEM-I stabilised soils were made. Results indicate that stabilisation using blast furnace slag based binders and alkali activation resulted in the most enhanced engineering performances; whereby alkali activation was seen to initiate pozzolanic reactions and subsequent mechanical property improvements with time, such as strength.

Keywords: *stabilisation, IBP's, sustainability, binder performance, alkali activation.*

1.0 Background

Large areas of many countries around the world are dominated by soft soils such as alluvium. These can become problematic when developed upon due to their low shear strengths and bearing capacities, potential to experience shrinkage/swelling, differential settlement and liquefaction when subjected to ground vibrations and cyclic loads. To remediate such ground conditions, numerous stabilisation techniques are available for use. This paper will concentrate on soil mixing using cementitious binders. Soil mixing was developed in Sweden during the 1970's by using lime and cement binders, and can improve a material's strength, durability, volume stability and permeability (Ahnberg et al., 2003). This technique has since been utilised internationally, particularly within soft soils that have high clay contents. Ultimately, deep mixing reduces a soil's moisture content and therefore decreases its likelihood of experiencing shrinkage/swelling. The strength and compaction properties are also improved (Sherwood, 1993 and Rogers et al., 2000). Deep soil mixing started in the UK during the early 1990's (Al-Tabbaa and Evans, 1998); whereby stabilised soil columns are created through injecting fluidised binder into the ground to the required treatment depth via rotary auger mixing (Figure 1). The drill's rotation direction is then reversed and retrieved to the ground surface whilst binder is pumped through the auger's mixing tool to mix the soil and binder together. The bladed mixing tool's fins are orientated so they incur compaction along the column during mixing. Deep mixed soils tend to have binder contents of 5 – 15 % weight by mass.

Portland cement (CEM-I) has long been used as a binder, which is preferred over lime in providing rapid strength enhancements (Jegandan et al., 2010). Soil water reacts with calcium silicates/aluminates within binders to produce strengthening calcium silica hydroxide (C-S-H) and calcium aluminate hydroxide (C-A-H) gels, respectively. These long-term reactions are "pozzolanic", which occur when soil pH levels are ≥ 10.5 (Davidson et al., 1965). Through progressive curing, stronger cementitious soil matrices are produced.

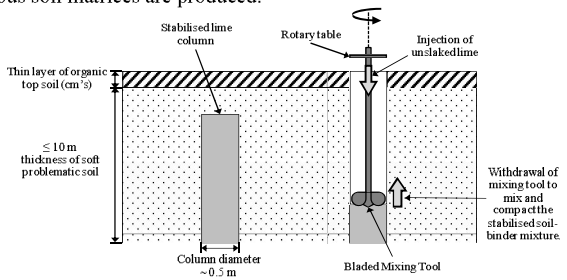

Figure 1: *Schematic of the deep dry mixing technique.*

Utilising CEM-I and lime as binders incurs numerous environmental problems, as their production requires large amounts of energy. Thus, there is a prerogative to find new binders that are more environmentally sustainable than CEM-I and lime, which should provide comparable engineering performances within similar curing times. An approach that has been recently utilised for choosing new binders is the reuse of industrial by-products (IBP's); preferably those that have alumino-silicate compositions. Rather than using lime to activate pozzolanic reactions and subsequent cementitious bond formation within IBP stabilised soils, work by Palomo et al. (1999) determined that using other alkalis such as sodium hydroxide/silicate would further enhance rates at which the soil's mechanical properties are enhanced. This paper summarises findings from a laboratory investigation, which assessed the strength and compressibility performances of alkali activated IBP-stabilised soft soil. An artificial silty sandy clay was manufactured in the laboratory to replicate alluvial soils, which are very common in the UK. Figure 2 presents information regarding the artificial soil's Atterberg limits and soil grading curve.

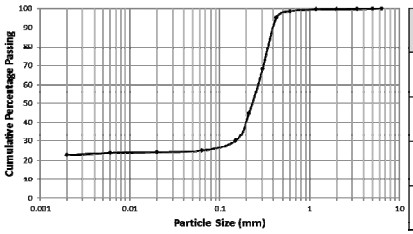

Atterberg Parameter	Value
Plastic Limit	11.46
Liquid Limit	23.48
Plasticity Index	12.02
Soil Classification (Casagrande Criteria)	CL

Figure 2: *Soil grading and Atterberg limits data obtained for the artificial alluvium tested, according to BS 1377: Part 2 (1990) procedures.*

Alluvium is unfavourable when constructed upon due to the high silt content and consequently low levels of strength and cohesion in wet and dry conditions. The synthetic soil comprised 70 % fine silica sand (provided by WBB Minerals Ltd) and 30 % grade E kaolin (provided by English China Clay International Europe Ltd).

2.0 Binder Materials

The IBP's used as binders for this study were ground granulated blast furnace slag (GGBS; provided by Frodingham Cement Ltd), pulverised fly ash (PFA; provided by ScotAsh Ltd) and red gypsum (RG; provided by Huntsman Tioxide Europe Ltd). GGBS is a latent hydraulic cement produced during the manufacture of pig iron, PFA is a synthetic material produced from combustion within coal-fired power plants, and RG is a waste product from Titanium Dioxide manufacture that is produced in filter cake form during sulphuric acid neutralisation. Table 1 summarises RG's chemical composition. For this study, three binder combinations using the aforementioned IBP's were tested during this study: GGBS-PFA, GGBS-RG and PFA-RG.

***Table 1**: The chemical composition of red gypsum. Courtesy of Hughes et al. (2011).*

Component	Content (% dry weight)	Component	Content (mg/kg)
Gypsum ($CaSO_4.2H_2O$)	58.5 – 59.3	Chromium (Cr)	500 – 800
Iron Oxide (Fe_2O_3)	32.9 – 36.6	Zinc (Zn)	200 – 400
Titanium (Ti)	1.0 – 1.3	Strontium (Sr)	100 – 300
Aluminium (Al)	0.1 – 0.8	Nickel (Ni)	50 – 60
Magnesium (Mg)	0.5 – 0.6	Cobalt (Co)	20 – 30
Manganese (Mn)	0.2 – 0.5	Barium (Ba)	1 – 3
Silicon (Si)	0 – 0.5	Lead (Pb)	1 – 2
Chlorine (Cl)	0.002 – 0.2		

Hughes et al. (2011) demonstrated that the use of lime as an alkali activator with a similar artificial soil and IBP binders did not consistently result in considerable strength improvements. The low strength development of some samples was thought to have been partly caused by insufficiently high pH levels produced by the lime activator. Thus, in line with work by Palomo et al. (1999), another activator was used for this study by mixing sodium hydroxide and sodium silicate at a ratio of 1:2.

3.0 Testing Methodology

3.1 Sample Preparation

Binders were added to the soil at 10 % by dry weight and mixed for 10 minutes using a rotary mixing machine. To produce alkali activated (AA) samples, the sodium hydroxide/silicate was added at 20 % by dry weight to the IBP's. Based on compaction testing (BSI, 1990), the soil had an optimum gravimetric water content of 15 %. For comparative purposes, both non-alkali activated (C) and CEM-I binders were tested. Post-mixing, the stabilised materials were tamped into a split sample mould and compressed using a hydraulic press. This technique produced samples with optimum bulk densities of 2.2 Mg/m^3 and consistent dimensions of 76 mm long 38 mm diameter for strength tests and 76 mm diameter 18 mm long samples for oedometer tests. Samples were then cured within sealed PVC moulds for 7, 14, 28 and 56 days, which were placed in a temperature controlled room (20 ^{o}C, 55 % relative humidity). Post-curing samples were extruded, cut to their required dimensions and immediately tested.

3.2 Compressive Strength

IBP-stabilised soils were tested for their compressive strength by utilising an INSTRON 5585H loading frame in adherence to BS 1377: Part 7 (BSI, 1990). The strain rate used for UCS tests was 0.3 mm/min. Three samples were tested for each binder combination after each curing period.

3.3 Shear Strength

Undrained triaxial testing was conducted on three samples for each IBP binder combination after each curing period, in accordance with BS 1377: Part 7 (BSI, 1990).

3.4 Compressibility

Samples also underwent oedometer testing to examine their levels of compressibility. Tests were conducted according to BS 1377: Part 5 (BSI, 1990). Four loading stages were subjected to each sample; 50, 100, 200 and 400 kPa.

3.5 Mineralogy and pH

Soil mixtures were tested for their pH levels prior to and after curing by using a Camlab Ultrameter 6P according to BS 1377: Part 3 (BSI, 1990). The mineralogy of samples post-strength testing was examined by using X-ray diffraction (XRD). The equipment used was a PANalytical X'Pert Pro diffractometer, fitted with an X'celerator and a secondary monochrometer, which used a copper k-alpha radiation wavelength of 1.54180 Å. To identify mineral phases within samples, the X'Pert Highscore Plus software was used in conjunction with the ICDD database (ICDD, 1999).

4.0 Results

4.1 Compressive Strength

Compressive strength testing results for the three binder combinations are presented in Figure 3, along with UCS values obtained for CEM-I and the non-stabilised soil for comparison.

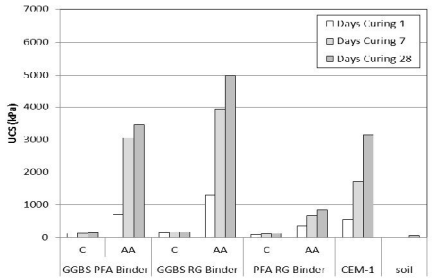

***Figure 3**: UCS behaviour for non-activated and alkali activated samples tested.*

Generally, Figure 3 demonstrates that using the sodium-hydroxide/silicate activator resulted in enhanced strength developments for each binder. Activated GGBS-RG and GGBS-PFA binders showed high strength developments of 5 MPa and 3.5 MPa, respectively after 28 days; both of which exceeded the strength achieved by the more traditional CEM-I binder. However, Figure 3 clearly shows that the PFA-RG binder combination was not as successful; whereby strengths of less than 1 MPa were produced after 28 days.

4.2 *Undrained Shear Strength*

Results from this study's "quick" undrained triaxial tests are presented in Figure 4. Relatively similar results to those shown in Figure 4 for compressive strength can be seen; whereby the alkali activated GGBS-RG and GGBS-PFA binder combinations produced the highest shear strengths after 28 days. Interestingly between 28 and 56 days, the strength of the activated GGBS-RG specimen decreased from 2.1 to 1.7 MPa. However, even after this strength reduction, the GGBS-RG binder's strength exceeded that of most other binders tested. The non-activated binder combinations showed low strength values ranging between 100 and 200 kPa. However, after 28 days Figure 4 shows evidence to suggest that the non-activated GGBS-PFA and GGBS-RG binders started to slowly develop higher strengths, increasing up to 300 – 400 kPa at 56 days.

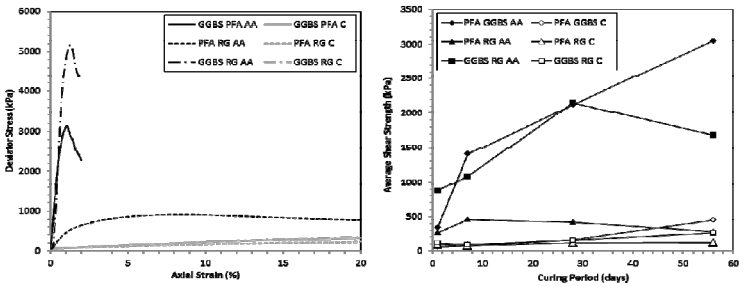

***Figure 4**: Deviator stress–axial strain behaviour after 28 days (left). Development of average shear strength over 28 days for all samples tested (right).*

4.3 *Compressibility*

An oedometer study was conducted to study the compressibility of non-activated and alkali activated specimens of each IBP binder combination. To gain an understanding of the compressibility characteristics for each soil-binder mixture, values for their volume compressibility coefficients (Mv) were calculated. Each soil-binder combination was tested after 28 days curing. An observation made for all samples was that they initially experienced rapid consolidation prior to secondary consolidation, which is typically uncharacteristic of clay soils. This thereby implies that the IBP-stabilised silty sandy clay samples behaved more like granular soils.

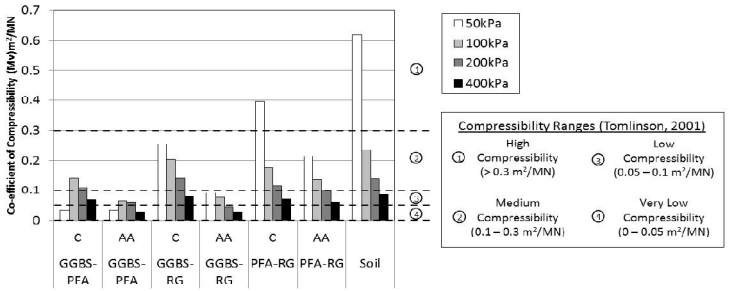

***Figure 5**: Oedometer testing results summary after 28 days.*

The non-stabilised soil was calculated to have an Mv value of 0.6 m^2/MN, which is classified by Tomlinson (2001) as being highly compressible. However, testing results in Figure 5 show that with the use of each alkali activated IBP binder combination, the compressibility of the soil decreased by a greater extent than non-activated samples. Alkali activated specimens produced Mv values ranging between 0.06 and 0.25 m^2/MN, which according to Tomlinson (2001) would be classified as having low to medium levels of compressibility. As seen in Figure 5, the GGBS-PFA-AA binder combination produced the most optimum performance in decreasing compressibility for each loading stage, followed closely by GGBS-RG-AA. However, the PFA-RG binder combination exhibited the poorest performances.

4.4 *pH Levels*

Bearing work done by Hughes et al. (2011) in mind, IBP-soil mixtures had their pH levels recorded post-strength testing after 28 days, in order to assess whether specimens required alkali activation to achieve a pH of 10.5 and subsequent strength enhancements through pozzolanic reactions.

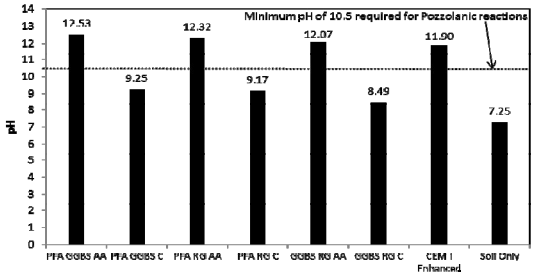

***Figure 6**: Summary of the average pH values obtained by all samples after 28 days.*

Samples' average pH values varied between 7.25 and 12.53 (Figure 6); whereby non-activated samples stabilised with GGBS-PFA, GGBS-RG and PFA-RG binders achieved average values of 9.3, 8.5 and 9.2, respectively. However, the activated versions of these binders achieved greater pH's of 12.5, 12.1 and 12.3, respectively.

4.5 Mineralogy

To examine the mineralogical properties of IBP-soil mixtures and determine whether cementitious bond formation caused improved strength performances after 28 days, XRD analysis was used. Analyses revealed quartz to be present within all samples. C-S-H minerals were observed within GGBS-PFA-AA and PFA-RG-C samples, aluminium oxide within PFA-RG-AA and calcium aluminium oxide hydrate within GGBS-RG-C. Given that Little et al. (2005) found the presence of Ettringite and/or Thaumasite minerals can lead to soil degradation through shrinkage/swelling, XRD studies also searched for such minerals. Only the GGBS-RG-AA sample was found to contain Ettringite. Another unfavourable mineral, Thenardite was seen within PFA-RG-AA samples, which can induce sulphate attack within concrete and masonry and cause strength degradations by expansion (Rodriguez-Navarro et al., 2000).

5.0 Discussion

5.1 Strength

From the compressive and shear strength testing results, significantly more cementitious bonds formed within alkali activated samples after 28 days compared with non-activated samples. The GGBS-PFA-AA binder produced the most enhanced strength performances, closely followed by GGBS-RG-AA; both of which exceeded strengths gained by CEM-I. PFA-RG samples exhibited very poor strength development over the 28 day testing period. Given that PFA and RG tended to produce encouraging strengths when combined with GGBS, the use of RG with PFA and sodium hydroxide/silicate activator within a silty sandy clay soil is ill advised. This may be attributed to numerous factors. Firstly, according to Fraay et al. (1989), the addition of PFA can delay strength gains due to pozzolanic reactions requiring up to 7 days to occur. Secondly, RG is not a natural pozzolanic material (Beretka et al., 1996); and finally the technique used to prepare RG for mixing may also be partly responsible for its poor performance when combined with PFA. RG's filter cake was initially oven dried, which in turn altered RG's micro-chemical structural properties by evaporating its natural structural water content, thereby weakening its mineralogical structure. Once dried, the RG was ground down using a pestle and mortar, which produced a coarser and less uniform powder compared with GGBS and PFA. For activated GGBS-PFA and GGBS-RG specimens, high stiffnesses accompanied high strength enhancements. Such high stiffnesses suggest that these high strength IBP-soil mixtures were likely to fail in a brittle manner, which is geotechnically disadvantageous when dynamically loaded. In addition, although high strengths were achieved for GGBS-PFA and GGBS-RG samples through alkali activation that had been cured at 20 ^{o}C, such strengths may be further improved if cured at higher temperatures, particularly within the first 5 hours of curing (Palomo et al., 1999).

5.2 Compressibility

Results from oedometer testing have shown that the use of each IBP binder combination decreased the initial untreated soil's high level of compressibility to low-medium levels of compressibility. However, alkali activated samples resulted in

greater compressibility reductions compared with non-activated samples. A similar oedometer study was conducted by Al-Tabbaa and Evans (1998). However, the Mv values recorded from this study are significantly different to those presented by Al-Tabbaa and Evans (1998), which were considerably smaller in magnitude and resembled those typically achieved by rocks. Thus, although Al-Tabbaa and Evans' (1998) stabilised soils produced high strengths and stiffnesses which would be appropriate for various geotechnical purposes, they would potentially be unfavourable when incorporated within railway embankments and dynamically loaded by train traffic. In such a situation, brittle failure may result. Hence, the Mv values obtained for alkali activated IBP-soil mixtures from this study, which behaved as very stiff clays; would be better suited to dynamic loading due to more compressional flexibility.

5.3 pH and Mineralogical Properties

Based on the strength testing and pH results, the evidence suggests that a soil's pH has an effect on its strength development. Compressive and shear strength values greater than 1 MPa were recorded for samples that had been alkali activated, which achieved a pH of at least 10.5. With that said however, although the PFA-RG-AA sample reached a pH of 12.3, high strength developments were not observed; thereby indicating that activation and increase in pH did not initiate pozzolanic reactions. If oxidising reactions occurred within the PFA-RG-AA sample, which ultimately prevented strength gain reactions from occurring; these samples may have required storage within air-tight containers prior to testing.

XRD results showed that C-S-H and calcium aluminium oxide hydrate gels were present within most samples, and can therefore be attributed to their strength enhancements, as suggested by Sherwood (1993). Results also showed that unfavourable minerals that can cause structural distress within calcium-based stabilised sulphate-bearing clay soils, were observed within certain samples but were relatively uncommon. Ettringite was only observed within GGBS-RG-AA and Thenardite within PFA-RG-AA. However, the presence of Ettringite within GGBS-RG-AA did not appear to result in any marked sample degradations. It is therefore possible that the presence of Ettringite resulted in strength enhancement, which would correspond with Wild et al.'s (1998) findings for samples of similar compositions.

6.0 Conclusions and Recommendations

This study has demonstrated that alkali activated IBP binders have good potential for use as environmentally sustainable replacements for CEM-I and lime in stabilising soft soils through soil mixing techniques. Testing results suggest that the strength, stiffness and compressibility of the activated IBP-soil mixtures would be suitable for construction purposes. Strength results suggest that from the IBP binder combinations studied, the alkali activated specimens achieved the most favourable strength values over 28 days, as clearly found for the GGBS-PFA binder. GGBS-RG-AA also showed high strength development. For engineering cases where high levels of strength and stiffness are required of a soil, the GGBS-PFA-AA binder combination would be recommended for use as a CEM-I/lime replacement.

However, care should be taken when selecting a binder, as this should depend on the engineering situation at hand. For instance, when designing foundations for high speed railway embankments where the ground is frequently dynamically loaded by passing train traffic, the specification of the embankment soil should be characterised by at least medium levels of stiffness, in order to prevent any unwanted brittle ground failures. For such scenarios, alkali activated GGBS-PFA or GGBS-RG binders would be suitable for use. Additionally, given the clear need to dispose of these industrial wastes, the use of these materials in soil mixing would be advantageous financially and environmentally.

Although the sodium-hydroxide/silicate activator utilised in this study proved to be effective in increasing pH levels for pozzolanic reactions to occur within most samples, it should be considered that there may be issues concerning its practical use on site and cost. Hence, further research into identifying/developing an alternative IBP activator with a high alkaline content would be recommended. Cementitious C-S-H gels thought to be responsible for strength gains in stabilised soils, were observed within certain samples during XRD analyses. Ettringite minerals were rarely found within samples, however they did not appear to contribute towards soil degradation. According to Hughes (2005), XRD is not preferable when searching for amorphous hydrated cement products and RG, due to low sensitivity. Hence, future mineralogical studies should also incorporate the use of SEM to justify XRD analyses.

Given the unforeseen poor performance of the PFA-RG binder from this study, it should be considered that IBP's be studied on a case-by-case basis in terms of being used as a binder in deep soil mixing. This should be adopted at least until an elaborate and consistent knowledge base has been developed. Ultimately, findings from the study are anticipated to assist the construction sector in developing the optimum sustainable IBP binder mix designs regarding quality and economics for problematic alluvial soils. However, to ensure this research is meaningful to the geotechnical academic and industrial communities, utilising IBP's as soil binders needs to be demonstrated on other known problematic soils. Such IBP's should also be demonstrated as being financially sustainable. A final recommendation for future study would be to conduct a number of field trials and a costing study for utilising promising IBP's for soil stabilisation compared with traditional materials.

References

Ahnberg, H., Johansson, S.-E., Pihl, H. and Carlsson, T., 2003, *"Stabilising effects of different binders in some Swedish soils"*, Ground Improvement, 7, No. 1, pp. 9-23.

Al-Tabbaa, A. and Evans, C. W., 1998, *"Pilot in situ auger mixing treatment of a contaminated site, Part 1: treatability study"*, Proceedings of the Institute of Civil Engineers, Geotechnical Engineering, 131, pp. 52-59.

Beretka, J., Cioffi, R., Marroccoli, M. and Valenti, G., 1996, *"Energy-saving cements obtained from chemical gypsum and other industrial wastes"*, Waste Management, 16, pp. 231-235.

BSI, 1990, BS: 1377 Incorporating Amendment No. 1, Methods of test for Soils for Civil Engineering Purposes, British Standards Institution, Milton Keynes.

Davidson, L. K., Demirel, T. and Handy, R. I., 1965, *"Soil Pulverization and Lime Migration in Soil Lime Stabilisation"*, Highway Research Record, 1965 (92), pp. 103-126.

Fraay, A. L. A., Bijen, J. M. and Haan, D. Y. M., 1989, *"The reaction of fly ash in concrete: a critical examination"*, Cement and Concrete Research, 1989 (19), pp. 235-246.

Hughes, P. N., 2005, *"The Use of Synthetic Red Gypsum as a Construction Material"*, PhD Thesis, School of Civil Engineering and Geosciences, Newcastle University, UK.

Hughes, P. N., Glendinning, S., Manning, D. A. C. and White, M. L., 2011, *"Use of red gypsum in soil mixing engineering applications"*, Proceedings of the Institution of Civil Engineers, Geotechnical Engineering, vol. 164, GE3, pp. 223-234.

ICDD, 1999, The Powder Diffraction File: Database of the International Centre for Diffraction Data, Sets 1 – 49. ICDD, Newtown Square, PA.

Jegandan, S., Liska, M., Osman, A. A-M. and Al-Tabbaa, A., 2010, *"Sustainable binders for soil stabilisation"*, Proceedings of the Institution of Civil Engineers, Ground Improvement, 163, G11, pp. 53-61.

Little, D. N., Herbert, B. and Kunagalli, S. N., 2005, *"Ettringite Formation in Lime-Treated Soils: Establishing Thermodynamic Foundations for Engineering Practice"*, Transportation Research Record: Journal of the Transportation Research Board, No. 1936: Soil Mechanics 2005, Transportation Research Board of the National Academies.

Palomo, A., Grutzeck, M. W. and Blanco, M. T., 1999, *"Alkali-activated fly ashes. A cement for the future"*, Cement and Concrete Research, vol. 29, pp. 1323-1329.

Rodriguez-Navarro, C., Doehne, E. and Sebastian, E., 2000, *"How does sodium sulphate crystallised? Implications for the decay and testing of building materials"*, Cement and Concrete Research, 30, pp. 1527-1534.

Rogers, C. D. F., Glendinning, S. and Holt, C. C., 2000, *"Slope stabilisation using lime piles – a case study"*, Ground Improvement, 4, pp. 165-176.

Sherwood, P. T., 1993, *"Soil stabilisation with cement and lime – state of the art review"*, Transport Research Laboratory, Department of Transport, HMSO publications, ISBN 0-11-551171-7.

Tomlinson, M. J., 2001, *"Foundation Design and Construction"*, 7th Edition, Pearson Education, Prentice Hall, ISBN 0-13-031180-4.

Wild, S., Kinuthia, J. M., Jones, G. I. and Higgins, D. D., 1998, *"Effects of partial substitution of lime with ground granulated blast furnace slag (GGBS) on the strength properties of lime-stabilised sulphate bearing clay soils"*, Engineering Geology, 51, pp. 37-53.

Appendix 2:

IS-GI 2012

Conference Paper

Alkali Activation of Industrial By-Products for use in Soil Stabilisation

P. Sargent, M. Rouainia, P. N. Hughes, and S. Glendinning

Drummond Building, School of Civil Engineering and Geosciences, Newcastle University, Newcastle upon Tyne, Tyne and Wear, NE1 7RU, United Kingdom.

E-mail: paul.sargent@ncl.ac.uk; m.rouainia@ncl.ac.uk; p.n.hughes@ncl.ac.uk; stephanie.glendinning@ncl.ac.uk

ABSTRACT

Presented in this paper is an overview of findings recently obtained from a laboratory study, which examined the potential of industrial-by-products and alkali activation for use in stabilising a synthetic soft soil. Geotechnical and mineralogical tests were performed on activated and non-activated samples for curing periods up to 56 days. Comparisons in performances to widely used CEM-I cement binders were made. Results from the study indicate that IBP-stabilisation (particularly with the use of ground granulated blast furnace slag) and alkali activation can improve soil's mechanical properties. Activation was observed to initiate pozzolanic reactions and subsequent strength enhancements with time. However, such improved material performances due to alkali activation did not always result in durability improvements.

Keywords: *soil stabilisation, IBP's, alkali activation, strength, durability.*

1.0 INTRODUCTION

Significant areas of land within flood plains in the UK predominantly comprise soft alluvial soils. Whilst wet or dry, such soils can present difficulties when loaded upon given their low strengths, poor bearing capacities and unfavourable shrinkage-swelling and differential settlement characteristics. To allow for any engineering development to occur on such poor quality soils, various stabilisation techniques may be adopted to improve the geotechnical properties of such soils. A technique that is popularly used in countries including Sweden and Japan, where soils are predominantly of poor quality is deep soil mixing. Amongst numerous other material properties, deep mixing is known for its ability to enhance a material's strength, durability and volume stability (Sherwood, 1993), and has been used in the UK since the early 1990's (Al-Tabbaa and Evans, 1998). Hence, this paper concentrates on the use of deep mixing.

Initially developed in Sweden during the 1970's, deep mixing uses cementitious and high-alkali binders such as lime and cement (Ahnberg et al., 2003). This technique would reduce the moisture contents and hence the potential of shrinkage-swelling within soft soils, thereby improving the soil's strength and compaction properties (Rogers et al., 2000). Generally, deep soil mixing contracts tend to use binder dosages of 5 – 15 % weight by mass within soils. To create deep mixed soil columns, a rotary auger is first drilled to a specified treatment depth. Once drilling has been completed, binder is then injected into the ground through the auger's bladed mixing tool to mix the soil and binder together, whilst the auger is retrieved and the drill's direction of rotation is reversed. The quality of the deep mixed column is further improved due to the auger's bladed mixing tool's fin orientation, which incurs a level of compaction during mixing. Figure 1 illustrates the deep soil mixing stabilisation process.

One of the most popular binders that has been widely used in soil mixing over the past 30 years is ordinary Portland cement (CEM-I); whereby Jegandan et al. (2010) state that it is favoured over lime with regards to its ability to provide considerable strength improvements over short time periods. Pore water within stabilised soil columns reacts with the calcium silicate/-aluminate based binders, resulting in the formation of calcium silica hydroxide (CSH) and/or calcium aluminate hydroxide (CAH) gels. Such gel forming reactions ultimately provide improved strengths within soils and are referred to as "pozzolanic". As stated by Davidson et al. (1965), Pozzolanic reactions take place over long time periods when soil pH conditions are ≥ 10.50. As stabilised soils undergo curing, stronger cementitious soil matrices result, referred to by Sherwood (1993) as "Geopolymer" materials.

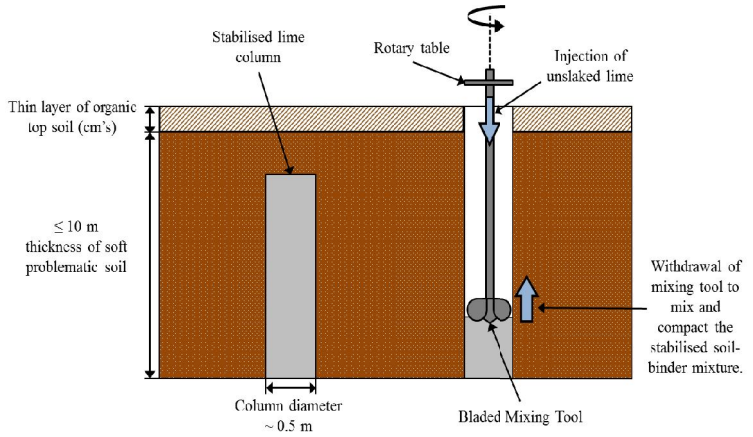

Figure 1*: Illustration of the deep dry mixing technique using lime.*

Although the usage of CEM-I and lime as soil binders in deep mixing have clearly demonstrated their ability to enhance the geotechnical properties of soft soils, a number of environmental issues have been identified in their use. One of the most concerning issues is related to the high amounts of energy required for their manufacture. On this basis, there has become the need to seek new more environmentally sustainable binder materials that would be able to produce improved engineering performances similar to those demonstrated by CEM-I and lime within similar curing periods. A recent more environmentally sustainable approach that has recently been adopted in selecting new binder materials is recycling industrial by-products (IBP's); whereby those that are pozzolanic in nature would be preferred.

To further improve the mechanical performances of deep mixed soils, the addition of alternative alkali materials to lime have also been sought to increase soil pH with a view to activating pozzolanic reactions and the subsequent formation of cementitious bonds. Encouraging work by Palomo et al. (1999) identified that sodium hydroxide and/or sodium silicate showed encouraging potential as alternative alkali activators for use in deep soil mixing, due to their observed ability to raise soil pH and increase rates of mechanical property improvement. Thus, the primary aim of this study was to assess the performance and viability of using alternative alkali activators (AA) within a deep mixed IBP-stabilised synthetic silty sandy clay.

2.0 SOIL AND BINDER MATERIAL CHARACTERISTICS

This study conducted geotechnical, chemical and mineralogical testing to determine the suitability and performance of a number of IBP's and alkali activation in stabilising an artificially manufactured silty sandy clay. This artificial soil was created by utilising a rotary mixer in the laboratory to typify a UK alluvium soil, which tends to be found abundantly on floodplains within river valleys where housing and industrial developments are common. Alluvium typically comprises high proportions of silt and/or clay, which has low levels of cohesion in both wet and dry conditions. This can inherently present wall failure hazards within excavations and slope instability for embankment projects. Additionally, such soft soils are often characterised by low levels of stiffness and consequently lead to problems associated with bearing capacity, should such soils be loaded upon. The artificial silty sandy clay consisted of 70 % fine silica sand and 30 % grade E kaolin, which were provided by WBB Minerals Ltd and English China Clay International Europe Ltd, respectively. The soil also had an optimum gravimetric water content of 15 %, based on compaction testing conducted in accordance with BS 1377: Part 4 (BSI, 1990). Data regarding the soil's grading curve and Atterberg limits are presented below in Figure 2.

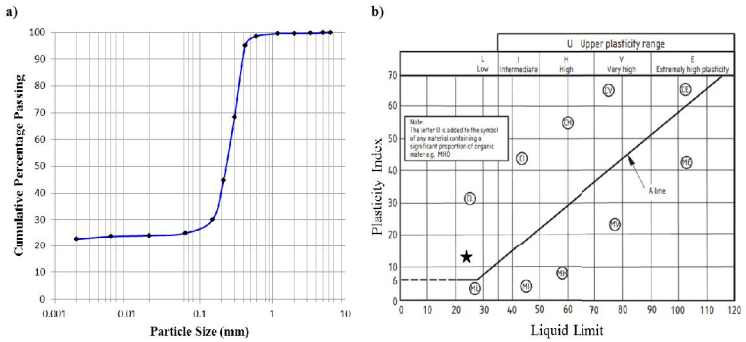

***Figure 2**: Particle size distribution and Atterberg limit data for the artificial alluvium tested (BSI, 1990).*

The IBP's utilised as binders for this study included ground granulated blast furnace slag (GGBS), pulverised fly ash (PFA) and red gypsum (RG). GGBS (supplied by Frodingham Cement Ltd) is a pozzolanic latent hydraulic cement produced from pig iron manufacture; the chemical composition of which closely resembles that of CEM-I. PFA, which was provided by ScotAsh Ltd, is a synthetic pozzolanic waste material that results from combustion within coal-fired power plants. Finally, large stockpiles of RG filter cake are found the world over, which are produced as by-products of sulphuric acid neutralisation during the manufacture of Titanium Dioxide (see Table 1 for the chemical composition of RG). For this project, RG was supplied by Huntsman Tioxide Europe Ltd.

***Table 1**: A summary of the chemical composition of red gypsum. Courtesy of Hughes et al. (2011).*

Component	Content (% dry weight)	Component	Content (mg/kg)
Gypsum ($CaSO_4.2H_2O$)	*58.5 – 59.3*	*Chromium (Cr)*	*500 – 800*
Iron Oxide (Fe_2O_3)	*32.9 – 36.6*	*Zinc (Zn)*	*200 – 400*
Titanium (Ti)	*1.0 – 1.3*	*Strontium (Sr)*	*100 – 300*
Aluminium (Al)	*0.1 – 0.8*	*Nickel (Ni)*	*50 – 60*
Magnesium (Mg)	*0.5 – 0.6*	*Cobalt (Co)*	*20 – 30*
Manganese (Mn)	*0.2 – 0.5*	*Barium (Ba)*	*1 – 3*
Silicon (Si)	*0 – 0.5*	*Lead (Pb)*	*1 – 2*
Chlorine (Cl)	*0.002 – 0.2*		

Recent studies, such as those by Hughes et al. (2011), have identified that utilising lime as an alkali activator within an IBP-stabilised alluvium resulted in inconsistencies with regards to significant strength developments. It may be considered that the relatively poor strength and durability performances observed for certain stabilised soil mixtures may have been attributed to the low pH levels produced by the lime activator used. Hence, based on the work by Palomo et al. (1999), this study used a sodium hydroxide - sodium silicate activator, which was prepared with a ratio of 1:2.

3.0 SAMPLE MIXING METHODOLOGY

To produce stabilised samples, binders were mixed with the artificial alluvium at a dosage of 10 % by dry weight for 10 minutes within a rotary mixer. For AA samples, the sodium hydroxide-sodium silicate mixture was added at a dosage of 20 % by dry weight of the IBP binder used. Non activated (C) IBP-stabilised samples and CEM-I stabilised samples were also prepared and tested for comparative purposes. Once the stabilised soil mixtures had been prepared, samples were then manufactured by tamping into split sample moulds and compressed using a hydraulic press to produce optimum sample bulk densities of 2.2 Mg/m^3. Once compressed, samples were then placed within wax-sealed PVC moulds and cured for periods of 7, 14 and 28 days within a temperature controlled room at 20 ^oC and 55 % relative humidity. For testing at each curing period, samples were extruded from their moulds and then trimmed to the required dimensions in accordance to the necessary BSI (1990) and ASTM (1996) standards.

ISSMGE - TC 211 International Symposium on Ground Improvement IS-GI Brussels 31 May & 1 June 2012

4.0 TESTING PROGRAMME AND RESULTS

Some of the important material properties to take into account when examining the engineering performance of the aforementioned stabilised soil mixtures include: compressive strength, durability, pH levels and mineralogy. For this study's experimental programme, the strength test conducted was unconfined (uniaxial) compressive strength (UCS) (BS 1377: Part 7: Clause 7, BSI 1990). UCS samples were retained post-testing after each curing period in order to determine any changes in water content over the 28 day testing programme (BS 1377: Part 2, BSI, 1990). For durability testing, samples were submerged in water and underwent wetting-drying cycles (ASTM, 1996, D 559 – 96 clause 5.3) and freezing-thawing cycles (ASTM, 1996, D 560 – 96 clause 5.3). pH levels (BS 1377: Part 3: Clause 9, BSI 1990) of samples were recorded to determine whether alkali activation was necessary to raise the pH up to 10.5 to initiate pozzolanic reactions and subsequent strength developments.

4.1 *Compressive Strength*

To assess the UCS performance of the deep mixed IBP binder-soil mixtures, testing was conducted in adherence to BS 1377: Part 7 (BSI, 1990). Samples of dimensions 76 mm (long) x 38 mm (diameter), were tested on a uniaxial Instron 5585H loading frame; whereby three repeats were conducted for each stabilised soil mixture after each curing period. A consistent strain rate of 0.5 mm min^{-1} was used for all UCS tests. After a 28 day curing period, testing results presented in Figure 3 indicate that activated samples containing the GGBS binder produced the most rapidly improved strengths compared with activated samples mixed with PFA, RG or CEM-I. The GGBS-AA sample achieved a compressive strength of 6339 kPa. Contrastingly, based on the low compressive strengths of 488 kPa and 344 kPa achieved for PFA-AA and RG-AA samples, respectively; alkali activation using sodium hydroxide – sodium silicate had negligible effects on strength development. Whether the PFA or RG stabilised samples had been activated or not; they were observed to have experienced remarkably slow rates of strength development.

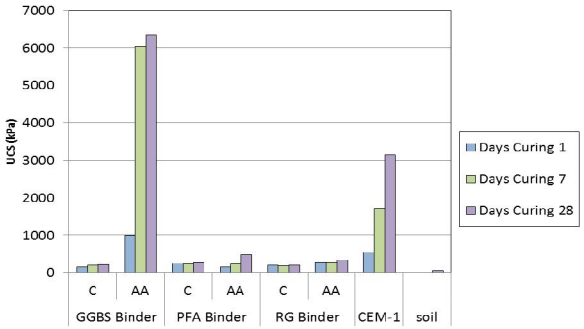

***Figure 3**: UCS behaviour for the non-activated and alkali activated samples tested.*

Work by Fraay et al. (1989) claims that for non-activated PFA samples, delays in strength development may occur as a result of PFA's inertness and that a curing period of at least 7 days would normally be required before any marked strength gains are observed. However, from the results presented in Figure 3, no clear significant strength enhancements were seen over the 28 day testing period. Finally with regard to the GGBS-AA and CEM-I stabilised samples that rapidly reached high strength values, these samples were observed to experience brittle failure; whereas those characterised by much slower strength development experienced more plastic behaviour upon failure.

4.2 *Wet-Dry and Freeze-Thaw Durability*

The durability testing programme studied changes in volume and water content of IBP-soil samples and their resistance to soil-cement losses when subject to wetting and drying (ASTM, 1996, D 559 – 96 clause 5.3) and freezing-thawing (ASTM, 1996, D 560 – 96 clause 5.3) cycles over a 24 day period. Testing

results from the wetting-drying component are presented in Figure 4 and Table 2. Other than the alkali activated GGBS and PFA samples which survived the full 12 testing cycles, all other IBP-stabilised samples disintegrated very shortly after their initial immersion in water. The water content and volumetric changes experienced by the GGBS-AA and PFA-AA samples remained relatively uniform over the testing period. The CEM-I stabilised sample initially exhibited very similar water content and volumetric change behaviour to the GGBS-AA and PFA-AA samples, but disintegrated after 4.5 cycles of testing.

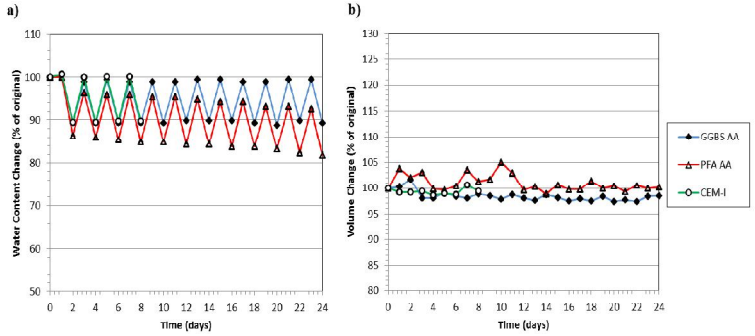

***Figure 4**:a) Water content and b) volumetric changes experienced by samples during wet-dry durability testing.*

The results from the freezing-thawing testing are shown in Figure 5 and Table 2. As observed during wetting-drying testing, the alkali activated GGBS and PFA samples were the only soil-binder mixtures to survive the full 12 cycles of testing and that all non-activated samples disintegrated upon first immersion. Unlike that seen during the wetting-drying testing, the RG-AA sample was able to survive 3 cycles; however this was accompanied by a significant increase in volume during the third cycle. With the exception of the GGBS-AA soil-binder mixture which exhibited the least change in water content and volume change; samples water contents generally showed more variation than that observed during wetting-drying testing, whereby the general trend showed decreasing water contents. The most notable water content observation from the freeze-thaw programme was the dramatic decrease in PFA-AA's water content, which occurred between the seventh and twelfth cycles. Generally, considerably higher fluctuations in volume were recorded for samples during freezing-thawing testing compared with wetting-drying testing; whereby the sample which exhibited the greatest amount of variation was also found to be PFA-AA. As similarly seen during wetting-drying testing, the CEM-I sample survived 4.5 cycles and showed relatively little volume change and a slight reduction in water content.

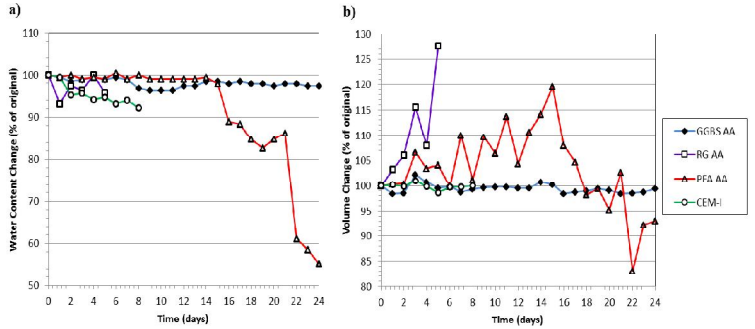

***Figure 5**: a) Water content and b) volumetric changes experienced by samples during freeze-thaw durability testing.*

***Table 2**: Summary of the average number of cycles survived by the soil-binder mixtures tested during the wetting-drying and freezing-thawing testing programme.*

Soil – Binder Mixture	Average no. of cycles survived	
	Wetting-Drying	Freezing-Thawing
Soil + GGBS-AA	12	12
Soil + GGBS-C	0	0
Soil + PFA-AA	12	12
Soil + PFA-C	0	0
Soil + RG-AA	0	3
Soil + RG-C	0	0
Soil + CEM-I	4.5	4.5

4.3 *Moisture Content*

To ensure that the moisture content within the samples tested were sufficiently high to allow for hydration and the development of cementitious bonds, UCS samples were retained post-strength testing for moisture content determination according to BS 1377: Part 2 (BSI, 1990) procedures. However, given the mineralogical and chemical structure of RG-based samples, a slight deviation from the BSI (1990) procedure was required in order to measure their moisture contents. Drying RG samples at 110 ^{o}C would consequently remove RG's structural water and convert the gypsum to anhydrite; thereby potentially resulting in inaccurate moisture content data. Therefore, for this study it was decided that RG samples be dried at a lower temperature of 45 ^{o}C for double the length of the standard drying period.

According to the data presented in Table 3, IBP-stabilised samples were measured to have moisture contents of 11 to 14 % over the 28 day testing period, regardless of whether they were alkali activated or not. Generally, each IBP-stabilised sample experienced very little variation from their initial moisture content over the 28 days, which severely contrasts to the distinct reduction in moisture content by the CEM-I stabilised sample. Hence, this would indicate that sufficient water was present within the IBP-stabilised samples for hydration reactions to occur during testing.

***Table 3**: Summary of the average variations in water content with increasing curing time experienced by the soil-binder mixtures studied.*

Soil – Binder Mixture	Water Content (%)		
	1 day curing	7 days curing	28 days curing
Soil + GGBS-AA	*12.9*	*12.3*	*12.2*
Soil + GGBS-C	*12.8*	*12.9*	*12.7*
Soil + PFA-AA	*11.2*	*12.6*	*12.7*
Soil + PFA-C	*11.7*	*12.3*	*12.1*
Soil + RG-AA	*14.1*	*14.5*	*14.1*
Soil + RG-C	*12.5*	*13.3*	*12.9*
Soil + CEM-I	*15.29*	*13.25*	*11.92*

4.4 *pH Levels*

A recent study by Hughes et al. (2011) revealed that soft soils mixed with IBP binders whose pH levels were lower than 10.50 often resulted in poor strength improvements; thereby indicating that the addition of further alkalis would be required to activate pozzolanic reactions and thus CSH/CAH bond formation. Hence during this study, UCS samples were retained post-UCS testing after 28 days and tested for their pH in adherence to BS 1377: Part 3 (BSI, 1990) procedures. Samples were tested by using a Camlab Ultrameter 6P; the results are presented in Figure 6. The range of pH values recorded from this testing programme varied between 6.23 and 11.90. Non-activated samples had average pH levels of 6.23, 9.0 and 9.77 for RG-C, GGBS-C and PFA-C, respectively; thereby indicating that pozzolanic reactions did not occur within these samples. Whereas for these samples alkali activated equivalents, each achieved pH

levels that were in excess of 10.50; specifically values of 11.10, 11.47 and 11.70 for RG-AA, GGBS-AA and PFA-AA, respectively. Additionally, the pH value achieved by the CEM-I stabilised sample (11.90) was comparable to the pH values obtained by the three alkali activated IBP-soil mixtures

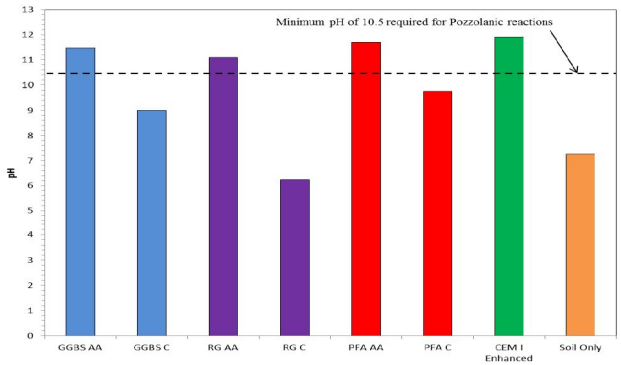

***Figure 6**: Bar chart showing the average pH values obtained by all non-activated and alkali activated samples over a curing period of 28 days.*

5.0 DISCUSSION

5.1 *Strength*

Compressive strength testing results generally suggest that more cementitious bonds were formed over the 28 day curing period within alkali activated samples compared with those which had not. Overall the GGBS-AA binder was seen to produce the most improved strengths over the 28 day testing period, surpassing those reached by the conventionally used CEM-I binder. Non-activated PFA-based samples exhibited delayed compressive strength gains, which are thought to be the result of PFA being inert and with a minimum of 1 week being required for such developments to become apparent (Fraay et al., 1999).

The poor UCS performances and plastic behaviour characteristics of RG-stabilised samples were consistently recorded over the testing period and were therefore not considered to be attributable to delayed strength gains. This would suggest that RG as a lone binder was not suitable for seeking improved engineering performances within soft alluvium, even when alkali activated using sodium hydroxide/sodium silicate. Factors which are likely to have contributed towards such performances include chemical compositional changes to RG during sample preparation; specifically the removal of RG's natural water content as its filter cake was dried, thereby resulting in a degraded mineralogical structure. Another factor associated with RG's sample preparation which may have contributed towards its poor performance was that once its original filter cake form had been dried, it required grinding down to a powder using a mortar and pestle. This in turn may have produced a powder that was less uniform in terms of particle size compared with the GGBS and PFA powders also used during this study. Away from RG's method of preparation for mixing, it should also be considered that a study by Beretka et al. (1996) showed RG not to have a pozzolanic nature and thus may be expected not to produce as impressive strength performances as other IBP binders such as GGBS.

Alkali activation was observed to cause strength and therefore stiffness enhancements within GGBS samples. However, the high stiffness nature of GGBS-AA samples inherently meant that they were likely to experience brittle failure and therefore considered to be potentially unsuitable, should they be dynamically loaded upon. Such observations in material behaviour upon sample failure would suggest that a denser network of cementitious bonds and CSH/CAH gels were present within alkali activated samples. Hence, the results obtained from the UCS programme infer that the strength of IBP-stabilised soils and the overall performance of alkali activation are predominantly controlled by the length of curing (in agreement with findings by Hughes et al., 2011); their level of alkali activation and the chemical/water composition of the soil and IBP's used.

5.2 *Durability*

Both wetting-drying and freezing-thawing durability results demonstrated that the GGBS-AA binder provided the most improved durability performance when added to the artificial alluvium, closely followed by PFA-AA. In severe contrast, RG-stabilised samples provided negligible improvements in durability, based on the disintegration of RG-AA and RG-C samples upon immersion during wetting-drying testing and the RG-C sample during freeze-thaw testing. Although the RG-AA sample survived 3 cycles of freeze-thaw testing before disintegrating, this performance would still be classed as poor and unacceptable for construction standards. As discussed above for strength, the method used to prepare RG for mixing resulted in a non-uniform coarse-grained material, and thereby characterised by a lower density and higher permeability compared with GGBS or PFA powders. This consequently enabled water to more freely infiltrate RG-stabilised samples whilst submerged during testing and therefore be at high risk of disintegration before completing the 12 cycle wetting-drying/freeze-thaw testing periods. This occurrence has been recorded by Hughes (2005), whereby a GGBS-RG-AA sample failed in a brittle manner during thawing after the seventh cycle of freeze-thaw testing. Ultimately, water which entered the sample had frozen, causing contraction and consequently sample cracking. Hughes (2005) was also of the view that this sample degradation may also have been caused by reactions between RG and hydrated compounds, thereby forming unfavourable Ettringite along with shrinkage and/or swelling. Hence, as shown by the GGBS-AA sample; alkali activation demonstrated its ability to produce denser and less permeable soils and therefore decrease the chances of water absorption and sample shrinkage/swelling. However, as the results from RG-AA and PFA-AA samples suggest, alkali activation using the sodium hydroxide/sodium silicate mixture did not consistently result in improved durability properties.

5.3 *pH and Mineralogy*

pH and UCS testing results indicate that alkali activation was required to allow pozzolanic reactions and subsequent strength enhancements to occur. This would suggest that a soil's pH strongly influences any potential strength development it may experience. Compressive strengths greater than 1 MPa were only recorded for samples in this study that had been alkali activated and had achieved a pH $\geq$ 10.50, namely GGBS-AA (11.47); thereby permitting pozzolanic activity. However, some samples with sufficiently high pH levels for pozzolanic activity to occur, such as PFA-AA and RG-AA specimens, did not develop high strengths. A study by Wilkinson et al. (2010b) suggests that the strength of certain stabilised soils may increase as pH decreases. This therefore puts the relationship between soil pH and strength development under further scrutiny. Should any oxidation and/or pH degradation processes occur with stabilised soils, it may be possible for pozzolanic reactions along with any associated strength improvement to become impeded. Thus, it is strongly advised that samples be well sealed and stored within air-tight containers and that the precise quantities of alkali activator to be added to soils pre-mixing are accurately calculated, to ensure the pH will remain $\geq$ 10.50 over an adequate curing period (i.e. minimum of 28 – 56 days).

Previous mineralogical studies by Rodriguez-Navarro et al. (2000), Little et al. (2005) and Hughes (2005) have shown that through analysis techniques such as XRD, minerals including Ettringite, Thaumasite and Thenardite may be found within stabilised clay soils where calcium-based binders have been used. The presence of the aforementioned minerals within stabilised soils or concrete would be considered as highly unfavourable, as they can potentially lead to material degradation through shrinkage, swelling, sulphate attack and severely compromise the engineering integrity of the material in question. Although a mineralogical analysis was not conducted as part of this study, it is highly recommended that mineralogical techniques such as scanning electron microscopy and XRD be conducted in future studies in searching for the presence of potentially structurally unfavourable minerals within stabilised soil specimens. Additionally, it would be interesting to search for any correlation between the formation of structurally unfavourable minerals and pH during such mineralogical studies, as Hughes (2005) suggested that Ettringite or Thaumasite tend to form within soils characterised by low pH levels.

5.4 *Moisture Content*

To allow the hydration of binders and the formation of cementitious gels/minerals within stabilised soils, it is necessary for a suffice amount of water to be present. For this study, samples were initially mixed so that they had a moisture content of 15 %. Post-UCS testing for each curing period, sample's moisture contents were recorded. It was generally found that moisture contents decreased over the 28 day curing period by only 1 – 3 %. Given this relatively low reduction in moisture content, the samples tested are interpreted as containing enough water for hydration. It should also be noted that a proportion of samples' moisture contents is depleted due to pozzolanic reactions; involving calcium hydroxide being transferred

by water to amalgamate with aluminate and siliceous minerals. These undergo dissolution to produce cementitious CAH/CSH gels. From this study, certain alkali activated samples (e.g. GGBS-AA) and the CEM-I sample showed higher compressive strengths with decreasing moisture contents. This observation is in agreement with a study by Duxson et al. (2007), who concluded that water is consumed during the dissolution of geopolymer-based reactions. This would also indicate that AA samples tend to have lower moisture contents than C samples; although it should be borne in mind that this may not always be the case, whereby C samples' moisture content may be equally depleted by evaporation pre-testing. One final factor which may influence a sample's water content and hydration reactions is the negative pore pressures generated when compacting samples within the split-sample mould. Such negative pore pressures have also been documented by Hughes et al. (2011), which may result in higher strengths being achieved. Hughes et al. (2011) also state that soils with high clay contents would inherently have low levels of permeability and thus greatly inhibit the amount of water available within the soil for hydration.

6.0 CONCLUSIONS

Based on the results obtained from the laboratory testing programme carried out, a number of conclusions can be made:

- The use of IBP binders and alkali activation with a sodium hydroxide/sodium silicate mixture have demonstrated their plausibility in being successfully used as more environmentally sustainable replacements for lime and CEM-I in soft soil stabilisation. Namely, the strength and durability performances shown by the GGBS-AA specimens were commendable and would be suitable for construction specifications.
- The replacement of CEM-I with IBP binders for deep dry soil mixing projects could be accomplished with very little plant or equipment modifications, along with negligible degradation in the overall efficiency of the soil mixing process. However, the use of sodium silicate solution as an alkali activator on site may present financial and practicality problems. An alternative high-alkali waste product in the form of a powder would be preferred both in terms of the environment and finance.
- From the IBP binders tested, the GGBS-AA mixture proved to be the most effective in producing high strength gains of > 6 MPa and effective resistance to wet-dry and freeze-thaw cycles over 28 days. Hence, GGBS-AA would be the most suitable replacement for CEM-I in projects where engineering specifications require high strength and stiffness levels. However, other engineering scenarios where medium levels of stiffness are required, for instance high speed railway line foundations which frequently experience dynamic loading induced by passing trains; GGBS-AA would not be suitable as brittle failure of stabilised soil columns may result.
- pH testing results confirmed alkali activation was required to increase the pH of stabilised soils to at least 10.50, in order for pozzolanic activity to potentially take place. Evidence from this study suggest that pH bears an influence on a stabilised soil's strength development; whereby increasing pH allows pozzolanic reactivity and subsequent increases in strength. However, findings from other recent studies contend that this does not always apply; thereby warranting further investigation.
- Alkali activation using sodium hydroxide and sodium silicate did not harmoniously enhance sample durability. Given the poor overall geotechnical performances of the PFA and RG binders, careful evaluations ought to be conducted for IBP's when being considered for selection as binders for deep soil mixing projects. Additionally, careful consideration must be paid towards both the soil that is to be stabilised and the loading conditions to be imposed over stabilised soil columns, on an individual case basis. This approach is recommended to be taken until a more extensive and detailed understanding has been developed on binder/alkali activator properties for soil stabilisation.
- Findings from this study are expected to be valuable to the construction sector in procuring the most optimum sustainable binder mix designs for deep soil mixing, in terms of quality and economics for problematic soft alluvium soils. However, if this research is to be of use to the geotechnical community, future works should focus on demonstrating the potential of IBP binders within other documented problematic soils and determining whether utilising IBP binders is financially feasible compared with more traditional binders, by conducting a series of field trials and costing studies.

REFERENCES

Ahnberg, H., Johansson, S.-E., Pihl, H. and Carlsson, T., 2003, *"Stabilising effects of different binders in some Swedish soils"*, Ground Improvement, 7, No. 1, pp. 9-23.

Al-Tabbaa, A. and Evans, C. W., 1998, *"Pilot in situ auger mixing treatment of a contaminated site, Part 1: treatability study"*, Proceedings of the Institute of Civil Engineers, Geotechnical Engineering, 131, pp. 52-59.

American Society for Testing and Materials (ASTM), 1996, *Designation: D 559 – 89 Standard Test Methods for Wetting and Drying Compacted Soil-Cement Mixtures*, Annual Book of ASTM Standards, 4.08, West Conshocken: Pa.

American Society for Testing and Materials (ASTM), 1996, *Designation: D 560 – 96 Standard Test Methods for Freezing and Thawing Compacted Soil-Cement Mixtures*, Annual Book of ASTM Standards, 4.08, West Conshocken: Pa.

Beretka, J., Cioffi, R., Marroccoli, M. And Valenti, G., 1996, *"Energy-saving cements obtained from chemical gypsum and other industrial wastes"*, Waste Management, 16, pp. 231-235.

BSI, 1990, BS: 1377 Incorporating Amendment No. 1, Methods of test for Soils for Civil Engineering Purposes, British Standards Institution, Milton Keynes.

Davidson, L. K., Demirel, T. and Handy, R. I., 1965, *"Soil Pulverization and Lime Migration in Soil Lime Stabilisation"*, Highway Research Record, 1965 (92), pp. 103-126.

Duxson, P., Fernandez-Jimenez, A., Provis, J. L., Lukey, G. C., Palomo, A. and Deventer, J. S. J, 2007. Geopolymer technology: the current state of the art. Journal of Materials Science, Advances in Geopolymer Science and Technology. 42, 2917-2933.

Fraay, A. L. A., Bijen, J. M. and Haan, D. Y. M., 1989, *"The reaction of fly ash in concrete: a critical examination"*, Cement and Concrete Research, 1989 (19), pp. 235-246.

Hughes, P. N. and Glendinning, S., 2004, *"Deep dry mix ground improvement of a soft peaty clay using blast furnace slag and red gypsum"*, Quarterly Journal of Engineering Geology and Hydrogeology, 37, pp. 205-216.

Hughes, P. N., 2005, *"The Use of Synthetic Red Gypsum as a Construction Material"*, PhD Thesis, School of Civil Engineering and Geosciences, Newcastle University, UK.

Hughes, P. N., Glendinning, S., Manning, D. A. C. and White, M. L., 2011, *"Use of red gypsum in soil mixing engineering applications"*, Proceedings of the Institution of Civil Engineers, Geotechnical Engineering, vol. 164, GE3, pp. 223-234.

Jegandan, S., Liska, M., Osman, A. A-M. and Al-Tabbaa, A., 2010, *"Sustainable binders for soil stabilisation"*, Proceedings of the Institution of Civil Engineers, Ground Improvement, 163, G11, pp. 53-61.

Little, D. N., Herbert, B. and Kunagalli, S. N., 2005, *"Ettringite Formation in Lime-Treated Soils: Establishing Thermodynamic Foundations for Engineering Practice"*, Transportation Research Record: Journal of the Transportation Research Board, No. 1936: Soil Mechanics 2005, Transportation Research Board of the National Academies.

Palomo, A., Grutzeck, M. W. and Blanco, M. T., 1999, *"Alkali-activated fly ashes. A cement for the future"*, Cement and Concrete Research, vol. 29, pp. 1323-1329.

Rodriguez-Navarro, C., Doehne, E. and Sebastian, E., 2000, *"How does sodium sulphate crystallised? Implications for the decay and testing of building materials"*, Cement and Concrete Research, 30, pp. 1527-1534.

Rogers, C. D. F., Glendinning, S. and Holt, C. C., 2000, *"Slope stabilisation using lime piles – a case study"*, Ground Improvement, 4, pp. 165-176.

Sherwood, P. T., 1993, *"Soil stabilisation with cement and lime – state of the art review"*, Transport Research Laboratory, Department of Transport, HMSO publications, ISBN 0-11-551171-7.

Wilkinson, A., Haque, A. and Kodikara, J., 2010b, *"Stabilisation of clayey soils with industrial by-products: part B"*, Proceedings of the Institution of Civil Engineers, Ground Improvement, 163, G13, pp. 165-172.

Appendix 3:

Engineering Geology

Journal Paper

Contents lists available at SciVerse ScienceDirect

Engineering Geology

journal homepage: www.elsevier.com/locate/enggeo

The use of alkali activated waste binders in enhancing the mechanical properties and durability of soft alluvial soils

Paul Sargent [a,*], Paul N. Hughes [a], Mohamed Rouainia [a], Maggie L. White [b]

[a] School of Civil Engineering and Geosciences, Drummond Building, Newcastle University, Newcastle upon Tyne, Tyne and Wear, NE1 7RU, UK
[b] Materials Analysis Group, School of Chemical Engineering and Advanced Materials, Herschel Building, Newcastle University, Newcastle upon Tyne, Tyne and Wear, NE1 7RU, UK

ARTICLE INFO

Article history:
Received 11 August 2011
Received in revised form 3 August 2012
Accepted 13 October 2012
Available online 7 November 2012

Keywords:
Stabilised soils
Sustainability
Performance
Alkali activation

ABSTRACT

This paper presents recent work in utilising industrial by-products as sustainable binders for use in deep soil mixing, to enhance the geotechnical properties of soft soils. The study has used geotechnical and mineralogical tests to determine the performance of the binders when incorporated into an artificial silty sand soil. Comparisons with the strength and durability of untreated and stabilised soils have been made. The study indicates that from the by-products tested, soils stabilised with alkali activated blast furnace slag resulted in the greatest strength and durability improvements; with other materials tested showing smaller improvements. The addition of alkali activators has been observed to allow pozzolanic reactions to occur, which has led to improved mechanical properties; primarily strength, which increased with time. The durability of the soil was improved by the additions of by-products, though alkali activation did not cause significant additional increase in durability.

1. Introduction

In many countries, large areas of the ground surface are covered by soft soils (e.g. alluvium and peats). These can be problematic when built upon, due to their unfavourable bearing capacity, shrink/swell, settlement and durability characteristics. To improve such conditions, a number of stabilisation techniques are available for use, including compaction/consolidation, mechanical stabilisation and soil mixing with cementitious binders (Sherwood, 1993). This paper focuses on soil mixing, specifically deep dry soil mixing.

Deep soil mixing has used lime and cement as the primary binder since the 1970s, which have been extensively used internationally. Techniques commonly utilised include column installation and slurry pressure injection. These decrease soil moisture contents; thereby reducing their likelihood of shrinkage/swelling and enhancing strength and compaction properties (Glendinning and Rogers, 1996; Threadgold, 1996; Rogers et al., 2000; Ahnberg et al., 2003). Deep dry mixing started in the UK during the 1990s (Al-Tabbaa, 2003); whereby it creates stabilised soil columns through injecting a binding agent (Figure. 1). To introduce binders into the ground, a rotary mixing auger is drilled to the treatment depth. The drill's rotation direction is then reversed and retrieved whilst a binder is pumped through the auger drill bit and mixes the binder and soil. The drill bit's fins are orientated so compaction occurs along the column during mixing.

Portland Cement (CEM-I according to BS EN: 197-1; BSI, 2000) and lime have long been utilised as binders; whereby the former is considered more favourable in providing rapid strength enhancements (Rogers et al., 2000; Hossain, 2010; Jegandan et al., 2010). Deep mixed soils typically have binder contents of 5–15% by mass, although the dosage used depends upon numerous factors including the soil's organic content, mineralogy and water content. The presence of soil water and calcium silicates/aluminates within binders reacts to form hydration products such as calcium silica hydroxide (C-S-H) and calcium aluminate hydroxide (C-A-H) gels. Such cementitious gels continue to form over long periods of time via pozzolanic reactions, which occur when soil pH levels are ≥10.5 (Davidson et al., 1965). The soil-binder mixtures progressively cure and produce stronger, cementitious soil matrices known as "Geopolymers" (Sherwood, 1993). Should any further water percolate around or through the deep mixed columns, through curing the cementitious gels will be able to resist dissolution and therefore soil erosion. Deep mixing has a wide number of applications, such as providing supporting walls for excavations, foundation engineering, hydraulic cut-off walls, liquefaction mitigation and environmental remediation. Japan extensively uses deep mixing for numerous applications, one of which was the construction of the 15 km long Trans-Tokyo Bay Highway; whereby the soft alluvial clay foundation soil was treated using a cement slurry to safeguard the tunnels. UCS values after 28 days curing reached up to 2 MPa (CDIT, 2002). Elsewhere, deep mixed soil columns have been used for stabilising failed levees and floodwalls along Orleans Avenue Canal in New Orleans, USA after Hurricane Katrina in 2005. By using a high strength cement binder, deep mixed shear panels were extended through the levee fill into the underlying beach sands (McGuire et al., 2012). For the purpose of this paper, the intended application of deep mixing using the new IBP-based binders is to stabilise soft foundation soils beneath road or railway embankments.

* Corresponding author. Tel.: +44 7815 714237; fax: +44 191 222 5322.
E-mail addresses: paul.sargent@newcastle.ac.uk (P. Sargent), p.n.hughes@newcastle.ac.uk (P.N. Hughes), m.rouainia@newcastle.ac.uk (M. Rouainia), maggie.white@newcastle.ac.uk (M.L. White).

0013-7952/$ – see front matter © 2012 Elsevier B.V. All rights reserved.
http://dx.doi.org/10.1016/j.enggeo.2012.10.013

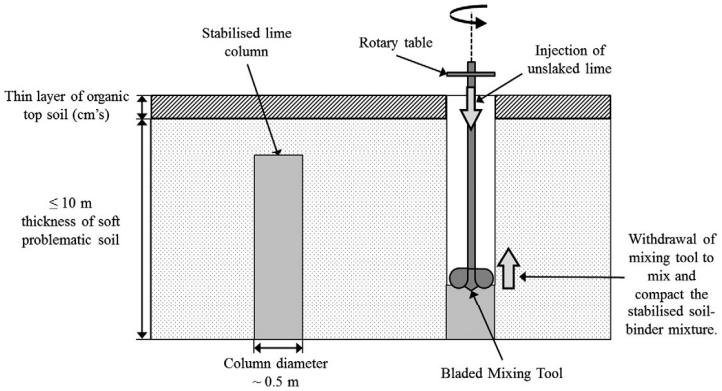

Fig. 1. Schematic of the deep dry soil mixing technique.

Negative environmental and financial issues are associated with utilising CEM-I and lime as binders. McLellan et al. (2011) recently conducted a sustainability comparison study between CEM-I and geopolymer cements in terms of their costs and carbon emissions; whereby the three main factors considered were energy (direct fuel and electricity consumption), greenhouse gas emissions and financial cost. Also considered in the study were factors including technical performance, leaching, water usage, hazardous material content and the volume of waste produced. A number of previous works were considered by McLellan et al. (2011); notably that of Weil et al. (2009) who assessed the financial cost and CO_2 emissions (kg $CO_{2\text{-eq}}/m^3$) produced for feedstock and transport. Weil et al. (2009) determined that for a geopolymer comprising 78% gravelly soil and 22% binder (9.6% GGBS, 2.4% PFA, 3.5% reactive waste, 1.4% Na_2SiO_3, 1% NaOH and 4% deionised water), a reduction of 131 kg $CO_{2\text{-eq}}/m^3$ was observed for the combined feedstock and transport of the binder compared with that produced for CEM-I. Thus, McLellan et al. (2011) concluded that geopolymers have high potential for reducing the environmental impacts of cement production. Based on a proposed Australian geopolymer mix, McLellan et al. (2011) estimated a significant greenhouse gas emission reduction of 44–64% compared with CEM-I.

Hence, there becomes a need for identifying more sustainable binders to replace CEM-I and lime; specifically in terms of lower energy consumption, greenhouse gas emissions, production and transport costs. These binders should provide strength and durability performances that are either comparable or surpass those of CEM-I and lime within similar curing times. A popular route for selecting new binders has been to recycle industrial by-products (IBP's); preferably those which are alumino-silicate based (i.e. pozzolanic). Based on findings by Palomo et al. (1999), the introduction of alternative alkalis such as sodium hydroxide (NaOH) and sodium silicate (Na_2SiO_3) to these IBP's, can potentially further enhance the rate at which the mechanical properties of stabilised soils are improved by increasing soil pH; thereby allowing pozzolanic reactions and cementitious bonding to occur.

2. Materials

This paper presents results from a laboratory study, which investigates the mechanical strength and durability of alkali activated IBP-stabilised soil. For consistency an artificial silty sand was produced in the laboratory. This soil type was chosen for study as alluvial soils containing large quantities of silt present difficult ground conditions for construction purposes; whereby in both wet and dry conditions it has low levels of cohesion which can cause wall collapses within excavations and slope instability. These soils can also have low strength and stiffness leading to bearing capacity problems. Alluvial soils are found in abundance across the UK, especially on floodplains within river valleys which tend to be where housing and industrial developments are concentrated.

The IBP binders used in the study were pulverised fly ash (PFA), ground granulated blast furnace slag (GGBS) and red gypsum (RG). PFA is a synthetic pozzolanic material that is produced from combustion processes occurring within coal-fired power stations, which for this study was supplied by ScotAsh Ltd. GGBS is a latent hydraulic cement produced during pig iron manufacture, whose chemical composition partly resembles that of CEM-I cement (GGBS used in this study was supplied by Frodingham Cement Ltd). RG is a by-product of Titanium Dioxide manufacture (an extensively used white pigment), which occurs in a filter cake form during sulphuric acid neutralisation, this is produced in the UK by Huntsman Tioxide Europe Ltd. The chemical composition of RG can be seen in Table 1.

Previous studies (Hughes et al., 2010, 2011) have investigated the use of lime as an alkali activator in a range of similar soils/IBP binders. In these studies, whilst some soil/binder combinations exhibited significant mechanical improvement not all IBP's investigated could be seen to improve the strength of all the soils investigated. The low strength development could at least be partially attributed to insufficiently high pH being generated by the lime activator. Durability was also

Table 1
Summary of the chemical composition of red gypsum.
After Hughes et al. (2011).

Component	Content (% dry weight)	Component	Content (mg/kg)
Gypsum ($CaSO_4.2H_2O$)	58.5–59.3	Chromium (Cr)	500–800
Iron Oxide (Fe_2O_3)	32.9–36.6	Zinc (Zn)	200–400
Titanium (Ti)	1.0–1.3	Strontium (Sr)	100–300
Aluminium (Al)	0.1–0.8	Nickel (Ni)	50–60
Magnesium (Mg)	0.5–0.6	Cobalt (Co)	20–30
Manganese (Mn)	0.2–0.5	Barium (Ba)	1–3
Silicon (Si)	0–0.5	Lead (Pb)	1–2
Chlorine (Cl)	0.002–0.2		

identified as a potential concern when using these binders. Therefore in this study an alternative alkali activator was added to the IBP's by mixing NaOH flakes and Na_2SiO_3 solution. For comparison purposes, non-activated binders and CEM-1 were tested in addition to activated samples.

3. Methodology

3.1. Soil characterisation

The artificial soil was produced by mixing fine silica sand (produced by WBB Minerals Ltd) with grade E kaolin (produced by English China Clay International Europe Ltd) at a ratio of 70:30. Based on the particle size distribution of the soil (see Figure 2), it may be classified as a silty sand according to BS 5930 (BSI, 1999) criteria. In terms of the soil's Atterberg limits, the soil had a liquid limit of 23.48 and a plasticity index of 12.02, thereby indicating that the artificial silty sand was of low plasticity.

To gain an understanding of the silty sand's capacity to react with binders and ultimately produce cementitious gels, cation exchange capacity (CEC) and specific surface area testing were conducted. CEC provides an estimate of the number of sites on clay minerals within a soil where cation exchange can occur. Inherently, soils with high surface area values (i.e. those characterised by higher clay contents) result in higher CEC values. Hence, knowledge about the CEC and surface area properties of a soil provides an insight into its potential for undergoing future reactions between soil particles and the cementitious binder, and therefore the formation of cementitious gels. The method used for CEC analysis was BS: 7755, Section 3.12:1996, ISO 13536:1995, using barium chloride solution buffered at a pH of 8.1; whereby a CEC value of 1.96 cmol/kg (or 1.96 meq/100 g) was determined. Through the use of this CEC value and Eq. (1) as stated by Meunier (2005):

$$\sigma_{CEC} = \left[\qquad\right]/2ab \tag{1}$$

where e = the elementary charge, which has a constant value of 1.6022×10^{-2} C. a and b are unit cell parameters for the clay mineral in the x–y plane, whereby for kaolinite a = 0.531 nm and b = 0.92 nm. Values were taken from Meunier (2005).the CEC-related charge density (σ_{CEC}) for the artificial silty sand was calculated to be 0.0032 C m^{-2}.

According to Cooper (2009), such a low CEC value is representative of soils characterised by low organic matter contents and relatively low clay/high sand contents; whereby such properties can be expected from river alluvium deposits. The surface area of a soil can influence its physical and chemical characteristics, whereby in terms of CEC, larger surface area provides more exchangeable surfaces. Generally, the higher the soil's clay content, the greater the surface area; and thus has a major impact on the soil CEC. For determining the artificial silty sand's surface area, the Brunauer Emmett Teller (BET) nitrogen absorption method was adopted, which produced a very low value of 2.275 m^2/g.

According to a study by Ersahin et al. (2006), low surface area and CEC values can be expected of alluvial soils; particularly those which are classed as sandy loams (comprising approximately 10% clay, 30% silt and 60% sand). However, the surface area and CEC values obtained for the artificial silty sand from this study are even lower than those documented by Ersahin et al. (2006). This can be explained by the large proportion of sand sized particles within the artificial soil and the relatively little silt and clay content.

3.2. Sample preparation

To create test samples alkali activated and non-activated binders were added to the soil at 10% by dry weight and mixed using a rotary mixing machine for 10 min, water was added to the mixture to achieve an overall gravimetric water content of 15%. The activator was created by mixing NaOH and Na_2SiO_3 at a ratio of 1:2, which was added to the IBP binders at a concentration of 20% by dry weight.

Samples were created by tamping and compressing the stabilised soils into split-sample moulds. The moulds were then placed in a hydraulic press to compact the material to the correct dimensions. This allowed the production of samples with consistent dimensions, water contents and density at relatively rapid rates. In the case of strength tests 38 mm diameter × 76 mm long were created. 76 mm diameter × 18 mm thick samples were created for compressibility testing. Based on optimum compaction criteria for the artificial silty sand, all samples had a bulk density of 2.2 Mg/m^3, a dry density of 1.9 Mg/m^3 and an initial gravimetric moisture content of 15%. According to Tomlinson (2001), the dry density of the artificial silty sand falls within the category of fine and silty sands (1.75–2.15 Mg/m^3).

For this study, IBP's were used both individually and mixed together in order to identify the most effective combination. Table 2 summarises the soil-binder mixtures examined and their respective concentrations.

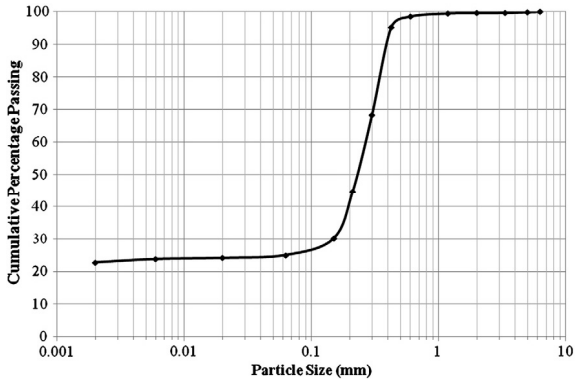

Fig. 2. Soil grading curve of the artificial silty sandy clay.

According to Hansson et al. (2001), construction specifications in deep mixing usually require strength improvements to be acquired within 28 days. Hence, samples were cured within sealed PVC sample moulds for periods of 7, 14, 28 and 56 days, and were placed within a temperature controlled room (55% relative humidity, 20 °C ambient air temperature). Once samples had been cured, they were extruded, cut to the appropriate dimensions and then tested.

3.3. Laboratory testing

A range of laboratory tests were conducted to assess the performance of the binders being investigated. Strength and stiffness were assessed via unconfined compressive strength (UCS) (BS 1377: Part 7: Clause 7, BSI, 1990) and undrained triaxial (BS 1377: Part 7: Clause 8, BSI, 1990). Compressibility was assessed by oedometer testing (BS 1377: Part 5, BSI, 1990). Durability was assessed by wetting–drying and freeze–thaw durability tests (ASTM-D 559 and ASTM D560, ASTM, 1996a,b). The pH level of soil mixtures was tested both before and after curing using a Camlab ultrameter 6P (BS 1377: Part 3, BSI, 1990). Finally, X-ray diffraction analysis (XRD) was used to determine sample mineralogy of samples retained after strength testing. X-ray diffraction analysis was carried out with a PANalytical X'pert Pro diffractometer fitted with an X'celerator and secondary monochrometer, using copper k-alpha radiation of wavelength 1.54180 Å. Phase identification was carried out using X'Pert Highscore Plus software and the ICDD database, sets 1–49 (ICDD, 1999).

4. Results

4.1. Strength and stiffness

Fig. 3 shows stress strain plots from the UCS testing of the individual IBP binder soil mixes. Fig. 4 shows the average maximum strengths attained compared with soils mixed with CEM-1 and untreated soil. When the IBP's were used individually as binders, alkali activation had little effect on the strength of RG samples. The strength of the alkali activated PFA samples increased with time whereas the non-activated PFA samples did not. Compared with the natural performance of the artificial silty sand, the benefits in using activated PFA or RG binders appear to be negligible. The alkali activated GGBS samples showed the largest and most rapid strength and stiffness improvements with curing time. After 28 days curing, the activated GGBS binder exhibited twice the strength of standard CEM-1 cement, averaging 6 MPa after 28 days. However, as similarly observed for the non-activated PFA and RG, non-activated GGBS showed very little strength gain over the testing period. In general, the behaviour of the activated GGBS samples after each curing period upon failure was brittle, compared with the more ductile behaviour observed for other stabilised mixtures.

Presented in Fig. 5 is a selection of stress strain plots from the UCS testing of combined IBP binder soil mixes, and in Fig. 6 a summary of average maximum strengths with curing time compared with soils mixed with CEM-1 and untreated soil. Alkali activation clearly increased the strengths developed in all of the combined IBP binders. The combination of GGBS–RG exhibited the highest strength (5 MPa after 28 days) and GGBS–PFA also showed significant strength gain (3.5 MPa after 28 days), both of these combinations exhibited higher strengths than the CEM-1 binder. Contrastingly, the combination of PFA and RG exhibited the smallest strength gains; whereby Fig. 5 also shows these samples having the lowest levels of stiffness.

As similarly seen for the UCS testing of the individual binders, the behaviour of samples which contained a GGBS-based binder and had been alkali activated exhibited brittle behaviour upon failure. Contrastingly, the activated PFA–RG samples were characterised by more ductile behaviour at failure.

Table 2
Summary of the binder compositions used for laboratory testing. (Note: C denotes non-alkali activated samples and AA denotes alkali activated samples).

Mix	Composition
PFA–C	100% PFA
PFA–AA	100% PFA
RG–C	100% RG
RG–AA	100% RG
GGBS–C	100% GGBS
GGBS–AA	100% GGBS
PFA–RG–C	50% PFA, 50% RG
PFA–RG–AA	50% PFA, 50% RG
PFA–GGBS–C	50% PFA, 50% GGBS
PFA–GGBS–AA	50% PFA, 50% GGBS
GGBS–RG–C	50% GGBS, 50% RG
GGBS–RG–AA	50% GGBS, 50% RG
CEM-1	100% CEM-1

4.2. Compressibility

Oedometer studies were conducted in accordance with BS 1377: Part 5 (BSI, 1990). Both non-activated and activated soil-binder mixtures of GGBS–RG, GGBS–PFA and PFA–RG were tested. The coefficients of volume compressibility (M_v) – defined as the volume change per unit volume per unit increase in effective stress (Craig, 2004), was calculated to gain an understanding of the compressible nature of IBP-stabilised silty sand. Samples were allowed to cure for 28 days and then subjected to 50, 100, 200, 400 and 800 kPa loading stages. Compression curves from oedometer testing are shown in Fig. 7 and a summary of the calculated M_v values is shown in Fig. 8.

According to Fig. 7, the compression curve for the untreated silty sand is located below the compression curves for all of the stabilised soil mixtures tested. This is the result of more compression being experienced by the silty sand compared with the other stiffer stabilised samples.

With regards to the compression indices (C_c) exhibited by samples over the course of oedometer testing, the stabilised samples have higher values compared with that for the untreated silty sand. When comparing the C_c values obtained for the stabilised samples, the alkali activated GGBS–RG and GGBS–PFA samples have the lowest values; whereas their respective non-activated samples along with the non-activated and activated PFA–RG samples had considerably higher C_c values. This generally indicates that the activated GGBS–RG and GGBS–PFA binders were much less compressible compared with the untreated silty sand and the other binder combinations. Additionally, the C_c values obtained for the non-activated GGBS–RG, GGBS–PFA and PFA–RG were comparable with that obtained for the untreated silty sand. This would therefore suggest that alkali activation is certainly required in order to observe any marked reduction in compression and therefore C_c value.

Fig. 8 shows that all of the binders tested reduced the compressibility of the silty sand soil and that the alkali activated binders reduced the compressibility of the soil by a greater extent than the non-activated binders. The initial M_v of the untreated soil was calculated to be 0.6 m^2/MN, which is typical of normally consolidated alluvial clays and can be considered highly compressible (Tomlinson, 2001). In the samples mixed with alkali activated IBP binders, the compressibility was reduced to an M_v of between 0.06 and 0.21 m^2/MN and could therefore be considered to be a soil of low to medium compressibility (Tomlinson, 2001).

Of the alkali activated binders, the GGBS–PFA binder is the most effective in reducing compressibility with GGBS–RG slightly less effective and PFA–RG significantly less effective.

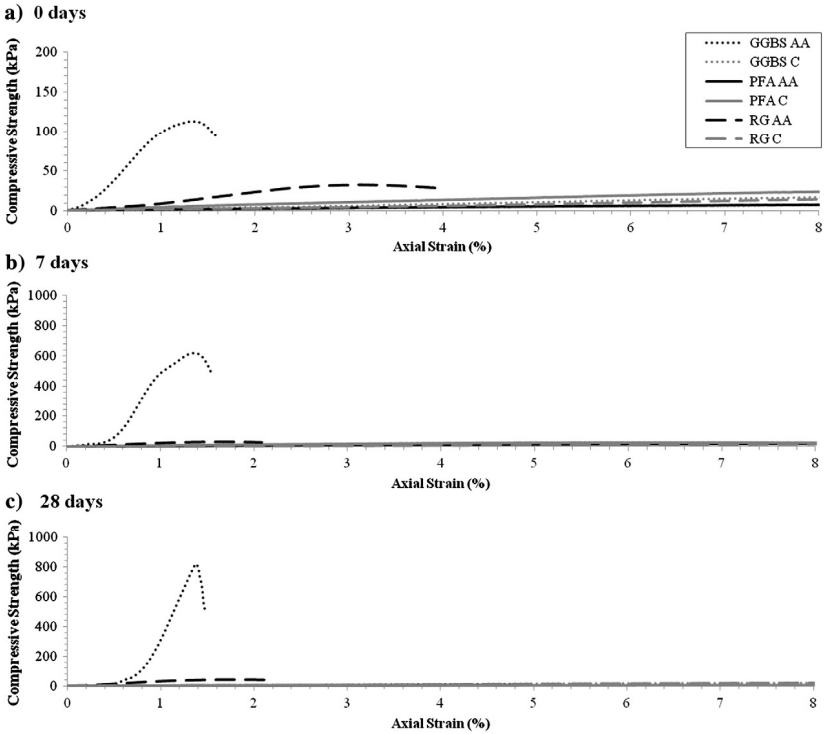

Fig. 3. Stress strain plots from UCS testing for single IBP binder mixes after curing periods of: a) 0 days, b) 7 days and c) 28 days.

4.3. Durability

4.3.1. Wetting–drying

Wetting–drying durability testing was conducted to determine soil cement losses, changes in volume and water contents due to wetting and drying cycles. Wetting–drying cycles actively occur up to depths of 3.5 m; however this is likely to vary between locations due to in-situ soil and vegetation conditions (Clarke and Smethurst, 2010). For temperate maritime climates, such as that experienced in the UK, rainfall occurs throughout the year and therefore any related surface water is likely to percolate through the sub-surface. Thus, in locations where deep mixed columns are installed, there is potential for water to percolate through or around the columns, causing swelling during wet periods and shrinkage during drier periods. Therefore, should IBP binders be mixed into a problematic soil via deep mixing, it is important that they are able to endure such wetting–drying cycles and prevent the failure of the deep mixed columns, along with any adversities to any overlying loads or structures.

Considering the UK's temperate maritime climate, it may be considered that the ASTM 559 standard for conducting wetting–drying durability testing is fairly extreme. However, the standard followed in this study can be considered as more representative of climatic conditions in other countries around the world. Results from the wetting and drying tests are shown in Figs. 9 and 10 and Table 3.

Of the individual IBP binders non activated GGBS, PFA and RG all disintegrated upon their first immersion in water as did alkali activated RG. Alkali activated GGBS and PFA survived for the full 12 cycles during

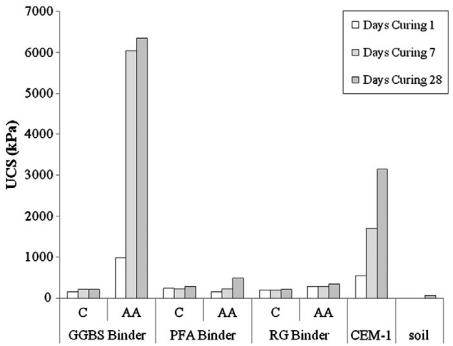

Fig. 4. Average maximum unconfined compressive strengths for single IBP binders (average of three tests per curing period).

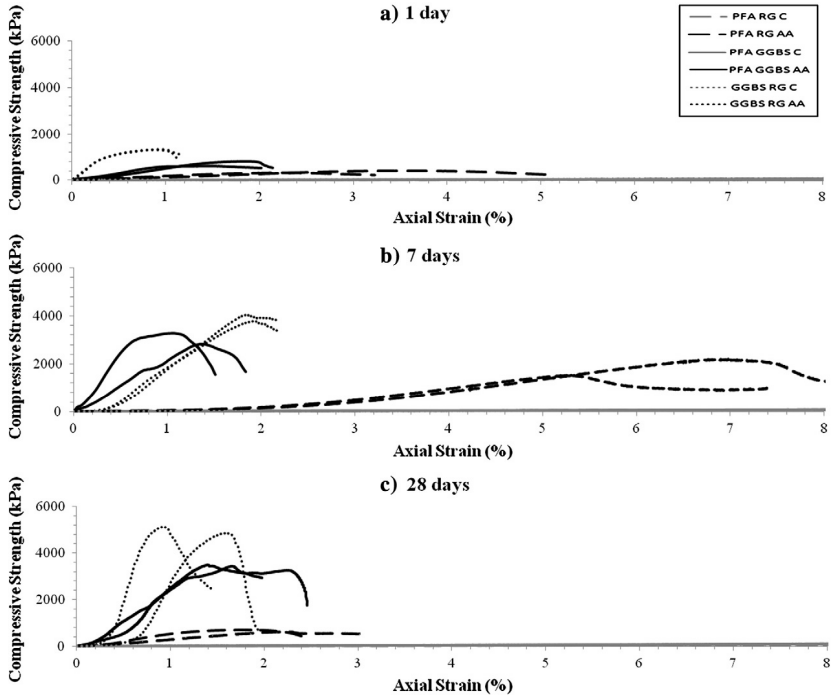

Fig. 5. Stress strain plots from UCS testing for combined IBP binder mixes after curing periods of: a) 0 days, b) 7 days and c) 28 days.

which their water content and volume remained reasonably constant. Of the combined IBP binders all the non-activated samples disintegrated during the first cycle of testing. Alkali activated PFA–RG survived for 6 cycles but displayed a rapid reduction in volume during preceding cycles. Alkali activated GGBS–RG and GGBS–PFA survived the full 12 cycles. Specimens mixed with CEM-I initially showed reasonably constant water content and volume however these disintegrated at 4 and 5 cycles.

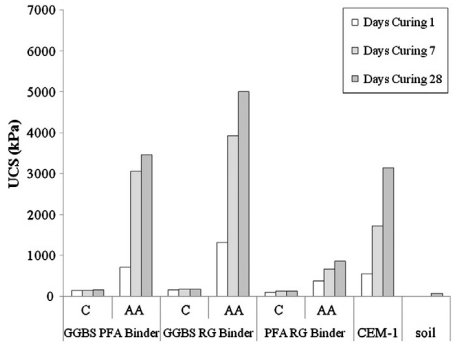

Fig. 6. Unconfined compressive strengths for combined IBP binders.

4.3.2. Freezing–thawing

Freezing–thawing testing aimed to determine samples' resistance to soil–cement losses, volume and water content changes due to repeated freezing–thawing of stabilised soils. In a worst-case scenario, freeze–thaw processes within UK soils could occur up to a depth of 2 m. Thus, for cases where deep mixed columns are to be installed; should any water percolate through or around the columns, shrinkage, swelling and subsequent physical weathering may be imposed along their upper lengths within the shallow sub-surface. Similar to the wetting–drying durability testing, the ASTM 560 standard for investigating the freeze–thaw durability of the IBP stabilised silty sand may be deemed as being slightly extreme in terms of representing climatic conditions that typically occur in the UK. The results from the freeze–thaw tests are presented in Figs. 11 and 12 and Table 4.

As similarly seen for the individual IBP binders during wetting–drying testing, all non-activated samples disintegrated upon their first immersion in water. The alkali activated RG binder however survived 3 cycles, the alkali activated PFA exhibited a significant reduction in water content and variation in volume after the 7th cycle. The alkali activated GGBS binder sample survived for the full 12 cycles and showed only slight fluctuations in water content and volume.

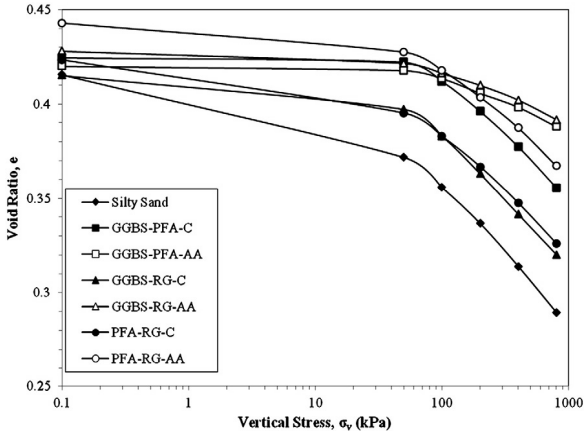

Fig. 7. Oedometer compression curves of the natural and stabilised silty sand samples.

With the exception of GGBS–PFA, the non-activated combined IBP binders exhibited low durability. Non-activated PFA–RG survived for 4 cycles and non-activated GGBS–RG survived for 8 cycles. The alkali activated combined binders survived the full 12 cycles with the exception of GGBS–RG, which disintegrated after 9 cycles. Despite surviving 12 cycles, the PFA–RG–AA and GGBS–PFA–C specimens showed significant variation in water content and volume throughout testing. Only the GGBS–PFA–AA specimen showed consistent water content and volume over 12 cycles.

Samples stabilised with CEM-I survived 4 cycles; whereby little variation was observed in volume. However, samples showed a slight decrease in water content over the 4 cycles survived.

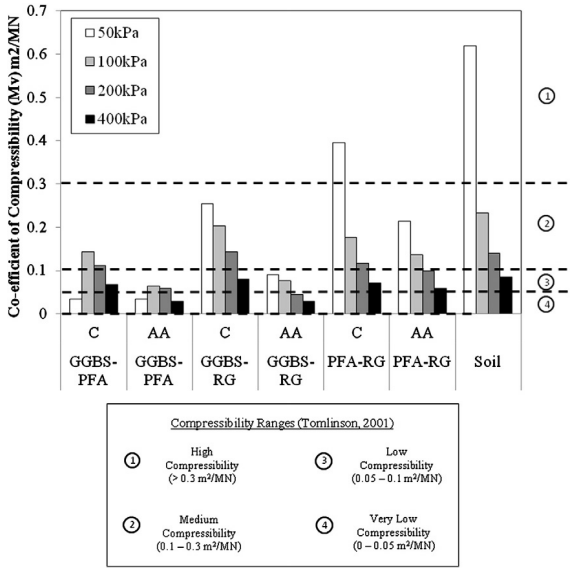

Fig. 8. Summary of the M_v values (m^2/MN) calculated from oedometer tests.

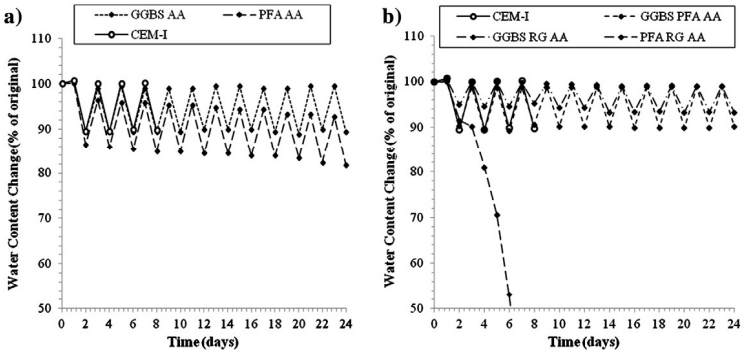

Fig. 9. Water content changes experienced during wetting–drying testing by: a) single binders and b) multi binders.

4.4. Water content testing

In order to determine whether there was sufficient water within the samples for continuing hydration and formation of cementitious gels, sub-samples were retained for water content testing immediately after strength testing. Testing was carried out in general accordance with BS 1377: Part 2 (BSI, 1990). Where samples contained gypsum, an adjustment to the testing procedure was made. Given that the conventional test requires samples to be dried at 110 °C, exposure to such high temperatures will cause the conversion of gypsum to anhydrite and lead to an incorrect water content reading. Therefore gypsum samples were dried at 45 °C for twice the standard drying time.

From Table 5, most samples had water contents ranging between 12 and 14% over the 28 day curing period. However, a few samples had water contents of ~11% (PFA–AA/C) and 16% (PFA–RG–AA). This indicates that there was sufficient water within the samples for hydration to occur throughout the testing periods.

4.5. pH testing

Previous studies (Hughes et al., 2011) have identified that insufficient pH (<10.5) within soils stabilised with pozzolanic material can result in low strength development. Therefore in this study, sub-samples were retained after strength testing at 28 days and their pH checked in accordance with BS 1377: Part 3 (BSI, 1990). pH results are shown in Fig. 13.

Average pH values of 9.0, 6.23 and 9.7 were recorded for non-activated GGBS, RG and PFA-stabilised soils, respectively; whereas values of 11.47, 11.1 and 11.7 were achieved for their respective activated mixtures. pH values obtained for activated samples comprising two IBP's were greater than those above; whereby GGBS–PFA, GGBS–RG and PFA–RG samples ranged between 12.4–12.7, 11.9–12.4 and 12.1–12.5, respectively.

4.6. Mineralogy

The 28 day cured UCS samples were retained after strength testing for a qualitative XRD analysis to examine the mineralogy of the combined IBP-stabilised samples, specifically focussing on determining whether cementitious minerals (such as C-S-H and C-A-H) were present within the samples, which have been documented in the literature to cause strength development within stabilised soils. Additionally, attention was paid towards searching for any problematic minerals such as Ettringite, which is known for its potential to cause soils to swell and ultimately lead to the structural degradation of its matrix through sulphate attack. The results of the analysis (Table 6) demonstrate that

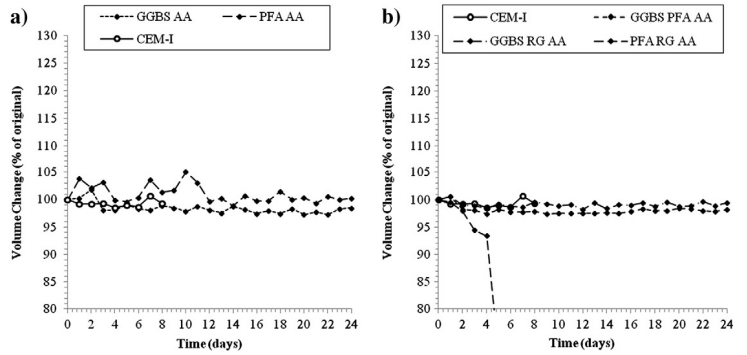

Fig. 10. Volume changes experienced during wetting–drying testing by: a) single binders and b) multi binders.

Table 3
Average number of testing cycles survived by soil-binder mixtures during wetting–drying testing.

Binder mixture	No. of cycles survived
GGBS–AA	12
GGBS–C	0
PFA–AA	12
PFA–C	0
RG–AA	0
RG–C	0
GGBS–RG–AA	12
GGBS–RG–C	12
GGBS–PFA–AA	12
GGBS–PFA–C	0
PFA–RG–AA	5
PFA–RG–C	0
CEM-I	4.5

alkali activated binders which exhibited the highest strength gains during UCS testing also contained common hydrated cement minerals. Conversely, samples which exhibited lower strengths during UCS testing did not appear to show any evidence of cementitious bond formation.

Analyses showed that kaolinite and quartz mineral phases were present within all samples, which was expected given that they were the artificial silty sand's two key constituents. Cementitious C-S-H minerals were observed within GGBS–PFA–AA and PFA–RG–C samples, aluminium oxide within PFA–RG–AA and calcium aluminium oxide hydrate within GGBS–RG–C. Thenardite was observed within PFA–RG–AA samples, which is an anhydrous sodium sulphate mineral that causes unfavourable sulphate attack within concrete and masonry, consequently reducing strength through expansion and leading to degradation (Rodriguez-Navarro et al., 2000).

5. Discussion

5.1. Strength

Testing results indicate that more cementitious bonds formed over 28 days within all alkali activated samples. RG samples showed disappointing strength developments and plastic behaviour; thereby suggesting that its use along with alkali activation as a single binder within artificial alluvium is not recommended. RG's poor performance was at least partly attributed to the method in which its filter cake was prepared for testing; whereby it was dried and then ground down to a powder using a mortar and pestle. This may have produced a powder that was coarser and less uniform than the GGBS or PFA powders used. Drying the filter cake would have altered RG's microchemical structural properties, which comprises water; whereby a large proportion of RG's natural water content would have evaporated and consequently weakened its mineralogical structure. As determined by Beretka et al. (1996), RG is not pozzolanic and has not been greatly researched for use as a binder. Thus, this study examined RG's use in combination with GGBS and PFA to form binders. Strengths significantly improved when RG was combined with GGBS and had been activated; whereas those achieved by PFA–RG samples were much smaller. Although Hughes (2005) found GGBS–RG to be more favourable than CEM-I, GGBS–AA specimens from this study showed strength enhancements to exceed those of both GGBS–RG and CEM-I, reaching compressive strengths of over 6 MPa after 28 days.

According to Fraay et al. (1989), PFA retards cementitious bond development; whereby pozzolanic reactions can take over a week to initiate, resulting in initial slow strength developments. However, this was not observed during this study. Given that Fraay et al.'s (1989) experiments were not activated to raise water pH and initiate pozzolanic reactions, the use of alkali activators for PFA in this study resulted in sudden strength gains within the first week of testing.

With reference to the values obtained for the artificial silty sand's low CEC, charge density and surface area, it appears that they resemble a sandy loam alluvial soil according to Ersahin et al. (2006). With such a low clay and high sand content within the artificial soil, this in turn presents a significantly limited number of sites within the soil for cation exchange and subsequent hydration and pozzolanic reactions to occur. Thus, it is possible that the addition of the alkali activator within certain IBP-soil mixtures has over-compensated for the lack of cation exchange surfaces available by increasing the soil's pH, which has ultimately led to the dissolution of silica from the clay particles and subsequent formation of cementitious gels. There are a number of previous studies which have used (low-alkaline) PFA as a binding agent and have shown much more encouraging strength performances than that observed in this paper; notably that by Horpibulsuk and Raksachon (2010). Although their study used cement in combination with the PFA, Horpibulsuk and Raksachon (2010) stabilised a silty clay comprising 2% sand, 45% silt and 53% clay. Therefore, based on basic CEC theory in terms of soil stabilisation, Horpibulsuk and Raksachon's (2010) soil would have provided a significantly higher number of cation exchange sites than that provided by this study's artificial silty sand. Should a future artificial soil be manufactured with a different clay of higher CEC, it is postulated that the performance of the alkali activated PFA binder would surpass that observed in this paper.

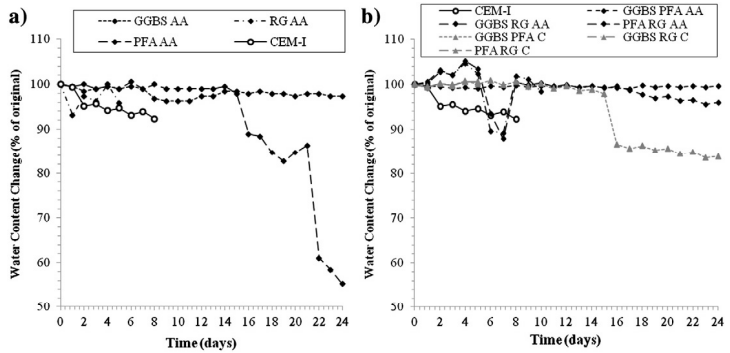

Fig. 11. Water content changes experienced during freezing–thawing testing by: a) single binders and b) multi binders.

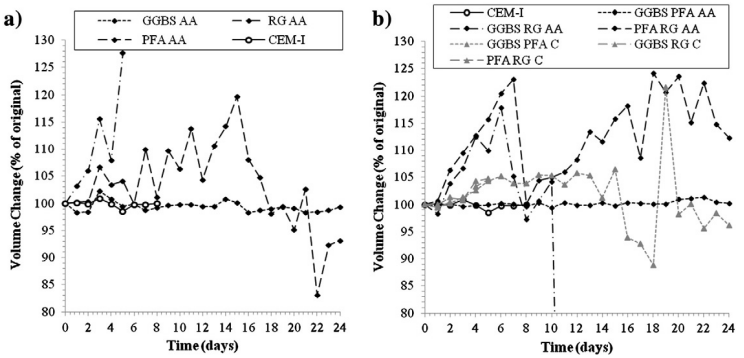

Fig. 12. Volume changes experienced during freezing–thawing testing by: a) single binders and b) multi binders.

In addition to strength enhancements, alkali activation caused considerable increases in stiffness; as observed for GGBS–AA samples. Such soils were liable to experience brittle failure, which can be geotechnically unfavourable, e.g. when dynamically loaded. According to Rowles and O'Connor (2003), higher silica to alumina ratios result in higher compressive strengths being achieved by alkali activated samples; thereby explaining the low strengths achieved by PFA during this study, which comprises mainly silica and alumina (i.e. a low silica to alumina ratio). Additionally, higher silica ratios within a material have been documented to enhance elasticity (Rowles and O'Connor, 2003).

Results from both shear and compressive strength testing have demonstrated that the length of curing imposed on samples has a considerable influence on the final strengths achieved, and ultimately on the performance of the alkali activation (Hughes et al., 2011). Even though alkali activation during this study increased strength gain rates for numerous samples that had been cured at 20 °C, work by Palomo et al. (1999) suggests that if samples are cured at higher temperatures, specifically during the first 5 h of curing, reaction rates are increased even further and therefore result in further improved strength properties. However, the practicality of applying such heating conditions on site may be limited and could also potentially be financially and environmentally costly; thereby defeating the objective of sustainability.

5.2. Compressibility

According to criteria stated by Tomlinson (2001), the study's oedometer results demonstrated that each binder improved the artificial soil's initially high level of compressibility to at least a medium to low level of compressibility. Alkali activated specimens also resulted in much greater improvements than those which had not, particularly those which contained the GGBS–PFA binder. Thus, as similarly observed during compressive strength testing after 28 days curing, alkali activated GGBS–PFA oedometer samples exhibited the least amount of compression due to its high level of stiffness; which was closely followed by activated GGBS–RG samples. Although the activated and non-activated PFA–RG samples produced lower Mv values than those achieved by the untreated silty sand after each loading stage, the compression indices for the PFA–RG samples were still comparable with that of the silty sand. Therefore, rather than creating cementitious bonds to reduce compressibility, the PFA–RG binder has acted as a bulking agent. As outlined in the discussion of the strength results, it is anticipated that improved compressibility performances of the GGBS and PFA binders may be observed within a soil that has a higher surface area and cation exchange capacity. However, stabilised soils with high strengths and stiffness after 28 days curing may experience unfavourable brittle failure, should any large static or dynamic stresses

Table 4
Average number of testing cycles survived by soil-binder mixtures during freezing–thawing testing.

Binder mixture	No. of cycles survived
GGBS–AA	12
GGBS–C	0
PFA–AA	12
PFA–C	0
RG–AA	3
RG–C	0
GGBS–RG–AA	8.75
GGBS–RG–C	7.5
GGBS–PFA–AA	12
GGBS–PFA–C	12
PFA–RG–AA	12
PFA–RG–C	3.75
CEM-I	4.5

Table 5
Average changes in water content observed with increasing curing time for non-activated and alkali activated soil-binder mixtures.

Binder	Water content (%) with increasing curing time			Reduction in water content (%)
	1 day	7 days	28 days	
GGBS–AA	12.90	12.30	12.20	0.70
GGBS–C	12.80	12.90	12.70	0.10
PFA–AA	12.70	12.60	11.20	1.50
PFA–C	12.30	12.10	11.70	0.60
RG–AA	14.50	14.10	14.10	0.40
RG–C	13.30	12.90	12.50	0.80
GGBS–PFA–AA	13.0	12.12	11.85	1.15
GGBS–PFA–C	13.68	12.68	11.12	2.56
GGBS–RG–AA	12.11	11.41	11.08	1.03
GGBS–RG–C	13.95	13.65	11.45	2.50
PFA–RG–AA	13.10	12.51	12.04	1.06
PFA–RG–C	13.46	13.46	12.64	0.82
CEM-I enhanced	15.29	13.25	11.92	3.37

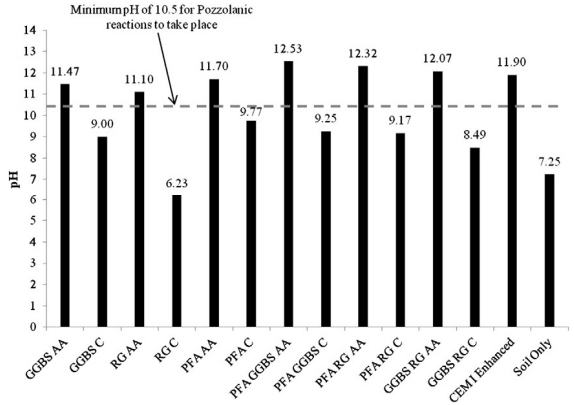

Fig. 13. Bar chart showing the average pH values obtained by all non-activated and alkali activated samples over a curing period of 28 days.

be exerted. Should further oedometer testing be conducted on these IBP binders, it would be the intention of the authors to conduct a testing procedure comprising a number of unloading and reloading stages in order to more accurately define each binder's compressibility and swelling behaviour.

5.3. Durability

Overall, the addition of alkali activated GGBS or GGBS–PFA binders to the artificial silty sand produced the most enhanced durability performances. Albeit a GGBS-based binder, a brittle failure was observed for a GGBS–RG–AA sample whilst thawing, due to crack formation during freezing. Samples containing RG or PFA–RG binders were considered the least durable, due to their premature disintegration during wetting–drying testing and disintegration for an activated specimen after the third cycle during freeze–thaw testing. As previously discussed, the technique used to prepare RG produced non-uniform coarse-grained samples that were potentially less dense and more permeable than GGBS or PFA. This would have enabled water to permeate through RG-stabilised samples and consequently result in swelling; thereby making the material prone to disintegration. The presence of thenardite within activated PFA–RG samples may have also promoted sample swelling and degradation during durability testing.

As generally demonstrated by samples mixed with GGBS, GGBS–PFA and GGBS–RG, alkali activation proved successful in producing denser and less porous/permeable materials, which reduced the likelihood of water absorption and consequent sample degradation through shrinkage and swelling due to wetting–drying and freezing–thawing cycles. However, based on the soil and binder dosages examined, the future potential of RG and PFA as binders in enhancing the durability performance of sandy soils appears to be limited and therefore requires further research.

Table 6
Summary of the cementitious and problematic mineral phases found during XRD analyses of samples.

Binder mixture	Cementitious mineral phases recorded
GGBS–RG–AA	Calcium sulphate hydrate, calcium aluminium oxide hydrate
GGBS–RG–C	Ettringite
GGBS–PFA–AA	Calcium silicate hydrate
GGBS–PFA–C	Gypsum
PFA–RG–AA	Aluminium oxide and thenardite
PFA–RG–C	Calcium silicate
CEM-I	Portlandite and calcium silicate hydrate

5.4. Water content

For binders to hydrate and cementitious bonds to form within stabilised samples, sufficient quantities of natural soil water are required within samples. When the stabilised samples were produced, their initial water contents were recorded to be approximately 15%. After each curing period, sample's water contents were measured after compressive strength testing. Generally, water contents decreased over 28 days by a maximum of only 3%; thereby suggesting that all samples contained sufficient quantities of water for hydration reactions to occur and therefore the formation of cementitious bonds.

Part of activated sample's water contents gets consumed by pozzolanic reactions (Duxson et al., 2007), whereby calcium hydroxide is transported via water to combine with siliceous and aluminate minerals, which dissolve to form strengthening C-S-H/C-A-H gels. During this study, samples' compressive strengths increased with decreasing water content, which corresponds with Duxson et al.'s (2007) findings. In addition, Duxson et al. (2007) determined that water gets consumed during dissolution of geopolymeric reactions; whereby solid aluminosilicates break down through alkaline hydrolysis, resulting in silicate and aluminate species. This also suggests that activated samples have lower water contents than non-activated samples. However, this may not always apply and that non-activated samples may lose similar volumes of water via evaporation before testing.

Albeit there is clearly evidence for slight decreases in samples' water contents, which may be attributed to hydration and pozzolanic reactions; based on the low surface area and CEC of the artificial silty sand, it may be possible that the binders which demonstrated relatively poor performances in this study may be more successful within other soils characterised by higher clay contents. This would be due to more cation exchange sites being available for cementitious bonds to form as a result of hydration and pozzolanic reactions; causing greater water content reductions compared with those observed in this study over similar curing periods.

As all samples were produced through compaction within a mould, it is possible that negative pore water pressures may have developed during this process, as seen by Hughes et al. (2011). This in turn may have slightly increased the strength values recorded. For soils which have higher clay contents than the samples tested during this study, these would be characterised by low levels of permeability and would significantly limit the amount of water accessible for hydration reactions to occur in the field (Hughes et al., 2011).

5.5. Mineralogy and pH

Previous studies have shown that a soil's pH may strongly influence its strength development; whereby higher UCS values (i.e. > 1 MPa) are achieved by alkali activated samples whose pH values are > 10.5; thereby allowing long-term pozzolanic reactions to occur. However, a number of samples with high pH levels did not achieve high compressive strengths; e.g. RG–C, RG–AA and PFA–RG–AA specimens. If oxidising reactions and subsequent pH reduction occur within IBP-stabilised samples, pozzolanic reactions and strength gains can become inhibited. It is therefore essential to make an assessment of the quantity of alkali activator to be added to soils prior to treatment to ensure that pH remains above 10.5 for a sufficient period for curing to occur.

Mineralogically, XRD analyses from this study provided evidence for the existence of cementitious calcium silicate hydrate and calcium aluminium oxide hydrate minerals within certain alkali activated samples. Thenardite was observed within a PFA–RG–AA sample, which can cause sulphate attack and strength degradations within concrete (Rodriguez-Navarro et al., 2000) and therefore potentially cemented soils. No thaumasite was observed within any samples, however ettringite was only observed within one GGBS–RG–AA sample. The presence of ettringite and/or thaumasite within calcium-based stabilised sulphate-bearing clay soils can cause structural distress (Little et al., 2005). However, in the case of this study and that by Wild et al. (1998) for clay–lime–GGBS–gypsum systems with high lime–low GGBS compositions, Ettringite may not have weakened the soils by swelling, but instead strengthened them.

5.6. Alkali activator

The alkali activator used in this study comprised two parts sodium silicate solution to one part sodium hydroxide; whereby its effectiveness in raising pH and producing strength improvements has been seen, particularly for GGBS-based binders. The addition of these constituents to any commercial binder would have an associated cost and add to the complexity and risk of the mixing process. Particularly for the sodium silicate solution component, this alkali can be expensive to produce and the environmental impact resulting from its manufacture can be fairly significant (Habert et al., 2011). Additionally, given that the sodium silicate used was in liquid-form, it would not be applicable to deep dry mixing. Hence, substituting these with a high alkalinity waste-based powder would be desirable to make these binders more commercially viable and easier to use on site. According to Habert et al. (2011), using sodic slags as a replacement for sodium silicate may be a viable option.

6. Conclusions and recommendations

From the laboratory experiments conducted within this study the following conclusions can be drawn.

- Alkali activated cements have the potential to be used as replacements for CEM-I and lime in stabilising soft soils in construction projects. Strengths and stiffnesses achieved by soils improved with these binders would be sufficient for construction specifications.
- Waste based binders could be substituted for CEM-1 and lime in the dry deep mixing process with only minimal modification to existing plant and equipment or a reduction in the efficiency of the installation process.
- Whilst the sodium hydroxide–sodium silicate activator used within this study was shown to be effective in raising pH to a sufficient level within the samples, there may be some difficulties in using it on site from a cost/practicality basis — specifically in terms of the sodium silicate. Substituting these with a high alkalinity waste based powder would have clear advantages.
- Of the mixtures tested, the alkali activated GGBS binder exhibited the highest strength gains. However, alkali activated GGBS–PFA and GGBS–RG also exhibited high strengths. Some engineering specifications require high strengths and stiffnesses and in these cases using activated GGBS would be the most logical replacement for CEM-1 and lime. With that said, there are also engineering scenarios such as the foundations for high speed rail lines where the dynamic loading of the ground caused by passing train traffic requires lower stiffness to prevent brittle failure of the ground. In these cases using activated GGBS–PFA or GGBS–RG within problematic silty sandy soils would be preferable. Also, taking into account the need for disposal of these materials, using activated GGBS–PFA and activated GGBS–RG in ground improvement may be more desirable from an environmental and costs perspective.

Acknowledgements

The authors would like to thank ScotAsh Ltd, Frodingham Cement Ltd and Huntsman Tioxide Europe Ltd for providing the materials tested. We would also like to thank master's degree students M Dixon, A Onibonje, H King and D Alazigha for their assistance in the laboratory. Thanks also go to St. James's Investments (London, UK) for sponsoring P. Sargent whilst this paper was being produced.

References

Ahnberg, H., Johansson, S.-E., Pihl, H., Carlsson, T., 2003. Stabilising effects of different binders in some Swedish soils. Ground Improvement 7, 9–23.
Al-Tabbaa, A., 2003. Soil mixing in the UK 1991–2000: state of practice report. Ground Improvement 7, 117–126.
American Society for Testing and Materials (ASTM), 1996. Designation: D 559–89 standard test methods for wetting and drying compacted soil–cement mixtures. Annual Book of ASTM Standards, 4.08. West Conshocken: Pa.
American Society for Testing, Materials (ASTM), 1996b. Designation: D 560–96 standard test methods for freezing and thawing compacted soil–cement mixtures. Annual Book of ASTM Standards, 4.08. West Conshocken: Pa.
Beretka, J., Ciolfi, R., Marroccoli, M., Valenti, G., 1996. Energy-saving cements obtained from chemical gypsum and other industrial wastes. Waste Management 16, 231–235.
BSI, 1990. BS: 1377 Incorporating Amendment No. 1, Methods of Test for Soils for Civil Engineering Purposes. British Standards Institution, Milton Keynes.
BSI, 1999. BS: 5930, Incorporating Amendment No. 1, Code of Practice for Site Investigations. British Standards Institution, Milton Keynes.
BSI, 2000. BS EN: 197-1 Incorporating Amendments No.1 and 2, Composition, Specifications and Conformity Criteria for Common Cements. British Standards Institution, Milton Keynes.
CDIT, Coastal Development Institute of Technology, 2002. The Deep Mixing Method: Principle, Design and Constructions. A. A. Balkema, The Netherlands.
Clarke, D., Smethurst, J.A., 2010. Effects of climate change on cycles of wetting and drying in engineered clay slopes in England. Quarterly Journal of Engineering Geology & Hydrogeology 43, 473–486.
Cooper, T.H., 2009. Unit 12 Chapter 2 — Cation exchange and cation exchange capacity. [online] Available at http://www.swac.umn.edu/classes/soil2125/doc/s12ch2.htm [Last accessed 20th June 2012].
Craig, R.F., 2004. Soil Mechanics, Seventh edition. Spon Press, Taylor & Francis Group978-0-415-32703-9.
Davidson, L.K., Demirel, T., Handy, R.L, 1965. Soil pulverization and lime migration in soil lime stabilisation. Highway Research Record 92, 103–126.
Duxson, P., Fernandez-Jimenez, A., Provis, J.L., Lukey, G.C., Palomo, A., Deventer, J.S.J., 2007. Geopolymer technology: the current state of the art. Journal of Materials Science, Advances in Geopolymer Science and Technology 42, 2917–2933.
Ersahin, S., Gunal, H., Kutlu, T., Yetgin, B., Coban, S., 2006. Estimating specific surface area and cation exchange capacity in soils using fractal dimension of particle-size distribution. Geodema 136, 588–597.
Fraay, A.L.A., Bijen, J.M., Haan, D.Y.M., 1989. The reaction of fly ash in concrete: a critical examination. Cement and Concrete Research 19, 235–246.

Glendinning, S., Rogers, C.D.F., 1996. Deep stabilisation using lime. In: Dixon, N., Glendinning, S., Rogers, C.D.F. (Eds.), Lime Stabilisation. Thomas Telford, London, pp. 127–138.
Habert, G., d'Espinose de Lacaillerie, J.B., Roussel, N., 2011. An environmental evaluation of geopolymer based concrete production: reviewing current research trends. Journal of Cleaner Production 19, 1229–1238.
Hansson, T., Parry, L., Graham, M., Troughton, V., Eriksson, H., 2001. Limix: a deep dry mixing system used at channel tunnel rail contract 440. Proceedings of Underground Construction 2001 Symposium and Exhibition, London. Institute of Materials, Minerals and Mining, London.
Horpibulsuk, S., Raksachon, Y., 2010. Fly ash as a dispersing material in cement stabilization. Ground improvement and geosynthetics, proceedings of sessions of Geoshanghai 2010: ASCE Geotechnical special publication no. 207, pp. 137–142.
Hossain, K.M.A., 2010. Development of stabilised soils for construction applications. Proceedings of the Institution of Civil Engineers, Ground Improvement 163, 173–185.
Hughes, P.N., 2005. The Use of Synthetic Red Gypsum as a Construction Material. PhD Thesis, School of Civil Engineering and Geosciences, Newcastle University, UK.
Hughes, P.N., Glendinning, S., Manning, D.A.C., Noble, B.C., 2010. Production of 'green' concrete using red gypsum and waste. Proceedings of the Institution of Civil Engineers, Engineering Sustainability 163, 137–146.
Hughes, P.N., Glendinning, S., Manning, D.A.C., White, M.L., 2011. Use of red gypsum in soil mixing engineering applications. Proceedings of the Institution of Civil Engineers, Geotechnical Engineering 164, 223–234.
ICDD, 1999. The Powder Diffraction File: Database of the International Centre for Diffraction Data, Sets 1–49. ICDD, Newtown Square, PA.
Jegandan, S., Liska, M., Osman, A.A.-M., Al-Tabbaa, A., 2010. Sustainable binders for soil stabilisation. Proceedings of the Institution of Civil Engineers, Ground Improvement 163, 53–61.
Little, D.N., Herbert, B., Kunagalli, S.N., 2005. Ettringite formation in lime-treated soils: establishing thermodynamic foundations for engineering practice. Transportation research record: journal of the transportation research board; soil mechanics 2005. Transportation Research Board of the National Academies 1936, 51–59.
McGuire, M., Templeton, E., Filz, G., 2012. Stability analyses of a floodwall with deep-mixed ground improvement at Orleans Avenue Canal, New Orleans. ISSMGE — TC 211 International Symposium on Ground Improvement IS-GI Brussels, 31st May & 1st June 2012, vol. 2, pp. 199–209.
McLellan, B.C., Williams, R.P., Lay, J., van Riessen, A., Corder, G.D., 2011. Costs and carbon emissions for geopolymer pastes in comparison to ordinary portland cement. Journal of Cleaner Production 19, 1080–1090.
Meunier, A., 2005. Clays. Springer Publishing, Berlin Heidelberg New York3-540-21667-7.
Palomo, A., Grutzeck, M.W., Blanco, M.T., 1999. Alkali-activated fly ashes. A cement for the future. Cement and Concrete Research 29, 1323–1329.
Rodriguez-Navarro, C., Doehne, E., Sebastian, E., 2000. How does sodium sulphate crystallised? Implications for the decay and testing of building materials. Cement and Concrete Research 30, 1527–1534.
Rogers, C.D.F., Glendinning, S., Holt, C.C., 2000. Slope stabilisation using lime piles — a case study. Proceedings of the Institution of Civil Engineers, Ground Improvement 4, 165–176.
Rowles, M., O'Connor, B., 2003. Chemical composition of the compressive strength of aluminosilicate geopolymers synthesised by sodium silicate activation of metakaolinite. Journal of Materials Chemistry 13, 1161–1165.
Sherwood, P.T., 1993. Soil Stabilisation with Cement and Lime — State of the Art Review. Transport Research Laboratory, Department of Transport. HMSO Publications0-11-551171-7.
Threadgold, L., 1996. Slope stabilisation using reinforced lime piles. In: Dixon, N., Glendinning, S., Rogers, C.D.F. (Eds.), Lime Stabilisation. Thomas Telford, London, pp. 176–183.
Tomlinson, M.J., 2001. Foundation Design and Construction, Seventh edition. Pearson Education, Prentice Hall0-13-031180-4.
Weil, M., Dombrowski, K., Buchwald, A., 2009. Life-cycle analysis of geopolymers. In: Provis, J.L., Van Deventer, J.S.J. (Eds.), Geopolymers: Structures, Processing, Properties and Industrial Applications. Woodhead Publishing Limited, Cambridge, England, pp. 194–210.
Wild, S., Kinuthia, J.M., Jones, G.I., Higgins, D.D., 1998. Effects of partial substitution of lime with ground granulated blast furnace slag (GGBS) on the strength properties of lime-stabilised sulphate bearing clay soils. Engineering Geology 51, 37–53.

Appendix 4:

Alkali Activated Cements

Book Chapter

The development of alkali-activated mixtures for soil stabilisation

21

P. Sargent
AECOM, Newcastle upon Tyne, UK

21.1 Introduction

Chemical (admixture) stabilisation introduces cementitious materials to soft problematic soils, with a view to improving their engineering properties including strength and durability. Portland cement (CEM-I; BS EN: 197-1) and lime have long been utilised as binders; the former is considered more favourable in providing rapid strength enhancements (Rogers *et al.*, 2000; Hossain, 2010; Jegandan *et al.*, 2010). The presence of soil water and calcium silicates/aluminates within the binders react to form hydration products including calcium silica hydroxide (C-S-H) and calcium aluminate hydroxide (C-A-H) gels.

Negative environmental and financial issues are associated with utilising CEM-I and lime as binders; specifically high energy consumption, financial cost, greenhouse gas and carbon emissions. The continued use of these binders is not sustainable. Hence, there is a need to identify more environmentally and financially sustainable replacement binders. These binders should provide engineering performances that are either comparable or surpass those of CEM-I and lime within similar curing times.

A popular route for selecting new binders has been to recycle industrial by-products (IBPs), preferably those which are alumino-silicate based (i.e., pozzolanic). The introduction of alternative alkali activators such as sodium hydroxide to these IBPs, can increase the rate at which the mechanical properties of stabilised soils are improved by increasing soil pH, thereby allowing pozzolanic reactions and cementitious bonding to occur (Palomo *et al.*, 1999).

The primary aim of this chapter is to present the most up-to-date literature on the development and use of alkali-activated cements as binders for chemical soil stabilisation. The first few sections address the basic mechanisms of chemical soil stabilisation, traditionally used binders and this technique's applicability in geotechnics. Findings from recent research on sustainability in terms of environmental and financial costs will then be presented, outlining the need for new sustainable binders. The final sections will then present findings from recent laboratory-based research on the development of new alkali-activated cement mixtures, in addition to possible future trends in this research area.

Handbook of Alkali-activated Cements, Mortars and Concretes. http://dx.doi.org/10.1533/9781782422884.4.555

21.2 Basic mechanisms of chemical soil stabilisation

There are five main reactions which occur between the binder and the soil to be stabilised: cation exchange, flocculation/agglomeration, hydration, pozzolanic reactions and potentially carbonation. Cation exchange and flocculation/agglomeration occur immediately upon mixing and can last for up to a few hours afterwards. Hydration takes place up to one month post-mixing, whereas pozzolanic reactions occur over a longer time-scale, i.e. months or years.

21.2.1 Cation exchange

Immediately upon mixing, the introduction of a binder to the soil releases calcium ions, which can exchange with metal ions (e.g., Na^+ and Al^{3+}) incorporated within the soil's clay lattice (Rogers and Glendinning, 1996). This process is referred to as cation exchange, which results in numerous physical changes to the soil. One of the first changes to occur is a reduction in the electric double (adsorbed water) layer surrounding clay particles (Rogers and Glendinning, 1996). The physical arrangement of clay particles dictates the size of the electric double layer; parallel arrangements allow larger envelopes to form compared with 'edge-to-face' arrangements. A reduction in the electric double layer thickness means that clay particles are less prone to the addition of water. The second change experienced is flocculation, whereby van der Waals forces overcome the repulsion of the negatively charged clay particles, bringing them into close proximity with each other and further reducing the thickness of the adsorbed water layer (Figure 21.1).

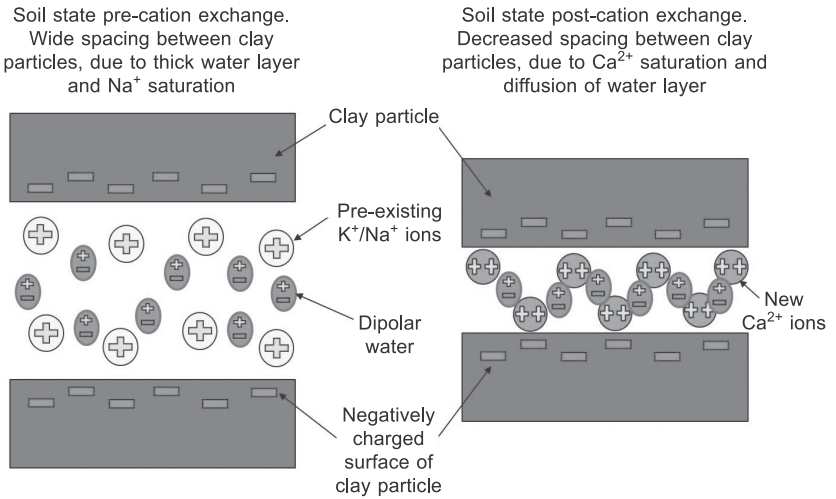

Figure 21.1 Diagram demonstrating cation exchange within soils, which occurs immediately upon introducing a binder such as lime or cement.

The aforementioned changes result in numerous textural and strength changes within the soil; namely a transition from a medium–high plastic clay to a more granular and friable soil characterised by a lower plasticity index. This results in an increase in the friction angle between agglomerate matter and consequently an increase in shear strength (Rogers and Glendinning, 1996).

Some of the most common cations involved in cation exchange include aluminium (Al^{3+}), calcium (Ca^{2+}), magnesium (Mg^{2+}), potassium (K^{+}), ammonium (NH_4^{+}), sodium (Na^{+}) and hydrogen (H^{+}). A cation's adsorption potential is influenced by valence and atomic weight, whereby the higher these values, the higher the cation's adsorption level.

21.2.2 Flocculation

Flocculation/agglomeration occurs immediately post-mixing, involving the restructuring of negatively charged clay particles which are surrounded by a positively charged cation shell. The cation shell's thickness depends on the level of charge; the higher the charge the thicker the shell. Initially, the clay particles are dispersed and occur in a parallel arrangement, due to their negative surface charge and positively charged cation shells repelling each other. This repulsion may be overcome by van der Waals forces, causing particles to flocculate and give a new edge-to-face orientation (Figure 21.2).

There are two divisions of flocculators: good flocculators are ions with larger hydrated radii and higher valences (≥2+) (Sumner and Naidu, 1998), including Ca^{2+} and Mg^{2+}; poor flocculators include ions with smaller hydrated radii and lower valences, including Na^{+} and K^{+}. As a result of flocculation, soils gain improved

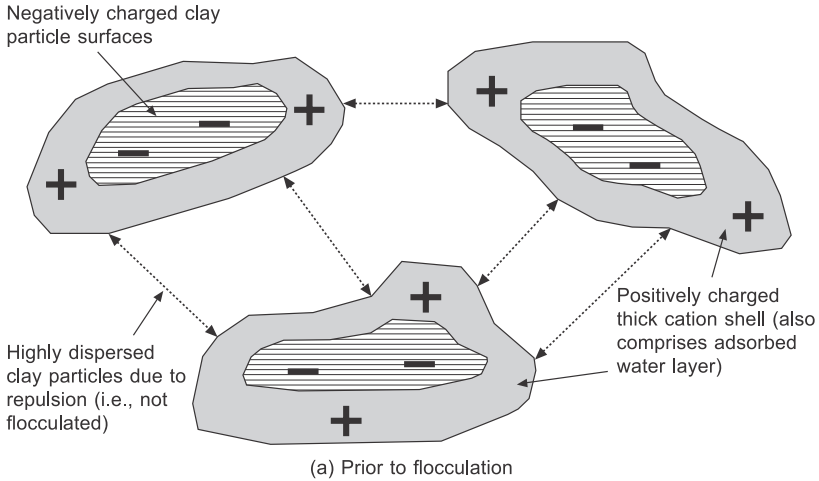

Figure 21.2 Illustration of the state of a soil (a) prior to and (b) post flocculation.

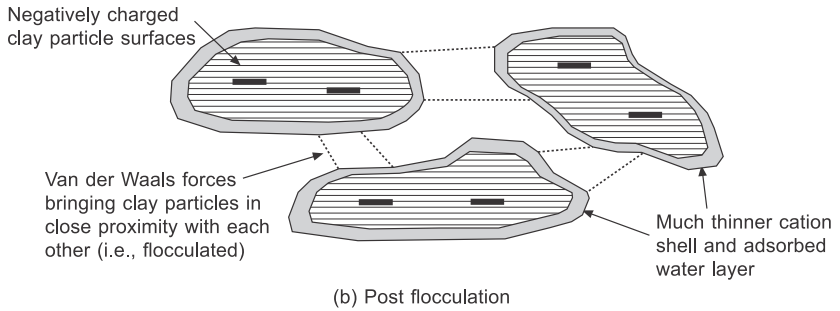

Figure 21.2 Continued

engineering performances, specifically by increasing the plastic limit, increasing shear strength and the development of a granular texture.

21.2.3 Hydration

Hydration occurs when combining water with lime or cement (Eq. 21.1). The hydration of quicklime is exothermic (Figure 21.3); whereby occasionally the amount of heat produced can cause a soil's pore water to boil (Bergado *et al.*, 1996). Upon mixing, the soil's water content instantly decreases as the water is consumed during hydration. This drying process is key in improving soft soils with high moisture contents. According to Bergado *et al.* (1996), the moisture content of the soil must be sufficiently high in order for the quicklime to be completely slaked. There must also be sufficient amounts of water post-evaporation due to the heat produced during slaking, to ensure that ion exchange occurs between calcium ions of hydrated lime and alkali ions of clay minerals (Bergado *et al.*, 1996).

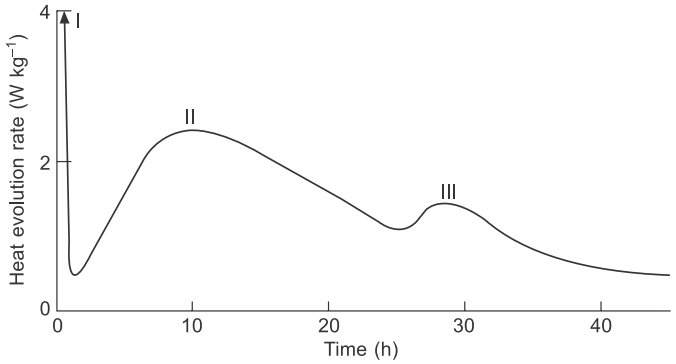

Figure 21.3 Heat evolution during hydration of ordinary Portland cement at 20°C and a water–cement ratio of 0.4. Note the three maxima (I, II and III) in hydration reaction rates. Courtesy of Bye (2011). Reproduced with permission from the Institution of Civil Engineers.

$$CaO + H_2O \rightarrow Ca(OH)_2 + Heat \quad (21.1)$$

The calcium oxide reaction product from Eq. (21.1) dissociates in the pore water, which increases its electrolytic concentration and pH (Eq. 21.2), thereby dissolving SiO_2 and Al_2O_3 from the soil's clay particles (Bergado *et al.*, 1996). These will collectively allow ion exchange, flocculation and pozzolanic reactions to occur (Bergado *et al.*, 1996).

$$Ca(OH)_2 \rightarrow Ca^{++} + 2(OH)^- \quad (21.2)$$

There are two mechanisms involved during hydration: 'through solution' and 'topochemical' (Kurtis, 2007). Through solution involves the dissolution of anhydrous compounds towards their ionic constituents, hydrate formation within the solution and ultimately their precipitation, given their low solubility (Kurtis, 2007). The topochemical mechanism (solid state hydration) involves reactions that occur on anhydrous cement compound surfaces whilst not going into solution (Kurtis, 2007). Five key phases occur upon mixing cement with soil water; firstly the cement particles undergo dissolution followed by increases in ionic concentration levels within the water. Once ionic concentrations have become sufficiently high, compounds develop within solution, whereby once ionic concentration has become saturated these compounds precipitate as solid hydration products. These products form close to or on the surfaces of anhydrous cement particles (Kurtis, 2007).

Four main strength-producing compounds exist within CEM-I, two are silicate-based, two are aluminate-based. Tricalcium silicate (C_3S) hydrates and hardens quickly and accounts for any early setting and strength gains (3 hours–14 days post-mixing).

The second main hydrated cement compound is dicalcium silicate (C_2S) which hydrates and hardens relatively slowly. Rather than contributing towards initial strength gains, the strengthening effects of C_2S are observed at a later stage; normally between 7 and 14 days (Kurtis, 2007). Higher levels of heat are associated with C_3S hydration than with C_2S. The two aluminate-based hydrated cement compounds are tricalcium aluminate (C_3A) and tetracalcium aluminoferrite (C_4AF), whereby the former releases considerable amounts of heat during the first couple of days of curing and is most useful in terms of initial strength development; whereas, the C_4AF hydrates quickly and decreases the clinkering temperature, contributing very little towards strength development (Kurtis, 2007).

All four of the aforementioned compounds are important for providing strength gains. Immediately upon mixing, the cement hydrates very rapidly and produces primary cementitious products (a.k.a. major hydration products), these being hydrated calcium silicates (C_2SH_x and $C_3S_2H_x$) and aluminates (C_3AH_x and C_4AH_x) and hydrated lime (Bergado *et al.*, 1996). The cement particles then create bonds between adjacent cement grains and undisturbed soil particles during the hardening phase, ultimately creating a stronger soil–cement skeleton.

By hydrating both C_3S and C_2S, C-S-H and calcium hydrates (CH) are produced (Figure 21.4); however, C_2S produces significantly lower amounts of CH, which is vital for durability purposes within sulphate-bearing soils (Kurtis, 2007). As is

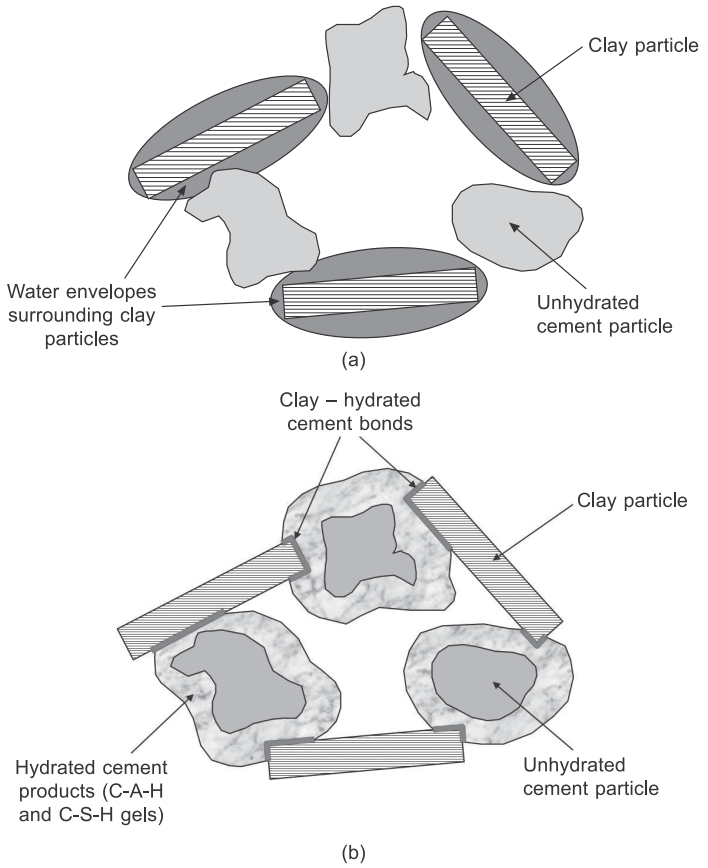

Figure 21.4 The typical state of a soil mixed with cement (a) prior to hydration and (b) after a few weeks curing, whereby the cement has reacted with the soil water and produced hydrated cementitious gels.

commonly known for most chemical reactions, temperature influences the rate of hydration.

C-S-H gels are generally poorly understood regarding their mineralogical structure, due to their wide variation from amorphous to poorly crystalline (Kurtis, 2007). C-S-H is the primary strengthening mineral within CEM-I via ionic and van der Waals bonds, whereby it takes up to 60% of the hydrated cement paste and takes up large surface areas of up to 700 m^2/g (Kurtis, 2007).

According to Kurtis (2007), as the hydration rates of the aforementioned five phases can significantly differ, factors such as the rate of cement hardening, the amount of time required for cement to stiffen and the setting time will ultimately depend on the cement composition. Cement hydration also leads to an increase in

the soil pore water's pH as a direct consequence of the dissociation of the hydrated lime (Bergado *et al*., 1996).

21.2.4 Pozzolanic reactions

Pozzolanic reactions occur over long time scales (months to years). The main mechanism involves the transportation of calcium hydroxide via water within the soil to combine with the aluminate and/or silicate clay minerals (Duxson *et al*., 2007). The high surface area aluminate and silicate minerals are pozzolan phases, which in the presence of water and an alkali (e.g., calcium) produce cementitious materials, comprising calcium silicates and aluminate hydrates (Bergado *et al*., 1996). Any dissolved Ca^{2+} ions within the soil then react with any dissolved SiO_2 and Al_2O_3 located on clay particles to produce hydrated gels of C-S-H and C-A-H, which cement soil particles together as can be seen in Figure 21.5.

$$Ca^{2+} + 2(OH)^{-} + SiO_2 \rightarrow C\text{–}S\text{–}H \quad (21.3)$$

$$Ca^{2+} + 2(OH)^{-} + Al_2O_3 \rightarrow C\text{–}A\text{–}H \quad (21.4)$$

Pozzolanic reactions consume part of the soil's water content. This is preferable in terms of engineering performance of the stabilised soil, as the material becomes stiffer and less susceptible to volume shrinkage/swelling. The soil–binder mixtures cure and produce stronger, cementitious soil matrices known as 'geopolymers' (Sherwood, 1993), which will be able to resist dissolution and soil erosion.

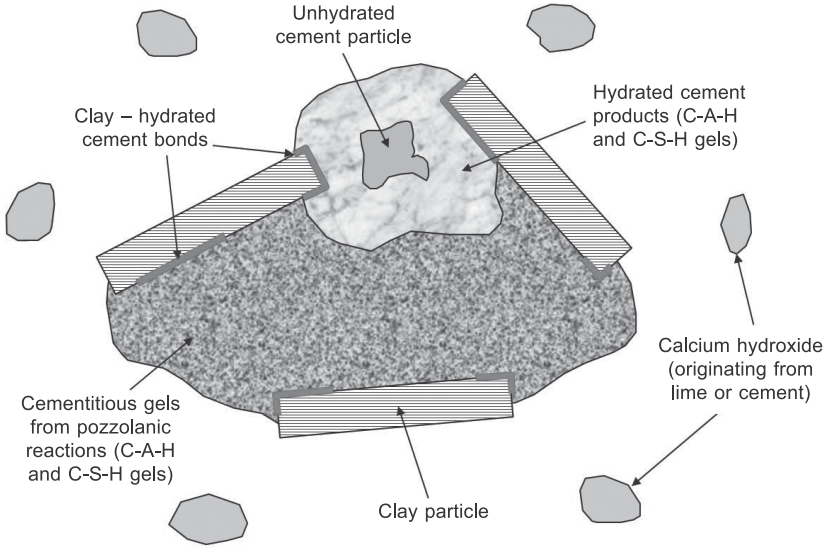

Figure 21.5 Cementitious bonding products formed during hydration and long-term pozzolanic reactions.

According to Bergado *et al*. (1996) and Diamond and Kinter (1965), pozzolanic reactions are not complete until five years post-mixing. The solubility potential of silicates and aluminates within the soil, their likelihood of reacting with lime/cement and cementitious bond formation rely heavily on soil pH. According to Davidson *et al*. (1965), pozzolanic reactions only occur when soil pH is ≥10.5, as this is when SiO_2 and Al_2O_3 become soluble. Broms (1984) and Palomo *et al*. (1999) suggest that if samples cure at higher temperatures during the first 5 hours post-mixing, reaction rates are increased, resulting in further improved strengths.

21.3 Chemical stabilisation techniques

Chemical treatment is a versatile ground improvement technique, which is suitable for stabilising various soils up to 25 m depth. A key advantage of this technique is that a large range of binders are available for selection, each having their own unique set of physicochemical properties that are advantageous in stabilising a soil. Both the soil's and binder's material properties must be carefully studied prior to stabilisation, as a binder may show impressive strength gains within one soil and damaging effects in another.

21.3.1 Surface and shallow soil mixing

Surface and shallow mixing are low cost techniques for enhancing the mechanical properties of soft soils, which cover large areas (Topolnicki, 2004). Surface mixing involves the incorporation of a lime or cement-based binder (dry or wet) within the top 250 mm of soil at air temperatures > 7°C (Figure 21.6). This technique has long been used in the United States and Australia for treating soft subgrades.

Prior to mixing, the binder may be applied by spreading either a dry powder or slurry. Soils which are most suitable for surface mixing are characterised by clay contents > 10%, plasticity index (PI) > 20, an activity PI–clay content ratio > 0.75 and a sulphate content < 1%.

For stabilising the subgrade, the typical binder dosage should be > 2.5%. Once the binder has been mixed into the soil, an uneven surface is produced. Thus, a roller follows behind the mixer to compact the stabilised soil. The main advantage of using surface mixing is negating the need to remove poor soil away from site. Onsite stabilisation reduces the amount of binder/aggregate that would be required if significant quantities of poor soil were to be replaced. Depending on the soil and binder type, additional binder may be introduced to increase strength gain rates. Numerous disadvantages are associated with surface mixing, the most serious of which is dust and atmospheric pollution caused by plant equipment.

Shallow mixing involves treatment up to 3 m depth, whereby large diameter augers and mass mixers stabilise a specific volume of soil (Topolnicki, 2004), commonly called 'mass stabilisation'. The uppermost soil layers may be insufficiently strong to support heavy mixing equipment. Therefore mass mixers/augers should either be

Figure 21.6 Photograph of surface mixing taking place at a site in India (courtesy of Wirtgen Group, 2014).

suspended from a crane or mounted to a cantilever. It is normal practice to initially stabilise a 2 m wide × 5 m long × 3 m deep block of soil that is positioned onsite so it is within the crane's operational range (Topolnicki, 2004). One major disadvantage with shallow mixing is high emissions. To reduce such emissions, mixing tools may be fitted with a hood/bottom-opened cylinder, temporary low-pressure blowers, vacuum pumps, dust collectors, fume incinerators and activated carbon scrubbers (Topolnicki, 2004).

21.3.2 Deep soil mixing

Deep soil mixing (DSM) is used for various geotechnical applications on- and offshore, ranging from environmental remediation to ground improvement for construction purposes including foundations, excavation wall support, liquefaction mitigation, slope stabilisation and embankment hydraulic cut-off walls. DSM involves the mechanical disturbance of a soil via auger mixing up to depths of 25 m (Quasthoff, 2012). Once the auger has been drilled to the required depth, its rotation direction is then reversed and retrieved whilst a binder is pumped through the auger drill bit. The auger's rate of rotation and binder flow must remain constant during mixing, to ensure homogeneous stabilised soil columns are produced. Various auger drill bits are available for use in DSM; whereby the drill bit used depends upon the DSM column diameter required and the soil being stabilised. The fins of the all drill bits are orientated to ensure compaction occurs along the column's length upon auger retraction.

DSM has numerous advantages over other deep ground improvement techniques, including its applicability within a wide variety of soils and its minimal environmental impact due to low levels of vibration, noise and spoil. DSM has high levels of productivity, making it economical for larger projects (Topolnicki, 2004). The desired engineering properties of DSM soils are easily adjustable, as are the column spacing and their installation pattern (Figure 21.7).

For chemical treatment, there are dry and wet mixing methods. Dry mixing involves a dry binder being injected under compressed air into the surrounding soil via nozzles at the tips of the auger mixing tool's blades (Figure 21.8). A similar

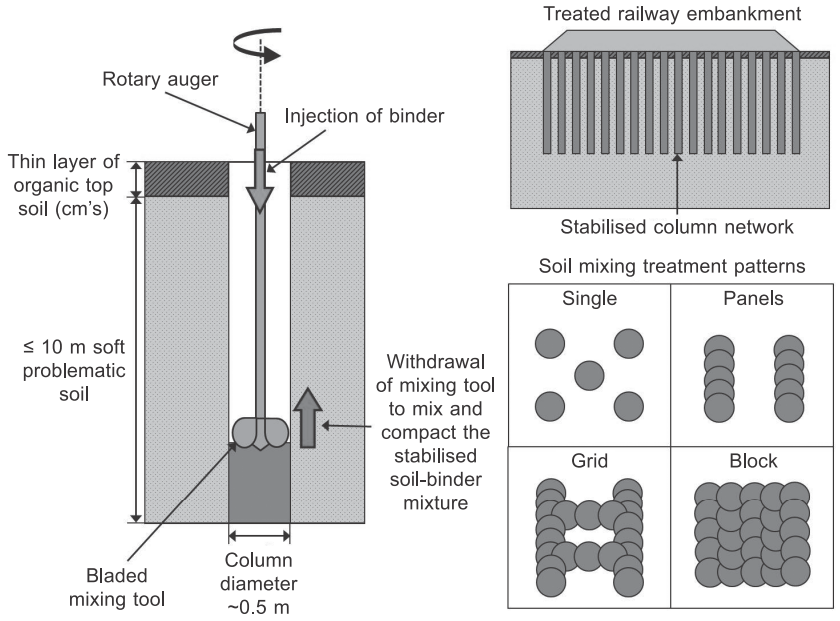

Figure 21.7 Illustration of the DSM technique and its application in ground improvement.

Figure 21.8 Dense network of solidified DSM columns (courtesy of Treviicos, 2013).

process is involved for wet mixing, whereby the binder slurry is supplied from a delivery pump. However, more expensive plant equipment is required, namely a water tank, a temporary storage tank and large silos (Topolnicki, 2004). When determining whether to use wet or dry mixing, the soil's moisture content must be considered. Cohesive soils with moisture contents of 60–200% are most suited for dry mixing (Topolnicki, 2004).

For soils with moisture contents < 20% and/or lower than the soil's plastic limit, the volume of water within the soil would be insufficient for hydration. For DSM projects where high strength columns are essential, wet mixing should be used as it provides higher levels of homogeneity due to longer mixing times. Dry mixing tends to be used when using either a combination of cement and lime or IBPs as binders.

Dry mixing is preferred over wet mixing in regions where long periods of cold temperatures, freeze and thaw cycles are experienced (e.g., Scandinavia) as water-based delivery systems are prone to freezing (Topolnicki, 2004; Quasthoff, 2012). When installing DSM columns through harder stratified soils, wet mixing should be used as the slurry acts as a lubricant, aids and ensures higher torque capacity and consistent strengths along the length of the columns (Topolnicki, 2004).

Since DSM was pioneered in Scandinavia and Japan during the 1960s, the technique has become increasingly popular. Countries including Belgium, Germany, China and US commonly use the technique (Topolnicki, 2004); whereas the UK has only used it since the 1990s (Al-Tabbaa, 2003). For dry and wet DSM, lime and cement have predominantly been used as binders since the 1970s, based on their high strength performance. Where DSM is used for environmental remediation, cementitious binders are substituted with chemical oxidation agents and reactive materials (Topolnicki, 2004).

The strength of DSM soils depends on numerous factors, including the blade rotation number, the mixing energy used, the binder dosage and soil type (Topolnicki and Pandrea, 2012). Table 21.1 summarises the expected engineering properties of DSM soils after 28 days.

Table 21.1 Summary of typical unconfined compressive strength (UCS) and permeability values expected after 28 days curing for various soil types and binder dosages

Soil type	Binder dosage (kg/m^3)	Expected permeability, k (ms^{-1})	Expected UCS (MPa)
Sludge	250–400	1×10^{-8}	0.1–0.4
Peat/Organic silts and clays	150–350	5×10^{-9}	0.2–1.2
Soft clays	150–300	5×10^{-9}	0.5–1.7
Medium–hard clays	120–300	5×10^{-9}	0.7–2.5
Silts and silty sands	120–300	1×10^{-8}	1.0–3.0
Fine–medium sands	120–300	5×10^{-8}	1.5–5.0
Coarse sands and gravels	120–250	1×10^{-7}	3.0–7.0

Source: Data courtesy of Geo-Con, Inc. (1998) and FHWA (2001).

21.4 Soil suitability for chemical treatment

The characteristics of both the stabilisation reactions and the end-products are controlled by numerous key factors associated with the nature of the soil; namely mineralogy, soil grading, cation exchange capacity (CEC) surface area and moisture content. Given that such properties vary greatly between soils, chemical stabilisation may not be suitable for treating all soils.

From Figure 21.9, chemical treatment may be used for soils comprising fine clays to medium/coarse sands. Soils which are deemed suitable for soil mixing include most silts, clays, peats and some non-cohesive granular soils. Soils are required to have a moisture content of ≥20% for DSM to be effective (Quasthoff, 2012). Generally, cohesive fine grained soils achieve better engineering performances after chemical treatment compared with non-cohesive coarse grained soils.

To understand a soil's capacity to react with binders and ultimately produce cementitious gels, workers including Sargent *et al.* (2013) have determined that it is necessary to conduct specific surface area and CEC analyses. Other factors including the organic and sulphate contents of soils also have a role in assessing whether a soil is suitable for chemical treatment.

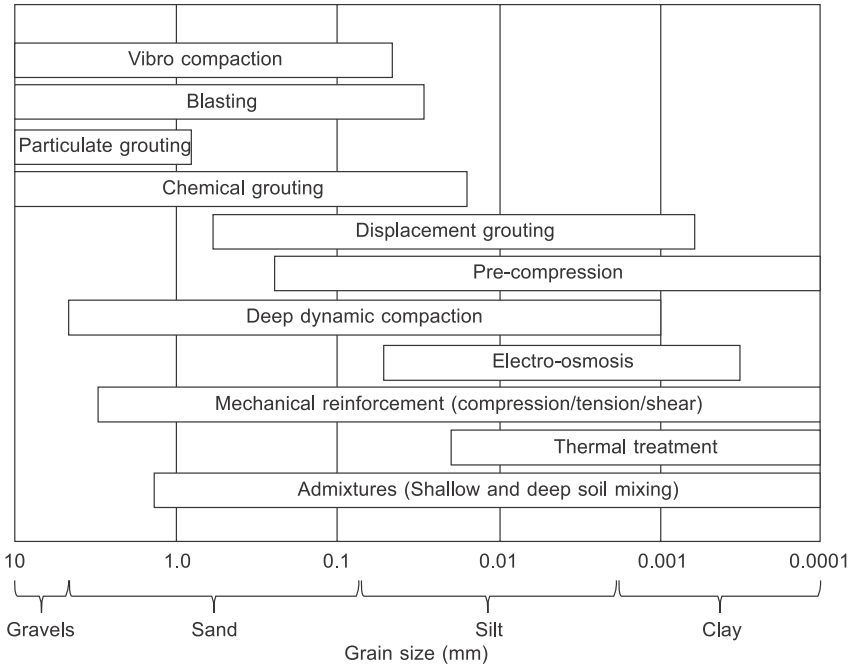

Figure 21.9 Graph showing the influence of a soil's PSD on the applicability of ground improvement techniques which can be used.

21.4.1 Surface area and cation exchange capacity

Quantifying the specific surface area of a soil provides insights into its CEC and particle size distribution. Clay particles have high surface areas, therefore soils with high surface area values indicate high clay contents. This implies that the soil's CEC is likely to be high, suggesting that the soil would be well suited to chemical stabilisation. One of the most widely used techniques for determining the specific surface area of soils is the Brunauer Emmett Teller (BET) method, which involves nitrogen gas adsorption on particle surfaces (Brunauer *et al.*, 1938).

CEC provides an estimate of the net negative charge on soil particulate matter as a result of isomorphous substitution and broken bonds at boundaries (Terzaghi *et al.*, 1996), i.e. the number of sites within a soil which are able to attract, retain and exchange cations. Large proportions of most soils comprise clay minerals and organic matter, both of which are characterised by negative surface charges, implying that they must attract cation elements of the opposite charge. Cations which neutralise negative surface charges within water are able to be exchanged with other cations, which depends upon the cation concentrations within the soil water and their electrovalences (Terzaghi *et al.*, 1996).

Out of kaolinite, illite and montmorillonite, montmorillonite has the highest CEC (Table 21.2), due to its structure comprising multiple single unit sheets (Terzaghi *et al.*, 1996).

Soils containing clay minerals with high CEC values will experience more significant mechanical changes upon mixing compared with those containing clay minerals with low CEC values (Rogers and Glendinning, 1996). Low CEC values are representative of soils characterised by low organic matter contents and low clay/high sand contents (Figure 21.10), which can be expected from river alluvium deposits (Cooper, 2009). A soil's surface area can influence its physical and chemical characteristics, whereby a larger surface area provides more cation exchange surfaces.

Knowledge about the CEC and surface area properties of a soil provides an insight into its potential cementitious gel formation. By using CEC values obtained from laboratory testing and Eq. (21.5) (Meunier, 2005), the CEC-related charge density (σ_{CEC}) may be calculated:

$$\sigma_{\mathrm{CEC}} = \frac{e(\mathrm{CEC} \times 10^{-2})}{2\,ab} \tag{21.5}$$

where e = the elementary charge, which has a constant value of 1.6022×10^{-2} C,

Table 21.2 Summary of cation exchange capacity values of the three principal clay minerals

Clay mineral	Cation exchange capacity (meq/g)
Kaolinite	0.03–0.1
Illite	0.2–0.3
Montmorillonite	0.8–1.2

Source: Values courtesy of Terzaghi *et al.*, 1996. Reproduced with permission from John Wiley & Sons, Inc.

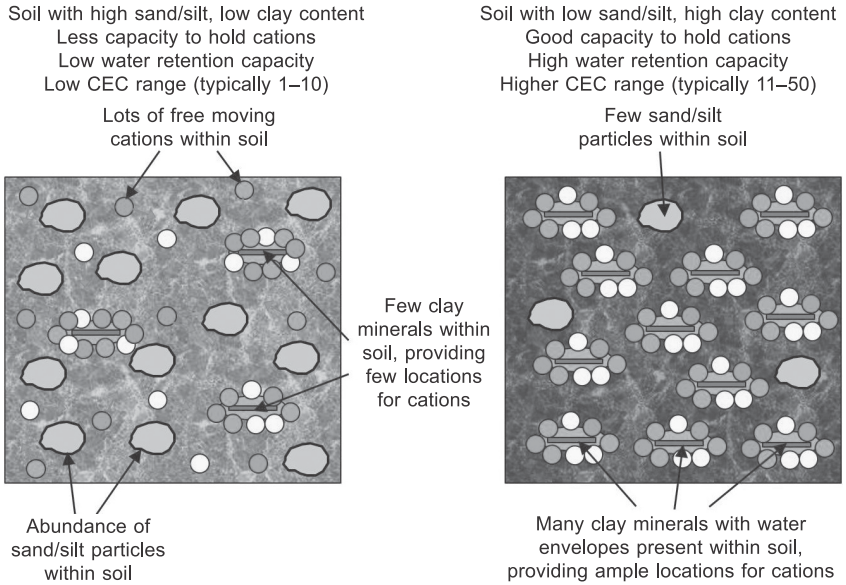

Figure 21.10 Schematic showing how cation exchange capacity varies between soils that are predominantly composed of sand/silt and those of mainly clay particles.

and a and b are unit cell parameters for the clay mineral in the x-y plane, where for kaolinite a = 0.531 nm and b = 0.92 nm; values taken from Meunier, 2005.

Following Table 21.3, low surface area, organic matter and CEC values can be expected of sandy and silty soils such as loam and alluvium (Ersahin *et al.*, 2006).

Table 21.3 Summary of surface area, organic matter and CEC characteristics typically expected for various soils

Soil No.	Particle size distribution (%)			Texture class	Specific surface area (m^2/g)	Organic matter (%)	Cation exchange capacity (cmol/kg)
	Clay	Silt	Sand				
1	61.2	11.4	27.3	C	234.1	2.0	37.4
2	35.7	11.3	53.0	SiCL	122.6	1.8	22.8
3	14.0	27.5	58.5	SiL	68.4	1.3	14.6
4	35.0	26.0	39.0	CL	133.7	2.4	26.1
5	7.7	58.3	34.0	SL	43.0	0.65	11.0
6	49.0	25.0	26.0	SCL	146.0	2.4	19.3
7	18.0	33.0	49.0	L	53.4	1.2	14.8

Note: C = Clay, SiCL = Silty clay loam, SiL = Silty loam, CL = Clay loam, SL = Sandy loam, SCL = Sandy clay loam and L = Loam. The texture classification scheme used by Ersahin *et al.* (2006) was that of the USDA.
Source: Adapted from Ersahin *et al.*, 2006. Reproduced with permission from Elsevier.

21.4.2 Other factors

Although CEC and surface area have a considerable role in dictating a soil's suitability for chemical treatment, other parameters to consider include particle size distribution, organic and sulphate contents.

Soils containing high fines contents which are chemically treated produce the most impressive strengths (Puppala *et al*., 2008). This is related to surface area characteristics; whereby soils with higher surface areas are characterised by relatively high CEC values, which are ideal for cementitious bonding and strength development.

Chemical treatment has long been applicable for soft clayey soils with high degrees of total organic matter (TOM). However, the level of improvement gained for soils with high TOM values will be of lower magnitude compared with that achieved by soils with low TOM values. Delle Site (2000) provides a conversion factor of 1.724 to convert total organic carbon (TOC) values to TOM.

TOM interferes with the chemical reactions occurring between the soil and binder. The higher the degree of a soil's organic matter decomposition (OMD), the stronger the soil will be upon stabilisation. Prior to stabilisation, a soil's TOM value affects its Atterberg limits and pH (Puppala *et al*., 2008). Oven and air drying such soils increases acidity and reduces plasticity. Once treated with lime-cement, Puppala *et al*. (2008) documented poor strength developments, which were attributed to the soil becoming more plastic rather than more acidic. A large fraction of a soil's organic content comprises humified material, which has adverse effects on strength development (Puppala *et al*., 2008). The presence of lime in organic soils inhibits strength development, as it increases organic solubility, resulting in higher degrees of homogenisation in terms of organic distribution within the soil (Puppala *et al*., 2008). Hence for organic soils, the use of CEM-I is preferred over lime or lime-cement.

The final aspect of a soil's chemistry to consider is sulphate content. Soils with sulphate contents > 3000 ppm are problematic, whereby ettringite formation is inevitable. For such soils, Little and Nair (2009) recommend that whilst it is impossible to fully solubilise all sulphates, water should be used to thoroughly mix the soil to ensure that sulphates and all possible ettringite formation sites are homogeneously distributed.

Sulphates occur as gypsum but are not uniformly distributed through the soil column; they most commonly occur in seams or as lenses. Climate has an impact on ion movement within soils; whereby in dry arid climates where evaporation is common, sulphates are located within the shallow surface. For wet humid climates, sulphates may be found at greater depths due to water infiltration. However, capillary action can cause water and sulphate sources to rise towards the surface (Little and Nair, 2009). Local terrain, geological and hydrological conditions also influence sulphate distribution. In regions characterised by hilly topography, (gravitational) surface and sub-surface water flow are common, which results in soils with high moisture and sulphate contents, along with high potentials of ettringite formation and surface heave on valley floors.

Clay-rich soils have higher moisture-retention capabilities, and higher sulphate and salinity contents compared with most other soils (Little and Nair, 2009). These characteristics are key for ettringite and thaumasite production, which are hydrous calcium aluminate sulphate (Aft) minerals as can be observed in Figure 21.11 (Wilkinson *et al*., 2010a). These cause volumetric expansion within soils that have been stabilised with calcium-based binders (Little and Nair, 2009). In contrast to soils containing high organic contents, the presence of lime does not inhibit strength development as it decreases organic solubility and does not interfere with chemical reactions between the soil and lime (Puppala *et al*., 2008).

The high surface areas of ettringite and thaumasite provide high reactivity rates, which allow reactants to become available as soluble ions (Little and Nair, 2009). Hence, ettringite formation in CEM-I concrete is rapid and relies on the matrix sulphate content, whereas for stabilised soils, ion availability in solution depends on the soil's mineralogy, degree of initial flocculation and dissolution properties (Little and Nair, 2009).

In chemical stabilisation, there are two phases of ettringite formation (Little and Nair, 2009); the first occurs during initial hydration and does not present any damaging effects. The second stage occurs later in the curing process when the soil's cemented matrix has been established, which may lead to deterioration. The environmental and weathering conditions which soil particles are subjected to create higher levels of heterogeneity compared with CEM-I, meaning that fewer ions are available in solution to produce ettringite in stabilised soils compared with cement pastes (Little and Nair, 2009). Thus, ettringite does not form as rapidly in stabilised soils as it does in cement.

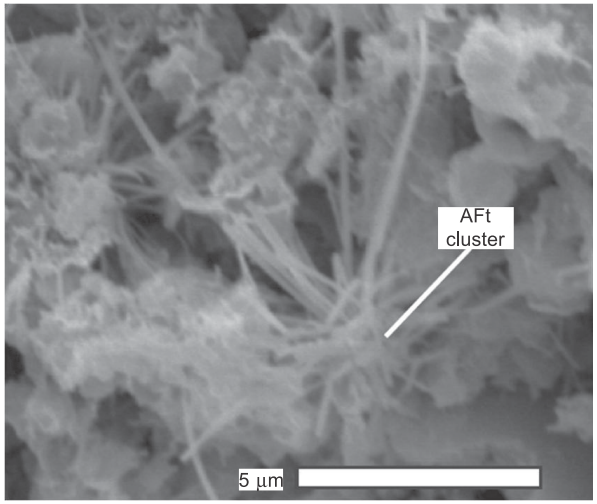

Figure 21.11 Ettringite (AFt) formation within PFA-stabilised Ginifer soil after 28 days. Courtesy of Wilkinson *et al*. (2010a). Reproduced with permission from the Institution of Civil Engineers.

No single binder will necessarily be suited for stabilising all problematic soil types, due to the natural complexity of soils. It is common for binders to comprise two or three materials, as the chemistry of a single material may not be as efficient in creating the ideal conditions for cementitious bond formation compared with the use of two or three materials. A soil's chemistry and basic geotechnical classification dictate the binder design to be used for its stabilisation. It is strongly advised that EuroSoilStab (2002) be studied prior to treatment, in order to select the most appropriate binder mix for stabilising the problematic soil at hand.

21.5 Traditional binder materials

Since the 1960s, there have been various binders that have been widely used, depending on the soil type to be stabilised. The ideal binder should bond soil particles together and waterproof the material. However, not all binders are able to do both within all soils. The performance of binders whose primary aim is to bond soil particles depends upon the strength of the stabilised soil's matrix, whether bonds form between soil particles and the matrix and whether individual or agglomerations of soil particles are bonded with each other (Sherwood, 1993). Binders will not completely waterproof a soil; however, they will ensure less water absorption, whereby their purpose is to ensure that the soil's moisture content is kept to a minimum. The performance of such binders is measured by how much the soil's permeability has been reduced (Sherwood, 1993).

The presence of soil water and calcium silicates/aluminates within binders reacts to form C-S-H and C-A-H gels via long-term pozzolanic reactions when soil pH levels are ≥ 10.5 (Davidson *et al.*, 1965). The mixtures then cure and produce stronger, cementitious soil matrices known as 'geopolymers' (Sherwood, 1993). Cement and lime have long been utilised as binders, where the former is more favourable in providing rapid strength enhancements (Rogers *et al.*, 2000; Hossain, 2010; Jegandan *et al.*, 2010). The primary components of Portland cement are tri- and di-calcium silicates. Other constituents may be added to produce advanced cement blends that are more suitable than type-I cement (CEM-I) for specific engineering purposes. CEM-I is most commonly used in soil stabilisation, due to its availability and low cost over other cements (Bergado *et al.*, 1996).

Lime originates from the calcination of chalk or limestone, where calcitic lime may be utilised as either quicklime or slaked lime. Lime treatment is generally used to modify expansive soils by drying the soil and allowing for compaction (Christopher *et al.*, 2006). Additionally, lime may be used to prepare soils for subsequent cement stabilisation (Christopher *et al.*, 2006).

Both lime and cement are available as fine grained powders, making them ideal for dry soil mixing. However, they may also be combined with water to produce slurries (Sherwood, 1993). This eliminates dust emissions and produces more homogeneous soil–binder mixtures, although using slurries is less applicable in highly saturated soils compared with dry powders.

21.6 Alkali-activated waste products as environmentally sustainable alternatives

Negative environmental issues are associated with utilising CEM-I and lime in soil stabilisation, as their production requires large amounts of energy. Dust and sulphur dioxide (SO_2) aerosol emissions from manufacturing plants can pose serious health risks including long-term respiratory diseases. SO_2 is also a primary contributor to trans-boundary pollution via acid rain. CEM-I/lime manufacture also produces high CO_2 emissions, accounting for 5–7% of global CO_2 emissions (Bye, 2011; McLellan *et al.*, 2011). Heavy elements including lead are present within the raw materials and fuels involved in cement manufacture (Bye, 2011), which can be toxic at high concentrations. Environmental pollution has been regulated in the UK since 1805 by the UK Alkali Act and by the Integrated Pollution Prevention and Control Directive (IPCC) in the EU (Bye, 2011).

It has become a priority for the cement/lime manufacture and construction industries to develop new cementitious binders and become more environmentally sustainable (energy consumption and greenhouse gas emissions). New binders should provide engineering performances that are either comparable or surpass those of CEM-I and lime within similar curing times. A popular route for selecting new materials has been the development of geopolymers, which are synthetic alkali alumino-silicates produced when combining a solid alumina-silicate with a highly concentrated aqueous alkali hydroxide or silicate solution (Duxson *et al.*, 2007). Geopolymers commonly use alumino-silicate based (i.e., pozzolanic) industrial by-products (IBPs) (Bye, 2011), which are able to produce high compressive strengths, low shrinkage levels, acid and fire resistance and low thermal conductivity (Duxson *et al.*, 2007; Weil *et al.*, 2009). Also, IBP geopolymers production costs are up to 30% lower than that for CEM-I (Duxson *et al.*, 2007). McLellan *et al.* (2011) conducted a sustainability comparison study between CEM-I and Australian geopolymers, which revealed that geopolymers reduced greenhouse gas emissions by 44–64%.

Popularly used IBPs include ground granulated blast furnace slag (GGBS) from pig iron manufacture, steel slag (SS) and pulverised fly ash (PFA) from coal combustion in power plants, where type C PFA is preferred over type F PFA due to its higher reactivity and better cementitious properties (McCarthy *et al.*, 1984). Red gypsum (RG) as a waste from titanium dioxide (TiO_2) manufacture has recently been developed as a binder (Hughes *et al.*, 2011; Gazquez *et al.*, 2013). From the aforementioned materials, GGBS and type C PFA tend to be the most preferred binders due to the high strengths which they typically achieve. With regard to SS, type F PFA and RG, these tend to be used in combination with other cementitious wastes (GGBS) to produce higher strengths, due to factors including low tricalcium silicate content (Shi *et al.*, 2006). Ashes produced from burning certain organic materials including rice husk and wood may also be used as binders, due to their high levels of pozzolanicity and reactivity, in addition to their high CaO and silica contents (Abu Bakar *et al.*, 2011; Zain *et al.*, 2011; Supancic and Obernberger, 2012).

Certain IBPs require alkali activation in order to initiate pozzolanic reactions, cementitious bond formation and to increase the rate at which mechanical properties

are improved by increasing soil pH (Palomo *et al.*, 1999). Such materials may be sourced naturally or synthetically, although the latter incurs high costs and negative environmental impacts. Alkali silicates (sodium silicate) are the most useful activators. Lime and metakaolin are less popular due to environmental impacts, poor early strength development, long setting times (Moranville-Regourd, 1998; Shi *et al.*, 2006) and the fact that metakaolin requires large volumes of water, which increases a soil's porosity and decreases its stiffness (Duxson *et al.*, 2007).

21.7 Financial costs of traditional versus alkali-activated waste binders

Financial cost in terms of energy consumption, transportation and market price is a significant factor to consider in determining whether alkali-activated geopolymers can become sustainable replacements for CEM-I/lime. If geopolymers are to become serious competitors, their financial cost must be similar to or lower than that for CEM-I and lime. The inclusion of alkali activators within geopolymers significantly increases their overall cost due to the amount of fuel and electricity required in their production (Figure 21.12) (McLellan *et al.*, 2011).

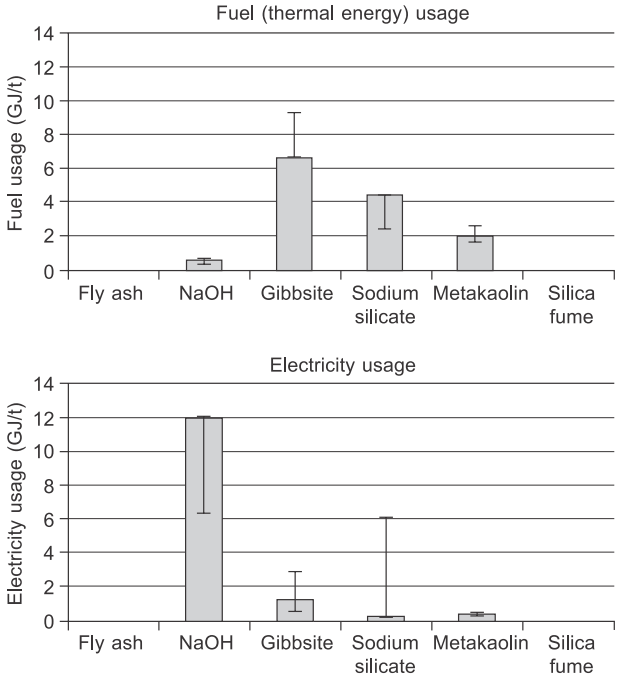

Figure 21.12 Energy usage for geopolymers feedstock production in Australia. Reprinted from McLellan *et al.* (2011), Copyright © 2011, with permission from Elsevier.

However, given that IBPs have no production costs and make up > 80% by dry weight of geopolymers, their inclusion compensates for the high cost of alkali materials. For the Australian geopolymers studied by McLellan *et al.* (2011), the overall cost of most mixtures was not much greater than that of CEM-I, although their transportation costs were considerably higher (Figure 21.13). This therefore raises doubts about the merits of using geopolymers. However, McLellan *et al.*'s (2011) findings were restricted to production and transportation within Australia, where transportation distances can vary greatly. Hence, McLellan *et al.*'s (2011) findings may not be truly representative of transportation costs incurred in other parts of the world where geopolymers are manufactured.

Wherever geopolymers are intended for use, careful assessments should be conducted to ensure that the distances between the binder source and treatment site are minimised, as this influences their overall sustainability, market price

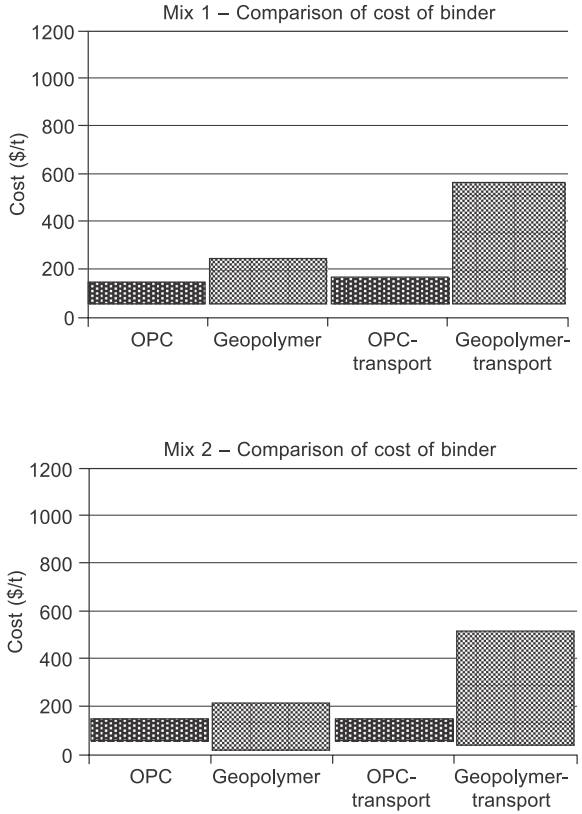

Figure 21.13 Summary of the overall costings for the four Australian geopolymers compared with CEM-I. Reprinted from McLellan *et al.* (2011), Copyright © 2011, with permission from Elsevier.

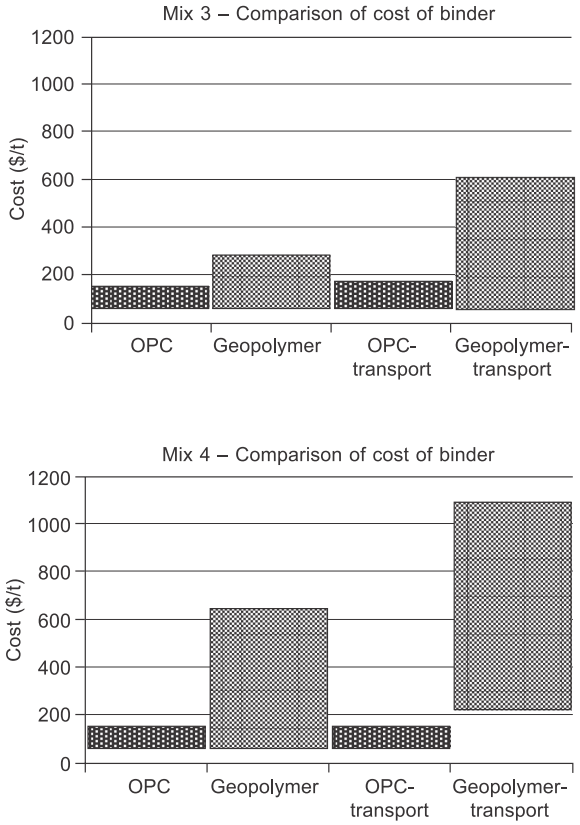

Figure 21.13 Continued

and competitiveness against CEM-I/lime. The market price of NaOH and sodium silicate are considerably higher than other alkalis and IBPs. However, alkalis are only required in small quantities to activate pozzolanic reactions. To summarise, although the inclusion of alkalis within geopolymers can incur high costs due to their production and transport and appear to make geopolymers less able to compete against CEM-I/lime, geopolymers are capable of achieving strengths which surpass those of CEM-I/lime.

21.8 Recent research into the engineering performance of alkali-activated binders for soil stabilisation

There is extensive literature on the laboratory investigation of chemically stabilised soils. There are two main types of laboratory investigations which are conducted

on chemically treated soils: those which examine the mechanical (engineering) performance and those which examine how the mineralogy of stabilised soils change with curing, in order to account for engineering performance enhancements. A number of studies from both types of investigation are presented here.

21.8.1 Al-Tabbaa et al. – Cambridge University, UK

Some of the first studies on the laboratory characterisation of stabilised soils in the UK using IBP-based binders were those by Al-Tabbaa and Evans (1998, 1999). Their studies aimed to develop soil–grout mixtures that were suitable for stabilising soils (made ground, sands and gravels) in terms of strength and environmental remediation, which had been contaminated with organic compounds and heavy metals on a former chemical works site in West Drayton, Middlesex. There was also an emphasis on using as little cement/grout as possible to meet economic and environmental criteria. The binders used included CEM-I, PFA, bentonite and lime to increase soil pH. A soil–grout ratio of 5:1, a water–dry grout ratio of 0.42:1 and a soil–dry grout ratio of 5:1/7:1 were always maintained. After 28 days curing, the mixtures tested reached unconfined compressive strength (UCS) values of 350–1100 kPa, leachate pH values of 6.5–10.5, reasonable wet-dry but poor freeze-thaw durability performances, low permeabilities of $0.2–2.0 \times 10^{-9}$ ms^{-1} and low M_v values of 2×10^{-6} m^2/kN. These results suggested that the treatment methodology employed by Al-Tabbaa and Evans (1998) was appropriate for treating the West Drayton site. This led to their 1999 paper, which simplified (in terms of the contaminants present) and homogenised the West Drayton site's conditions, thereby allowing correlations to be made between the 1998 treatability study and the properties of the lab-scale *in-situ* treated soil, and secondly between the lab and field-scale modelling of the soil stabilisation conducted.

21.8.2 Hughes et al. – Newcastle University, UK

Hughes and Glendinning (2004) stabilised a site near Sandling in Kent (UK) characterised by 5 m of problematic peaty soils, which underlie a section of the Channel Tunnel Rail Link (CTRL). Given the poor ground conditions and the CTRL's importance, stabilised soils were required to achieve minimum undrained shear strengths of 100 kPa and a Young's modulus of 10 MPa after 28 days (Hughes and Glendinning, 2004). The study's main aim was to assess RG's suitability when combined with GGBS as an alternative to lime/CEM-I, in terms of cost and engineering performance. Hughes and Glendinning (2004) conducted both field and laboratory testing using a range of GGBS/RG ratios at a dosage of 200 kg m^{-3}. Once 27 DSM columns had been installed, Hughes and Glendinning (2004) conducted *in-situ* standard column penetration (SCPT) and cone penetration tests after 7 and 56 days curing. Cores were recovered from the columns for laboratory testing; namely quick undrained unconsolidated triaxial, durability (wet-dry and freeze-thaw) pH and mineralogical analyses (XRD, SEM).

Hughes and Glendinning (2004) documented a good correlation between the *in-situ* SCPT and laboratory undrained shear strengths. However, there were a few exceptions where there was a poor correlation (Figure 21.14), whereby laboratory strengths were higher than the *in-situ* strengths. This may be attributed to continued strength development of laboratory samples between sample recovery and their testing (Hughes and Glendinning, 2004). Additionally, the unusually low laboratory strengths may be due to sample disturbance and weakening during transport.

Using a GGBS–RG ratio of 75:25 produced the most impressive strengths, which met the required design criteria and exceeded those achieved by using CEM-I (Hughes and Glendinning, 2004). Durability results were also encouraging, as little damage was incurred to the columns and the GGBS–RG's overall performance was comparable to CEM-I.

Although pH may have an impact on DSM column strength development, pH values > 10.5 did not guarantee higher shear strengths (Hughes and Glendinning, 2004). Humic acids within the peaty soils interfered with the soil–cement reactions (Hughes and Glendinning, 2004), which may explain the low pH and strength values of certain mixtures. Using an alkali activator is recommended to raise the pH of such samples and thus promote pozzolanic reactions.

Further to their 2004 study, Hughes *et al.* (2011) investigated RG's effectiveness in terms of strength/stiffness development over 28 days at 55% RH when combined with GGBS, PFA and basic oxygen steel slag (BOSS). The RG–IBP ratios varied

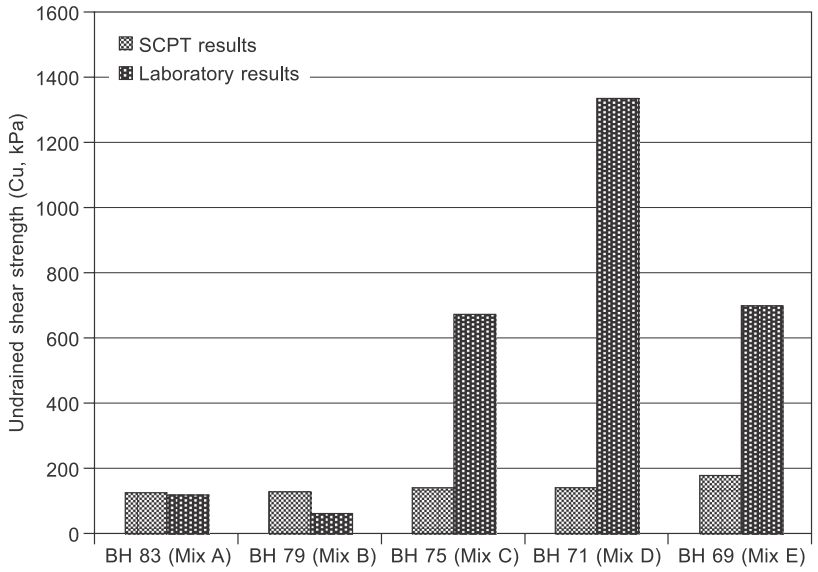

Figure 21.14 Variations in undrained shear strengths obtained for five GGBS-RG columns from *in-situ* SCPT and laboratory testing. Taken from Hughes and Glendinning (2004). Reproduced with permission from the Geological Society of London.

between 9:1 and 5:5; whereby 1% calcium hydroxide was also added to ensure pH was > 10.5. UCS results revealed that the most effective mixture was RG–GGBS at a ratio of 10:90 and moisture content of 35%, which produced strengths of 39.7 MPa. For the lower moisture contents tested by Hughes *et al.* (2011), RG–BOSS mixtures produced the highest UCS values, which produced highly brittle failures that could prove problematic when dynamically loaded. Although the highest strengths were achieved by RG–GGBS using a ratio of 10:90; Hughes *et al.* (2011) deemed the RG–GGBS ratio of 50:50 to be most favourable as it used as much IBP material as possible, whilst achieving high strengths.

Further to the above, Hughes *et al.* (2011) assessed RG–GGBS's performance in stabilising numerous UK soils, including an artificial alluvium, London Clay, Northumberland Glacial Till and Irish Moss Peat. For triaxial testing, confining pressures of 100 kPa and a strain rate of 1.23 mm/min were used. Samples were wet and dry cured for up to 112 days, whereby for the former an 18 kPa surcharge was exerted on top of samples to simulate realistic confining pressures beneath the water table.

For stabilised artificial alluvium samples, soak- and dry-cured samples achieved strengths of ~ 2.7 MPa and 5 MPa, respectively (Figure 21.15). Their rate of stiffness development was slower than that for CEM-I stabilised samples. For stabilised till samples, these developed lower undrained shear strengths (0.5 MPa) than those recorded for CEM-I-stabilised samples (3 MPa); any considerable strength developments were only observed after 28 days.

Significantly lower shear strength values were obtained for stabilised peat samples, even when additional lime was incorporated. However, such results were expected given the high water and organic contents and low pH levels, which inhibit pozzolanic

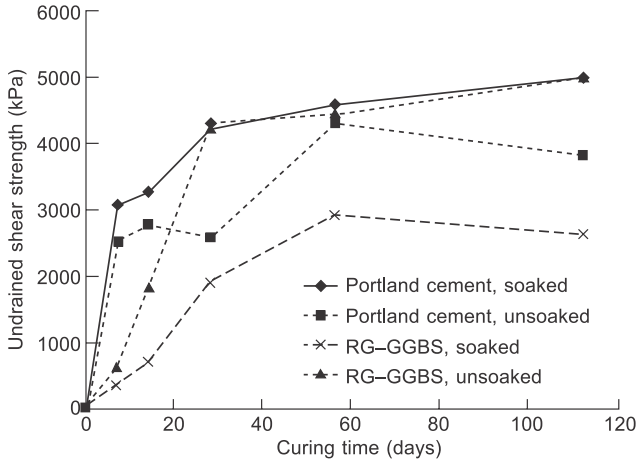

Figure 21.15 Undrained shear strength development of stabilised silty sand samples tested by Hughes *et al.* (2011). Taken from Hughes *et al.* (2011). Reproduced with permission from the Institution of Civil Engineers.

reactions. The highest undrained shear strength recorded after 14 days was 10 kPa for samples containing 30% lime. Similar to stabilised peat, negligible strength developments were observed for stabilised London Clay, reaching ≤150 kPa which was 10 times lower than that achieved by CEM-I samples. These results indicate that further work on binder chemistry and dosage is required for stabilising London Clay and soft organic peat soils.

21.8.3 Horpibulsuk et al. – Suranaree University of Technology, Thailand

Horpibulsuk *et al*. (2010) suggested that strength development within stabilised soils may be split into three zones (Figure 21.16(a)):

1. an active zone within which the volumes of pores < 0.1 μm decreased through incorporating a binder and the development of cementitious minerals;
2. an inert zone within which pore size distribution and volume of cementitious minerals undergo negligible change with increasing cement dosage and hence minimal strength enhancements; and
3. a deterioration zone where the amount of pore water present is insufficient for hydration given the relative excess of binder.

The cluster theory states that there are two pore types within stabilised soils: inter- (>0.01 μm) and intra-aggregate (<0.01 μm) (Horpibulsuk *et al*., 2010). Immediately post-mixing, the volume occupied by inter-aggregate pores decreases due to clay–cement agglomeration formation whilst the volume of larger inter-aggregate pores increases. With cementitious mineral growth, inter-aggregate pores become occupied and the soil's total pore volume decreases. Horpibulsuk *et al*. (2010) confirmed this after 7 days curing, where large pore volumes and total pore volumes within samples decreased as the volume of small pores (<0.01 μm) increased due to cementitious mineral growths (Figure 21.16(b)).

Horpibulsuk *et al*. (2011) investigated UCS development of PFA-biomass ash stabilised Bangkok clay, whereby the effects of various water contents (89, 119 and 149%), cement (0–30%) and PFA/biomass ash (0–60%) dosages were investigated for curing periods of up to 120 days at 20°C. An optimum PFA content of 25% produced the highest strengths (1900 kPa for 89% moisture content) after 28 days. Using this PFA dosage was also the most economic mixture, as it reduced the amount of binder required to stabilise the soil by 16% compared with using CEM-I. Horpibulsuk *et al*. (2011) observed that the relationship between sample strength, their clay-water/cement ratio and curing times was useful in estimating laboratory strengths and the required cement dosages within soils of different *in-situ* and field moisture contents (Figure 21.17).

PFA-stabilised soil mixes are expected to achieve strengths of 0.6–3.0 MPa after 28 days (Horpibulsuk *et al*., 2011). In relation to CEC, ash, silt and sand particles within such mixtures are non-interacting particles given their low specific surface areas and non-electrical nature, whereas cement and clay particles are able to undergo

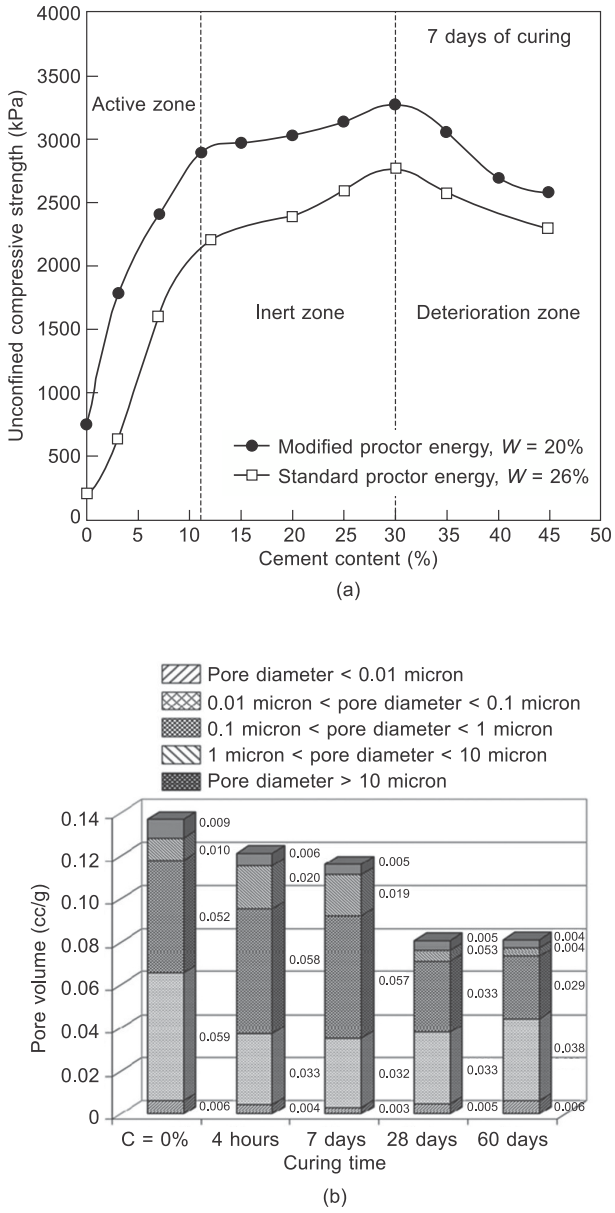

Figure 21.16 (a) Three zones of strength development within cemented soils; (b) chart showing pore size distribution for samples stabilised with 10% CEM-I. Reprinted from Horpibulsuk *et al*. (2010), Copyright © 2010, with permission from Elsevier.

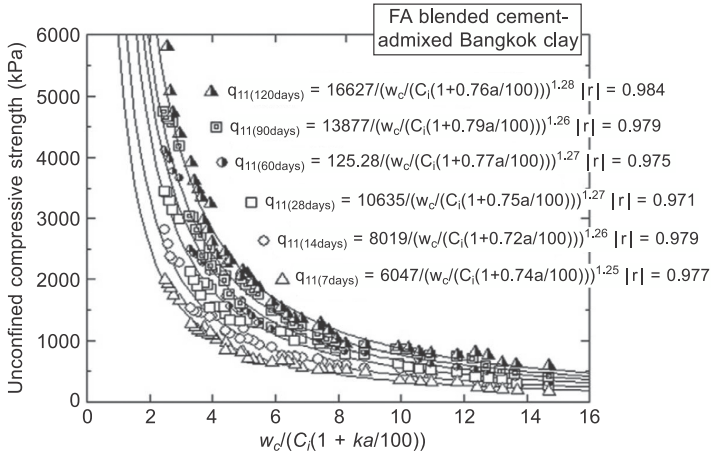

Figure 21.17 Relationship between unconfined compressive strength and clay-water/cement ratio for PFA-cement stabilised Bangkok clay. Reprinted from Horpibulsuk *et al.* (2011), Copyright © 2011, with permission from Elsevier.

physicochemical interactions with soil water. As a result of the clay's interactions, a micro-fabric develops which strengthens when cement is mixed into the soil, thereby creating large clay–cement agglomerations (Horpibulsuk *et al.* (2011).

Although PFA is silica and alumina rich, its pozzolanicity is very low. This contrasts with how many previous authors and industrial standards have characterised PFA as having good pozzolanicity levels (e.g. ASTM D5239-04). Rather than the conventional pozzolanic strength gain mechanism of $Ca(OH)_2$ produced via hydration by cements, PFA is only able to disperse large clay–cement agglomerations. This leads to increases in the reactive surface area of cement particles and subsequent strength enhancements. Horpibulsuk *et al.* (2011) confirmed this through the use of SEM, mercury intrusion porosimetry and thermal gravimetric analyses. Thus, Horpibulsuk *et al.* (2011) proposed a new hypothesis on how strength develops within blended cement–clay admixtures, whereby the strengths achieved depend solely on the clay-water/cement ratio. Hence, given PFA's poor pozzolanicity, the equivalent cement content within a stabilised soil depends on the dispersing potential of the material, which is controlled by the PFA content (Horpibulsuk *et al.*, 2011).

21.8.4 Ahnberg – Swedish Geotechnical Institute

Many previous laboratory studies which have examined the strength of stabilised soft soils have used UCS, due to its simplicity, low cost and usefulness in comparing the effects of different binders/other factors in influencing their strengths. However, Ahnberg (2007) amongst others believes that to develop a more detailed understanding of stabilised soil's mechanical behaviour, triaxial testing is more appropriate given that they fail in shear.

Little literature exists on yield stresses within stabilised soils and their effects on strength behaviour. Yield stresses within stabilised soils are largely influenced by cementation (Ahnberg, 2007). However, stresses acting on stabilised soils during curing also play a role. To examine the impact of these factors, effective stress path and shear strength behaviour of stabilised soils, Ahnberg (2007) carried out consolidated drained and undrained triaxial testing on two stabilised Swedish post-glacial clays, characterised by moisture contents of 80–90%, plastic and liquid limits of 24% and 68% respectively, high clay contents (>60%), low organic contents (1%), sensitivities of 20–25 and low undrained shear strengths (8–15 kPa).

The dry binder mixtures used by Ahnberg (2007) included CEM-II, quick lime, CEM-II+quick lime, CEM-II+GGBS, CEM-II+PFA and GGBS+quick lime, where the composite binders comprised a 50:50 ratio of each material. The binder dosage used for both soils was 100 kg/m^3. Ahnberg (2007) used two curing methods; most samples were stored within sealed plastic tubes and cured for 1, 28 and 360 days at 8°C according to Swedish testing standards. However, some CEM-II and quick lime-stabilised samples were cured within triaxial cells under numerous vertical stresses. Prior to shearing, Ahnberg (2007) mounted samples within the triaxial cells and subjected them to K_0 consolidation and curing under the same stresses for 28 days, where effective confining pressures of 20–60 kPa and vertical effective stresses of 40–120 kPa were applied. For comparison, Ahnberg (2007) also stored non-stressed stabilised samples for 28 days which were saturated from both ends. Given stabilised soil's high stiffnesses and low permeabilities, Ahnberg (2007) saturated samples by using back pressures of ≥400 kPa. Subsequently, samples were consolidated for 7.5 h to achieve a K_0 of 0.5. For shearing, a constant strain rate of 0.02%/min was used for all tests. A variation in shear strength was recorded for the different stabilised mixtures; ranging from 50 to 1500 kPa (Figure 21.18).

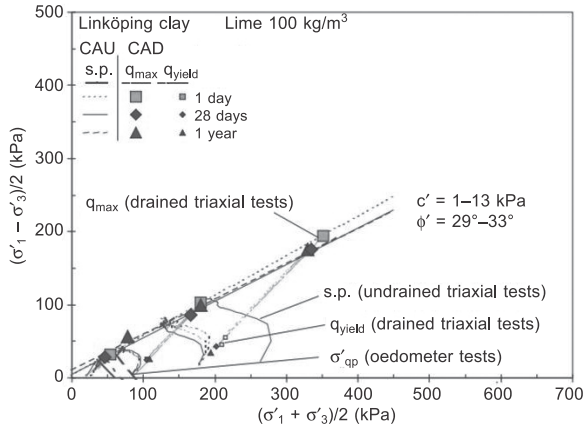

Figure 21.18 Measured effective stress paths in the *s*–*t* plane for stabilised Linköping clay mixtures. Taken from Ahnberg (2007). © 2008 Canadian Science Publishing or its licensors. Reproduced with permission.

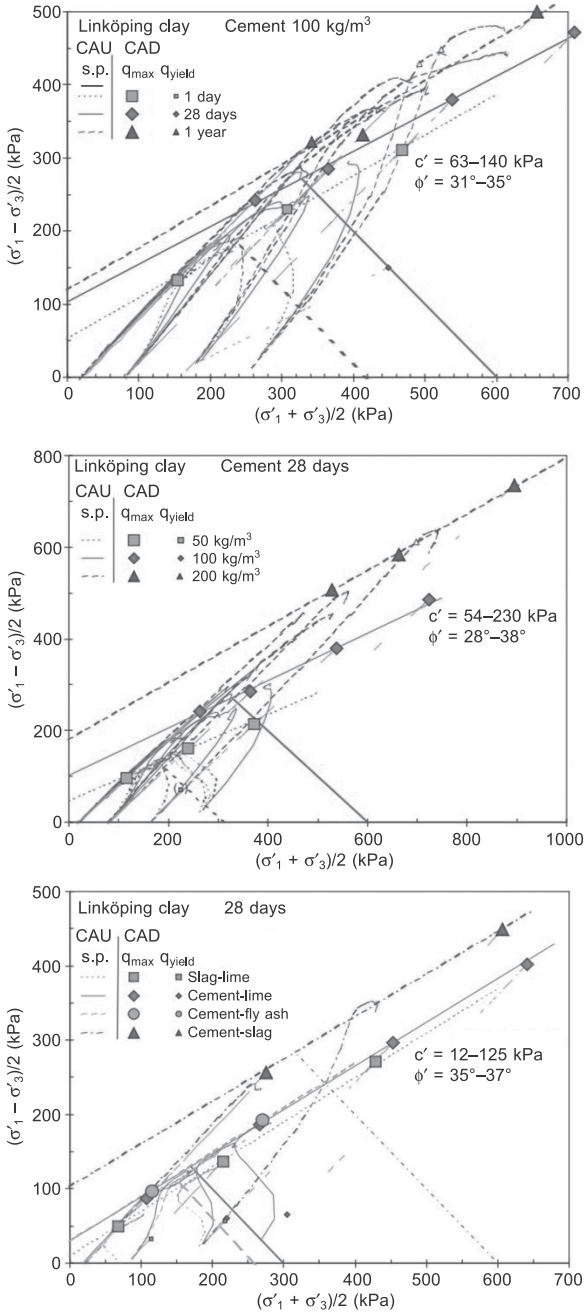

Figure 21.18 Continued

Samples which had been consolidated at stresses lower than their yield stresses behaved in an overconsolidated manner, whereas those which had been consolidated at stresses higher than their yield stresses behaved as normally consolidated soils. The majority of yield stress values were evaluated from oedometer tests, which depicted a stress dependency of stabilised soil's undrained shear strength behaviour.

Ahnberg (2007) recorded high effective friction angles (30–36°) and effective cohesion values (up to 175 kPa). Such increases in effective cohesion were attributed to simultaneous increases in undrained shear strength. However, Ahnberg (2007) noted this did not always apply, namely for lime-stabilised mixtures where the use of lime had negligible strengthening effects. Such poor performances are common when using high lime dosages within soils containing high moisture contents. Locat *et al*. (1990) confirmed that high lime dosages result in long-term strength increases only for soils with high moisture contents (Figure 21.19).

Drained triaxial tests revealed that yield points for lower strength samples were recorded at low strains, whereas failure occurred at much greater strains. However, Ahnberg (2007) noticed that yielding became less distinguishable within higher strength samples, where it occurred at stresses and strains close to failure.

Although significant variations in strength were seen by Ahnberg (2007) due to factors including soil type, binder type and curing period, relatively similar stress–strain behaviour was recorded for the different stabilised mixtures. This was linked to samples' degree of overconsolidation. For samples under drained conditions which failed at smaller strains, large reductions in shear strength with increasing strain post-failure were seen. Ahnberg (2007) noted this behaviour for samples that had been consolidated at lower stresses than their yield stresses.

Under undrained conditions, Ahnberg generally recorded little changes in deviator

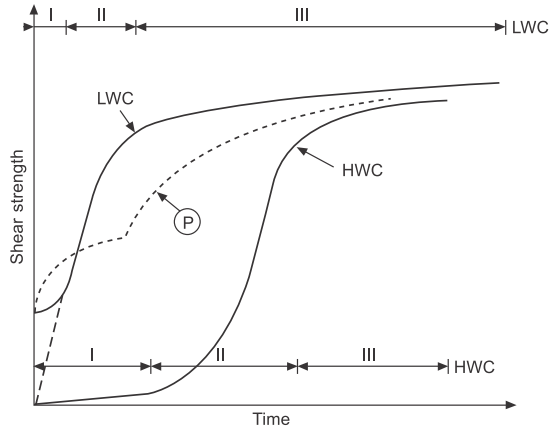

Figure 21.19 A mechanical conceptual model of shear strength development within lime-stabilised sensitive clays at both low and high moisture contents. (LWC: low water content; HWC: high water content; P: Perret model for silty soils.) Taken from Locat *et al*. (1990). © 2008 Canadian Science Publishing or its licensors. Reproduced with permission.

stress post-failure. The strains experienced at failure for normally consolidated untreated and stabilised samples were similar, as both experienced near-perfect plastic behaviour with no considerable strength degradations post-failure (Ahnberg, 2007). For highly overconsolidated samples, brittle behaviour was experienced at small strains, followed by significant strength degradation post-failure.

Ahnberg (2007) identified a 'phase-transformation' point during undrained tests where changes in pore pressure were zero and the stress paths of overconsolidated samples changed direction to follow the critical state line. Ahnberg interpreted this as depicting a yield surface and that Larsson's (1977) yielding model closely described this behaviour.

Ahnberg (2007) assumed that the effects of increased external stresses are related to the compression of the stabilised soil, inferring that increased stresses due to external loads ought to be applied shortly after stabilisation. This ensures that the material becomes compressed, allowing for cementation and increases in yield and overall shear strength to occur.

21.8.5 Wilkinson et al. – Department of Transport/Monash University, Australia

Wilkinson *et al.* (2010b) studied pH, plasticity and undrained shear strength development of various soil–binder mixtures with curing. Four soil types were stabilised; two high plasticity (Ginifer and Leeville), one low plasticity (Boambee) and one engineered clay soil (Table 21.4). The binders used included lime, lime-activated GGBS and lime activated PFA, which were added to the soils at a dosage of 10% by dry weight.

Table 21.4 Summary of the geotechnical, chemical, CEC and mineralogical characteristics of the soils stabilised by Wilkinson *et al.* (2010a,b)

Soil	Plasticity index (%)	Clay mineralogy	Cationic exchange capacity (meq/100 g)	pH at 1:3 soil/water ratio	Organic carbon content (%)
Ginifer	68.8 (high)	Smectite dominant	33.1	8.25	0.08 (low)
Leeville	47.9 (high)	Smectite dominant	18.1	5.38	1.22 (high)
Boambee	31.1(low)	Kaolinite dominant	6.0	4.45	0.35 (high)
Engineered soil	59.0 (high)	Kaolinite dominant	18.2	8.2	0

Source: Reproduced with permission from the Institution of Civil Engineers.

Davidson *et al.* (1965) determined that for pozzolanic reactions to occur within stabilised soils, a minimum pH of 10.5 was required. Based on the four soils' pH values in Table 21.4, each required alkali activation. Initial pH values post-stabilisation all exceeded 12 but degraded towards 11.5 over one year. Hence, pozzolanic reactions could occur within all samples and a relationship existed between decreasing soil pH with increasing strength as curing progressed. The mechanism by which this occurs involves calcium hydroxide acting as an electrolyte to fuel modification reactions and as a caustic agent, allowing stabilisation to occur through increasing pH for pozzolanic reactions (Rogers and Glendinning, 2000; Wilkinson *et al.*, 2010b). Pozzolanic reactions then consume hydroxyl ions from soil and binder particle surfaces, which combine with pore water to precipitate cementitious minerals.

Wilkinson *et al.*'s (2010b) results show that the most successful binder in the short and long term was lime-activated GGBS (Figure 21.20). Ginifer soil, which had been stabilised with this binder, produced the highest undrained shear strengths out of all twelve mixtures tested, where 388 kPa was achieved after 28 days.

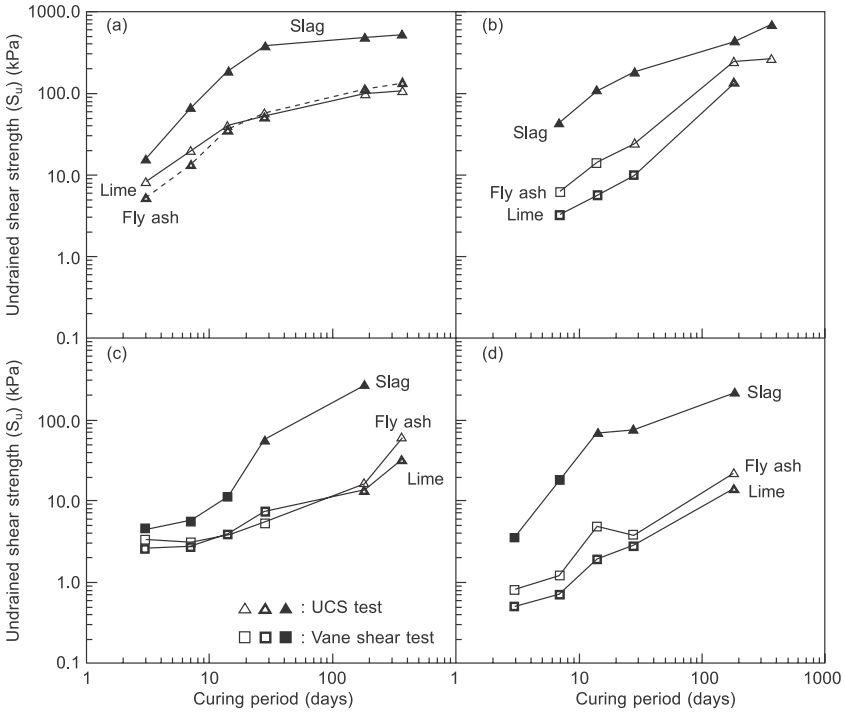

Figure 21.20 Undrained shear strength development of all stabilised soil mixtures tested by Wilkinon *et al.* (2010b): (a) Ginifer, (b) Engineered clay, (c) Leeville, (d) Boambee. Taken from Wilkinson *et al.* (2010b). Reproduced with permission from the Institution of Civil Engineers.

Activated PFA and lime binders exhibited similar performances within smectite-based clays, whereas activated PFA produced preferable performances over lime for the kaolinite-dominated soils. Work by Bell (1996) on the lime stabilisation of clay soils determined that smectite has higher short-term pozzolanicity compared with kaolinite, which can be attributed to smectite's higher surface area and CEC. These characteristics along with the higher organic carbon content of the Ginifer soil may be the root causes behind the GGBS-activated engineered soil producing higher strengths than the GGBS-activated Ginifer soil after 1 year curing.

Plasticity testing revealed that clay particles had been altered during cementation (as confirmed by SEM imagery), as the smectite-bearing soils demonstrated reductions in PI values due to smectite consumption. Contrastingly, kaolinite-bearing soils exhibited increases in PI values as cementation occurred.

21.8.6 Verástegui Flores et al. – Ghent University, Belgium

A triaxial study was conducted by Verástegui Flores and van Impe (2009) on artificially cemented kaolin clay samples, in order to distinguish between the material behaviour of stabilised and untreated kaolin. Untreated samples had a moisture content of 57.7% to simulate a very soft soil. Verástegui Flores and van Impe (2009) used a more advanced triaxial set-up than Ahnberg (2007), which involved the use of bender elements to gain insights into the small strain stiffness behaviour of cemented soils. The binder used was CEM-I at dosages of 5–20% by dry mass.

Once the samples were saturated, Verástegui Flores and van Impe (2009) isotropically consolidated untreated samples to an effective stress of 50 kPa prior to shearing. Treated samples containing binder dosages of 10% and 20% were isotropically consolidated under effective stresses of 100 kPa and 300 kPa, respectively. During consolidation, values of initial shear stiffness (G_0) were recorded through the use of bender elements; whereby shear waves were generated by 1 cycle of a sinusoidal electrical pulse at a frequency of 10 kHz (Verástegui Flores and van Impe, 2009). Initially high G_0 values were observed to decrease with increasing isotropic consolidation stresses to a minimum value, straight after which they increased. Verástegui Flores and van Impe (2009) stated that this behaviour is typical of non-cemented frictional soils, and that the transition from G_0 decreasing to increasing again denotes the point at which the material's structure degrades from cemented to non-cemented behaviour, defining the yield stress (p'_y) (Figure 21.21(a)).

At low confining pressures, shear strength behaviour was influenced by the level of cementation; whereas at higher confining pressures the behaviour was influenced by isotropic consolidation stresses. All treated samples produced a linear peak failure envelope, which was located above that defined for untreated samples (Figure 21.21(b)). Based on this observation, Verástegui Flores and van Impe (2009) interpreted that an unbound granular macrostructure existed within cemented samples. Verástegui Flores and van Impe's (2009) findings should therefore encourage the use of bender elements on soils stabilised with alkali-activated IBPs in the future, to gain further insights into their mechanical behaviour at small strains.

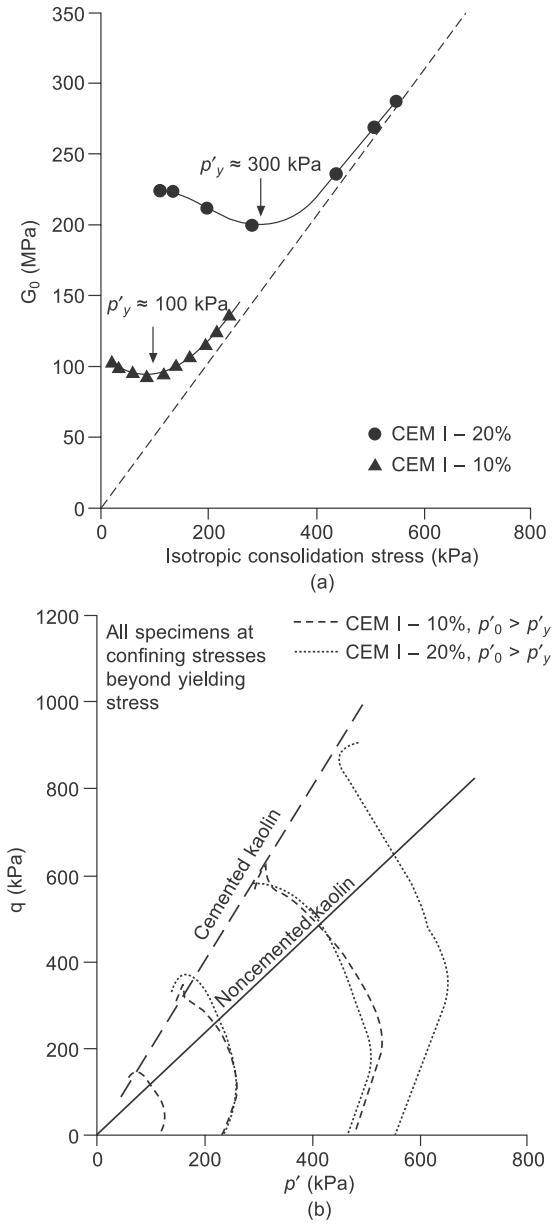

Figure 21.21 (a) Bender element measurement of G_0 for CEM-I stabilised kaolin mixtures; (b) Effective Cambridge stress path plot of treated and untreated kaolin samples. Reprinted from Verástegui Flores and van Impe (2009). Copyright © 2009, with permission from IOS Press.

21.8.7 Sargent et al. – Newcastle University, UK

Sargent *et al.* (2013) investigated the mechanical strength and durability of an artificial silty sand stabilised with various alkali-activated IBP binder mixtures. The artificial silty sand replicated alluvial soils typically found in the UK, which present difficult ground conditions for construction purposes. The soil was characterised by a gravimetric moisture content of 15%, PI of 12.02, CEC of 1.96 meq/100 g and a surface area of 2.275 m^2/g.

The IBPs used by Sargent *et al.* (2013) were PFA, GGBS and RG, where each was activated and tested individually and in combination with each other. Hughes *et al.* (2010, 2011) revealed that the use of lime as an alkali activator does not consistently result in improved engineering performance, due to insufficiently high pH values. Thus, based on work by Palomo *et al.* (1999) and Hughes *et al.* (2010, 2011), Sargent *et al.* (2013) used an alkali activator comprising NaOH flakes and Na_2SiO_3 solution.

UCS results presented in Figure 21.22 reveal that activated GGBS samples exhibited the highest and most rapid strength improvements of 6 MPa after 28 days curing, which was twice the strength of CEM-I. Other mixtures which showed encouraging strength results were activated GGBS–RG and GGBS–PFA with strengths of 5 and 3.5 MPa, respectively. The behaviour of the activated GGBS samples after each curing period upon failure was brittle, compared with the more ductile behaviour observed for other mixtures. Given that the soil had a low clay–high sand contents, this presented a limited number of sites for cation exchange and subsequent hydration/pozzolanic reactions to occur. Thus, activation within certain mixtures overcompensated for the lack of cation exchange surfaces available by increasing pH, which led to the dissolution of silica from the clay particles and subsequent formation of cementitious gels.

Sargent *et al.* (2013) also conducted oedometer testing on the aforementioned mixtures; whereby, according to Tomlinson (2001), results in Figure 21.23 show that each binder improved the soil's initial high level of compressibility to at least low to medium levels.

Alkali-activated specimens resulted in much greater improvements, particularly those containing GGBS–PFA due to high stiffness levels. Although the activated and non-activated PFA–RG samples produced lower M_v values than those achieved by the untreated soil after each loading stage, their compression index values were still comparable with that for the silty sand. Hence, rather than creating cementitious bonds, the PFA–RG binder acted as a bulking agent.

Durability testing revealed that the addition of activated GGBS or GGBS–PFA produced the most enhanced performances (Figures 21.24 and 21.25). These samples were dense and characterised by low porosities/permeabilities, which reduced the likelihood of water absorption and consequent sample degradation. RG and PFA–RG binders (activated or not) were the least durable, which was linked with RG's preparation technique, whereby a non-uniform coarse-grained powder was produced. The RG was less dense and more permeable than GGBS or PFA, which would have allowed water to permeate through samples and result in disintegration.

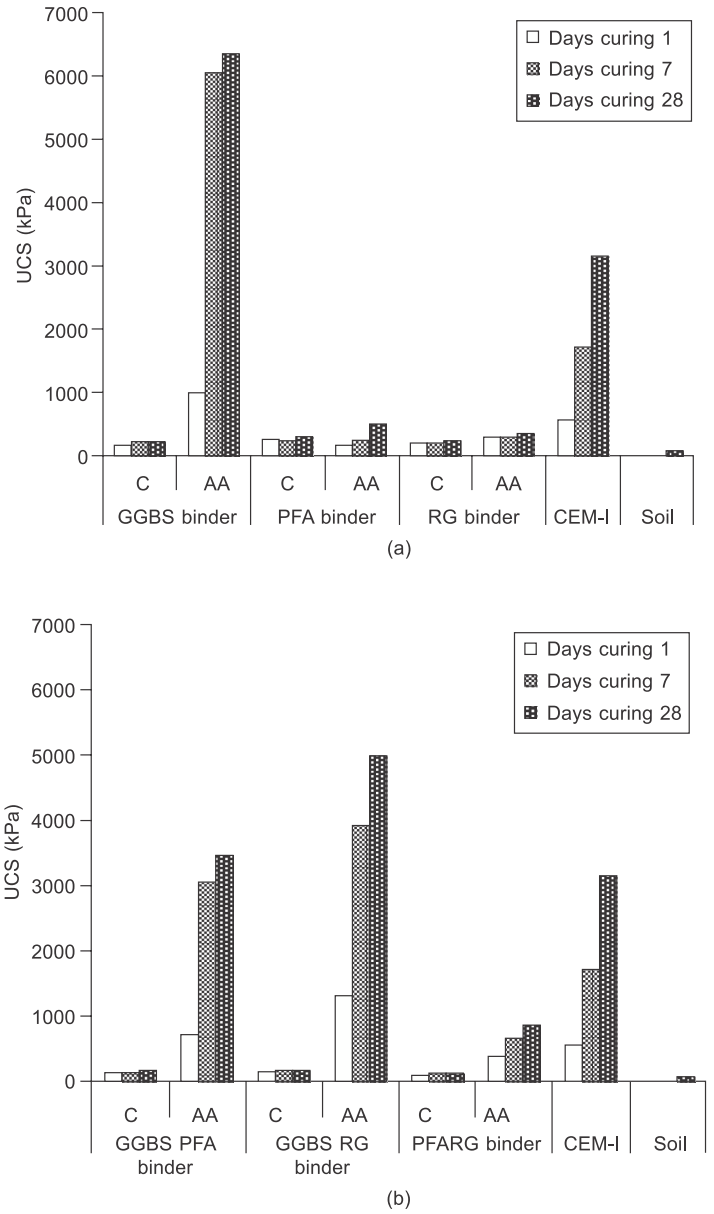

Figure 21.22 UCS development with increasing curing time for (a) individual and (b) combined IBP binders in both controlled (C) and alkali-activated (AA) states. Reprinted from Sargent *et al.* (2013), Copyright © 2013, with permission from Elsevier.

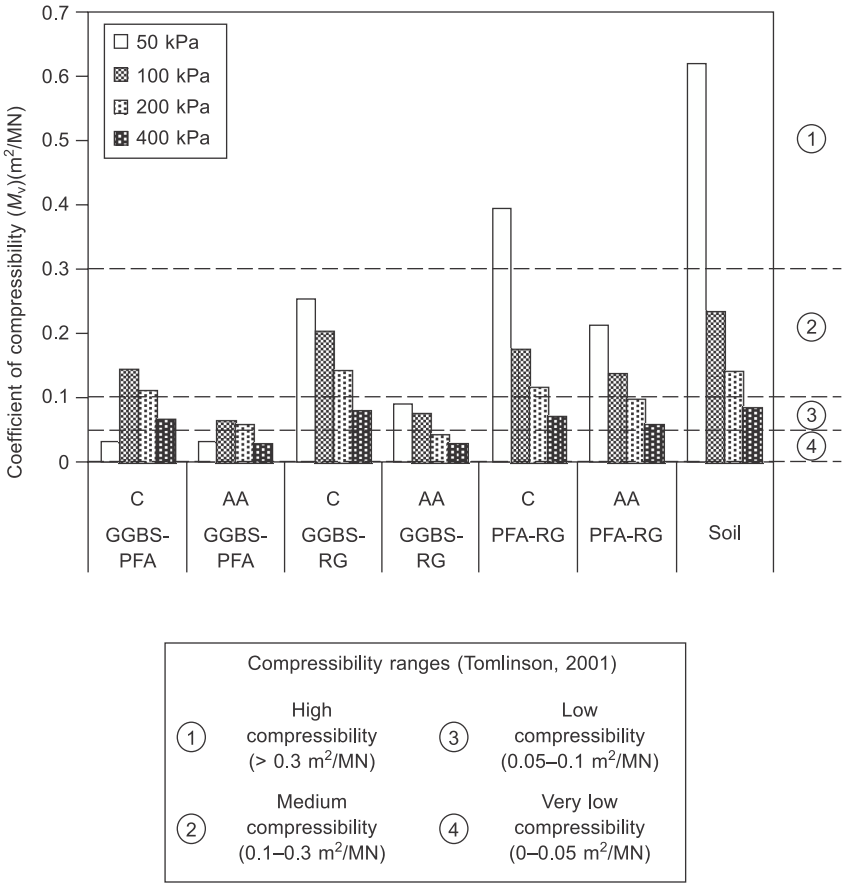

Figure 21.23 M_v values (m²/MN) for alkali-activated IBP mixtures. Reprinted from Sargent *et al.* (2013), Copyright © 2013, with permission from Elsevier.

The addition of constituents including sodium hydroxide and sodium silicate to existing commercial binders would have an associated cost and add to the complexity of DSM processes. Given that the sodium silicate used by Sargent *et al.* (2013) was in liquid form, it would not be applicable to dry DSM. Hence, substituting this with an alternative high alkalinity waste-based powder would be preferable. Habert *et al.* (2011) suggest that sodic slags could be viable replacements.

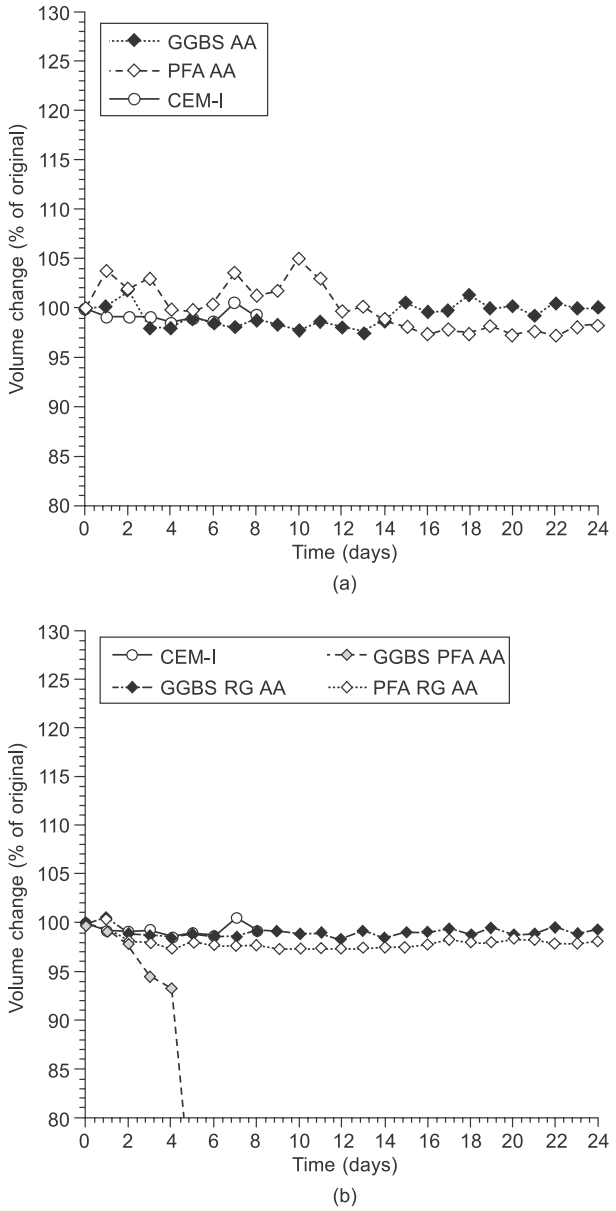

Figure 21.24 Volume changes recorded for samples containing (a) individual and (b) combination binders during wet-dry durability testing. Reprinted from Sargent *et al.* (2013), Copyright © 2013, with permission from Elsevier.

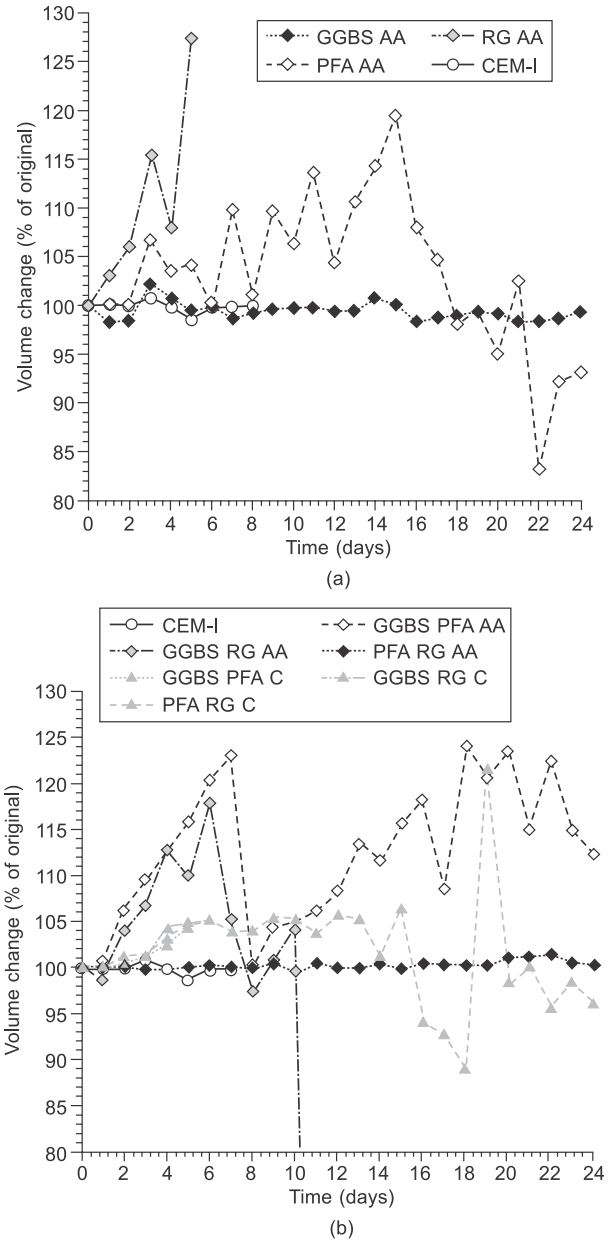

Figure 21.25 Volume changes recorded for samples containing (a) individual and (b) combination binders during freeze-thaw durability testing. Reprinted from Sargent *et al*. (2013), Copyright © 2013, with permission from Elsevier.

21.9 Recent research into the mineralogical and microstructural characteristics of alkali-activated binders for soil stabilisation

21.9.1 Al-Tabbaa et al. – Cambridge University, UK

Following their 1998 study, Al-Tabbaa and Evans (1999) used XRD and SEM techniques to examine the microstructural and physico-chemical characteristics of the same stabilised mixtures after 7 and 28 days curing.

XRD and SEM results (Figure 21.26) confirmed the presence of hydrating cementitious compounds, and that the presence of most contaminants within the soil–grout mixtures did not inhibit the development of cementitious minerals. However, the presence of lead nitrate appeared to inhibit cementitious mineral growth as much as mineral oil and lead nitrate combined (Al-Tabbaa and Evans, 1999).

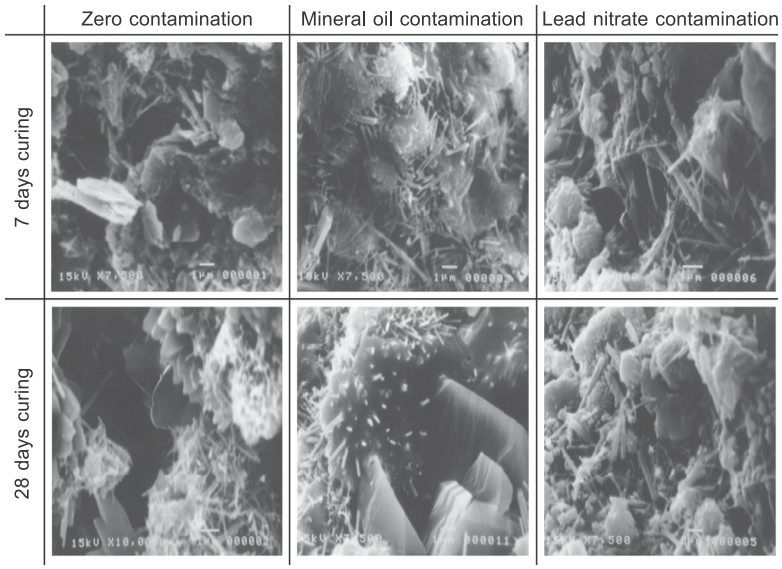

Figure 21.26 SEM micrographs of West Drayton soil in both uncontaminated and contaminated states after 7 and 28 days curing. Adapted from Al-Tabbaa and Evans (1999). Reproduced with permission from the Institution of Civil Engineers.

21.9.2 Hughes et al. – Newcastle University, UK

In addition to their geotechnical testing, Hughes and Glendinning (2004) conducted SEM and XRD analyses on samples recovered from the 27 DSM columns installed. XRD analyses revealed no evidence of ettringite or thaumasite within any of the samples, indicating that the GGBS–RG columns were not susceptible to sulphate attack

for up to 56 days post-treatment. However, the detection of hydrated cementitious minerals within samples was not possible by using XRD, due to their amorphous nature.

SEM techniques (including the EDS point elemental analysis tool) identified hydrated cementitious minerals infilling void spaces due to pozzolanic reactions. Some of the SEM micrographs taken showed the presence of a few needle-shaped minerals (Figure 21.27), which suggested the presence of ettringite/thaumasite. However, the SEM-EDS system determined these minerals as RG and posed no threat towards the soil's mechanical structure.

Hughes *et al.* (2011) also conducted XRD and SEM analyses on treated and untreated samples of artificial silty sand, Northumberland till, London Clay and Irish peat (Table 21.5). From Hughes *et al.*'s (2011) SEM-EDS analyses on polished sections of the mixtures in Table 21.5, little mineralogical differences existed between samples containing RG–GGBS or CEM-I. Hughes *et al.* (2011) did not recommend the use of the EDS tool, as it can only identify elements with atomic numbers > 5, and is thus unable to detect hydrogen.

The effectiveness of RG–GGBS in producing improved engineering performances was influenced by soil mineralogy and pH. For the artificial alluvium tested, the addition of lime was needed to raise the pH to > 10.5. In contrast, the mineralogy (specifically sulphate content) of the Northumberland glacial till, peat and London Clay caused pH levels to decrease with curing, where the lime added was insufficient

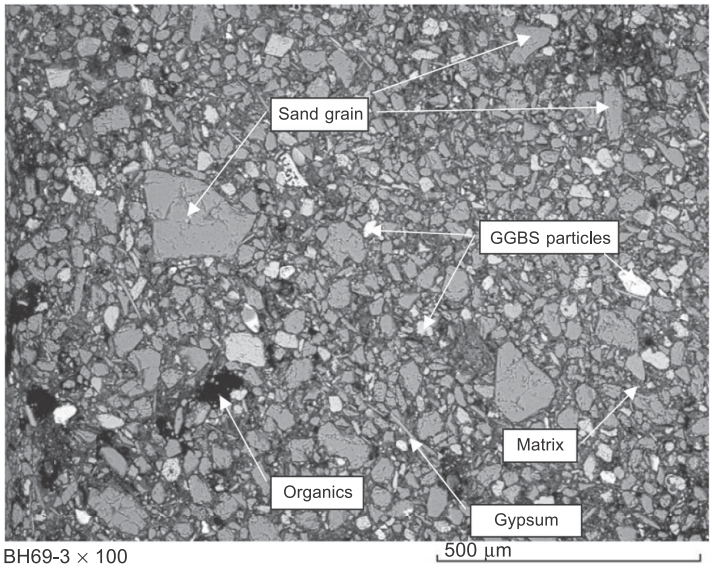

Figure 21.27 SEM micrograph of a polished sample section, which has been EDS analysed. Taken from Hughes and Glendinning (2004). Reproduced with permission from the Geological Society of London.

Table 21.5 Summary of mineral phases observed in each sample analysed by Hughes *et al.* (2011) using XRD

	RG-GGBS stabilised		CEM-I stabilised	
	Dry-cured	***Soak-cured***	***Dry-cured***	***Soak-cured***
Artificial alluvium	Kaolinite, Gypsum, Ettringite, Quartz and C-S-H	Kaolinite, Gypsum, Ettringite, Quartz and C-A-O-H	Kaolinite, Portlandite, Calcite, Quartz, C-S-H and C-A-O-H	Kaolinite, Portlandite, Calcite, Quartz, Calcium Silicate and C-A-O-H
London Clay	Gypsum, Ettringite, Quartz and Muscovite	–	Kaolinite, Calcite, Ettringite, Quartz, Muscovite and C-S-H	Ettringite, Quartz, Muscovite and Calcite
Northumberland Glacial Till	Kaolinite, Gypsum and Quartz	Kaolinite, Gypsum, Ettringite, Quartz and C-S-H	Kaolinite, Portlandite, Calcite, Quartz and C-S-H	Kaolinite, Portlandite, Calcite, Quartz and C-S-H

The symbol (–) denotes no sample was analysed.
Reproduced with permission from the Institution of Civil Engineers.

to raise pH levels, resulting in the unsuccessful activation of the RG–GGBS. Although the strengths achieved were lower compared with CEM-I, Hughes *et al.* (2011) believed that RG–GGBS should still be considered as a sustainable alternative to CEM-I which meets construction specifications.

Wax-sealing samples for curing was more effective in preventing sample evaporation compared with cling film wrapping samples, as adopted by Rahman *et al.* (2008). Hughes *et al.*'s (2011) RG preparation method was more effective than that adopted by Rahman *et al.* (2008) in producing higher strengths, which involved oven drying the moist RG filter cake at 40°C and then manually grinding it into a powder. The strengths of activated GGBS mixtures exceeded those achieved by CEM-I. Hence, the performance of the activated GGBS may conceal any effects due to the presence of RG.

21.9.3 Wilkinson et al. – Department of Transport/Monash University, Australia

Similar to Hughes *et al.* (2004, 2011), Wilkinson *et al.* (2010a,b) investigated the use of lime-activated PFA and GGBS to stabilise numerous Australian clayey soils. SEM and XRD were used to examine mineralogical changes within stabilised mixtures at various curing periods up to 1 year. SEM images revealed the occurrence

of flocculation and agglomeration once they had been stabilised. Wilkinson *et al.* (2010a) also observed the development of neoform products including AFt (aluminate ferro tri-) phases (ettringite and thaumasite; Figure 21.28), calcium hydroxide (Figure 21.28(b)), AFm (aluminate ferrite mono-) phases (i.e., strätlingite and calcium monosulphate hydrate; Figure 21.29(a)) and C-S-H (Figure 21.29(b)), where these products grew within pore spaces binding the soil structure together.

The abundance of AFt, AFm and C-S-H mineral phases increased with curing, where C-S-H minerals were most abundant after 182 days (Wilkinson *et al.*, 2010a). XRD analyses also confirmed the changing mineralogy of samples with time (Figure 21.30).

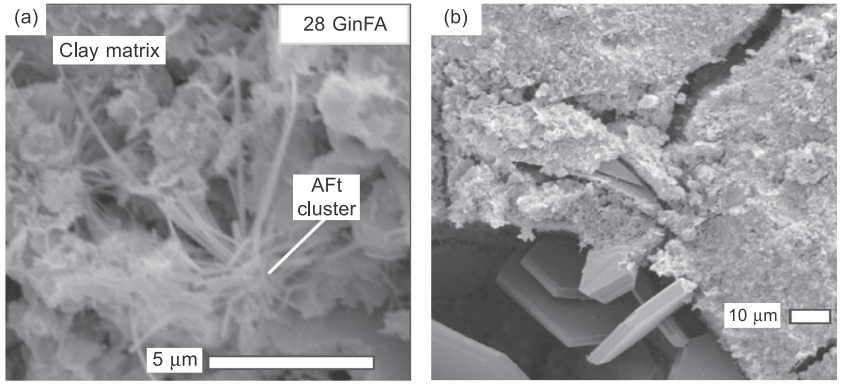

Figure 21.28 SEM images of (a) AFt phase ettringite and (b) CH minerals. Taken from Wilkinson *et al.* (2010a). Reproduced with permission from the Institution of Civil Engineers.

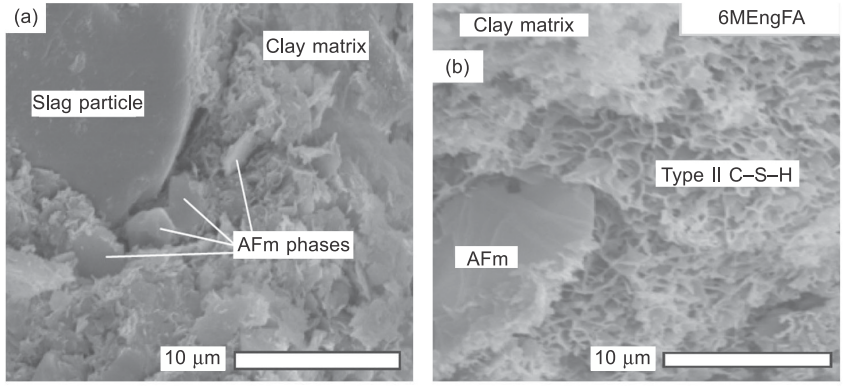

Figure 21.29 SEM images of (a) AFm phase and (b) type II C-S-H minerals. Taken from Wilkinson *et al.* (2010a). Reproduced with permission from the Institution of Civil Engineers.

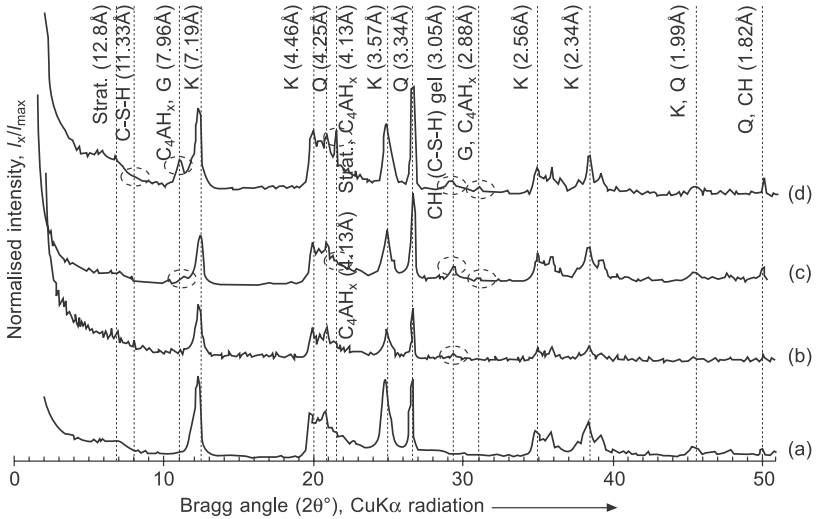

Figure 21.30 XRD traces of samples analysed by Wilkinson *et al.* after various curing periods: (a) untreated clay at 0 days, (b) with hydrated lime at 6 months, (c) activated PFA at 1 year and (d) activated GGBS at 6 months. (K = kaolinite, Q = quartz, G = gypsum, C_4AH_x = calcium aluminate oxide (carbonate) hydroxide.) Courtesy of Wilkinson *et al.* (2010a). Reproduced with permission from the Institution of Civil Engineers.

Overall, the activated PFA and GGBS were seen to influence the type and form of growing mineral phases. Finally, soil organic content was observed to hinder cementitious mineral growths and thus subsequent strength developments.

21.9.4 Sargent et al. – Newcastle University, UK

Previous studies have shown that a soil's pH may strongly influence its strength development, as higher UCS values (>1 MPa) are achieved by alkali-activated samples whose pH values are > 10.5. pH testing after 28 days showed that alkali activation was required to ensure that each mixture reached a minimum pH of 10.5 for pozzolanic reactions to occur. Whilst sufficiently high pH values were recorded for samples which achieved high UCS values (GGBS and GGBS–PFA), numerous samples with high pH levels did not achieve high strengths (RG–AA and PFA–RG–AA). Oxidising reactions and subsequent pH reductions can hinder pozzolanic reactions and strength gains. It is therefore necessary to fully assess the quantity of activator to be added to stabilised soil mixtures prior to treatment to ensure that pH remains > 10.5 for a sufficient curing period (Sargent *et al.*, 2013).

Mineralogically, XRD analyses from Sargent *et al.*'s (2013) study provided evidence for the existence of C-S-H and calcium aluminium oxide hydrate minerals within certain activated samples. Thenardite was observed within a PFA–RG–AA

sample, which can cause sulphate attack and strength degradations within concrete (Rodriguez-Navarro *et al*., 2000). No thaumasite was observed within any samples; however, ettringite was observed within one GGBS–RG–AA sample. The presence of ettringite/thaumasite within calcium-based stabilised sulphate-bearing clay soils can cause structural distress (Little *et al*., 2005). However, in the case of Sargent *et al*.'s (2013) study and that by Wild *et al*. (1998) for clay–lime–GGBS–gypsum systems with high lime–low GGBS compositions, Ettringite may strengthen soils.

21.9.5 Zhang et al. – Worcester Polytechnic Institute, USA/ Northwest A&F University, China

Similar to Sargent *et al*. (2013), Zhang *et al*. (2013) stabilised a low-plasticity synthetic clay soil in the laboratory and subjected it to UCS, volumetric strain, and mineralogical/microstructural testing; specifically XRD and SEM-EDX (energy dispersive X-ray spectroscopy). The stabiliser used for their study was metakaolin at dosages of 3–15%; whereby samples were cured for up to 28 days in cling film. For samples containing a Si/Al ratio of 1.7 and a 15% binder dosage, impressive 28-day UCS values of 31 MPa were achieved, even though cling-filming samples for curing is less desirable than wax-sealing and the fact that Duxson *et al*. (2007) believe that metakaolin should not be used in geopolymers due to the large volumes of water required and the consequent increase in the material's porosity.

The use of SEM-EDX was successful in qualitatively identifying the presence of cementitious gels within samples and that sample homogeneity (and thus strength) was enhanced through increasing binder dosage. As shown in Figure 21.31, sodium

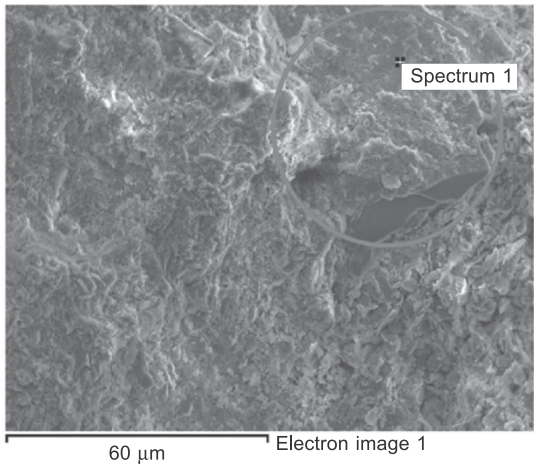

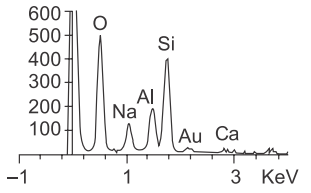

Element	Weight%	Atomic%
O K	52.62	67.21
Na K	6.37	5.66
Al K	9.57	7.25
Si K	25.03	18.21
Ca K	2.48	1.26
Au M	3.94	0.41
Totals	100.00	

Figure 21.31 EDX spectra of metakaolin geopolymers after 28 days curing. Reprinted from Zhang *et al*. (2013), Copyright © 2013, with permission from Elsevier.

was detected in all EDX analyses of metakaolin-stabilised samples, which is likely to be associated with the geopolymer gels (Zhang *et al*., 2013).

Upon blending the metakaolin with the soil, the reaction was observed to be rapid due to the metakaolin's fineness and high amorphous content (Zhang *et al*., 2013). Regarding XRD analyses, Zhang *et al*. (2013) recorded a negligible difference between stabilised and untreated samples, indicating that there was no reaction between the metakaolin and the soil minerals and that the strength enhancements were attributed solely to geopolymer gels. However, metakaolin is a costly material, which has been documented to be unsuitable for chemical stabilisation (Duxson *et al*., 2007) and must be used at high dosages (>11%) to produce comparable performances as using 5% CEM-I (Zhang *et al*., 2013). Hence, other alkalis ought to be used for activating IBP-based geopolymers.

21.10 Conclusions and future trends

This chapter has presented a detailed review of the processes and materials typically involved in chemical soil stabilisation, in addition to the development of new more sustainable alkali-activated mixtures as alternatives to lime and CEM-I. The key points to note are summarised below:

- Factors including high levels of versatility, low dust and noise emissions make DSM techniques ideal for improving ground conditions characterised by soft clayey and/or organic soils. This technique has been used successfully in stabilising local ground conditions for numerous major engineering projects, including the construction of the CTRL and the repair of levees in New Orleans after Hurricane Katrina in 2005.
- To ensure that the soil and binder react and that maximum engineering improvements will be achieved, a detailed understanding of the various binder materials available for use in chemical treatment is essential. Additionally, thorough assessments of the soil must be made in terms of particle size distribution, surface area/reactivity, mineralogical and chemical characteristics. Soils which are ideally suited to chemical treatment contain fines (>10% clays of smectite or montmorillonite composition), low organic and sulphate contents as organics can interfere with cementation reactions and sulphates can produce unfavourable minerals including ettringite and thaumasite.
- Although lime and CEM-I have been used in previous projects and produced high strengths and durabilities, there are numerous environmental and financial problems associated with their production and usage. The production of these materials incurs high costs due to their high levels of energy consumption and high greenhouse gas and carbon emissions. Hence, their continued use as binders is unsustainable and there becomes a need for identifying new sustainable binders; specifically in terms of lower energy consumption, greenhouse gas emissions, production and transport costs. To ensure that such materials are going to be competitive, they should provide engineering performances that are either comparable or surpass those of CEM-I and lime within similar curing times.
- Research into developing new alternative materials has been ongoing since the mid-1990s. One of the most preferred routes for selecting new binders has been recycling IBPs to form geopolymers. Such binders could be substituted for CEM-I and lime with only

minimal modification to existing plant and equipment or a reduction in the efficiency of the installation process.

- Recent laboratory and field-based research has demonstrated that IBPs have great potential as sustainable lime/CEM-I replacements. However, the inclusion of alkali activators is necessary to enhance the rates at which their mechanical properties are improved by increasing pH. This thereby promotes the conditions required for pozzolanic reactions and cementitious bonding to occur. Alkali-activated GGBS is known to produce excellent short- and long-term engineering performance, which comfortably surpass those exhibited by lime and CEM-I.
- For any chemical soil stabilisation project involving the use of alkali-activated mixtures, one should be aware that the cost of producing alkali activators is quite high. It is common for geopolymer components to come from various locations, meaning that the distances between sourcing plants and the stabilisation site can be considerable. Given that modern transportation costs are high, careful planning must be conducted to keep the aforementioned distances down to a minimum. This will ensure that the use of geopolymers remains more sustainable and competitive than lime or CEM-I.

References

Abu Bakar, B. H., Ramadhansyah, P. J. and Megat Azmi, M. J., 2011. Effect of rice husk ash fineness on the chemical and physical properties of concrete. *Magazine of Concrete Research* 65 (5), 313–320.

Ahnberg, H., 2007. On yield stresses and the influence of curing stresses on stress paths and strength measured in triaxial testing of stabilized soils. *Canadian Geotechnical Journal* 44, 54–66.

Al-Tabbaa, A., 2003. Soil mixing in the UK 1991–2000: state of practice report. *Ground Improvement* 7, 117–126.

Al-Tabbaa, A. and Evans, C. W., 1998. Pilot *in situ* auger mixing treatment of a contaminated site – Part 1: Treatability study. *Geotechnical Engineering* 131, 52–59.

Al-Tabbaa, A. and Evans, C. W., 1999. Laboratory-scale soil mixing of a contaminated site. *Journal of Ground Improvement* 3, 119–134.

Bell, F. G., 1996. Lime stabilisation of clay minerals and soils. *Engineering Geology* 42 (4), 223–237.

Bergado, D. T., Anderson, L. R., Miura, N. and Balasubramaniam, A. S., 1996, *Soft Ground Improvement in Lowland and Other Environments*, American Society of Civil Engineers – ASCE Press, Reston, VA.

Broms, B. B., 1984. Stabilization of soft clay with lime columns, Proc. Seminar on Soil Improvement and Construction Techniques in Soft Ground, Nanyang Technological Institute, Singapore.

Brunauer, S., Emmett, P. H. and Teller, E., 1938. Adsorption of gases in multimolecular layers. *Journal of the American Chemical Society* 60, 309–319.

Bye, G., 2011. *Portland Cement*, 3rd edn. Institution of Civil Engineers, London.

Christopher, B. R., Schwartz, C. and Boudreau, R., 2006. *Geotechnical Aspects of Pavements*. National Highway Institute, Federal Highway Administration, US Department of Transportation, Washington D.C. Publication No. FHWA NHI-05-037, May.

Cooper, T. H., 2009. Unit 12 Chapter 2 – Cation exchange and cation exchange capacity.

[online]. Available at <http://www.swac.umn.edu/classes/soil2125/doc/s12ch2.htm> (accessed 6 July 2014).

Davidson, L. K., Demirel, T. and Handy, R. I., 1965. Soil pulverization and lime migration in soil lime stabilisation. *Highway Research Record* 92, 103–126.

delle site, A., 2000. Factors affecting sorption of organic compounds in natural sorbent/water systems and sorption coefficients for selected pollutants: a review. *J. Hys. Chem. Ref. Data* 30 (1), 187–439.

Diamond, S. and Kinter, E. B., 1965. Mechanisms of soil-lime stabilization – an interpretative review, *Highway Research Record* 92, 83–102.

Duxson, P., Fernandez-Jimenez, A., Provis, J. L., Lukey, G. C., Palomo, A. and Deventer, J. S. J, 2007. Geopolymer technology: the current state of the art. *Journal of Materials Science, Advances in Geopolymer Science and Technology* 42, 2917–2933.

Ersahin, S., Gunal, H., Kutlu, T., Yetgin, B. and Coban, S., 2006. Estimating specific surface area and cation exchange capacity in soils using fractal dimension of particle-size distribution. *Geoderma* 136, 588–597.

EuroSoilStab, 2002. Development of design and construction methods to stabilise soft organic soils: design guide soft soil stabilisation. CT97-0351. Project No. BE 96-3177.

FHWA-RD-99-167, 2001. An introduction to the deep soil mixing methods as used in geotechnical applications: volume 3 – verification and properties of treated soil. Prepared by Geosystems (D. A. Bruce) for US Department of Transportation, Federal Highway Administration, p.163.

Gazquez, M. J., Bolivar, J. P., Vaca, F., Garcia-Tenorio, R. and Caparros, A., 2013. Evaluation of the use of TiO_2 industry red gypsum waste in cement production. *Cement & Concrete Composites* 37, 76–81.

Geo-Con., Inc., 1998. Promotional information.

Habert, G., d'Espinose de Lacaillerie, J. B. and Roussel, N., 2011. An environmental evaluation of geopolymer based concrete production: reviewing current research trends. *Journal of Cleaner Production* 19, 1229–1238.

Horpibulsuk, S., Rachan, R., Chinkulkijniwat, A., Raksachon, Y. and Suddeepong, A., 2010. Analysis of strength development in cement-stabilized silty clay from microstructural considerations. *Construction and Building Materials* 24, 2011–2021.

Horpibulsuk, S., Rachan, R. and Suddeepong, A., 2011. Assessment of strength development in blended cement admixed Bangkok clay. *Construction and Building Materials* 25, 1521–1531.

Hossain, K. M. A., 2010. Development of stabilised soils for construction applications. *Ground Improvement* 163, 173–185.

Hughes, P. N. and Glendinning, S., 2004. Deep dry mix ground improvement of a soft peaty clay using blast furnace slag and red gypsum. *Quarterly Journal of Engineering Geology and Hydrogeology* 37, 205–216.

Hughes, P. N., Glendinning, S., Manning, D. A. C. and Noble, B. C., 2010. Production of 'green' concrete using red gypsum and waste. *Engineering Sustainability* 163, 137–146.

Hughes, P. N., Glendinning, S., Manning, D. A. C. and White, M. L., 2011. Use of red gypsum in soil mixing engineering applications. *Geotechnical Engineering* 164, 223–234.

Jegandan, S., Liska, M., Osman, A. A-M. and Al-Tabbaa, A., 2010. Sustainable binders for soil stabilisation. *Ground Improvement* 163, 53–61.

Kurtis, K., 2007. Portland Cement Hydration; PowerPoint presentation from the School of Civil Engineering, Georgia Institute of Technology, Atlanta, Georgia. Available at <people.ce.gatech.edu/~kk92/hyd07.pdf> (accessed 10 December 2013).

Larsson, R., 1977. Basic behaviour of Scandinavian soft clays. Report 4, Swedish Geotechnical Institute, Linköping, Sweden.

Little, D. N. and Nair, S., 2009. NCHRP web-only document 145: Recommended Practice for Stabilization of Sulfate Rich Subgrade Soils. Contractor's Final Task Report for NCHRP Project 20-07. National Co-operative Highway Research Program, Transportation Research Board of the National Academies, Washington, DC.

Little, D. N., Herbert, B. and Kunagalli, S. N., 2005. Ettringite formation in lime-treated soils: establishing thermodynamic foundations for engineering practice. *Transportation Research Record: Journal of the Transportation Research Board* 1936, 51–59.

Locat, J., Berube, M. A. and Choquette, M., 1990. Laboratory investigations on the lime stabilization of sensitive clays: shear strength development. *Canadian Geotechnical Journal* 27, 294–304.

McCarthy, G. J., Swanson, K. D., Keller, L. P. and Blatter, W. C., 1984. Mineralogy of Western fly ashes. *Cement and Concrete Research* 14 (3), 471–478.

McLellan, B. C., Williams, R. P., Lay, J., van Riessen, A. and Corder, G. D., 2011. Costs and carbon emissions for geopolymer pastes in comparison to ordinary portland cement. *Journal of Cleaner Production* 19, 1080–1090.

Meunier, A., 2005. *Clays*, Springer Verlag, Berlin, Heidelberg.

Moranville-Regourd, M., 1998. Cements made from blast furnace slag. In Hewlett, P. (ed.) *Lea's Chemistry of Cement and Concrete* Arnold, London, 633–699.

Nair, S. and Little, D. N., 2009. Water as the key to expansion of ettringite in cementitious materials. *Transportation Research Record: Journal of the Transportation Research Board* 2104, 55–62.

Palomo, A., Grutzeck, M. W. and Blanco, M. T., 1999. Alkali-activated fly ashes: a cement for the future. *Cement and Concrete Research* 29, 1323–1329.

Puppala, A. J., Madhyannapu, R. S., Nazarian, S., Yuan, D. and Hoyos, L., 2008. Deep Soil Mixing Technology for Mitigation of Pavement Roughness. Texas Department of Transportation & Federal Highway Administration. Report No. FHWA/TX-08/0-5179-1.

Quasthoff, P., 2012. State of the art in 'dry soil mixing' – basics and case study. ISSMGE – TC 211 International Symposium on Ground Improvement, IS-GI, Brussels, 31 May – 1 June 2012, Vol. 3, 285–298.

Rahman, M. W., Ghataora, G. S., Chapman, D. N., Tyrer, M., Claisse, P. and Ganjian, E., 2008. Gypsum waste reduction through stabilization for trench backfill. Proceedings of GeoCongress 2008: Geotechnics of Waste Management and Remediation. ASCE, 320–327.

Rodriguez-Navarro, C., Doehne, E. and Sebastian, E., 2000. How does sodium sulphate crystallise? Implications for the decay and testing of building materials. *Cement and Concrete Research* 30, 1527–1534.

Rogers, C. D. F. and Glendinning, S., 1996. Modification of clay soils using lime. In Dixon, N., Glendinning, S. and Rogers, C. D. F. (eds), *Lime Stabilisation*. Thomas Telford, London, 99–114.

Rogers, C. D. F. and Glendinning, S., 2000. Lime requirement for stabilization. *Transportation Research Record* 1721. Paper No. 00-0604, 9–18.

Rogers, C. D. F., Glendinning, S. and Holt, C. C., 2000. Slope stabilisation using lime piles – a case study. *Ground Improvement* 4, 165–176.

Sargent, P., Hughes, P. N., Rouainia, M. and White, M., 2013. The use of alkali activated waste binders in enhancing the mechanical properties and durability of soft alluvial soils. *Engineering Geology* 152, 96–108.

Sherwood, P. T., 1993. *Soil Stabilisation with Cement and Lime – State of the Art Review*. Transport Research Laboratory, Department of Transport. HMSO publications, London.

Shi, C., Krivenko, P. V. and Roy, D., 2006. *Alkali-Activated Cements and Concretes*. Taylor & Francis, Abingdon.

Sumner, M. E. and Naidu, R., 1998. *Sodic Soils*. Oxford University Press, New York.

Supancic, K. and Obernberger, I., 2012. Wood ash utilization as a binder in soil stabilization for road construction – first results of large-scale tests. Proceedings of ASH 2012 conference, Stockholm, Sweden, 25–27 January.

Terzaghi, K., Peck, R. B. and Mesri, G., 1996. *Soil Mechanics in Engineering Practice*, 3rd edn. John Wiley & Sons, New York.

Tomlinson, M. J., 2001. *Foundation Design and Construction*, 7th edn, Pearson Education, Harlow.

Topolnicki, M., 2004. *In situ* soil mixing. In Moseley, M. P. and Kirsch, K. (eds) *Ground Improvement*, 2nd edition. Spon Press, London, 331–428.

Topolnicki, M. and Pandrea, P., 2012. Design of in-situ soil mixing. ISSMGE – TC 211 International Symposium on Ground Improvement, IS-GI, Brussels, 31 May – 1 June 2012, Vol. 3, 309–316.

Treviicos, 2013. Soil Mixing. Available at <http://www.treviicos.com/viewdoc.asp?co_id=1095> (accessed 6 July 2014).

Verástegui Flores, R. D. and van Impe, W. F., 2009. Stress–strain behaviour of artificially cemented kaolin clay. In Hanza, M. *et al.* (eds) Proceedings of the 17th International Conference on Soil Mechanics and Geotechnical Engineering, 283–286.

Weil, M., Dombrowski, K. and Buchwald, A., 2009. Life-cycle analysis of geopolymers. In Provis, J. L. and Van Deventer, J. S. J. (eds), *Geopolymers: Structures, Processing, Properties and Industrial Applications*. Woodhead Publishing Limited, Cambridge, 194–210.

Wild, S., Kinuthia, J. M., Jones, G. I. and Higgins, D. D., 1998. Effects of partial substitution of lime with ground granulated blast furnace slag (GGBS) on the strength properties of lime-stabilised sulphate bearing clay soils. *Engineering Geology* 51, 37–53.

Wilkinson, A., Haque, A. and Kodikara, J., 2010a. Stabilisation of clayey soils with industrial by-products: Part A. *Ground Improvement* 163, 149–163.

Wilkinson, A., Haque, A. and Kodikara, J., 2010b. Stabilisation of clayey soils with industrial by-products: Part B. *Ground Improvement* 163, 165–172.

Zain, M. F. M., Islam, M. N., Mahmud, F. and Jamil, M., 2011. Production of rice husk ash for use in concrete as a supplementary cementitious material. *Construction and Building Materials* 25, 798–805.

Zhang, M., Guo, H., El-Korchi, T., Zhang, G. and Tao, M., 2013. Experimental feasibility study of geopolymer as the next-generation soil stabilizer. *Construction and Building Materials* 47, 1468–1478.

Appendix 5:

Small Strain Triaxial Testing

A5.1 Introduction

The academic literature extensively highlights that, due to strain levels around geotechnical structures being fairly small (Figure A5.1), it is essential to determine soils' geotechnical parameters at very small strains and to understand how stiffness varies with changing stress and strain conditions (Clayton, 2011).

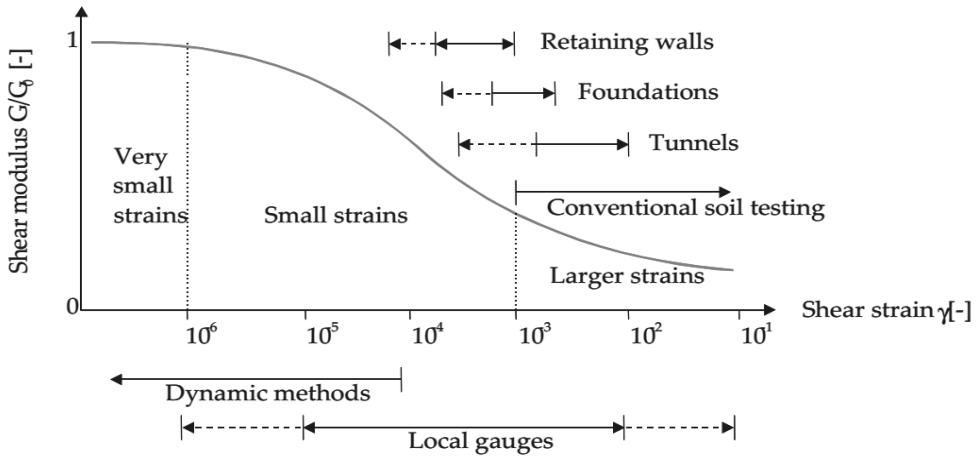

Figure A5.1: Typical variations in stiffness and strain ranges for geotechnical structures and laboratory strain measuring devices. Adapted from Clayton (2011).

Per Mayne et al. (2009), small strain measurements during triaxial tests by using local LVDT's have revealed that soils are considerably stiffer than previously thought from conventional techniques. For instance local strain measurements on North Sea Clay produced E_u values of 600 MPa, compared with the much lower E_u value of 48 MPa obtained using global LVDT's. Additionally, local strain measurements confirm that the Poisson's ratio of soils is smaller and that $E_0 = 2G_0/(1+\upsilon)$ applies at the very start of deviatoric stress-strain curves at small strain levels (Mayne et al., 2009).

Hence, monotonic triaxial tests using local LVDT's and bender elements were conducted at Bristol University to complement the triaxial testing conducted at Newcastle University and gain insights into the small strain behaviour of the Lanton alluvium both in its untreated and GGBS-NaOH stabilised states. This testing was particularly important, given that local small strain measurements produce higher, more representative stiffness measurements for a geomaterial and remove errors

associated with bedding errors, top cap-load cell seating, apparatus compliance, rod friction, the compressibility of porous stones and specimen boundary restraint effects.

The testing programme at Bristol included 2 small strain triaxial tests on undisturbed and reconstituted samples of Lanton alluvium under drained and undrained conditions. Due to time restrictions associated with this research, the author spent a period of one month visiting Bristol to carry out the required tests. However, during the first two weeks of this period many equipment calibrations needed to be conducted. Also, numerous leaks were encountered with the triaxial cell apparatus. Hence, only one undrained triaxial test on the untreated undisturbed and GGBS-NaOH stabilised Lanton alluvium was possible.

A5.2 Methodologies

A5.2.1 Triaxial apparatus

The conventional effective stress path equipment used for this testing was a hydraulic triaxial apparatus, after Bishop and Wesley (1975). Similar connections between samples and the back pressure lines as those used for the ELDYN apparatus at Newcastle were established. However, to reduce saturation and consolidation times and to effectively remove any air bubbles from within the back pressure system and samples, two thin nylon tubes were connected to both the top cap and base pedestal.

As with Newcastle, a 10–16 bar compressor was used to supply the cell, ram and back pressures for the apparatus. The air pressures provided were applied in the form of hydraulic pressures via air-water interfaces. To manage and control the cell, back and hydraulic ram pressures, a similar pressure control system to that used by Gasparre (2005) was utilised, comprising three separate stepper-motor driven manostats that were computer controlled via relay outputs from the data logger and control card. The software used to control, monitor and record raw data from the tests was Triax, as developed by Professor D. Toll from Durham University (1993).

During saturation and consolidation, the hydraulic ram was used to maintain a constant connection between the submersible load cell and sample top cap. The hydraulic ram used two interface systems. The dedicated pressure controller was used to increase air pressure within the air-water bladder interface, which then increased water pressure leading into a water-oil interface. The resulting pressurised oil caused the large piston within the base of the Bishop Wesley cell to rise, along with the sample base pedestal; resulting in sample compression. To conduct strain-rate controlled tests, a constant rate of strain pulser (CRSP) was used instead of the hydraulic ram. This is a stepper-motor driven pump connected directly to the hydraulic system and controls the flow of water leading into the water-oil interface and hence the movement of the piston at the base of the Bishop-Wesley cell. The viscosity of the oil used was sufficient to ensure minimal time delays were experienced between applying a ram pressure and the resulting ram movement and sample straining.

Fully calibrated Druck pressure transducers of 15 bar capacity were fitted to the triaxial apparatus to monitor cell, back, hydraulic ram and pore pressures at both the top and bottom of samples throughout triaxial tests. A single volume change unit was attached to the triaxial apparatus, which was an ICVC with a maximum capacity of 100 ml. Similar to the ICVC unit used for the ELDYN apparatus at Newcastle University, this ICVC contained a belloframe and sealed piston, which moved up and down per volumetric increases and reductions within the sample, respectively (based on the assumptions that samples were fully saturated and that water is incompressible). An LVDT was fixed to the side of the ICVC unit to accurately monitor volumetric strains experienced by samples. Figures A5.3–A5.4 display detailed schematics of the Bishop Wesley triaxial apparatus used at Bristol University.

An external LVDT was mounted to the base of the Bishop Wesley cell. The armature rested on an arm that was fixed to the lowering/rising hydraulic ram to measure axial strains experienced by samples. Additionally, local axial and radial strains were measured by mounting LVDT's and their associated calipers onto samples (Cuccovillo and Coop, 1997) by using an instant contact adhesive (Evo-Stik Multi Purpose Impact). These provided vital insights into the behaviour of the samples at small strains and to reduce errors associated with bedding, end-effects and machine compliance, which are commonly observed when using external LVDT's. Two axial LVDT's were mounted diametrically opposite each other within the middle third of

samples (Figure A5.2), which is considerably less restrained than towards the sample ends. The LVDT's armatures were fixed to a lower mount. The lower and upper mounts contained screws, which enabled adjustments to the gauge length to be made prior to filling the triaxial cell with water. To more easily resolve very small strains once shearing commenced and to allow for the Triax software to log changes in axial strain in the most sensitive range of the LVDT's, all the LVDT's were reset to their electrical zero by making the necessary adjustments within the LVDT's amplifiers. Care was taken to ensure that all LVDT cables were clear from interfering with other LVDT's and the radial caliper. All external and local LVDT's were calibrated using a micrometer.

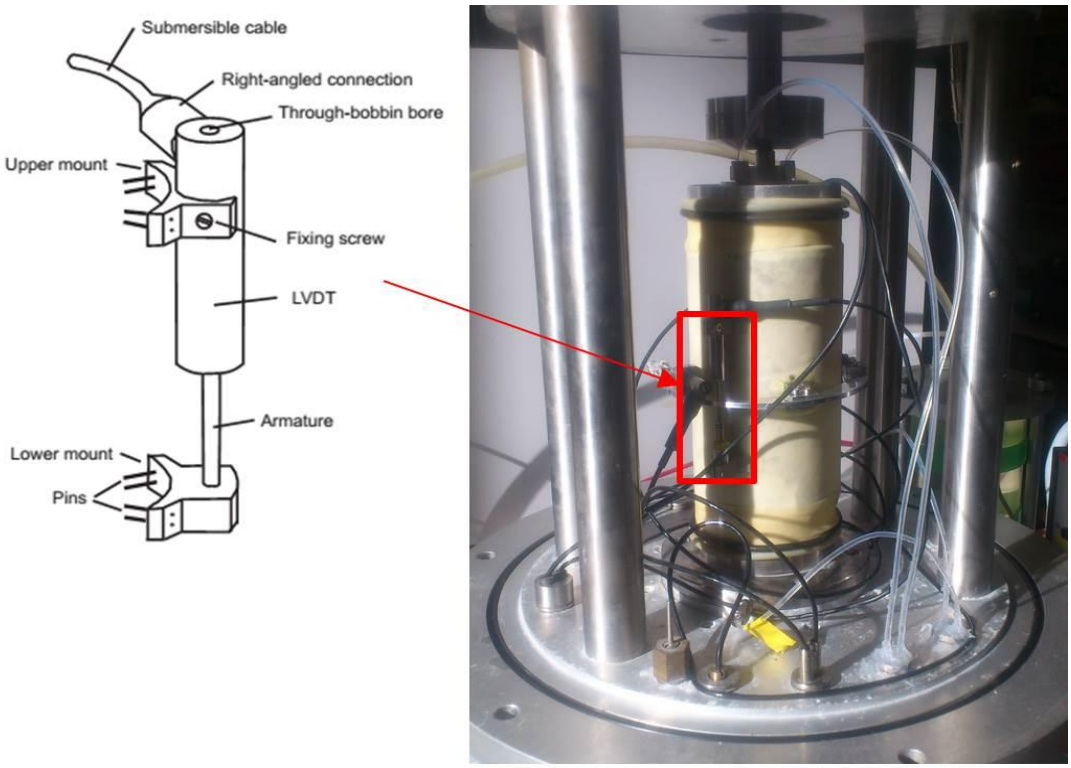

Figure A5.2: Mounting of two axial and one radial local LVDT's on samples for small strain measurement. LVDT schematic courtesy of Cuccovillo and Coop (1997).

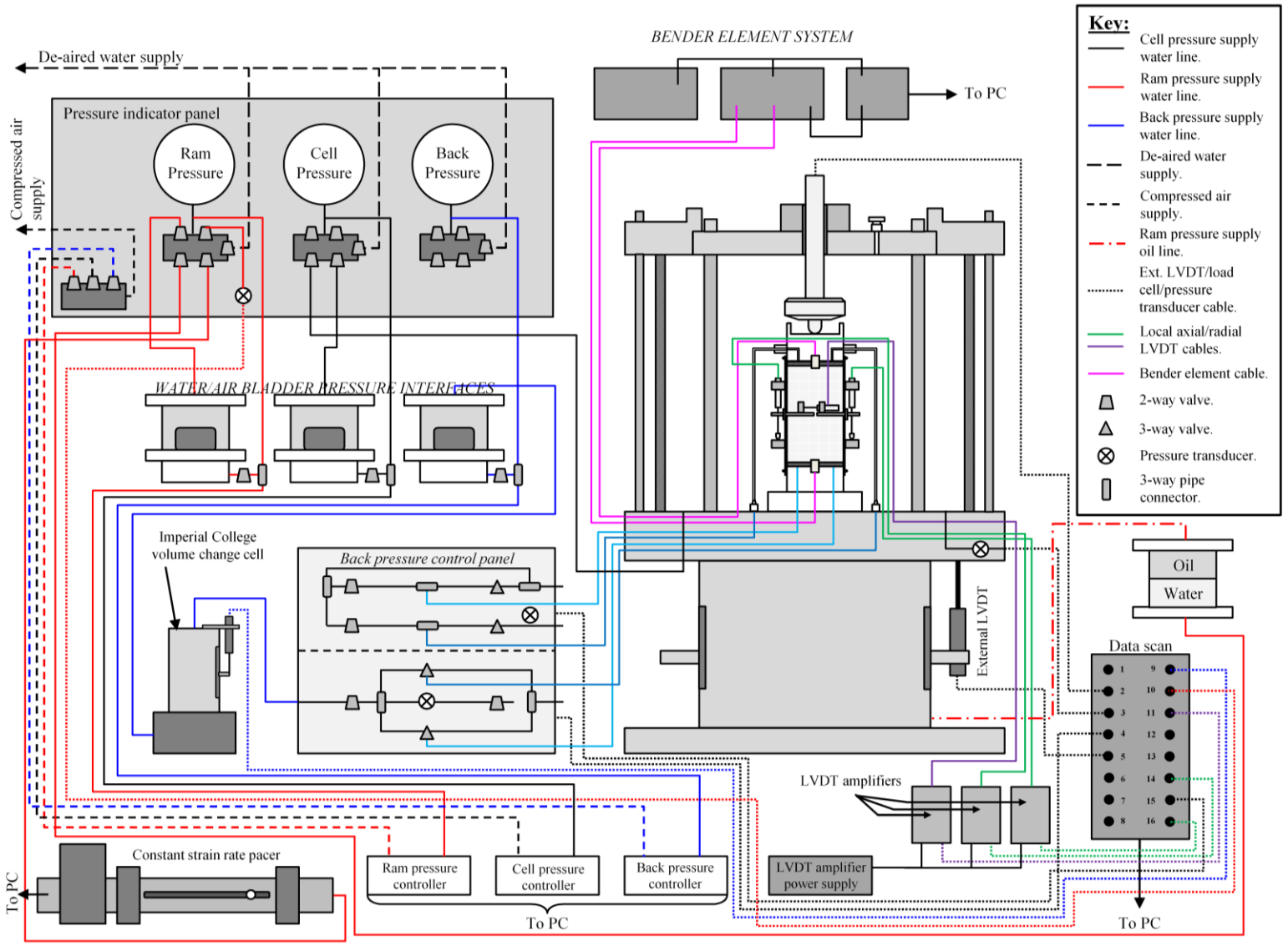

Figure A5.3: Schematic of Bishop-Wesley triaxial apparatus (including small strain LVDT's and bender elements) used at Bristol University.

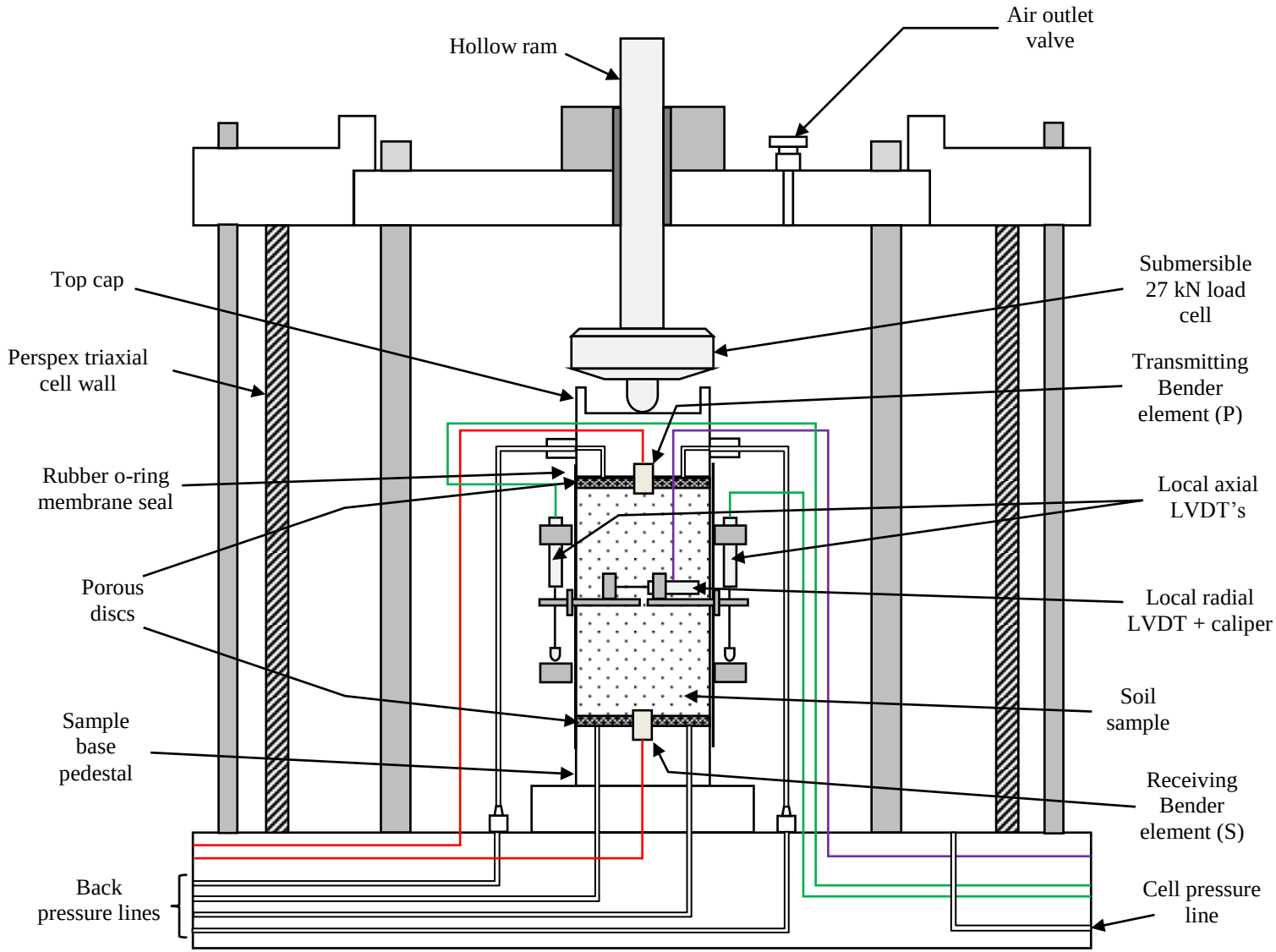

Figure A5.4: Detailed schematic of the Bishop-Wesley triaxial cell at Bristol University.

Two sets of bender elements were installed within the base pedestal (Figure A5.5a) and top cap to measure changes in the shear stiffness of samples throughout sample preparation and testing. The bender element transducers comprised two thin laminated piezoceramic plates based within epoxy-filled aluminium pots, which sent shear (S) waves through a sample.

(a) 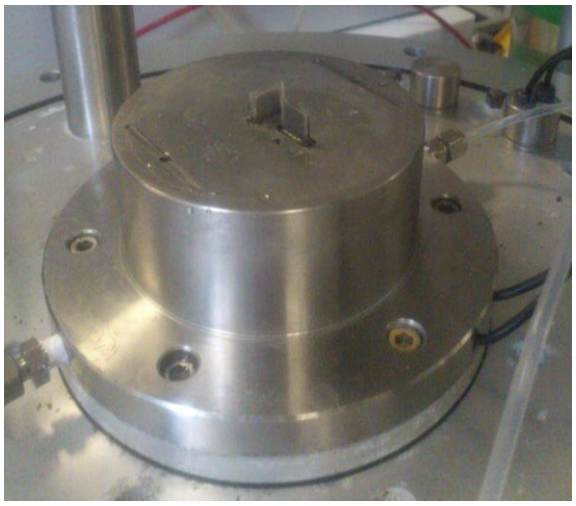

(b) 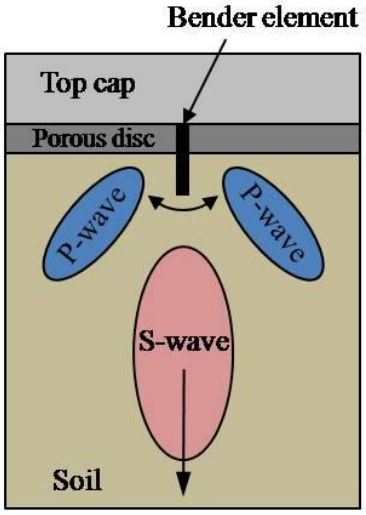

Figure A5.5: (a) Bender elements for measuring G_{max} within the vv and vh planes of samples, protruding from the base pedestal; (b) transverse and in-plane directions of generated S and P-waves (after Lee and Santamarina, 2005).

For each set of bender elements, a transmitter (parallel – P) and receiver (series – S) are required. The transmitter located within the top cap had a voltage applied to it (in the form of a sine wave signal burst) from a SIGLENT SDG 1010 function/arbitrary waveform generator via a custom-built three channel bender signal routing unit. This caused the bender element to vibrate at a specified ultrasound frequency normal to the face of the piezoceramic plates and thereby send two P-wave side lobes normal to their plane (one in compression, one in rarefraction) and an S wave frontal lobe through the sample, per Figure A5.5b (Lee and Santamarina, 2005). The receiver at the sample base receives the S-waves sent through the sample and sends the signal to a digital oscilloscope (Picoscope) and was analysed within the its associated Picoscope 6 software to calculate the travel time (t_s) between the signal being sent and received. A labelled schematic of the bender element apparatus used for triaxial tests is presented in Figure A5.6.

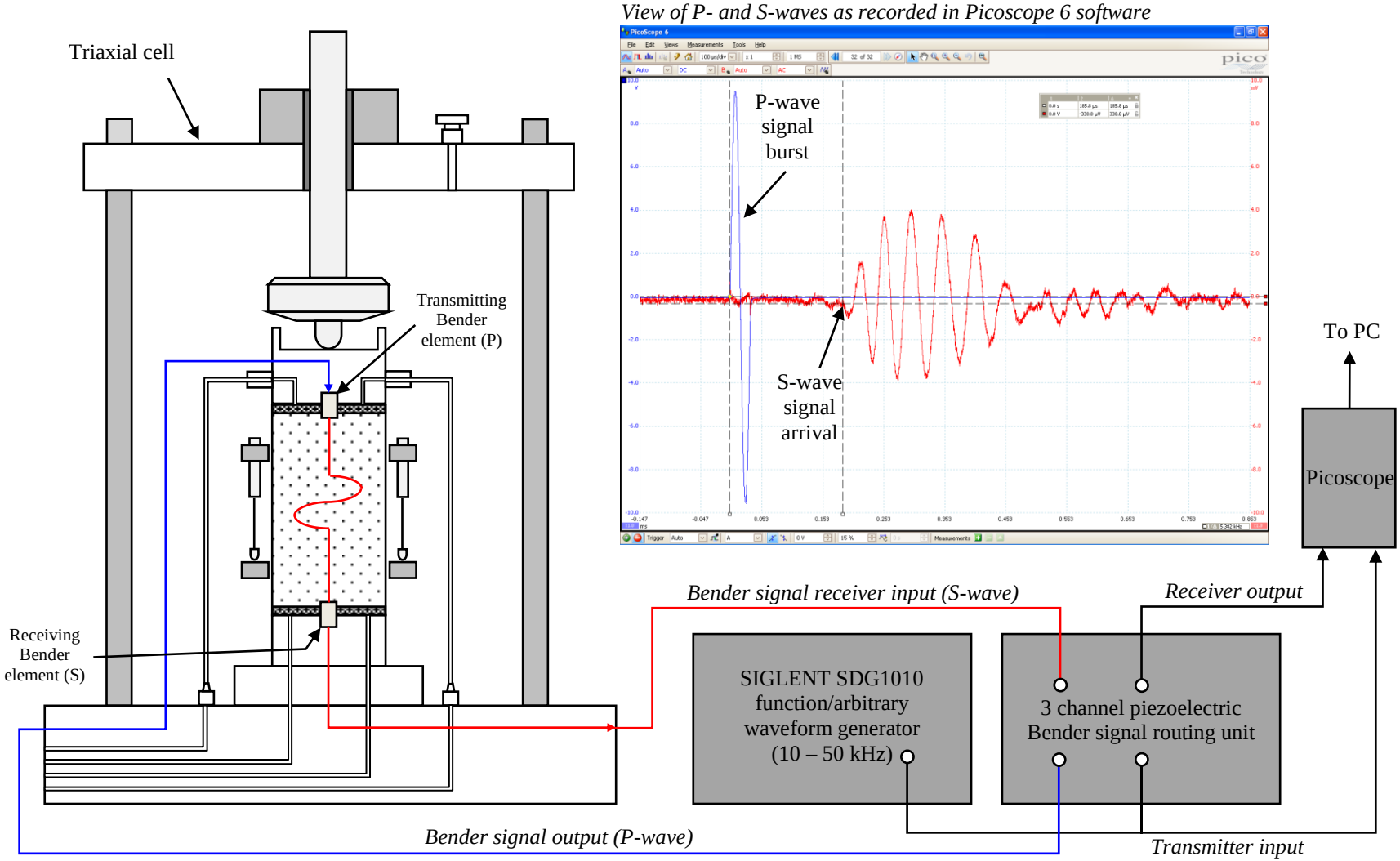

Figure A5.6: Bender element apparatus and set-up used within Bishop Wesley triaxial apparatus at Bristol University.

P-waves can reflect off cell walls and therefore interfere with the arrival of S-waves. The level of interference depends on the cell geometry, the soil specimen's state of stress and saturation (Lee and Santamarina, 2005). Generally, the magnitude of P-wave reflections within output signals is greater when the soil sample is dry. Per Snelling et al. (2011), using P and S waves is ideal in characterising the stiffness of soils. However, given the small area of the bender element tip which excites a soil, P-wave signals are not as strong as those received for S-waves. Additionally, for saturated soils, a water propagated P-wave can potentially conceal the P-wave travelling through the material (Snelling et al., 2011). Therefore, P-waves should not be considered when determining initial soil stiffnesses.

To ensure that the bender element tests conducted at Bristol University produced the highest quality S-wave signals and therefore more accurate estimations of initial shear stiffness values (i.e. G_{max}), it was imperative that the bender elements were calibrated. The materials used for calibration were 100 mm diameter – 200 mm long cylindrical samples of aluminium and Lucite, per calibrations conducted by Arroyo et al. (2010). Care was taken to ensure an accurate level of in-plane alignment was achieved between the source and receiver bender elements at either end of the samples. Frequencies used for the source bender element's signal bursts during the calibration process were between 5 and 50 kHz. The shear wave velocities obtained for the aluminium and Lucite samples were very similar to those documented by Arroyo et al. (2010); namely 3078 m/s and 1351 m/s, respectively.

Once bender element calibration was completed, the soil samples were ready for testing. Through personal communication with Nash and Diambra (2013), a minimum number of three wavelengths (λ) are required to pass through a sample during a bender element test. Based on pre-existing knowledge of the density and stiffnesses of the materials being tested, estimations of their associated shear wave velocities (V_s) were made. Such estimations were then used to identify the range of frequencies used during bender element tests, via the following equation:

Frequency: $$F = \frac{V_s}{\lambda}$$ (**Equation A5.1**)

Besides the frequency values obtained from these calculations, a series of bender element tests were also conducted on samples prior to submerging them in water to determine which frequencies produced the best quality S-wave signals. Based on these findings, source signal bursts using frequencies of 10, 20 and 30 kHz were used for all bender element tests conducted on all samples to allow for direct comparisons. The GDS BEAT tool was predominantly used as a convenient method for analysing the bender element data sets, by using the time and frequency domain techniques. However, the time-domain analysis of the data sets was conducted manually by the author for comparative purposes.

A5.2.2 Sample preparation

For undisturbed samples tested at Bristol University for small strain measurements, once the samples were sealed within a latex rubber membrane, measurements and a series of markings were lightly drawn onto the membranes with an extra fine nib permanent marker pen to indicate the intended positions for the local axial LVDT mounts, the radial LVDT caliper and finally to ensure that the bender elements within the top cap and base pedestal were accurately aligned with each other. The upper and lower mounts for both local axial LVDT's were fixed to the membrane by an instant contact adhesive (Evo-Stik Multi Purpose Impact). Once the adhesive had set after an hour of drying, the local axial LVDT's were fitted. Subsequently, the radial caliper was mounted to the samples, whilst taking additional care not to disturb the local axial LVDT's already mounted. Once the contact adhesive had set, the local radial LVDT was fitted.

The porous discs used at Bristol had two slots drilled out at their centre, to allow for the bender elements to protrude from the base pedestal/top cap, through the porous disc and into the base/top of the samples. However, a gap was observed between the protruding bender element and the porous disc, as observed in Figure A5.7. Neglecting the presence of this gap would probably have resulted in the porous discs and sample moving during testing, in addition to unfavourable coupling and reflection issues during testing when bender element measurements were to be taken. Thus, the gap was carefully infilled with small amounts of either moistened fine grained sand,

untreated or GGBS-NaOH stabilised Lanton alluvium. Given the soft nature of the untreated Lanton alluvium, no slots were required to be made within the top or bottom faces of samples, as the protruding bender elements within the top cap and base pedestal would simply push into soil. Coupling between the sample and the bender elements was of good quality prior to filling the triaxial cell with water, as evidenced by the strength of the received S-wave signals.

Figure A5.7: Infilling of gaps between bender elements and porous discs to avoid sample movement and increase sample-bender element coupling.

As the stabilised alluvium was characterised by a much higher stiffness compared with the untreated alluvium, bender elements would not simply push into the ends of the stabilised samples. This problem has also been observed by GDS on the bender element testing of sandstone (GDS, 2014) (Figure A5.8). Hence, similar to that conducted by GDS (2014), slots were carved out of both ends of the samples using a Stanley knife to house the bender elements (Figure A5.9). Once some initial bender tests had been conducted to establish that a good degree of coupling existed between the bender elements and the stabilised sample and that the strength of received S-wave signals was sufficiently strong, the triaxial cell was ready for filling with water.

As samples were subjected to increasing cell pressures during saturation and consolidation and compression during shearing, the level of coupling between the samples and the bender elements improved further.

Figure A5.8: Slots carved out of ends of a sandstone specimen. Taken from GDS (2014).

Figure A5.9: Stabilised sample with slots carved out for inserting the bender elements.

All LVDT cables, bender element cables and nylon back pressure lines within the triaxial cell were carefully arranged to ensure that none had any risk of moving and interfering with any of the local LVDT's and the small strain measurements made during testing.

The data acquisition/control software used for triaxial testing was Triax. To ensure similar constant deviator stress conditions were maintained during saturation and consolidation as conducted at Newcastle with the GDS equipment, the "Hold Cell and Back" and "Increase Cell and Back" functions ensured that the ram pressure adjusted automatically to maintain a q value of 0 kPa. Once the test files had been set up, the triaxial cell was carefully placed over the sample, sealed by tightening the necessary bolts, the submersible load cell was docked with the top and finally the triaxial cell was filled with de-aired water ready for the first cell pressure increment required in the saturation process.

Once samples had been encapsulated and sealed within a membrane, measurements for the intended positions of the local axial LVDT mounts, the local radial LVDT caliper and the in-plane alignment of the bender elements were lightly drawn onto the membranes with an extra fine nib permanent marker pen. All of the LVDT mounts and caliper were secured to the membrane by using the Evo-Stik Multi Purpose Impact adhesive. Once adhesive had dried, all of the LVDT's were fitted whilst taking care to ensure that none of the LVDT's or their cables interfered with one another.

A5.2.3 Testing procedures

The same testing procedures conducted at Newcastle for saturating, isotropically consolidating and shearing samples were also followed for small strain triaxial tests conducted at Bristol (please refer to Chapter 3 for details). The results obtained from small strain triaxial tests are presented forthwith.

A5.2.4 Bender element data analysis

To determine the G_{max} value of the untreated and stabilised Lanton alluvium at the start of shearing, the time taken for the generated S-wave to pass through the material between the transmitting and receiving bender elements (i.e. the arrival time) first required determination. From the literature, there is no single standard method for interpreting bender element data to determine S-wave arrival times. This presents major difficulties in calculating representative G_{max} values for geomaterials. The two most commonly used methods for interpreting bender element tests are time-domain and frequency domain (cross-correlation) approaches. The time domain method assumes no reflected/refracted waves are detected. The arrival time of a plane wave front is estimated as the time difference between the generation of the sine wave pulse signal at the transmitter bender element and the detection of the S-wave at the receiving bender element. The arrival of the received signal tends to be characterised by an initial downward deflection relative to the travel time (x) axis, which arises from the "near field effect". This effect is caused by wave front spreading and coupling between waves that are characterised by similar particle motions but propagating at different velocities (Gasparre, 2005; Rees et al., 2013). There has been much debate regarding which point on the received signal should be taken as the first arrival. Per Gasparre (2005), using low frequencies for transmitting signals makes detecting the first arrival considerably more challenging compared with higher frequencies. According to researchers at Bristol University and Rees et al. (2013), there are four points of interest on the received signal (per Figure A5.10) which may be used for determining the arrival time:

1) Point A is the time recorded for the first deflection.
2) Point B is the time recorded for the first bump maximum (i.e. the point corresponding to the first most negative output).
3) Point C is the time recorded for when the output signal first crosses the travel time (x) axis with an output signal of zero.
4) Point D is the time recorded for the first major peak in output signal.

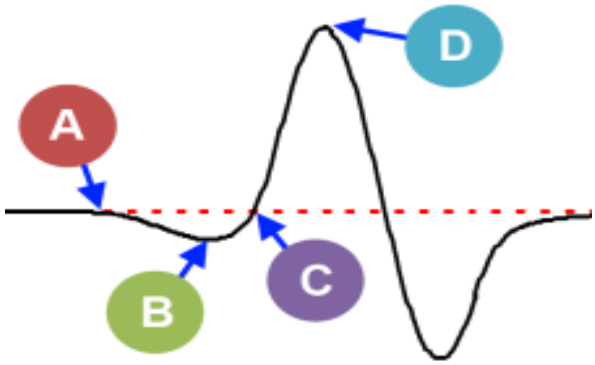

Figure A5.10: Idealised S-wave signal containing the "near field effect", with four possible areas of interest for taking wave arrival times. Courtesy of Rees et al. (2013).

Besides issues associated with frequency, other factors known to influence determining accurate arrival times include shear wave reflections from the top and bottom platens of the triaxial apparatus within which the benders are installed. Also shear waves may not take direct paths between the transmitting and receiving bender elements (Greening and Nash, 2004). Hence, the development of frequency domain approaches through using cross-power spectrum and cross-correlation functions (Rees et al., 2013) may also be used to determine S-wave arrival times. Greening and Nash (2004) view this technique as providing a clearer understanding of the relationship between the transmitting and receiving bender signals compared with the time-domain method, particularly when using the π point and continuous sweep methods (Figure A5.11). To determine S-wave arrival times through this method, a continuous harmonic signal is transmitted through samples at various frequencies. The points at which the received and transmitted waves are both in phase and 180 degrees out of phase correspond to the maximum "cross correlation" between the signals recorded at the two points (Gasparre et al., 2005).

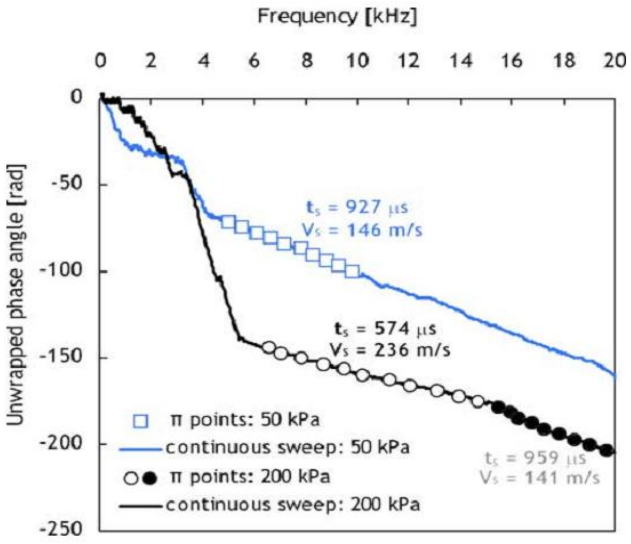

Figure A5.11: Demonstration of frequency domain derived S-wave arrival times. Taken from Viana da Fonseca et al. (2008).

A free bender element analysis tool (BEAT) has recently been developed by GDS Ltd. as an add-in for Microsoft Excel to analyse and interpret multiple bender element data sets using both of the aforementioned time and frequency domain techniques to provide useful comparisons (Rees et al., 2013). The tool produces travel time reports in the form of numerical values for travel time estimations and graphical visualisations of the transmitting and receiving bender elements. Bender element tests were conducted by Rees et al. (2013) on a triaxial sample of Leighton Buzzard sand which had been isotropically consolidated using varying frequencies. The BEAT tool was used by the author to interpret the data obtained and demonstrated that a good agreement was found between calculated V_s and G_{max} values, thereby indicating that the BEAT tool is useful in interpreting bender element data; albeit Rees et al. (2013) strongly recommend that engineering judgements should still be taken when documenting shear stiffness values.

It is clear that further work needs to be conducted into devising a standard means for analysing raw bender element data. Numerous methods have been suggested to try and accurately determine S-wave arrival times. The time- and frequency-domain techniques tend to be the most popularly used; albeit slight disparities in V_s values tend to be observed between the two methods. Based on the encouraging findings by Rees et al. (2013) on using the GDS BEAT tool in analysing bender element tests on

Leighton Buzzard sand, the BEAT tool will be used to analyse raw bender element data. Additionally, the author personally analysed all of the bender element data using the time-domain technique. Each of the four possible points of S-wave arrivals (per Figure A5.10) were identified. Through personal communication with Nash and Diambra (2013), based on their extensive experience in the use and interpretation of bender elements, it is strongly recommended that when using the time-domain technique, the most suitable point to take on the received signal as the first S-wave arrival is point B, the first bump maximum.

Once the arrival time (t_s) for the received S-wave has been determined, it may then be used to calculate the shear wave velocity (V_s) for the S-wave via the following formula:

Shear wave velocity: $$V_s = \frac{l}{t_s}$$ (**Equation A5.1**)

where l is the separation between the tips of the transmitting and receiving bender elements. According to workers at Bristol University and research by Arroyo et al. (2010), a high level of coupling is required in the successful transmission of shear waves through samples by using bender elements. This has been directly related to the extent of bender element intrusion within samples, besides accurate in-plane alignment of the transmitter and receiver. Thus, the 10 mm wide, 12 mm long, 1.5 mm thick bender elements protruded 5 mm into samples. The value obtained for V_s may then be used along with the known density of the soil (ρ) to calculate the initial shear stiffness of the material (G_{max}) via the following formula:

Initial shear stiffness: $$G_{max} = \rho V_s^2$$ (**Equation A5.2**)

A5.3 Results and analysis

A5.3.1 Untreated undisturbed Lanton alluvium

A5.3.1.1 Shearing behaviour

The axial strain experienced by the sample was measured by LVDT's both globally and locally, whereby local LVDT's were mounted directly onto the sample. The deviatoric stress – axial strain response of the undisturbed sample under undrained conditions is presented in Figure A5.12.

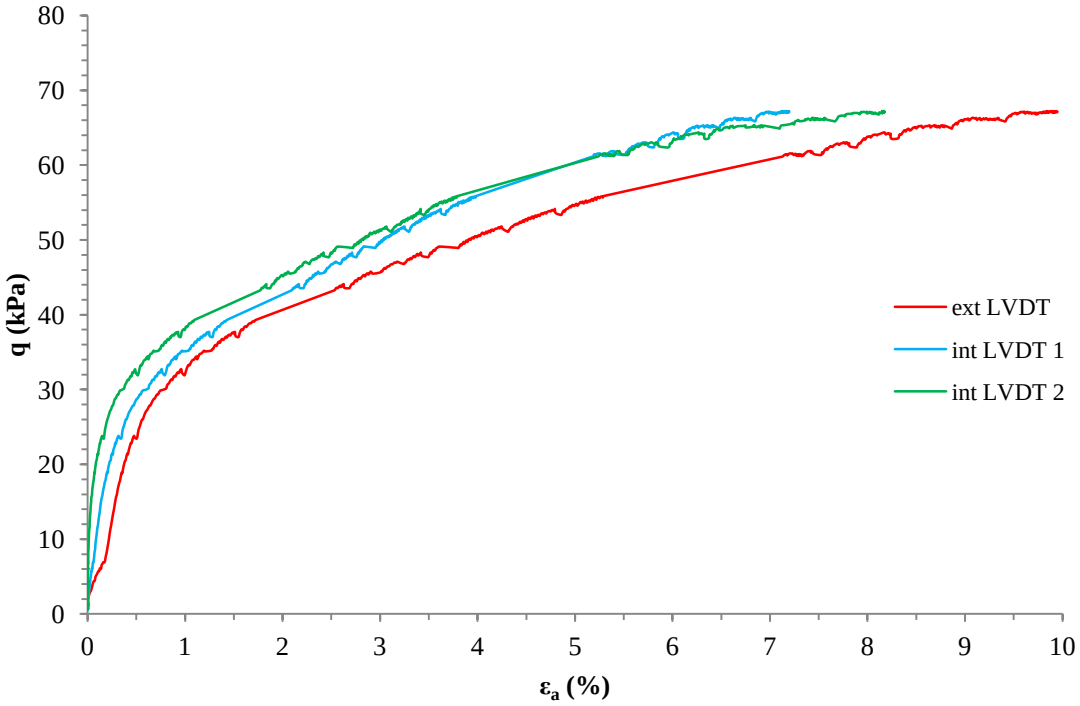

Figure A5.12: Deviatoric stress-strain behaviour of undrained undisturbed small strain sample of Lanton alluvium, using external and local LVDT axial strain measurements.

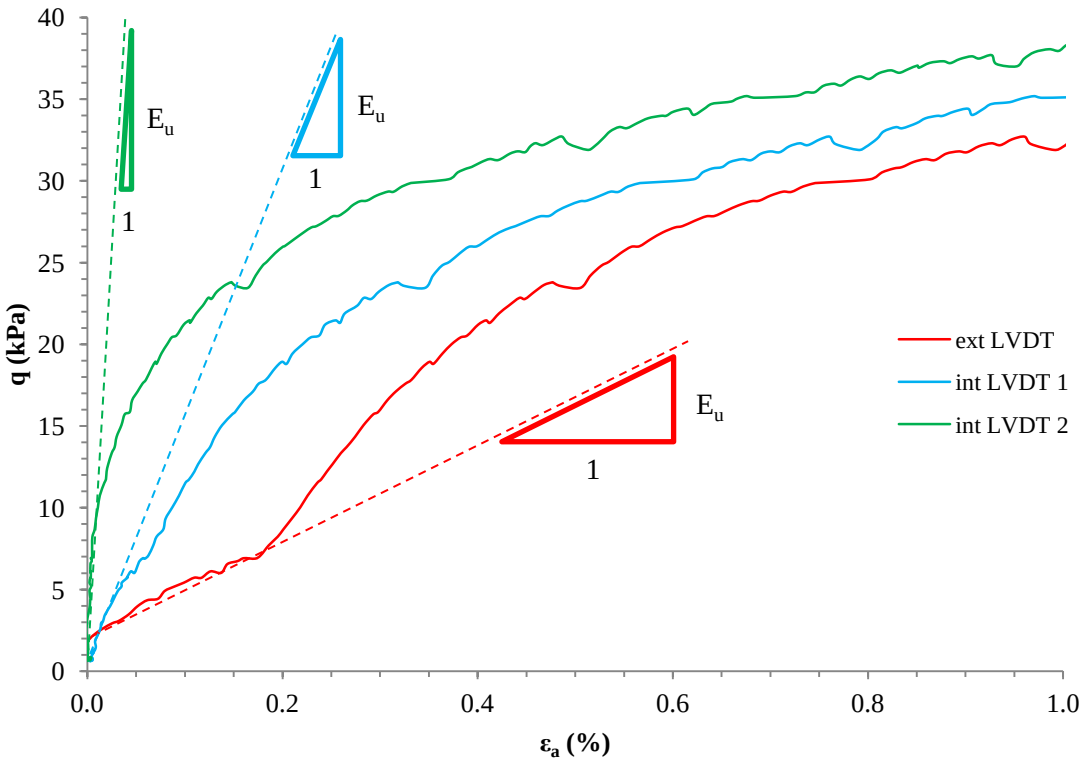

Figure A5.13: Considerably stiffer deviatoric stress-strain response observed for Lanton alluvium when using local rather than external axial strain measurements.

Certainly at shear strains up to 0.2%, much lower secant Young's modulus values were derived from external LVDT measurement (3 MPa) compared with the much stiffer values derived from both local LVDT's 1 (15.2 MPa) and 2 (130 MPa). At larger strains >1%; the three sets of deviatoric stress–strain measurements are seen to converge. These higher stiffnesses and deviatoric stress–strain curve convergence is seen in Figure A5.13.

A slight difference can be observed between the stiffnesses measured by local axial LVDT's 1 and 2; therefore an average of the two data sets was taken for the purpose of measuring small (axial) strain stiffnesses within the sample throughout testing. As observed for undrained reconstituted and undisturbed samples tested at Newcastle, the deviatoric stress–strain behaviour of the sample demonstrates clear evidence of work hardening up to the point of failure (i.e. maximum effective stress ratio) and critical state being achieved. The deviatoric stress–strain behaviour of the undisturbed Lanton alluvium may also be expressed regarding radial strains (Figure A5.14), according to local strains measured by the radial LVDT positioned half way up the sample.

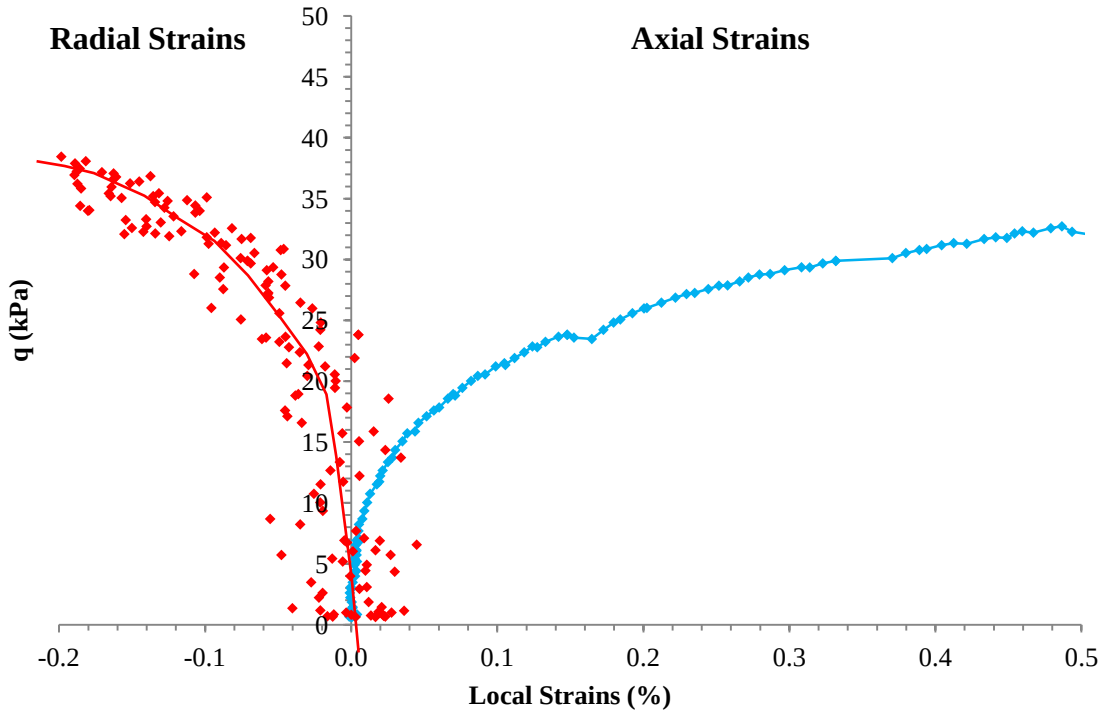

Figure A5.14: Relationship between deviatoric stress and average local axial and local radial strains.

Albeit there appears to be more scatter for the radial strain data, there is almost a mirror image between the deviatoric stress – axial strain behaviour of the soil and its deviatoric stress – radial strain response. However, the radial stiffness appears to be higher than that recorded for the axial stiffness, which in turn produced a Poisson's ratio of approximately 0.5. Although values of 0.5 are theoretically possible for stiff saturated clays during CIU triaxial compression tests, such a value would be considered too high for a soft silty alluvial soil; whereby 0.3 - 0.35 would typically be expected (Bowles, 1977). However, a soil's Poisson's ratio is permitted to be >0.5 during CID triaxial tests where samples experience dilation during shearing (Briaud, 2013). The higher than expected radial stiffnesses may be partially attributed to a combination of factors, the first being the stiffness of the latex rubber membrane encasing the sample which restricts radial deformation in response to axial strain. Secondly, given the degree of data scatter within the radial strain data set shown on Figure A5.12, there may be the implication that the chosen position for the best-fit curve of the data is not true and therefore provides an over-estimate of the Poisson's ratio. Small levels of frictional resistance created by the linear core moving in and out of the LVDT's body work may also partially explain the higher radial stiffnesses.

Alternatively, there may be the natural factor of stiffness anisotropy within the soil. Further testing with horizontally mounted bender elements at the centre of the sample would be required to investigate these postulates further. The maximum deviatoric stress recorded for the sample was 67 kPa, producing an undrained shear strength of 33.5 kPa. These values were closely comparable to those recorded for the undisturbed samples tested at Newcastle.

The pore pressure response of the undrained sample was monitored at both the top and bottom of the sample. The pore pressure data presented in Figure A5.15a is an average of the pore pressures measured at the top and bottom of the sample. Pore pressures increased up to 34 kPa at a shear strain of 1.5%; after which the pore pressures slowly decreased to approximately 30 kPa with increased straining until sample failure.

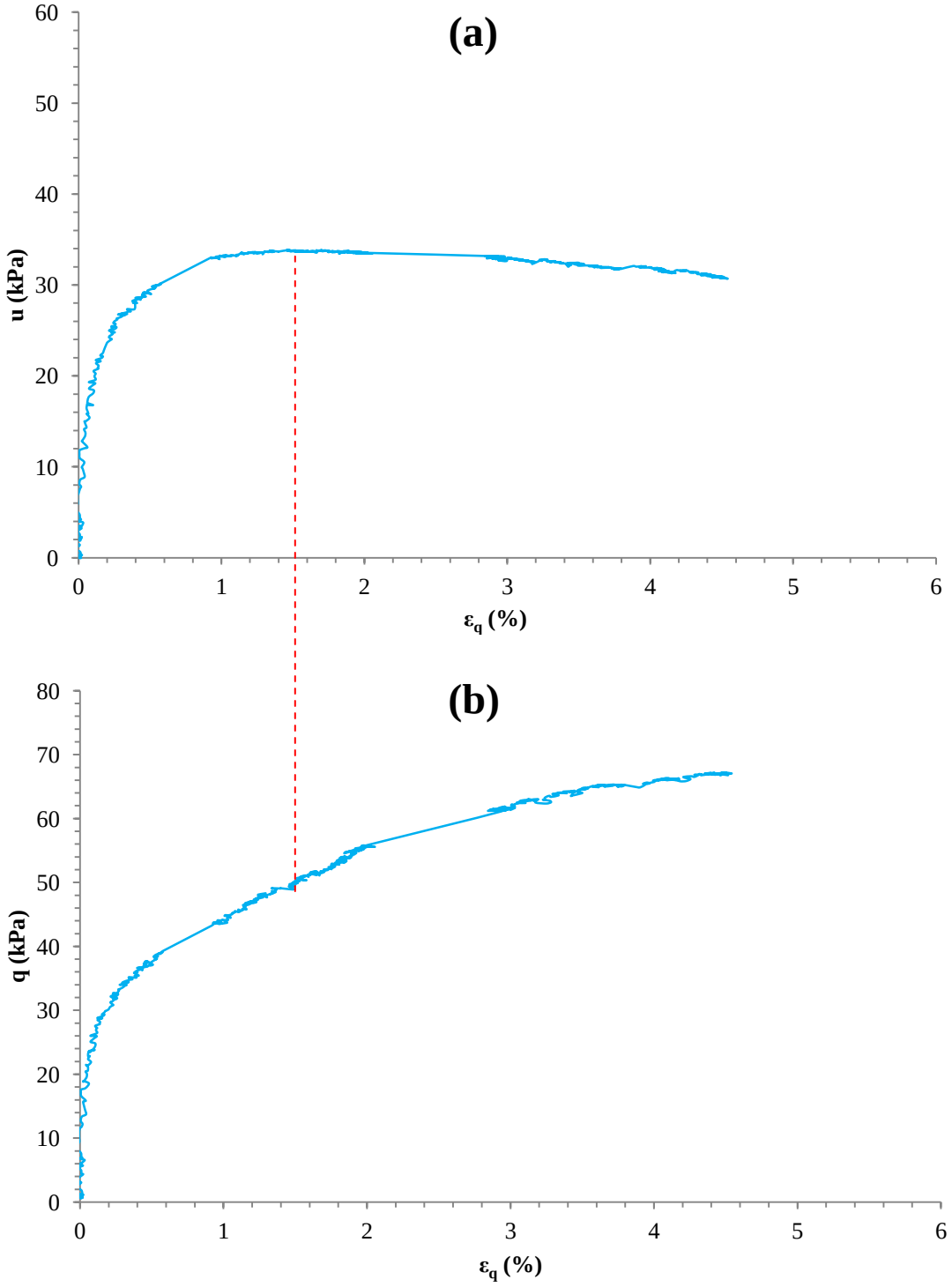

Figure A5.15: Pore pressure behaviour of undrained undisturbed small strain sample of Lanton alluvium.

Within q-p' stress space, the shape of the sample's undrained stress path (Figure A5.16) is very similar to those in Figure 7.25 for undisturbed samples tested at Newcastle, which clearly illustrates the soil experienced strain hardening. The peak pore pressure occurred in coincidence with the soil approaching its critical state, where the effective stress path experienced a transition in behaviour from gradually decreasing mean effective stress values with increasing deviatoric stress towards mean effective and deviatoric stresses increasing simultaneously. Also, the soil's failure envelope lies just beneath the CSL, as derived from extensive testing conducted at Newcastle.

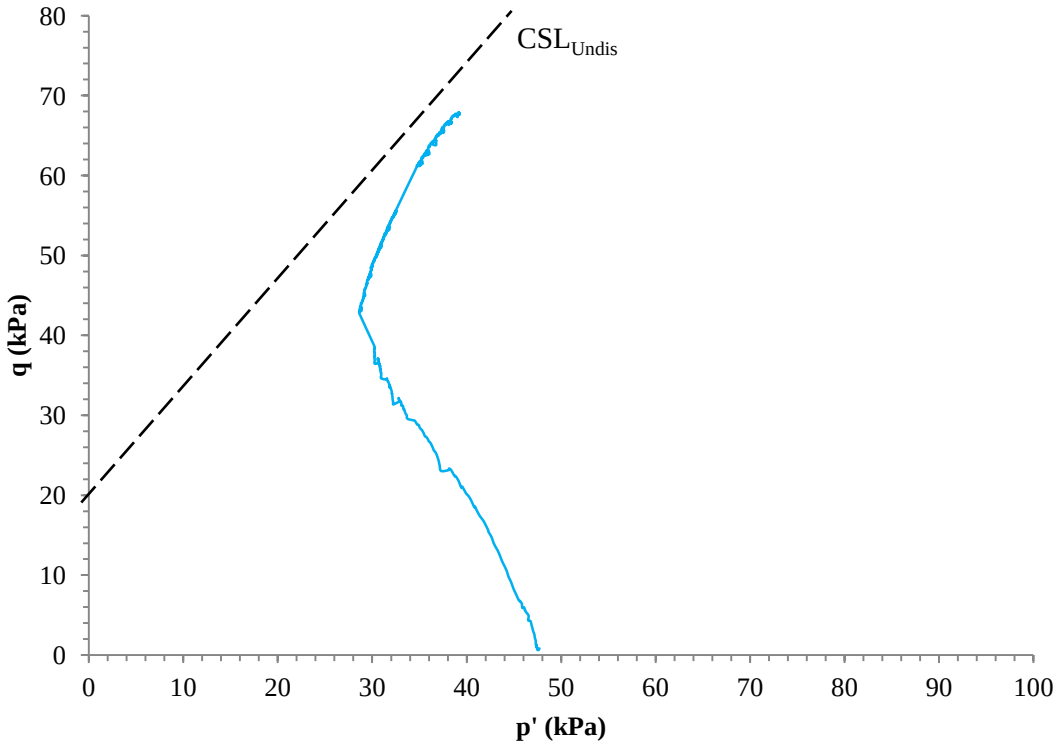

Figure A5.16: Undrained effective stress path for the undisturbed sample tested at Bristol within the q-p' stress plane. The CSL for undisturbed samples (CSL_{Undis}) derived from testing conducted at Newcastle is superimposed.

Based on the M value for the slope of the effective stress path at critical state, c' and φ' values of 0.49 kPa and 33^{o} were obtained for this sample. The φ' value lies comfortably within the φ' range defined from the triaxial testing at Newcastle; whereas the c' value is lower than the c' range of 2.81–9 kPa recorded at Newcastle.

However, such a low c' value of 0.49 kPa is not atypical of silty sand soils such as Lanton alluvium. Such low c' values were observed for the reconstituted undrained samples tested at Newcastle.

A5.3.1.2 Bender elements

To gain insights into the changing shear stiffness of Lanton alluvium throughout the triaxial testing process, bender element measurements were taken at every stage of sample preparation, at the end of saturation and finally at the end of consolidation (prior to the initiation of shearing). Unfortunately, no bender element measurements could taken during shearing as there were multiple leaks within the bender element cables (Figure A5.17). This was caused by previous users of the equipment over-tightening the cables as they passed through the access ring into the triaxial cell, causing several tears along the cable sleeves which pressurised cell fluid could penetrate. Table A5.1 summarises the sample conditions encountered for each bender element measurement taken.

Figures A5.18–A5.19 present the raw P-wave and S-wave signal data for each bender element measurement conducted at frequencies of 10, 20 and 30 kHz. Superimposed on these signal traces are a series of manually drawn lines, which identify the possible arrival times for the S-waves. Based on the S-wave signals in Figures A5.18–A5.19, using a frequency of 30 kHz generally produced the most stable signals on the Picoscope. Figures A5.20–A5.24 present a summary of the GDS BEAT time and frequency domain analyses for all the 30 kHz frequency bender element measurements taken.

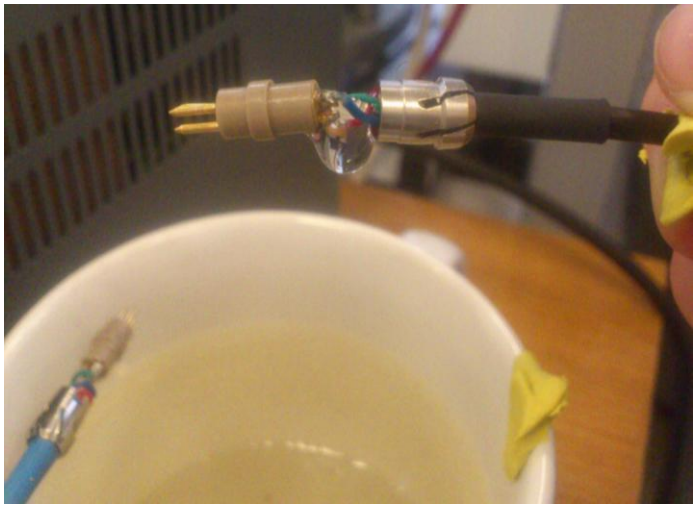

Figure A5.17: Water leaks through bender element cables.

Table A5.1: Details of bender element tests conducted on the undisturbed Lanton alluvium sample.

BE test no.	Date & time	Frequencies used (kHz)	Voltage peak to peak (V)	Sample condition	Sample height (mm)	Bender element separation (mm)
1	23/10/13 23.30	10, 20, 30	20	Sample docked, membrane, no LVDT's attached, no cell, no water. $\rho = 1.81$ Mg/m^3	177.03	167.03
2	24/10/13 00.04	10, 20, 30	20	Sample docked, membrane, LVDT's attached, no cell, no water. $\rho = 1.81$ Mg/m^3	177.03	167.03
3	24/10/13 01.33	10, 20, 30	20	Sample docked, membrane, LVDT's attached, cell full, CP = 9.85kPa. $\rho = 1.83$ Mg/m^3	177.017	167.017
4	24/10/13 14.56	10, 20, 30	20	Sample docked, membrane, LVDT's attached. SATURATED (CP = 300.17kPa, PWP = 292.4kPa, load = 7.19N). $\rho = 1.83$ Mg/m^3	176.631	166.631
5	25/10/13 17.11	10, 20, 30	20	Sample docked, membrane, LVDT's attached. CONSOLIDATED (CP' = 50kPa). $\rho = 1.89$ Mg/m^3	172.81	162.81

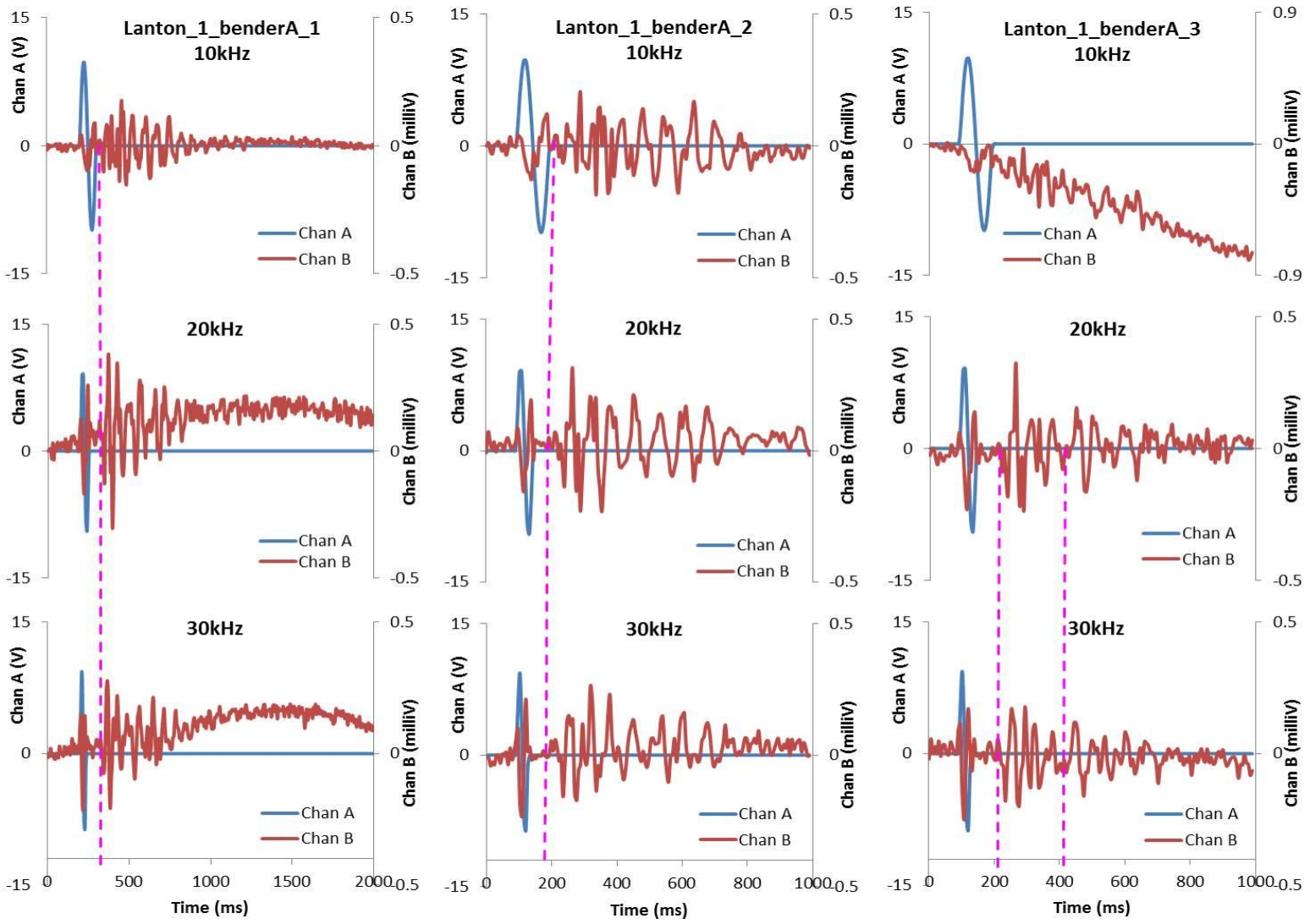

Figure A5.18: Source and received signals obtained from bender element tests 1 – 3.

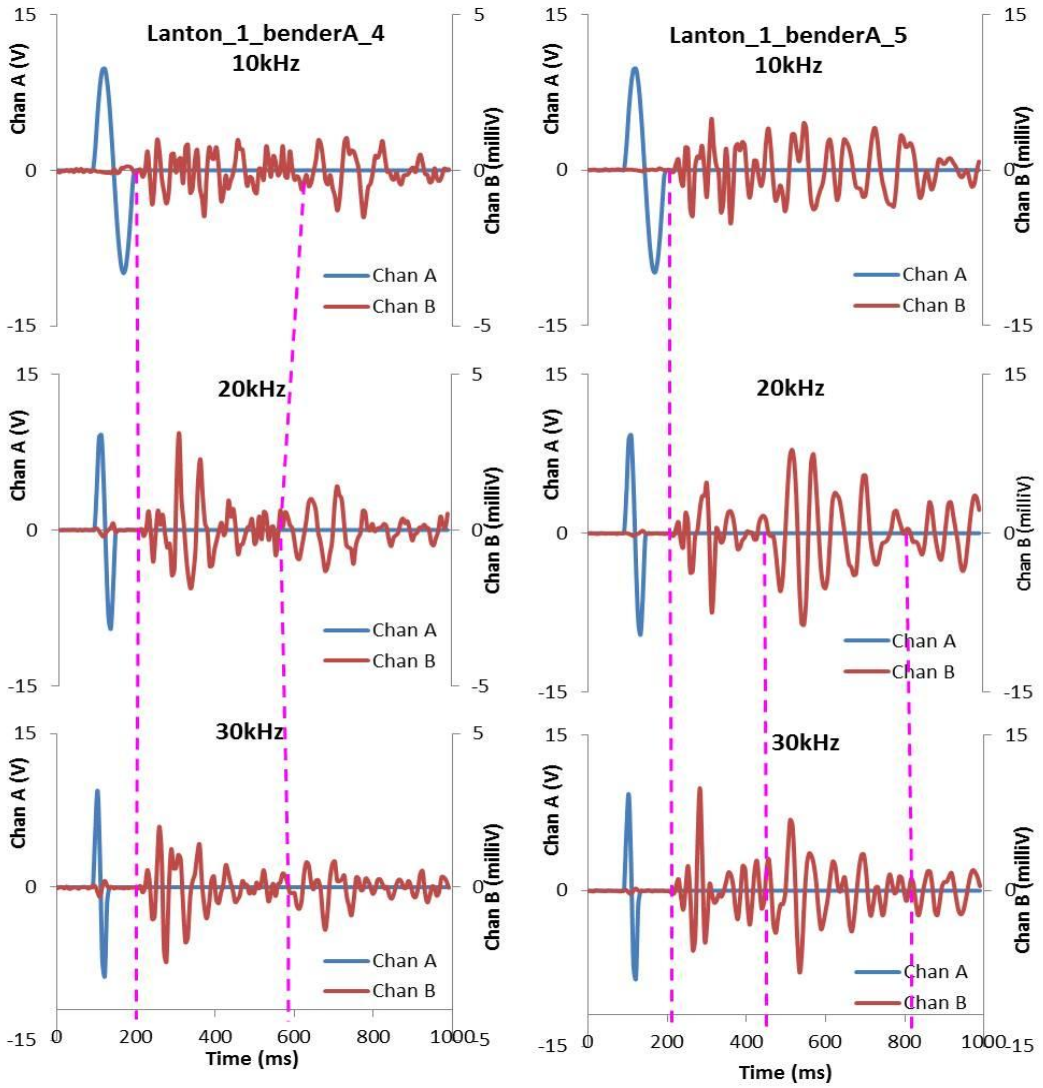

Figure A5.19: Source and received signals obtained from bender element tests 4 – 5.

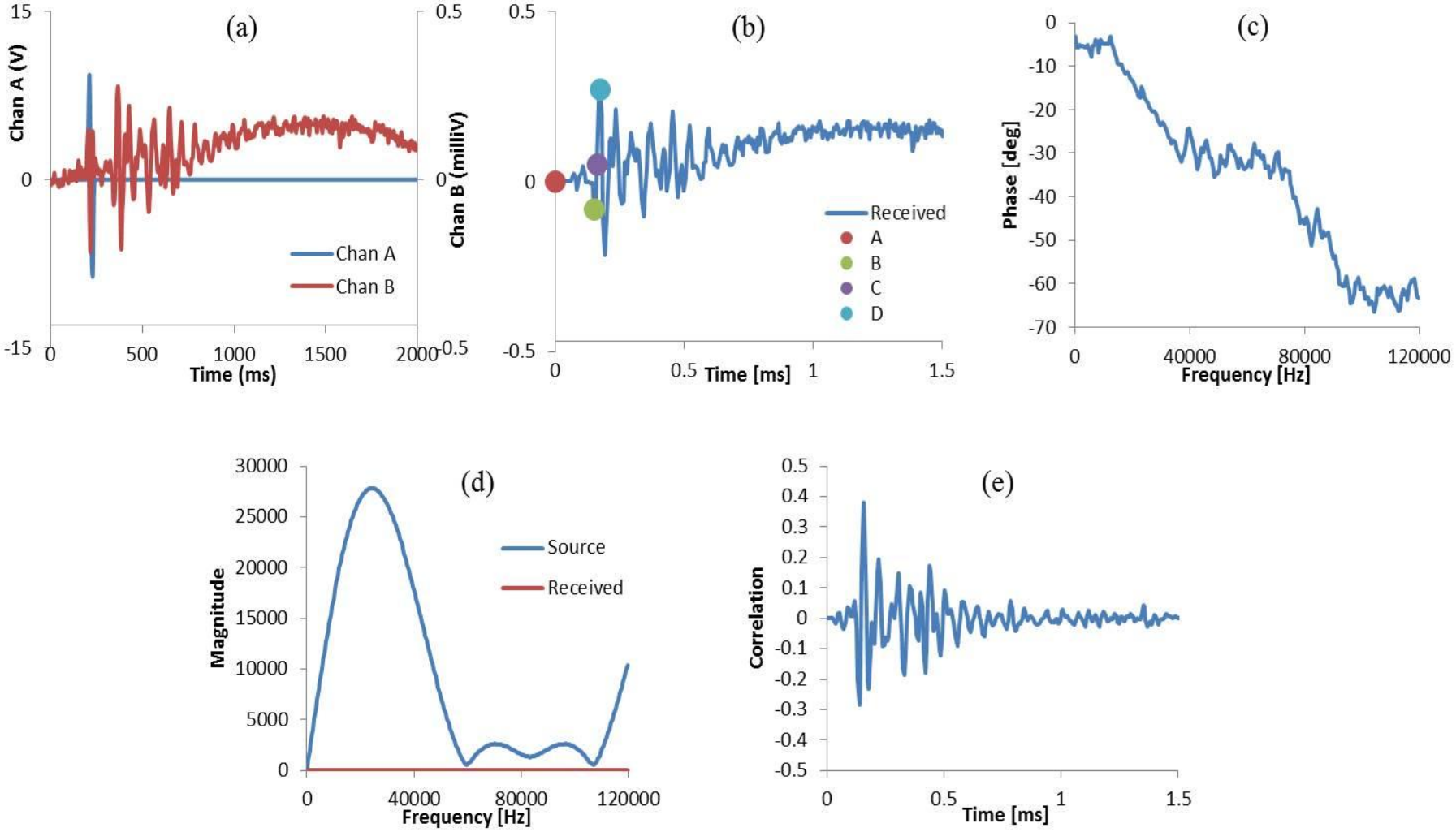

Figure A5.20: GDS BEAT Interpretation of bender element test 1 at 30 kHz, using time and frequency domain techniques: (a) raw signal time-domain data; (b) BEAT interpretation of possible S-wave arrival times; (c) unwrapped phase; (d) frequency spectrum; (e) cross correlation.

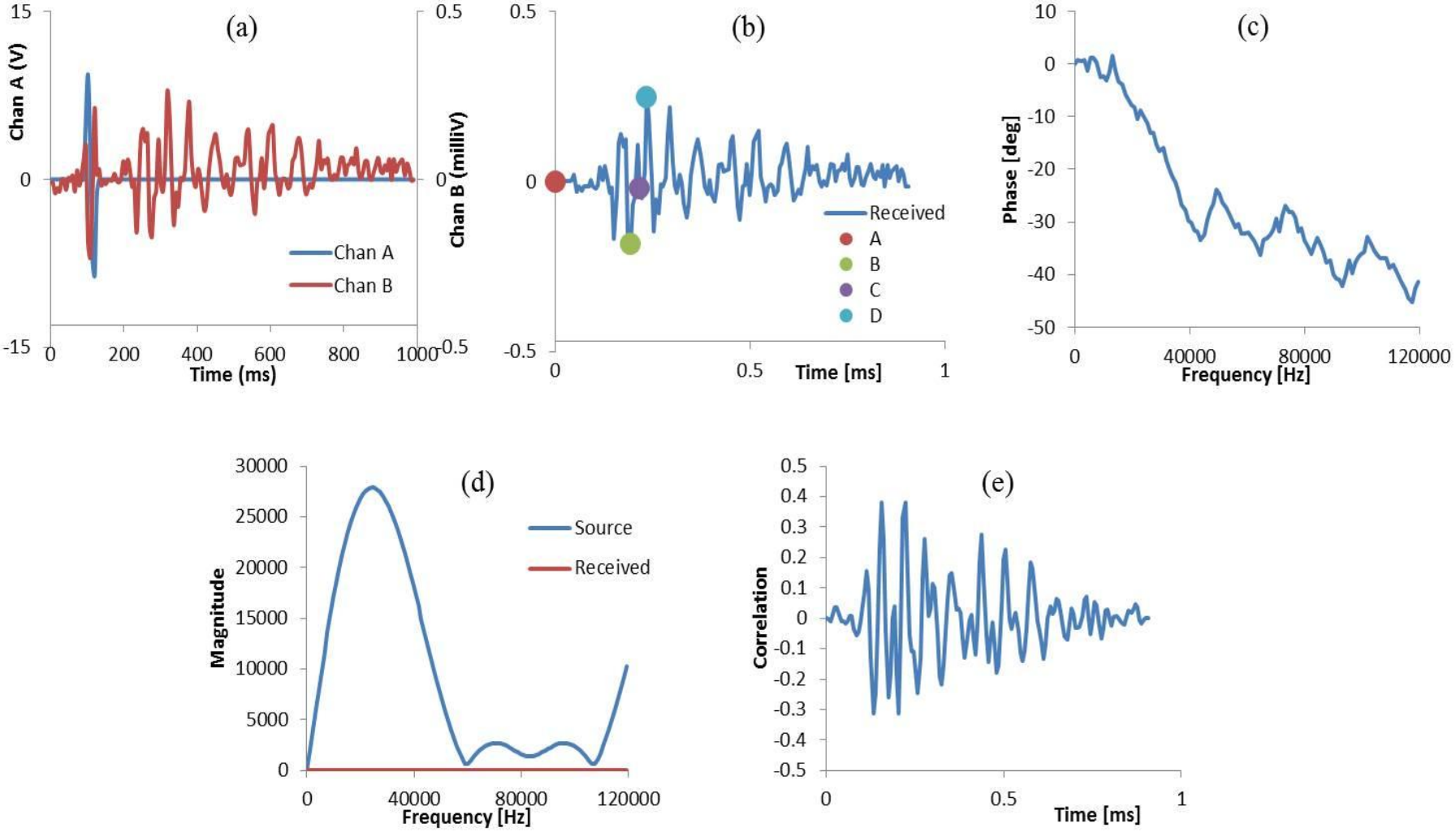

Figure A5.21: GDS BEAT Interpretation of bender element test 2 at 30 kHz, using time and frequency domain techniques: (a) raw signal time-domain data; (b) BEAT interpretation of possible S-wave arrival times; (c) unwrapped phase; (d) frequency spectrum; (e) cross correlation.

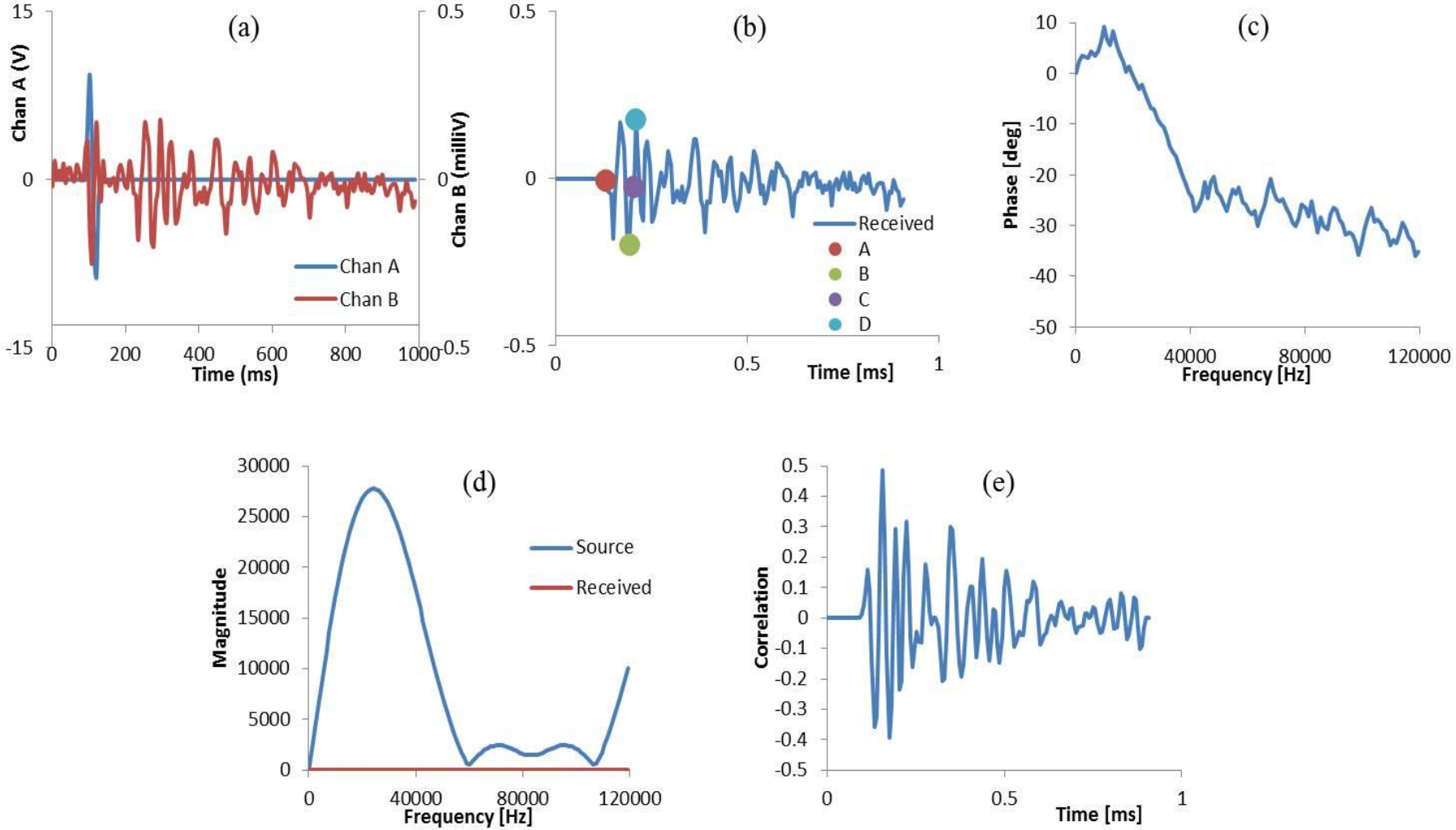

Figure A5.22: GDS BEAT Interpretation of bender element test 3 at 30 kHz, using time and frequency domain techniques: (a) raw signal time-domain data; (b) BEAT interpretation of possible S-wave arrival times; (c) unwrapped phase; (d) frequency spectrum; (e) cross correlation.

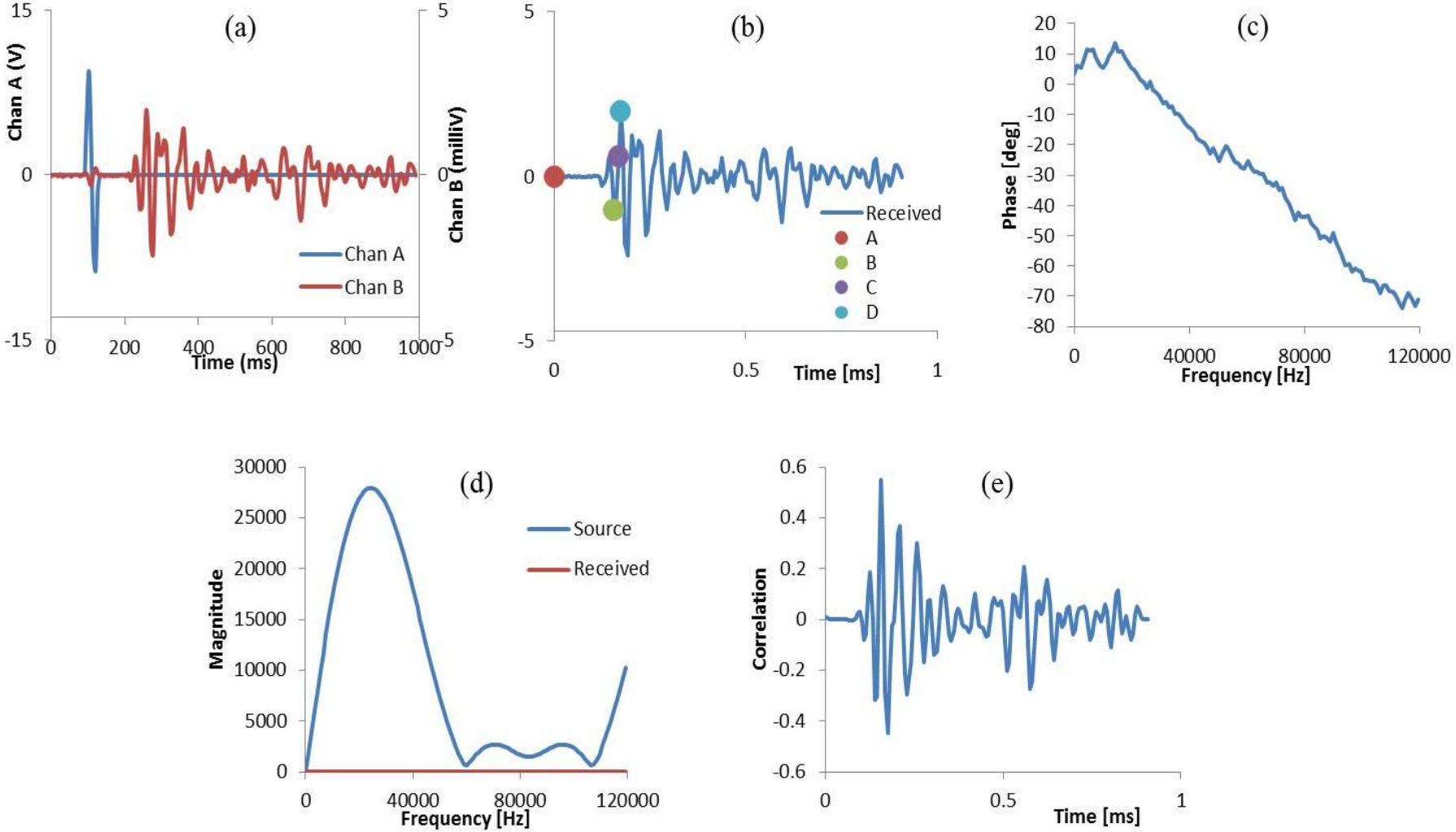

Figure A5.23: GDS BEAT Interpretation of bender element test 4 at 30 kHz, using time and frequency domain techniques: (a) raw signal time-domain data; (b) BEAT interpretation of possible S-wave arrival times; (c) unwrapped phase; (d) frequency spectrum; (e) cross correlation.

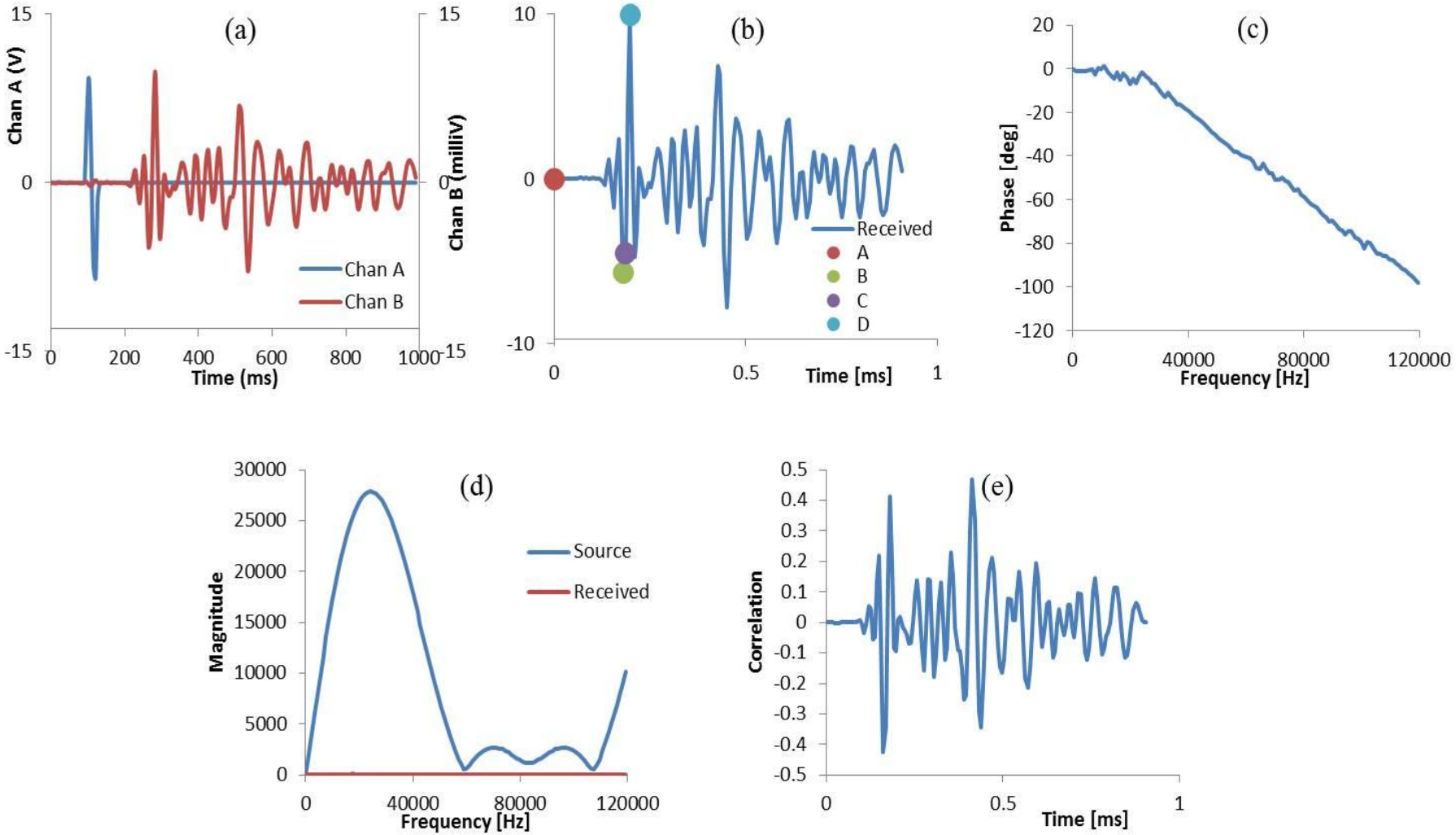

Figure A5.24: GDS BEAT Interpretation of bender element test 5 at 30 kHz, using time and frequency domain techniques: (a) raw signal time-domain data; (b) BEAT interpretation of possible S-wave arrival times; (c) unwrapped phase; (d) frequency spectrum; (e) cross correlation.

Per Figures A5.18–A5.19, the morphology of the received signals are much more complex and far less idealistic compared with the typical signal morphology presented by Rees et al. (2013). The signals are generally characterised by many peaks of varying magnitude (i.e. interference/noise), which inherently makes it difficult to accurately determine the true S-wave arrival time. With regards to time-domain analyses (Figures A5.20–A5.24), the GDS BEAT demonstrated varying degrees of difficulty in identifying the correct positions for the four possible points of S-wave arrivals in each of the bender tests. Mostly, the BEAT tool identified the time of initial deflection as 0 milliseconds, which is incorrect as this is the time at which the transmitting P and S-wave signal is produced. In this case, it is likely that the BEAT tool has identified a small trace in the received signal due to electromagnetic coupling. Commonly known as "crosstalk", this phenomenon between the transmitting and receiver bender elements manifests as a received signal with an early component, which is quasisimultaneous with the transmitted (input) signal (Lee and Santamarina, 2005). Regarding identifying the first major peak within the received signals, BEAT simply identified the peak of the highest magnitude. It is the opinion of the author that this is incorrect, as there are several peaks prior to the largest peak which could be considered major based on their degree of deflection from the time axis. For bender tests 2, 3 and 5, a similar observation was made regarding identifying the first bump maximum within the signals; whereby BEAT took the largest peak beneath the x-axis.

According to Chan (2012), whilst using higher frequencies (>5 kHz) for the transmitting signal reduces near-field effects, they also produce interference particularly prior to the first major deflection. Considerable degrees of interference are also observed after the first deflection, as seen by Vilhar and Jovicic (2009) (Figure A5.25).

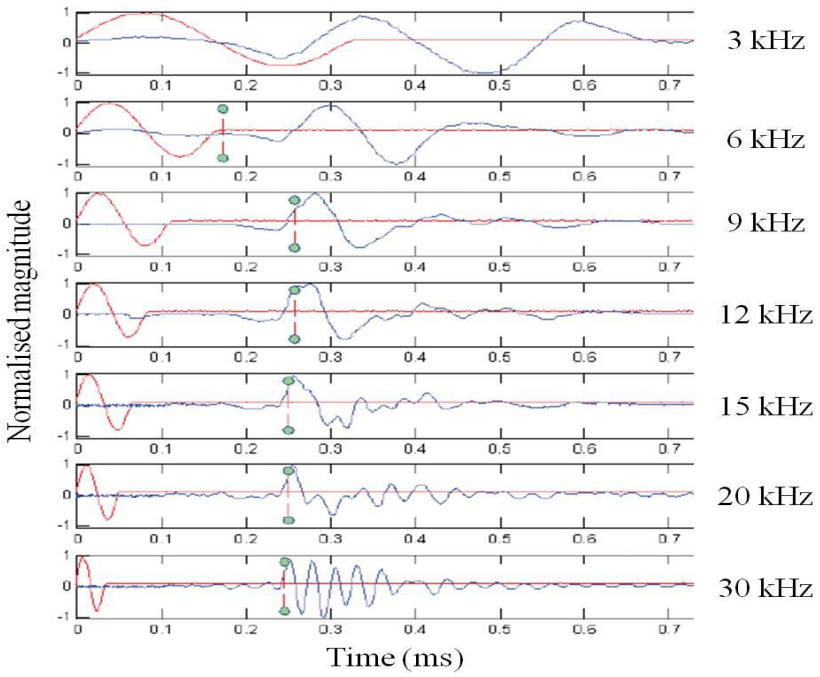

Figure A5.25: Interference patterns typically associated with increasing input frequencies for bender element measurements. Taken from Vilhar and Jovicic, (2009).

The interference patterns observed for a frequency of 30 kHz within Figure A5.25 is remarkably similar to the interference observed within the bender element measurements 1–5 (Figures A5.20–A5.24). Per Chan (2012), when using higher frequencies, a soil's energy-absorption is generally insufficient to sustain any prolonged and effective dynamic interaction between the soil and the bender elements. This consequently results in the attenuation of the received S-wave signal. In an attempt to compensate for this, a gain of x8 was used to amplify the received signals.

For bender element measurements 4 and 5, there appears to be a second signal event. Additionally, for bender measurement 5, there is also evidence suggesting a third signal event occurred within the received S-wave signal. Per Figure A5.19, these events are separated by similar time differences and are most clearly seen when using frequencies of 20 and 30 kHz. Evidence for signal attenuation is apparent within all bender element measurements at all three frequencies; particularly for bender measurements 4 and 5 where the second and third signal events are of lower magnitude compared with the first major event. Given the similar morphology of the second and third events and their similar time separations, these multiple signal events are S-wave reflections.

When using the time-domain technique, S-wave reflections present difficulties in determining the true travel times for S-waves. However, Lee and Santamarina (2005) stated the presence of such multiple S-wave reflections may provide a means of overcoming uncertainties in determining travel times by using the cross correlation and the frequency domain techniques. Based on the sample information and tip-to-tip separation of the bender elements (Table A5.1), Table A5.2 below summarises the arrival times, shear wave velocities and G_{max} values obtained for all five bender element measurements taken at 30 kHz by using the time and frequency domain techniques via GDS BEAT.

For a silty sand soil such as Lanton alluvium, the calculated G_{max} values within Table A5.2 seem far too high for this material, as such high G_{max} values would normally be expected for soft rocks. Lenart and Vilhar (2007) conducted bender element measurements on the Bostanj alluvial silty sand from Slovenia, which was similar to Lanton alluvium regarding its geotechnical index properties. The similar PSD curves for the Bostanj and Lanton alluvial soils are displayed in Figure A5.26.

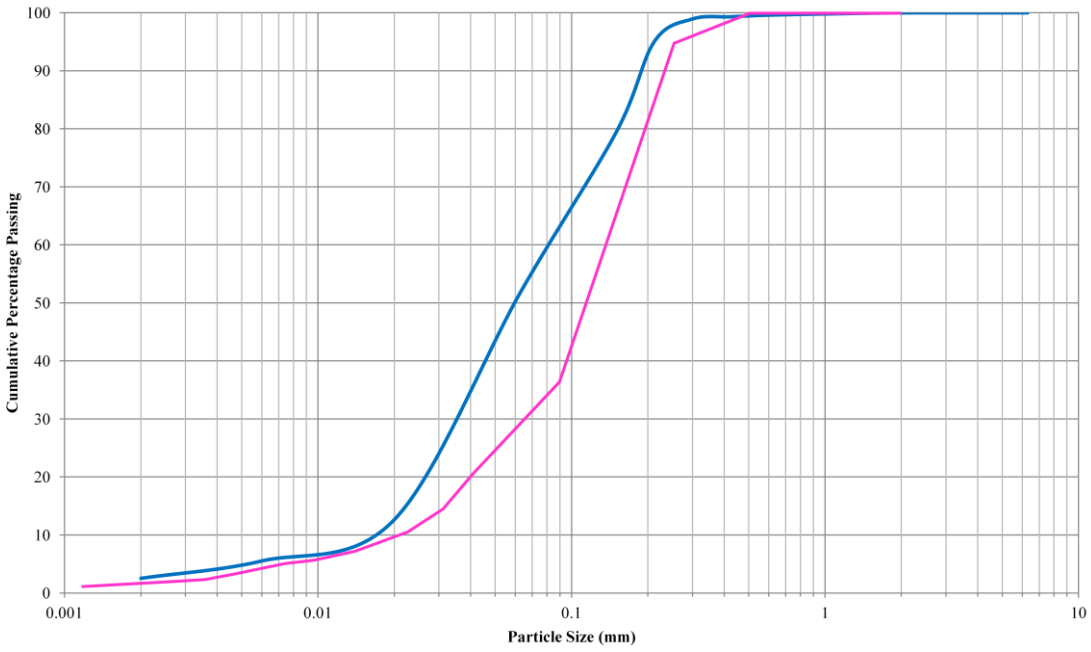

Figure A5.26: PSD curves for Lanton alluvium (blue) and the Bostanj alluvium (pink) tested by Lenart and Vilhar (2007).

Table A5.2: Summary of the S-wave arrival times, shear wave velocities and G_{max} values obtained by GDS BEAT for the five bender element measurements taken for the undisturbed Lanton alluvium.

	Time-domain analysis															**Frequency-domain analysis**		
	A (initial deflection)			**B (first bump max)**			**C (first zero cross)**			**D (first major peak)**			**Cross-correlation**					
Bender test no.	***t* (*μs*)**	***V_s* (*m/s*)**	***G_{max}* (*MPa*)**	***t* (*μs*)**	***V_s* (*m/s*)**	***G_{max}* (*MPa*)**	***t* (*μs*)**	***V_s* (*m/s*)**	***G_{max}* (*MPa*)**	***t* (*μs*)**	***V_s* (*m/s*)**	***G_{max}* (*MPa*)**	***t* (*μs*)**	***V_s* (*m/s*)**	***G_{max}* (*MPa*)**	***t* (*μs*)**	***V_s* (*m/s*)**	***G_{max}* (*MPa*)**
1	0	-	-	150	1114	2118	162	1031	1816	174	960	1574	156	1071	2075	172	971	1707
2	0	-	-	192	870	1293	216	773	1021	234	714	870	156	1071	2075	181	923	1542
3	132	1265	2985	192	870	1292	204	819	1145	210	795	1080	156	1071	2137	189	884	1456
4	0	-	-	156	1068	1949	168	1207	2490	174	958	1566	156	1068	2114	145	1149	2446
5	0	-	-	180	905	1397	186	1233	2598	198	822	1154	414	393	293	172	947	1697

Based on findings by Lenart and Vilhar's (2007) for the Bostanj soil and bender element measurements taken by Saldago et al. (2000) for Ottowa sand with up to 5% fines content, G_{max} values ranging between 25 and 80 MPa may be expected for silty sand alluvial soils at initial mean effective stresses of 50 kPa. Hence, all the time and frequency-domain derived G_{max} values in Table A5.2 for Lanton alluvium are almost two orders of magnitude too high. Although multiple S-wave reflection events can be observed with confidence for bender element measurements 4 and 5, the BEAT tool couldn't calculate a more realistic S-wave arrival time via cross-correlation, contrary to findings by Lee and Santamarina (2005).

Based on these findings and given the complexity of the S-wave signal morphologies, the author manually analysed the bender element measurements taken at 30 kHz by using the time-domain technique. The author adopted the same approach as Rees et al. (2013) in identifying the initial deflection, first bump maximum, first zero-crossing and first major peak as the four possible locations for the true S-wave arrival. Figure A5.27 presents a comparison between the locations typically taken by GDS BEAT for the aforementioned four possible S-wave arrival times and those taken by the author.

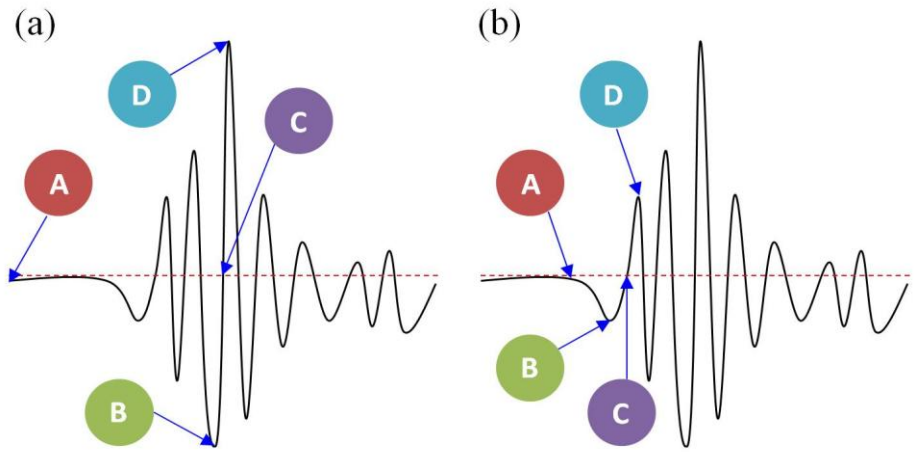

Figure A5.27: Locations taken for the initial deflection (A), first bump maximum (B), first zero crossing (C) and first maximum peak (D) within received S-wave signals according to: (a) GDS BEAT and (b) visually by the author.

As bender element measurements 4 and 5 were taken when the sample of Lanton alluvium was fully saturated and consolidated, the author conducted a time-domain

analysis on these two sets of measurements at a frequency of 30 kHz only. Bender measurements 1–3 were not selected for further analysis as the triaxial cell had not been placed over the sample. Therefore, most of the interference observed within the output signals for these bender measurements could be attributed to everyday human activities and other pieces of working equipment within the geotechnical lab at Bristol. Table A5.3 summarises the S-wave arrival times, S-wave velocities and G_{max} values obtained by the author for bender element measurements 4 and 5 taken at 30 kHz by using of the time-domain technique.

Based on the short arrival times in Table A5.3 for the first signal events within bender measurements 4 and 5, the derived G_{max} values are comparable to the very high values derived from GDS BEAT. Hence, these values are considered to be too high and not truly representative of the soft Lanton alluvium. The G_{max} values obtained for the first reflections (second events) within the output signals for measurements 4 and 5 are an order of magnitude lower than those obtained for the first signal event. Albeit the G_{max} values obtained are much lower than those typically expected for soft rocks or concrete, the G_{max} range of 170–415 MPa per Table A5.3 would typically be expected for much stiffer overconsolidated soils such as glacial tills (Femern, 2011), especially at such low initial mean effective stresses of 50 kPa. By examining the third reflection observed within the output signal for bender measurement 5, the G_{max} values range between 82 and 92 MPa. These values may be considered as more realistic for alluvial soils, as they are comparable to the G_{max} values recorded by Lenart and Vilhar (2007) on the Bostanj soil.

Further to recommendations from Nash and Diambra (2013), the point taken on the output signal for bender measurement 5 as being the most likely S-wave arrival is point B, the first bump maximum. Hence, under an initial mean effective stress of 50 kPa, the G_{max} value of 89.1 MPa was taken for Lanton alluvium. This value is plotted on the following small strain shear stiffness degradation plots at a shear strain value of 0.0001%. Further bender element measurements of Lanton alluvium's changing shear stiffness are clearly required; particularly during shearing which would further add to small strain stiffness degradation data provided by local axial and radial LVDT's. Future bender element measurements should also be conducted at various frequencies <10 kHz, with a view to reducing the level of interference observed within output signals, as recorded in this research study and by Vilhar and Jovicic, (2009).

Table A5.3: Summary of the S-wave arrival times, shear wave velocities and G_{max} values obtained by the author for bender element measurements 4 and 5 taken at a frequency of 30 kHz for the undisturbed Lanton alluvium.

	Time-domain analysis											
	A (initial deflection)			**B (first bump max)**			**C (first zero cross)**			**D (first major peak)**		
Bender test no.	***t* (μs)**	***V_s* (m/s)**	***G_{max}* (MPa)**	***t* (μs)**	***V_s* (m/s)**	***G_{max}* (MPa)**	***t* (μs)**	***V_s* (m/s)**	***G_{max}* (MPa)**	***t* (μs)**	***V_s* (m/s)**	***G_{max}* (MPa)**
4 1st event	126	1322.5	3235.5	132	1262.4	2948.1	138	1207.5	2697.3	144	1157.2	2477.2
4 2nd event (reflection)	498	334.6	207.1	528	315.6	184.3	534	312.0	180.1	546	305.2	172.3
5 1st event	120	1356.75	3479.1	132	1233.4	2875.3	138	1179.8	2630.7	144	1130.6	2416.0
5 2nd event (1st reflection)	378	430.7	350.6	390	417.5	329.4	414	393.3	292.3	426	382.2	276.1
5 3rd event (2nd reflection)	738	220.6	92.0	750	217.1	89.1	762	213.7	86.3	780	208.7	82.3

A5.3.1.3 Small strain stiffness degradation

The secant shear stiffness degradation behaviour of the undisturbed Lanton alluvium sample under undrained conditions from small strain to large strain ranges is presented in Figure A5.28. The G_{sec} data obtained for shear strains <0.01% is considered much more representative of Lanton alluvium's behaviour, based on the much higher stiffnesses derived from higher resolution local strain measurements compared with the measurements obtained from triaxial testing at Newcastle.

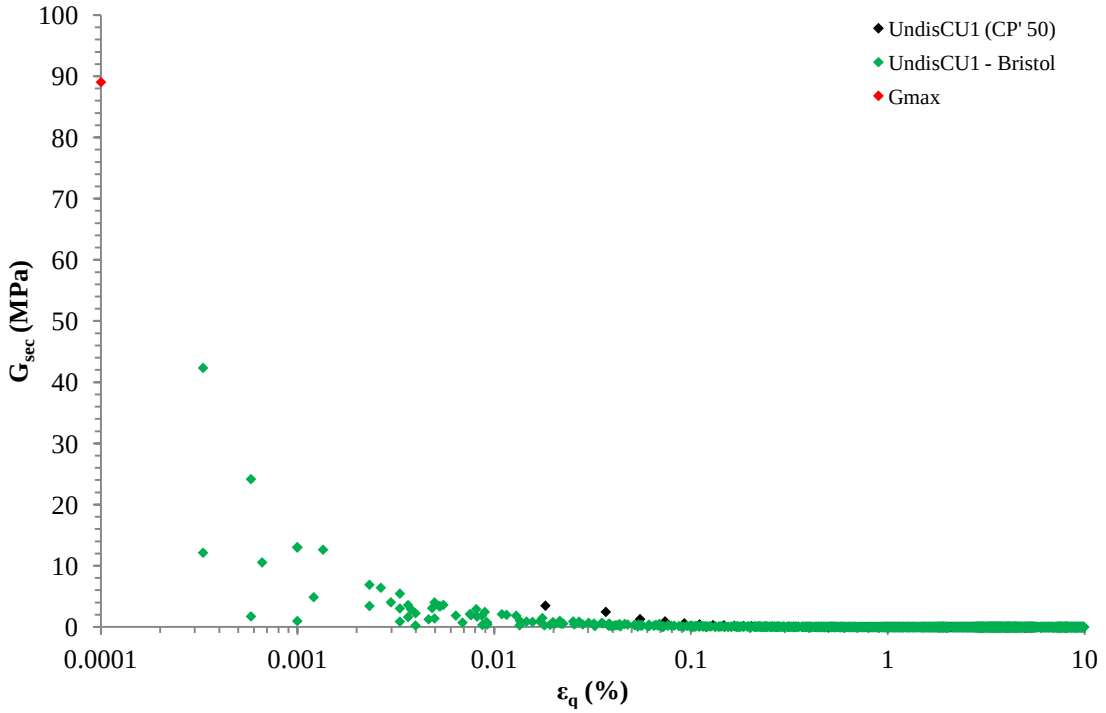

Figure A5.28: Secant shear stiffness degradation behaviour for the undrained undisturbed small strain Lanton alluvium sample. Undisturbed undrained sample tested at Newcastle, UndisCIU1 (p'0 50) superimposed for comparison.

The G_{max} value of 89.06 MPa obtained from bender element measurement 5 is plotted on Figure A5.28 at a small shear strain value of 0.0001%. Based on testing results from Newcastle, the highest shear stiffnesses of 3.5 MPa were achieved at shear stiffnesses of 0.02% shear strain, whereas the lowest stiffnesses were achieved after reaching shear strains >0.2%. However, as can be seen from the small strain test conducted at Bristol, considerably higher stiffnesses were recorded within the small

strain range (<0.002%); whereby the lowest stiffnesses were achieved at strains >0.02%. These features of the soil's behaviour can be more clearly seen in Figure A5.29, whereby the secant shear stiffness data has been normalised with respect to the sample's p'_0 value.

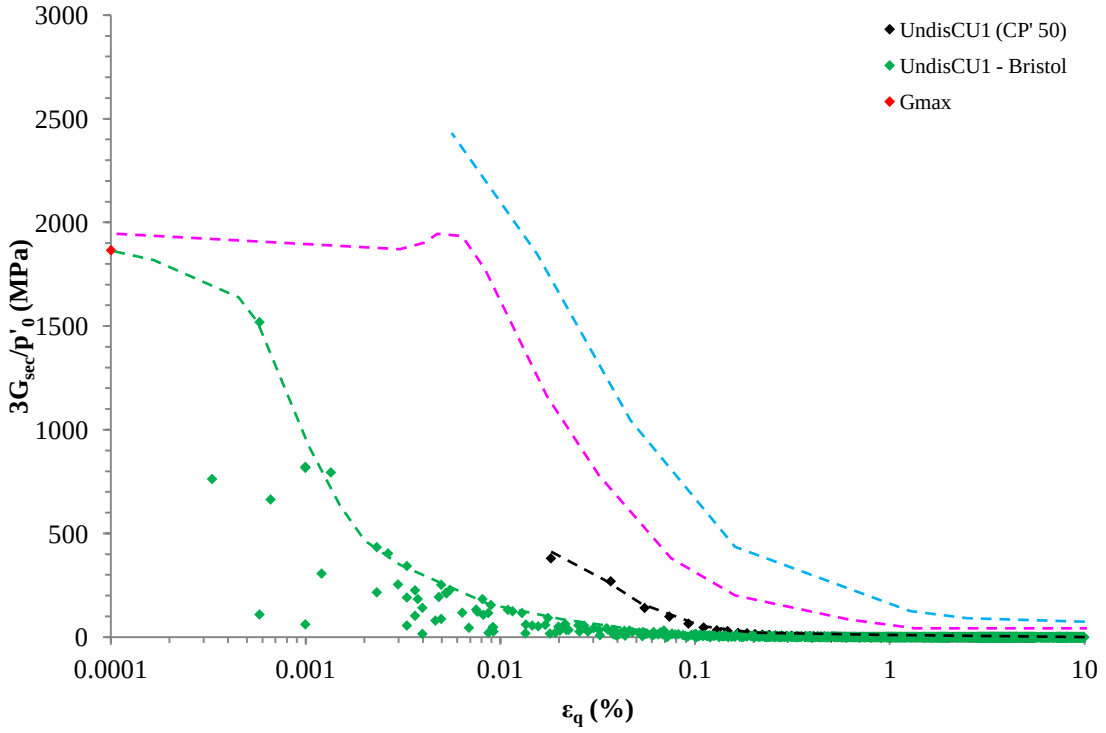

Figure A5.29: Normalised secant shear stiffness degradation behaviour for the undrained undisturbed Lanton alluvium tested at Bristol (small strain = green) and Newcastle (black). Curves obtained by Gasparre (2005) for London clay (pink) and by Simpson and Rouainia (2012) for Northumberland glacial till (blue) are superimposed.

Slightly more data scatter is observed within the testing data obtained from Bristol compared with that from Newcastle, particularly within the small strain range (Figures A5.28–A5.29). However, an approximate trace for Lanton alluvium's shear stiffness degradation curve may be defined from the data obtained from Bristol, which is much more reliable than that from Newcastle. Although the initial shear stiffness and degree of structure within Lanton alluvium is comparable to that measured by Gasparre (2005) for sub-unit B2(a) of London Clay, Lanton alluvium's stiffness can be seen to degrade at a considerably quicker rate. Almost 75% of the soil's stiffness, and

inherently its structure, are lost after just 0.002% shear strain had been experienced. This highly sensitive behaviour to monotonic loading complements findings from oedometer testing (chapter 5), which contrasts to the behaviour of London clay, whose initial structure and highest stiffnesses are retained up to shear strains of approximately 0.01%. Small strain stiffness testing conducted by Simpson and Rouainia (2012) on Northumberland glacial till imply that it has considerably higher stiffnesses at small and large strains compared with Lanton alluvium and London clay; although further testing is required to define the till's G_{max} value and ultimately the point at which initial structure and shear stiffnesses start to degrade with shear straining.

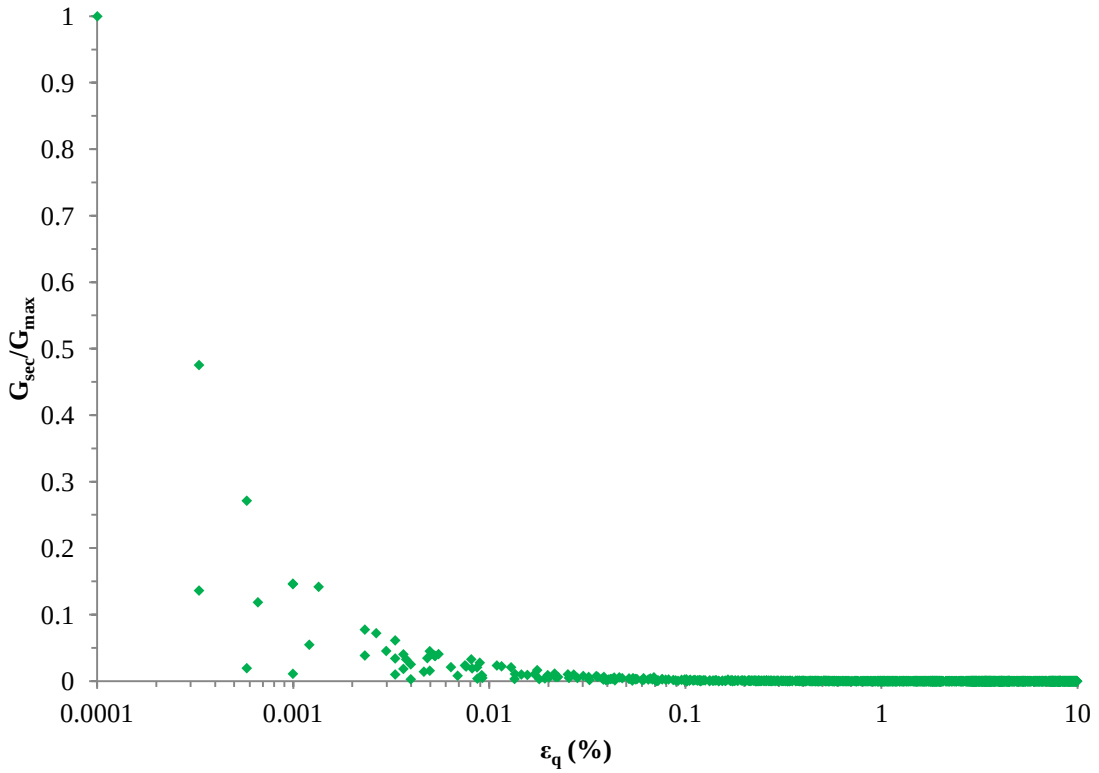

Figure A5.30: Secant shear stiffness degradation behaviour for undrained undisturbed small strain Lanton alluvium sample, normalised by its G_{max} value.

The shear stiffness degradation curves in Figures A5.28–A5.29 and the deviatoric stress–strain curves in Figures A5.12–A5.13 highlight the problematic issues associated with measuring small – large strain soil stiffnesses by using conventional triaxial testing methods and global strain measurements. Factors including sample

bedding errors, top cap-load cell seating, apparatus compliance, rod friction, the compressibility of porous stones and specimen boundary effects (whereby there is much restraint at sample ends and relatively little within the middle third) all have detrimental effects on measuring true soil stiffnesses. Other minor factors including the restraining effects presented by the membrane and filter paper also have an effect on the measured soil stiffness; although correction factors can be applied for these per BS 1377 (BSI, 1990). Hence, given the importance of small strain around geotechnical structures during their design and levels of anisotropy within soils, using local strain measurements and bender elements in triaxial testing should be considered as a standard procedure. Using other laboratory methods to examine small strain behaviour and initial shear stiffnesses, such as resonant columns and hollow cylinder are also encouraged. As there is always the possibility of initial structure within soils being partially or totally removed during their transport from the field to the lab, in-situ field testing techniques including the pressure-meter test and dynamic testing methods are recommended.

A5.3.2 Stabilised Lanton alluvium

A5.3.2.1 Shearing behaviour

Axial strains experienced by stabilised Lanton alluvium during shearing were measured both globally and locally by using local LVDT's mounted directly onto the sample. Figure A5.31 displays the deviatoric stress – axial strain response of the sample according to global (external) and local strain measurements. Within the first 1% of axial strain experienced by the sample, there is a considerable difference between the stiffnesses measured by the local LVDT's compared with those measured by the external LVDT. There is a marked difference in the stiffnesses measured by local LVDT's 1 and 2, although such discrepancies are not unheard of in advanced triaxial testing. By taking the most linear portion of the deviatoric stress – strain curves after axial strains of 0.4% had been experienced (Figure A5.32); and taking an average of the stiffnesses measured by both local LVDT's, the E_u values measured

using local and global strain measurements were 2912 and 177 MPa, respectively. At larger strain levels of 1–1.5%, the stress – strain curves converge. The deviatoric stress – axial strain curves in Figures A5.31–A5.32 demonstrate that the sample predominantly experienced work hardening, although a peak deviatoric stress and post-peak softening was also observed; similar to the observations made for undrained tests conducted at Newcastle. Besides axial strains, the deviatoric stress development within the sample can also be related to radial strains (Figure A5.33), which were measured half way up the sample by another local LVDT mounted to the sample via a radial caliper.

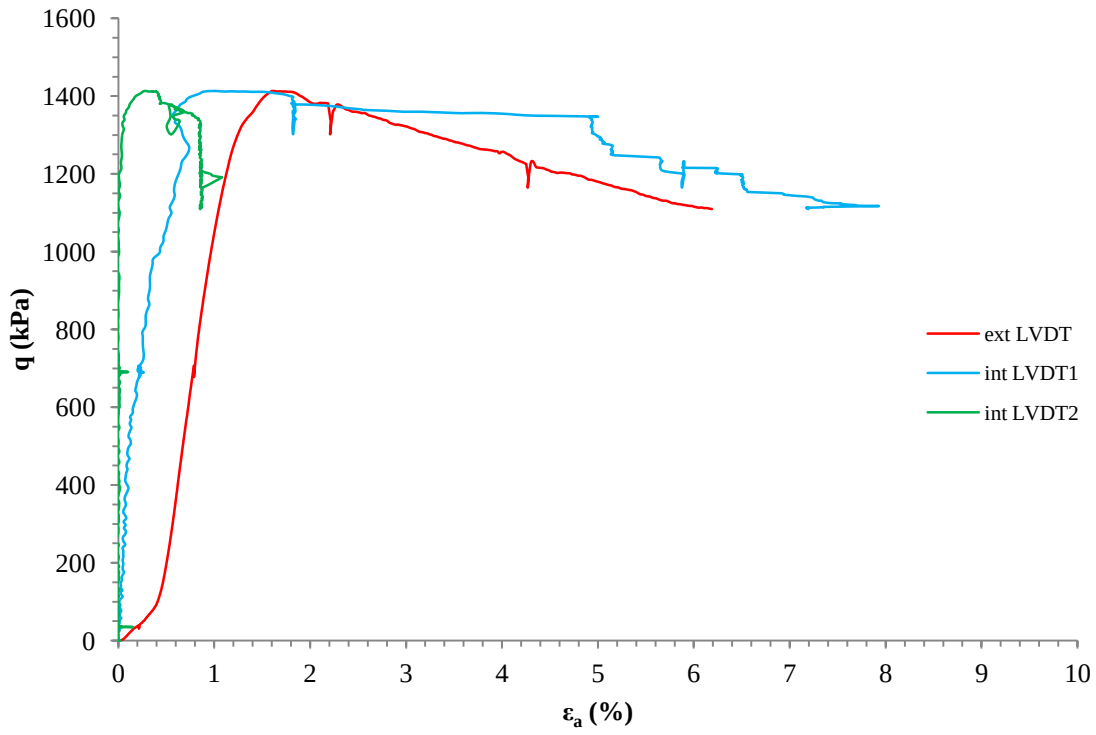

Figure A5.31: Deviatoric stress-strain behaviour of undrained GGBS-NaOH stabilised small strain sample of Lanton alluvium, using external (ext) and local (int) LVDT axial strain measurements.

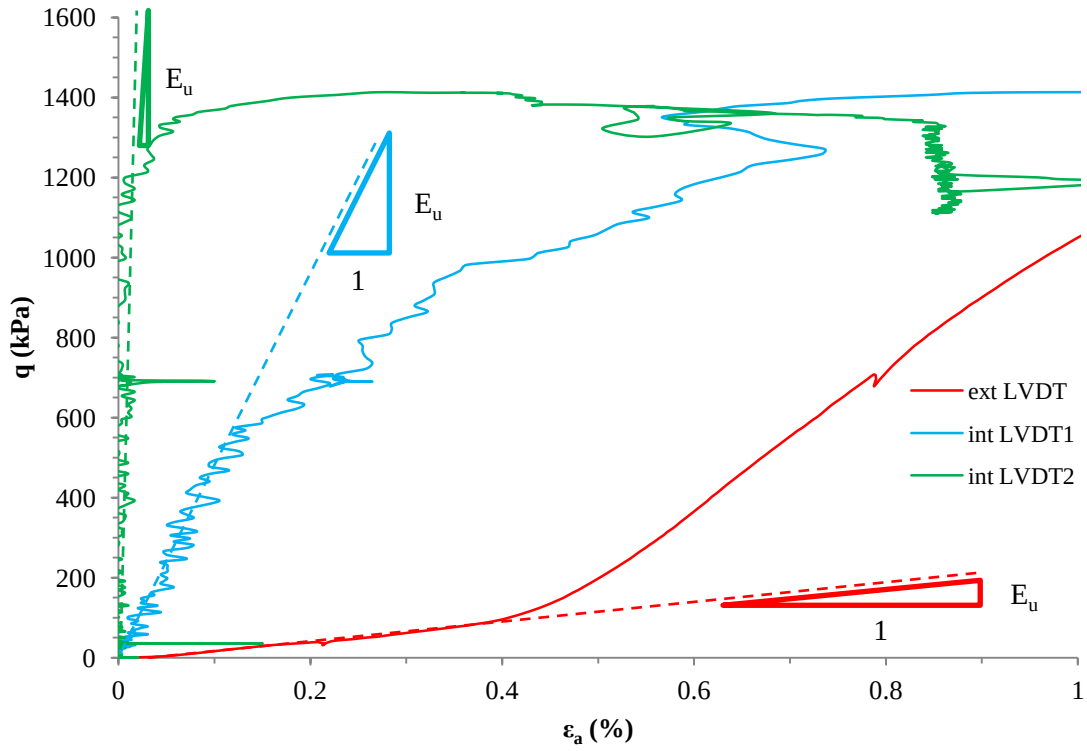

Figure A5.32: Stiffer deviatoric stress-strain response observed for GGBS-NaOH stabilised Lanton alluvium when using local over external axial strain measurements.

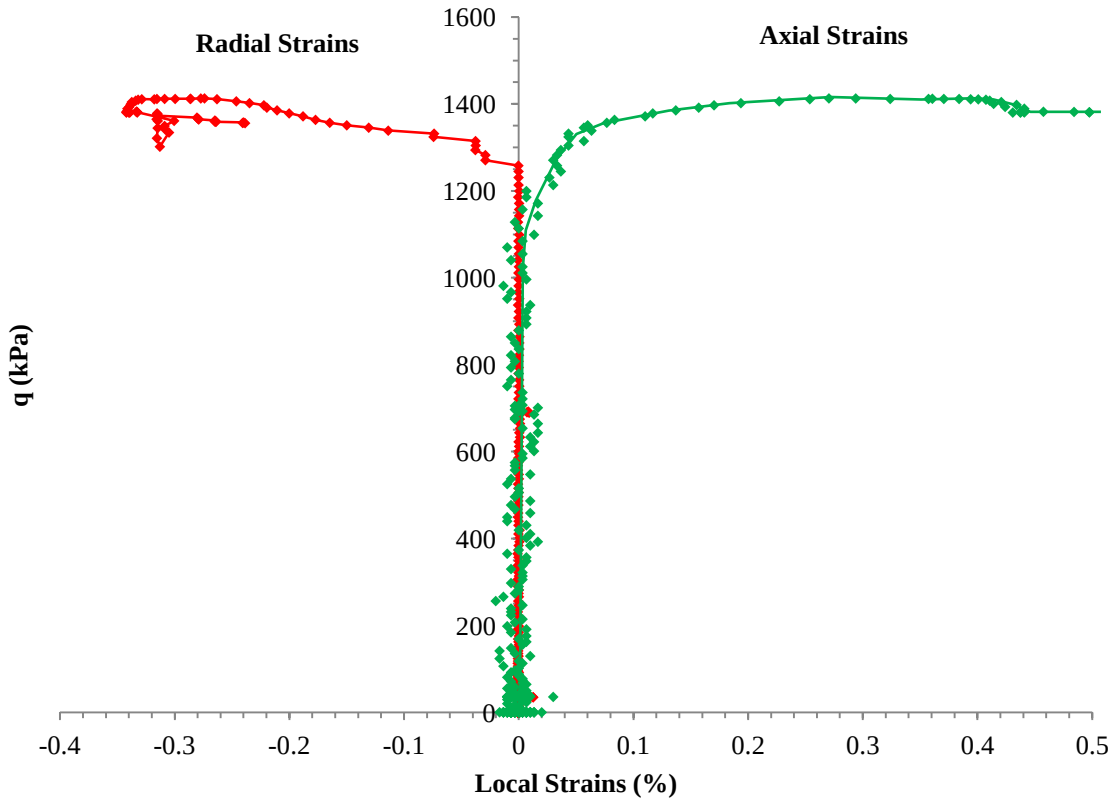

Figure A5.33: Relationship between deviatoric stress and local axial (green) and radial (red) strains.

The peak deviatoric strength of the sample (1412 kPa) was very similar to those measured at Newcastle (1280–1600 kPa) for undrained tests also conducted at an effective confining stress of 50 kPa. Per Figure A5.33, there almost appears to be a mirroring behaviour for the sample's radial and axial strain behaviour with the development of deviatoric stresses. Arguably, the radial stiffness is slightly higher for deviatoric stress levels ranging between 1100 and 1300 kPa, which in turn produced Poisson's ratio values which slightly exceeded 0.5, as similarly observed for the untreated Lanton alluvium in section A5.3.1.1. This condition is theoretically impossible under undrained conditions in soil mechanics for linear elastic behaviour, although based on the results presented above and in Chapter 8, the GGBS-NaOH stabilised Lanton alluvium is not a linear elastic material. The marked difference between the stiffnesses measured by the two local axial LVDT's could be attributed to sample anisotropy; albeit the level of anisotropy is expected to be low, given that the sample was well mixed during its production to achieve maximum levels of homogeneity. Factors more likely to be responsible for the difference in stiffness measured in the radial and axial planes include calibration error and frictional resistance caused by the LVDT's core moving in and out of the LVDT's main body. Given the high stiffness of the stabilised soil, restraining effects on the material's radial strain response due to the latex rubber membrane would have been negligible.

The pore pressure behaviour of the sample was measured from both the top and bottom of the sample during testing. The average of the two measurements was taken and is shown in Figure A5.34. This shows that pore pressures increased up to a steady peak value of approximately 42 kPa, which was maintained between shear strains of 0.35 and 0.5%. However, at 0.5% shear strain the pore pressure was observed to suddenly decrease towards negative values (i.e. suction) as shear strains increased towards 3.5%. Such a sudden reduction in pore pressure may be attributed to the formation of the shear plane within the sample.

This pore pressure behaviour correlates well with that observed for undrained tests conducted at Newcastle under p'_0 conditions of 50 kPa, which is typical of densely cemented soils and rocks when they are close to approaching their rupture point and start to undergo dilation (Mesri et al., 1972; Rios et al., 2014).

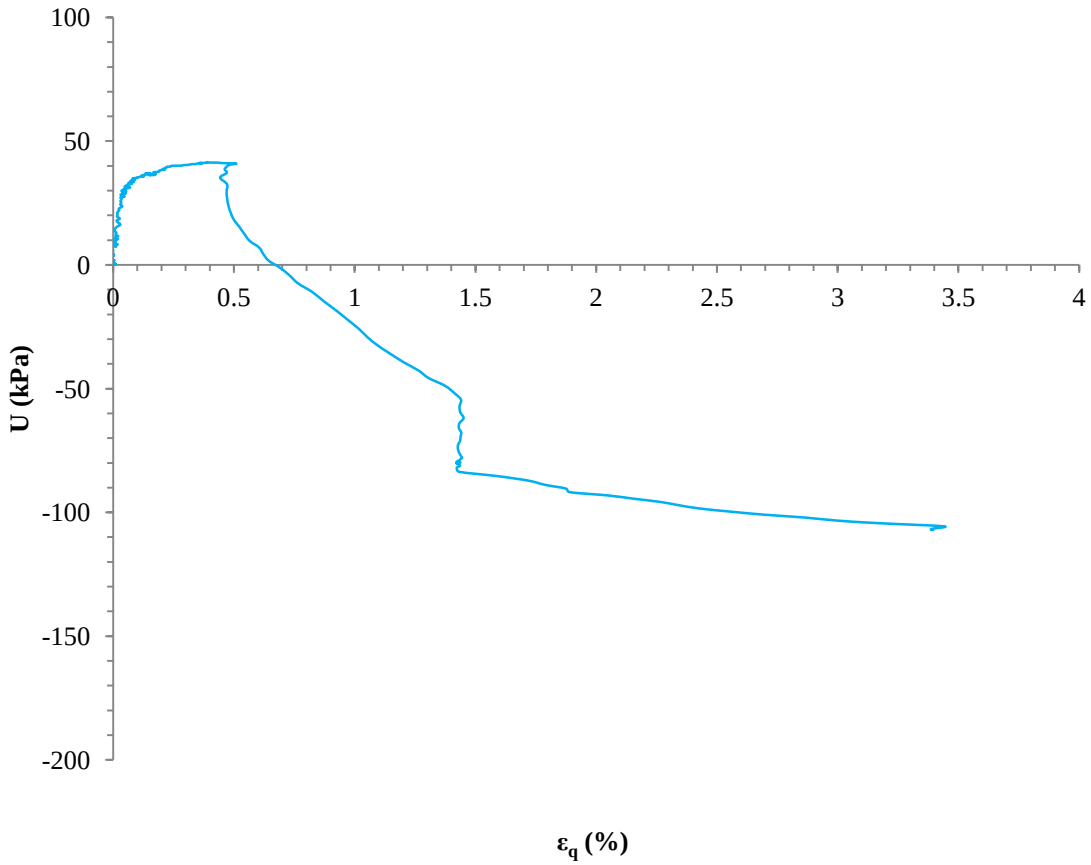

Figure A5.34: Pore pressure behaviour of small strain GGBS-NaOH stabilised sample of Lanton alluvium.

The shape of the effective stress path taken by the sample in q-p' stress space (Figure A5.35) closely resembles those observed for samples tested at Newcastle under p'_0 conditions of 50 kPa; whereby the sample appears to follow a drained path until a phase transformation occurs. This transformation indicates the sample had reached its failure envelope. With increased straining, the mean effective stress increased slightly as the deviatoric strength reduced; thereby indicating that the sample had then reached its critical state, followed closely by complete sample failure when the deviatoric strength of the material decreased significantly. This again proves that for this material, the CSL and failure envelope (yield locus) surfaces do not coincide.

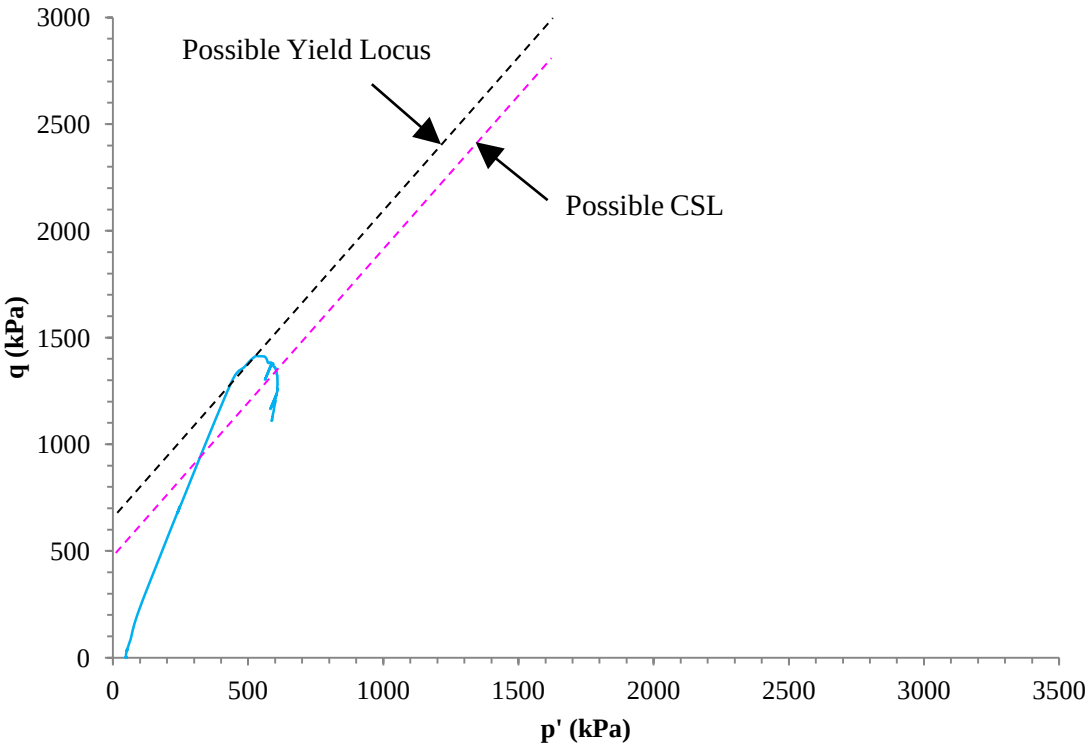

Figure A5.35: Undrained stress path, possible yield locus and CSL within the q-p' stress plane for all GGBS-NaOH stabilised Lanton alluvium samples.

A5.3.2.2 Bender elements

Bender element measurements were taken for the sample at every stage of the sample preparation process and at the end of saturation and consolidation. Similar bender element cable leaks due to their over-tightening as they passed through the triaxial cell's access ring were experienced during the test when cell pressures exceeded 300 kPa. Hence, no bender element measurements of stabilised Lanton alluvium's changing shear stiffness could be taken during shearing.

Table A5.4 presents a summary of the stabilised sample's conditions for each bender element measurement taken between the start of saturation and end of consolidation; along with the frequencies and the input signal voltages used.

Table A5.4: Details of bender element tests conducted on the GGBS-NaOH stabilised Lanton alluvium sample after 28 days curing.

BE test no.	Date & time	Frequencies used (kHz)	Voltage peak to peak (V)	Sample condition	Sample height (mm)	BE separation (mm)
3	10/10/13 16.00	10, 20, 30	20	Sample docked, membrane, LVDT's attached, cell full, CP = 50 kPa. ρ = 1.91 Mg/m^3	179.18	169.18
4	11/10/13 11.00	10, 20, 30	20	Sample docked, membrane, LVDT's attached, cell full, CP = 187 kPa. ρ = 1.91 Mg/m^3	179.16	169.16
5	14/10/13	10, 20, 30	20	Sample docked, membrane, LVDT's attached, cell full, CP = 237 kPa. ρ = 1.91 Mg/m^3	179.27	169.27
6	17/10/13 11.27	10, 20, 30	20	Sample docked, membrane, LVDT's attached, cell full, SATURATED - CP = 510 kPa. ρ = 1.91 Mg/m^3	179.22	169.22
7	18/10/13 10.49	10, 20, 30	20	Sample docked, membrane, LVDT's attached, cell full, CONSOLIDATED – CP' = 50 kPa. ρ = 1.91 Mg/m^3	178.51	168.51

Displayed in Figures A5.36–A5.37 are the raw P- and S-wave signal data obtained for each bender element measurement taken. Drawn onto these figures are a series of lines, which identify the likely S-wave arrival times using the time-domain technique for each of the three frequencies used and how increasing frequency potentially effects the arrival time recorded. Albeit more signal interference was observed within the received S-wave signals when using a higher frequency of 30 kHz, their signal traces on the Picoscope were much more stable compared with those taken when using frequencies of 10 or 20 kHz. Hence, time and frequency domain analyses using GDS BEAT were conducted on bender element measurements which used a 30 kHz frequency. The results are presented in Figures A5.38–A5.42.

The geometry of the received S-wave signals in Figures A5.36–A5.37 become increasingly complex with increasing frequency, due to higher levels of noise and interference. The received signals from tests using a frequency of 10 kHz were characterised by the simple idealistic signal geometry typically expected for S-waves, per Rees et al. (2013). Additionally, slightly higher levels of interference may be observed within the S-wave signals produced for bender element measurements 3–5, due to everyday human activities and other pieces of equipment in operation causing slight vibrations within the geotechnical laboratory at Bristol. Additionally, when higher confining pressures were used within the triaxial cell, this also appeared to suppress the effects of any external sources of interference. Although the signals produced using higher frequencies were characterised by higher levels of noise/interference, near-field effects were reduced and the signals were still strong enough to determine initial deflection S-wave arrival times fairly accurately when using the time-domain technique for analysing the data.

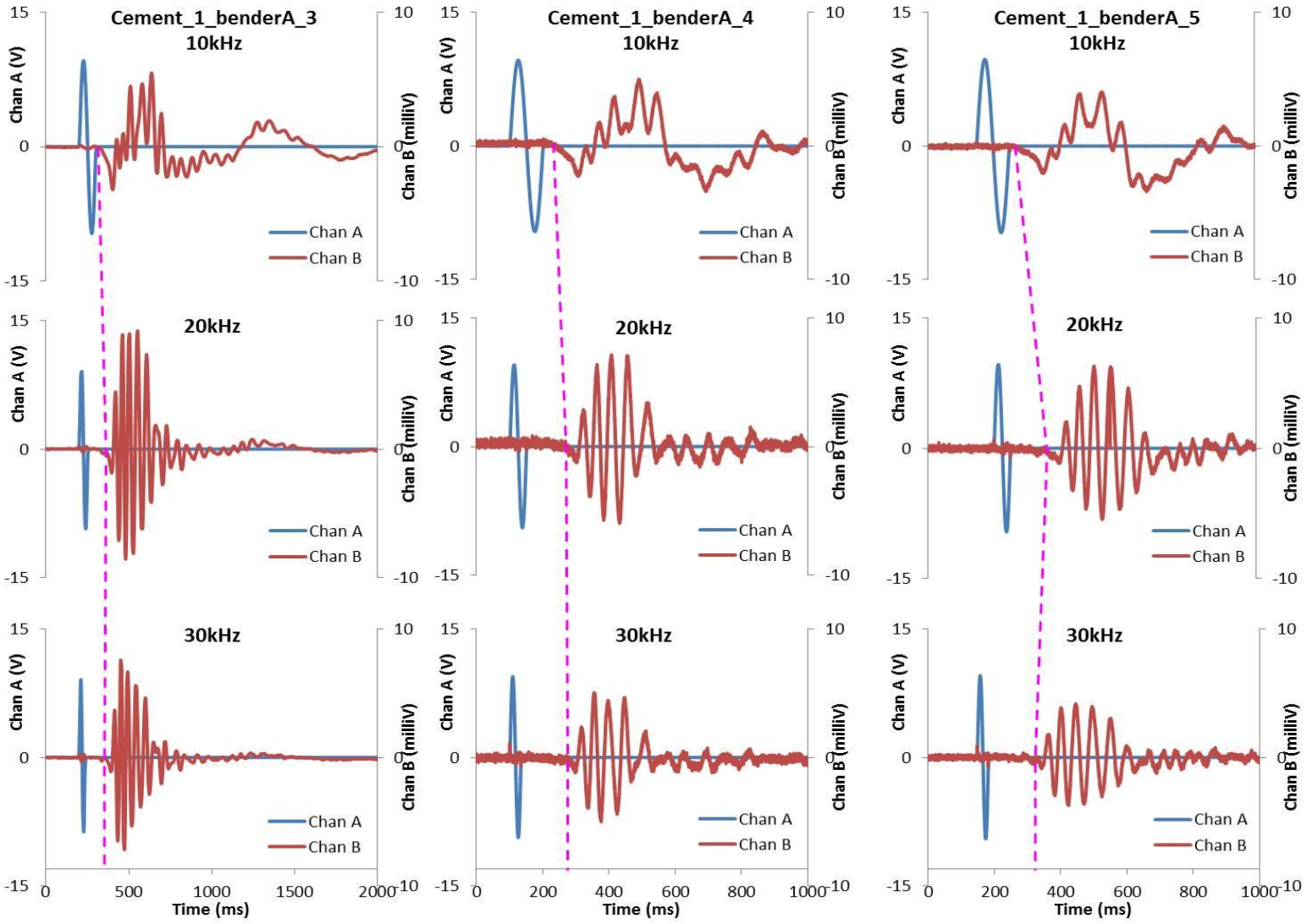

Figure A5.36: Source and received signals obtained from bender element tests 3 – 5.

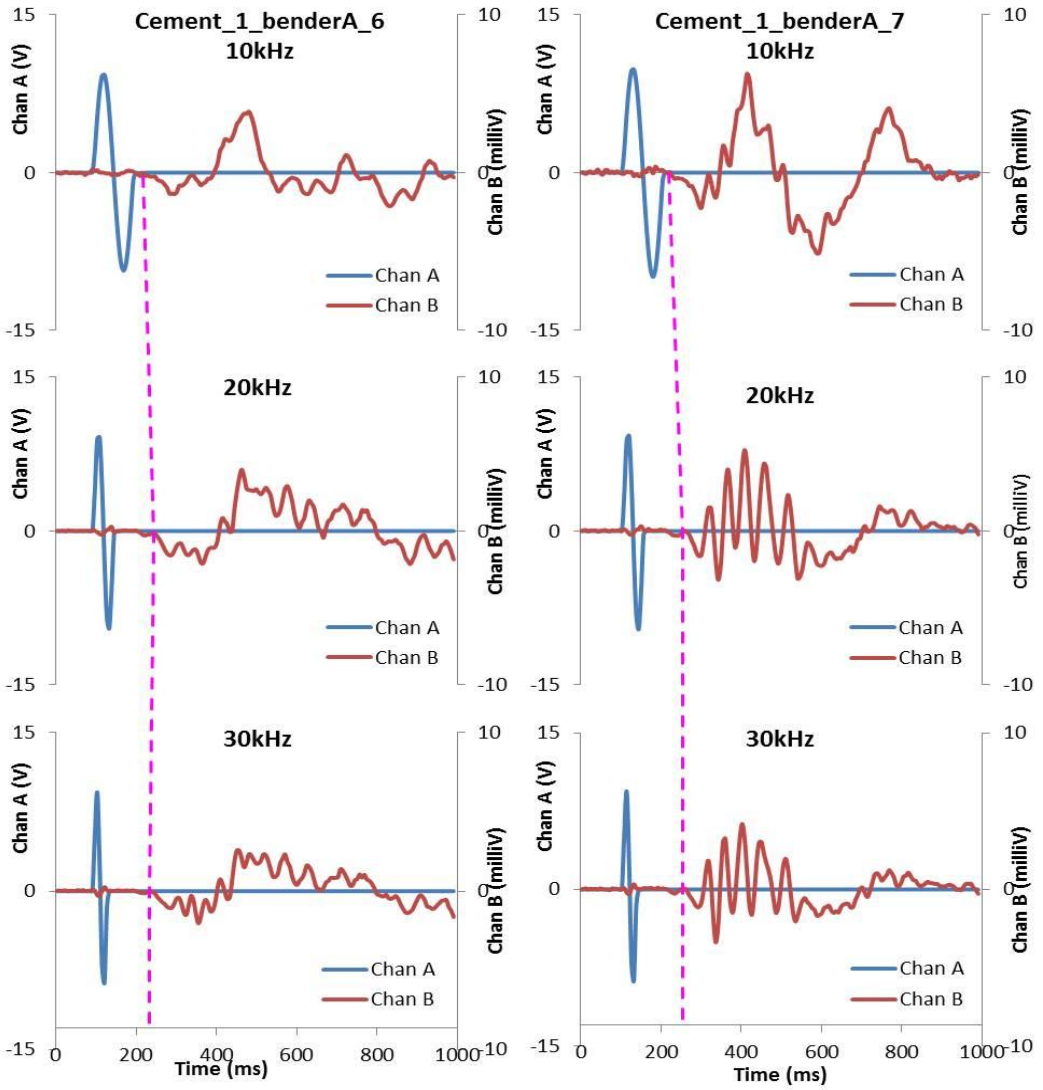

Figure A5.37: Source and received signals obtained from bender element tests 6 – 7.

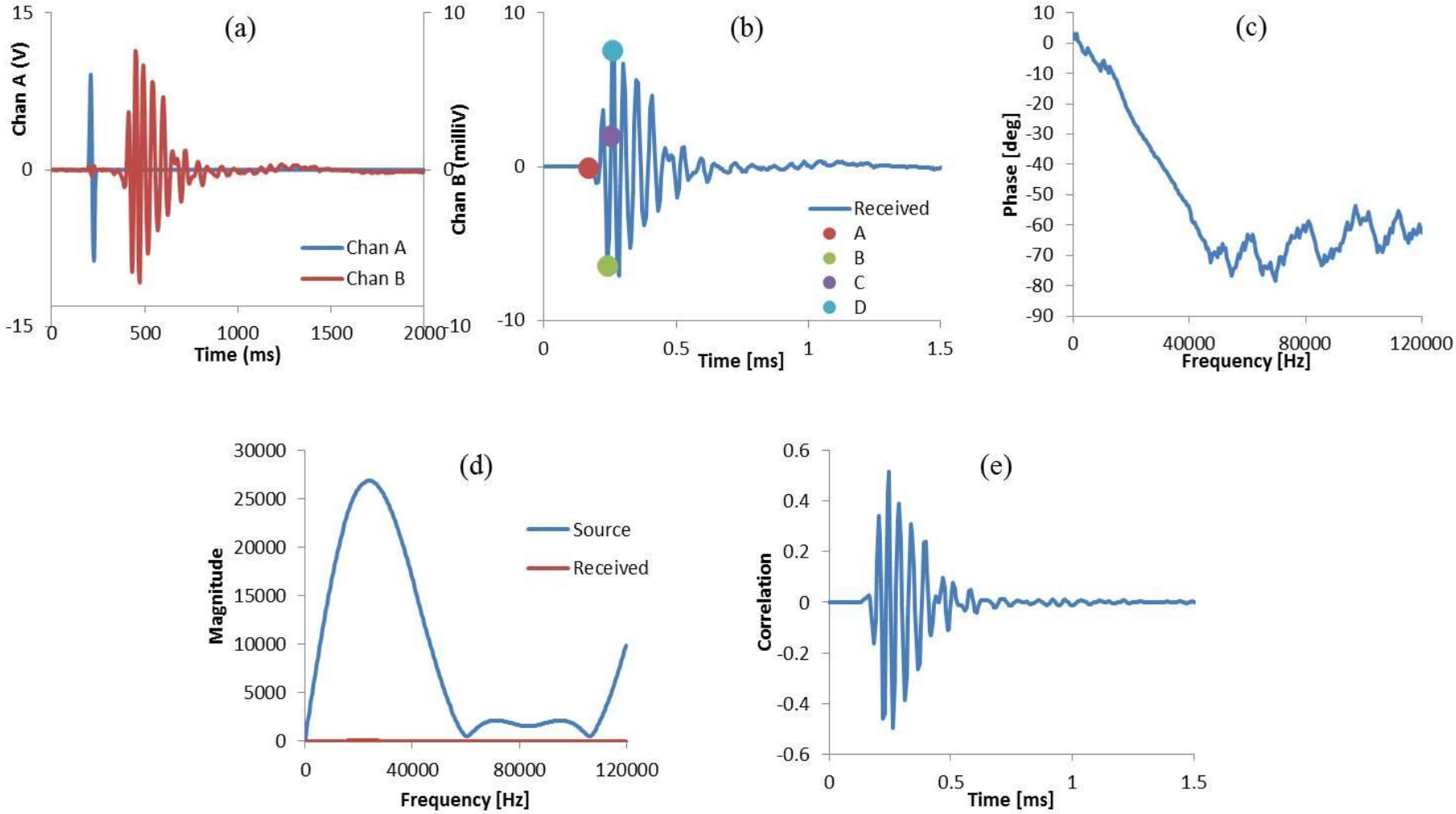

Figure A5.38: GDS BEAT Interpretation of bender element test 3, using time and frequency domain techniques: (a) raw signal time-domain data; (b) BEAT interpretation of possible S-wave arrival times; (c) unwrapped phase; (d) frequency spectrum; (e) cross correlation.

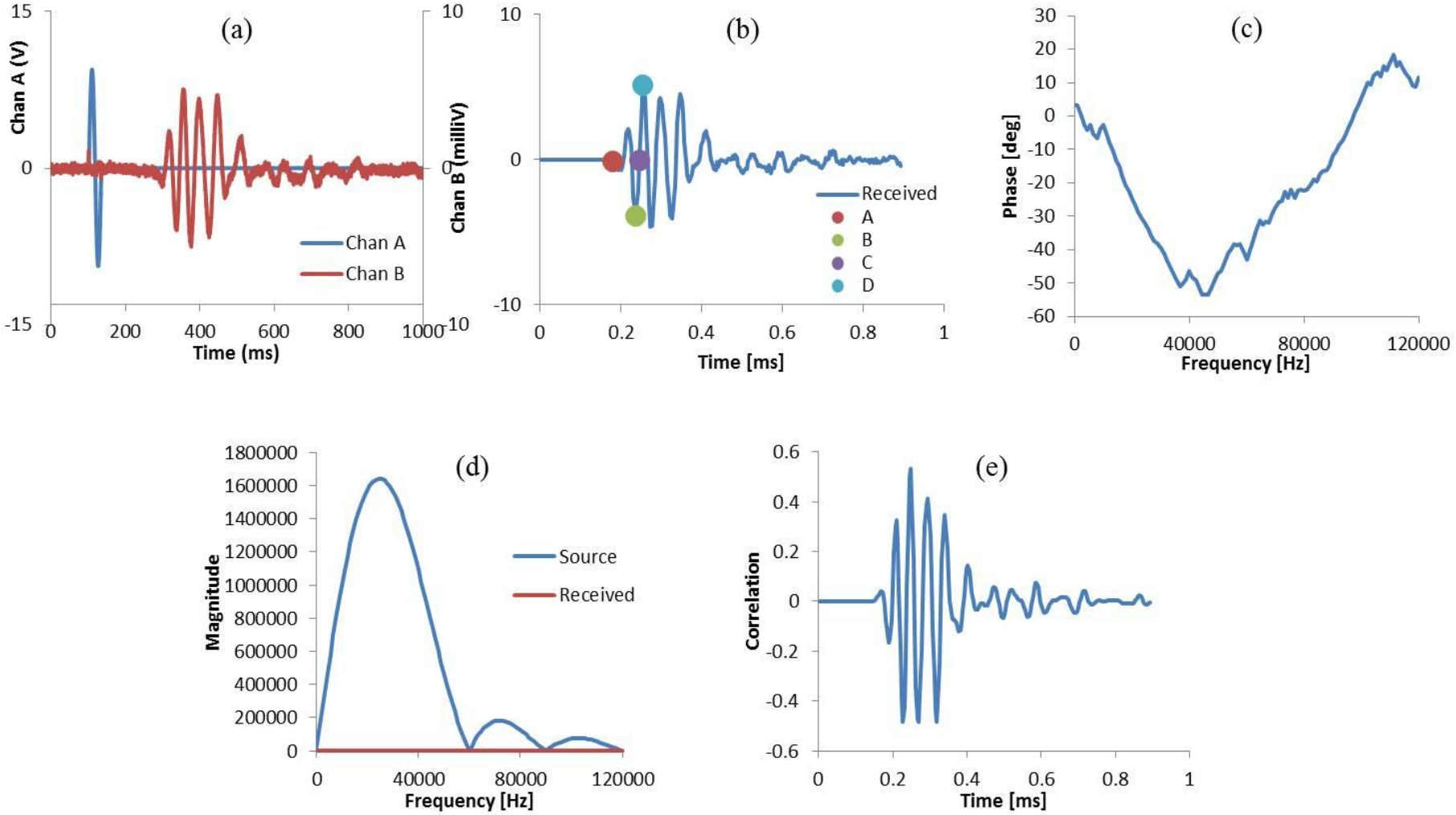

Figure A5.39: GDS BEAT Interpretation of bender element test 4, using time and frequency domain techniques: (a) raw signal time-domain data; (b) BEAT interpretation of possible S-wave arrival times; (c) unwrapped phase; (d) frequency spectrum; (e) cross correlation.

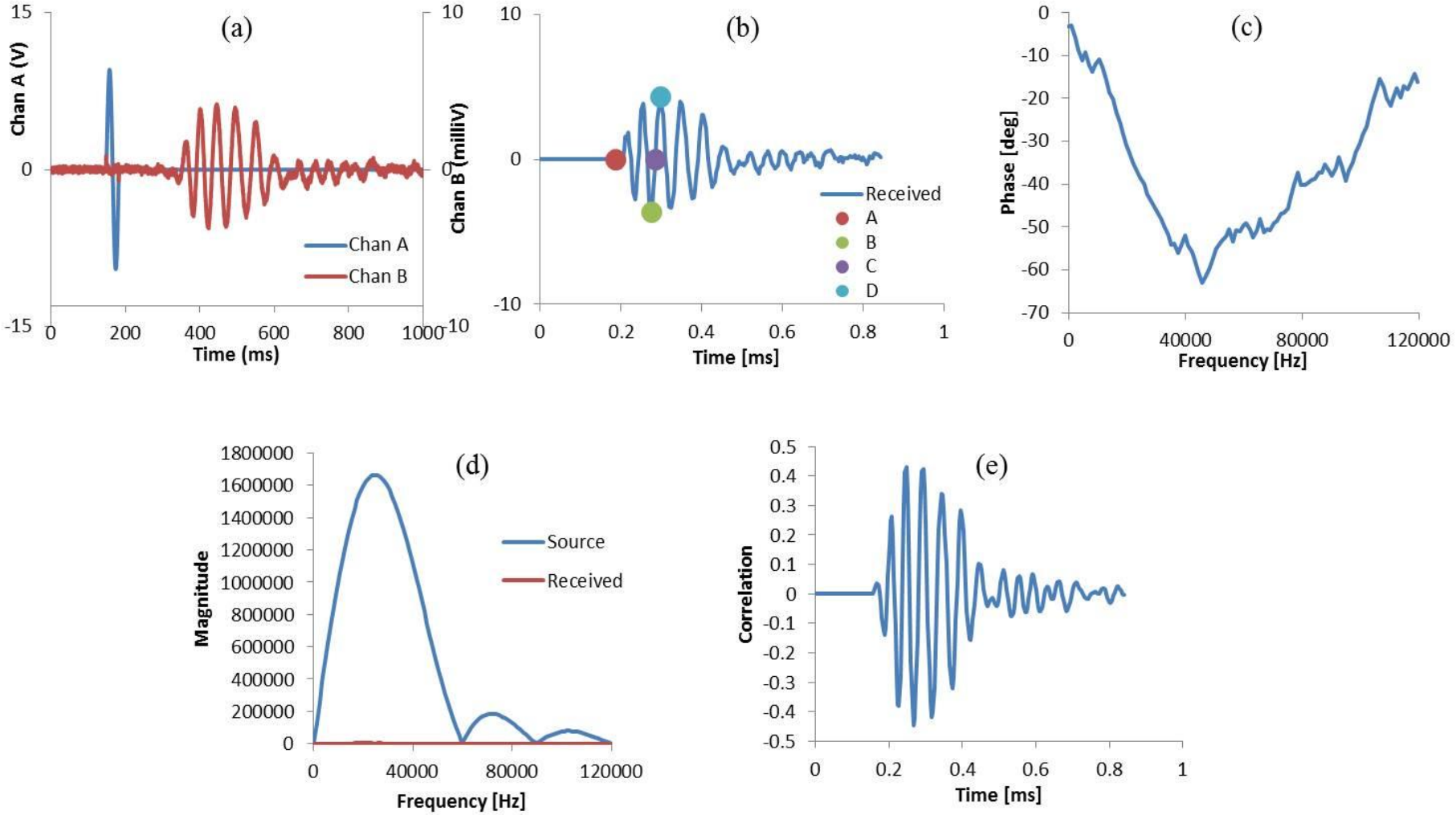

Figure A5.40: GDS BEAT Interpretation of bender element test 5, using time and frequency domain techniques: (a) raw signal time-domain data; (b) BEAT interpretation of possible S-wave arrival times; (c) unwrapped phase; (d) frequency spectrum; (e) cross correlation.

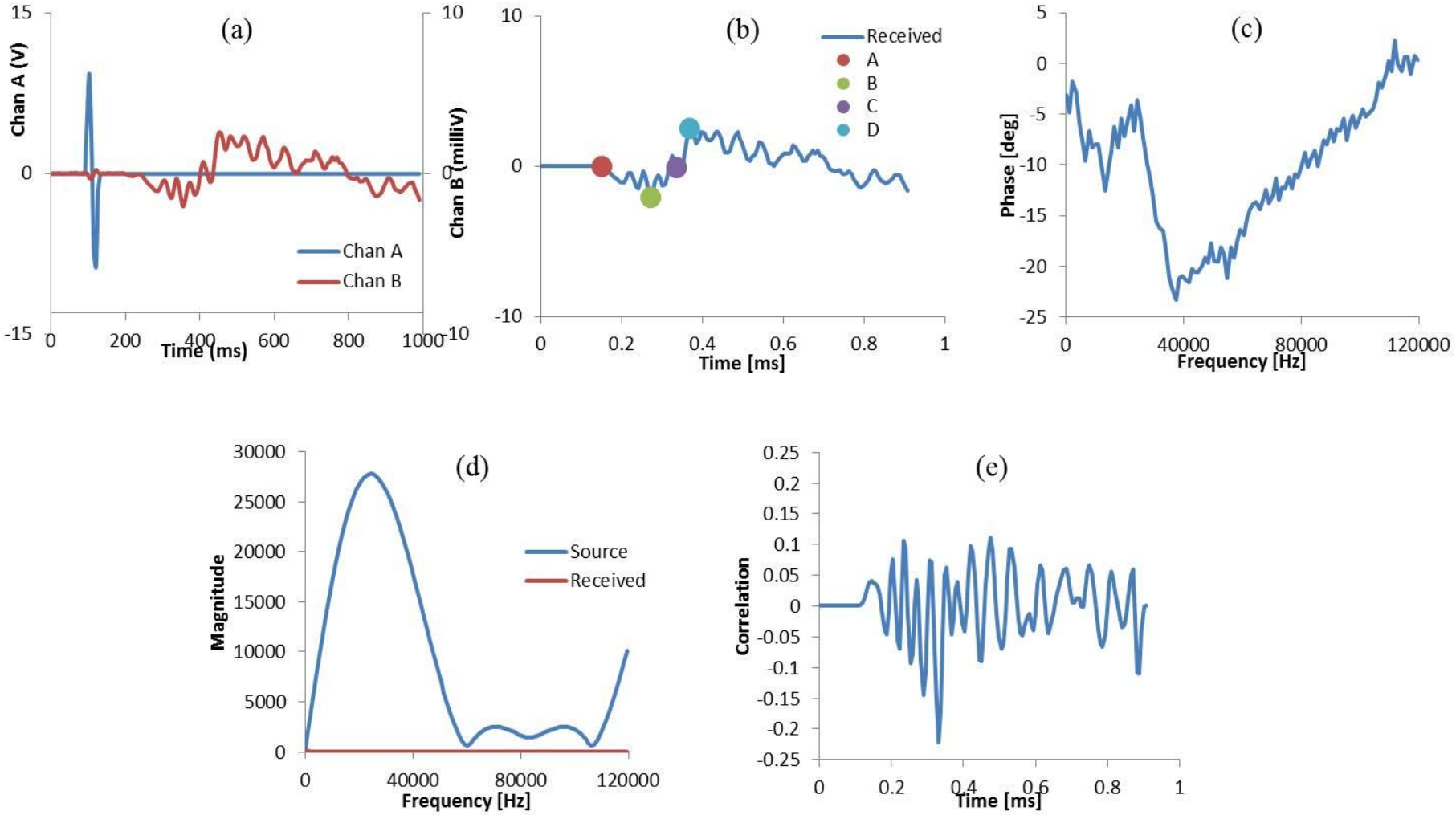

Figure A5.41: GDS BEAT Interpretation of bender element test 6, using time and frequency domain techniques: (a) raw signal time-domain data; (b) BEAT interpretation of possible S-wave arrival times; (c) unwrapped phase; (d) frequency spectrum; (e) cross correlation.

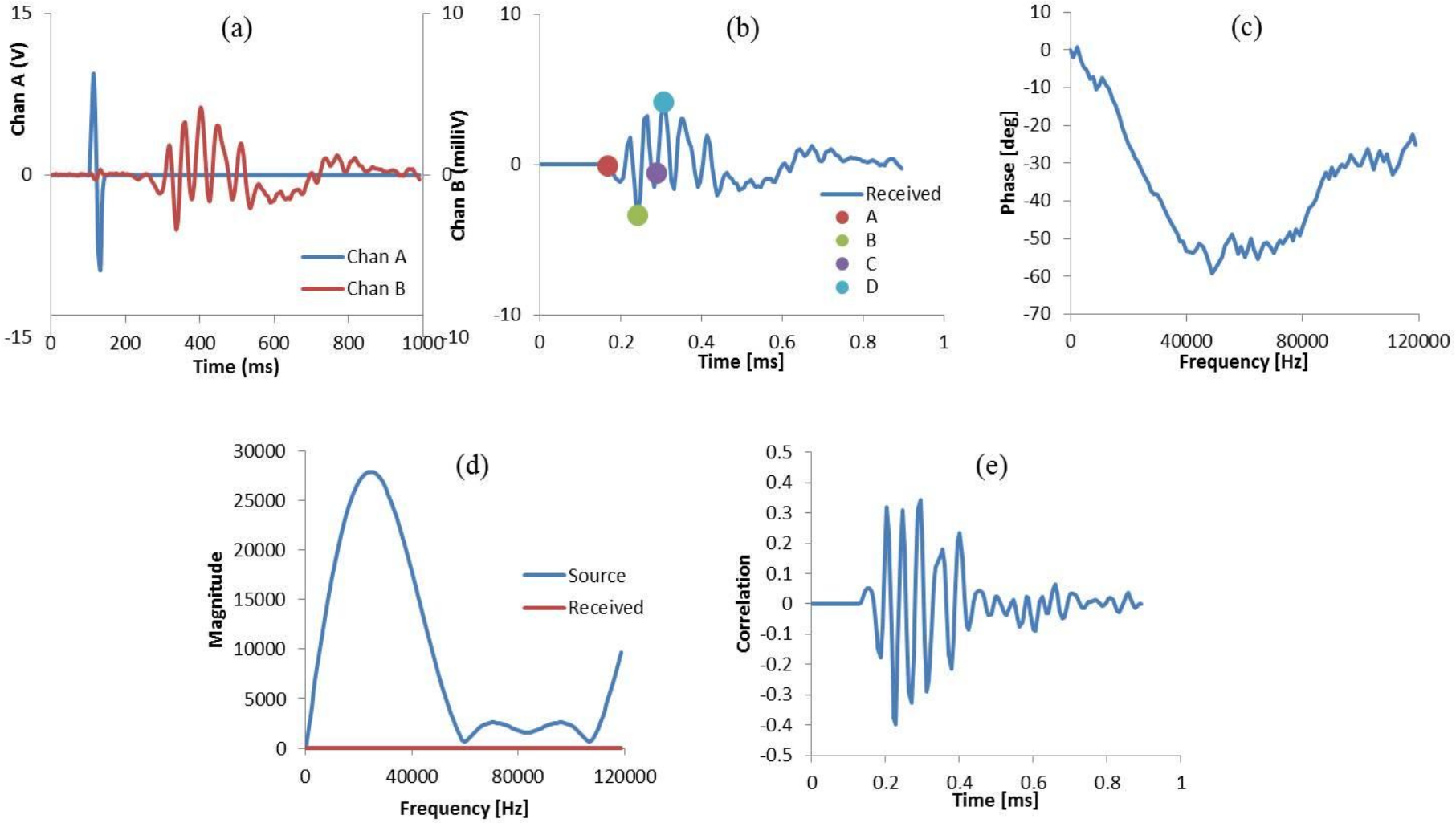

Figure A5.42: GDS BEAT Interpretation of bender element test 7, using time and frequency domain techniques: (a) raw signal time-domain data; (b) BEAT interpretation of possible S-wave arrival times; (c) unwrapped phase; (d) frequency spectrum; (e) cross correlation.

Generally, the arrival times for the initial deflection within the S-wave signals using frequencies of 10 kHz were slightly shorter than those recorded when using higher frequencies of 20 and 30 kHz; the arrival times for which were very comparable. The effect of using higher frequencies resulted in shorter wavelengths being produced for the P-wave signal and consequently, the time difference between the start and the end of the received S-wave signal patterns became shorter. Contrary to findings by Chan (2012), attenuation of the received S-wave signals was not observed with increasing frequency. Unlike the author's visual observations and analyses and BEAT analyses on bender element measurements taken for untreated undisturbed Lanton alluvium in the previous chapter, there was no clear evidence of any S-wave reflections within the stabilised sample. BEAT also demonstrated far less difficulty in identifying the arrival times of initial deflection for S-waves. There was a good correlation between the initial deflection arrival time which the BEAT determined with that determined by the author. BEAT also successfully removed effects due to electromagnetic coupling "crosstalk" between the transmitting and receiving bender elements. A summary of the arrival times, S-wave velocities and G_{max} values for bender element measurements 3–7 at 30 kHz obtained by BEAT via the time and frequency domain techniques is shown in Table A5.5.

With the exception of bender element measurement 6, the BEAT experienced some difficulty in identifying the arrival times for points corresponding to the first bump maximum, first zero crossing and first maximum peak. For the first bump maximum and first major peak, BEAT tended to take the arrival times corresponding to the largest magnitude peaks in the negative and positive y-direction, respectively. The time taken by BEAT for the first zero crossing was taken as the point where the signal passed through the time axis half way between the largest magnitude peaks in the negative and positive y-direction. Based on the academic literature and findings from bender element measurements taken for untreated undisturbed Lanton alluvium in the previous chapter, the author deemed the BEAT arrival times for the first bump maximum, first zero crossing and first maximum peak to be slightly too slow. Hence, the visual analysis technique presented in Figure A5.27 was adopted to more accurately determine S-wave arrival times for bender element measurements 3–7 taken for the stabilised Lanton alluvium.

Table A5.6 presents a summary of the S-wave arrival times, S-wave velocities and G_{max} values obtained for bender measurements 3–7 taken at a frequency of 30 kHz, through using the time-domain technique. When comparing the G_{max} values displayed in Tables A5.5–A5.6, there are some considerable stiffness discrepancies. In general the initial shear stiffnesses measured visually by the author were higher than those derived by BEAT. The highest stiffness values for each bender measurement were obtained for the initial deflection when using the time-domain analysis technique. Due to the fact that bender element measurements 3–5 were taken prior to the sample reaching its fully saturated or consolidated states, the G_{max} values derived from these measurements should not be taken as the true initial shear stiffness of the material prior to shearing.

Table A5.5: Summary of the S-wave arrival times, shear wave velocities and G_{max} values obtained by GDS BEAT for the five bender element measurements taken for the undisturbed Lanton alluvium.

	Time-domain analysis															**Frequency-domain analysis**		
	A (initial deflection)			**B (first bump max)**			**C (first zero cross)**			**D (first major peak)**			**Cross-correlation**					
Bender test no.	***t (μs)***	***V_s (m/s)***	***G_{max} (MPa)***	***t (μs)***	***V_s (m/s)***	***G_{max} (MPa)***	***t (μs)***	***V_s (m/s)***	***G_{max} (MPa)***	***t (μs)***	***V_s (m/s)***	***G_{max} (MPa)***	***t (μs)***	***V_s (m/s)***	***G_{max} (MPa)***	***t (μs)***	***V_s (m/s)***	***G_{max} (MPa)***
3	168	1007	1933.2	240	704.9	947.3	252	671.4	859.2	258	655.7	819.7	246	687.7	901.6	232	729.2	1013.7
4	180	939.8	1683.9	236	716.8	979.6	245	690.5	908.9	254	666	845.7	247	684.9	894.3	234	722.9	996.4
5	186	910.1	1577.1	276	613.3	716.3	285	593.9	671.7	298	568	614.4	246	688.1	901.6	221	765.9	1117.1
6	150	1128.2	2424.4	270	626.8	748.3	336	503.6	483.2	366	462.4	407.2	474	357	242.8	222	762.3	1106.8
7	168	1003	1924.6	240	702.1	943	288	585.1	654.9	306	550.7	580.1	294	573.2	628.4	215	783.8	1175.1

Table A5.6: Summary of the S-wave arrival times, shear wave velocities and G_{max} values obtained visually by the author for bender element measurements 3 – 7 taken at a frequency of 30 kHz for the 28 day cured GGBS-NaOH Lanton alluvium.

	Time-domain analysis											
	A (initial deflection)			**B (first bump max)**			**C (first zero cross)**			**D (first major peak)**		
Bender test no.	***t*** ***(μs)***	***V_s*** ***(m/s)***	***G_{max}*** ***(MPa)***	***t*** ***(μs)***	***V_s*** ***(m/s)***	***G_{max}*** ***(MPa)***	***t*** ***(μs)***	***V_s*** ***(m/s)***	***G_{max}*** ***(MPa)***	***t*** ***(μs)***	***V_s*** ***(m/s)***	***G_{max}*** ***(MPa)***
3	162	1044.3	2079.1	198	854.5	1391.8	210	805.6	1237.3	222	762.1	1107.1
4	179	944.5	1700.9	201	841.6	1350.4	206	822	1288.2	216	781.7	1165.1
5	187	905.2	1560.3	196	863.6	1420.3	206	822.9	1289.5	215	786.2	1177.1
6	156	1084.8	2241.5	270	626.8	748.3	354	478	435.3	366	462.4	407.2
7	150	1123.4	2414.2	198	851.1	1385.4	204	826	1305	216	780.1	1164.2

As interference from high frequencies can cause difficulties in identifying the first deflection within the S-wave signal (Chan, 2012), the G_{max} values obtained visually by the author or from BEAT for the initial deflection should be used with caution. Per the methodology used in the previous chapter, the first bump maximum was selected as the point of interest on S-wave signals; and is most likely to be the true S-wave arrival time; as recommended by Nash and Diambra (2013). Therefore, according to the author's visual analysis of bender measurement 7, stabilised Lanton alluvium had a G_{max} value of approximately 1385 MPa at a small strain level of 0.0001%, under an effective confining pressure of 50 kPa. Although there was a significant stiffness discrepancy of over 400 MPa between this value and that obtained by BEAT for the same point of interest using time-domain analysis, a much closer correlation was evident between the author's G_{max} value and that obtained by BEAT through the frequency-domain technique (1175 MPa).

Such high G_{max} values do not seem unreasonable for Lanton alluvium stabilised with 7.5% GGBS-NaOH. G_{max} values >1000 MPa were recorded by Cuccovillo and Coop (1997) for an intact rock sample of cemented calcarenite and Trhlikova et al. (2012) measured G_{max} values of approximately 700 MPa for pure Nevada sand, which had been stabilised with only 4% cement. However, further bender element analyses on GGBS-NaOH stabilised Lanton alluvium at various effective confining stresses is required; especially as the results in Chapter 8 demonstrate that the strength and stiffness of the material during shearing is influenced by increasing effective confining pressures when such values exceed 200 kPa. The focus should be on using bender elements to measure the initial and changing shear stiffnesses during shearing at lower frequencies (i.e. not exceeding 20 kHz), so as to reduce noise/interference effects and to complement the small strain stiffness data obtained from local axial/radial LVDT measurements. Additionally, future efforts should also focus on attempting to increase the level of correlation between the G_{max} values obtained by the engineer and those derived from the GDS BEAT tool.

A5.3.2.3 Small strain stiffness degradation

Figure A5.43 displays the secant shear stiffness degradation behaviour of 28 day cured GGBS-NaOH stabilised Lanton alluvium tested at Bristol, produced through using local (axial and radial) strain and bender element measurements. Unlike the stiffness degradation data obtained from undrained triaxial tests at Newcastle (Figure 8.12), considerably higher shear stiffness values were captured at smaller shear strain levels (i.e. <0.001%). Additionally, Figure A5.43 shows the sample reached its minimum shear stiffness after 0.05% shear strain was experienced. This is at least one order of magnitude smaller than the shear strains measured at Newcastle at which shear stiffnesses reached their steady state minimum. Given the much higher resolution of the shear stiffness data obtained from Bristol compared with that obtained from Newcastle, the much higher stiffnesses in Figure A5.43 are considered more accurate.

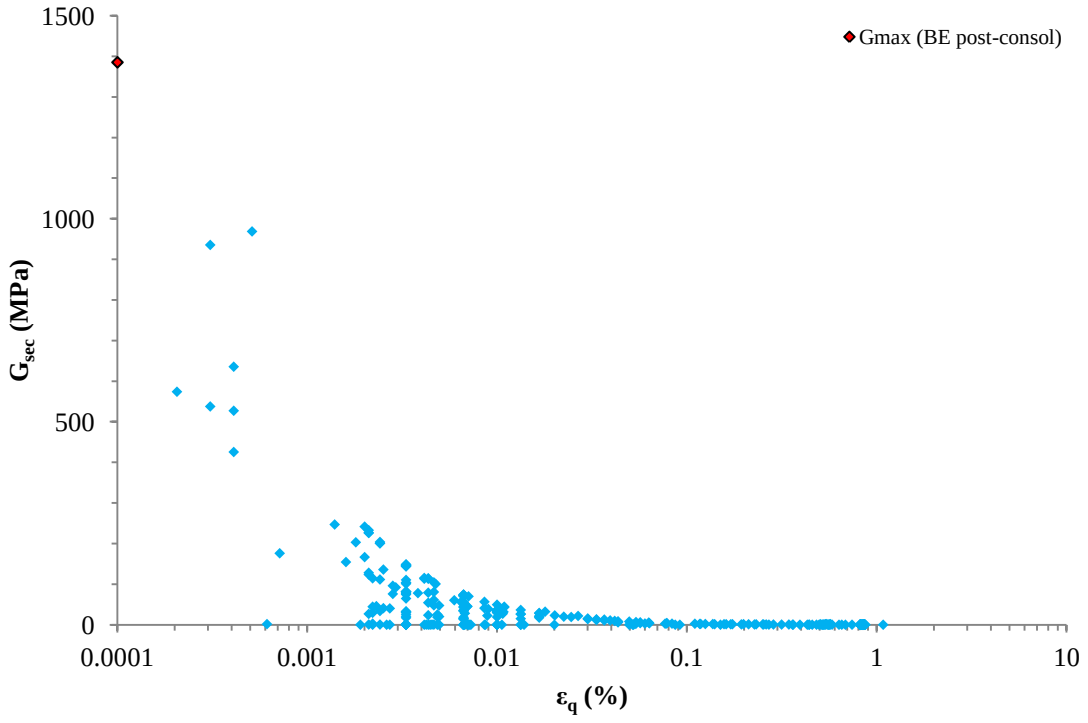

Figure A5.43: Secant shear stiffness degradation behaviour for undrained small strain GGBS-NaOH stabilised Lanton alluvium sample. G_{max} value presented was obtained from bender element (BE) measurements.

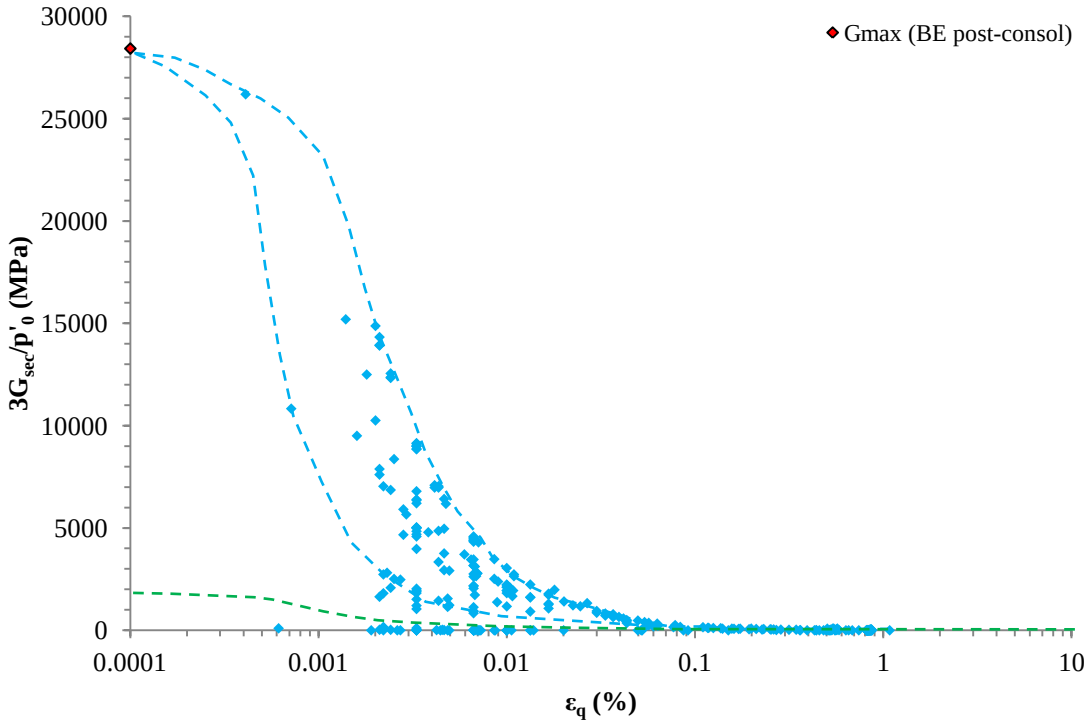

Figure A5.44: Secant shear stiffness degradation behaviour for undrained small strain GGBS-NaOH stabilised Lanton alluvium sample (blue) normalised by its corresponding p'_0 value. Normalised scant shear stiffness degradation curve for undisturbed Lanton alluvium (green) superimposed.

As with the Newcastle data, the raw shear stiffness data in Figure A5.43 was normalised with respect to the sample's p'_0 of 50 kPa. The normalisation of shear stiffness data obtained for stabilised Lanton alluvium samples tested at p'_0 = 50 kPa was unsuccessful in producing less data scatter and therefore in defining a tighter fitting curve with a higher degree of correlation. The same observation is evident in Figure A5.44, albeit a stiffness degradation curve for the material can be defined. For comparison, the small strain secant shear stiffness degradation curve for untreated undisturbed Lanton alluvium has been superimposed on Figure A5.44. Although the r_0 value for the untreated undisturbed soil is considered to be higher than that for the stabilised soil, the level of improvement regarding the material's shear stiffness due to the GGBS-NaOH cementitious binder is very impressive for shear strains between 0.0001 and 0.1%. The G_{sec} data for stabilised Lanton alluvium has also been normalised with respect to the G_{max} value of 1385 MPa derived from bender element measurements. The results of this normalisation are presented in Figure A5.45, along

with the normalised results for untreated undisturbed Lanton alluvium sample for comparison purposes.

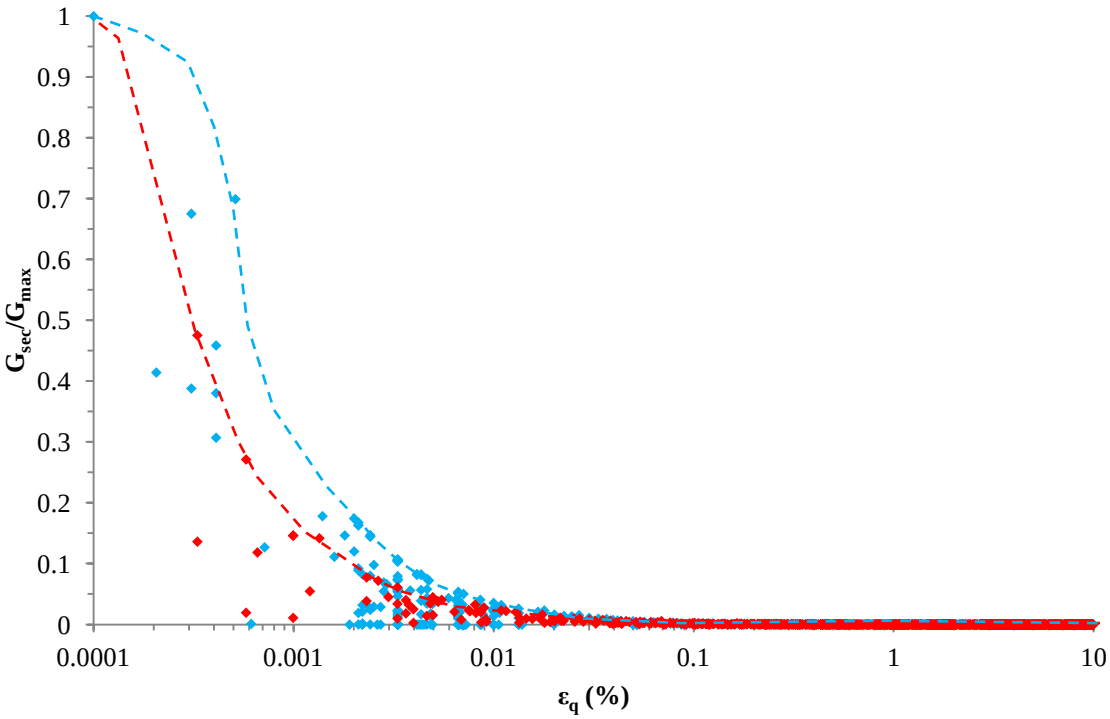

Figure A5.45: Secant small strain shear stiffness degradation behaviour for undrained GGBS-NaOH stabilised (blue) and untreated undisturbed (red) Lanton alluvium samples, normalised by their G_{max} values.

The G_{max}-normalised G_{sec} data sets in Figure A5.45 show that within the strain ranges of 0.0001–0.01%, the shear stiffness degradation curve for the stabilised soil is shifted towards the right, relative to the position of untreated undisturbed Lanton alluvium's curve; whereby its threshold shear strain is higher due to its cement content and thus higher strength.

A5.4 Summary

From oedometer and triaxial testing results in chapters 5 and 7, respectively, undisturbed Lanton alluvium has been deemed to be a very sensitive soil whose initial

sedimentation structure and shear stiffnesses degrade very easily upon the application of very small loads and shear strains. This explains the very steep curve in Figure A5.45 for shear strains between 0.0001 and 0.001%. However, for the stabilised soil, once its cemented structure breaks down, it does so reasonably quickly; thereby causing it's shear stiffness degradation curve to steepen towards an almost vertical angle. Regarding the rate of internal structure loss for the two materials, although the stabilised soil is characterised by significantly higher initial G_{max} values, its cemented structure is lost within a shorter time compared with the natural structure of undisturbed untreated Lanton alluvium. The shear stiffness degradation curves for the untreated and stabilised Lanton alluvium converge at shear strains of 0.02% and achieve their minimum steady state shear stiffnesses at approximately 0.04% shear strain.

The significant differences between the shear stiffnesses measured from triaxial tests at Newcastle and Bristol point towards the need to measure strains and stiffnesses via local rather than global LVDT's measurements. The higher apparent stiffnesses measured by the Newcastle triaxial tests for stabilised Lanton alluvium at larger strains will probably be attributable to factors including apparatus compliance and specimen boundary restraint effects. Restraining effects presented by the membrane were corrected for per BS 1377 (BSI, 1990); although given the high stiffness of the stabilised samples, the restraining effect caused by the membrane is thought to have been negligible. Further monotonic testing on this material is required, specifically involving local strain measurements and bender elements to better define the small strain stiffness behaviour of GGBS-NaOH stabilised Lanton alluvium after 28 days curing and how this potentially changes with increasing effective confining stresses.